ACTA RADIOLOGICA

FOUNDED IN 1921 BY GÖSTA FORSSELL

OFFICIAL ORGAN OF THE RADIOLOGICAL SOCIETIES OF DENMARK FINLAND NORWAY AND SWEDEN

DIAGNOSIS

INDICES to Vol 16 (1975)

January March May July September November

Contents of Volume 16 — DIAGNOSIS

Contents of Volume 16 — DIAGNOSIS

Lungs Pleura, Mediastinum and Chest walls

Bones and Joints (incl soft tissue)

Subject index to Volume 16 — Diagnosis

ROENTGEN DIAGNOSIS

Nervous system

Digestive tract (incl biliary tract and spleen)

Heart and Vessels (incl lymphatic vessels)

CONTRAST MEDIA

MISCELLANEOUS

Ear, Nose and Throat

Ophthalmology

Uro genital system

ISOTOPES

TECHNIQUE

List of Supplements to Acta Radiologica

Nos 173–346

(Issued November 1975)

For Suppl Nos 1–172 inclusive, see list issued December 1960, in Vol 54, fasc 6

The supplements are published from time to time and are not included in the subscription rate Prices and year of publication of numbers already issued are detailed below

173 ERIK ODEBLAD BJORN WESTIN and SVEN ERIK ENGLUND Disappearance measurements Theoretical technical, biological and medical aspects 1959 *Price Sw Kr 30*

174 LARS BILLING and ERIK SEVERIN Slipping epiphysis of the hip A roentgenological and clinical study based on a new roentgen technique 1959 *Price Sw Kr 35*

175 ÅKE HA[illegible]

17[illegible]

Sw Kr 25

177 PEKKA VUORINEN The roentgenographic slit methods A survey and analysis of procedures based on the use of a narrow bundle of roentgen rays (scanography) 1959 *Price Sw Kr 25*

178 BENGT H O ROSENGREN Determination of cell mass by direct X ray absorption 1959 *Price Sw Kr 25*

179 S HULTBERG, O DAHL, R THORAEUS, K J VIKTERLÖF and R WALSTAM Kilocurie cobalt 60 therapy at the Radiumhemmet Equipment, technique and dose measurements 1959 *Price Sw Kr 35*

180 BENGT LILJA Motor activity of the stomach 1959 *Price Sw Kr 25*

181 PER AMUNDSEN The diagnostic value of conventional radiological examination of the heart in adults (Appendix by R G CARPENTER An account of the statistical analysis of the relative heart volumes of 755 patients in various disease groups) 1959 *Price Sw Kr 20*

182 H M TRUBY Acoustico-cineradiographic analysis considerations with especial reference to certain consonantal complexes 1959 *Price Sw Kr 35*

183 ERIK BOIJSEN Angiographic studies of the anatomy of single and multiple renal arteries 1959 *Price Sw Kr 30*

184 GUSTAF NOTTER A technique for destruction of the hypophysis using Y^{90} spheres A radiologic, endocrine and histologic study 1959 *Price Sw Kr 35*

185 BENGT LILIEQUIST The subarachnoid cisterns An anatomic and roentgenologic study 1959 *Price Sw Kr 35*

186 BENGT LILIEQUIST Pontine angle tumour Encephalographic appearances 1959 *Price Sw Kr 30*

187 HOLGER SKÖLDBORN On the design physical propert[illegible]

1[illegible]

189 OLOV DAHL and KARL JOHAN VIKTERLÖF Attainment and value of precision in deep radiotherapy Some fundamentals with special reference to moving beam therapy with 200 to 250 kV roentgen rays and cobalt 60 gamma radiation 1960 *Price Sw Kr 35*

List of Authors

List of Supplements to Acta Radiologica

Nos 173–346

(Issued November 1975)

For Suppl Nos 1 172 inclusive see list issued December 1960 in Vol 54, fasc 6

The supplements are published from time to time and are not included in the subscription rate Prices and year of publication of numbers already issued are detailed below

173 Erik Odeblad Björn Westin and Sven Erik Englund Disappearance measurements Theoretical technical biological and medical aspects 1959 *Price Sw Kr 30*

174 Lars Billing and Erik Severin Slipping epiphysis of the hip A roentgenological and clinical study based on a new roentgen technique 1959 *Price Sw Kr 35*

175 Åke Hanngren Studies on the distribution and fate of C^{14} and T labelled p-aminosalicylic acid (PAS) in the body 1959 *Price Sw Kr 25*

176 Lars Björk Cineradiographic studies on the Fallopian tubes in rabbits 1959 *Price Sw Kr 25*

177 Pekka Vuorinen The roentgenographic slit methods A survey and analysis of procedures based on the use of a narrow bundle of roentgen rays (scanography) 1959 *Price Sw Kr 25*

178 Bengt H O Rosengren Determination of cell mass by direct X ray absorption 1959 *Price Sw Kr 25*

179 S Hultberg O Dahl, R Thoraeus, K J Vikterlöf and R Walstam Kilocurie cobalt 60 therapy at the Radiumhemmet Equipment technique and dose measurements 1959 *Price Sw Kr 35*

180 Bengt Lilja Motor activity of the stomach 1959 *Price Sw Kr 25*

181 Per Amundsen The diagnostic value of conventional radiological examination of the heart in adults (Appendix by R G Carpenter An account of the statistical analysis of the relative heart volumes of 755 patients in various disease groups) 1959 *Price Sw Kr 20*

182 H M Truby Acoustico-cineradiographic analysis considerations with especial reference to certain consonantal complexes 1959 *Price Sw Kr 35*

183 Erik Boijsen Angiographic studies of the anatomy of single and multiple renal arteries 1959 *Price Sw Kr 30*

184 C [illegible]
radi[illegible]

185 [illegible]
195[illegible] *[illegible] Sw Kr 35*

186 Bengt Liliequist Pontine angle tumour Encephalographic appearances 1959 *Price Sw Kr 30*

187 Holger Sköldborn On the design physical properties and practical application of small condenser ionization chambers 1959 *Price Sw Kr 30*

188 Jens Nielsen Anno Aetatis Suae LX Papers dedicated to Jens Nielsen professor of radiotherapy at the University of Copenhagen on his sixtieth anniversary December 19 1959 *Price Sw Kr 40*

189 Olov Dahl and Karl Johan Vikterlöf Attainment and value of precision in deep radiotherapy Some fundamentals with special reference to moving beam therapy with 200 to 250 kV roentgen rays and cobalt 60 gamma radiation 1960 *Price Sw Kr 35*

List of Authors

309 LAURI PATOMÄKI A mathematical model for radiation fields of telecobalt treatment units—With special reference to the isodoses of Rocus 1971 *Price Sw Kr 35*

310 RADIOBIOLOGIC INVESTIGATIONS Edited by Erik Lindgren and Bernhard Tribukait 1971 *Price Sw Kr 45*

311 HALVOR VERMUND Enhancement of radiation effects by chemotherapy 1971 *Price Sw Kr 35*

312 PERTTI KASKI Osteomedullography of the tibia 1971 *Price Sw Kr 40*

313 PROCEEDINGS OF THE SIXTH CONFERENCE OF THE NORDIC ASSOCIATION OF CLINICAL PHYSICS held in Århus Denmark 1970 Edited by C B Madsen and K Liden. 1972 *Price Sw Kr 45*

314 BIRGER HELIN Heart volume in human kidney transplantation 1972 *Price Sw Kr 25*

315 UNO WEGELIUS Angiography of the hand Clinical and postmortem investigations 1972 *Price Sw Kr 35*

316 P E S PALMER Haemangiosarcoma of Kaposi 1972 *Price Sw Kr 35*

317 JUHANI RAUSTE Lymphographic findings in granulomatous inflammations and connective tissue diseases—Differential diagnosis between these diseases and lymphomas 1972 *Price Sw Kr 30*

318 OVE MATTSSON Formation of the tomographic image—With special reference to blurring 1972 *Price Sw Kr 35*

319 PROGRESS IN VETERINARY RADIOLOGY Proceedings of the 2nd International Conference of Veterinary Radiologists held in Stockholm 1970 Edited by Sten Erik Olsson 1972 *Price Sw Kr 45*

320 TJAKKO KUIPERS Carcinoma of the uterine cervix Aspects of clinical oncology in patients referred for radiation therapy 1972 *Price Sw Kr 50*

321 BO LUNDSTROM Angiographic abnormalities following percutaneous needle biopsy of the kidney 1972 *Price Sw Kr 40*

322 LARS BLOMQUIST Mode of accumulation of iodophenylalanines in the exocrine pancreas and a[illegible]

[illegible] resistant and skin tumor susceptible mice 1973 *Price Sw Kr 35*

325 NILS GUNNAR LINDQUIST Accumulation of drugs on melanin. 1973 *Price Sw Kr 40*

326 JOHN ERIK JOHNSSON Hysterography and diagnostic curettage in carcinoma of the uterine body 1973 *Price Sw Kr 40*

327 ERIC BERGQUIST Tentorial notch and adjacent major vessels in carotid angiography 1973 *Price Sw Kr 45*

328 O HASSLER and S O HIETALA Angiographic abnormalities in the urinary bladder wall after irradiation Part I Animal experiments Part II Clinical investigation 1973 *Price Sw Kr 45*

329 OLOF ECKERDAL Tomography of the temporomandibular joint—Correlation between tomographic image and histologic sections in a three-dimensional system 1973 *Price Sw Kr 40*

330 JORMA RANTANEN Radiation injury of connective tissue—A biochemical investigation with experimental granuloma 1973 *Price Sw Kr 40*

331 FRANZ PAUL PROBST Congenital defects of the corpus callosum—Morphology and encephalographic appearances 1973 *Price Sw Kr 50*

[illegible]

[illegible] measure

[illegible] KOTTMEIER Carcinoma of the uterine corpus—A retrospective survey of individualized therapy 1973 *Price Sw Kr 40*

335 Metrizamide, a non ionic water soluble contrast medium—Experimental and preliminary clinical investigations 1973 *Price Sw Kr 50*

336 Sven Scheller and Lars Mårtenson Traumatic dislocation of the patella A radiographic investigation 1974 *Price Sw Kr 50*

337 Ossi Korhola Myocardial scintigraphy and estimation of regional blood flow with xenon 133 1974 *Price Sw Kr 40*

338 Kurt Åstrand and Sven Reichmann Optimised tomography Theoretical and practical analyses of the elimination of depiction errors in tomography 1974 *Price Sw Kr 40*

339 Ilkka Suramo Lymphography in tuberculosis 1974 *Price Sw Kr 40*

340 Eeva Nordman ^{75}Se sodium selenite scintigraphy in diagnosis of tumours 1974 *Price Sw Kr 45*

341 Ilpo Lauteala Pelvimetry with image intensifier camera A low radiation dose method 1974 *Price Sw Kr 50*

342 Anders Möller Pneumography in paraventricular and intraventricular tumours of the posterior fossa 1974 *Price Sw Kr 60*

343 Håkan Jorulf Roentgen diagnosis of intraperitoneal fluid A physical, anatomic and clinical investigation 1975 *Price Sw Kr 55*

344 *Skeletal development, growth rate and hip dysplasia Experimental investigations* with special reference to the effect of estrogens growth hormone and nutrition Edited by Sten Erik Olsson 1975 *Price Sw Kr 70*

345 Hans Kuisk and Faiz M Khan Nominal standard dose and tumor standard dose Tables for radiation therapy planning and analysis 1975 *Price Sw Kr 65*

346 Computer tomography of brain lesions Edited by Erik Lindgren 1975 *Price Sw Kr 73*

ACTA RADIOLOGICA

OFFICIAL ORGAN OF THE RADIOLOGICAL SOCIETIES OF
DENMARK, FINLAND, NORWAY AND SWEDEN

Vol 16 Fasc 1	DIAGNOSIS	1975 January

ORBITAL PHLEBOGRAPHY

IV. The cavernous sinuses and adjacent venous sinuses of the skull base

JAN BRISMAR

The cavernous sinuses and adjacent basal venous sinuses may be affected in various disorders in and close to the base of the skull Sufficient information concerning these sinuses may be achieved by carotid angiography only in a minority of cases, and thus, phlebography is often indicated Two different phlebographic routes to the basal sinuses have been used, the anterior approach via the orbital veins and the posterior via the inferior petrosal sinuses

The technique of angular vein puncture for orbital phlebography introduced by DEJEAN & BOUDET (1951) may also be used for examination of the cavernous sinus (BREGEAT et coll 1952) This technique was used by several authors (BÉTOULIÈRES et coll 1957, ARSENI et coll 1965, ARON-ROSA et coll 1966, 1967) although even the ipsilateral cavernous sinus was not always demonstrated Frontal vein puncture, introduced by VRITSIOS (1961) and modified by VIGNAUD (1970), has improved the results of orbital phlebography (BRISMAR 1974 a, b, c) as well as of examinations of [illegible] PISCOL 1970, ENGEL [illegible] be obtained when [illegible] technique, provided that the superior ophthalmic veins were unobstructed

From the Section on Neuroradiology (Director S Cronqvist), Department of Diagnostic Radiology (Director Prof O Olsson) University Hospital S-221 85 Lund, Sweden

Submitted for publication 21 December 1973

(LLOYD) Bilateral filling of the cavernous sinuses and the adjacent basal sinuses (SHIU et coll 1968, WAGA et coll 1970, CLAY et coll 1972, VIGNAUD et coll 1972 b) may also be achieved with the method of inferior petrosal sinus catheterization via the internal jugular vein (HANAFEE et coll 1965) Alternatively, the inferior petrosal sinuses may be catheterized via the femoral vein (TAKAHASHI & TANAKA 1971) These two methods are complementary if the orbital veins or the basal sinuses are occluded However, in some seven per cent of cases (SHIU et coll) the anatomy of the inferior petrosal sinus prevents the use of the posterior approach Furthermore, while no complications have been described in association with the frontal vein puncture, SHIU et coll in 100 patients examined with inferior petrosal sinus catheterization reported one patient with a lateral medullary syndrome developing during the examination, presumably due to rupture of one of the pontine veins, in two other cases contrast medium extravasated into the subdural space but without any serious consequences Frontal vein puncture is simpler than inferior petrosal sinus catheterization and may also be performed on out-patients Thus, the former method seems to be preferable as the primary method of approach

Reports on the normal phlebographic appearance of the basal sinuses of the skull are partly contradictory and do not always agree with classical anatomic descriptions Lateral displacement of the cavernous sinus has been used as a sign of pituitary tumors (SHIU et coll , WAGA et coll), although no normal values for the transverse diameter of the pituitary fossa, as defined by the medial borders of the cavernous sinuses, are given in the literature

As several problems remain regarding phlebography by injection of contrast medium into a frontal vein for examination of disorders in and close to the base of the skull the present investigation was undertaken to (1) evaluate the value of the method to demonstrate the basal veins of the skull, (2) arrive at a deeper knowledge of the normal phlebographic anatomy of the cavernous sinus and adjacent basal venous sinuses, and (3) determine the normal transverse diameter of the pituitary fossa, as assessed from the medial borders of the cavernous sinuses

Anatomy

While the detailed anatomy of the cavernous sinus is still a matter of dispute, especially with respect to the positions of the cranial nerves and the carotid artery in relation to the 'cavernous tissue', the general arrangement of the basal venous sinuses is not a matter of controversy among anatomists (HAFFERL 1969) The nomenclature used in the present report appears in Fig 1

The cavernous sinuses (CS) are located on each side of the sella turcica, extending from the superior orbital fissure to the apex of the pyramid The upper and lateral walls of the sinus are formed by the dura, the upper part of the medial wall consists of a septum towards the pituitary fossa while the infero-medial part borders on the lateral surface of the body of the sphenoidal bone Anteriorly, each cavernous sinus

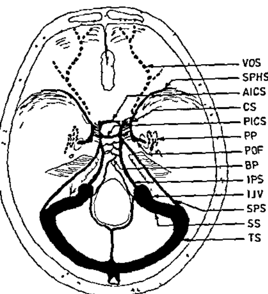


Fig 1 Basal venous sinuses AICS = anterior intercavernous sinus, BP = basilar plexus, CS = cavernous sinus IJV = internal jugular vein, IPS = inferior petrosal sinus, PICS = posterior intercavernous sinus, POF = plexus of the foramen ovale, PP = pterygoid plexus, SPHS = sphenoparietal sinus, SPS = superior petrosal sinus, SS sigmoid sinus, TS = transverse sinus, VOS = superior ophthalmic vein

is connected to the superior ophthalmic vein (VOS) which leaves the orbit through the superior orbital fissure and often also to the sphenoparietal sinus (SPHS) that follows the free edge of the smaller sphenoidal wing The sphenoparietal sinus is often joined by the middle cerebral veins, which, however, may also enter the cavernous sinus separately The venous plexus of the foramen ovale and adjacent foramina (POF) connects the lateral part of the cavernous sinus with the pterygoid plexus (PP) From the superior posterior part of the cavernous sinus, the superior petrosal sinus (SPS) runs in its sulcus to the sigmoid sinus, while the larger inferior petrosal sinus (IPS) leaves the inferior posterior part of the cavernous sinus, and passes in the sulcus with its name to the anterior part of the jugular foramen, where it empties in the internal jugular vein (IJV)

The two cavernous sinuses are interconnected through the anterior (AICS) and posterior intercavernous sinuses (PICS) located in the sellar diaphragm at the anterior and posterior edge of the sella turcica, and through the basilar plexus (BP), which is a venous network on the clivus This plexus is also connected with the inferior petrosal sinuses and the deep cervical veins

Material

In order to obtain a 'normal material', patients with a disorder possibly affecting the veins at the base of the skull, or with an intraorbital disorder causing an occlusion of the intraorbital veins, were not included Examinations without satisfactory technical quality permitting a detailed evaluation of the anatomy of the cavernous sinuses and the adjacent basal sinuses were also excluded Thus out of the initial

(LLOYD) Bilateral filling of the cavernous sinuses and the adjacent basal sinuses (SHIU et coll 1968, WAGA et coll 1970, CLAY et coll 1972, VIGNAUD et coll 1972 b) may also be achieved with the method of inferior petrosal sinus catheterization via the internal jugular vein (HANAFEE et coll 1965) Alternatively, the inferior petrosal sinuses may be catheterized via the femoral vein (TAKAHASHI & TANAKA 1971) These two methods are complementary if the orbital veins or the basal sinuses are occluded However, in some seven per cent of cases (SHIU et coll) the anatomy of the inferior petrosal sinus prevents the use of the posterior approach Furthermore, while no complications have been described in association with the frontal vein puncture, SHIU et coll in 100 patients examined with inferior petrosal sinus catheterization reported one patient with a lateral medullary syndrome developing during the examination, presumably due to rupture of one of the pontine veins, in two other cases contrast medium extravasated into the subdural space but without any serious consequences Frontal vein puncture is simpler than inferior petrosal sinus catheterization and may also be performed on out-patients Thus, the former method seems to be preferable as the primary method of approach

Reports on the normal phlebographic appearance of the basal sinuses of the skull are partly contradictory and do not always agree with classical anatomic descriptions Lateral displacement of the cavernous sinus has been used as a sign of pituitary tumors (SHIU et coll, WAGA et coll), although no normal values for the transverse diameter of the pituitary fossa, as defined by the medial borders of the cavernous sinuses, are given in the literature

As several problems remain regarding phlebography by injection of contrast medium into a frontal vein for examination of disorders in and close to the base of the skull the present investigation was undertaken to (1) evaluate the value of the method to demonstrate the basal veins of the skull, (2) arrive at a deeper knowledge of the normal phlebographic anatomy of the cavernous sinus and adjacent basal venous sinuses, and (3) determine the normal transverse diameter of the pituitary fossa, as assessed from the medial borders of the cavernous sinuses

Anatomy

While the detailed anatomy of the cavernous sinus is still a matter of dispute, especially with respect to the positions of the cranial nerves and the carotid artery in relation to the 'cavernous tissue', the general arrangement of the basal venous sinuses is not a matter of controversy among anatomists (HAFFERL 1969) The nomenclature used in the present report appears in Fig 1

The cavernous sinuses (CS) are located on each side of the sella turcica, extending from the superior orbital fissure to the apex of the pyramid The upper and lateral walls of the sinus are formed by the dura, the upper part of the medial wall consists of a septum towards the pituitary fossa while the infero-medial part borders on the lateral surface of the body of the sphenoidal bone Anteriorly, each cavernous sinus

Table

Incidence of filling of basal venous sinuses in the 'normal material SPHS – sphenoparietal sinus, CS = cavernous sinus AICS = anterior and PICS = posterior intercavernous sinuses, BP = basilar plexus POF = plexus of the foramen ovale IPS = inferior and SPS = superior petrosal sinuses, IJV = internal jugular vein

	n	Veins filled		
		Bilaterally		Unilaterally
SPHS	26	12		7
CS	26	26		0
AICS	26		21	
PICS	26		18	
BP	26		25	
POF	26	20		4
IPS	25	23		1
SPS	25	0		2
IJV	24	21		2

the digital compression was ineffective, and in the fourth no axial view was exposed as the patient was old and in a bad condition and without symptoms or signs of a disorder affecting the basal sinuses

Results

Bilateral filling of the cavernous sinuses and their interconnections (the anterior and posterior intercavernous sinuses and the basilar plexus), and of the plexus of the foramen ovale was obtained in a majority of cases In most cases also the inferior petrosal sinuses were completely filled to the internal jugular veins (Table)

The cavernous sinus Provided there is no obstruction of flow from the site of injection to the cavernous sinuses, and provided the compression is effective, an adequate bilateral demonstration of the cavernous sinus should always be achieved with the author's technique The sinus was best observed in the axial view (Fig 3 b) where it, in the normal material, always appeared as a roughly rectangular structure with a longitudinal defect caused by the intracavernous part of the internal carotid artery (Fig 4) The lateral part was anteriorly connected to the ophthalmic veins and the sphenoparietal sinus, while postero-laterally it was connected with the plexus of the foramen ovale The medial part, located somewhat posterior to the lateral one, was anteriorly connected to the anterior and posterior intercavernous sinuses while posteriorly it was connected to the basilar plexus and to the inferior petrosal sinus

In the a p view (Fig 3 a) the cavernous sinus was often masked by the angular and anterior facial veins and by the intraorbital veins

In the straight lateral view (Fig 3 c) the two sinuses were superimposed However, an antero-inferior and a postero-superior part, separated by the carotid artery, could

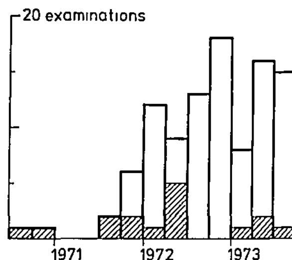


Fig 2 Distribution of unisatisfactory examinations (hatched) in the total series of 101 examinations 1971 1973

material of 101 examinations in 94 patients there remained 26 patients, 10 females and 16 males, constituting the 'normal material'

The relevant veins and sinuses were included in the projections used with the following exceptions in the axial view in one patient the petrosal sinuses and the jugular veins were not included, and in another patient not the jugular veins The number of examinations remaining for an analysis of the anatomy of these veins thus amounted to 25 and 24, respectively Four children were included in the 'normal material' (age one day, four months, two years and four years) The oldest patient was 71 years of age

Method and technical results

A complete examination of the cavernous sinuses is included in the technique for orbital phlebography used by the present author It has been described in detail previously (BRISMAR 1974 a), to which report the reader is referred

Measurements of the transverse diameter of the pituitary fossa, were performed on the axial films without correction for magnification The film-focus distance was about 100 cm, and the head of the patient rested on the automatic film changer During the latter part of this series, linear angio-tomography has also been performed in the a p projection in several cases

The examinations have been classified as adequate or incomplete Those with only fragmentary or unilateral demonstration of the cavernous sinus and its drainage and those without an axial view have been assigned to the incomplete ones

As the examination technique was gradually worked out during the series, incomplete examinations were more common at the beginning and due to too slow injection of contrast medium, defective external compression, or absence of adequate views Among the last 70 examinations, only four were classified as incomplete In one of these, the injection of contrast medium was partly perivascular, in another the collaterals over the midline in the forehead were underdeveloped, in the third case

Table

Incidence of filling of basal venous sinuses in the 'normal material' SPHS = sphenoparietal sinus, CS = cavernous sinus, AICS = anterior and PICS posterior intercavernous sinuses, BP = basilar plexus POF = plexus of the foramen ovale, IPS = inferior and SPS = superior petrosal sinuses, IJV = internal jugular vein

	n	Veins filled		
		Bilaterally		Unilaterally
SPHS	26	12		7
CS	26	26		0
AICS	26		21	
PICS	26		18	
BP	26		25	
POF	26	20		4
IPS	25	23		1
SPS	25	0		2
IJV	24	21		2

the digital compression was ineffective, and in the fourth no axial view was exposed as the patient was old and in a bad condition and without symptoms or signs of a disorder affecting the basal sinuses

Results

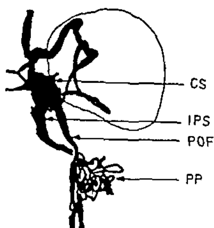
Bilateral filling of the cavernous sinuses and their interconnections (the anterior and posterior intercavernous sinuses and the basilar plexus), and of the plexus of the foramen ovale was obtained in a majority of cases In most cases also the inferior petrosal sinuses were completely filled to the internal jugular veins (Table)

The cavernous sinus Provided there is no obstruction of flow from the site of injection to the cavernous sinuses, and provided the compression is effective, an adequate bilateral demonstration of the cavernous sinus should always be achieved with the author's technique The sinus was best observed in the axial view (Fig 3 b) where it, in the normal material, always appeared as a roughly rectangular structure with a longitudinal defect caused by the intracavernous part of the internal carotid artery (Fig 4) The lateral part was anteriorly connected to the ophthalmic veins and the sphenoparietal sinus, while postero-laterally it was connected with the plexus of the foramen ovale The medial part, located somewhat posterior to the lateral one, was anteriorly connected to the anterior and posterior intercavernous sinuses while posteriorly it was connected to the basilar plexus and to the inferior petrosal sinus

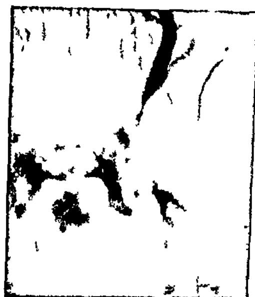
In the a p view (Fig 3 a) the cavernous sinus was often masked by the angular and anterior facial veins and by the intraorbital veins

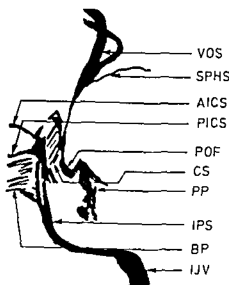
In the straight lateral view (Fig. 3 c) the two sinuses were superimposed However, an antero-inferior and a postero superior part, separated by the carotid artery, could





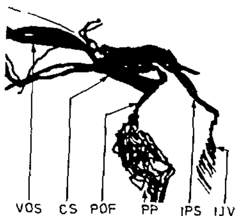
a





b





c

Fig 3 Normal case a) A p b) axial c) lateral views (For abbreviations see Fig 1)



Fig 4 Angiotomography of the cavernous sinus in two normal cases A p projection Left Plexus of the foramen ovale filled bilaterally (←)

be identified The degree of tortuosity of the artery thus influenced the appearance of the sinus The antero-inferior part of the sinus was anteriorly connected to the ophthalmic veins and posteriorly to the plexus of the foramen ovale The latter connection ran from the cavernous sinus at right angles downwards The postero-superior part was posteriorly connected to the inferior petrosal sinus which in the lateral view was superimposed on the dorsal contour of the clivus In some cases the superior petrosal sinus was observed to originate from the postero-superior part of the cavernous sinus and to project along the superior contour of the petrous bone

The anterior and posterior intercavernous sinuses and the basilar plexus were best separated on the axial view (Fig 3 b) They were demonstrated in 21, 18 and 25 cases respectively, out of the 26 in the normal material The two intercavernous sinuses, together with the medial parts of the cavernous sinuses, in the axial view, outline an oval area corresponding to the pituitary fossa The basilar plexus, located on the posterior aspect of the clivus may appear as a single vein (Fig 5) or as a venous network (Fig 3 b) The relative sizes of these three interconnections between the two cavernous sinuses may vary considerably (Fig 5)

Transverse diameter of the pituitary fossa The lateral boundaries of the pituitary fossa are formed by the upper parts of the medial walls of the cavernous sinuses, while its anterior and posterior boundaries, as well as its floor, consist of the bony walls of the sella turcica The two intercavernous sinuses were located close to the anterior and posterior parts of the sellar diaphragm The transverse diameter of the pituitary fossa was measured as the maximum transverse distance between the two cavernous sinuses between the anterior and posterior intercavernous sinuses in the axial view In a few cases, measuring was difficult due to a tortuous carotid artery displacing a part of the sinus medially (Fig 6) but also in those cases the fossa could be identified and measured The transverse diameter of the pituitary fossa averaged 17 8 mm ± 2 0 mm SD for adults (Fig 7) The diameter in a one day old girl was 11 mm, in a 4-month old boy 13 mm and in two boys, 2 and 4 years of age, 15 mm

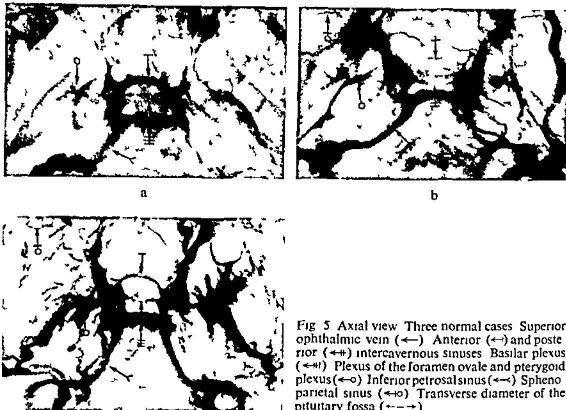


Fig 5 Axial view Three normal cases Superior ophthalmic vein (←) Anterior (↤) and posterior (↞) intercavernous sinuses Basilar plexus (↞) Plexus of the foramen ovale and pterygoid plexus (←o) Inferior petrosal sinus (←<) Sphenoparietal sinus (←o) Transverse diameter of the pituitary fossa (←–→)

The sphenoparietal sinus was demonstrated in 19 patients (in 12 bilaterally) out of 26 It was most easily identified in the axial view (Figs 3 b, 5), where it ran in a smooth curve following the free edge of the smaller sphenoidal wing In the a p view it was superimposed on the superior orbital fissure, and could easily be mistaken for the lacrimal vein In several cases this sinus appeared to join the internal part of the superior ophthalmic vein before entering the cavernous sinus

Plexus of the foramen ovale and the pterygoid plexus Contrast medium passed from the cavernous sinus via the plexus of the foramen ovale to the pterygoid plexus in 24 of the 26 normal cases, in 20 of these bilaterally This venous route was often wider than the inferior petrosal sinus and was often better filled It thus appears as if the plexus of the foramen ovale forms an important drainage of the cavernous sinus This plexus is easy to recognize in all the projections used (Fig 3) In the axial view (Figs 3 b, 5) it appeared as one or several veins leaving the lateral part of the cavernous sinus and via the foramen ovale and adjacent foramina joining the pterygoid plexus, located lateral to the sinus In the lateral view (Fig 3 c) it was seen to leave the inferior part of the cavernous sinus at right angles and proceeded downwards to the pterygoid plexus In the a p view it ran a course directed downward laterally (Fig 3 a) and was always located lateral to the inferior petrosal sinus

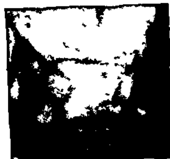


Fig 6 Ectatic carotid arteries, bilaterally causing a double medial contour of the cavernous sinus in the axial view

The superior petrosal sinus was observed, only unilaterally, in two out of the normal 25 cases, both were children, one one day-old (Fig 8), the other two years of age This sinus ran backwards, in the sulcus bearing its name, on the superior aspect of the pyramid, to empty into the sigmoid sinus, and had a characteristic straight appearance in all views

The inferior petrosal sinus could be observed in 24 of 25 normal cases, in one only unilaterally It may be doubled or tripled unilaterally (Fig 5) or bilaterally, it may terminate directly into the internal jugular vein or end in a venous net communicating with this vein In the axial view, the inferior petrosal sinus ran in a smooth curve backward laterally from the medial posterior part of the cavernous sinus to the internal jugular vein, in the lateral view it was projected over the posterior aspect of the clivus In the a p view it passed downward laterally medial to the plexus of the foramen ovale

Internal jugular vein In 21 of 24 normal cases filling of the internal jugular vein was achieved in 2 further cases the vein was filled unilaterally A better demonstration of these veins may be obtained if the amount of contrast medium injected is increased to 20 ml

Discussion

Arseni et coll applied the technique of angular vein puncture and demonstrated the cavernous sinus in 21 out of 40 cases Using the same technique, Boudet (1953) stated that absence of filling of this sinus was not always pathologic According to Lloyd, adequate filling of the cavernous sinuses should always be expected with the frontal vein approach, provided the superior ophthalmic veins were unobstructed This latter statement is in agreement with the results of the present investigation

The term 'cavernous sinus' was introduced by Winslow (1732) as he considered the interior structure of the sinus to be similar to that of the corpus cavernosum penis The sinus is classically described as a blood filled channel on each side of the sella turcica completely surrounding the horizontal part of the internal carotid artery

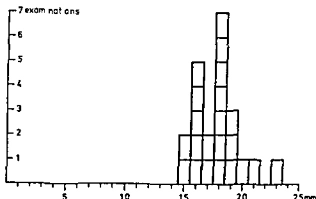


Fig 7 Measurements of the transverse diameter of the pituitary fossa in the normal material Figures not corrected for magnification

as well as the abducens (6th) nerve and divided by numerous trabeculae (DUKE-ELDER 1952, HAFFERL 1969) These 'numerous interlacing bands considerably *narrow and retard the current of blood*' (CAMPBELL 1933) and may thus 'favour the lodgement of thrombi' (DUKE-ELDER)

At histology BALÓ (1950), however, could find no true cavernous tissue in the walls of the human cavernous sinus and only a few trabeculae were found by BUTLER (1957) in an autopsy material Among 34 adult cavernous sinuses BEDFORD (1966) found abundant trabeculae only in 6 cases, while in the rest of the cases the sinus was virtually an unbroken venous channel with only a few trabeculae between the medial side of the carotid artery and the floor of the cavernous sinus OLIVIER & PAPAMILTIADÈS (1951), like BONNET (1955), on the contrary claimed that the cavernous sinus in fact consisted of a plexus of veins and that no proper sinus did exist

The conception of a venous network was supported by MERCIER et coll (1970) using dissection, serial sections, corrosion preparations and radiologic technique in a material of 30 cavernous sinuses Their results from histologic examination of the same material, however, supported the classical opinion of a sinus with abundant trabeculae

The position of the carotid artery and the abducens nerve in the cavernous sinus is also a matter of dispute, *while there is agreement that the third, fourth, and fifth* cranial nerves are located in the lateral wall of the sinus WEIZENHOFFER (1932) thus placed the artery in the medial wall of the sinus while BRASH (1951) argued that the artery, as well as the sixth nerve, are situated in the lateral wall Other authors (THOREK 1951) claim that the sixth nerve is located in the lateral wall of the sinus, separated from the carotid artery which lies within the sinus BEDFORD in 34 adults found that in 26 cases both the carotid artery and the sixth nerve were located outside the lumen of the sinus in its lateral wall In five cases, the carotid artery was located within the lumen of the sinus and the sixth nerve in the lateral wall and in only three cases both structures were inside the lumen of the cavernous sinus

MERCIER et coll in their material stated that the carotid artery, always with the sixth nerve on its lateral side, although having various positions in the sinus, was always separated from both the lateral and the medial wall by venous tissue (Fig 9)



a



b

Fig 8 Girl one day of age a) Axial b) lateral views Superior petrosal sinus (→) Plexus of the foramen ovale (→) Inferior petrosal sinus (↔)

The results obtained in the present investigation support the opinion of MERCIER et coll that venous tissue exists not only medial to but also lateral to the carotid artery (Fig 4) Phlebographically, the cavernous sinus appears as a continuous venous channel It is an open question whether trabeculae or venous walls, too thin to be demonstrable with the technique applied, do exist within this channel

Three different types of cavernous sinuses have been described previously a plexiform venous arrangement (considered to be most frequent), double (or triple) parallel veins and a single vein (BOUDET, BÉTOULIÈRES et coll, ARSENI et coll, OFFRET & ARON ROSA, OFFRET et coll, DEBAENE 1972) Later, ARON ROSA et coll (1966, 1967) stated also that the cavernous sinus, in the lateral view, was divided into two compartments separated by the intracavernous part of the carotid artery, one antero-inferior and one postero-superior part These opinions were based on experiences gained with a technique implying a relatively slow injection of contrast medium This tends to produce a laminar flow, that would, in combination with a compartment structure of the cavernous sinus, explain the conceptions stated In fact, in the first few cases in the present series contrast medium was injected through a scalp vein needle, and results similar to those of BETOULIÈRES et coll were obtained However, during the rest of this series using a rapid injection of contrast medium, the cavernous sinus could always be bilaterally demonstrated with the appearance of a proper sinus surrounding the carotid artery

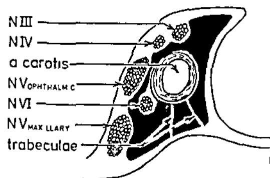


Fig 9 Sagittal section of the cavernous sinus Lumen of the sinus in black, only a few trabeculae are indicated

Recently VIGNAUD et coll (1972 a) by angiotomography in the a p projection could improve the demonstration of the intracavernous structures, the third and sixth nerves as well as the carotid artery could be identified in one normal case These observations have been corroborated by the tentative application of a p linear angiotomography in several cases out of the present series, there is a substantial increase in detailed anatomic information on the cavernous sinus Experiences with angiotomography will be further discussed in a forthcoming report

As venous tissue exists medial to the carotid artery outlining the lateral wall of the pituitary fossa, the intercavernous distance in the axial view may be used as a measure of the transverse diameter of the fossa Except for WEIZENHOFFER (1932), who does not mention the basis for his statement, all authors seem to agree that normally the sinus extends medially to the artery In the present material, in all cases filling of the cavernous sinuses was obtained medial as well as lateral to the carotid artery The distance between the intracavernous part of the carotid artery and the midline has also been used as a measure of the transverse diameter of the pituitary fossa (CHASE & TAVERAS 1961, BULL & SCHUNK 1962) The course of the carotid artery in the cavernous sinus is, however, variable and in only 65 per cent of normal cases does it overlie the floor of the sella turcica (CHASE & TAVERAS 1963) Furthermore, tortuous arteries may invade the pituitary fossa and the distance between the arteries may in such cases be reduced to 4 mm (BERGLAND et coll 1968) Thus, the location of the carotid artery is no reliable measure of the transverse diameter of the pituitary fossa and, as stressed by BERGLAND et coll, the only method to evaluate this diameter is to use the cavernous sinuses

In patients with a shallow sella turcica and a weak or incomplete sellar diaphragm most of the cavernous sinus is often situated below the level of the floor of the sella turcica (CHASE & TAVERAS 1961) In such cases the diaphragm will offer little resistance to the upward expansion of a pituitary tumor and, consequently, the lateral displacement of the cavernous sinuses will be less dominating Furthermore, a pituitary tumor may displace only part of the cavernous sinus laterally, thus causing a cavitation of the medial contour of the cavernous sinus in the a p view The use of the intercavernous distance in the axial view as a measure of the transverse diameter of the pituitary fossa is therefore sometimes not quite exact Serial frontal angiotomo

graphy in a p projection would better disclose the relation between the pituitary fossa and the cavernous sinuses in the individual case, as indicated by preliminary results

Except for the cavernous sinus, the basal venous sinuses of the skull have not received much interest in earlier reports on phlebography Exceptions are the reports of SHIU et coll, GIUDICELLI et coll (1972), THERON et coll (1972) and RABISCHONG et coll (1972) SHIU et coll used bilateral transjugular inferior petrosal sinus catheterization (HANAFEE et coll) for examination of the cavernous sinus As the type of drainage of the inferior petrosal sinuses into the jugular veins influences the results of the examination performed with this technique, an analysis of the drainage was given In their material, the inferior petrosal sinus drained directly into the jugular bulb in 45 per cent of the cases, into a vein connecting the jugular bulb with the deep cervical plexus in 24 per cent, and directly into the cervical plexus in 7 per cent The inferior petrosal sinus existed as a plexus of veins draining into the jugular bulb as well as into the cervical plexus in 24 per cent of their cases

In the present series, the plexus of the foramen ovale seemed to be an important drainage route for the cavernous sinus The importance of this plexus is not evident from textbooks on anatomy At phlebography this plexus has sometimes been a source of confusion MORRIS & WYLIE (1973) have mistaken it for the inferior petrosal sinus, while ARON ROSA et coll (1966, 1967) and VIGNAUD, as evident from their illustrations, for the superior petrosal sinus It is apparent from the present investigation that the superior petrosal sinus is only rarely filled during frontal phlebography The internal jugular veins have in this material been filled in the majority of cases, and frontal vein phlebography has been used by the present author to analyse patent venous drainage of the skull in cases with ventriculo-atrial shunts and possibly occluded jugular veins

Conclusions

Orbital phlebography by the frontal vein approach is a safe and reliable method of examining also the cavernous sinuses and adjacent basal venous sinuses of the skull In cases without an obstruction of the superior ophthalmic veins, an adequate filling of the cavernous sinuses should always be achieved if the technique is correctly applied The phlebographic anatomy of the cavernous sinus has proved to be quite constant

The intercavernous distance (width of the pituitary fossa) in normal subjects in this material amounted to 17 8±2 0 mm SD measured directly on the film This distance is of importance for deciding whether an enlargement of the pituitary gland exists

The drainage routes of the cavernous sinus are always evident Not only the inferior petrosal sinus, but also the plexus of the foramen ovale were demonstrated in the majority of cases in this series This plexus evidently constitutes an important drainage route for the cavernous sinus

SUMMARY

Frontal phlebography has been used to examine the cavernous sinuses and adjacent basal venous sinuses of the skull The method has proved to be simple and effective The normal phlebographic anatomy of the basal sinuses and their drainage has been revised in a material of 26 cases A normal range for the transverse diameter of the pituitary fossa has been established

ZUSAMMENFASSUNG

Es wurde die frontale Phlebographie verwendet, um die cavernosen Sinus und die anliegenden basalen venosen Sinus des Schadels zu untersuchen Die Methode erwies sich als einfach und effektiv Die normale phlebographische Anatomie der basalen Sinus und deren Abfluss wurden an einem Material von 26 Fallen nachgepruft Der normale Bereich des transversalen Diameters der Hypophyseneisenkung wurde festgestellt

RÉSUMÉ

La phlébographie frontale a ete utilisée pour examiner les sinus caverneux et les sinus veineux adjacents de la base du crâne Cette methode s'est montree simple et efficace L'anatomie phlébographique normale des sinus basaux et leur drainage ont été étudiés sur une série de 26 cas L'auteur a etabli les variations normales du diametre transversal de la fosse pituitaire

REFERENCES

ARON-ROSA D, OFFRET G, RAMÉE A, METZGER J, AARON C et ROSA A La phlebographie orbitaire Bull Soc Ophtal Fr (1967) Suppl

— RAMÉE A et METZGER J La phlébographie orbitaire *In* L exploration neuroradiologique en ophtalmologie, p 136 Edité par P Guillot H Saraux et R Sedan Masson et Cie, Paris 1966

ARSENI C, MIHAILESCU N, SIMIONESCU M and LE-XUAN-TRUNG Orbital phlebography Acta neurochir 12 (1965), 521

BALO J The dural venous sinuses Anat Rec 106 (1950), 319

BEDFORD M A The 'cavernous' sinus Brit J Ophthal 50 (1966), 41

BERGLAND R M, RAY B S and TORACK R M Anatomical variations in the pituitary gland and adjacent structures in 225 human autopsy cases J Neurosurg 28 (1968), 93

BÉTOULIÈRES P, BOUDET CH, PALEIRAC R, GARBAY B et LONJON P Etude anatomo-radiologique du sinus caverneux J Radiol Électrol 38 (1957) 726

BONNET P La loge caverneuse et les syndromes de la loge caverneuse Arch Ophtal (Paris) 15 (1955), 357

BOUDET CH Premiers résultats de phlébographie orbitaire Thèse, Montpellier 1953

BRASH J C Cunningham's text-book of anatomy, 9th ed, p 1347 Oxford University Press, London 1951

phlébographie

15 (1974), 369

its tributaries

Acta radiol Diagnosis 15 (1974), 481

— (c) Orbital phlebography III Topography of intraorbital veins Acta radiol Diagnosis 15 (1974) 577

Bull J W D and Schunk H The significance of displacement of the cavernous portion of the internal carotid artery Brit J Radiol 35 (1962) 801

Butler H The development of certain human dural venous sinuses J Anat (Lond) 91 (1957) 510

Campbell E H The cavernous sinus anatomical and clinical considerations Ann Otol Rhinol Laryng (St Louis) 42 (1933) 51

Chase N E and Taveras J M Cerebral angiography in the diagnosis of suprasellar tumors Amer J Roentgenol 86 (1961) 154

— — Carotid angiography in the diagnosis of extradural parasellar tumors Acta radiol Diagnosis 1 (1963) 214

Clay C Théron J et Vignaud J Intéret de la jugulographie et de la phlébographie orbitaire dans la pathologie du sinus caverneux Arch Ophtal (Paris) 32 (1972) 123

Debaene A Étude neuroradiologique des tumeurs de la région du sinus caverneux Thèse, Marseille 1972

Dejean Ch et Boudet Ch Du diagnostic des varices de l orbite et de leurs complications par la phlébographie Bull Soc franç Ophtal 64 (1951) 374

Duke Elder S Text book of ophthalmology, vol 5 p 5445 Kimpton London 1952

Engel P Mise en evidence du sinus caverneux par phlebographie antérieure Neurochirurgie 18 (1972) 639

Giudicelli G Resche F, Louis R et Salamon G Radioanatomie du sinus caverneux Neurochirurgie 18 (1972) 599

Hafferl A Lehrbuch der topographischen Anatomie Springer Verlag Berlin 1969

Hanafee W Rosen L M Weidner W and Wilson G H Venography of the cavernous sinus orbital veins and basal venous plexus Radiology 84 (1965) 751

Lloyd G The localization of lesions in the orbital apex and cavernous sinus by frontal venography Brit J Radiol 45 (1972) 405

Mercier R Patouillard P Vanneuville G et Aussilhou A Contribution à l etude du sinus caverneux par l utilisation simultanée de plusieurs modes d investigation C R Ass Anat 149 (1970) 877

Morris L and Wylie I Tomography of the cavernous sinuses Brit J Radiol 46 (1973) 424

Offret G et Aron Rosa D Le phlebogramme orbitaire Arch Ophtal (Paris) 25 (1965) 85

— — Metzger J et Doyon D Le phlebogramme orbitaire Acta radiol Diagnosis 5 (1966) 441

Olivier E et Papamiltiades M Le système caverneux veineux de la région latéro-sellaire C R Ass Anat 38 (1951) 769

Piscol K Hamer J und Tornow K Die kraniale retrograde Phlebographie Acta neurochir 22 (1970) 195

Rabischong P Clay C Vignaud J et Paleirac R Approche hémodynamique de la signification fonctionnelle du sinus caverneux Neurochirurgie 18 (1972) 613

Shiu P Hanafee W Wilson G and Rand R Cavernous sinus venography Amer J Roentgenol 104 (1968) 57

[illegible] gy 3 (1971) 1

[illegible] Philadelphia 1951

Tornow K und Piscol K Technik und Wert der retrograden Phlebographie bei raumfordernden Prozessen im Sellabereich Radiologe 10 (1970) 470

VIGNAUD J Phlébographie orbitaire par ponction directe d une veine du front *In* Progrès récents en angiographie cérébrale, p 49 Edité par H Fischgold, J Metzger et M L Aubin Laboratoires Schering Sepps 1970

— CLAY C, AUBIN M L et KORACH G (a) Opacification du sinus caverneux Intéret de la tomographie simultanee J Radiol Électrol 53 (1972), 51

— DOYON D, AUBIN M L et CLAY C (b) Opacification du sinus caverneux par voix postérieure Neurochirurgie 18 (1972), 649

VRITSIOS A A new method for demonstrating ophthalmic veins, facial veins, and superficial venous system of the head (In Greek) Arch ophthal Hetair borei hellad 12 (1961) 223

WAGA S, KIKUCHI H, HANDA J and HANDA H Cavernous sinus venography Amer J Roentgenol 109 (1970), 130

WEIZENHOFFER A Contralateral cavernous sinus thrombosis N Y St J Med 32 (1932) 139

WINSLOW J B Exposition anatomique de la structure du corps humain, vol 2 p 31 Prevost, London 1732

FROM THE DEPARTMENT OF NEURORADIOLOGY, KAROLINSKA SJUKHUSET, S-104 01 STOCKHOLM, SWEDEN.

ANATOMY OF THE CRANIAL NERVES IN THE BASAL CISTERNS

A radiologic post-mortem investigation

ARNE GREPE

The new water-soluble contrast medium, Metrizamide, designed for the subarachnoid space and with a low neurotoxic effect (Acta radiol Suppl 335, 1973) may be assumed to allow clinical cisternography to be more extensively used in a near future It will also allow a more detailed examination of the anatomy and in particular the contents of the intracranial basal cisterns Detailed information concerning the normal intracisternal structures as seen at clinical radiography will then be needed This can to a large extent be gained and confirmed only by post mortem examinations, which is the reason for the present investigation

The gross anatomy of the subarachnoid cisterns as demonstrated at encephalography was described by LILIEQUIST (1959) but little interest has hitherto been evidenced for the structures within the cisterns Cranial nerves identified at encephalography were described by DI CHIRO (1961), EPSTEIN (1966), METZGER (1967), NEUMANN (1968) and FISCHGOLD et coll (1969), but these observations were not compared to post-mortem findings This lack of confirmation may explain why the descriptions were incomplete and sometimes incorrect, as in the monograph of EPSTEIN

Submitted for publication 18 December 1973

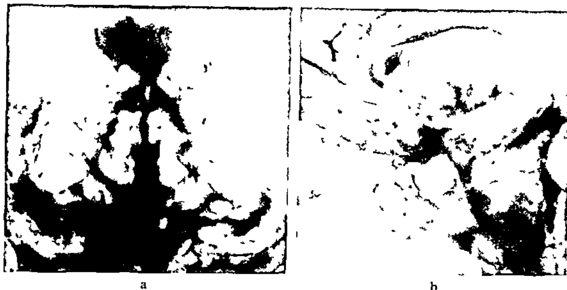


Fig 1 Post mortem cisternography *Distribution of contrast medium in the basal cisterns after percutaneous suboccipital injection* a) A p view with beam direction parallel to the skull base b) Lateral view The interhemispheric and the Sylvian fissures were filled as well as the basal parts of the ventricular system

The same absence of basic anatomic correlation is found in the literature on cisternography performed with oily contrast media In the last decade a large number of reports have been issued on expansive lesions in the cerebellopontine angle (BAKER 1963, 1972, GASS 1963, 1968, SCANLAN 1964, REESE & BULL 1967, BRITTON et coll 1968, BURROWS 1969, HASTINGS-JAMES 1969) Oily contrast media are not ideal as has been admitted by some of these authors These media are non resorbable and their use is thus restricted to the posterior intracranial fossa, also they are not completely removable Furthermore, the physical properties of these media render them unsuitable because of high viscosity and high attenuation of radiation HASTINGS-JAMES when analysing the anatomic structures visible within the cisterns, found that the vessels, particularly the arteries, were easily identified but stated that the cranial *nerves are rarely demonstrated in radiography*

In the report of BAKER (1963), a drawing of the intracisternal course of the facial and statoacoustic nerves is inaccurate, moreover, these nerves when seen in another of the illustrations are not indicated, thus demonstrating that the course of these nerves was not clear to the author

A critical review of previous publications on the normal anatomy of the cranial nerves as seen at clinical radiography performed with negative or positive contrast media thus supports the opinion that post-mortem cisternography is needed for correct assessment of the topographic anatomy

A report on the topography of the optic chiasm and the acoustic nerves in vivo and post-mortem was given by the present author (1967) but only that part dealing with the anatomy of the cerebellopontine angle was published (GREPE 1969) The prospects for cisternography with a water-soluble contrast medium as a clinical method has

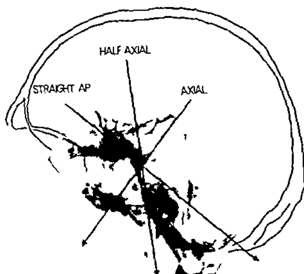


Fig 2 Injected specimen removed en bloc and subsequently submitted to radiography including tomography in projections indicated The half axial projection represents the superior inferior direction

prompted a review of this material and a further analysis of the results obtained The investigation originally performed to evaluate the intracisternal topographic anatomy of the cranial nerves also indicates suitable projections for demonstration of the individual cranial nerves as well as the value of tomography

Material and Methods

A technique for post mortem radiography of the intracranial basal cisterns was elaborated and standardized in a preliminary series of 5 cases which were not otherwise included in the material This technique was then applied on 8 cadavers without history of brain or cranial nerve disorders constituting the present material

The brain and brain stem were fixed in situ by formalin injections through the four neck arteries With the cadaver in supine position the cisterna magna was punctured with a coarse needle and 30 ml of the cerebrospinal fluid removed The cadaver was then turned to the prone position the head end tilted down 15° and 40 to 60 ml of a warmed suspension of barium sulphate in gelatin solution (1 volume part of Micropaque in 9 parts of a gelatin solution 10 per cent) was gently injected by hand through the suboccipital needle Cisternal filling was controlled by radiography in two planes (Fig 1) In all cases the warmed contrast suspension filled the intracranial basal cisterns before solidifying In some cases an incomplete filling of the declive parts of the ventricular system also occurred The vault of the skull was opened with a low circumferential sawcut just above the skull base The basal part of the brain, including the basal ganglia, and the skull base were then removed in one piece, the bony structures being gently chiselled out (Fig 2)

After further formalin fixation the injected brain skull base specimens were subjected to conventional radiography and supplementary linear tomography in four

	Axial r	Axial t	Half Axial r	Half Axial t	Straight A P r	Straight A P t	Lateral r	Lateral t
I	0/0	0/0	0/0	0/0	0/0	0/0	0/0	0/0
II	0/6	0/7	5/1	6/1	0/0	0/0	6/1	8/0
III	3/0	5/3	2/1	6/0	0/0	0/0	7/0	8/0
IV	0/0	0/0	0/0	0/0	0/0	0/0	0/0	0/0
V	1/3	4/2	3/1	5/2	1/3	5/3	6/1	5/3
VI	0/0	1/0	1/0	2/0	0/0	0/0	0/0	0/0
VII	3/1	7/1	1/1	8/0	0/3	0/8	0/0	0/0
VIII	3/1	7/1	1/1	8/0	0/3	0/8	0/0	0/0
IX	0/1	3/5	0/0	1/2	0/0	1/0	0/0	0/0
X	0/1	3/5	0/0	1/2	0/0	1/0	0/0	0/0
XI	1/2	3/5	0/0	1/2	0/0	1/0	0/0	0/0
XII	0/0	0/0	0/0	0/0	0/0	1/0	0/0	0/0
Σ	11/15	33/29	13/5	38/9	1/9	9/19	19/2	21/3

Fig 3 Identification of individual cranial nerves at post mortem cisternography Number of complete (= upper left of quadrant) and incomplete (= lower right of quadrant) identifications in the four projections without (r) and with tomography (t) with regard to each cranial nerve pair and summarized below, to cranial nerve structures as a whole

projections (Fig 2) with a Mimer II equipment Preliminary experience indicated that a tomographic angle of 10° yielded the best survey information on the topographic anatomy of the cranial nerves All specimens were examined with this angle but in order to demonstrate the anatomic structures in closer detail 16° and 31° were also used Tomographic sections were made at 5 mm intervals, the magnification factor was constantly 1 4

The following four projections were used, the central ray of the beam always aligned to pass through the centre of the interpeduncular fossa

A) Straight a p view The beam direction was parallel with the skull base along the supraorbito-meatal line

B) Half-axial a p view The central beam formed a 45 angle with the skull base Tomographic sections in this projection are roughly perpendicular to the brain stem

C) Axial view The beam direction was perpendicular to the skull base, i e to that of projection A Tomographic sections in this projection were *parallel with the* average plane of extension of the cisterns traversed by the cranial nerves

D) Lateral view

The specimens were then cut into 1 cm thick slices, corresponding to one of the planes in which the tomography was carried out and including all planes The slices were submitted to radiography and to dissection

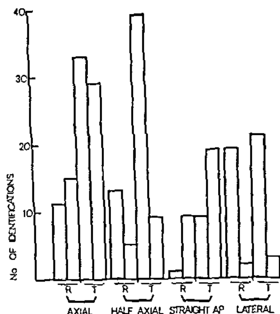


Fig 4 Identifications of the cranial nerves in various projections without (first two columns in each projection) and with tomography (the following two columns in each projection) Filled columns = cranial nerves completely assessable Unfilled columns = cranial nerves not fully assessable R = radiography without tomography T = tomography

The entire film-material was used to classify the individual cranial nerves as well as the different projections in three groups (Fig 3)

I Cranial nerve identifiable and assessable along the entire intracisternal course, or most of it

II Cranial nerve not completely distinguished Nerves depicted 'end on' in a projection that was more or less parallel with their course were also included in this group, as well as trigeminal nerve structures observed only within Meckel s cave

III Cranial nerves not identified

Results

Technical considerations

The individual cranial nerve pairs identified at radiography with and without tomography in the four projections are listed in Fig 3 In the axial and half-axial projections the cranial nerves were found to be completely assessable three times more often with tomography than without (33 against 11 and 38 against 13 identifications, respectively) The numbers of nerves that were partially assessable were under the same conditions nearly doubled (29 against 15 and 9 against 5, respectively) (Fig 4)

In the straight a p view the number of complete identifications (group I) was considerably increased, from 1 to 9, with the use of tomography and the number of incomplete identifications (group II) was roughly doubled, from 9 to 19

The results do not indicate that tomography improves the demonstration of the cranial nerves in the lateral projection as the complete identifications were only raised

from 19 to 21 and incomplete ones from 2 to 3 The results are not directly comparable, however In a true lateral projection the cranial nerves of both sides are superimposed They can only be separated in oblique views, or by use of tomography

Fig 3 indicates the projections that allow the best evaluation of the individual cranial nerves, besides offering information as to the value of tomography in each of the four projections Maximum information of the individual cranial nerves was gained in the following projections

I The olfactory tracts could not be identified in any case or any projection

II The optic tracts, nerves and chiasm were best observed in the half-axial and lateral views, without as well as with tomography A clear concept of the anatomy of the optic nerve structures could be obtained The axial projection was, however, indispensable for the evaluation of the relations of the nerve to adjacent structures within or close to the chiasmatic cistern

III The oculomotor nerves were most often identified in the lateral view, with tomography, however, they were better demonstrated and equally well in the lateral, half-axial and axial projections Like the optic nerve structures the oculomotor nerves could never be identified in the straight a p projection

IV The trochlear nerves could never be demonstrated, even when tomography was used

V The trigeminal nerves were most often demonstrated in the lateral projection without tomography but equally well in all projections when tomography was carried out Meckel's cave was filled bilaterally with contrast medium in 6 out of the 8 cases and faintly filled in one additional case It was bilaterally demonstrated in all projections at radiography with and without tomography but was most evident in the half-axial and lateral views

VI The abducens nerves were only observed in axial and half-axial views and then in only 1 and 2 cases, respectively

VII, VIII The facial and statoacoustic nerves accompany each other through the cerebellopontine cistern and could always be identified at tomography in the axial and half-axial projections They were considerably less often discerned when tomography was not used In the straight a p projection they were superimposed and furthermore obscured medially by the pons They were nevertheless partly assessable in all 8 cases in the straight a p projection with tomography, but in only 3 cases without Due to superimposition of the temporal bones these nerves could never be demonstrated in the lateral view whether tomography was used or not

IX, X, XI The glossopharyngeal, vagal and accessory nerves were only demonstrated in the axial view without tomography and then only in a few cases Using tomography, these nerves were more or less completely assessable in the axial projection, but less often in the half-axial and a p views They were never observed in the lateral view

XII The hypoglossal nerves were identified in one single case, in the straight a p projection at tomography

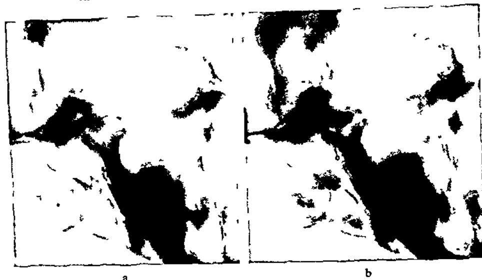


Fig 5 Post mortem cisternography, tomography in the lateral projection a) Midline, b) paramedian sections The optic chiasm (→) and the hypophyseal stalk (↔)are best seen in (a) the optic tract and nerve (⇸) are demonstrated in a sagittal paramedian tomographic section, as well as the rostral part of the oculomotor nerve (o→)

Anatomic considerations

The cranial nerves may be divided into three groups depending on the level at which they leave the brain or brain stem and the cisternal compartment which they traverse The basal cisterns will thus be divided into an upper, a middle and a lower cranial nerve compartment

Upper cranial nerve compartment The subarachnoid space through which the first four cranial nerve pairs pass before leaving the intracranial cavity constitutes a major part of the supratentorial basal cisterns and includes the chiasmatic, interpeduncular and ambient cisterns (supratentorial part), as well as the narrow subarachnoid space in the olfactory sulci (Figs 5, 6, 12, 13) These cisterns are traversed by the olfactory, optic, oculomotor and trochlear nerves However, only the optic and oculomotor nerves could be identified at post mortem cisternography These nerves emerge from the most superior mesencephalic part of the brain stem The optic tract and the external geniculate body demarcate laterally the border between the mesencephalon and the diencephalon In the lateral view the optic and the oculomotor nerves have a course that is more or less perpendicular to the clivus (Fig 5)

The optic nerves, tracts and chiasm (Figs 5, 6, 7, 9, 12, 13) form a flat cross shaped plate that obliquely traverses the chiasmatic cistern These structures have a large extension in the transverse direction and cause a high absorption gradient against contrast medium in the wide cistern behind the chiasm at examination in the lateral projection, irrespective of whether this medium is positive or negative Thus the optic nerves have long been recognized at encephalography in the lateral view At post-

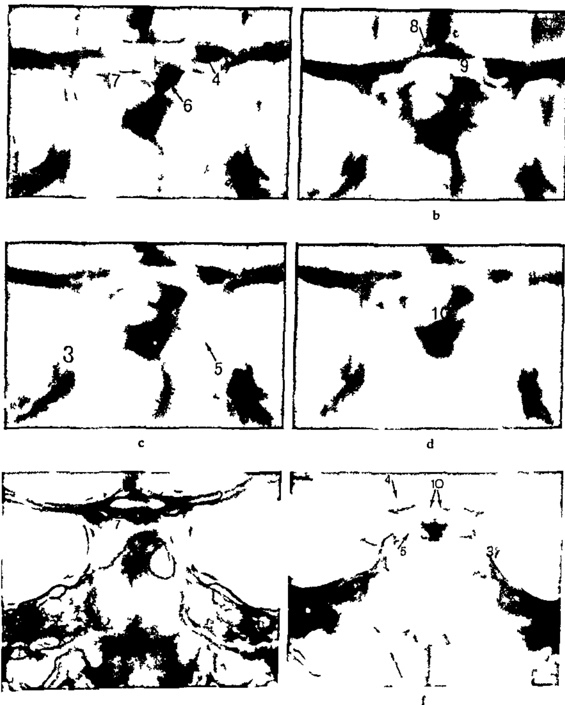


Fig 6 Post mortem c sternography in the axial projec the upper cran al nerve compartment (a–d) Spec m Sylvian f ssure (2) supra and infratentor al parts of c sterns (3) Opt c (4) and oculomotor (5) nerves D

I c d ve g g op c r cr cs hiasm in an upward med al in a slight up vard d rect on e oculomotor nerves run on anter or d rect on



Fig 7 Anterior part of the upper cranial nerve compartment Tomography in half axial projection a) Encephalography The lateral borders (→) of the optic tracts nerves and chiasm are delineated by air b) Post mortem cisternography The medial borders (→) are also visible The carotid siphon (→)

mortem cisternography the optic nerve structures in this view were more distinctly outlined than at encephalography Hence, in parasagittal tomographic sections the two optic tracts and nerves could be distinguished (Fig 5) This was also true to a certain degree of the carotid siphons

In the axial view the optic nerves (Fig 6) are depicted almost along their axis Tomography in this projection proved to yield considerable amounts of detailed information on the topographic anatomy The narrow subarachnoid space between the optic chiasm and the straight gyri harbouring the anterior cerebral arteries and the anterior communicating artery could be demonstrated In this view the diverging optic nerves were medially bordered by a thin slit like subarachnoid space Above the mamillary bodies the optic tracts converged towards the chiasm The optic tracts and the oculomotor nerves coursed parallel, the former on a converging course, the latter on a diverging one

Optic nerve structures are difficult to demonstrate at encephalography in a projection perpendicular to the intracisternal course (the half axial view) At tomography the optic nerve structures were completely demonstrated in the half axial view in 6 cases and partially in one case This was found to be the most informative projection with regard to the anatomy of the optic tracts, nerve and chiasm (Figs 7, 9)

The oculomotor nerves (Figs 5, 6, 8, 9) are considerably more slender than the optic nerves They emerge in the midline from the mesencephalon in the bottom of the interpeduncular fossa and pass through the cistern on diverging courses before entering the cavernous sinus at the level of the posterior clinoid process of the dorsum sellae Though slender, these nerves may sometimes be seen superimposed in the lateral projection at encephalography and were easily identified at post mortem cisternography (Fig 8) They could be observed separately in their entire intracisternal course in parasagittal tomographic sections (Figs 5, 8)

In the axial views not only the mid part but also the proximal as well as the distal parts of the oculomotor nerves were observed in all cases (Fig 6) They diverged laterally and anteriorly through the cistern

In the half axial projection (Figs 9, 12) the beam direction was almost perpendicular

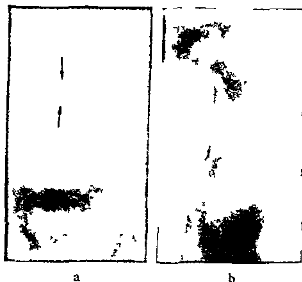


Fig 8 The oculomotor nerve in lateral view a) Encephalography The oculomotor nerves (→) are superimposed b) Post mortem cisternography One of the nerves lies in the tomographic section close to the midline

to the intracisternal route of these nerves (Fig 5) resulting in less foreshortening than in other projections, which facilitated a detailed evaluation

Middle cranial nerve compartment is composed of the subarachnoid space anterior and lateral to the pons, i e the pontine and the cerebellopontine cisterns (Figs 10, 12, 14) The group of cranial nerves passing through this compartment includes the trigeminal, abducens, facial and statoacoustic nerves They course through the subarachnoid space in directions that differ in the transversal as well as in the sagittal plane Consequently the relationship between the individual cranial nerve pairs differs according to the projection used

The abducens nerves (Figs 10, 12) are completely located within the pontine cistern They leave the brain stem in the midline in the groove between the pons and the medulla oblongata at the same level as the facial and statoacoustic nerves At cisternography the abducens nerves were demonstrated only in the axial and half-axial projections and in only a few cases They diverged through the cistern towards the lateral part of the clivus at the level of the petrous bone where they left the subarachnoid space and entered the cavernous sinus (Figs 10, 12) As their intracisternal course is more or less parallel with the skull base, these nerves are depicted with the least distortion in the axial projection The abducens nerves could never be identified in the a p or lateral views at cisternography and could not be identified even at radiography of frontal or sagittal slices

In every case the trigeminal nerves (Figs 10, 11, 12, 13, 14) were demonstrated at post-mortem cisternography in the lateral view when tomography was carried out When filled with contrast medium the subarachnoid space around the trigeminal nerve root and bordering the gasserian ganglion in Meckel's cave could always be demonstrated (Fig 11) The intracisternal part of the trigeminal nerve demarcates the upper border of the cerebellopontine cistern It forms an angle of about 15° with a plane which is perpendicular to the clivus and which coincides with the main exten-



Fig 9 Tomograph [illegible]

oculomotor nerves and the converging optic tracts (1) The hypophyseal stalk (2) in the midline behind the chiasm The mamillary bodies (3)

sion of the subarachnoid space within the cave In axial, half axial and a p views the trigeminal nerves were observed passing forward through the cistern on a slightly diverging course (Fig 10) In the half axial projection the beam direction is about perpendicular to the intracisternal route of the nerve This is also valid with regard to the cranial nerve structures visible within Meckel's cave Along its intracisternal course the nerve is flattened out before entering the cave and the separate nerve bundles of the nerve slightly diverge along the intracisternal route This appearance is still more evident within Meckel's cave where the nerve bundles spread on the surface of the ganglion In this projection as well as in the axial one the subarachnoid space within the cave has an appearance reminiscent of a 'lion's paw' (Fig 11)

The facial and statoacoustic nerves (Figs 10, 12, 13, 14) pass through the posterior part of the cerebellopontine cistern The intracisternal part is more than twice as long as the intracanalicular one The total length could be measured in the axial view and was about 30 mm after correction for magnification The nerves run parallel on a characteristically straight route through the cistern At cisternography they were found to be more or less assessable in the axial as well as the half axial views in all cases This was true with regard to the intracisternal as well as to the intracanalicular portion In the straight a p projection the facial and statoacoustic nerves were superimposed and furthermore the most medial parts of the nerves were obscured by the pons (Fig 10) Despite these limitations they were, however, partly identified in all cases They could never be observed in the lateral view [illegible]

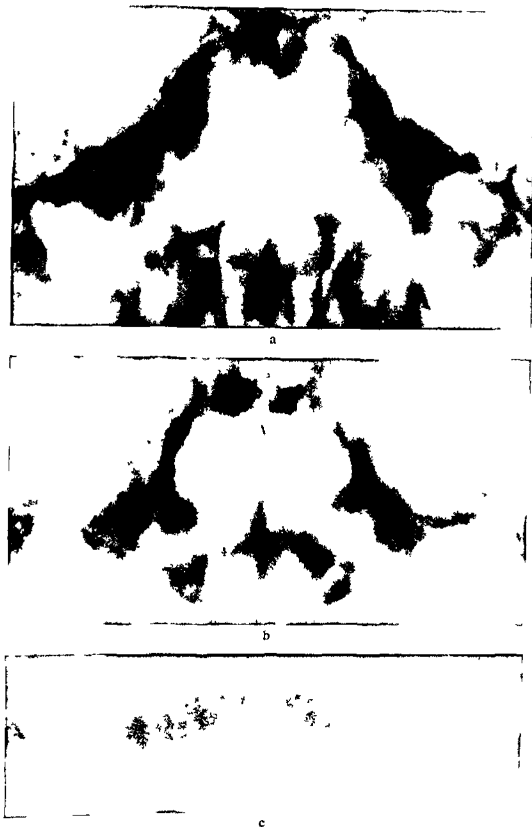
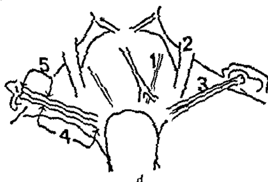


Fig 10 (For legend see opposite page.)



(Fig 13) They are consequently, like the abducens nerves, depicted with the least distortion in the axial projection In two sagittally sectioned specimens the angle formed by the trigeminal and facial statoacoustic nerves in the sagittal plane was 35° and 45°, respectively (Fig 13)

The nerves in the cerebellopontine cistern were not superimposed in the axial view but when the beam direction approaches or passes the half axial projection the medial parts of the trigeminal and facial statoacoustic nerves will become superimposed (Fig 10)

Lower cranial nerve compartment is composed of the subarachnoid space anterior and lateral to the medulla oblongata, i e the medullary cistern (Figs 15, 16 17) The cranial nerves passing through this compartment are the glossopharyngeal, vagal, accessory and hypoglossal nerves. The first three of these cranial nerve pairs (Figs 15, 16, 17) emerge from the brain stem in the posterior lateral s... the ...ndle of nerve ootlets ... medulla oblongata, rootlets of spinal origin (Fig 15) arising from cervical segments of the spinal cord entering the intracranial cavity through the foramen magnum The trunks formed by the glossopharyngeal, vagal and accessory nerves all leave the intracranial cavity through the jugular foramina The last cranial nerve pair, the hypoglossal nerves, emerges from the brain stem in the anterior lateral sulcus of the medulla oblongata anterior to the olive and leaves the intracranial cavity through the hypoglossal foramina

The glossopharyngeal, vagal and accessory nerves were best demonstrated in the axial projection (Fig 15) Tomography proved to be mandatory The trunks formed



Fig 11 Post-mortem cisternography, lateral view Parasagittal tomographic section *The trigeminal nerve (→) passes* through the uppermost part of the cerebellopontine cistern and enters Meckel's cave with gasserian ganglion bordered by contrast medium (o→)

by the glossopharyngeal and vagal nerves had *in this projection an almost straight* lateral course towards the jugular foramen The cranial and spinal rootlets forming the accessory nerve converged laterally upwards to the same foramen The nerves could be distinguished only once in the a p view, which is perpendicular to the axial projection They passed obliquely through the cistern in an anterior lateral direction and departed through the jugular foramen (Fig 16) Their appearance at cisternography in the a p projection could be verified at radiography of slices cut in the same planes as at tomography (Fig 14) They could not be distinguished in the lateral projection The hypoglossal nerves were demonstrated in one single case at tomography in the a p projection They passed through the medullary cistern in an anterior lateral direction parellel with the nerves departing through the jugular foramen (Fig 17) In the axial and half-axial views they could not be identified with certainty from the superimposed glossopharyngeal and vagal nerves emerging from the brain stem at the same level but posterior to the olive

Discussion

The possibilities to discern the cranial nerve structures have until now been rather limited despite the progress of encephalography including refined tomographic techniques or cisternography with oily contrast media The results hitherto published demonstrate the need for improvements of technique in the examination of the cranial nerve structures and a comparison between the results of clinical radiology and post-mortem examinations A non toxic resorbable water-soluble contrast medium would be well suited to meet some of these demands

To demonstrate the normal anatomy of the cranial nerves post-mortem it is mandatory to include in the specimen not only the subarachnoid space with its membranes and the adjacent structures of the brain but also the skull base This is necessary in order to ensure an undisturbed topography of the entire course of the cranial nerves and to establish a reference to the bony structures

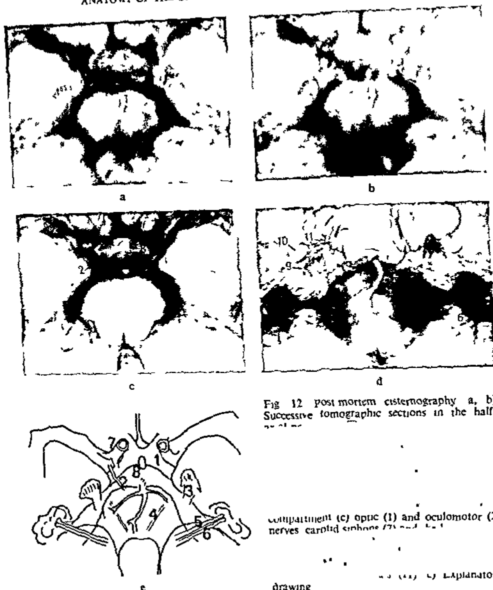


Fig 12 post mortem cisternography a, b) Successive tomographic sections in the half- ... compartment (c) optic (1) and oculomotor (2) nerves carotid siphons ... Explanatory drawing

A factor of importance for the demonstration of cranial nerves at cisternography is the attenuation capacity of the injected contrast medium If this is too high, the nerves may be hidden by the contrast medium particularly when the cisterns are capacious or when the central beam is parallel with the long extension of the medium-filled subarachnoid space (*Fig 10*) In preliminary experiments a suitable concentration of the contrast medium *for demonstration of* intracisternal structures was found to be about half of that utilized by LILIEQUIST (1959) *This would* correspond to a

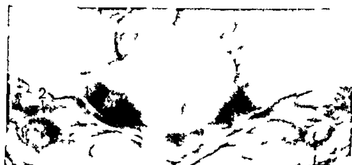


a



b

Fig 13 Radiography of slices a) Midline b) parasagittal structures a) The anterior border of the chiasm (→) *superimposed on* the optic nerves b) The intracisternal part (→) of the trigeminal nerve and the part within Meckel's cave (o→) The carotid canal (x→) The direction of the facial and statoacoustic (>→) nerves in the sagittal plane in this case forms an angle of about 45 with that of the trigeminal nerve more or less parallel with the skull base



a



b

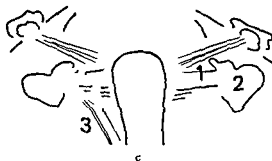
Fig 14 A p projection a) Section through middle cranial nerve compartment The trigeminal nerve (1) The facial and statoacoustic nerves (2) are faintly seen within the auditive meatus and are partly superimposed b) Section through lower compartment the facial (3) and statoacoustic (2) nerves The three cranial nerves (4) that depart through the jugular foramen (5) hypoglossal nerves (6) before departing through the hypoglossal foramen



a



b



c

Fig 15 Tomography in the axial projection parallel to and (a) close to (b) further away from the skull base c) Explanatory drawing In the two successive sections the trunks formed by the glossopharyngeal and vagal nerves (1) pass in a straight lateral direction through the medullary cistern towards the jugular foramen The accessory nerves (3) run in a more oblique superior lateral direction converging towards the same foramen On the left one of the spinal rootlets of the accessory nerve is probably in part superimposed on a vessel (→) The hypoglossal nerves cannot be identified

solution of a water soluble contrast medium containing about 100 mg iodine per ml

The unintentional partial filling of the ventricular system that occurred had a disturbing effect in one instance, the frontal horns were superimposed on nerve structures in the half axial view Filling of the ventricular system at post mortem cisternography may be prevented by catheterization and blocking of the aqueduct but will probably not be met with in clinical cisternography

The pressure used to inject the contrast medium was probably sufficient to compress the arteries and veins This is probably the reason why they were usually more difficult to identify than the nerves As the primary purpose of this investigation was



Fig 16 Tomography in a p projection a) Encephalography, b) post-mortem cisternography The superimposed glossopharyngeal, vagal and accessory nerves (→) pass in a straight anterior lateral direction towards the jugular foramen

the anatomy of the cranial nerves no precaution was taken to prevent the collapse of the vessels This may be done by injecting a gelatine solution This method will be used in future experiments in order to investigate the relationship between vessels and nerves *In vivo* the vessels are distended which probably explains the fact that they were better seen than the nerves at clinical cisternography (Fig 9)

The projections used were, with the exception of the axial one originally chosen in order to correlate the findings with those obtained at encephalography Therefore a p a half-axial projection was not included in the post-mortem examinations nor projections oblique to the sagittal plane Hence, optimal projections at clinical cisternography have to be further explored

This post-mortem investigation was initially made to form a basis for a correct understanding of anatomic structures revealed by tomography at encephalography *The information obtained suggests that tomography will be of considerable value in* clinical cisternography using water-soluble contrast media, but other supplementary techniques such as subtraction and stereoscopy may also be valuable auxillary procedures

The results of the present investigation may be compared with those currently obtained at encephalography and at cisternography with oily contrast media

The upper cranial nerve compartment has until now only been examined with air and other *gaseous contrast media Before the introduction of tomography in en*cephalography, the optic nerves were seen in the lateral projection only Tomography has made it possible to examine these structures both along their axis (METZGER 1967) and in the perpendicular direction (GREPE 1967) The demonstration of the optic



Fig 17 Tomography in a p projection Post mortem cisternography The hypoglossal nerves (→) have a course through the cistern that is parallel with that of the glossopharyngeal, vagal and accessory nerves (→)

chiasm by encephalography, especially when supplemented with hypocycloid tomography, in a projection along its axis has proved to be of considerable clinical value Theoretically, a demonstration of the optic nerve structures in a projection perpendicular to their axis would be of the same or even greater importance, but is difficult for anatomic and technical reasons and can only seldom be accomplished

Furthermore, the use of gaseous contrast media permits only the lateral borders of these structures to be seen (Fig 7) At post-mortem cisternography with positive medium the optic nerve structures could almost always be distinguished in axial and half axial views, the axial one giving more detailed information as to the relationship between the optic nerves and surrounding structures In the half-axial view, the optic nerve tracts nerves and chiasm were delineated by contrast medium along their entire intracisternal route Hence, even small expanding or atrophic lesions will probably be observable Another advantage lies in the fact that by utilizing a positive contrast medium the prerequisite will be present for the optic tracts and nerves to be demonstrated separately in the lateral projection

At encephalography the oculomotor nerves may sometimes be observed superimposed in the lateral view and separately in the half-axial projection when tomography is included In the present investigation the individual oculomotor nerves could be distinguished in the lateral projection, and their anatomy could be evaluated in greater detail in the half axial view Furthermore, these nerves could generally be seen in the axial projection in a large proportion of cases

At encephalography cranial nerves belonging to the middle cranial nerve compartment have until now been demonstrated only in the half axial projection LILIEQUIST observed the trigeminal nerve in the medial part of the cerebellopontine cistern NEUMANN (1968) using radiography with metal indicators in a post mortem investigation demonstrated the intracisternal route of the trigeminal nerve in relation to that of the facial statoacoustic nerves as seen at encephalography Cisternography was, however, not performed and this may explain why the characteristic fan-like appearance in the half-axial view (Fig 10) was not described The facial and statoacoustic nerves may be demonstrated at encephalography in a p projections with the beam parallel to the skull base particularly at tomography (GREPE 1969)

These cranial nerves are, with one exception—the abducens nerves—reported to be identified only in a small part of their intracisternal course, when oily contrast media are used It is the part closest to their exit from the subarachnoid space and even this only faintly visible judging from the illustrations published Those parts of

the nerves that are hidden in the dense contrast medium cannot be evaluated This may explain the following statement by HASTINGS-JAMES (1969) which also illustrates the difficulties encountered when evaluating cranial nerve structures using oily contrast media "*Whether the seventh and eighth nerve roots themselves become out*lined within the Pantopaque field is uncertain Since the whole length of the auditory nerve is only 17–19 mm of which about half lies within the bony canal, only a short length is available for visualization within the cistern, to project which in profile would probably require a half-axial view"

In the present material (Fig 10) the intracanalicular part of the facial and statoacoustic nerves was less than one third of their total length, which could be measured on the tomograms and was found to be about 30 mm after correction for magnification

The abducens, trigeminal, facial and statoacoustic nerves could be most often distinguished in the half-axial and axial projections In the lateral view only the trigeminal nerves could be identified because they alone were projected above the petrous bone As all these cranial nerves were observed along their entire intracisternal course and the trigeminal nerve structures also within Meckel s cave, clinical cisternography with water-soluble contrast media in the future is likely to allow more nerve structures to be distinguished than has hitherto been possible

Nerves within the lower cranial nerve compartment have seldom been reported to be observed at encephalography The same statement is valid with regard to examinations performed with oily contrast media The results at post-mortem cisternography indicate, however, that these nerves will probably be assessable when a contrast medium of suitable properties is available

Conclusions

The present investigation suggests that by using a suitable positive contrast medium, clinical cisternography will allow more information to be obtained in the examination of the cranial nerves than has hitherto been possible by encephalography or by cisternography with iodized oil In order to fully exploit the advantages of cisternography the contrast medium should have a suitable viscosity, surface tension, and, above all, adequate attenuation properties A water-soluble contrast medium is likely to meet these demands The use of positive contrast medium permits the cranial nerves to be demonstrated in other projections than at encephalography, particularly the axial and half-axial projections combined with tomography have been found useful

From the experience gained in this material it may be deduced that cisternography with a water-soluble contrast medium will probably elucidate the anatomy of the glossopharyngeal, vagus and accessory nerves, which previously have not been evidently demonstrated at roentgen examination in vivo The optic, oculomotor, trigeminal, facial and statoacoustic nerves, which are more or less demonstrable by

currently used methods will be demonstrable in other projections and in greater detail The olfactory, the trochlear and hypoglossal nerves will probably be most difficult to assess

SUMMARY

A post mortem radiologic investigation of the basal cisterns has been made with special regard to the cranial nerves The cisterns were removed in one piece together with the adjacent brain structures and the skull base The anatomy of the cranial nerves as seen at cisternography and the frequency of their identification have been analysed The application in clinical cisternography of the information obtained is discussed

ZUSAMMENFASSUNG

Eine post mortem rontgenologische Untersuchung der basalen Zisternen wurden unter besonderer Berucksichtigung der kranialen Nerven vorgenommen Die Zisternen wurden in einem Stuck zusammen mit den zugehorigen Gehirnstrukturen und der Schadelbasis ent fernt D e An

RÉSUMÉ

L auteur a fait un travail de recherche radiologique post mortem sur les citernes basales en vue d etudier spécialement les nerfs craniens Les citernes ont ete prélevees en un bloc avec les structures cerebrales adjacentes et la base du crane L'anatomie des nerfs craniens vue en cisternographie et la frequence de leur identification ont ete analysés L'auteur discute l application en cisternographie clinique des informations obtenues

REFERENCES

BAKER H L JR Myelographic examination of the posterior fossa with positive contrast medium Radiology 81 (1963) 791

— Cerebellopontine angle myelography J Neurosurg 36 (1972) 614

BRITTON B H HITSELBERGER W E and HURLEY B J Iophendylate examination of posterior fossa in diagnosis of cerebellopontine angle tumors Arch Otolaryng 88 (1968), 608

BURROWS E H Positive contrast examination (cerebell...

...STEIN B S Pneumoencephalography and cerebral angiography Year Book Medical Publ Inc Chicago 1966

— The trigeminal nerve shadow in the basal cisternogram Radiology 90 (1968), 42
GREPE A Encephalographic and post-mortem studies of the optic chiasm and the acoustic nerves Transactions of the VIIIth Symposium Neuroradiologicum Paris 1967 Résumé des communications 36 (1967)
— The normal anatomy of the cerebellopontine angle as studied radiologically *In* Nobel Symposium 10 Disorders of the skull base region Almqvist & Wiksell, Stockholm 1969
HASTINGS-JAMES R The anatomy of the posterior fossa in relation to positive contrast cisternography Radiology 92 (1969), 1065
LILIEQUIST B The subarachnoid cisterns An anatomic and roentgenologic study Acta radiol (1959) Suppl No 185
METRIZAMIDE A non ionic water-soluble contrast medium Acta radiol (1973) Suppl No 335
METZGER J Le signe du chiasma de face en pneumographie hypocycloïde Rev Neurol 117 (1967), 666
NEUMANN J Praktische Erfahrungen und diagnostische Moglichkeiten bei der Darstellung *der Trigeminuswurzel in PEG Erwachsener Wien Z Nervenheilk 26 (1968), 272*
REESE D F and BULL J W D Positive contrast demonstration of normal internal acoustic meatus, Meckel's cave and jugular foramen Amer J Roentgenol 100 (1967), 650
SCANLAN R L Positive contrast medium (Iophendylate) in diagnosis of acoustic neuroma Arch Otolaryng 80 (1964), 698

FROM THE DEPARTMENTS OF MEDICINE (DIRECTOR PROF A NORDOY) AND RADIOLOGY (DIRECTOR PROF H-J MAURER), INSTITUTE OF CLINICAL MEDICINE, UNIVERSITY HOSPITAL, N-9012 TROMSO, NORWAY

MENINGEAL REACTIONS FOLLOWING MYELOGRAPHY

Effects of detergent washing agent

H VIK MO and H-J MAURER

Serious complications following lumbar myelography with water soluble contrast media are relatively rare Acute meningeal reactions may result from the trauma of the procedure itself, contamination with micro-organisms, the irritative effect of the agent employed or the response to some irritant contaminating the equipment used (SWARTZ & DODGE 1965)

Five cases of severe meningeal reaction following myelography with Dimer-X have been encountered at this department and will now be reported and possible etiologic factors discussed

Material and Methods In the years 1970 to 1973 192 myelographies were carried out using dimeglumine iocarmate (Dimer X) The injection technique will be described in detail as this is a possible source of the meningeal reactions As premedication the patient received 1 1 ml ephedrine 5 per cent After washing the skin three times with Hibitane alcohol 0 5 per cent (chlorhexidin diglucon 0 5 g) the lumbar subarachnoid space was punctured with a disposable lumbar needle (ID 0 1 mm) Five ml cerebrospinal fluid were drained into a measuring glass cylinder and mixed with 5 ml Dimer-X This mixture was aspirated into a 10 ml disposable syringe and reinjected slowly

Submitted for publication 13 May 1974

Table 1

Clinical findings in 5 cases of chemical meningitis following myelography

Case No	Age	Sex	Predominating initial symptoms and signs	Time (h) from myelography to	
				initial symptoms and signs	lumbar puncture
1	42	M	Headache	3	72
2	42	M	Headache, nausea, fever	12	48
3	37	M	Spasms in the legs	24	48
4	61	M	Headache, fever	12	24
5	26	F	Headache, fever	24	144

The glass cylinder had been cleaned with water mixed with a washing agent and rinsed in water before autoclaving The manufacturer describes the washing agent as consisting of ionic as well as non-ionic detergents and alcohols

Discussion

The five cases had an acute meningeal reaction following myelography with fever, nausea, headache and nucheal rigidity (Table 1) The onset was rather acute, beginning 3 to 24 hours after myelography The symptoms and signs of meningeal irritation disappeared gradually within a few days up to a week No neurologic sequelae were encountered The CSF finding suggested a bacterial meningitis with cloudy fluid, markedly elevated white cell count and increased protein values (Table 2) The glucose level was found to be normal in 4 of the patients, but one patient had a low glucose level of 4 mg % The latter finding is usually encountered in bacterial meningitis, although low glucose levels have been observed in chemical meningitis (SWARTZ & DODGE 1965) GIBBONS (1969) reported two cases following spinal anesthesia with glucose values of 1 and 8 mg %, respectively Because of these initial findings a bacterial contamination as a result of inadequately sterilized equipment was first suggested and the patients received triple antibiotic treatment However, no bacteria were found except in one case where slight growth of saprophytic bacteria appeared, most probably based on later contamination The examination of the contrast medium gave no evidence of bacterial contamination and a bacterial etiology was thus considered less probable

An inflammatory reaction to a chemical irritant was then suggested In the myelographic procedure only disposable equipment was used except the glass cylinders for mixing the contrast medium with CSF These cylinders were cleaned in a solution with a detergent washing agent

Careful inspection of the cylinders after autoclaving revealed streaks of washing agent which drew attention to the possibility of CSF contamination There have been

Table 2

CSF in 5 cases with chemical meningitis following myelography The predominating cell type was granulocytes

Case No	Cells /µl	Glucose mg %	Protein mg %	Appearance	Bacteriology
1	1 660	45	220	Cloudy Xanthochrom	Negative
2	6 500	42	348	Cloudy Xanthochrom	Negative
3	600	68	295	Cloudy	Negative
4	6 300	4	544	Cloudy	Negative
5	1 810	54	112	Cloudy	Saprophyt bact

several reports suggesting that meningeal reactions may be caused by detergents used for cleaning of instruments for lumbar puncture WINKELMAN (1952) was the first to suggest that contamination of agents by surface active compounds, such as detergents, might produce meningeal reactions when introduced intrathecally He reported 11 cases with a syndrome of aseptic meningitis complicating spinal anesthesia and suggested that syringes cleaned in a detergent solution and inadequately rinsed in water before autoclaving retained enough detergent to act as an irritant Later GOLDMAN & SANFORD (1960) reported 5 patients with acute chemical meningitis possibly as a result of contamination of the equipment with a phenolic disinfectant DENSON et coll (1957) demonstrated experimentally that equipment soaked in various detergent solutions and autoclaved without washing may produce pathologic reactions in the meninges

Mild transient meningeal reactions have been reported in as much as 22 per cent of 630 Dimer X myelographies performed with Dimer X (GONSETTE 1971) Recently LEHTINEN & SEPPANEN (1972) found meningeal irritation in 5 5 per cent of 54 myelographies with Dimer X More serious acute meningeal reactions are rare, however IRSTAM (1973) reported one case of chemical meningitis among 300 myelographies with Dimer X, presumed to be caused by the contrast medium or by the lumbar puncture per se

It is not possible to prove beyond doubt that contamination of the equipment with the detergent washing agent is responsible for the acute meningeal reactions in the present five patients but it seems to be the most probable explanation A reaction to the contrast medium itself cannot be ruled out with certainty, however

Errors in the injection technique, especially contamination with chemical or bacterial agents, are the main cause of meningeal reactions From our experience it is concluded that a procedure of mixing CSF with the contrast medium outside a disposable syringe should be avoided and that only disposable equipment should be used in the myelography procedure

SUMMARY

Severe acute meningeal reaction following lumbar myelography are described Contamination of the cerebrospinal fluid with a detergent washing agent is the most probable etiology

ZUSAMMENFASSUNG

Schwere akute meningeale Reaktionen nach lumbaler Myelographie werden beschrieben Die Kontamination der cerebrospinalen Flussigkeit mit einem detergenten Spul-Agnes ist die wahrscheinlichste Ursache

RÉSUMÉ

Présentation de réaction meningée aigue grave après myélographie lombaire La contamination du liquide cérébro spinal avec un agent de lavage détergent est l etiologie la plus probable.

REFERENCES

DENSON J S, JOSEPH S I, KOONS R A, MURRY W E and BISSONNETTE H W Effects of detergents intrathecally Anesthesiology 18 (1957) 143

GIBBONS R B Chemical meningitis following spinal anesthesia J Amer med Ass 210 (1969), 900

GOLDMAN W W and SANFORD J P An 'epidemic' of chemical meningitis Amer J Med 29 (1960), 94

GONSETTE R An experimental and clinical assessment of water-soluble contrast medium in neuroradiology A new medium Dimer-X Clin Radiol 20 (1971), 44

IRSTAM L Side effects of water-soluble contrast media in lumbar myelography Acta radiol Diagnosis 14 (1973), 111

KUHLENDAHL H *Schaden durch Kontrastmittel bei der Myelographie In* Die Wirbelsaule in Forschung und Praxis, Band 41 Herausgegeben von H Junghanns Hippokrates Verlag, Stuttgart 1969

LEHTINEN E and SEPPÄNEN S Side effects of Conray Meglumin 282 and Dimer X in lumbar myelography Acta radiol Diagnosis 12 (1972) 12

MA [illegible] following Panto [illegible]

SWA [illegible] Engl J Med 272 (1965), 898

WINKELMAN N W Neurological symptoms following accidental intraspinal detergent injection Neurology 2 (1952) 284

FROM THE DEPARTMENT OF DIAGNOSTIC RADIOLOGY, UNIVERSITY OF LIVERPOOL, LIVERPOOL L69 3BX, ENGLAND

CONGENITAL ARTERIOVENOUS MALFORMATIONS OF THE UTERUS DEMONSTRATED BY ANGIOGRAPHY

J P BOTTOMLEY and G H WHITEHOUSE

Congenital arteriovenous malformations of the uterus are rare lesions, and there are only seventeen cases reported in the literature (DUBREUIL & LOUBAT 1926, GRAVES & SMITH 1927, REYNOLDS et coll 1949, GAINES & GREENWALD 1953, GARDNER 1954, WILLIAMS 1954, HOGE 1955) including those reviewed by SALM (1959) Although angiography has been extensively used in the examination of gynaecologic disease (LANG 1967), the angiographic demonstration of congenital arteriovenous malformations has been described on only two previous occasions (LIGGINS 1964, FRENCKEN & LANDMAN 1965) Preoperative diagnosis of the lesion will affect case management as well as facilitating any proposed surgical intervention Two cases, with conclusive angiographic findings, will now be discussed The clinical details of Case 1 have been described in full elsewhere (HIBBARD et coll 1972)

Case reports

Case 1 Th
mole at 22
curettings
one such examination haemorrhage was so severe as to require intrauterine packing No abnormality was found at hysterography on three occasions during this period

Submitted for publication 20 May 1974

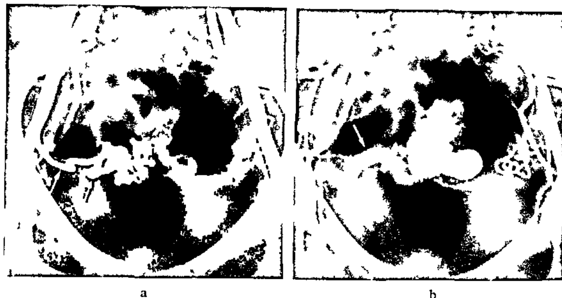


Fig 1 Case 1 a) Enlarged right uterine artery (→) supplying the uterine arteriovenous malformation b) Early filling of enlarged right uterine vein (→) Left uterine vein also filled

At the age of thirty years following resuscitation from an episode of shock due to uterine haemorrhage a percutaneous pelvic angiography was performed the catheter being introduced into the abdominal aorta 30 ml Urografin 60 % were injected An arteriovenous malformation consisting of a mass of serpiginous vessels was delineated in the area of the uterus The arterial supply was derived mainly from a tortuous and dilated right uterine artery The left uterine artery was also enlarged and supplied the vascular malformation (Fig 1 a) There was early filling of both uterine veins with contrast medium even when medium was still present within the arteries (Fig 1 b) The right uterine vein was greatly dilated Contrast medium persisted in some of the vessels of the abnormal plexus for several seconds

At subsequent laparotomy the uterine arteries and veins on both sides were found to be enlarged A pulsatile swelling 1 cm in diameter was visible on the postero lateral aspect of the right side of the uterus Hysterectomy was performed and section of the excised uterus showed many vascular channels up to 0 4 cm in diameter in the fixed state singly and in clusters within the myometrium Several of the vessels were thin walled and situated sub jacent to the endometrium No evidence of hydatidiform mole or trophoblastic tumour

Case 2 An 18 year old woman had a normal menstrual history prior to her admission to hospital with an incomplete abortion of a twelve week foetus A subsequent dilatation and curettage was uneventful Normal menstruation ensued until a second pregnancy This resulted in the complete abortion of a twin pregnancy of twenty weeks duration Dilatation and curettage was again uneventful but two months later she was again readmitted to hospital with prolonged and heavy uterine bleeding Normal endometrium at curettage but the persistent haemorrhage necessitated laparotomy Ovarian cystectomy for a bleeding *corpus* luteum cyst was performed Apart from some free blood in the peritoneal cavity no other abnormality was noticed Two months later uncontrollable uterine haemorrhage required readmission to hospital when she was found to have a haemoglobin of 75 % and normal blood coagulation tests With persistence of bleeding the haemoglobin level fell to 42 % and the patient required a blood transfusion By this time she had received eighteen units of blood over a six month interval



a



b



c

Fig 2 Case 2 a) ... left ... malf ... malf ... arterial phase Left uterine vein filled (→) c) Second angiography after left uterine artery ligation Left ovarian artery (→) and right uterine artery (↔) now supply the arteriovenous malformation

A survey film of the abdomen revealed no abnormality A percutaneous pelvic angiography was then performed a catheter being introduced into the abdominal aorta to the level of the tip of the third lumbar vertebra Thirty five ml Urografin 60% were injected An arteriovenous malformation was present in the left side of the uterus and left parametrium The vascular anomaly consisted of a cluster of vessels ... guration and was ... cular malformation ... was drained into ...

... the patient had normal menstruation during the seven months following laparotomy ... was then readmitted to hospital with a history of ...

external iliac artery also supplied the malformation The patient refused hysterectomy, but the haemorrhage ceased spontaneously soon after the angiography A subsequent hysterogram has been normal, and menstruation has also remained normal for six months

Discussion

Congenital arteriovenous malformations of the uterus present with haemorrhage per vaginam which is either spontaneous, associated with menstruation or follows curettage, usually in women of child bearing age On vaginal palpation, the uterus is soft and enlarged, and often pulsatile

At laparotomy, greatly dilated and tortuous vessels are found in close association with the uterus, and often in the parametrium Pulsation of the vascular mass is felt or even seen, and haemostasis is difficult

Pathologically, the vascular malformations are usually described as being of the 'circoid' type, as in both these cases, implying that the lesion is composed of multiple arteriovenous fistulas within a conglomeration of dilated vascular channels, which in some cases are large and described as 'cavernous', or the lesion may be more discreet with the component vessels being smaller than in the circoid type (SALM 1959)

Several vessels, such as the uterine, ovarian and hypogastric arteries may supply the vascular malformation, and will then be dilated and elongated The corresponding draining veins are also enlarged

The rarity of the lesion is reflected by the paucity of reported cases No arteriovenous malformations were found in the series of 345 cases of gynaecologic disease which were subjected to pelvic angiography by BORELL & FERNSTRÖM (1958)

In the two previous cases which were shown by angiography (LIGGINS, FRENCKEN & LANDMAN), the internal iliac arteries were dilated, and the enlarged uterine arteries supplied a large plexus of convoluted vessels within the uterus and parametrium, in which contrast medium remained for several seconds before passing into large veins At the same time, venous filling occurred while the arteries were still filled with contrast medium, indicating a degree of arteriovenous shunting (BORELL & FERNSTRÖM 1958) Similar appearances were also found in the two cases now described The possible multiplicity of feeding arteries is shown by Case 2 following ligation of the left uterine artery, which until then had been responsible for most of the arterial supply When aortography is performed the ovarian artery is filled in only 22 per cent of cases where aortic compression is not applied, and in 63 per cent of cases with aortic compression (BORELL & FERNSTRÖM) It is important that the aortic catheter be inserted sufficiently high to allow contrast medium to enter the ovarian arteries

Under normal conditions the diameter of the ovarian artery is only 1 5 mm, while the sum of the projected dimensions of the two uterine arteries in the non-pregnant state is 1 to 5 mm (FERNSTRÖM 1955)

There are other causes of arteriovenous shunts in the uterus and parametrium which have been demonstrated by angiography Retained placenta following ab-

dominal pregnancy (SMULEWICZ et coll 1971) and regions of necrotic villa in the placenta during uterine pregnancy (BORELL & FERNSTRÖM) may cause direct communications between arteries and veins A traumatic fistula between a uterine artery and vein may occur following caesarian section (HOWARD 1968) and after hysterectomy (MORLEY & LINDENAUER 1968) Multiple arteriovenous shunts may be demonstrable in carcinoma of the cervix and uterine body (LANG 1967) Rapid flow through arteriovenous fistula with enlarged supplying and draining vessels are often found in trophoblastic tumours (COCKSHOTT et coll 1964), but is then associated with bizarre appearances of the vessels and the presence of many irregular vascular spaces within the tumour The arteriovenous shunting on initial angiography may persist after successful chemotherapy in the case of trophoblastic tumours (COCKSHOTT & HENDRICKSE 1967) Neither of the two present cases had any clinical, operative, or pathologic findings to suggest any of these causes

Clinical awareness of uterine arteriovenous malformations will lead to earlier diagnostic confirmation by angiography A history of severe menorrhagia, metrorrhagia and uterine haemorrhage following curettage in a woman of childbearing age may suggest the condition, especially when associated with a bulky and pulsatile uterus, normal uterine curettings and normal hysterography The angiographic features are essentially those of such lesions occurring elsewhere in the body, with enlarged feeding arteries and draining veins, rapid filling of the veins, and some stasis of contrast medium within the plexus of abnormal vessels In none of the four cases now described has there been extravasation of contrast medium into the uterine cavity Presumably this is feasible if the uterine haemorrhage is of sufficient severity at the time of angiography

SUMMARY

Two cases of congenital arteriovenous malformations of the uterus are described, with details of their angiographic and operative identification The condition is rare, but should be considered in cases of severe uterine haemorrhage when more routine investigations have been normal

ZUSAMMENFASSUNG

Es werden zwei Fälle von kongenitalen arteriovenosen Missbildungen des Uterus mit deren angiographischen Einzelheiten und operativen Bestatigung beschrieben Das Vorkommen ist selten sollte aber bei Fallen mit schweren uterinen Blutungen, bei welchen Routineuntersuchungen normal ausgefallen waren erwogen werden

RESUME

Description de deux cas de malformations arterio veineuses congenitales de l'uterus avec des détails de leur diagnostic angiographique et operatoire Cette affection est rare et devrait être envisagee dans les cas d hemorragie utérine severe quand les examens plus courants ont été normaux

REFERENCES

BORELL U and FERNSTROM I The ovarian artery An angiographic study in human subjects Acta radiol 42 (1954), 253

— — Arteriovenous fistulae of the uterus and adnexae Acta radiol 49 (1958) 1

COCKSHOTT W P, EVANS K T and HENDRICKSE J P de V Arteriography of trophoblastic tumours Clin radiol 15 (1964), 1

— and HENDRICKSE J P de V Persistent arteriovenous fistulae following chemotherapy of malignant trophblastic disease Radiology 88 (1967) 329

DUBREUIL G and LOUBAT E Aneurysme circoide de l uterus Ann Anat path 3 (1926) 697

FERNSTRÖM I Arteriography of the uterine artery Acta radiol (1955) Suppl No 122

FRENCKEN V A M and LANDMAN G H M Circoid aneurysm of the uterus Specific arteriographic diagnosis Amer J Roentgenol 95 (1965), 775

GAINES J A and GREENWALD J C Uterine arteriovenous fistula Amer J Obstet Gynec 65 (1953), 997

GARDNER H I Circoid aneurysm of the uterus Amer J Obstet Gynec 68 (1954), 845

GRAVES W T and SMITH G V Circoid aneurysm of the uterus Amer J Obstet Gynec 14 (1927), 30

HIBBARD B M, JONES D P and SCARROW G D Circoid aneurysm of the uterus as a cause of menorrhagia J Obstet Gynaec Brit Cwlth 79 (1972), 855

HOGE R H Arteriovenous fistula of the uterus Sth med J (Bgham Ala) 48 (1955), 18

HOWARD L R Iatrogenic arteriovenous sinus of a uterine artery and vein Obstet Gynec 31 (1968), 255

LANG E K Arteriography in gynaecology Radiol Clin N Amer 5 (1967) 133

LIGGINS G C Uterine arteriovenous fistula Obstet Gynec 23 (1964), 214

MORLEY G W and LINDENAUER S M Arteriovenous fistula following pelvic operations Obstet Gynec 31 (1968), 722

REYNOLDS R T, OWENS C I and CANTAOR M O Arteriovenous aneurysm of the uterine artery and vein J Amer med Ass 141 (1949), 841

SALM R Diffuse cavernous haemangioma of the uterus J Path Bact 77 (1959), 111

SMULEWICZ J J, TAFRESHI M, CAGAN S H and HEDJAZI M Retained placenta following term abdominal pregnancy diagnosed by angiography Amer J Obstet Gynec 109 (1971), 1220

WILLIAMS G A Arteriovenous aneurysm of the uterus Amer J *Obstet Gynec 67 (1954)*, 68

FROM THE DEPARTMENT OF DIAGNOSTIC RADIOLOGY (DIRECTOR PROF B NORDENSTRÖM),
KAROLINSKA SJUKHUSET, S 104 01 STOCKHOLM, SWEDEN

LIVER BIOPSY WITH GUIDANCE IN SCANNING

A preliminary report

ULF ERASMIE

Liver scanning is a common method of examination of little discomfort to the patient In recent years it has been increasingly used for the analysis of a variety of diseases of the liver In the normal liver parenchyma the isotope uptake is homo geneous, in pathologic conditions the uptake is irregular, locally reduced, in the scan visible as defects Although isotope scanning is of limited value in establishing a differential diagnosis (CONN 1972, SAUER et coll 1973) it is considered a useful screening method with an accuracy of discovery of lesions generally stated to between 70 and 90 per cent (COVINGTON 1970, FERRANTE & MAXFIELD 1968) SAUER et coll could enhance the diagnostic accuracy by combining liver scanning with peritoneoscopy An expedient supplementary diagnostic examination is the percutaneous needle biopsy of the liver The frequency of complications of this method is stated to be low (CONN & YESNER 1963, LUNDQUIST 1971), although animal experiments have recorded a high rate of minor vascular sequelae (HELLEKANT & OLIN 1973) Previously percutaneous needle biopsy has been carried out following the recording of liver scans (CONN, COVINGTON, FERRANTE & MAXFIELD, THOMMERSEN 1973) Recently a method of percutaneous liver biopsy with scintigraphic control was published An isotopically tagged needle was used and the liver and the biopsy needles demonstrated con-

Submitted for publication 26 June 1974

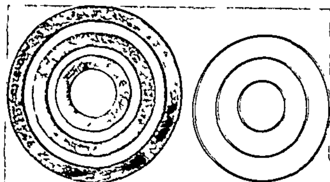


Fig 1 Indicator rings made of Wood s metal to the left and stainless steel to the right, 3, 6 and 9 cm inner diameter, respectively

currently on the scintillation camera with a *persistence oscilloscope during the* procedure (REYERSON 1974)

A method of introduction of the biopsy instrument into the liver under fluoroscopic control conducted by the scan is now presented The examination technique has been elaborated and applied on 19 patients

Method Scanning of the liver is performed by means of a scintillation camera with a persistence oscilloscope (Nuclear Chicago Pho gamma III with a 4 000 parallel hole collimator) Following the intravenous administration of 2 mCi $^{99}Tc^{m}$ sulfur colloid, recordings are made in a p , p a and lateral projections The biopsy area is indicated on the skin with guidance of the scan, the patient being placed supine or prone according to the projection in which the lesion is best visible Rings of metal of high radiation absorption serve as indicators, rings of Wood's metal (Bi 50 %, Pb 25 %, Cd 12 5 %, Sn 12 5 %) with an inner diameter of 30, 60 and 90 mm, a width of 10 mm and a thickness of 2 to 3 mm have been used (Fig 1) A ring with an inner diameter somewhat larger than the region of reduced isotope accumulation is selected and placed on the skin of the patient under the collimator and is visible after a short while on the oscilloscope The ring is subsequently carefully adjusted to a position right above the lesion of the liver (Fig 2) The inner outline of the ring is marked on the skin With the patient in unchanged position and the ring removed, the head of the gamma camera is revolved and the location of the lesion determined and marked on the skin in a perpendicular projection Due to the collimator having parallel holes, the rays are parallel and thus the metal ring is reproduced in the same scale as the liver, irrespective of the distance to the skin In direct comparison with the known ring diameter, estimation of dimensions can be made on the scan in levels parallel to the ring Thus, the diameter of a lesion with a reduced isotope uptake may be determined and the size of the liver be approximated

Liver biopsy is performed under fluoroscopy in a conventional roentgen laboratory with the patient placed in the same position as during the indication of the lesion Rings of identical dimensions are applied with surgical tape round the markings on the skin The indication rings being heavy and lumbering may preferably be exchanged for more slender rings of stainless steel The biopsy instrument is inserted from a suitable position, usually the right side, horizontally at level with the centre of the

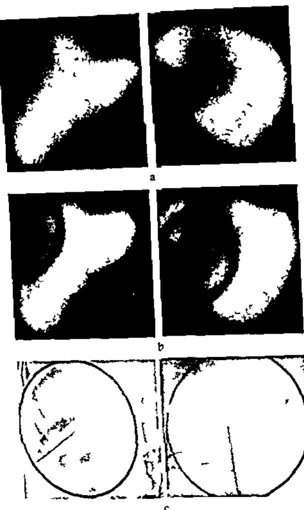


Fig 2. a) Liver scan frontal and lateral projections Large defect in the isotope uptake in the right lobe b) The same projections with indicator rings (Wood s metal) applied c) Films exposed in the same projections The biopsy needle introduced under fluoroscopic control The rings of Wood s metal have been replaced by stainless steel rings

side ring Under fluoroscopic control the instrument is introduced into the liver until its point is projected within the centre of the ring of the perpendicular plane The point of the needle should then be positioned centrally in the region of reduced isotope accumulation and permit sampling of tissue material

Results

Liver biopsy using the technique described has now been applied on 19 patients The right lobe was punctured in 18 patients and the left lobe in one patient Twelve cases had a single region of reduced isotope accumulation in their scans Seven cases had two or more such regions The diameter of the lesion punctured was between 3 and 6 cm in 8 cases 6 and 9 cm in 8 cases and more than 9 cm in 3 cases

Table

Distribution of biopsy diagnoses in 19 cases with liver scan

	No of cases
Primary or metastatic carcinoma	10
Bile obstruction	1
Distended gall bladder with a stone in its neck	1*
Local hepatitis following irradiation	1
Uncertain diagnosis	1
Normal liver cells	5

* Diagnosed by contrast injection through the biopsy needle

Cytology revealed carcinoma cells in 10 patients, in 5 normal liver tissue was obtained In 4 of these the isotope accumulation was only slightly reduced in the possible lesion and it is uncertain whether they should be considered pathologic A follow up of the these patients will give the answer A small but distinct region of reduced isotope accumulation in the left liver lobe was evident in the fifth case This patient was operated upon and it was found that the parenchyma was evidently thinner in the corresponding part of the liver, explaining the appearance of the scan Four cases remain In one of them a distended gall bladder with a stone in its neck was punctured In a further case cytology revealed signs of bile obstruction, and the third had probably a local hepatitis following irradiation In the remaining case the cytologic diagnosis was uncertain (Table) No complications in connection with the biopsies have been encountered

Discussion

Liver scanning is a useful screening method of high accuracy (COVINGTON, FERRANTE & MAXFIELD) On previous applications percutaneous biopsy has proved to be a diagnostically valuable supplement (CONN, COVINGTON, FERRANTE & MAXFIELD THOMMERSEN 1973)

Consequently it has been considered of value to describe a technique that makes it easy to introduce a biopsy instrument into a lesion detected at scintigraphy of the liver Since the method has been applied only on 19 patients until now, it is not possible to evaluate the accuracy of the technique at present, however, the results available are encouraging A similar technique may be used for biopsies from other organs and for field markings in radiation therapy

SUMMARY

A method to improve the accuracy of obtaining biopsy material of a lesion detected at liver scanning is presented The site of the lesion is determined in two orthographic projections during scintigraphy and indicated on the patient's skin With guidance of indicator fluoroscopy in two perpendicular projections percutaneous biopsy from any part of the liver may be performed

ZUSAMMENFASSUNG

Es wird eine Methode gezeigt um die Genauigkeit Biopsiematerial von einer bei der Leber Szintigraphie entdeckten Veranderung zu erhalten, zu verbessern. Der Platz der Veranderung wird bei der Szintigraphie in zwei orthographischen Projektionen bestimmt und auf der Haut des Patienten angezeichnet Unter Leitung von Indikator Durchleuchtung in zwei perpendikularen Projektionen konnen perkutane Biopsien von jedem Teil der Leber vorgenommen werden

RESUMÉ

Présentation d une méthode destinée a améliorer la précision de prelevements biopsiques d une lesion détectée par scintigraphie hépatique Le siege de la lesion est determine dans 2 projections orthogonales au cours de la scintigraphie et est indique sur la peau du malade La biopsie percutanée de n importe quelle region du foie est rendue possible par le guidage radioscopique dans 2 directions perpendiculaires

REFERENCES

CONN H O Rational use of liver biopsy in the diagnosis of hepatic cancer Gastroenterology 62 (1972) 142

— and YESNER R A reevaluation of needle biopsy in the diagnosis of metastatic cancer of the liver Ann intern Med 59 (1963) 53

COVINGTON E E The accuracy of liver photo scans Amer J Roentgenol 109 (1970), 742

FERRANTE W A and MAXFIELD W S Comparison of the diagnostic accuracy of liver scans, liver function tests and liver biopsies Sth med J 61 (1968) 1255

HELLEKANT CH and OLIN T Vascular complications following needle puncture of the liver An angiographic investigation in the rabbit Acta radiol Diagnosis 14 (1973) 577

LUNDQUIST A Fine needle aspiration biopsy of the liver Applications in clinical diagnosis and investigation Acta med scand (1971) Suppl No 520

REYERSON T W Percutaneous needle liver biopsy with scintigraphic control Radiology 110 (1974) 226

SAUER R FAHRLANDER H and FRIDRICH R Comparison of the accuracy of liver scans and peritoneoscopy in benign and malignant primary and metastatic tumours of the liver Scand J G

FROM THE DEPARTMENT OF DIAGNOSTIC RADIOLOGY III (DIRECTOR ASSOC PROF C-G HELANDER), SAHLGRENSKA SJUKHUSET, S-411 32 GOTHENBURG, AND DEPARTMENT OF PHYSICS, DIVISION IV A (DIRECTOR PROF. G BROGREN), CHALMERS UNIVERSITY OF TECHNOLOGY, S-402 20 GOTHENBURG, SWEDEN

INTENSIFYING SCREENS IN SOFT TISSUE RADIOGRAPHY

E DEICHGRÄBER, S REICHMANN and K-G STRID

Low voltage radiation is nowadays more and more being employed in soft tissue radiography The most important application is mammary radiography but the same technique is becoming increasingly common in examinations of the joints of the extremities FISCHER (1973 a, b) and FISCHER & BRAUN (1973) used a tube with a molybdenum target and non-screen film in examinations of joints of fingers and toes, wrist, elbow and the tendon of Achilles A tube with a tungsten rhenium target and low inherent filtration (0 5 mm Al) was used by REICHMANN et coll (1974) and DEICHGRÄBER & OLSSON (to be published) in examinations of finger joints (26 kV) and shoulder joints (40 kV) respectively

The radiation emitted at low tube potential involves comparatively large radiation doses to the patient A recording medium of as high sensitivity as possible is thus desirable The influence of different non-screen films on the image quality in mammary radiography was analysed by DEICHGRÄBER et coll (1974) In relation to the radiation dose required a superior image was obtained on industrial film of medium sensitivity Films of higher sensitivity gave rise to a disturbing quantum mottle, which definitely outweighed the gain in exposure reduction A recording medium with high capacity

Submitted for publication 5 March 1974

Table 1

Relative mAs values giving of three black-and white films optimal density

kV	Film	Density	Rel exposure
26	Mamoray T 3	2.0	1 0
	Curix RP 1	1 3	0 6
	Red Seal	1.3	0 4
40	Mamoray T 3	2 0	1 0
	Curix RP 1	1 3	0 6
	Red Seal	1 3	0 3

to absorb photons would increase the sensitivity without also increasing the quantum mottle This would be achieved by using intensifying screens, provided that they would not cause undue loss in image quality

Phantom tests

Two phantoms were made of square plastic bottles and contained vegetable oil with layer thickness of 3 and 7 cm respectively as measured in the beam direction Within the oil there were five nylon wires varying from 0 25 to 1 0 mm in diameter The bottles also contained small pieces of chalk embedded in an epoxy plastic A metal disc was placed on the upper side of each bottle, the disc being practically impenetrable to the radiation used The wires and the pieces of chalk were projected free of the discs Any blackening of the film occurring within the area of the disc image would reflect the degree of secondary radiation and other fog factors The *thinner of the phantoms was used in combination with a tube potential of 26 kV, the* thicker one with 40 kV

Four pairs of intensifying screens were tested It was considered of importance that the unsharpness resulting from light scattering within the phosphorus layer should be kept at a minimum, thus two high definition screens were chosen, viz Kodak X-omatic Fine and Siemens Rubin Super Kodak X-omatic screens have a rather regular crystalline texture, as compared with several other types (REICHMANN & HELANDER 1974 a) For this reason also Kodak X-omatic Regular was included in the tests although this screen presumably would give a higher degree of unsharpness due to its thicker phosphorus coating The fourth screen selected was Ilford Fluorazure since it had been found to yield a much higher light output (higher radiation to-light con version factor) when exposed to soft radiation, than calcium tungstate screens (LEVY & WEST 1933) The screens were placed in a vacuum cassette and tested together with four films a conventional roentgen film intended for 90 s processing time, Agfa Gevaert Curix RP 1, another black-and white film for ordinary clinical use, intended for a somewhat longer processing time, Ilford Red Seal, a film that previously had been shown to have a low grain mottle (REICHMANN & HELANDER 1974 b), Agfa Gevaert

Table 2

The figures indicate the exposure reduction obtained with intensifying screens compared to exposure without screens on the same film (in per cent)

kV	Film	Density	Screen	X omatic Regular	X omatic Fine	Rubin Super	Fluor azure
26	Mamoray	1.0	double	50	111	200	—
	Mamoray	2.0	double	48	100	167	14
	Mamoray	1.0	back	25	71	77	—
	Mamoray	2.0	back	26	63	63	—
	Mamoray	3.0	back	—	—	—	10
	Curix	1.0	double	6	12	18	—
	Curix	2.0	double	2.9	9	13	1.2
	Curix	1.0	back	—	13	9	—
	Curix	1.25	back	4.1	—	—	—
	Curix	2.0	back	3.5	16	11	—
	Curix	2.3	back	—	—	—	1
	Red Seal	1.0	double	8	15	23	—
	Red Seal	2.0	double	5	13	20	2.2
	Red Seal	1.0	back	8	17	22	—
	Red Seal	2.0	back	5	10	20	—
	Red Seal	2.5	back	—	—	—	1.5
40	Mamoray	2.0	double	19	63	100	—
	Mamoray	3.5	double	—	—	—	6
	Mamoray	1.0	back	31	77	83	19
	Mamoray	2.0	back	30	67	71	16
	Curix	1.5	double	1.3	6	6	0.5
	Curix	1.0	back	—	15	14	—
	Curix	1.5	back	2.7	14	11	1.0
	Red Seal	1.0	double	2.9	10	16	1.6
	Red Seal	2.0	double	2.2	8	9	0.9
	Red Seal	1.0	back	3.6	15	15	2.0
	Red Seal	2.0	back	3.3	16	14	1.2

Medichrome, finally, an industrial film of medium sensitivity which, previously had been shown to yield the best results when used without screens (DEICHGRÄBER et coll. 1974), Agfa Gevaert Mamoray T 3 (previous name Mamoray 2). This last film is not intended for exposure by light but none the less proved useful in combination with intensifying screens.

The influence of exposures on the density levels of three types of black and white films was determined by sensitometry, phantoms not being used. The optimum rendering of weak signals on ordinary black-and white films is expected to be obtained at the density $D=1.3$, therefore the exposure values giving that density at 26 kV and 40 kV were measured and compared with those giving the density of $D=2.0$ for industrial film. The results are given in Table 1. Table 2 presents the ex

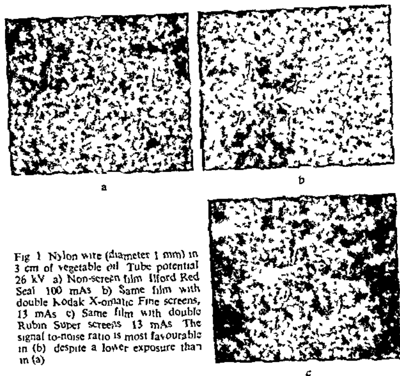


Fig 1 Nylon wire (diameter 1 mm) in 3 cm of vegetable oil Tube potential 26 kV a) Non-screen film Ilford Red Seal 100 mAs b) Same film with double Kodak X-omatic Fine screens, 13 mAs c) Same film with double Rubin Super screens 13 mAs The signal to-noise ratio is most favourable in (b) despite a lower exposure than in (a)

posure reduction obtained for the three types of film when used in combination with the various screens in relation to the same films exposed without screens The term 'intensification factor' has been avoided The reason is that the exposure reductions listed in Table 2 indicate that these vary considerably with the level of density It is evident that the exposure reductions were moderate when industrial film was used and that the high definition screens gave the lowest reduction, the Fluorazure screen gave a high light output

The screen film combinations were then tested on the phantoms The Fluorazure screen was omitted, however, since sensitometry had revealed it to produce an unduly high mottle level The remaining screens (Kodak X-omatic Fine and Regular, Siemens Rubin Super) were combined with the black and-white films (Mamoray T 3, Curix RP 1, Red Seal) and with the Medichrome film The target of the tube was 0 6 mm × 0 6 mm and the FFD 70 cm

The quality of the image recorded on industrial film without intensifying screens was definitely superior to all the roentgenograms taken with the other films, whether exposed with or without screens The most evident difference concerned the mottle level, which was lowest in the non-screen industrial film For the remaining conventional films an interesting observation was made In films exposed with double Kodak X omatic Fine screens the signal to-noise ratio was more favourable than in

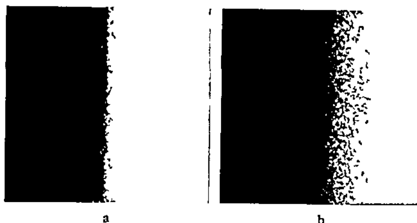


Fig 2 Microphotographs from a roentgenogram of a thin metal wire on industrial roentgen film exposed with back screen The image of the tube-side emulsion of the roentgen film (a) is much sharper than that of the back side emulsion (b), where the screen has contributed to the exposure (Magnification ×250)

films exposed without screens, although the total exposure dose was lower when the screens were used (Fig 1) With double screens the level of secondary radiation was lowered, owing to the filtering effect of the front screen (LAURELL 1932, LINDBLOM 1934, OOSTERKAMP 1946) This reduction contributed to a better signal-to-noise ratio Thus it cannot with certainty be maintained that the screen roentgenogram, in this case, was produced with the aid of a larger number of photons than the non-screen one Whatever the mechanism, the screens improved the signal-to-noise ratio and lowered the patient dose When industrial film was used, on the other hand, none of the screens improved the image quality In a comparison between the three conventional roentgen films (Curix, Red Seal, Medichrome), no significant difference appeared in roentgenograms taken under equal conditions

Rubin Super proved to produce a comparatively high mottle level (Fig 1 c) This was most evident when double screens were used Likewise, X-omatic Regular caused a rise in mottle, although a less disturbing one, possibly because this screen produced a higher degree of unsharpness than the other screens An image quality comparable to the reference recording medium (non-screen industrial film) was thus obtained only with Kodak-X-omatic Fine and industrial film in combination both at 26 kV and 40 kV It appears from Table 2, however, that the exposure reduction made possible with this combination is a modest one

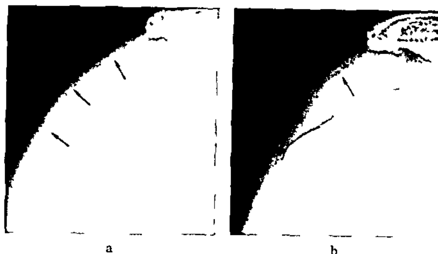
In soft tissue radiography it is suggested only to employ back screens (PRICE & BUTLER 1970) The image is then to a large extent produced by photons absorbed directly in the silver emulsion of the film It might be expected that the image would appear more distinct than when double screens are employed In an additional test series thin metal threads were exposed on industrial film at 26 kV and 40 kV potentials The same three screens were used as back screens as well as in pairs Films were also exposed without screens The films were analysed under the microscope at low

magnification In the front emulsion layer an extremely well defined image appeared when a back screen alone had been employed, whereas the silver layer in contact with the back screen presented a much more blurred image of the same thread (Fig 2) The loss of definition was considerable even with the finest screen Thus the introduction of one intensifying (back) screen seems likely to cause such a high loss of definition that addition of a front screen only slightly increases the total unsharpness At close inspection the images of the threads did not vary significantly in definition whether exposed with a back screen alone or with screen pairs

In summary All conventional roentgen films tested gave rise to a lower image quality than did non screen industrial film Kodak X omatic Fine screen improved the image quality when conventional films were employed However when combined with industrial film this screen caused a slight decrease in quality, mostly due to increased loss of detail Rubin Super introduced a high mottle level X omatic Regular caused more loss of definition than X omatic Fine The mottle level was also probably raised In combination with industrial film however, X omatic Regular appeared most suitable for further investigation X omatic Fine and Rubin Super were excluded since they reduced the exposure dose only modestly Rubin Super, moreover, caused increased mottle Therefore it was considered reasonable to supplement the experiments with clinical trials to determine if the reduction in quality introduced by the X omatic Regular screens has any diagnostic significance

Clinical experiences

The soft tissues of the shoulder joint were chosen for the clinical tests since these have proved somewhat difficult to demonstrate in non screen industrial film of medium sensitivity due to rather long exposure times needed Clinical experience with Mamoray T 3 has shown the optimum tube potential to be 40 kV (DEICHGRABER & OLSSON) The inherent filtering of the tube was equivalent to 0 5 mm Al The FFD was 70 cm Patients admitted for soft tissue examination of the shoulder were examined according to this technique in a p projection and served as a reference material For each shoulder an additional film was exposed for comparison with as near as possible identical centering Cassettes with double Kodak X omatic Regular screens were used As this procedure was found to increase the image contrast due to a lowered level of secondary radiation the tube potential was increased to between 40 and 50 kV Eight patients were examined Medichrome film being employed The thin fat tissue layer located on the lateral aspect of the shoulder joint beneath the deltoid muscle (Fig 3 a) was demonstrated in the reference films but was more or less indistinguishable in Medichrome films The image quality of these films was thus so poor that they were considered useless Next Mamoray T 3 films were used in 35 examinations with 50 to 60 kV being used At 60 kV the contrast obtained in films exposed with screens was approximately identical to that obtained in the reference material Well-developed fat tissue layers in the shoulder region were clearly visible



[illegible] a) Non

[illegible]

the arrow

even on films exposed with screens The unsharpness was more marked, however, which was most clearly evident in the bone structure Neither did this blur allow extremely thin fat tissue layers to be discerned, thus simulating a true disappearance, as occurring in conditions with a regional inflammatory edema (Fig 3 b) Consequently the use of screens produced an image quality, which might lead to false diagnoses This deterioration was not considered to be outweighed by the reduction of the exposure

Discussion

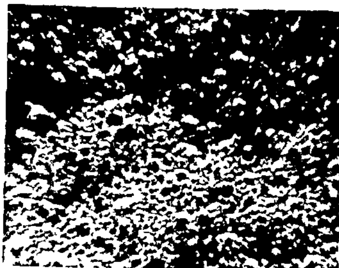
The purpose was to determine whether intensifying screens provide for increased absorption of photons as compared with non-screen film, so that the exposure may be reduced without undue loss in image quality The assumption that this should be possible proved to be true for films having a low silver content, i e films intended for conventional clinical diagnostic work Such films combined with one type of screens produced a definite improvement of image quality compared to exposure without screens, at the same time allowing a significant dose reduction Thus the basic idea proved to be correct However, the same principle could not be successfully applied to that type of film which ought to be used in most cases of soft tissue radiography, viz industrial film of medium sensitivity with a high silver content This film used without screens gave an image of extraordinary quality but with screens the image quality deteriorated because of loss of definition

The low voltage radiation employed in soft tissue radiography is easily absorbed Thus, at this energy level, even a thin phosphorus layer of an intensifying screen should be able to absorb a considerable number of photons In principle, it should

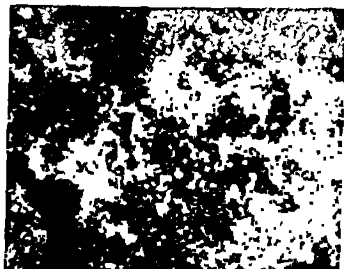
therefore be possible to make intensifying screens adapted for soft tissue radiography

Inhomogeneous crystalline texture of intensifying screens may introduce mottle into the image The phosphorus layer, therefore, must meet very high demands for homogeneity The lower the unsharpness caused by the screen, the higher these demands must be, because mottle may be rendered invisible by unsharpness (GOODENOUGH et coll 1972) The unsharpness introduced by screens varies inversely with the thickness of the phosphorus layer A thinner coating of the screens chosen for this investigation to reduce unsharpness to an acceptable degree decreased the light output so much that the reduction of the exposure became too small The present results indicate that the only screen film combination which could be considered acceptable yielded an exposure reduction of about 60 per cent of that used for non-screen industrial film Against this dose reduction must be weighed the special maintenance necessary for these screens In this type of diagnostic procedure the screens must be cleaned with utmost care Even the finest dust particles will be clearly reproduced in the films and may be confused with calcific deposits in the soft tissues The inherent conflict between light output and image unsharpness would indicate that available intensifying screens should not be used for soft tissue radiography This conclusion is probably true as regards the fluorescent substances of the screens used At low tube potential the light output of calcium tungstate and barium lead sulfate rapidly decreases (MATTSSON 1955) The modification of zinc sulfide used in the Fluorazure screen, on the other hand, gives a relatively high output when exposed to soft radiation Screens for soft tissue examinations should be based upon a fluorescent substance with a favourable light output for soft radiation Technical improvements should thus aim at the production of extremely thin phosphorus layers with a high light output

The unsharpness of the image introduced by intensifying screens is to a considerable extent caused by light scattering within the phosphorus layer The optical properties of this layer determine the degree of unsharpness The factors most often discussed are the thickness of the layer, the grain size, and the presence or absence of a reflecting coating at the boundary between the phosphorus layer and the screen base (HARTMANN 1931, KLUG 1937, SCHOBER & KLETT 1954, PIWONKA et coll 1965) Two additional factors deserve consideration The X-omatic screens were examined under the microscope at low magnification in reflected and transmitted light and the Kubin Super screen in reflected light only Other screens (CaWo Universal, CaWo Fin, Du Pont Par Speed, Siemens Saphir) were examined in the same way In reflected light refraction or reflection phenomena or both were observed at the boundary between the binding substance and the crystals (Fig 4 a) The conclusion was that they had different refractive indices Thus, all the screens were optically inhomogeneous, which should enhance light scattering This applied particularly to screens with more than one layer of crystals Furthermore, the binding material invariably was opaque Crystals at the surface of the layer were more easily observed in trans-



a



b

Fig 4 Microphotographs of intensifying screens in a) reflected light (Siemens Rubin Super) and b) *transmitted light* (CaWo Fin) Superficial crystals in (a) appear black with a halo of light that indicates differences in refractive index between crystals and binder In the bright areas of (b) no superficial crystals were present No sharp image of crystals of the deeper layers could be obtained, *owing to the opacity of the binder* (Magnification ×115)

mitted light than those situated in deeper layers, even if they were not covered by overlying crystals (Fig 4 b) This means that the opacity of the binder also should enhance light scattering

Further progress as regards intensifying screens suitable for soft tissue radiography should imply that fluorescent substances with a high light output for soft radiation be used The zinc sulfide of the Fluorazure screen (LEVY & WEST 1933) might be considered as well as the rare-earth oxysulfides described by BUCHANAN et coll. (1972) The fluorescent substance should be dispersed into a thin, preferably monocrystalline, layer of densely packed, minute and regular crystals The binder should be absolutely clear and possess the same refractive index as the crystals Colour substances may be added to the binder as usual, provided the binder not being opacified Another

possibility bears on the principle applied in the production of intensifying screens of cesium iodide in image intensifiers (STEVELS et coll 1973) Precipitation of a suitable fluorescent agent as needle crystals, all oriented in the beam direction should be favourable for constructing a screen for soft tissue radiography, once problems of a technical nature have been solved

The choice of the film type is of great importance The industrial film of medium sensitivity appears to be the most suitable one as a starting point for further investigation However, it should have to be modified so that it can be used in combination with screens prepared as suggested It is evident that further research for promotion of a refined technique of soft tissue radiography should include simultaneous attention to the qualities of films and intensifying screens

Acknowledgement

This investigation was supported by a grant from the Swedish Society of Medical Radiology

SUMMARY

Certain screen film combinations were tested in the low voltage range (26 to 40 kV, tungsten target) and compared with an optimal non screen industrial film The dose reduction was of no consequence as compared with the loss in image quality Some physical properties of the screens giving rise to the failure are discussed

ZUSAMMENFASSUNG

Gewisse Schirm Film Kombinationen wurden im Niedervoltbereich (26–40 kV, Tungsten Target) geprüft und mit einem optimalen nicht Schirm industriellen Film verglichen Die Verminderung in der Dosis war bedeutungslos verglichen mit dem Verlust in der Bild qualität Einige physikalische Eigenschaften der Schirme die zu dieser Verschlechterung führen werden diskutiert

RESUME

Les auteurs ont étudié certaines combinaisons d écrans et de films dans le domaine des bas voltages (26–40 kV anode en tungstène) et les ont comparées avec un film industriel sans écran optimal La réduction de dose est sans intéret quand on la compare avec la perte de qualité de l image Les auteurs examinent certaines propriétés physiques des écrans qui sont la cause de cet échec

REFERENCES

BUCHANAN R A FINKELSTEIN S I and WICKERSTEIN K A X ray exposure reduction using rare-earth oxysulfide intensifying screens Radiology 5 (1972) 185

DEICHGRABER E and OLSSON B Soft tissue radiography in painful shoulder To be published in Acta radiol Diagnosis

— REICHMANN S and BUREN M Film quality in mammary radiography Acta radiol Diagnosis 15 (1974) 93
FISCHER E Der Nachweis einer chronischen Insertionstendopathie am Epicondylus humeri durch Weichstrahlaufnahmen Fortschr Rontgenstr 119 (1973) 358
— Die progressive Sklerodermie der Finger im Weichstrahlbild Fortschr Rontgenstr 119 (1973) 372
— und BRAUN J Neue diagnostische Moglichkeiten an den Extremitaten durch Weichstrahlaufnahmen mit Mammographiegeraten Electromedica 3 (1973) 90
GOODENOUGH D J ROSSMANN K and LUSTED L B Radiographic application of signal detection theory Radiology 105 (1972) 199
HARTMANN J H Verstarkerfolien ihre Beurteilung und Eigenschaften Fortschr Rontgenstr 49 (1931) 758
KLUG H Vergleichende Untersuchung der gebrauchlichen Durchleuchtungsschirme und Verstarkerfolien Fortschr Rontgenstr 55 (1937) 191
LAURELL H Dunne Bleifolien als Sekundarblenden Acta radiol 13 (1932) 193
LEVY L and WEST D A new and much more rapid intensifying screen allowing great alterations in radiographic technique Brit J Radiol 6 (1933) 85
LINDBLOM K Secondary screening by means of filtering Acta radiol 15 (1934) 620
MATTSSON O Practical photographic problems in radiography Acta radiol (1955) Suppl No 120
OOSTERKAMP W J Eliminating scattered radiation in medical X ray photographs Philips Techn Rev 8 (1946) 97
PIWONKA R VOIGT G und PETRI E C Der Einfluss der wirklichen Korngrosse des Calciumwolframat Leuchtstoffes auf die Detailwiedergabe von Rontgen Verstarkerfolien Rontgen Bl 18 (1965) 79
PRICE J L and BUTLER P D The reduction of radiation and exposure time in mammography Brit J Radiol 43 (1970) 251
REICHMANN S and HELANDER C G (a) Homogeneity of intensifying screens Acta radiol Diagnosis 15 (1974) 449
— — (b) High voltage radiography Theory and clinical application Acta radiol Diagnosis 15 (1974) 561
STEVELS A L N DE PAUW A D M and DAAMS J L C Luminescent screen with pile structure Medicamundi 18 (1973) 149
SCHOBER H und KLETT C Untersuchungen uber die Zeichenscharfe von Verstarkerfolien Rontgen Bl 7 (1954) 214

FROM THE DEPARTMENT OF DIAGNOSTIC RADIOLOGY III (DIRECTOR CARL-GUSTAV HELANDER), SAHLGRENSKA SJUKHUSET, S-411 32 GOTHENBURG, AND THE DEPARTMENT OF PHYSICS, DIVISION IV A (DIRECTOR PROFESSOR GÖSTA BROGREN), CHALMERS UNIVERSITY OF TECHNOLOGY, S-402 20 GOTHENBURG, SWEDEN

CONTRAST FORMATION IN FLUOROSCOPIC VIDEODENSITOMETRY

III. Relation between roentgen tube potential and exposure rate to produce constant video level

BO LANTZ and KARL-GUSTAV STRID

In two previous papers (STRID & LANTZ 1973, LANTZ & STRID 1973) a mathematical model for the optimisation of contrast was presented and shown to describe the extinction due to iodine as determined by a videodensitometric method for tube potential values in the range 40 to 110 kV, tissue being simulated by water layers of varying thickness, and copper filters being used Good agreement between experimental data and the model was found, showing optimal iodine contrast at low tube potential (40 to 50 kV) and moderate copper filtering (0 4 to 0 7 mm) for water layers up to a thickness of 10 cm As far as optimal contrast is concerned, angiography should thus be performed at as low tube potential as possible and with slight copper filtering In clinical radiology, however, it is of utmost importance that the radiation dose received by the patient be reduced as far as possible The purpose of the present investigation was to determine the relation between iodine contrast formation in fluoroscopy and exposure rate in order to arrive at an acceptable compromise between high contrast and low patient dose

Submitted for publication 13 March 1974

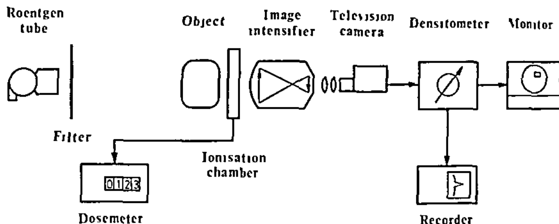


Fig 1 Block diagram of the experimental set up

Measuring systems

A videodensitometric system was used as described in detail previously (LANTZ & STRID) It consists of roentgenologic standard equipment (roentgen apparatus Triplex Angiomatic 1023/2 CE, Elema-Schönander, rhenium-target roentgen tube Bi 150/30/50 R, Siemens, 12 5 cm image intensifier Sirecon Duplex 25/15, Siemens, vidicon television chain Videomed I, Siemens), a logarithmating videodensitometer (constructed by Strand & Lantz) and a multi-channel strip-chart recorder (Mingograf 800) The intrinsic filtration of the tube was equivalent to that of 2 mm aluminium

For measuring the exposure rate an air ionisation chamber (Streustrahlenkammer, Physikalisch-Technische Werkstätten Dr Pychlau KG, No 20075, calibrated for the exposure-rate range 1 7–670 μR s^{-1}) was used in conjunction with a dosemeter (Simplex Dosimeter II, PTW)

The measurement set-up for the experiments is illustrated in Fig 1 The distance between the focus of the roentgen tube and the entrance plane of the image intensifier was 93 cm The ionisation chamber was placed in the centre of the irradiated field close to the input screen of the intensifier tube The various water layers were placed close to the ionisation chamber, and the copper filters close to the tube

Measurements

The exposure rate was registered by the dosemeter for tube potential values ranging from 40 kV to 110 kV at 10 kV intervals and copper filters with thickness ranging from 0 to 1 0 mm at 0 2 mm intervals The video level was adjusted by means of a cathode-ray oscilloscope to a value somewhat below the white level It was then kept constant on changing tube potential and filters by setting the tube current so as to yield a constant reading off the strip-chart recorder Voltage and current values were read directly from calibrated volt- and milliamperemeters in the roentgen generator

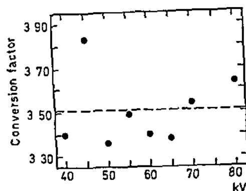


Fig 2 The [illegible]

The sampling window of the videodensitometer was placed centrally in the irradiated field The position and the size of the window remained the same throughout the measurements, and the gain of the video chain was not varied

The roentgen equipment used permitted a maximum of 5 mA, which precluded measurements to be carried out with low tube potential and heavy filtering, since the required video level could not be achieved

Calibration of the dosemeter system The calibration factor of the system of ionisation chamber and dosemeter was obtained from the manufacturer's test record

Throughout the investigation the irradiated field was confined by diaphragms to form a square 5 cm by 5 cm Since only part of the ionisation chamber volume was irradiated, preliminary measurements were performed to establish a conversion factor for dosemeter readings Unfiltered radiation being used, dosemeter readings were taken with the chamber completely irradiated and with the diaphragms inserted Over 40 to 80 kV the quotient of the readings appeared reasonably constant (Fig 2)

Correlation between exposure rate and mA In the experimental set-up, the ionisation chamber was placed immediately before the image intensifier However, the quantity of clinical interest is the skin dose, a measure of which is the exposure rate at the entrance surface of the water that simulates soft tissue in the model

Theoretically, the exposure rate depends linearly on the tube current at given value of the potential Thus, the exposure rate in an actual case would be

$$\dot{X} = (i/i_0)\,\dot{X}_0,$$

i being the actual current and $\dot{X}_0$ being the exposure rate measured in the absence of water and with the tube current i_0 To verify this relation experimentally, the exposure rate was measured as a function of the current The measurements confirmed (Fig 3) that the relation could be safely used for calculating the exposure rate at the entrance surface of the object (water layer) under the prevailing circumstances

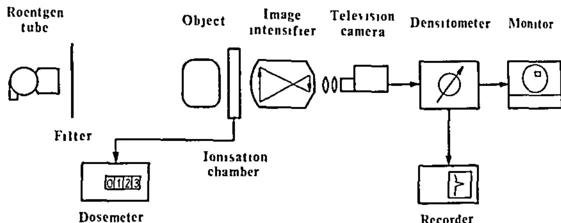


Fig 1 Block diagram of the experimental set up

Measuring systems

A videodensitometric system was used as described in detail previously (LANTZ & STRID) It consists of roentgenologic standard equipment (roentgen apparatus Triplex Angiomatic 1023/2 CE, Elema-Schonander, rhenium-target roentgen tube Bi 150/30/50 R, Siemens, 12 5 cm image intensifier Sirecon Duplex 25/15, Siemens, vidicon television chain Videomed I, Siemens), a logarithmating videodensitometer (constructed by Strand & Lantz) and a multi-channel strip-chart recorder (Mingograf 800) The intrinsic filtration of the tube was equivalent to that of 2 mm aluminium

For measuring the exposure rate an air ionisation chamber (Streustrahlenkammer, Physikalisch-Technische Werkstätten Dr Pychlau KG, No 20075, calibrated for the exposure-rate range 1 7–670 $\mu R\ s^{-1}$) was used in conjunction with a dosemeter (Simplex Dosimeter II, PTW)

The measurement set-up for the experiments is illustrated in Fig 1 The distance between the focus of the roentgen tube and the entrance plane of the image intensifier was 93 cm The ionisation chamber was placed in the centre of the irradiated field close to the input screen of the intensifier tube The various water layers were placed close to the ionisation chamber, and the copper filters close to the tube

Measurements

The exposure rate was registered by the dosemeter for tube potential values ranging from 40 kV to 110 kV at 10 kV intervals and copper filters with thickness ranging from 0 to 1 0 mm at 0 2 mm intervals The video level was adjusted by means of a cathode-ray oscilloscope to a value somewhat below the white level It was then kept constant on changing tube potential and filters by setting the tube current so as to yield a constant reading off the strip chart recorder Voltage and current values were read directly from calibrated volt- and milliamperemeters in the roentgen generator

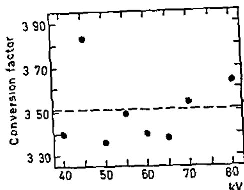


Fig 2 The ratio of the dosemeter reading with the ionisation chamber completely irradiated to that with a 5 cm by 5 cm field irradiated The average value $3\ 5 \pm 0\ 3$, was used as the conversion factor for dosemeter readings

The sampling window of the videodensitometer was placed centrally in the irradiated field The position and the size of the window remained the same throughout the measurements, and the gain of the video chain was not varied

The roentgen equipment used permitted a maximum of 5 mA, which precluded measurements to be carried out with low tube potential and heavy filtering, since the required video level could not be achieved

Calibration of the dosemeter system The calibration factor of the system of ionisation chamber and dosemeter was obtained from the manufacturer's test record

Throughout the investigation the irradiated field was confined by diaphragms to form a square 5 cm by 5 cm Since only part of the ionisation chamber volume was irradiated, preliminary measurements were performed to establish a conversion factor for dosemeter readings Unfiltered radiation being used, dosemeter readings were taken with the chamber completely irradiated and with the diaphragms inserted Over 40 to 80 kV the quotient of the readings appeared reasonably constant (Fig 2)

Correlation between exposure rate and mA In the experimental set up, the ionisation chamber was placed immediately before the image intensifier However, the quantity of clinical interest is the skin dose, a measure of which is the exposure rate at the entrance surface of the water that simulates soft tissue in the model

Theoretically, the exposure rate depends linearly on the tube current at given value of the potential Thus, the exposure rate in an actual case would be

$$\dot{X} = (i/i_0)\, \dot{X}_0,$$

i being the actual current and $\dot{X}_0$ being the exposure rate measured in the absence of water and with the tube current i_0 To verify this relation experimentally, the exposure rate was measured as a function of the current The measurements confirmed (Fig 3) that the relation could be safely used for calculating the exposure rate at the entrance surface of the object (water layer) under the prevailing circumstances

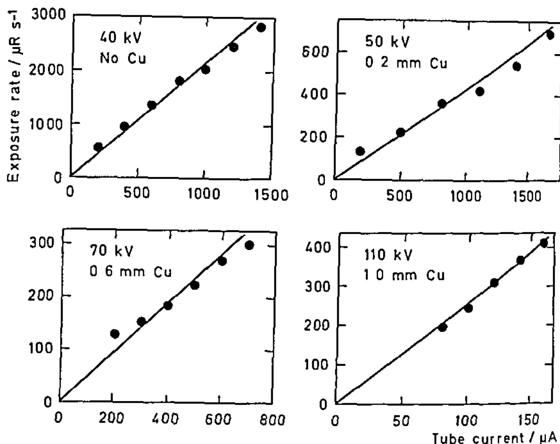


Fig 3 The relation between exposure rate and tube current for certain values of tube potential and copper filter thickness

Results

Dependence of the exposure rate on tube potential and filtering at constant video level Two circumstances were obvious from the measurements the extremely high exposure rate in the absence of copper filtering in the low potential range (40 to 70 kV) as compared with the high range (80 to 110 kV), and the marked effect of the copper filters in decreasing the exposure rate in the lower potential range (Fig 4) To yield the prescribed value of the video level in the television chain for a 5 cm water layer at 50 kV, the exposure rate 6 6 mR s^{-1} was required, and at 60 kV 4 5 mR s^{-1} Filtering with 0 2 mm Cu reduced the exposure rate required to 2 6 mR s^{-1} at 60 kV and to 0 78 mR s^{-1} at 100 kV

The water layer being increased to 10 cm, the exposure rate required to produce the prescribed video-level value increased 4 to 7 times, most in the low potential range Thus the exposure-rate values at 60 kV and 70 kV were 28 mR s^{-1} and 16

Fig 4 The exposure rate at the entrance surface of the object required to produce constant video level with unfiltered radiation (left) and with radiation filtered through 0 2 mm copper (right) The object (water layer) thickness was ●, 0 ▲, 5 cm ■, 10 cm

Fig 5 The exposure rate at the entrance surface of the object required to produce constant video level for a 5 cm (left) and a 10 cm (right) thick object (water layer)

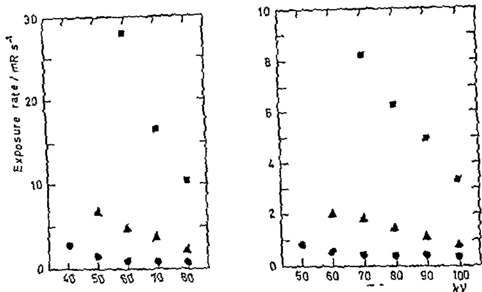


Fig 4 (For legend see opposite page)

Exposure rate / mR s⁻¹

Filter thickness / mm

☆ 50 kV ✶ 60 kV □ 70 kV ■ 80 kV ▼ 90 kV ○ 100 kV ● 110 kV

Fig. 5 (For legend see opposite page)

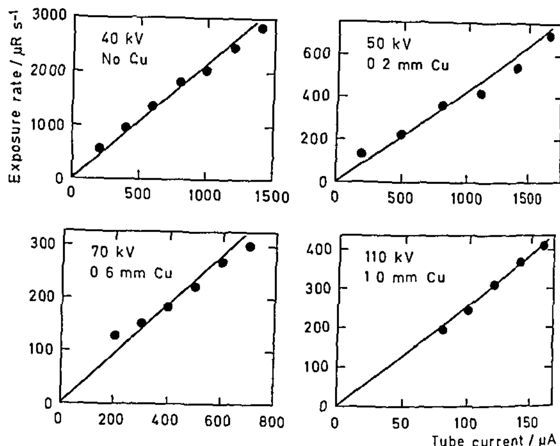


Fig 3 The relation between exposure rate and tube current for certain values of tube potential and copper filter thickness

Results

Dependence of the exposure rate on tube potential and filtering at constant video level Two circumstances were obvious from the measurements the extremely high exposure rate in the absence of copper filtering in the low potential range (40 to 70 kV) as compared with the high range (80 to 110 kV) and the marked effect of the copper filters in decreasing the exposure rate in the lower potential range (Fig 4) To yield the prescribed value of the video level in the television chain for a 5 cm water layer at 50 kV, the exposure rate 6 6 mR s^{-1} was required and at 60 kV 4 5 mR s^{-1} Filtering with 0 2 mm Cu reduced the exposure rate required to 2 6 mR s^{-1} at 60 kV and to 0 78 mR s^{-1} at 100 kV

The water layer being increased to 10 cm, the exposure rate required to produce the prescribed video level value increased 4 to 7 times most in the low potential range Thus the exposure rate values at 60 kV and 70 kV were 28 mR s^{-1} and 16

Fig 4 The exposure rate at the entrance surface of the object required to produce constant video ... through 0 2 mm copper (right) The ● ▲ ■

... quired to produce constant video

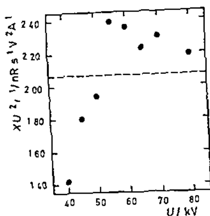


Fig 6

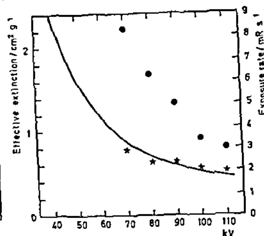


Fig 7

Fig 6 The quantity $B \equiv X/U^2 I$ as a function of the tube voltage

Fig 7 The effec

the exposure rate at the water layer entrance surface is decreased for a given value of the video level

Conclusion

The present investigation has shown that the exposure rate in fluoroscopic videodensitometry can be kept at a minimum with the tube voltage about 100 kV and with slight copper filtering (0 2 mm) The extinction due to iodine has its maximum in the tube potential range 40 to 50 kV with slight copper filtration (LANTZ & STRID 1973) Towards higher kV the extinction decreases to 20 to 50 per cent depending on the filters used In model experiments where the exposure cannot cause injury to a patient the low voltage range is preferable

In clinical radiology, however, the patient dose should always be considered This investigation has shown that the exposure rate required to produce a prescribed video level decreases rapidly with increasing voltage At low voltage, the exposure rate can be brought to a reasonably low value by means of slight copper filtering (0 2 to 1 0 mm) when the radiation penetrates soft tissue equivalent to 5 cm water It is difficult, however, in clinical practice to estimate the depth of the soft tissue, and the present results demonstrate the rapid increase in the exposure rate required to produce the desired video level when increasing the soft tissue thickness In spite of the decrease in iodine extinction for higher kV values (Fig 7), it is recommended that fluoroscopic examinations of the circulatory system be performed at 100 kV with 0 2 mm Cu filtering, in order to minimise the rate of exposure of the patient

mR s^{-1}, respectively, with no copper filtering. As for the 5 cm layer, the exposure rate with 10 cm water decreased with even slight copper filtering and was measured at 100 kV *with 0.2 mm Cu to be 3.4 mR s^{-1}. As a rule, however, the reduction of the* exposure rate was more dependent on an increase in tube potential than on an increase in filter thickness, particularly in the high potential range (80 to 110 kV), where *increasing the copper filtering only contributed slightly to lowering the ex*posure rate or even tended to increase it (Fig. 5).

Relation between the exposure rate and the potential and current. If characteristic radiation is disregarded, the spectral distribution of the radiation emitted from a target bombarded with electrons of kinetic energy $h\nu_0$ (h being Planck's quantum of action) is given by

$$I_\nu(\nu) = AZi(\nu_0 - \nu) \quad \text{for } \nu < \nu_0 \tag{1}$$

(STRID 1972, STRID & LANTZ 1973), $I_\nu(\nu)\,d\nu$ being the intensity of radiation in a frequency interval of width $d\nu$ centered around ν, A being a universal constant, Z the atomic number of the target metal and i the tube current. Integration of (1) yields the total intensity

$$I = \int_0^{\nu_0} I_\nu(\nu)\,d\nu = \tfrac{1}{2} AZi\nu_0^2 \tag{2}$$

Observing that ν_0 is proportional to the accelerating voltage, U, and taking the exposure rate, $\dot{X}$, proportional to the intensity, the following is obtained from (2)

$$\dot{X} = BiU^2, \tag{3}$$

where the constant B incorporates A and Z and geometrical factors.

The validity of (3) could be tested readily. The quantity $\dot{X}U^{-2}i^{-1}$, calculated from the values of the preliminary measurements with the ionisation chamber completely irradiated, is shown in Fig. 6. Under the conditions given (rhenium anticathode, 85 cm distance between the target and the centre of the chamber), (3) was concluded to hold *with $B = (2.1 \pm 0.6)$ μR s^{-1} kV^{-2} mA^{-1}. The deviations from (3) due to the* presence of characteristic radiation and to the intrinsic filtration of the roentgen tube will be discussed elsewhere.

Discussion

As could be expected, much higher exposure rate is required at low tube potential to produce *the prescribed video level, because low-energy photons are to a large* extent absorbed by the water layer. The soft radiation does not then contribute to the luminance but does contribute to the contrast. On filtering with copper, especially in *the low potential range*, the radiation effective in producing luminance will take a larger part of the exposure rate, the soft radiation being absorbed by the filter. Thus,

FROM THE SECTION OF DIAGNOSTIC RADIOLOGY, DEUTSCHE KLINIK FÜR DIAGNOSTIK,
D 6200 WIESBADEN, GERMANY

THE PANCREATOGRAPHIC EFFECT DURING PHARMACOANGIOGRAPHY OF THE PANCREAS

RUDOLF SCHMARSOW and PETER E PETERS

The differential diagnosis between chronic pancreatitis and carcinoma of the pancreas still remains a problem as pointed out by REUTER et coll (1970) BUCHELER et coll (1971) and TYLÉN (1973) The diagnosis of carcinoma is made even more difficult when associated with chronic pancreatitis (10 2 per cent, GAMBILL 1971) The vascular abnormalities occurring with both conditions are mainly the same, the intention was therefore to investigate the value of the pancreatographic effect

This effect has been observed occasionally at angiography of the pancreas performed without use of vasodilators or other drugs (RÖSCH et coll 1965, REUTER et coll 1969, 1970, HERNANDEZ et coll 1967 LECHNER et coll 1971) but considered of little val
sow (19

The f ... ugs to obtain a satisfactory pancreatic accumulation of contrast medium were performed by MCCUNE et coll (1959) with administration of Trypsin and Hypaque 90% intraaortically They achieved a satisfactory pancreatographic effect in 70 per cent Secretin was used by TAYLOR et coll (1969) UDÉN (1969) administered both secretin and pancreozymin and SCHMARSOW (1972) secretin trypsin and histamine A fairly satisfactory pancreatographic effect was achieved with the trypsine combination in 73 per cent of the cases

Presented at the XIII International Congress of Radiology Madrid, 1973 Submitted for publication 22 February 1974

SUMMARY

The exposure rate required to produce a prescribed value of the video level in a vidicon television chain during fluoroscopy was measured for water layers and copper filters of varying thickness The reduction of the patient exposure rate was found to be so large that, in spite of a reduction of the iodine extinction to 20 to 50 per cent of the value at 40 to 50 kV, examinations of the circulatory system are recommended to be performed at 100 kV with slight copper filtering

ZUSAMMENFASSUNG

Die Exponierungsleistung, die notwendig ist, um einen bestimmten Wert des Bild-Niveaus in einer Bildverstarker-Fernseh-Kette während der Durchleuchtung zu erhalten, wurde fur Wasserschichten und Kupferfilter verschiedener Dicke gemessen Die Verminderung der Exponierungsdosis des Patienten wurde als so wesentlich befunden, dass trotz einer Verminderung fur die Extinktion durch Jod auf 20 bis 50 Prozent des Wertes bei 40 bis 50 kV zur *Durchfuhrung von Untersuchungen des Zirkulationssystems 100 kV mit geringer Kupfer-*Filtrierung empfohlen wird

RÉSUMÉ

Le taux d'exposition necessaire pour obtenir une valeur déterminée du niveau de video dans une chaine de télévision vidicon pendant la radioscopie a été mesuré pour des couches d'eau et pour des filtres en cuivre de différentes épaisseurs La réduction de la dose d exposition du patient est si importante que les auteurs recommandent de faire les examens du système circulatoire à 100 kV avec une faible filtration de cuivre, bien que l'atténuation du rayonnement par l'iode soit comprise entre 20 a 50 pour cent de ce qu'elle est pour un rayonnement de 40 à 50 kV

REFERENCES

LANTZ B and STRID K-G Contrast formation in fluoroscopic videodensitometry II A comparison between theoretically computed and experimentally measured contrast Acta radiol Diagnosis 14 (1973), 625

STRID K G Optimisation of contrast in radiography Gothenburg Inst Phys Rep GIPR *081 (1972)*

— and LANTZ B Contrast formation in fluoroscopic videodensitometry I A mathematical model for optimising contrast in radiography Acta radiol Diagnosis 14 (1973) 395



a



b

Fig 1 Female aged 49 ...

of contrast medium administered were the same in both series It is thus apparent that the pancreatographic effect was enhanced by the drugs The superselective technique with injection of contrast medium into the hepatic and splenic arteries and in a few cases into the gastroduodenal and dorsal pancreatic arteries without drugs increased the frequency of the pancreatographic effect It appeared in 43 3 per cent of 30 cases but with drugs in 71 4 per cent of 28 cases With the addition of vaso dilatory drugs higher rates of the pancreatographic effect were achieved

Comparison of the type of pancreatographic effect and pancreatic function was made in 31 cases A homogeneous pancreatographic effect was achieved in 14 patients

Priscoline (tolazoline hydrochloride) has been employed as a vasodilator in peripheral arteriography (KAHN et coll 1965, JACOBS et coll 1967) and in visceral angiography to improve the filling of small arterial branches (KAHN et coll 1965, HAWKINS et coll 1973) and the filling of the superior mesenteric and portal veins (REDMAN et coll 1969) In the present investigation, secretin, priscoline, serotonin and caerulein were used to enhance the pancreatographic effect

Technique Selective angiography of the celiac axis and superior mesenteric artery was performed simultaneously or subsequently by the percutaneous transfemoral method with the thin wall red Kifa catheter (ID 1 40, OD 2 20 mm) or the Cordis cobra-catheter Seventy examinations were performed in 55 adult patients with possible pancreatic disorder clinically or indicated by function test (secretin-cholecystokinin-pancreozymin test) Two catheters, one in the celiac artery and one in the superior mesenteric artery, were used in 20 examinations, one in the hepatic and one in the splenic artery in 29 examinations In 12 examinations one catheter in the celiac artery only was used and of these the superior mesenteric artery was catheterized subsequently in 9 examinations

In most cases Itridal (Dominal 40 mg, Cyclobarbital-Calcium 140 mg, Phenyl dimethylpyrazolon 240 mg) was administered immediately before the angiography The average dosage of the different drugs was Secretin 1 5 IU/kg, priscoline 0 7 mg/kg, serotonin 0 7 γ/kg and caerulein 0 03 γ/kg They were combined as follows secretin and priscoline in 33 cases, secretin and serotonin in 7 cases, secretin and caerulein in 3 cases, priscoline only in 11 cases, and secretin only in 1 case One examination was performed before and another after the administration of the drugs in 17 cases, in the remaining 38 after drug administration only An AOT film changer was used with the following exposure rates 2 films/s for 2 s, 1 film/s for 1 s, interval of 5 s and then 1 film every third second for 9 seconds With a Contrac injector 60 to 70 ml Conray 60 were injected with a flow rate of 7 to 9 ml/s

Secretin is a polypeptid (proteohormone) which increases the blood flow in the pancreas Priscoline (tolazoline hydrochloride) is a sympatholytic vasodilator acting upon the alpha receptors of the postganglionic fibers (JACOBS et coll 1967) Serotonin (5-hydroxytryptamin) which is a 'biogenic' amine, a tissue hormone, depends for its action of the arterial tonus Vasodilatation occurs if the tonus is high, but if low, as in isolated organs, a vasoconstriction has been observed (BOCK et coll 1957, HOLTZ 1958)

Caerulein was recently isolated from the skin of an Australian amphibium (Hyla caerulea) and was synthetically produced by Farmitalia It is a dekapeptide and the action is similar to gastrin and cholecystokinin-pancreozymin It stimulates the secretion of the pancreas

Results

In a series of 174 celiac angiographies performed without drugs the pancreatographic effect was present in 18 4 per cent but in the present material of 55 cases with drugs the effect was produced in 74 5 per cent The injection technique and amount



Fig 3 Male aged 50 with inoperable carcinoma of the pancreas confirmed by laparoscopy Angiography with secretin and serotonin Irregular narrowing of the splenic and hepatic arteries as well as irregular gastroduodenal artery No pancreatographic effect

lipase was recorded immediately after the examination, less evident at the 24-hour control Secretin and priscoline had been administered in these cases and in both an excellent pancreatographic effect was demonstrated All patients examined with serotonin experienced different degrees of general bad feeling and one patient (100 γ) nearly came to a collapse

Comments

The effect on the pancreas of the different drugs employed at angiography was uniform, except regards serotonin At fluoroscopy it was observed that serotonin produced constriction of the vessels followed by a reactive dilatation a few minutes later But considering the general bad feeling after administration of serotonin, this series was not continued

With the addition of vasodilatory drugs the pancreatographic effect occurred in 74 5 per cent with the selective and in 71 4 per cent with the superselective technique Although the frequency is almost the same with both methods, the superselective technique seems to be preferred as without drugs the pancreatographic effect appeared in 43 3 per cent of the cases with this technique against 18 4 per cent with the selective one

A good correlation existed between the pathologic pancreatic function test and the mottled appearance of the pancreas in 6 cases Two patients were operated upon and a moderate fibrosis of the pancreas was found, which probably explains the mottled appearance If no *fibrosis is* present the pancreatographic effect is possibly homogeneous even when a chronic pancreatitis exists



Fig 2 Female aged 29, with chronic pancreatitis and small calcific

with a normal pancreatic function test, in 6 cases with a pathologic test a mottled appearance of the pancreas occurred However, in 11 patients with a pathologic function test the pancreatographic effect was homogeneous but in no case with a normal function test a mottled effect was observed Consequently there were 11 false negatives but no false positive

Two angiographies in each patient, one without drugs and one with drugs, for direct comparison of the effect on the vessels were performed in 17 cases The small pancreatic arteries were better filled in 58 8 per cent and the portal splenic and superior mesenteric veins in 70 6 per cent In addition the pancreatographic effect improved in 8 cases and occurred only following administration of drugs in 3 cases

No pancreatographic effect was achieved in two cases of carcinoma but arterial abnormalities were evident In both cases the whole pancreas seemed to be invaded by the neoplasm at operation and no resection was possible In one case of a hypovascular insuloma no accumulation of contrast medium was observed at the site of the tumor

Scanning of the pancreas with the isotope ^{75}Se methionin was carried out in 27 cases but no correlation between the scan and the pancreatographic effect was found

No serious complications were observed but a segmental infarction of the spleen occurred in one case The associated pains in the left upper part of the abdomen disappeared within two days without further discomfort Subintimal injection of the contrast medium in the hepatic and splenic arteries in three cases did not produce any discomfort to the patients Only in two cases a slight elevation of amylase and

kreatographische Effekt dieser Gruppe mit dem einer Serie von 174 bauchhohlenbezüglicher Angiographien ohne Pharmaka verglichen Mit Pharmaka trat der pankreatographische Effekt häufiger (74,5%) als ohne (18,4%) auf Die kleinen Pankreas-Arterien und Venen liessen sich besser mit Pharmaka darstellen Der pankreatographische Effekt scheint zur Differentialdiagnose der chronischen Pankreatitis und des Karzinoms des Pankreas von Wert zu sein

RÉSUMÉ

Les auteurs ont pratiqué l angiographie du pancréas chez 55 malades apres administration de différents agents pharmacodynamiques stimulant le débit sanguin dans le pancréas, ils ont compare l'effet pancréatographique dans ce groupe de malades avec celui d'une série 174 angiographies coeliaques sans agent pharmaco-dynamique Avec les agents pharmaco-dynamiques l'effet pancréatographique apparaît plus souvent (74,5 pour-cent) que sans (18,4 pour-cent) Les petites artères et les petites veines pancréatiques sont mieux mises en evidence avec les agents pharmaco dynamiques L'effet pancreatographique paraît avoir un intéret de diagnostic differentiel entre la pancreatite chronique et le cancer du pancreas

REFERENCES

BENNET J , CHÉRIGIE E , CAROLI J , DOYON D , ECONOMOPOULOS P , PLESSIER J et STOOPEN M La pancréatographie après stimulation par la Sécrétine intra-arterielle (a propos de 33 cas) Ann Radiol 10 (1967) 617

BOCK, K D , DENGLER H [illegible]
tryptamin auf Blutd [illegible]
Schmiedeberg's Arch [illegible]

BUCHELER E , BOLDT I , [illegible]
der Pancreastumoren

GAMBILL E E Pancreat[illegible] associated with pancreatic carcinoma a study of 26 cases Proc Mayo Clin 46 (1971), 174

HAWKINS I F and KAUDE J Selective pancreatic angiography (a comparison study using intra arterial tolazoline, epinephrine, high pressure injection, magnification technique and the valsalva maneuver) Book of Abstracts of the XIII International Congress of Radiology (Excerpta medica) Madrid, Spain 15-20 October 1973 Page 244, Paper No 672

HERNANDEZ Cl , ECARLAT B et BISMUTH V L'arteriographie des affections pancréatiques J Radiol Electrol 48 (1967), 327

HOLTZ P Über den gegenwärtigen Stand der Serotoninforschung Dtsch med Wschr. 83 (1958) 681

JACOBS J B and HANAFEE W N The use of Priscoline in peripheral arteriography Radiology 88 (1967) 957

KAHN P C and CALLOW A D Selective vasodilatation as an aid to angiography Amer J Roentgenol 94 (1965), 213

LECHNER G und POKIESER H Ergebnisse angiographischer Untersuchungen bei Pankreatitis Fortschr [illegible]

[illegible] ization of the pancreas by aortography. Ann [illegible]

[illegible] H C , REUTER S R and MILLER W J Improvement of superior mesenteric and portal vein visualization with Tolazoline Invest Radiol 4 (1969), 24

Table

Differentiation between carcinoma of the pancreas and chronic pancreatitis

	Pancreatographic effect	Arteries	Veins
Normal	Mostly present and homogeneous	Normal	Normal
Pancreatic carcinoma	Absent	Occlusion, vessel irregularities, rarely typical tumor vascularity	Occlusion with collateral circulation stenosis
Chronic pancreatitis	When mottled (confirmative)	Displacement (pseudocysts), vessel irregularities	Infrequently occlusion with collateral circulation, stenosis

In the two cases of carcinoma no pancreatographic effect was demonstrated and this effect was absent in the tumor region in a case of insuloma The few cases of malignancy in this material suggest that in carcinoma the pancreatographic effect is completely or partially absent and if in addition a vascular abnormality is present, the diagnosis of a carcinoma is most likely A homogeneous pancreatographic effect seems to exclude a carcinoma and the mottled effect indicates a chronic pancreatitis (the Table)

The absence of pancreatographic effect in carcinoma seems to be explained by the fact that the neoplasm is mostly hypovascular and that the neoplastic tissue has an almost homogeneous dense fibrous stroma, which impedes the accumulation of the contrast medium in this region

Acknowledgement

The authors are indebted to Byck and Gulden Co for providing the contrast medium (Conray) and to Agfa Gevaert for the films for this investigation

SUMMARY

Angiography of the pancreas was performed in 55 patients after the administration of different drugs stimulating the blood flow in the pancreas and the pancreatographic effect in this group was compared with that in a series of 174 celiac angiographies without drugs With drugs the pancreatographic effect appeared more frequently (74 5 per cent) than without (18 4 per cent) The small pancreatic arteries and veins were better demonstrated with drugs The pancreatographic effect seems to be of value for the differential diagnosis of chronic pancreatitis and carcinoma of the pancreas

ZUSAMMENFASSUNG

Eine Pankreasangiographie wurde bei 55 Patienten nach der Gabe von verschiedenen Pharmaka, die die Durchblutung des Pankreas stimulieren, vorgenommen und der pan-

kreatographische Effekt dieser Gruppe mit dem einer Serie von 174 bauchholenbezuglicher Angiographien ohne Pharmaka verglichen Mit Pharmaka trat der pankreatographische Effekt haufiger (74,5%) als ohne (18,4%) auf Die kleinen Pankreas-Arterien und Venen liessen sich besser mit Pharmaka darstellen Der pankreatographische Effekt scheint zur Differentialdiagnose der chronischen Pankreatitis und des Karzinoms des Pankreas von Wert zu sein

RÉSUMÉ

[illegible]

174 angiographies coeliaques sans agent pharmaco-dynamique Avec les agents pharmaco-dynamiques l effet pancréatographique apparait plus souvent (74,5 pour-cent) que sans (18,4 pour-cent) Les petites arteres et les petites veines pancreatiques sont mieux mises en évidence avec les agents pharmaco-dynamiques L'effet pancreatographique parait avoir un intéret de diagnostic différentiel entre la pancréatite chronique et le cancer du pancreas

REFERENCES

Bennet J, Cherigié E, Caroli J, Doyon D, Economopoulos P, Plessier J et Stoopen M La pancreatographie apres stimulation par la Secrétine intra artérielle (a propos de 33 cas) Ann Radiol 10 (1967), 617

Bock, K D, Dengler H, Kuhn H M und Matthes K Die Wirkung von 5 Hydroxy-tryptamin auf Blutdr[illegible] Schmiedeberg s Arch

Bucheler E, Boldt I, F [illegible] der Pancreastumoren und der Pancreatitis Fortschr Rontgenstr 115 (1971), 726.

Gambill E E Pancreatitis associated with pancreatic carcinoma a study of 26 cases Proc Mayo Clin 46 (1971), 174

Hawkins I F and Kaude J Selective pancreatic angiography (a comparison study using intra arterial tolazoline, epinephrine, high pressure injection, magnification technique and the valsalva maneuver) Book of Abstracts of the XIII International Congress of Radiology (Excerpta medica) Madrid, Spain 15–20 October 1973 Page 244, Paper No 672

Hernandez Cl, Ecarlat B et Bismuth V L'arteriographie des affections pancréatiques J Radiol Electrol 48 (1967), 327

Holtz P Über den gegenwärtigen Stand der Serotoninforschung Dtsch med Wschr 83 (1958), 681

Jacobs J B and Hanafee W N The use of Priscoline in peripheral arteriography Radiology 88 (1967), 957

Kahn P C and Callow A D Selective vasodilatation as an aid to angiography Amer J Roentgenol 94 (1965), 213

Lechner G und Pokieser H Ergebnisse angiographischer Untersuchungen bei Pankreatitis Fortschr Rontgenstr 114 (1971), 49

McCune W S and Stanbro W W Visualization of the pancreas by aortography Ann Surg 150 (1959), 561

Redman H C, Reuter S R and Miller W J Improvement of superior mesenteric and portal vein visualization with Tolazoline Invest Radiol 4 (1969), 24

Table

Differentiation between carcinoma of the pancreas and chronic pancreatitis

	Pancreatographic effect	Arteries	Veins
Normal	Mostly present and homogeneous	Normal	Normal
Pancreatic carcinoma	Absent	Occlusion, vessel irregularities, rarely typical tumor vascularity	Occlusion with collateral circulation stenosis
Chronic pancreatitis	When mottled (confirmative)	Displacement (pseudocysts), vessel irregularities	Infrequently occlusion with collateral circulation stenosis

In the two cases of carcinoma no pancreatographic effect was demonstrated and this effect was absent in the tumor region in a case of insuloma The few cases of malignancy in this material suggest that in carcinoma the pancreatographic effect is completely or partially absent and if in addition a vascular abnormality is present, the diagnosis of a carcinoma is most likely A homogeneous pancreatographic effect seems to exclude a carcinoma and the mottled effect indicates a chronic pancreatitis (the Table)

The absence of pancreatographic effect in carcinoma seems to be explained by the fact that the neoplasm is mostly hypovascular and that the neoplastic tissue has an almost homogeneous dense fibrous stroma, which impedes the accumulation of the contrast medium in this region

Acknowledgement

The authors are indebted to Byck and Gulden Co for providing the contrast medium (Conray) and to Agfa Gevaert for the films for this investigation

SUMMARY

Angiography of the pancreas was performed in 55 patients after the administration of different drugs stimulating the blood flow in the pancreas and the pancreatographic effect in this group was compared with that in a series of 174 celiac angiographies without drugs With drugs the pancreatographic effect appeared more frequently (74 5 per cent) than without (18 4 per cent) The small pancreatic arteries and veins were better demonstrated with drugs The pancreatographic effect seems to be of value for the differential diagnosis of chronic pancreatitis and carcinoma of the pancreas

ZUSAMMENFASSUNG

Eine Pankreasangiographie wurde bei 55 Patienten nach der Gabe von verschiedenen Pharmaka, die die Durchblutung des Pankreas stimulieren, vorgenommen und der pan-

FROM THE DEPARTMENT OF DIAGNOSTIC RADIOLOGY, THE LABORATORY FOR PATHOLOGY AND THE DEPARTMENT OF GYNECOLOGY, THE NORWEGIAN RADIUM HOSPITAL, OSLO, NORWAY.

LYMPHOGRAPHY IN THE DIAGNOSIS OF METASTASES FROM CARCINOMA OF THE UTERINE CERVIX STAGES I AND II

ALF KOLBENSTVEDT

A reliable method of demonstrating early lymph node metastasis from carcinoma of the cervix would certainly lead to a reconsideration of the staging procedure and perhaps also the choice of treatment Several authors (DOLAN 1964, FUCHS & BÖÖK-HEDERSTRÖM 1964, CHAVANNE et coll 1967, PIVER et coll 1971) have discussed the value of lymphography, but their opinions differ widely KOLBENSTVEDT & KNUDSEN (1974) discussed the reasons for this disagreement In a material of 9 187 iliac lymph nodes removed by pelvic lymphadenectomy from 300 patients KOLBENSTVEDT (1974) found that 98 9 per cent contained contrast medium and that all solitary metastases were located in regions ordinarily demonstrated by injection of contrast medium into a lymph vessel of the foot

Therefore, in theory, a reliable lymphographic diagnosis of lymph node metastasis should be possible, provided the metastasis has reached a certain minimum size

Based on the available literature, LÜNING et coll (1971) presented a comprehensive list of abnormal lymphographic appearances and presumed significance They discussed partial or total lymph flow obstruction size, shape, structure or outline of lymph nodes and nodal defects However, confirmation by microscopy of the nodes

Submitted for publication 2 May 1974

REUTER S R and BOOKSTEIN J J Differential problems in the angiographic diagnosis of carcinoma of the pancreas Radiology 96 (1970), 93

— REDMAN H C and BOOKSTEIN J J Differential problems in the angiographic diagnosis of carcinoma of the pancreas Radiology 96 (1970), 93

— — and JOSEPH R R Angiographic findings in pancreatitis Amer J Roentgenol 107 (1969), 56

ROSENBUSCH G und CEN M Zoliakographie mit Sekretin Moglichkeiten der Pharmako-angiographie in der Pankreasdiagnostik Fortschr Rontgenstr 110 (1969) 639

SCHMARSOW R Angiography of the pancreas following the administration of secretin trypsin and histamine Acta radiol Diagnosis 12 (1972), 175

TAYLOR D A, MACKEN K L and FIORE A S Angiographic visualization of the Secretin stimulated pancreas Radiology 87 (1966), 525

TYLÉN U Angiographic differentiation between inflammatory disease and carcinoma of the pancreas Acta radiol Diagnosis 14 (1973), 257

UDÉN R Effect of Secretin in celiac and superior mesenteric angiography Acta radiol Diagnosis 8 (1969), 497

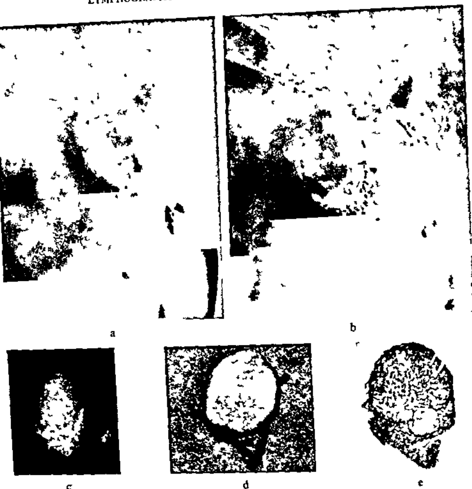


Fig 1 Case illustrating method of ens nne ex

The larger of the diameters found by histologic section and radiography of the specimen is given as the size of the metastases

Results and Discussion

General

A total of 209 lymph nodes containing metastasis were removed from 77 of the 300 patients

The accuracy of lymphography compared with the evaluation at operation after

Table 1

Age distribution

Age groups	10–19	20–29	30–39	40–49	50–59	60–69
No of patients	1	13	62	132	72	20

was sometimes lacking As such a confirmation must be considered essential for adequate evaluation of the lymphography a comparison between the lymphographic findings and microscopy forms the basis of this report

Materials and Methods

During the period February 1970 to March 1973 inclusive, 300 patients with carcinoma of the uterine cervix stages Ib (275), IIa (19) and IIb (6) were treated by radium insertions followed six weeks later by radical hysterectomy and pelvic lymphadenectomy The age distribution is given in Table 1 Bilateral lymphography was performed during the first hospitalization period Films of the pelvic and abdominal regions were exposed in anteroposterior, oblique and lateral projections immediately after injection of contrast medium and again 24 hours later The examination was unilateral in nine cases due to technical difficulties Immediately before the operation a new series of films was taken to reveal any alterations in the appearance of the nodes The roentgen unit was a Triplex optimatic 1023, Siemens Elema, with a Siemens Pantix 150/100 tube with focus 1 4 mm² Exposure data FFD 100 cm, 50–60 kV, 640 mA, 0 4 s for a p projection of the abdominal region When considered necessary, tomography and screening under compression with exposures in special projections were performed as supplementary examinations Further details concerning the lymphographic method and the procedure used in ensuring exact lymphographic and histologic correlation by means of specimen radiography were given by KOLBENSTVEDT & KNUDSEN A case demonstrating the method is illustrated in Fig 1 Problems related to lymphography and pelvic lymph node dissection were dealt with by KOLBENSTVEDT & KOLSTAD (1974)

Preoperatively, the films were classified as positive, negative or uncertain The practical result of classifying a node as uncertain was an effort to ensure its removal An average of 30 6 lymph nodes per patient were removed and subjected to microscopy

The opinions concerning lymph node involvement, based on palpatory and visual findings during the operation, were recorded

The size of lymph nodes and contrast defects referred to in the present report was measured on the films without correction for geometric enlargement, so as to correspond with measurements given in the literature (ELKE et coll 1972, FUCHS 1972)

Table 4

Influence of number of lymph nodes containing metastasis on diagnostic accuracy

Number of metastases	No of patients			
	Lymphography positive	Lymphography uncertain	Lymphography negative	Total
Solitary	8	12	10	30
Two or more	14	11	22	47
Total	22	23	32	77

spread did not seriously affect lymph flow and complete blockage was exceptional in the present series, which mainly consisted of stage Ib carcinoma

Detailed analysis

Persistent contrast medium in lymph vessels 24 hours after injection, wide afferent vessels and extravasation of medium are related to partial lymph flow obstruction CHAVANNE et coll and BUJAR & ROXIN (1970) considered these abnormalities non-specific and partly related to the speed of injection FRISCHBIER (1972) however considered them to be valuable when found together He reported a combination of, for example, persistent filling of lymph vessels and extravasation of contrast medium to be due to metastasis in 88 per cent of cases If, in addition, a region without filled nodes was present, a diagnosis of metastasis could be made with almost 100 per cent certainty

The relation of these abnormalities to metastasis in the present series (injection speed 3 ml per h on each foot) is given in Table 5 The table states whether a metastasis was present corresponding to the signs of partial obstruction, a connection could not be proved None of the signs by itself would indicate metastasis in more than about one third of the cases, even when they were taken together, metastasis still was only confirmed in one third (8 of 24)

A 3 mm arbitrary upper limit for lymph vessel calibre was adopted most vessels were considerably narrower The general width of a vessel is given, not the one with local dilatations Normally, the widest vessels were located between the inguinal and external iliac regions The widest vessel in a patient without metastasis was 5 mm with a local cystic dilatation to 9 mm

The frequent occurrence of the mentioned abnormalities in patients without metastasis indicates that they are unreliable BUJAR & ROXIN attributed greater significance to widening and persistent contrast medium in collateral lymph vessels

Interruption or displacement of lymph vessels and development of collaterals were less frequently encountered The relative frequency of metastasis appears in Table 6 Complete obstruction with formation of collaterals is considered one of the most

Table 2

Accuracy in the diagnosis of lymph node metastasis

	Lymphography				Evaluation after node dissection			
	Correct diagnosis	Uncertain diagnosis	Incorrect diagnosis	Total	Correct diagnosis	Uncertain diagnosis	Incorrect diagnosis	Total
No of patients without metastasis	165	49	9	223	194	14	15	223
No of patients with metastasis	22	23	32	77	32	9	36	77
Total	187	72	41	300	226	23	51	300
Per cent	62 3	24 0	13 7		75 3	7 7	17 0	

node dissection is given in Table 2 Lymphography was less exact than macroscopic evaluation of the specimen, but, as would be expected, neither method was as exact as microscopy The smallest metastasis diagnosed lymphographically was 4 mm, while the largest, measuring 2 5 cm, was not observed Most authors consider that a metastasis must have a diameter of at least 5 to 10 mm to be detected lymphographically (KOEHLER et coll 1964)

The size of the largest metastasis was more important for lymphographic accuracy than the number of nodes involved (Tables 3, 4) A solitary deposit with an expansive growth within a node was less difficult to diagnose than one growing infiltratively and with early dissemination of smaller foci to other nodes In general, metastatic

Table 3

Influence of size of the largest metastasis on diagnostic accuracy

Size of largest metastasis	No of patients			
	Lymphography positive	Lymphography uncertain	Lymphography negative	Total
< 5 mm	0	11	13	24
5–10 mm	4	7	11	22
> 10 mm	18	5	8	31
Total	22	23	32	77



Fig. 2 Right anterior oblique projection of left iliac region Abnormal collaterals due to infiltration by metastases.

strated In seven of the ten enlarged nodes with metastasis in Table 7 additional abnormalities such as nodal defects were present PATRIQUIN (1967) found no normal nodes measuring more than 2 cm while FUCHS et coll (1969) reported a normal size up to 3 cm in inguinal and iliac nodes and FUCHS & BOÖK-HEDERSTRÖM a maximum length of 4 cm in lumbar nodes with a width, however, never exceeding 1 5 cm In the present series the largest normal appearing, non metastatic lymph node was a common iliac node 4 cm long with a minimum width of 2 cm Generally, the nodes were smaller when measured on films 6 weeks after lymphography In one case with excessive extravasation of contrast medium, however, an increase in size was noted, possibly due to reactive hyperplasia caused by chemical irritation Some nodes, for example the presacral and gluteal are normally small and may, when enlarged, still be smaller than normal nodes in other regions Thus, the evaluation of enlargement requires experience

The normal granular lymph node structure was thoroughly analysed by TJERNBERG (1962) and LAMARQUE et coll (1967) It is caused by contrast medium droplets in the marginal, intermediary and medullary sinuses which surround the lymphatic lobules and their follicles The structure of one or more nodes may differ from the rest by having a coarser granulation Such nodes are often almost round, and have a distinct marginal sinus These changes may be due either to a nonspecific inflammatory reaction or to a reactive hyperplasia representing a defence mechanism against toxic and metabolic products from tumor cells (FUCHS et coll 1969) GERTEIS (1972) subdivided the node structure into eight subgroups He reported frequent occurrence

Table 5

Frequency of metastasis in relation to three common signs of partial lymph flow obstruction

Lymphography	No of patients with abnormality	No of patients in whom abnormality corresponded to metastasis
(1) Contrast medium in lymph vessels 24 h after injection	182	48 (26 4 %)
(2) Lymph vessels wider than 3 mm	70	15 (21 4 %)
(3) Extravasation of contrast medium	77	26 (33 8 %)
(4) Combination of (1) (2), and (3)	24	8 (33 3 %)

reliable abnormalities indicating metastasis (FUCHS et coll 1969, PIVER et coll) This combination only occurred once in the present series Total blockage was seen twice, once without metastasis In the latter case no vessels or nodes could be demonstrated above the fifth lumbar vertebra No explanation could be found for this at microscopy A knowledge of normal variations of lymphatic trunks is necessary when evaluating collaterals, and therefore normally occurring by-passes, blind loops, vessels to the obturator node and presacral anastomoses (KOLBENSTVEDT 1975) are not included in Table 6 Though abnormal collaterals (Fig 2) were only present in 14 patients, the occurrence of metastasis in 10 of these indicates the importance of this abnormality Displacement of lymphatics was most often due to tortuous arteries, which may be recognized in the lumbar and common iliac regions

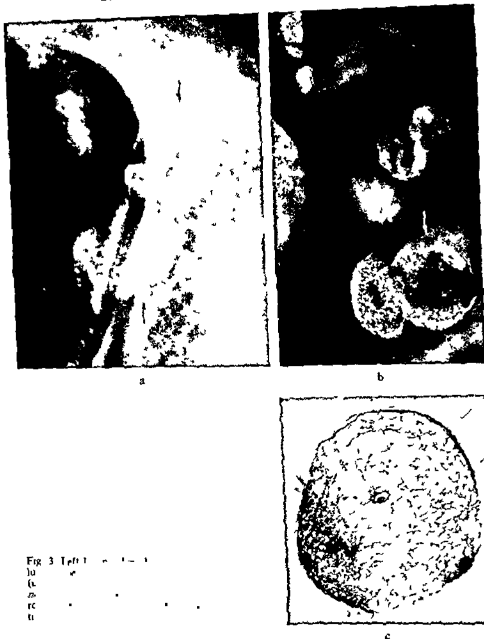
The shape, size, structure and outline of lymph nodes, and absence of normally filled nodes are criteria which have been the subject of controversy Most normal lymph nodes are somewhat flattened like an almond According to WILJASALO (1965) lymph nodes with metastases larger than 0 5 cm are rounded, globular or grapelike and may be diagnosed with more than 90 per cent accuracy by measurements in several projections In the present material the shape of lymph nodes with metastasis as a rule deviated from the globular, which made these measurements of doubtful value (KOLBENSTVEDT 1975)

In Table 7, enlargement or structural changes are only included when present in one or a few nodes, but not taken into account when found in all nodes demon-

Table 6

Frequency of proven metastasis in relation to interruption displacement and formation of collaterals

Lymphography	No of patients with abnormality	No of patients with abnormality due to metastasis
(5) Interruption of lymph vessels	12	4 (33 3 %)
(6) Displacement	17	4 (23 5 %)
(7) Collaterals	14	10 (71 4 %)



a

b

c

Fig 3 Left l ... l
lu
(l
n
rc
ti

The inguinal nodes are often the site of defects, probably becau se the ...
filter stations fro...
most cau...
frequently ... dation (Fig 3) that they have been called the

Table 7

Frequency of proven metastasis in relation to size, structure, outline and absence of lymph nodes normally demonstrated (empty region)

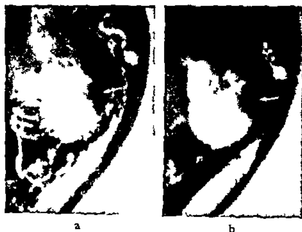
Lymphography	No of patients with abnormality	No of patients with abnormality proved due to metastasis
(8) Enlargement	27	10 (37 0 %)
(9) Coarse lymph node structure	70	13 (18 6 %)
(10) Combination of (8) and (9)	16	6 (37 5 %)
(11) Irregular outline of node	39	4 (10 3 %)
(12) 'Empty region'	28	6 (21 4 %)
(13) (12) combined with (3), (5) or (6)	14	5 (35 7 %)

of small foci of carcinoma cells in the coarsely granulated lymph nodes In the present material coarse granulation was noted in one or more nodes in 70 patients In these patients metastases occurred less frequently than in the total group Microscopically the sinuses were found to be widened and full of contrast medium as though inflow was easier than outflow Areas with follicular hyperplasia and sinus histiocytosis were also common, but small metastatic foci of carcinoma cells were only found in 15 of 89 such nodes

An irregular lymph node outline often described in the literature as 'moth-eaten' (JACKSON et coll 1961) occurred in 39 patients, four of whom had metastasis corresponding to the irregularity As a rule, lipomatous infiltration or nonspecific inflammatory changes were disclosed histologically The sign may also be due to incomplete filling with contrast medium

The lymphatic system is subject to innumerable variations and therefore it is generally agreed that the absence of a node or a node group which is usually filled with contrast medium is without significance unless additional signs of lymph flow obstruction are present In the present series such an 'empty region' was noted in 28 patients, 22 without metastasis In these 22 cases the empty region occurred twice as often on the left as on the right side and particularly in the region around the left iliac bifurcation Here, a gap of 5 to 7 cm without nodes was observed in 6 patients At microscopy, as a rule, no nodes were found corresponding to these empty regions When this absence of nodes was combined with extravasation of contrast medium, interrupted or displaced vessels, metastasis was more frequent, but still occurred in less than half of the patients An empty region combined with formation collaterals occurred only twice, both times due to metastasis

Nodal defects may have several causes, the most frequent alternatives to metastasis being lipomatous or fibrous infiltration or nonspecific inflammatory reaction In the latter case areas with follicular hyperplasia may be surrounded by sinuses filled with contrast medium in the more normal-appearing parts of the node



a b

Fig 6 Metastatic defect surrounded by a halo a) Fill ng phase Defect (arrow) not traversed by lymphat cs b) Retent on phase with defect M croscopy showed metastas s





a b c

Fig 7 Left il
halo has appe
Intermed ary

method in the diagnosis of metastasis PIVER et coll admitted that ab cesses or casea tion necros s might give both filling and retention defects but added that in a pa tient with carcinoma of the cervix metastasis must be the primary consideration

GERTEIS (1972) described silent zones (stumme Zonen) as perimetastatic areas not containing contrast medium Such zones might cause evident nodal defects and in exceptional cases permit the demonstration of metastases smaller than 1 mm In the present series the reverse phenom
purposes When a metastasis
the surrounding sinuses cont

were displaced and stretched



Fig 4



Fig 5 a



Fig 5 b

Fig 4 Left superior and inferior gluteal lymph nodes with defects due to benign lesions

Fig 5 Right superficial inguinal lymph node with non metastatic defect a) Filling phase The intermediary and medullary sinuses are traversing the defect towards the hilum It is thus not a true filling defect b) Retention phase with nodal defect The node in question was not removed No metastasis was found in the iliac nodes No sign of recurrence two years later

semilunar nodes (KINMONTH 1972) Possibly, by passing of the inguinal region may explain the appearance of the lateral lacunar nodes (FRISCHBIER 1966) In the present series the gluteal nodes were also found to be frequent sites of non metastatic defects (Fig 4) About half of the patients in whom the gluteal nodes were demonstrated, had a defect in one or more of these nodes One reason may be that the nodes receive afferent vessels not only from the visceral organs, but also from the deep and superficial layers of the posterior part of the thigh (ROUVIÈRE 1932) The defects in the lateral lacunar nodes were never due to metastasis, and those in the gluteal nodes only twice Defects in these nodes are, therefore, not included in the following analysis of nodal defects in the pelvic and lumbar lymph nodes

Several criteria have been suggested to distinguish metastatic from non metastatic nodal defects In the early literature defects due to metastasis were described as having an irregular outline (AVERETTE et coll 1962) while in more recent reports a sharp outline has been considered more suggestive (FUCHS 1972)

The appearance of lymph node defects in films exposed immediately after injection was described by SCHAFFER et coll (1963) and has received much attention in recent years If a nodal defect is due to lipomatous infiltration, it will be traversed by lymphatics in the filling phase (Fig 5), while if due to metastasis this should not be the case (Fig 6) This difference, between filling defects which appear both in the lymphangiogram and the lymphadenogram and retention defects which occur in the lymphadenograms only, was emphasized as a distinction of great importance by GERTEIS (1967) He further stated (1972) that these facts had long been overlooked, and that this was one reason why many authors consider lymphography an uncertain



Fig. 10 False positive finding in the right iliac region a) Lymph node with defect (arrow) b) Six weeks later The defect appears larger c) Microscopy (× 3.5) reveals a central core of lipomatous tissue with a sharp border

If it was infiltrating, the outline was irregular, if not, the outline was more regular Defects in enlarged nodes were due to metastasis in 5 of 9 cases, if the defect was larger than 1 cm in 5 of 6

The differentiation between retention and filling defects was relatively easy in the inguinal and lateral lacunar lymph nodes (Fig 5) In the more cranially situated nodes it was increasingly difficult (Figs 11, 12) and only considered possible in 61 of 105 patients The difficulties in making definite differentiations were due partly to superimposed vessels which obscured the defect, and partly to the fact that all nodes were

Table 8

Frequency of proven metastasis in relation to various types of lymph node defects

Lymphography	No of patients with abnormality	No of patients with abnormality due to metastasis
[illegible]		
[illegible]	105	33 (31.4%)
[illegible]	9	5 (55.5%)
[illegible]	21	17 (81.0%)
[illegible]	27	2 (7.4%)
[illegible]	27	6 (22.2%)
[illegible]	42	16 (38.1%)
[illegible]	24	13 (54.2%)
[illegible]	5	4 (80.0%)
(23) Retention and filling defect	41	12 (29.3%)
(24) Defect surrounded by contrast halo	20	6 (30.0%)
[illegible]	32	18 (56.3%)



a



b

Fig 8 Right lumbar region a) Initial film b) Radiography six months after pelvic lymphadenectomy A defect surrounded by a halo has appeared Microscopy of the lymph node showed metastasis



a



b

Fig 9 Left iliac region a) Lymph node with defect b) Radiography six weeks later The defect has grown Microscopy Metastasis

around the expansive process so that a zone of increased accumulation of medium could be observed resembling a halo (Figs 6, 7, 8)

Taking advantage of the fact that lymph nodes remain filled for months and even years after injection of contrast medium, MacDonald et coll (1968) reported serial radiography to be useful They found successive enlargement during an observation period, or change from normal to abnormal appearance, of particular diagnostic value

Table 8 gives the results in the present series with regard to nodal defects Of all lymphographic abnormalities listed in Tables 5 to 8 the growth (Fig 9) or appearance (Figs 1, 7, 8) of nodal defects was the most reliable indication of lymph node metastasis being present in 21 patients and due to metastasis in 17 A limiting factor was the relatively rare occurrence it was present in only 22 1 per cent of the 77 patients with metastases In four cases a false impression of growth was due to decrease of the contrast medium surrounding a defect (Fig 10) Appearance or growth of a defect surrounded by a halo was due to metastasis in 11 of 13 cases Most of the correct positive diagnoses of this series were due to changes in the nodes during the observation period Repeat radiography is therefore essential if lymphography for diagnostic purposes is performed in stage Ib carcinoma The same is felt to be true in stage IIa, while no definite conclusion can be drawn from the six patients in stage IIb

The size and outline of nodal defects was found to be important defects smaller than 1 cm with irregular outline were due to metastasis in only 2 of 27 patients On the other hand defects larger than 1 cm with regular outline were due to metastasis in 13 of 24 patients The outline of a metastasis was dependent on the mode of growth

nodes with defects (except gluteal and lateral lacunar nodes) appear in Table 9 Though not specific, the halo was present in half of the defects due to metastasis and only in one fifth of defects due to benign conditions

Conclusion

The diagnostic accuracy of lymphography in the total series of 300 patients with carcinoma of the cervix stages I and II was not sufficiently high to be solely relied upon in the choice of treatment Combined with the findings at operation however, lymphography was considered of value it was always aimed at removing nodes classified as positive or uncertain

It should be emphasized that this conclusion is based on lymphography in early stages of carcinoma of the cervix, and that it is not automatically valid for more advanced stages and for primary malignant disease in other organs

Accuracy depended on the size of the metastasis and had little to do with the number of nodes involved The appearance or increase in size of a nodal defect during a six week period was the most reliable indication of metastasis This, however, appeared only in 22 1 per cent of the patients with secondary spread

A perimetastatic halo occurred in about half of the defects due to metastasis More than half of the patients with nodal defects greater than 1 cm and with a regular outline had metastasis while irregular defects smaller than 1 cm as a rule were non metastatic

Differentiation between filling and retention defects was difficult in most pelvic nodes and the great importance attributed to such a distinction could not be confirmed In this series mainly consisting of stage Ib carcinoma complete obstruction with formation of collaterals was rare Greater accuracy may be expected in more advanced stages of carcinoma of the cervix

SUMMARY

The [illegible]
with c[illegible]
formed [illegible] macroscopic correlation was assured by means of radiography of the lymphadenectomy specimen The criteria of metastatic infiltration were critically evaluated.

ZUSAMMENFASSUNG

[illegible]



Fig 11 Left iliac region with large lymph node metastasis a) *Filling phase Defect obscured by lymph vessels* b) Retention phase The defect due to metastasis is evident

Fig 12 Right iliac region a) Filling phase *Defect obscured by lymph vessels b) Retention* phase The defect is evident This defect was not due to metastasis but to a nonspecific inflammatory reaction

not satisfactorily demonstrated in the filling phase Defects visible on the six week films only could not be classified Even in patients where a differentiation between filling and retention defects was considered possible, metastases were equally frequent in the two groups While lymphatics could be seen traversing defects due to *lipomatous infiltration, they were not seen in the frequent defects due to local areas* of follicular hyperplasia presumably caused by nonspecific inflammatory reaction There is no evidence in this series that the differentiation between filling and retention defects constitutes a break-through in diagnostic reliability

The halo sign, when present, was due to metastasis in more than half of the patients It was not present in metastases growing by infiltration TJERNBERG described rings of contrast medium surrounding rabbit lymph node follicles enlarged through inflammation Since no description of similar observations in human lymph nodes could be found, a closer analysis was felt justified The results of an analysis of pelvic

Table 9

Presence of halo in 130 lymph nodes with metastatic and non metastatic defects

	No of lymph nodes	
	Halo present	Halo not present
Metastasis	20	21
No metastasis	14	75

— and KNUDSEN O S A method for lymphographic and histologic correlation Experience from 300 patients treated by pelvic lymphadenectomy Gynec Oncol 2 (1974), 9

— and KOLSTAD P Pelvic lymph node dissection under peroperative lymphographic control Gynec Oncol 2 (1974), 39

LAMARQUE J L, PAGES A, PUJOL H, GINESTIE J-F et COMBES C Anatomie radiologique et valeur semiologique des images ganglionnaires en lymphographie J Radiol Électrol 48 (1967), 253

LUNING M, WILJASALO M und WIEDEMANN F H Problematik der lymphographischen Metastasendiagnostik — Metastasenkriterien Radiol diagn 3 (1971), 315

MACDONALD J S, LAUGIER A and SCHLIENGER M Observations on the growth of tumours in lymph nodes changing from normal to abnormal while remaining opacified after

PIVER M S, WALLACE S and CASTRO J R The accuracy of lymphangiography in carcinoma of the uterine cervix Amer J Roentgenol 111 (1971), 278

ROUVIERE H Anatomie des lymphatiques de l homme Masson et Cie, Paris 1932

SCHAFFER B, KOEHLER P R, DANIEL C R, WOHL G T, RIVERA E, MEYERS W A and SKELLEY J F A critical evaluation of lymphangiography Radiology 80 (1963), 917

TJERNBERG B Lymphography An animal study on the diagnosis of V × 2 carcinoma and inflammation Acta radiol (1962) Suppl No 214

WILJASALO M Lymphographic differential diagnosis of neoplastic diseases Acta radiol (1965) Suppl No 247

RÉSUMÉ

L'auteur examine l'exactitude de la lymphographie dans le diagnostic de métastase sur 300 malades atteintes de cancer du col de l'utérus au stade Ib et II Toutes ces malades ont subi une lymphadénectomie pelvienne La corrélation entre la lymphographie et l examen microscopique a été établie par radiographie des pièces de lymphadénectomie L'auteur étudie de façon critique les critères d'infiltration métastatique

REFERENCES

AVERETTE H E, HUDSON R C, VIAMONTE JR M I, PARKS R E and FERGUSON J H Lymphangioadenography (lymphography) in the study of female genital cancer Cancer 15 (1962), 769

BUJAR H et ROXIN T Modalités d'interprétation des aspects vasculaires en lymphographie *J Radiol Électrol 51 (1970)*, 247

CHAVANNE G, PELLIER D et VALETTE M La lymphographie dans les stades I et II du cancer du col utérin Étude de 150 cas opérés et vérifiés histologiquement J Radiol Électrol 48 (1967), 137

DOLAN P A Lymphography Brit J Radiol 37 (1964), 405

ELKE M, HUG I und SCHMID P Volumetrische Verlaufskontrollen an normalen Lymphknoten Radiol diagn 5 (1972), 614

FRISCHBIER H J Die Lymphographie Moglichkeiten und Grenzen der Metastasendiagnostik beim weiblichen Genitalkarzinom Geburtsh u Frauenheilk 26 (1966) 1255

— Wertbestimmung der verschiedenen Metastasenkriterien Radiol *diagn* 5 (1972), 591

FUCHS W A Frage der artspezifischen lymphographischen Metastasenkriterien bei bestimmten Organtumoren Radiol diagn 5 (1972), 627

— and BOOK-HEDERSTRÖM G Lymphography in the diagnosis of metastases with special reference to the carcinoma of the uterine cervix Acta radiol Diagnosis 2 (1964), 161

— DAVIDSON J W and FISCHER H W Lymphography in cancer Springer Verlag, Berlin Heidelberg, New York 1969

GERTEIS W The frequency of metastases in carcinoma of the cervix and the corpus In Progress in lymphology, p 209 Edited by A Ruttimann Georg Thieme Verlag, Stuttgart 1967

— *Darstellungsmethoden des Lymphgefasssystems und praktische Lymphographie In* Handbuch der allgemeinen Pathologie Band 3, Teil 6, S 595 Herausgegeben von H Meesen Springer Verlag, Berlin, Heidelberg, New York 1972

JACKSON L, WALLACE S, SCHAFFER B, GOULD J, KRAMER S and WEISS A J The diag*nostic value of lymphangiography* Ann intern Med 54 (1961), 870

KINMONTH J B The lymphatics Diseases, lymphography and surgery Edward Arnold Ltd, London 1972

KOEHLER P R, WOHL G T and SCHAFFER B Lymphangiography A survey of its current [illegible] 1716

KO [illegible] ionstration of the [illegible]

Normal lymphographic variations of [illegible] and [illegible] lymph nodes Acta radiol Diagnosis 15 (1974), 662

A critical evaluation of the projection difference index in the lymphographic diagnosis of lymph node metastases Acta radiol Diagnosis In press

Table 1

Previous reports comparing lymphangiography (L) cavography (C) and urography (U)

Reference	No of cases	Kind(s) of tumor	Abnormalities % at		
			L	C	U
BAUM et coll (1963)	40	Genito urinary	70	30	30
HOPF & FUCHS (1970)	136	Epithelial	30	17	26
LEE et coll (1971)	24	Carcinoma of cervix	75	83	—
MASSELOT et coll (1971)	60	Testicular	55	31	38
BAUM et coll (1963)	34	Malignant lymphoma	65	43	20
SCHWARZ et coll (1965)	100	Malignant lymphoma	73	38	14
HOPF & FUCHS (1970)	58	Malignant lymphoma	62	36	10
BROWER & SEALE (1974)	55	Hodkin s disease	37	25	5

be that filling of the right paraaortic lymph nodes is frequently scant above the third lumbar vertebra (FUCHS & PFAMMATER 1970) Cavography thus may add information in this silent area Furthermore, evaluation of the lymphangiography is often difficult, owing to the polymorphism of pathologic lymph nodes (WILJASALO 1969, ABRAMS 1971) a fair number of the examinations being evaluated as equivocal Cavography then facilitates the interpretation of the lymphographic films (and vice versa)

Examination of the spleen and lymph nodes in the splenic pedicle is not possible by lymphangiography Laparotomy in the staging of Hodgkin's disease has been described in recent reports (GLATSTEIN et coll 1969, KADIN et coll 1971, LANDBERG et coll 1974), where splenectomy, lymph node and liver biopsy was also performed It has become evident that involvement of the spleen is common as well as of lymph nodes in the splenic hilum and in the paraaortic region A rather large material of operated cases providing the opportunity of pathologic verification of the radiologic findings, has initiated this report on the value of lymphangiography, cavography and urography

Material and Methods

The material consists of 89 patients with Hodgkin's disease verified by biopsy (52 males, 37 females, mean age at examination 36 years, median age 29 years, range 6 to 78 years) examined during the years 1969 through 1972 Patients not subjected to lymphangiography because of clinically advanced disease were excluded

Lymphangiography was performed according to KINMONTH (1952) and KINMONTH et coll (1955) with small modifications (BAUM et coll 1963) Cavography was performed the day after lymphangiography The contrast medium was injected by hand through wide bore needles inserted into both femoral veins Routinely, anteroposterior, oblique and, in about half the cases, lateral films with the patient supine were exposed about a second after end of injection Other projections were used if neces-

FROM THE DEPARTMENT OF DIAGNOSTIC RADIOLOGY (DIRECTOR· PROF OLLE OLSSON),
UNIVERSITY HOSPITAL, S-221 85 LUND, SWEDEN.

CAVOGRAPHY AND LYMPHANGIOGRAPHY IN HODGKIN'S DISEASE

SVEN LAURIN

Radiation therapy has long been accepted as the treatment of choice in Hodgkin's disease, when systemic spread is not present (SMITHERS 1973) The disease often seems to arise from a single focus, spreading to contiguous lymph nodes, finally involving spleen, liver, bone marrow and other extra-lymphatic sites Meticulous determination of the full extent of the disease is mandatory for adequate treatment, i e irridation 'en bloc', if possible The deep abdominal lymph nodes are involved in about 40 per cent of untreated cases (KADIN et coll 1971, LANDBERG et coll 1974) In the diagnosis of this engagement, lymphangiography, phlebography of the inferior vena cava and urography may be used Combination of these three methods of examination in various kinds of malignant disease has been reported previously by BAUM et coll (1963), BATTEZZATI et coll (1963), MAHAFFY (1964), WILSON et coll (1965), CORINALDESI et coll (1966), PERTTALA & TORSTI (1968), HOPF & FUCHS (1970), LEE et coll (1971), MASSELOT et coll (1971) and with the interest particularly focused on malignant lymphoma by LEE et coll (1964), SCHWARZ et coll (1965) and BROWER & SEALE (1974) The authors conclude that lymphangiography is generally of greater value than the other two methods (Table 1) but that an increase of diagnostic information is gained when the three methods are combined (PERTTALA & TORSTI 1968, HOPF & FUCHS 1970, ABRAMS 1971, MASSELOT et coll 1971) The explanation may

Submitted for publication 25 February 1974



Fig 2. Female aged 16 Hodgkin s disease involving cervical nodes and mediast[illegible]
[illegible]
ab [illegible]
ve [illegible]
d)

unilateral pyelonephritis, no abnormality was found at cavography Occlusion of the left common iliac vein was demonstrated in two cases, indicating thrombosis, but neither was considered due to tumor An indentation of the posterior wall of the vena cava in one case was originally considered to indicate a mass lesion at L1–L2 (Fig 1) However, no tumor or enlarged lymph nodes were found at laparotomy At repeat examination one year later the appearance was unchanged, thus probably representing a normal variation

Lymph node engagement was demonstrated in the paraaortic region to the right of L1 and L2 in 20 instances altogether, both at cavography and lymphangiography in 4 at cavography only in 10 (Fig 2), and at lymphangiography only in 6 In 14 pathologic cases no abnormality was encountered at this level at either examination

Diagnostic laparotomy was performed in 36 cases (29 of these have been reported by LANDBERG et coll Lymphangiography had been reported abnormal in 12 cases, cavography in 8 cases, and urography in 4 cases At operation the abnormalities were verified except that one additional abnormal case was found (Fig 3), and, as mentioned before, an anatomic variation of vena cava was erroneously interpreted as a pathologic lesion Thus all three radiologic examinations failed to demonstrate pathology in one case, and one cavography was falsely abnormal

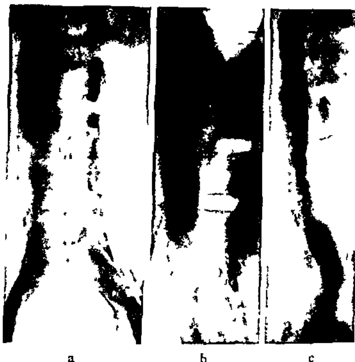


Fig 1 Male, aged 28, Hodgkin's disease involving neck and axilla Lymphangiography negative Cavography a) A p projection, no abnormality b) Oblique, c) lateral projection Indentation of the posterior wall of the vena cava at L1–L2, larger than the ususal indentation from the renal artery, initially interpreted as lymph node enlargement No tumor found at exploration Unchanged one year later

sary Excellent filling of the entire urinary tract was obtained on films exposed after the phlebography

In evaluating the films the criteria of RUTTIMANN & DEL BUONO (1962) and WILJASALO (1969) were applied The anatomy and pathology of the inferior vena cava has been described by HELANDER & LINDBOM (1959) and by FERRIS et coll (1969) Equivocal lymphangiographic examinations were considered non-pathologic, as were doubtful cavographies

Results

Of the 98 lymphangiographies, 87 were performed with bilateral injection and 11 were unilateral Femoral vein injection on one side only, at cavography, was made in three instances A groin wound impeded femoral vein puncture in one case, extravasation of contrast medium and hematoma formation precluded a successful repuncture of the femoral vein in two cases Urography was not performed in two cases Nine patients were completely examined a second time No serious complications were encountered, however, embolization of contrast medium to the lungs occurred fairly often at lymphangiography without clinical symptoms or signs

No abnormality was encountered in all three examinations 61 times, abnormality in all three 12 times Lymphangiography alone was pathologic 8 times, lymphangiography and cavography pathologic, urography normal 8 times In 5 instances lymphangiography and urography were abnormal but vena cava was of ordinary appearance There were 4 cases without pathology at lymphangiography but with abnormalities at cavography or urography or both One of the latter displayed signs of

Table 2

Abnormalities at lymphangiography (L) cavography (C) and urography (U)

Reference	Lymphangiography		Cavography		Urography		Ratio C/L (per cent)
	No	Per cent	No	Per cent	No	Per cent	
BAUM et coll (1963)	14 26	54	5 18	28	3/26	11	52
LEE et coll (1964)	67/104	65	30 64	47	13 87	13	72
HOPF & FUCHS (1970)	26 42	62	16 42	38	3 42	7	61
BROWER & SEALE (1974)	19 52	37	12/48	25	2/42	5	68
In all	126 224	56	63/172	37	21/197	11	66
Present series	33 98	34	21/98	21	17/96	17	65

The use of cannulas instead of catheters at cavography could be a draw-back since a cannula may slip out or perforate the wall, causing extravasation Only twice, however, did this preclude a successful examination on both sides

As earlier reports have indicated (HAYT 1966), layering of the heavy contrast medium along the dorsal part of the inferior vena cava occurs Lateral films exposed with horizontal beam direction greatly facilitated evaluation

In this material only 30 per cent of the cases had radiologic evidence of extension below the diaphragm Previous reports (LEE et coll 1964, LANDBERG et coll 1974) suggest involvement of abdominal nodes in 40 to 50 per cent of cases The reason for the lower rate in the present material is the exclusion of clinically advanced cases The diagnostic accuracy of lymphangiography was as high as that reported by ABRAMS (1971)—one false negative out of 36 operated cases, and three false negatives out of 32 not operated Previous reports (Table 1) comparing the diagnostic accuracy of lymphangiography with cavography and urography have given somewhat diverging results, depending on the kind of tumor examined In materials of malignant lymphomas in general, BAUM et coll (1963), SCHWARZ et coll (1965), HOPF & FUCHS (1970) reported pathologic findings at lymphangiography in about 65 per cent at cavography in about 50 and at urography in about 15 per cent, in Hodgkin's disease the result was quite similar (Table 2) BROWER & SEALE (1974), however, reported a lower number of abnormal findings, close to the results in the present series They stated that when lymphangiography was abnormal, cavography was also abnormal in 66 per cent In the present material lymphangiography was positive in 34 per cent (33/98) cavography in 21 (21/98), and urography in 17 per cent (17/96) Thus, when lymphangiography indicated tumor, cavography was abnormal in two thirds of the cases

Several authors comment on the value of cavography, some describing it as indispensable (LEE et coll 1964, PERTTALA & TORSTI 1968, HOPF & FUCHS 1970, LEE et coll 1971) From a perusal of the literature it is evident that its complementary value is greater in tumors of epithelial and testicular origin than in malignant lym-



Fig 3 Female, aged 41 Hodgkin s disease involving cervical and mediastinal nodes a) Lymphangiography Para aortic nodes with somewhat coarse and foamy structure but not definitely pathologic b) Two months later, postoperative film Lymph nodes enlarged with defects and increase of foaminess, evidently pathologic Operation extension to spleen, splenic hilar nodes and para aortic nodes

The 53 patients not operated upon were observed clinically Thirty-two had ordinary lymphangiographies, including the 2 cases with cavography demonstrating thrombosis Of these patients, 5 died from the disease, and 6 are alive having had at least one relapse, the remainder have been observed for 3 years on the average, without signs of recurrence At least three of those who relapsed possibly had abdominal engagement at, or soon after, lymphangiography Thus there may be 10 per cent false negatives In the non-operated group the number of false abnormalities cannot be evaluated since all patients considered abnormal were treated

Discussion

The retroperitoneal space is difficult to examine both clinically and radiologically The indirect methods—barium examination of the stomach and colon, as well as urography (KEMP HARPER 1960, LOWMAN 1965)—do not reveal small mass lesions, nor does retroperitoneal gas insufflation (DAVIDSON et coll 1959) Phlebography of the inferior vena cava and of the pelvic veins provides more information (HELANDER & LINDBOM 1959, FUCHS 1961, SHEEHAN et coll 1961), since the caval vein is large and surrounded by lymph nodes, but lesions may only be demonstrated on the right side by this method Lymphangiography on the other hand provides bilateral demonstration of both lymphatics and lymph nodes in the pelvic and retroperitoneal space

No lymph vessel could be cannulated on one side in 11 cases This is close to the rate reported by SCHWARZ et coll (1965) The examinations were performed by several different physicians during the years and initial lack of experience with this technique accounts for most of the failures However, enough contrast medium usually passed from the contralateral side to permit evaluation of both sides

BAUM S, BRON K, WEXLER L and ABRAMS H Lymphangiography, cavography and urography Comparative accuracy in the diagnosis of pelvic and abdominal metastases Radiology 81 (1963), 207

BROWER A C and SEALE D L. A critical appraisal of radiographic studies employed in the staging of patients with Hodgkin's disease Radiology 110 (1974), 97

CORINALDESI A, MARANI A, RIMONDI C e ZARABINI G E Risultati diagnostici della linfoadenografia e della flebografia parietale nello studio di neoplasie sistemiche e metastatiche della regione retroperitoneale (In Italian) Ann Radiol diagn 39 (1966), 209

DAVIDSON J K, HAVARD C W H and SCOTT R B Radiological demonstration of enlarged retroperitoneal lymph nodes Lancet (1959), I, p 1008

FERRIS E, HIPONA F, KAHN P, PHILIPPS E and SHAPIRO J Venography of the inferior vena cava and its branches Williams & Wilkins, Baltimore 1969

FUCHS W A Der diagnostische Wert der Cavographie Radiol Clin 30 (1961), 129

— und PFAMMATTER TH Die topographische Röntgenanatomie der inguinalen und retroperitonealen Lymphknoten Radiologe 10 (1970) 262

GLATSTEIN E, GUERNSEY J M, ROSENBERG S A and KAPLAN H S The value of laparotomy and splenectomy in the staging of Hodgkin s disease Cancer 24 (1969), 709

HAYT D Upright inferior vena cavography Radiology 86 (1966) 865

HELANDER C G and LINDBOM Å Venography of the inferior vena cava Acta radiol 52 *(1959) 257*

HOPF M A und FUCHS W A Die Lymphographie, Cavographie und Urographie als Kombinationsuntersuchung Radiologe 10 (1970), 280

KADIN M GLATSTEIN E and DORFMAN R Clinicopathologic studies of 117 untreated patients subjected to laparotomy for the staging of Hodgkin s disease Cancer 27 (1971), 1277

KEMP HARPER R A Radiology in the diagnosis of retroperitoneal tumors Clin Radiol 11 (1960) 69

KINMONTH J B Lymphangiography in man Clin Sci 11 (1952), 13

— KEMP HARPER R A and TAYLOR G W Lymphangiography by radiological methods J Fac Radiol 6 (1955), 217

LANDBERG T MOLLER T, BENGMARK S, BORJESSON B, OLSSON A, CAVALLIN-STÅHL E, AHLSTRÖM C G, ÅKERMAN M, JONSSON K, LUNDERQUIST A and NAVERSTEN Y Staging laparotomy with splenectomy in Hodgkin s disease Acta chir scand 140 (1974), 205

LEE B NELSON J and SCHW[illegible]
graphy and [illegible]

LEE [illegible]
[illegible] (1971), 284

LOWMAN R Retroperitoneal tumors A survey and assessment of roentgen techniques Radiol Clin N Amer 3 (1965), 543

MAHAFFY R G A *comparison* of the diagnostic accuracy of lymphography, cavography and pelvic venography Brit J Radiol 37 (1964), 422

MASSELOT J BERGIRON C [illegible]
la cavographie et de [illegible]
naires [illegible]

PERTTALA [illegible]
diagn

phomas The overall gain in information is about 11 per cent at most In Hodgkin's disease it has been stated that cavography demonstrates the tumor in 4 to 5 per cent of cases when lymphangiography does not In this material cavography did not reveal any pathology in cases with normal lymphangiography which is contrary to several previous reports However, the same results were also reported by ABRAMS (1971)

The routine use of both cavography and lymphangiography in the evaluation of Hodgkin's disease does not seem warranted Lymphangiography, being the more informative examination, is to be preferred Cavography to corroborate lymphangiographic findings still remains valid Thus, in the author's opinion, cavography in Hodgkin's disease can be limited to cases with an equivocal or technically unsatisfactory lymphangiography

SUMMARY

In a material of 89 patients with Hodgkin's disease, 98 combined examinations including lymphangiography, cavography and urography, were performed Lymphangiography disclosed signs of expansive lesion 33 times, cavography 21 times and urography 17 times The diagnostic accuracy of lymphangiography was high Routine cavography in Hodgkin's disease is not advocated, it may be restricted to cases with equivocal lymphographic findings

ZUSAMMENFASSUNG

An einem Material von 89 Patienten mit Hodgkin'scher Erkrankung wurden 98 kombinierte Untersuchungen einschliesslich Lymphangiographie, Cavographie und Urographie vorgenommen Die Lymphangiographie deckte Zeichen von expansiven Veranderungen 33 mal auf, die Cavographie 21 mal und die Urographie 17 mal Die diagnostische Genauigkeit der Lymphangiographie war hoch Routinemassig vorgenommene Cavographie bei den Hodgkin'schen Erkrankung wird nicht befurwortet sie kann auf die Falle mit zweideutigen lymphographischen Befunden beschrankt werden

RÉSUMÉ

Sur une serie de 89 malades atteints de maladie de Hodgkin 98 examens associes comprenant la lymphangiographie, la cavographie et l urographie ont eté pratiqués La lymphographie a montre des signes de lésions expansives 33 fois, la cavographie 21 fois et l urographie 17 fois La précision diagnostique de la lymphangiographie a été elevee La cavographie systematique dans la maladie de Hodgkin n est pas conseillee, elle peut être réservee aux cas ou les signes lymphographiques sont équivoques

REFERENCES

ABRAMS H Lymphangiography in lymphoma *In* Angiography p 1389 Edited by H Abrams Little, Brown & Co, Boston 1971

BATTEZZATI M, DONINI I, BELARDI P, BECCHI G und MUGGIATI L Die Phlebolymphographie der Leisten-Becken-Region Fortschr Rontgenstr 98 (1963) 705

FROM THE DEPARTMENT OF DIAGNOSTIC RADIOLOGY (DIRECTOR PROF O OLSSON), UNIVERSITY HOSPITAL, S-221 85 LUND, SWEDEN

FREQUENCY OF THROMBOSIS AND POST-THROMBOTIC CONDITIONS OF THE FOOT AT PHLEBOGRAPHY

JAN GÖTHLIN and STEFAN ZURBRIGGEN

Thrombosis in the veins of the foot is not uncommon, but the frequency has been unknown except in autopsy materials To obtain an estimation of the frequency in an unselected material also the foot was examined at ascending phlebography of the leg

Methods and Material In 350 patients referred for ascending phlebography, films in a p and lat projections were obtained after injection of 10 ml meglumine metrizoate (Isopaque Cerebral, Nyegaard, Norway) The patients were in standing position with stasis applied immediately beneath or around the malleoli A teflon cannula was used in order to avoid extravasation (GÖTHLIN 1972) (For further details of the technique see BRISMAR & GÖTHLIN 1972) Ninety five patients were referred for examination because of possible thrombosis, 62 for post thrombotic conditions, 166 for insufficiency of perforating veins and 27 with various disorders

Results

Fresh thrombosis was the clinical diagnosis in 95 cases, 60 of these (68 per cent) and 43 (69 per cent) of the 62 cases with possible post thrombotic conditions proved to be roentgenologically abnormal

Submitted for publication 23 July 1974

RÜTTIMANN A und DEL BUONO M S Die Lymphographie mit öligem Kontrastmittel Fortschr Röntgenstr 97 (1962), 551
SCHWARZ G, LEE B and NELSON J Lymphography, cavography and urography in the evaluation of malignant lymphoma Acta radiol Diagnosis 3 (1965), 138
SHEEHAN F R, LESSMAN E M and LESSMAN F P Comparative study of intraosseous cavography and intravenous pyelography in demonstration of retroperitoneal lymphoma Radiology 77 (1961), 757
SMITHERS D Hodgkin's disease A review of change over 40 years Brit J Radiol 46 (1973), 911
WILJASALO S Lymphographic polymorphism in Hodgkin's disease Acta radiol (1969) Suppl No 289
WILSON W, TEMPLETON A, RIDINGS R and JANSEN C Combined lymphography inferior vena cavography and urography for retroperitoneal and pelvic tumor evaluation Missouri Med 62 (1965), 290

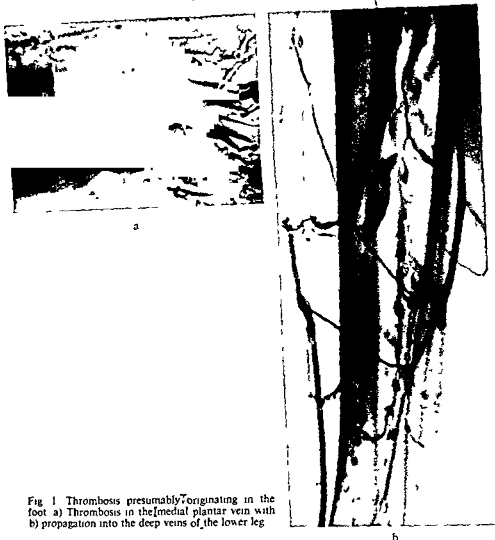


Fig 1 Thrombosis presumably originating in the foot a) Thrombosis in the medial plantar vein with b) propagation into the deep veins of the lower leg

part of the lower limb, the thrombosis was located both laterally and medially in the foot In cases with thromboses presumably originating in foot veins and ascending to the veins of the lower limb (Fig 1, Table 2), the pain spread only to the calf and was not located more distally as in the former group

In descending thromboses the pain started proximally in the lower leg and spread distally (Table 3) These findings were evident in 14 cases The origin of the thrombosis was impossible to determine in 7 cases

Post thrombotic conditions were located in foot veins only in 10 cases (23 per cent), in veins of the foot and lower leg in 17 cases (40 per cent) and in the lower leg only in 16 cases (37 per cent)

Table 1

Thrombosis limited to the veins of the foot

No	Localization	Pain	
		Onset	Spread
1	V plant lat	Lat malleolus	Planta pedis
2	V plant med	Med malleolus	Planta pedis
2	V plant med + lat	Med + lat malleolus	Distally in the lower limb
1	V plant med + lat + other veins	Med + lat malleolus	Distally in the lower limb

Table 2

Thrombosis ascending from the foot

No	Localization	Pain	
		Onset	Spread
1	V plant lat + v tib ant	Lat malleolus	Calf
1	V plant med + v tib post	Med malleolus	Calf
7	General veins of the foot + veins in the lower limb	Planta pedis	Calf

Table 3

Thrombosis descending to the foot

No	Localization	Pain	
		Onset	Spread
8	Lower limb + foot	Calf	Foot
3	*Lower limb + foot*	*Thigh*	*Calf foot*
3	Lower limb + foot	Thigh	Calf
7	Lower limb + foot	Not possible to determine	Not possible to determine

In 6 cases (10 per cent) the fresh thrombosis was limited to the veins of the foot, while in 30 (50 per cent) the thrombosis was located in the veins both of the foot and the limb Forty per cent of the thromboses (24 cases) were demonstrated in veins of the lower leg only The onset and spread of pain in cases with thrombosis in the foot veins only was correlated with the localization of thrombosis (Table 1) With a lateral localization of thrombosis, the pain started laterally and spread to the planta pedia Medial pain occurred at medial thrombosis and spread even here into the planta pedis When the pain began behind both malleoli and spread to the distal

cent and in veins behind the medial malleolus in 17 per cent of the cases in an autopsy material DENNECKE, OLOW and PAYR stressed the importance of pain in the foot and ankle as an indicator of deep vein thrombosis NEUMANN advanced the opinion that the thrombosis of the plantar veins continuing into the deep veins of the lower leg was more likely to cause pulmonary embolism than thrombosis of the veins of the muscle of the thigh The present material included an elderly man with pulmonary embolism where the only source found was fresh thrombosis of the plantar veins (Fig 2)

As thrombosis of the veins of the foot is common either isolated or extending into the venous system of the leg it is advisable to perform foot phlebography of the foot routinely in cases of possible thrombosis The clinician should be observant when patients complain of pain in the sole of the foot or behind the malleoli Early treatment may prevent further spread to more proximal veins

SUMMARY

In 350 consecutive ascending phlebographies thrombosis was demonstrated in 60 6 of which were limited to the foot The veins of the foot is an overlooked place for the origin of thrombosis and emboli

ZUSAMMENFASSUNG

Bei 350 nacheinander vorgenommenen ascendierenden Phlebographien wurde bei 60 eine Thrombose nachgewiesen die bei 6 sich auf den Fuss beschrankte Die Venen des Fusses sind ein nicht beachteter Platz fur den Ursprung einer Thrombose und Embolie

RESUME

Sur 350 phlebographies ascendantes consecutives une thrombose a éte mise en evidence dans 60 cas dans 6 de ces cas elle était limitée aux pieds Les veines du pied sont un point de départ meconnu pour l origine de thrombose et d embol

REFERENCES

BRISMAR J and GOTHLIN J Phlebography and thrombosis of the deep veins of the foot J Brit Rad ol 45 (1972) 199

DENNECKE K Der Plantarschmerz als Fruhsymptom einer beginnenden Thrombose des Unterschenkels Munch med Wschr 76 (1929) 1912

GÖTHLIN J The comparative frequency of extravasal injection at phlebography with steel and plastic cannula Clin Radiol 23 (1972) 183

NEUMANN R Ursprungszentren und Entwicklungsformen der Bein Thrombosen Arch path Anat 301 (1938) 708



Fig 2 Patient with pulmonary emboli Symptoms and signs of thrombosis of the foot No other source of embolism demonstrable except thrombosis in the medial plantar vein of the foot

Discussion

DENNECKE (1929), OLOW (1930), PAYR (1930) and TSCHMARKE (1931) described tenderness in the sole of the foot as the earliest clinical sign of thrombosis of the lower leg In the present material the pain started behind one or both malleoli with spread to the sole of the foot or distally in the leg, but not into the calf when the thrombosis was limited to foot veins (Table 1) When the thrombosis was located laterally the pain began behind the lateral malleolus, when it was located medially behind the medial malleolus, but when bilateral the pain was experienced distally in the leg In the patients with ascending thrombosis of foot veins (Table 2) the pain spread to the calf, where, however, no thrombosis of the veins was demonstrated This may indicate that thrombosis does not begin as often in the veins of the calf as is commonly assumed

The descending thrombosis (Table 3) gave pain beginning in the thigh or calf and spreading distally As in the former group, it seems justified to assume that a differentiation between ascending and descending thrombosis is possible based on the migration of the pain

Thirty six of 60 verified fresh thromboses (60 %) were located solely in or involving the veins of the foot This means that in most thrombosis of the lower leg the foot veins are also engaged This opinion is supported also by the distribution of the post thrombotic conditions The veins in the foot and the lower leg together were abnormal in 63 per cent of the cases which corresponds fairly well to the figures for fresh thrombosis That the post thrombotic conditions are more common than fresh thrombosis may be due to difficulties in diagnosing the latter in the acute stage and to the fact that the thrombosis later extends into the foot veins, resulting in easily demonstrable post thrombotic conditions

The common occurrence of thrombosis in the veins of the foot has been pointed out by NEUMANN (1938) who found thrombosis of the deep plantar veins in 71 per

A C T A   R A D I O L O G I C A

OFFICIAL ORGAN OF THE RADIOLOGICAL SOCIETIES OF
DENMARK, FINLAND NORWAY AND SWEDEN

Vol 16 Fasc 2 | DIAGNOSIS | 1975 March

BECQUEREL AND THE DISCOVERY OF RADIOACTIVITY

FOLKE KNUTSSON

Antoine Henri Becquerel (1852–1908) was trained as a physicist, and succeeded his father in 1892 as professor of physics at the Museum d'Histoire naturelle in Paris From 1895, he was professor at the Ecole polytechnique in Paris He had earlier cooperated with his father in the latter's research work, which was in large part concerned with the physical nature of the phosphorescent phenomena In 1885, he published a report on his own observations on the connection between absorption of light and phosphorescent radiation in his experiments with uranium

The Nobel Prize in Physics for 1903 was awarded to Becquerel for 'the discovery of spontaneous radioactivity' and to Marie and Pierre Curie for 'work on the radiation phenomena discovered by Becquerel'

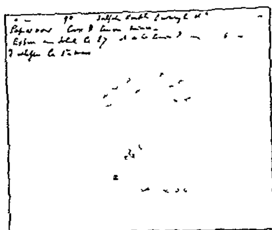
Becquerel reviewed his work under the title, 'On a new property of matter, radioactivity', in his Nobel address in Stockholm on 11 December 1903 When, early in 1896, he learned of the implications of Rontgen's discovery, his interest was aroused especially by the observation that the new form of radiation was seen simultaneously with the fl[illegible] ium tube in con- [illegible] 'whether or not [illegible] material emit similar radiation' Using uranium salts, which were available in satisfactory quantities and with which he had had previous

From the Department of Diagnostic Radiology (Director Prof H Lodin) Akademiska Sjukhuset University of Uppsala, S-750 14 Uppsala Sweden Submitted for publication 7 June 1974

OLOW J Concernant le diagnostic de la thrombose crural Acta obstet Gynec Scand 10 (1930), 159

PAYR E Gedanken und Beobachtungen uber die Thrombo Embolifrage Zbl Chir 57 (1930), 961

TSCHMARKE G Erfahrung uber den Fußsohlen Druckschmerz als Fruhsymptom der Thrombose Munch med Wschr 11 (1931), 2135



This image was prod iced on 1 March 1896 A
plate under a layer of
it was then placed in
and developed The c
salt must have been
covery of radioactivit

of uranium salt on photographic plates wrapped in paper As the sun only appeared occasionally, however, he could not carry out his plan of exposing them to sunlight, but placed them instead, for safe keeping, in a drawer This deviation from the routine procedure applied in the other experiments was to be of *significance* for the discovery As the sun did not shine on the following days either, he decided nevertheless on 1 March, to develop the plates Knowing that the phosphorescent light from the uranium salt he had used *only persisted for 1/100th* second at the most after

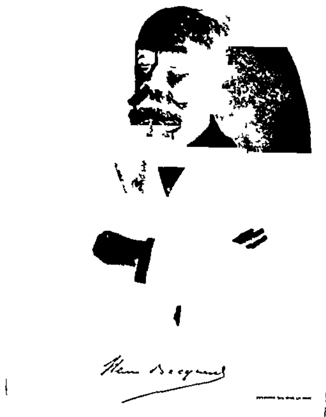
of the

He ir that the radiation had been in progress while the plates were lying in the box This *observation on 1 March*, which was made largely by accident, as a result of a temporary *change in the* experimental routine which did not form part of the original plan for the investigations meant in actual fact the

covery of

prepara

develop evidence of a radiation of the same intensity as in experiments where *prolonged exposure* to sunlight had been applied The logical conclusion was that the light rays which arise in connection with phosphorescence were not the cause of the phenomenon As *an* explanation he suggested the possibility that there could be invisible rays with much longer persistence than the extremely short lived light rays, and that they *might* be of the same type as those discovered by Röntgen At the meeting on 18 May he was able to report that uranium



experience, he placed a thin layer of the salt on a photographic plate wrapped in special paper as a protection against light, and exposed it to sunlight for several hours in order to produce strong and prolonged phosphorescence After developing the plate, he observed that the uranium salt had emitted a radiation which had passed through the paper wrapping, and that the salt layer was depicted on the plate He thought at first that this might be due to the phosphorescence produced by solar energy, but he added that 'it was not long before I concluded that the radiation did not come from an external source of energy such as light, heat, or electricity' He came to the conclusion that it was a matter of 'a spontaneous phenomenon of a new type'

Becquerel gave a detailed account of his first results, which were obtained in Feb ruary and March of 1896, at several meetings of the Paris Academy of Sciences By examining these reports, which were recorded in the minutes, it is possible to follow in detail both the way in which the experiments were organized, and the results that were obtained It is interesting to note the irrelevant circumstances that accidentally played a decisive part on the occasion when the discovery was made

On 26 and 27 February, Becquerel prepared a few experiments by placing a layer

ROM THE DEPARTMENTS OF NEUROSURGERY (DIRECTOR PROF L LEKSELL) AND NEURO-RADIOLOGY (DIRECTOR PROF T GREITZ), KAROLINSKA SJUKHUSET, S 104 01 STOCKHOLM, SWEDEN

STEREOTACTIC EXPLORATION OF BRAIN TUMOURS BY ULTRASOUND

ERIK OLOF BACKLUND, BO LEVANDER and TORGNY GREITZ

As various stereotactic procedures are used more and more in the management of brain tumours, demands for an accurate classification have increased This is of special importance when a tumour is to be treated with closed radiation surgery (BACKLUND 1973) Stereotactic biopsy is a useful method for obtaining samples for histologic and cytologic examination, employed at the Department of Neurosurgery in deeply situated brain tumours before the definite treatment program is determined However before the biopsy it is often desirable to get information about the inner structure of the tumour, to reveal and localize possibly occurring cysts etc

The various echoencephalographic characteristics of different tumours may be the base for such structural evaluation The intention of the present [illegible]

[illegible] presented as well A very brief report on the technique has been given previously (BACKLUND & LEVANDER 1970)

Method

The operative system developed by LEKSELL (1971) is used for the stereotactic procedures The outline of the tumour and the most important anatomic structures

Submitted for publication 27 July 1973

salt which had been kept in the dark for two months was still emitting radiation with undiminished intensity His investigations had by that time led to the view that the activity was to be explained by the presence of the element, uranium, in the substance

SUMMARY

A description is given of Becquerel s discovery of radioactivity Like Rontgen, Becquerel was also favoured by chance, in his discovery

ZUSAMMENFASSUNG

Becquerel's Entdeckung der Radioaktivitat wird beschrieben Ebenso wie Rontgen wurde Becquerel bei seiner Entdeckung durch einen Zufall begunstigt

RÉSUMÉ

Description de la découverte de la radio activité par Becquerel Comme Rontgen, Becquerel a lui aussi été favorisé par la chance dans sa découverte

REFERENCES

BECQUEREL A H Sur les radiations émises par phosphoréscence C R Acad Sci (Paris) 122 (1896), 420 (Lecture held on 24 February 1896)

— Sur les radiations invisibles émises par les corps phosphorescents C R Acad Sci (Paris) 122 (1896), 501 (Lecture held on 2 March 1896)

— Sur quelques propriétés nouvelles des radiations invisibles emises par divers corps phosphorescents C R Acad Sci (Paris) 122 (1896) 559 (Lecture held on 9 March 1896)

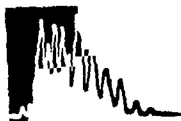
— Sur les propriétes différentes des radiations invisibles émises par les sels d uranium, et du rayonnement de la paroi anticathodique d un tube de Crookes C R Acad Sci (Paris) 122 (1896), 762 (Lecture held on 30 March 1896)

— Emission de radiations nouvelles par l uranium métallique C R Acad Sci (Paris) 122 (1896), 1086 (Lecture held on 18 May 1896)

— Sur une propriété nouvelle de la matière, la radio activité Conference Nobel Les Prix Nobel 1903 P A Norstedt & Soner, Stockholm 1906



a



b



c

spikes c) Chromophobe pituitary adenoma at removal found to be degenerated and partially hemorrhagic After the initial spike corresponding

needle guide is now replaced in the semicircular arc by the 2 25 MHz transducer of the Echoencephaloscope ME 800 (LKB Medical AB, Stockholm, Sweden) The tip of the transducer is protected by a sterile rubber glove after the application of electrode paste and can thus be inserted through the burr hole onto the dural surface The diameter of the transducer is 14 mm The axis of the beam is geometrically defined in the stereotactic system and identical with the puncture track With the apparatus used the distance from the dural surface to various echoproducing structures can be measured with great accuracy by moving on the oscilloscope screen an index point the relative position of which is continuously displayed in millimeters by a counter Representative echograms are recorded by a Polaroid camera The interpretation of the recordings is facilitated by the following method

A second stereotactic instrument is adjusted to be identical with that of the pa-

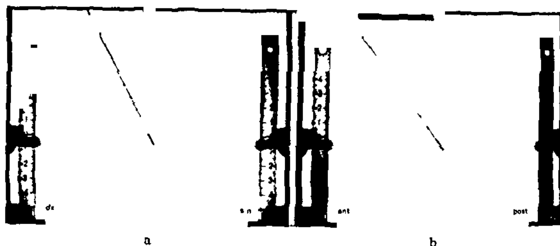


Fig 1 a) a p and b) lateral projections of the frame with the 'ruler' The latter is positioned at the angles of the predetermined puncture track

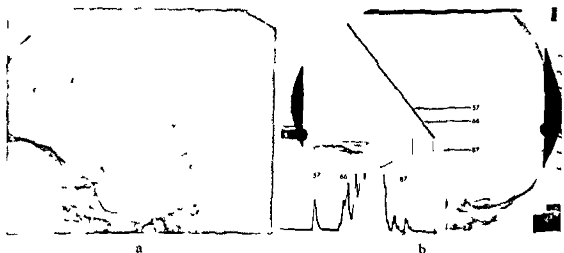


Fig 2 a) Encephalography Large irregular suprasellar tumour with calcifications probably a

in its vicinity are transferred to the stereotactic roentgen films from those of the previous neuroradiologic examinations The target point is chosen safely within the boundaries of the tumour The location of the burr hole for the echoencephalography and the puncture is determined, considering that (a) a puncture via the burr hole through the target should not jeopardize important normal structures surrounding the tumour, and (b) the puncture track and its extension beyond the target should pass through representative parts of the tumour

The determination of the stereotactic coordinates and the application of the semicircular arc of the instrument is performed according to conventional routine The

With a modified fixation technique, the stereotaxic frame may be applied sufficiently stable on the skin surface only This makes possible repeated transcutaneous controls of the cyst dimensions after intracavitary irradiation (BACKLUND et coll 1972) Other possible objects for similar long term control will be patients treated with closed radiation surgery In such cases the degree and extension of the gradually appearing radiation necrosis may be echographically demonstrated

SUMMARY

A report upon a new technique for investigation of brain tumour anatomy by means of stereotactically directed ultrasound is presented with some illustrative cases Information obtained with this technique has been found useful when deciding the treatment program for the tumour

ZUSAMMENFASSUNG

Es wird uber eine neue Technik zur Untersuchung der Anatomie von Hirntumoren mit Hilfe stereotaktisch gerichteten Ultraschalls zusammen mit einigen illustrativen Fallen berichtet Die mit dieser Technik erhaltenen Informationen wurden bei der Entscheidung des Behandlungs Programms des Tumors als nutzlich befunden

RÉSUMÉ

Les auteurs présentent une nouvelle technique d'examen de l anatomie des tumeurs cérébrales au moyen d ultra sons dirigés par stéréotaxie et donnent quelques exemples Les *informations obtenues* par cette technique ont éte considérees comme utiles pour decider le programme de traitement de la tumeur

REFERENCES

BACKLUND E O Indications for and results of treatment *with stereotaxic* radiosurgery *In* Diagnosis and treatment of pituitary tumors, p 263 Excerpta Medica Amsterdam 1973

— and LEVANDER B Echoencephalographic sounding of *the puncture track in* stereotaxic

—

Treatment by stereo-

DY[illegible] Intra-operative ultrasonic encephalography of cerebral mass lesions Bull Los Angeles *neurol Soc 3 (1966)* 14

GLASSER E [illegible]

LE[illegible]

LO[illegible] YOOO I [illegible]

scanning for detection

troencephalograms anc

tient, its needle replaced by a thin steel tube, in the lumen of which a row of small lead spheres are fixed at intervals of exactly 10 mm With this 'ruler', positioned at angles identical to that of the puncture track and with the tip corresponding to the target point or somewhat beyond this point, films in a p and lateral projections are taken (Fig 1) By directly measuring the distance between the semicircular arc of the patient-instrument and the dura, it is possible to indicate on the ruler the point corresponding to the dural surface By superimposing the films of the ruler frame upon the stereotactic films of the patient, and by 'plotting' the echo data along the ruler scale, the positions of various echoproducing anatomic structures can usually be identified (Fig 2)

Results

The general appearances and the characteristics of the transdural echograms in the present material of about 150 recordings correspond well with previously reported results (DYCK et coll 1966, WALKER & UEMATSU 1966, MULLER 1969, LOMBROSO et coll 1970, GLASSAUER & SCHLAGENHAUFF 1970) Typical 'M-echoes' have generally been recorded from solid tumour components whereas cyst walls have been represented by distinct single spikes Cysts with liquid contents are usually represented by a zone devoid of echoes (Fig 3 a) A cystic tumour with cholesteatomatous contents, however, displayed an M-echo with a 'slope' configuration (Fig 3 b) In chromophobe adenomas which have been found to contain cysts and hemorrhages at a later removal, the echogram indicated such degenerative changes (Fig 3 c)

Discussion

Stereotactic ultrasound examination has proved to be useful in the planning of the further management of the patient Evidence of a cystic lesion in cases of craniopharyngioma has indicated fine needle puncture and intracavitary isotope treatment In cases of solid tumours, the choice of instrument for the subsequent biopsy was facilitated

The nature of a pathologic process may also be indicated but further investigations of the correlations between the features of the echo and the histologic character of the lesion are needed MÜLLER (1971) has stated that the differentiation between a coagulated clot and a liquid mass in cases of intracerebral hemorrhage is possible In such cases, with the technique presented, various parts of the expanding lesion may be selectively explored by stereotactic direction of ultrasound and followed by attempts at needle aspiration only in those regions of the mass, where liquid blood is to be expected The exact depth and thickness of such areas is also obtained by the stereotactic technique employed

Assessment of the exact depth may also be of value in cases of foreign bodies within the brain, not demonstrable at roentgen examination, when stereotactic extraction is to be performed

FROM THE DEPARTMENT OF DIAGNOSTIC RADIOLOGY (DIRECTOR PROF H LODIN) AKADEMISKA SJUKHUSET, S 750 14 UPPSALA, SWEDEN

THE CRANIAL INDEX ACCORDING TO CRONQVIST COMPARED TO ECHO-VENTRICULOGRAPHY FOR DETERMINATION OF HYDROCEPHALUS

K BERGSTRÖM and H JORULF

Different methods are employed for simple and rapid determination of the size and growth of the skull in infants and children in the assessment of hydrocephalus Dilatation of the ventricular system will not, however, invariably produce significant evidence of an increase in the size or growth of the skull as determined by simple measurement of its circumference or by its assessment in roentgenograms GORDON (1966) described a roentgenologic method for calculating the volume of the skull in children A nonvolumetric index for evaluation of the skull size in children was presented by CRONQVIST in 1968, normal values obtained by this method were reported for different age groups of up to five years also by AUSTIN & GOODING (1971) SJÖGREN (1967) described a means of determining the size of the ventricular system by diagnostic ultrasound

The purpose of this investigation was to compare the cranial index according to CRONQVIST in hydrocephalic patients with the ventricular size as estimated by ultrasound (SJÖGREN et coll 1968, MOSTAFAWY 1971)

Cranial index by the Cronqvist method Three parameters of the neurocranium are

Submitted for publication 29 November 1973

MÜLLER H P Transdurale Echolotung von Hirntumoren mittels einer zweidimensionalen A Scan Technik Schweiz med Wschr 99 (1969) 1017
— Die transdurale Echoenzephalographie Verlag Hans Huber Bern 1971
TANAKA K YUKISHITA K and ITO K Diagnosis of brain tumor by A scope indication method *In* Diagnosis of brain disease by ultrasound Shindan to chityo sha Tokyo 1968
WALKER A E and UEMATSU S Dural echo-encephalography J Neurosurg 25 (1966) 634

Table 1

Number of subjects in the four different age groups The numbers within brackets refer to hydrocephalic patients

Age	No of patients
0–1 month	56 (28)
1–7 months	64 (34)
7–12 months	24 (17)
1–5 years	22 (12)
Total	166 (91)

Material The material comprised 166 children evaluated by the cranial index method and echo-ventriculography They were divided into four age groups, Table 1, to match the changing cranial index with increasing age (AUSTIN & GOODING) Fifty nine patients were also examined by encephalography, 52 of these were hydrocephalic The ventricular size determined by ultrasound corresponded to that registered at encephalography both in the hydrocephalic and normal groups In 39 hydrocephalic patients the ventricular size was estimated only by ultrasound These patients were also clinically classified as hydrocephalic The total hydrocephalic group thus comprised 91 patients

Results

The upper normal limits of both cranial and echo-ventricular indices have been correspondingly assigned to +1 sigma

The relationship between the cranial and echo indices in the four different age groups with regression lines and correlation coefficients is displayed in Fig 2 The upper normal limit for the echo index by the Sjögren method and the cranial index according to AUSTIN & GOODING also appear in the figures

In the infant group of 56 individuals up to one month of age (Fig 2 a) 27 cases had normal cranial and echo indices and in 13 cases both indices were above the normal upper limits Thus in 40 out of 56 patients both indices were within normal or pathologic limits On the other hand, in 15 infants the cranial index was within normal limits but the echo index was increased One patient with normal ventricular size (also verified by encephalography) had an increased cranial index, but had a giant hemisphere The midline structures in this case were displaced on echo-ventriculography

Out of 65 infants 1 to 7 months of age (Fig 2 b) 29 had normal cranial and echo indices and in 17 both indices were above the normal upper limits Sixteen hydrocephalic patients had normal and two decreased cranial indices In this age group

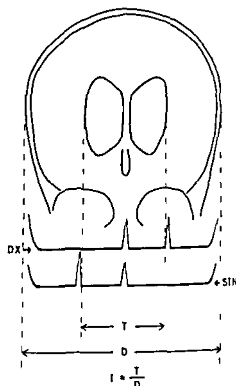


Fig. 1. Principle of echo ventriculography. D = external diameter of the head. T = distance between lateral ventricle echoes. I = lateral ventricle echo index.

measured and related to the width of the mandible according to the formula

$$\frac{L + H + W}{M} \times 10$$

where L is the greatest inner length of the skull, H the greatest inner height and W the greatest inner width, M is the greatest inner distance between the margins of the necks of the mandible.

Cronqvist reported the normal index variations to be 51 to 56 in children below seven years of age. Austin & Gooding correlated this index with the age of the child and found a decreasing index with increasing age. Thus in the first month of life the index was reported to be 57 ± 5 and at five years of age 53 ± 5.

Echo index. The midline and the width of the ventricular system are determined by A-scan echoencephalography. The ultrasonically determined external diameter of the patient's head is used as reference dimension for the measurements of the ventricular echoes (Fig. 1). It is thus possible to express the size of the ventricles in relation to the transverse cranial diameter, the upper normal limit of this index (T/D) is 0.33 (Sjögren 1968). Echoencephalography by the technique described is a simple and accurate method for determining the size of the ventricular system, especially in children under two years of age, it may also reveal complex cerebral malformations. A comparative investigation between cerebral pneumography and echoencephalography in infants and children was published by Sjögren et coll. (1968).

Table 2

Results in the whole material. EI = echo index CI = cranial index The figures within brackets represent percentage

Age	No of patients	EI normal		EI pathologic	
		CI not increased	CI pathol	CI not increased	CI pathol
0–1 month	56	27 (48)	1	15 (27)	13 (23)
1–7 months	64	29 (45)	1	12 (27)	17 (27)
7–12 months	24	6 (25)	1	8 (33)	9 (38)
1–5 years	22	9 (41)	1	5 (23)	7 (32)
Total	166	71 (43)	4	45 (27)	46 (28)

Twenty two children comprised the age group 1 to 5 years (Fig 2 d), in 16 of them both the cranial and echo indices were within normal limits or were increased Five subjects were hydrocephalic but had a normal cranial index One child had a normal ventricular size but a slightly increased cranial index, he was healthy but had a large skull

Table 2 summarizes the values from Fig 2 In 117 out of 166 patients both cranial and echo indices were either within or above normal limits, 46 of these were hydrocephalic and 71 normal A strikingly large number of hydrocephalic children in all age groups had cranial indices that were not increased For the whole material the number with no increase in the cranial index amounted to 27 per cent, but for the hydrocephalic group of 91 subjects the corresponding figure was 50 per cent Three hydrocephalic children had decreased cranial indices

Discussion

The cranial indices of normal children of different ages in the present investigation were in agreement with those reported by AUSTIN & GOODING All but 2 of 73 normal children had a normal cranial index, the 2 belonged to families with large skulls Of the remaining 48 patients with increased cranial indices, 46 were hydrocephalic and 2 pathologic in other respects (one with a malformed brain and one with bilateral subdural effusions) This means that an increased cranial index is highly suggestive of hydrocephalus although a normal or decreased cranial index does not necessarily exclude hydrocephalus Of the 91 hydrocephalic children 42 had normal and three decreased cranial indices, i e 50 per cent were false negatives

Conclusions A combination of cranial and echo indices will provide more accurate information in neuropaediatric subjects than assessment of one of the indices

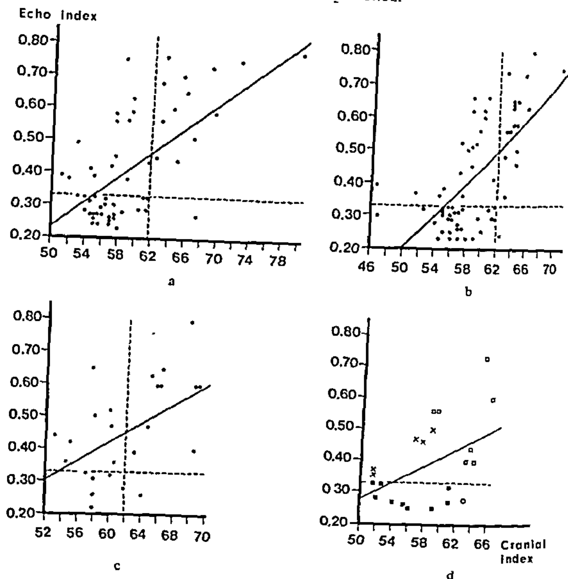


Fig 2 Correlation between cranial and echo indices in four age groups with regression lines Horizontal broken lines indicate the upper normal echo indices and vertical broken lines the upper nor-

indices increased, O normal echo index and increased cranial index, × increased echo index and normal cranial index

one patient appeared normal at echo-ventriculography but had a slightly enlarged neurocranium as had several members of his family.

In the group of 25 infants 7 to 12 months of age (Fig. 2 c) 16 had both cranial and echo indices within normal limits or both indices increased Eight infants with dilated ventricles had a normal cranial index One infant with a normal ventricular size but increased cranial index had bilateral subdural effusions at angiography.

ROM THE DEPARTMENTS OF NEURORADIOLOGY (DIRECTOR T GREITZ) AND CLINICAL NEUROPHYSIOLOGY (DIRECTOR L WIDEN), KAROLINSKA SJUKHUSET, S 104 01 STOCKHOLM, SWEDEN

METRIZAMIDE-PHENOTHIAZINE INTERACTION

Report of a case with seizures following myelography

TOMAS HINDMARSH, ARNE GREPE and LENNART WIDEN

Convulsions constitute the most serious immediate clinical complication in the use of water soluble contrast media in the subarachnoid space Metrizamide, a non-ionic compound designed for the subarachnoid space has been shown to have a low neurotoxic effect in extensive animal investigations (Acta radiol Suppl No 335, 1973) At the time of writing more than 1 000 clinical examinations have been carried out with this medium Most of these examinations have been restricted to the lumbar region but several have been extended to the thoracic, cervical and intracranial parts of the subarachnoid space So far no single case with clinical manifestation of seizures has been observed in the four departments where clinical trials have been run, with the exception of one incidence, the subject of the following report This case presents features of special interest, that warrant a discussion of clinical routine in examinations with metrizamide

Case report

A male, 25 years of age, was referred for complete myelography because of atypical pa
of two years duration in the left
the left si
of epilep
psychiatr
months
the day before the examination 50 mg of the drug

Submitted for publication 2 April 1974

alone A large number of hydrocephalic subjects have a normal cranial index A normal echo index and an increased cranial index should raise the possibility of a subdural effusion or brain malformation

SUMMARY

The CRONQVIST cranial index with the normal values for different age groups according to AUSTIN & GOODING is compared with the ventricular index estimated by ultrasound in a series of 166 neuropaediatric subjects aged 0 to 5 years A large number of hydrocephalic patients has a normal cranial index The cranial index alone is thus an unreliable method for the screening of hydrocephalus

ZUSAMMENFASSUNG

Es wurde der CRONQVIST Schadel Index mit den normalen Werten fur verschiedene Alters gruppen nach AUSTIN & GOODING mit dem durch Ultraschall bestimmten Ventrikel Index in einer Reihe von 166 neuropadiatrischen 0 bis 5 Jahre alten Kindern verglichen Eine grosse Anzahl von Patienten mit Hydrozephalus hatte einen normalen Schadel Index Der Schadel Index alleine ist somit eine unzureichende Skreening Methode zur Feststellung eines Hydrocephalus

RÉSUMÉ

L'index crânien de CRONQVIST avec ses valeurs normales pour les differents groupes d age suivant AUSTIN & GOODING a ete compare avec l'index ventriculaire estimé par les ultrasons sur une serie de 166 sujets neuropediatriques âges de 0 à 5 ans Un grand nombre du sujets hydrocéphaliques a un index crânien normal L'index crânien à lui seul est donc une methode infidèle pour depister l hydrocéphalie

REFERENCES

AUSTIN J H M and GOODING C A Roentgenographic measurement of skull size in children Radiology 99 (1971), 641

CRONQVIST S Roentgenologic evaluation of cranial size in children Acta radiol Diagnosis 7 (1968), 97

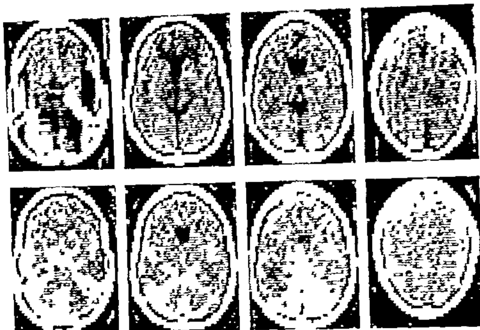
GORDON I R S Measurement of cranial capacity in children Brit J Radiol 39 (1966), 377

MOSTAFAWY A Pediatric sonoencephalography Springer, Berlin Heidelberg New York 1971

SJOGREN I Echoencephalography in paediatric practice with special regard to measurement of the ventricular size Acta paediat scand (1967) Suppl No 178

— Echoencephalographic measurements of ventricular size in children Develop Med Child Neurol *10 (1968)*, 145

— BERGSTROM K and LODIN H Echoencephalography in infants and children Comparison with cerebral pneumography in measuring ventricular size Acta radiol (1968) Suppl No 278



Computer ass s ed ax [illegible]
w th m
and 7 7
the pos

large doses of phenoperidine (0 25–0 4 mg/kg body weight) was demonstrated by NILSSON & INGVAR (1966) to evoke epileptogenic activity in the EEG of curarized cats

An interaction between the analgetic agent chosen for the dog experiments and the contrast medium was postulated and prompted a further investigation with cisternal application of metrizamide in dogs in N_2O analgesia with and without halothane with exclusion of potentially seizure-provoking drugs (GREPE & WIDEN 1973 b) Although the circumstances in other respects were essentially identical with those in the first series with cisternal application of metrizamide no epileptogenic activity was recorded in the latter series

The investigations by GREPE & WIDÉN thus indicated an interaction between metrizamide and phenoperidine promoting epileptic activity in dogs when high doses of the analgetic agent were given Phenothiazine is not chemically related to phenoperidine but may like this drug provoke epileptic activity when administered in high doses (GOODMAN & GILMAN 1966) The dose of the phenothiazine derivative given was low (75 mg daily) but if a synergism exists between this drug and metrizamide the medication may be considered as a contributory factor to provoke the epileptic convulsions

had been administered, the day of the examination only 25 mg chlorpromazine was given after the first attack of seizures

Before examination a steroid preparation was given (Solu-Cortef 100 mg) on account of a history of allergy, which was not, however, specific for iodine or contrast media No other premedication was given Sixteen ml of metrizamide in a concentration of 170 mg I/ml (2 7 g iodine) was administered by the lumbar route for examination of the entire spinal subarachnoid space During the examination, with tilting the position of the patient's head was arranged so as to keep the level of the intracranial subarachnoid space above that of the cervical region Due to a break-down of equipment, the application of contrast medium in the cervical region was considerably prolonged The subarachnoid space was well filled with contrast medium to the level of the foramen magnum and some medium was also observed around one of the cerebellar hemispheres The patient experienced a mild headache but no other signs or symptoms were recorded The pulse and the blood pressure were stable After myelography the patient was positioned according to the adopted routine with the headend of the bed raised about 30° Three and a half hours after the administration of metrizamide, the patient suffered a grand mal seizure, which lasted about one minute and stopped spontaneously Roentgen examination of the skull after this attack gave no evidence of contrast medium intracranially A further five hours later, 8½ hours after administration of metrizamide, the patient had a second grand mal seizure, after which 10 mg diazepam was administered intravenously The following day the patient complained of pain in the back and small compression fractures of the vertebral bodies of Th5 to Th8 were seen on roentgen films Twenty-four hours after the administration of metrizamide no increase in CSF cell count could be demonstrated

Discussion

The use of water-soluble contrast media hitherto accepted for examination of the subaracnnoid space has been hampered by the neurotoxic effects of these media, above all epileptic seizures (Baumgartner 1970, Praestholm & Lester 1970 Ahlgren 1971, Boisen & Lindholmer 1971, Geller 1971, Gonsette 1971, Skalpe 1971, Irstam 1973, Skalpe & Talle 1973) Considerably lower neurotoxic effect of the new non-ionic water-soluble contrast medium metrizamide has been demonstrated in extensive experimental investigations (Acta radiol Suppl No 335, 1973) even when the contrast medium was applied in the subarachnoid space over the cerebral cortex (Gonsette 1973, Oftedal & Kayed 1973) However, Grepe & Widén (1973 a) using intracranial subarachnoid application of the medium in dogs during neurolept analgesia provoked abundant epileptogenic activity in the EEG and also clinical seizures During the early experiments in this series phenoperidine was administered intermittently (about 0 1 mg/kg/h) The epileptogenic activity in the EEG, which followed the application of the contrast medium often increased after an injection of phenoperidine and sometimes an EEG seizure was provoked In three dogs an intermittent dose of phenoperidine (1 mg), administered before the injection of the contrast medium, elicited a few discharges of epileptogenic type (sharp waves)

The doses of phenoperidine employed in the animal experiments, required to obtain a satisfactory analgesia, exceeded the doses used in clinical anaesthesiologic practice about 7 times expressed in mg/kg/h The intravenous administration of

After these precautions were taken no clinical epileptic effects were observed, not even when the radiologic exploration was extended to the intracranial basal cisterns (GREPE 1975) It may be a matter of dispute whether the prophylactic administration of diazepam is necessary in patients who are not predisposed to convulsive manifestations

Anaesthesia using phenoperidine has considerable advantages in patients submitted to neuroradiologic and neurosurgical procedures Whether the relatively low dose of the analgetic agent used in clinical anaesthesiologic practice may provoke epileptogenic changes in the EEG in connection with intrathecal administration of metrizamide is the subject of a forthcoming investigation

Conclusion Circumstantial evidence indicates that the occurrence in one patient of grand mal seizures following subarachnoid administration of metrizamide might have been due to an interaction between the contrast medium and a phenothiazine derivative Until otherwise proved phenothiazine derivatives ought to be discontinued before examination with metrizamide

SUMMARY

One single clinical complication of grand mal seizures in conjunction with the subarachnoid administration of the new non ionic contrast medium metrizamide is reported in a patient who had been taking chlorpromazine An interaction between the contrast medium and phenothiazine derivatives is considered probable

ZUSAMMENFASSUNG

Die einmalige klinische Komplikation eines Grand Mal Anfalls im Zusammenhang mit der subarachnoidalen Anwendung des neuen nicht-ionisierten Kontrastmittels metrizamide bei einem Patienten der Chlorpromazin genommen hatte, wird beschrieben Eine Wechselwirkung zwischen dem Kontrastmittel und den Phenothiazin-Derivaten wird als wahrscheinlich angesehen

RÉSUMÉ

Les auteurs présentent un seul cas de complication de crise de grand mal en rapport avec l'administration sous arachnoïdienne du moyen de contraste non ionique au métrizamide chez un malade qui prenait de la chlorpromazine Les auteurs considèrent qu'une interaction entre le moyen de contraste et les dérivés de la phénothiazine est probable

REFERENCES

AHLGREN P Lumbal myelografi med Conray Meglumin 282 og Dimer X (In Danish) Paper read at the meeting of the Nordic Society of Medical Radiology, Reykjavik, June 1973

Following myelography the contrast medium is eliminated from the subarachnoid space partly by being absorbed through its membranes, partly—and probably dominating under normal conditions—by being transported with the CSF circulation through the arachnoid granulations With the aid of computer assisted transverse axial tomography it has been demonstrated that metrizamide after spinal subarachnoid administration moves cephalad and reaches the basal cisterns and the sylvian fissures within 3 hours (GREITZ & HINDMARSH 1974) in patients examined with the same technique and the same amount of contrast medium as the present case (Fig) Still more contrast medium could be expected to be present in the intra cranial cerebrospinal fluid pathways in the latter patient at the time of the grand mal seizures as the application time in the cervical region was prolonged

In a series of 34 patients examined with metrizamide for lumbar myelography (140 mg I/ml) HINDMARSH (1975) reported signs of epileptogenic activity in the EEG of one patient after the examination A few discharges of sharp waves appeared during a 12 minute long recording This female patient was taking a phenothiazine derivative in a daily peroral administration, dixyrazine 10 mg × 3 She was the only patient on this type of medication in this series and the only one to display epileptogenic activity in the EEG

Metrizamide as such may induce minor and transient response in the EEG consisting of an increased amount of slow wave activity The incidence of these changes in records obtained 24 hours after the injection of metrizamide was 32 per cent after lumbar myelography (HINDMARSH) Similar changes in the EEG have been reported by GONSETTE (1973) and KAADA (1973) to occur in a frequency of 16 per cent This response has nothing in common with the concept of epileptogenic EEG activity

Clinical seizures or epileptogenic activity in the EEG related to spinal intrathecal administration of metrizamide thus seem to be of rare occurrence and so far related to the additional administration of drugs which are capable of provoking seizures or lowering the seizure threshold The two patients with clinical or EEG epileptic manifestations described above were both on long term treatment with phenothiazine derivatives The concentration in the central nervous system of these drugs and their potent metabolites cannot be estimated accurately in these patients However, chlorpromazine is known to pass the blood-brain barrier readily (WASE *et coll* 1956, SJÖSTRAND et coll 1965, LINDQUIST 1973) The biologic half-life of the phenothiazines is very long and various metabolites are detectable in the urine 6 to 12 months after discontinuation of these drugs (GOODMAN & GILMAN 1966) Hence, the pharmaco *logic prerequisites* for an interaction between metrizamide and phenothiazines seem to have been prevalent in these cases

The case with clinical seizures was the very first in our series in which myelography was extended to include the thoraco cervical subarachnoid space Patients on phenothiazines or similar medication have since had this medication discontinued before examination Furthermore, patients examined above the lumbar region have from then on always been given diazepam before, during and after the examination

FROM THE NEUROROADIOLOGIC SECTION, DEPARTMENT OF DIAGNOSTIC RADIOLOGY (DIRECTOR PROF O OLSSON), UNIVERSITY HOSPITAL, S 221 85 LUND, AND THE DEPARTMENT OF NEUROLOGY (DIRECTOR PROF E KUGELBERG), KAROLINSKA SJUKHUSET, S-104 01 STOCKHOLM, SWEDEN

COMPUTER ASSISTED AXIAL TOMOGRAPHY IN CEREBROVASCULAR LESIONS

S CRONQVIST, J BRISMAR, K KJELLIN and C E SÖDERSTRÖM

Computer assisted axial tomography is a new radiologic non-invasive method for examination of the brain This method was first presented in 1972 at the Annual Congress of the British Institute of Radiology (AMBROSE & HOUNSFIELD 1973), more extensive reports on the system, its clinical application and radiation dose were published by HOUNSFIELD (1973), AMBROSE (1973) and PERRY & BRIDGES (1973), respectively The method is based upon measurement of the roentgen photons transmitted through the brain, even slight differences in absorption of photons can be recorded and by means of a computer an image is constructed displaying the attenuation levels of the brain tissue on a scale from white to black The subarachnoid space, the interhemispheric fissure and the ventricular system represent areas of low absorption, i e they appear dark Tissue with higher absorption is depicted as lighter areas *The sensitivity of the method is evident from the fact that it is possible* to distinguish between the cortex and the white matter, which appear as lighter and darker areas, respectively

Intracranial lesions alter the attenuation properties of the tissue Increased absorption has been evidenced in blood clots, in calcium deposits, in metastases and in meningiomas An absorption lower than normal is encountered in necrosis, edema,

Submitted for publication 13 March 1974

BAUMGARTNER J, BRAUN J P, CARON J, CECILE J, FISCHGOLD H, GONSETTE R, HIRSCH J F, LEGRE J et METZGER J Radiculographie au Dimer-X Premiers resultats après 630 examens J Radiol Electrol 51 (1970), 557

BOISEN E og LINDHOLMER E Alvorlige myelografikomplikationer med jodtalaminmeglumin (In Danish) Nord Med 85 (1971), 520

GELLER G Komplikationen bei der lumbalen Myelographie mit Conray 282 (Contrix 28) Fortschr Rontgenstr 114 (1971), 568

GOODMAN L S and GILMAN A The pharmacological basis of therapeutics Third edition p 162 Macmillan Comp, New York 1965

GONSETTE R An experimental and clinical assessment of watersoluble contrast medium in neuroradiology A new medium—Dimer-X Clin Radiol 22 (1971), 44

— Biologic tolerance of the central nervous system to metrizamide Acta radiol (1973) Suppl No 335, p 25

— Metrizamide as contrast medium for myelography and ventriculography Preliminary clinical experiences Acta radiol (1973) Suppl No 335, p 346

GREITZ T and HINDMARSH T Computer assisted tomography of intracranial CSF circulation using a water-soluble contrast medium Acta radiol Diagnosis 15 (1974) 497

GREPE A Cisternography with the non ionic water-soluble contrast medium metrizamide A preliminary report Acta radiol Diagnosis 16 (1975), 146

— and WIDÉN L (a) Neurotoxic effect of intracranial subarachnoid application of metrizamide and meglumine iocarmate An experimental investigation in dogs in neurolept analgesia Acta radiol (1973) Suppl No 335, p 102

— — (b) Effects of cisternal application of metrizamide An experimental investigation in dogs in N_2O analgesia with and without Halothane Acta radiol (1973) Suppl No 335, p 119

HINDMARSH T Lumbar myelography with meglumine iocarmate and metrizamide A double blind investigation Acta radiol Diagnosis 16 (1975)

IRSTAM L Side effects of water-soluble contrast media in lumbar myelography Acta radiol Diagnosis 14 (1973), 647

KAADA B Transient EEG abnormalities following lumbar myelography with metrizamide Acta radiol (1973) Suppl No 335, p 380

LINDQUIST N G Accumulation of drugs on melanin Acta radiol (1973) Suppl No 325

Metrizamide, a non-ionic water-soluble contrast medium Acta radiol (1973) Suppl No 335

NILSSON E and INGVAR D H Cerebral blood flow during neurolept analgesia in the cat Acta anaesth scand 10 (1966), 47

OFTEDAL S-I and KAYED K Epileptogenic effect of water-soluble contrast media An experimental investigation in rabbits Acta radiol (1973) Suppl No 335 p 45

PRAESTHOLM J and LESTER J Water-soluble contrast lumbar myelography with meglumine iothalamate (Conray) Brit J Radiol 43 (1970), 303

SJOSTRAND S E, CASSANO G B and HANSSON E The distribution of ^{35}S-chlorpromazine in mice studied by whole body autoradiography Arch int Pharmacodyn 156 (1965), 34

SKALPE I O Lumbar myelography with Conray Meglumin 282 Report of 100 examinations with special reference to the adverse effects Acta neurol scand 47 (1971), 569

— and TALLE K Lumbar radiculography with meglumine iocarmate (Dimer X) A clinical report with special reference to the adverse effects J Oslo City Hosp 23 (1973), 121

WASE A W, CHRISTENSEN J and POLLEY E The accumulation of S^{35}-chlorpromazine in brain Arch Neurol (Chic) 75 (1956), 54

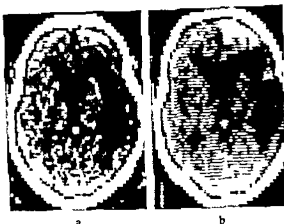


Fig 1 Right sided infarction which 9 weeks later (b) is better defined Increasing ventricular size

was the determination of its nature and accordingly the diagnosis was graded as definite (+ + +), highly probable (+ +) and probable (+) A non hemorrhagic infarct (I) was considered present in 15 of the 32 patients, an intracerebral hematoma (H) in 7 and a hemorrhagic infarct (HI) in 7 patients No absorption abnormality could be observed in 3 patients (Table 2) Regularly more than one section was made permitting also an evaluation of the extension of a lesion in the sagittal plane, thus giving a conception of the volume of the brain tissue affected

In cases with infarction the region with decreased attenuation generally corresponded to the region of supply of a relatively large artery, usually the middle cerebral (Fig 1) or the posterior cerebral artery (Fig 2) The size of the lesion varied In one case with a proven occlusion of the middle cerebral artery close to its main branching the region with decreased absorption extended from the posterior part of the frontal lobe backwards into the temporal, parietal and lateral occipital lobes In another case with only an expressive aphasia a decrease of absorption was noted within a small well defined region in the posterior part of the left temporal lobe corresponding to the area supplied by the temporal posterior artery In infarcts situated centrally in the brain the decrease of absorption could be confined to a small area (Fig 3) The outlining of an infarction was most often irregular and ill defined

When the area affected was initially small or only caused a slight decrease in absorption a complete normalisation was sometimes noted at a repeat examination Even large infarcts could be seen to change their form, eventually appearing more well defined (Fig 1) and smaller or larger with increasing time from the onset of the clinical symptoms and signs In 3 cases with a previous cerebrovascular lesion on the side contra lateral to the presently engaged, the time interval between the first lesion and the scan was 6 months, 13 months and more than two years, respectively In all these cases a region of decreased absorption was still seen on the side of the old lesion, in one case extending along the Sylvian fissure, in two through the territory supplied by the middle cerebral artery Abnormalities caused by a vascular occlusion may

Table 1

Days after onset of symptoms in 32 patients (73 examinations)

Days after onset	0–5	6–10	11–15	16–20	21–25	26–30
No of examinations	15	10	7	9	7	5
Days after onset	31–40	41–50	51–60	< 60	Unknown	
No of examinations	5	2	3	5	5	

cysts and is reported to occur also in gliomas and astrocytomas It has also been demonstrated that different types of cerebrovascular lesions have a different appearance Infarcts are thus characterized by an area with decreased and intracerebral hematoma with an area of increased attenuation (AMBROSE & HOUNSFIELD 1973 AMBROSE 1973) Recently reports from clinical series have appeared from the Massachusetts General Hospital and from the Mayo Clinic confirming these observations

The possibility of differentiating between intracerebral hematoma, non hemorrhagic infarct and hemorrhagic infarct will be discussed in this report Specific interest was directed to the progress and regress of changes with time

Material Thirty-two patients with clinically possible cerebrovascular lesions have been examined, 21 men and 11 women, aged 44 to 80 years, 22 were more than 60 years of age Seventeen patients were examined once, the remaining 15 between two and seven times at different intervals after the onset of symptoms (Table 1) In all 73 examinations have been performed

Results

The criteria established by AMBROSE were used, i e cerebral infarction is a region of decreased absorption and intracerebral hemorrhage is a region of increased absorption If both occurred simultaneously, a hemorrhagic infarction was considered likely The size of the lesion, as evident on the scan, was found to influence its perception and the certainty of the diagnosis The smaller the lesion the more difficult

Table 2

Diagnoses in the 32 patients

Diagnoses	No of cases	Definite +++	Highly probable ++	Probable +	Neg
Infarct	15	7	5	3	
Hematoma	7	4	1	2	
Hemorrhagic infarct	7	6	1		
Neg	3				3
	32	17	7	5	3

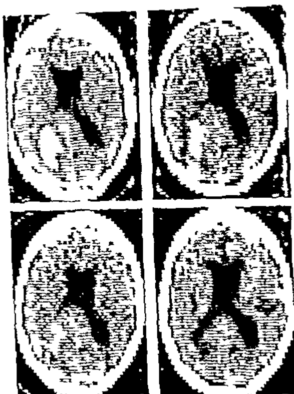


Fig 6 Repeat examinations in a case with intracerebral hemorrhage Gradual regression of the increased attenuation within 5 weeks The latest examination (lower right) displays a region with decreased absorption corresponding to the initial extension of the hematoma Narrow border of decreased absorption circumscribing the lesion at the first examination (upper left) possibly due to edema

system which seemed to be almost completely filled by blood (Fig 5) The attenuation of the intraventricular blood was equal to that of the intracerebral component

Three cases were examined on the day of the hemorrhage, the hematoma already then appearing as an area of increased absorption Repeat examinations were in one case performed on the third, fifth, sixth and seventh day without any change in attenuation The others were followed for a longer time and the locally increased absorption, indicating the hematoma, was seen to gradually diminish The whole region originally affected could still be observed also at late examinations but then as a region with decreased absorption (Fig 6) The outlining towards surrounding tissue became with time less evident and its margin less defined, i e changes developed similar to those encountered in recent infarcts

A hemorrhagic infarct was considered present whenever more or less irregular regions of increased and decreased absorption occurred (Fig 8) The part with increased absorption was usually located at the periphery of a region with decreased absorption but in some cases to its central part In only one instance these characteristics were found at an early examination performed on the second day after the onset of the symptoms In the other cases diagnosed as hemorrhagic infarct and examined more than once the initial examination performed during the first five



Fig 2

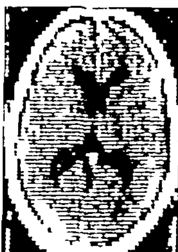


Fig 3



Fig 4



Fig 5

Fig 2 Infarction characterized by locally decreased absorption corresponding to region supplied by the right posterior cerebral artery

Fig 3 Right sided central infarction demonstrated as a vague and ill defined region with slightly decreased absorption

Fig 4 Bilateral regions of decreased absorption, on the right side due to occlusion of the middle cerebral artery six months earlier, on the left side due to a recent infarction

Fig 5 Intracerebral hemorrhage with rupture into the ventricular system The hematoma is seen on the right side as an irregular well defined region of increased absorption Areas of increased absorption partly filling the ventricular system as sign of intraventricular blood clots

thus be persistent, at least when—as in these cases—major arteries are engaged (Fig 4)

The 7 intracerebral hematomas were in three cases confined to the frontal lobes, in two to the region of the basal ganglia, in one to the thalamic region and in another one to the central part of the occipital region but without direct relation to the extension of the larger cerebral arteries The diagnosis was considered as definite, i e (+ + +), in 3 cases, the hematoma then had a rounded, slightly elongated form with somewhat irregular but well defined borders It was surrounded by a narrow rim of decreased absorption, immediately around the hematoma In two cases, with a very extensive central hemorrhage, the region of decreased absorption was seen to extend further peripherally The bleeding had also penetrated into the ventricular



deformed

The Sylvian fissure, normally appearing as a region of decreased absorption, was frequently not possible to identify at the side of the lesion This, as well as displacement, deformation or dilatation may be encountered also in the absence of decreased or increased absorption signifying a focus In cases with uncertain changes in absorption the presence of such findings could facilitate the evaluation of the scan

Discussion

Computer assisted axial tomography is a non invasive method and seems to be equal to and in some aspects superior to other neuroradiologic techniques Some difficulties are however apparent, partly of technical nature and partly connected with the interpretation of the resulting image

Table 3

Locally increased absorption within an infarction possibly signifying a hemorrhagic component is rarely seen before the fifth day after the onset of symptoms

Case No	Days after onset of symptoms									
	0–5	6–10	11–15	16–20	21–25	26–30	31–39	40–49	50–59	< 60
1	I	(H)I	HI	HI	(H)I		(H)I			(H)I
2	I	I	(H)I	HI	I					I
3	I			I	HI				I	
4		I			HI			HI		I
5	I	HI		(H)I		(H)I				
6	HI	HI								

I – infarct
H – hematoma
HI – hemorrhagic infarct

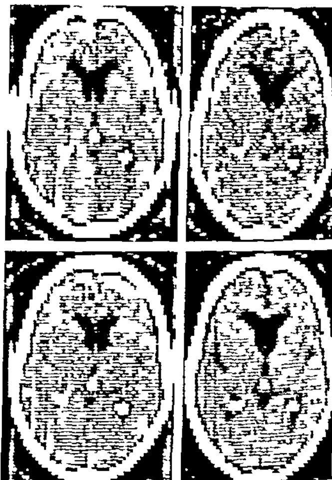


Fig 7 Same case as in *Fig* 6 Change of the position of the left choroid plexus with time (in this case within 5 weeks)

days merely demonstrated locally decreased absorption signifying a non hemorrhagic infarct After five days or more increased absorption also appeared In a few cases the increase was transitory in others it persisted and was present even after 46 days (Table 3)

Abnormalities not only appeared as changes of tissue absorption but also as a distortion of the normal anatomy The choroid plexus which due to calcific deposits often appear as small extremely high absorbing structures symmetrically localized on both sides of the midline were often displaced on the side of the lesion (Fig 7) Displacement and deformation of the ventricular system often occurred Ventricular dilatation was a common finding and at repeat examinations could be seen to increase with time (Fig 4) Such changes were encountered in 20 of the 32 patients Most often two or all three different modes of abnormality i e displacement deformation and dilatation were found simultaneously

In cases in which more than one examination was performed it could be noted that the displacement of the ventricular system decreased as well as the deformation Dilatation on the other hand increased in frequency with time and was also seen to progress probably as a sign of local or generalized atrophy (Table 4)

an edema only gradually develops and it is interesting to note that the increased absorption appearing in the so called hemorrhagic infarcts, in most of the cases was not found in the acute stage

Edema appears as a decrease in absorption It probably accounts for the narrow border of diminished attenuation surrounding an intracerebral hemorrhage The presence of edema in infarcts is indicated by the fact that they are initially ill defined but tend to become better circumscribed with time and also may appear smaller which suggests a regression of the edema

In two cases with blood in the cerebral spinal fluid at lumbar puncture, tomography on the day after the hemorrhage demonstrated regions of high absorption not only in the brain tissue but also in the ventricular system The sections obtained permitted an exact demonstration of the site at which the rupture of the intracerebral hematoma had occurred

The fact that a cerebrovascular lesion in addition to attenuation changes also cause a distortion of the normal anatomy should be stressed since this may be utilized as an aid in the diagnostic evaluation Displacement, deformation and dilatation are best demonstrated on a section parallel to the orbito-meatal line, including the choroid plexus and the pineal body On this section also the anterior part of the Sylvian fissure and the main regions supplied by the middle cerebral artery are demonstrated

In a forthcoming report, based on an extended patient material, the findings of computer assisted axial tomography in cerebrovascular lesions will be compared with the corresponding clinical and cerebrospinal fluid findings, especially those obtained by CSF spectrophotometry The last mentioned method has been found to have a high diagnostic significance in cerebrovascular lesions (Söderström & Kjellin 1972 Kjellin & Söderström 1973, 1974) This will possibly deepen our knowledge of the normal variations of the attenuation capacity of the brain tissue and involve a better understanding of the background to the images produced by the computer assisted tomography

Acknowledgements

The equipment has been put at our disposal by Statens Medicinska Forskningsråd and the Wallenberg Foundation

SUMMARY

C[illegible] cere[illegible] incr[illegible] hem[illegible] appeared Increase[illegible] three cases no abn[illegible] could be demonstrated Infarctions could be observed [illegible] of edema In [illegible] years after the onset of the symptoms intracerebral hemorrhages regressed slowly

Table 4

Time relation of anatomic changes

Case No	Day	Disloc	Deform	Dilat
5	3	+	+	0
	10	(+)	+	0
	18	0	0	+
4	10	+	+	+
	22	0	(+)	+
	46	0	0	+
	92	0	0	+
1	4	+	+	0
	7	+	+	0
	10	0	+	0
	24	0	+	+
	59	0	0	+

An adequate device for satisfactory fixation of the head is not yet available Correct positioning of the head of the patient is therefore rendered difficult Identical sections are thus not easy to obtain at repeat examinations, which may lead to incorrect conclusions when comparing the findings at different examinations

It was found difficult to exactly assess the extension of a lesion in the sagittal plane using multiple sections This difficulty may be overcome by increased experience By means of the computer it may even be possible to find an objective method for recording the height of a lesion

On sections close to the base of the skull, regions with increased absorption due to a cerebral lesion may be difficult to distinguish from similar alterations caused by bony structures The same problem is encountered in cerebral lesions localized close to the lateral aspect of the sphenoid ridge—the pterion region This structure often causes an elongated area of increased absorption between the inner table of the skull and the Sylvian fissure Its presence in this region, often engaged in occlusion of the middle cerebral artery, may lead to an erroneous diagnosis of a hemorrhagic infarct Another cause to a wrong conception may be compressed brain tissue In one case with an extremely large infarction involving the frontal, parietal, central and occipital regions on one side and extending into the contralateral frontal lobe, an area of increased absorption appeared laterally to the lesion in the last mentioned lobe This was supposed to be caused by the expansivity of the lesion compressing the brain tissue

Locally increased attenuation occurring within an infarct and in the present material considered as probably a hemorrhagic component may similarly be a sign of compression of tissue The cause of such a compression might be an edema developing secondary to the vascular lesion It is known (LINDGREN 1958) that such

PERRY B J and BRIDGES C Computerized transverse axial scanning (tomography) Part 3 Radiation dose considerations Brit J Radiol 46 (1973), 1048
SODERSTRÖM C E och KJELLIN K Den diagnostiska signifikansen av likvorspektrofotometri vid vaskulära nervsjukdomar (In Swedish) Abstract in the Proceedings of the Annual general meeting of the Swedish Society of Medical Sciences 1972, p 301
X ray diagnosis peers inside the brain Technology Review New Scient 54 (1972), 207

ZUSAMMENFASSUNG

Eine komputer unterstutzte Tomographie wurde bei 32 Patienten mit einer klinisch moglichen cerebro vaskularen Schadigung vorgenommen Eine geringere Absorption als Zeichen einer Infarcierung wurde bei 15 eine geringere Absorption als Zeichen einer Blutung bei 7 Patienten gefunden In anderen 7 Fallen war das gleichzeitige Auftreten einer erhohten und erniedrigten Absorption deutlich die als hamorrhagische Infarcierung diagnostiziert wurde Eine erhohte Absorption kann auch auf einem Kompressionseffekt oder einem Oedem beruhen In drei Fallen konnte kein abweichendes Bild nachgewiesen werden Infarcierungen konnten Jahre nach Einsetzen der Symptome beobachtet werden intra kraniale Blutungen gingen langsam zuruck

RESUME

Trente deux malades présentant des signes cliniques faisant penser à des lésions cerebro-vasculaires possibles ont subi une *tomographie axiale transverse traitee par* ordinateur On a trouvé une diminution de l absorption comme signe de ramollissement dans 15 cas et une augmentation de l absorption comme signe d hémorragie dans 7 cas Dans 7 autres cas on a trouve simultanément des signes d augmentation et de diminution de l absorption qui ont été diagnostiqués comme ramollissement hémorragique L augmentation de l absorption pourrait aussi dépendre d un effet de compression par l oedème Dans 3 cas on n a pas trouvé d absorption anormale On pourrait observer des ramollissements des années apres le début des symptomes les hemorragies intracérébrales ont régresse lentement

REFERENCES

AMBROSE J Computerized transverse axial scanning (tomography) Part 2 Clinical application Brit J Radiol 46 (1973) 1023

— and HOUNSFIELD G Computerized transverse axial tomography Brit J Radiol 46 (1973) 148

BAKER H L CAMPBELL J K HOUSER D W REESE D F SHEEDY P F and HOLMAN C B Computer assisted tomography of the head An early evaluation Mayo Clin Proc 49 (1974) 17

HOUNSFIELD G N Computerized transverse axial scanning (tomography) Part 1 Description of system Brit J Radiol 46 (1973) 1016

KJELLIN K and SÖDERSTROM C E Diagnostic significance of the CSF spectrophotometry in cerebrovascular diseases *In* X International Congress of Neurology p 167 International Congress Series No 296 Excerpta Medica Amsterdam 1973

— — Diagnostic significance of CSF spectrophotometry in cerebrovascular diseases J Neurol Sci 23 (1974) 359

LINDGREN S Course and prognosis in spontaneous occlusion in cerebral arteries *Acta* psychiat scand 33 (1958) 343

NEW F J, SCOTT W R SCHNUR J A DAVIS K R and TAVERAS J M Computerized axial tomography with the EMI scanner Radiology 110 (1974) 109

OLDENDORF W H Isolated flying spot detection of radiodensity discontinuities displaying the internal structural pattern of a *complex object I R E Transactions on Bio* medical Electronics 8 (1961) 68

fossa (BAKER 1963, 1972, GASS 1963, SCANLAN 1964, HITSELBERGER & HOUSE 1967, REESE & BULL 1967, STITT et coll 1968, HASTINGS-JAMES 1969) However, oily contrast media were found to be unpracticable for use above the tentorial level as they could not be removed after the examination Even when strictly confined to the infratentorial region these media cannot be completely evacuated Furthermore, the physical properties such as viscosity, surface tension and attenuation capacity of the iodized oils make them less than optimal Therefore the information obtained with gas or with iodized oils is incomplete especially with regard to more slender structures and narrow spaces A water-soluble contrast medium with suitable physical properties is likely to offer more information

Recently a new water-soluble contrast medium, metrizamide, which is well tolerated by neural tissue, has become available for experimental investigations and preliminary clinical trials This non ionic compound is designed for examination of the subarachnoid space and has been found to have low neurotoxic effects (Acta radiol Suppl No 335, 1973) Experiences in experimental investigations in dogs (GREPE & WIDÉN 1973 a, b) and in clinical myelography (HINDMARSH, to be published) seemed to justify the use of metrizamide also for examination of the basal cisterns of the posterior cranial fossa

Material and Methods

The material comprises 11 patients, 6 males and 5 females, varying in age between 29 and 61 years The indication for the examination usually was to exclude the presence of an expanding lesion in the basal cisterns or to obtain more information about the site, size and shape of a known tumour by establishing its relationship to surrounding anatomic structures

Anti-convulsive prophylaxis with diazepam was given, usually 10 mg before, 10 mg during and 5 mg every 4 hours up to 20 hours after the examination, otherwise no premedication was given With one exception the patients were examined without general anesthesia

The procedure was performed with a Mimer II equipment (Siemens Elema) supplied with a chair, rotatable in two planes around a transverse horizontal as well as around a longitudinal axis The chair could also be transformed into a stretcher, rotatable around the transverse axis

Metrizamide was administered to the intracranial basal cisterns following either lumbar, suboccipital or foramen ovale puncture In the concentrations used, metrizamide is heavier than CSF Irrespective of the route of administration a layering between contrast medium and CSF will occur The general principle in examining the intracranial subarachnoid space must therefore be one of a fractional examination, only one part at a time being examined The region of interest should, as far as possible, be positioned so as to form a pouch directed downwards in order to avoid escape of contrast medium

FROM THE DEPARTMENT OF NEURORADIOLOGY (DIRECTOR T GREITZ), KAROLINSKA SJUKHUSET, S-104 01 STOCKHOLM, SWEDEN

CISTERNOGRAPHY WITH THE NON-IONIC WATER-SOLUBLE CONTRAST MEDIUM METRIZAMIDE

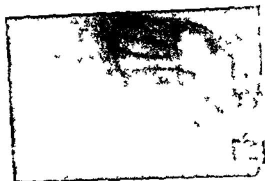
A preliminary report

ARNE GREPE

Although the intracranial basal cisterns have long been demonstrated by encephalography (DYKE & DAVIDOFF 1934, LILIEQUIST 1959) they still constitute a challenge to radiologic exploration The superimposition by bony structures of the skull base and the low contrast differences obtained by thin layers of gas are two concurrent factors limiting the possibilities to distinguish and to assess details of the intracisternal anatomy The efforts to overcome these obstacles have followed two lines—continuous improvement in the encephalographic technique on the one hand and the use of positive contrast media on the other In particular the introduction and development of tomography has made it possible to extract more encephalographic information of anatomic detail in the basal cisterns (DI CHIRO 1961, METZGER 1967, FISCHGOLD et coll 1969)

Water soluble contrast media have not been used in the basal cisterns because of their neurotoxic effects Iodized oils do not have this early noxious potential but with regard to long term effects their removal from the subarachnoid space after examination as far as possible is recommended Once introduced by MALIS (1958) for examination of the foramen magnum region the intracranial use of the oily media was soon extended to include the whole subarachnoid space in the posterior cranial

Submitted for publication 2 April 1974



a



b

Fig 2 Same patient as in Fig 1 Metriz

projections were taken subtraction technique being employed in the first of these views and tomography and stereoscopy in both Following removal of the needle the patients were turned with the head and neck hyperextended for examination in the axial projection in the prone position The turning manoeuvre was performed with care to keep the contrast medium within the cisterns of the posterior fossa

The approach through foramen ovale was used in 5 patients The puncture was usually performed during a very short general anesthesia using Brietal Sodium In one patient the entire examination was carried out in neurolept analgesia during continuous EEG control In 2 patients with large expanding lesions in the pontine angle one meningioma and one acoustic neurinoma the position was supine The other 3 patients one with a small acoustic neurinoma referred for a follow up examination after radiation surgery and two with the syndrome of trigeminal neuralgia were examined in the sitting position These three patients had the head and neck hyperextended to enable axial projection of the posterior cranial fossa In order to get the posterior surface of the petrous bone horizontal the chair was rotated forward about 70 and around the longitudinal axis about 30 to the contralateral side The head of the patient was rotated in the same direction about 15 Mainly axial oblique

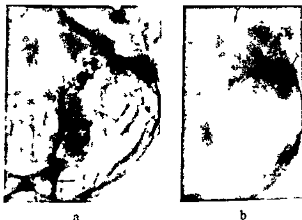


Fig 1 Distribution of contrast medium to the basal cisterns after lumbar injection of 6 ml metrizamide 300 mg I/ml Axial projection a) without and b) with tomography Laminar flow of medium along lowermost part of cervical subarachnoid space (→) with filling of the subarachnoid space around the cerebellar hemisphere (+→) and the cerebellopontine cistern (o→)

The lumbar approach was used in 2 patients with possible pontine angle lesion The patients were placed in the lateral recumbent position on the side to be examined Following puncture at the L3–L4 level the head end of the couch was tilted 10° downwards In both cases initial subtraction in the axial projection of the posterior cranial fossa was arranged for, i e the patient kept the head and neckhyperextended In one patient the head was kept straight in this position, in the other patient it was rotated 45° with the face towards the couch Metrizamide 300 mg I/ml was slowly injected in an amount of 5 to 6 ml and the flow of the medium to the intracranial cisterns was controlled with fluoroscopy Axial, oblique axial and lateral stereoscopic projections were used, supplemented by subtraction technique in the axial projection In one patient tomography was performed in the axial and lateral projections

The suboccipital approach was used in 4 patients, 3 with acoustic neurinoma and 1 with trigeminal neuralgia They were examined on the stretcher, two patients prone and the other two patients in the lateral recumbent position During the puncture the patient's head was kept straight and flexed In one patient following puncture in the prone position, the head was subsequently turned 45° to the side contralateral to the side of the lesion, in the other patient the head was kept straight By elevation of the head end of the stretcher before injection, the posterior surface of the petrous bone of the first patient and the clivus of the second patient was brought roughly to the horizontal position A total amount of 3 to 4 5 ml metrizamide 300 mg I/ml was injected slowly in an attempt to administer the medium selectively to the cerebello-pontine or pontine cistern

The other two patients both had acoustic neurinomas in the pontine angle, one a small tumour, one a very large one The examination was performed in the lateral recumbent position, the patients keeping the head straight and flexed The head end of the couch was lowered about 5° in order to obtain flow of CSF at the puncture and to achieve a suitable intracranial distribution of the contrast medium In both patients the amount of metrizamide injected did not exceed 4 ml The application of the medium was controlled by fluoroscopy in the lateral projection in order to avoid metrizamide distribution above the tentorial level Lateral and half-axial p a

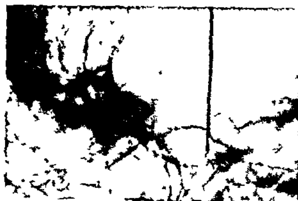
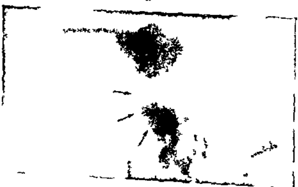


Fig 4 Cisternography with sub occip tal inject on of 4 ml metri zamide 300 mg I/ml patient in lateral recumbent position, half axial p a view Small tumour (→) at the entrance of the in ternal aud tory meatus partly superimposed by contrast me dium around the cerebellar hemisphere



a



b

F g 5 Encephalography (tomography) in a) half axial and b) lateral project ons in a patient with a large acoust c neurinoma (→)

imposition of cerebellar structures on the basal cisterns occurred in most projec tions which in combination with the low intracranial concentration of metrizamide made assessment of intracisternal details *difficult* The presence of an expanding le sion in the pontine angle could however be excluded with confidence in both *patients* The decrease in concentration caused by the dilution of the *contrast* me dium as met with in these two examinations also seemed to impair the *possibilities*



a b

Fig 3 a) Encephalography b) Selective distribution of metrizamide to the cerebellopontine cistern after suboccipital injection of 3 ml metrizamide 300 mg I/ml with patient in prone oblique position Half axial p a views Small lobulated tumour (→) at the entrance (→) of the internal auditory meatus (not filled with contrast medium)

axial and lateral projections were used Subtraction technique, stereoscopy and tomography were included when possible

As the route through foramen ovale was the one chosen for the very first administrations of metrizamide to the basal cisterns, the concentration and particularly the amount of contrast medium injected varied, the concentration being between 170 and 300 mg I/ml and the total amount between 0 35 and 5 5 ml

After-care Irrespective of route of administration, the patient was moved into a supine half-sitting position after the examination to direct the contrast medium to the spinal subarachnoid space The patient was kept in bed with the head end raised and was observed for 20 hours The day after the examination the patient was interviewed and examined with regard to clinical signs EEG recordings were not considered useful because of interference from the heavy anti-convulsive prophylaxis with diazepam Possible long term effects have not been assessable so far due to the relatively short observation time (not exceeding 3 months)

Results

Metrizamide administered by the *lumbar route* could be moved from the injection site to the intracranial basal cisterns by the effect of gravity However, a continuous mixing of metrizamide and CSF was apparent, probably partly by diffusion and partly due to a wash out by the CSF circulation The latter effect was evident within the spinal canal but was still more accentuated intracranially (Fig 1) When the medium reached the cranial cavity it spread around the cerebellar hemisphere and in addition filled the basal cisterns on the lowermost side (Fig 2) Filling of the narrow subarachnoid space around the cerebellar hemisphere evidently depended on the position of the head This compartment of the subarachnoid space was more extensively filled when the head was kept straight than when the head was rotated with the face towards the stretcher Once filled with contrast medium, this compartment could not be emptied during the examination As a consequence a disturbing super-

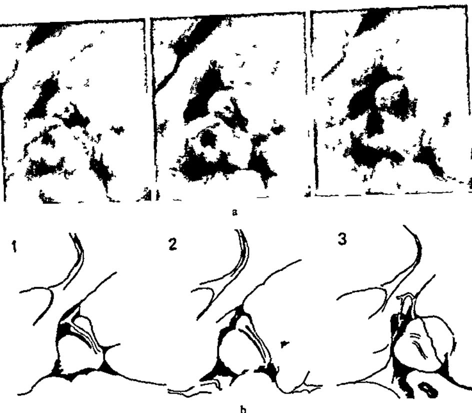


Fig 7 Same patient as in Figs 5 and 6 Cisternography in the lateral recumbent position after suboccipital injection of 3 5 ml metrizamide 300 mg I ml a) Consecutive tomographic sections in the sagittal plane b) Explanatory drawings Lobulated tumour invaginates and deforms the cerebellar hemisphere Relationship of vessels to the tumour clearly demonstrated

the projection of choice The diagnostic procedure did not seem to interfere with the result of the blocking subsequently performed in patients with trigeminal neuralgia

Supplementary techniques Irrespective of the site of injection very complex images were obtained when the region of interest was superimposed on contrast medium surrounding the cerebellar hemisphere and also on the bony structures of the skull base For this reason supplementary techniques as subtraction, tomography and stereoscopic views were used and proved to be of considerable value Tomography in the lateral projection yielded detailed information on the relationship of a large tumour to adjacent structures (Figs 6 7, 8) The stereoscopic views used in all projections proved to be indispensable for analysis of the superimposed anatomic structures in detail including the course of the surrounding vessels

Acute clinical tolerance The introduction of metrizamide into the cisterns caused a local sensation of pressure in those cases in which the amount of contrast medium exceeded 3 ml This sensation was of low intensity and was transitory, it usually dis-



Fig 6 Same patient as in Fig 5 … recumbent position a… amide 300 mg I/ml …

of directing the medium to various intracranial locations or bringing it back to the spinal subarachnoid space after the examination

The suboccipital approach yielded significantly higher intracranial concentration of metrizamide than the lumbar one In one patient with a small acoustic neurinoma examined in the prone position with the head turned 45° to the contralateral side, a selective distribution of the contrast medium to the cerebello-pontine cistern was obtained (Fig 3) In the other patient the clinical problem was to establish the relationship between a tortuous basilar artery and the trigeminal nerve root in a case of trigeminal neuralgia, during examination in the prone position the head was kept straight to get a uniform distribution of contrast medium to the pontine cistern In this patient the contrast medium also filled the chiasmatic cistern

As to the previously mentioned 2 patients with acoustic neurinomas examined in the lateral recumbent position, the small tumour was more difficult to assess in detail than the large one The difficulties encountered with the small tumour were due to superimposition of contrast medium surrounding the cerebellar hemisphere (Fig 4) The large tumour in the same location could, however, be evaluated in detail with regard to site, size, shape and relationship to surrounding structures, particularly to the cerebellar hemisphere and to vessels surrounding the tumour (Figs 5, 6, 7, 8) These details could be assessed not only in the half-axial p a projection but in the lateral projection as well The definition in the axial projections following the turning manoeuvre was, however, not adequate from the diagnostic point of view

The approach through the foramen ovale was used in the first examinations with cisternal application of metrizamide because the high selectivity of this approach permitted the use of small doses in comparatively low concentrations These examinations were made to exclude operable lesions in patients with trigeminal neuralgia referred for percutaneous phenol blocking of the gasserian ganglion As no adverse reactions were recorded initially, the amount and the concentration of metrizamide were successively raised in later examinations to the level later used with the suboccipital approach

The foramen ovale route was thus used also in cases of known or possible expansive lesions in the pontine angle With this approach the examinations were more time-consuming as the puncture procedure required general anesthesia One obvious advantage was that the position of the needle permitted subtraction technique in

In the analysis of the potentials of a water soluble contrast medium for use in the basal cisterns, the influence of the site of injection was first examined Intracranial selective administration of contrast medium in sufficient concentration following lumbar puncture would constitute a major advantage However, from the limited experience from two examinations using the lumbar approach it may be stated that this route of administration does not give a sufficiently high intracranial concentration of the medium

The contrast medium could be moved by gravity into the basal cisterns but the intracranial concentration of the medium was too low to be diagnostic with regard to small structures Still this result was better than that obtained by GONSETTE (1973) who claimed that it was impossible even to move the contrast medium to the cervical area after lumbar injection The present results are in accordance with those of HINDMARSH who moved the contrast medium into the cervical subarachnoid space but often had to use a supplementary lumbar injection of the medium to be able to examine the cervical region in full extent The techniques reported to be used in examinations with oily contrast media cannot be adopted when using metrizamide

The limited information of intracranial structures obtained following lumbar administration of metrizamide indicates that this route probably will not give satisfactory results Hence, from these preliminary experiences it was concluded that even the use of larger amounts of medium administered from a lumbar puncture would not essentially improve the results, furthermore, this would imply increased amounts of medium also supratentorially Whether a concentration of the medium higher than 300 mg I/ml can be used has yet to be evaluated by animal experiments before it may be contemplated clinically.

The results obtained with suboccipital injection of contrast medium demonstrated this, more selective, route of administration to be superior to the lumbar one Whether the patient should be examined in the prone or the lateral recumbent position is evidently not only dependent on the region of the basal cisterns which is the object of examination but also on the site and size of the expanding lesion

This has to be fully surrounded by the contrast medium to be assessable When the posterior fossa is the object of examination, the medium injected has to be collected in the compartment of interest while the distribution of medium to the supratentorial subarachnoid space is kept to a minimum This postulates that a fair estimate of the size of the lesion can be made, in order to enable the choice of an adequate technique, this was also the case in the tumour cases included In patients with trigeminal neuralgia examination with metrizamide was used instead of encephalography to exclude an expanding lesion affecting Meckel's cave or the cerebellopontine cistern

T [illegible]
inv [illegible]
rel [illegible] of the needle furthermore restricts the number of projections

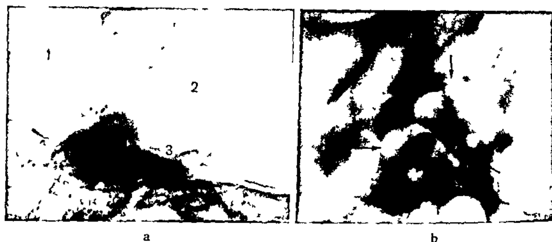


Fig 8 a) Normal anatomy in the sagittal plane as demonstrated by post mortem cisternography b) Comparison with the change produced by the expansive lesion (→) in the pontine angle (same patient as in Figs 5-7) 1 = uncus, 2 = cerebellar hemisphere, 3 = facial and statoacoustic nerves

appeared within half an hour Otherwise the examination did not produce any discomfort which could be attributed to the presence of the contrast medium Most of the patients, however, experienced headache localized to the frontal region 3 to 4 hours after the examination, sometimes in combination with slight nausea These late appearing symptoms were, with one exception, of a slight to moderate intensity and disappeared after administration of light analgetics In one patient a more widespread supratentorial distribution of the medium (Fig 10) caused no symptoms during the examination A late frontal headache was rather intense but not accompanied by objective signs, it had completely disappeared the following day

Discussion

The appearance of the basal cisterns is used to evaluate neural structures within or bordering on this compartment of the subarachnoid space Another type of clinical problem concerns the patency of the CSF pathways In the investigation of structures bordering the cisterns gas usually offers full information but due to the small absorption differences only in a limited number of projections, even when the examination is supplemented by tomography This limitation of gaseous media becomes still more evident when details of the intracisternal anatomy are the subject of examination For this purpose a contrast medium giving steeper absorption gradients is preferable, to achieve this positive contrast media have to be employed Until now only iodized oils have been available for intentional use in the cisterns, although water-soluble media have been applied for ventriculography The attenuation of oily media are, however, usually too high Furthermore, other physical properties, particularly the high surface tension characterizing these media, make them less suitable for penetration and adequate demonstration of narrow compartments within the subarachnoid space

which can be used until the needle has been removed The first of these two viewpoints carries weight enough to demand strict indications for this diagnostic procedure, which to-day seems justified only when encephalography or any other radiologic method with a lower rate of complications cannot give the same information Suboccipital puncture should be controlled with fluoroscopy to ensure optimal security, this is the case particularly when the anatomy in the cisterna magna is known from previous vertebral angiography or encephalography.

The limited number of projections available with the suboccipital technique may be overcome by using a suitable catheterization technique The method for selective ventriculography using the chain guide technique (CORRALES 1973) may be used also for selective injection in the cisterna magna with the intention to fill the cisterns However, a transcerebral approach can never be justified only to achieve selective injections in the cisterna magna

In examination of the cerebello-pontine cisterns a high selectivity is obtained when metrizamide is administered through a needle introduced in the subarachnoid space in Meckel's cave The route through the foramen ovale for exploration of the basal cisterns with positive contrast media has previously been proposed by JELASIC (1955) and JIMENEZ et coll (1966) using iodized oils Whether this approach is superior to the suboccipital one cannot be evaluated at this stage In patients with trigeminal neuralgia referred for injection treatment with phenol blocking of the gasserian ganglion, the same injection needle can evidently be used for a diagnostic procedure and for a subsequent therapeutic one According to our very limited experience, metrizamide cisternography carried out with one and the same needle does *not interfere* with the result of the phenol blocking This is the subject of an investigation in progress (HÅKANSSON & GREPE)

No objections can be raised about the transganglionic approach for cisternography and phenol blockings in patients with trigeminal neuralgia Although nothing seems [illegible]

[illegible] only be used in combination with a therapeutic puncture or possibly in case a suboccipital puncture fails or is contraindicated

In the present series the axial projection was only used following a turning manoeuvre in the patients with suboccipital injection of the contrast medium, which may explain the decrease in concentration of the medium in comparison with the situation before the patient was moved Obtaining the axial projection by hyperextending the head and neck when the patient is still in the lateral recumbent position may be assumed to improve the quality of the images

Additional information obtainable with supplementary techniques such as tomography, stereoscopy and subtraction have to be thoroughly analysed The extent to which tomography in the lateral projection furnished new information about the anatomy of the pontine angle when the superimposed petrous bones were blurred out was striking Also the stereoscopic views seemed to be of great help in analysing



a



b

Fig 9 Cisternography approach through the foramen ovale Total injection of 3 5 ml metrizamide 300 mg I/ml Small acoustic neurinoma (→) in oblique a) axial and b) frontal views

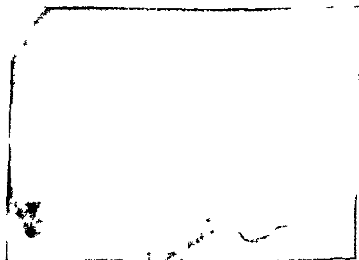


Fig 10 Unintentional filling of the supratentorial CSF pathways following suboccipital injection of 3 ml metrizamide 300 mg I/ml

which can be used until the needle has been removed The first of these two viewpoints carries weight enough to demand strict indications for this diagnostic procedure which to day seems justified only when encephalography or any other radiologic method with a lower rate of complications cannot give the same information Suboccipital puncture should be controlled with fluoroscopy to ensure optimal security, this is the case particularly when the anatomy in the cisterna magna is known from previous vertebral angiography or encephalography

The limited number of projections available with the suboccipital technique may be overcome by using a suitable catheterization technique The method for selective ventriculography using the chain guide technique (CORRALES 1973) may be used also for selective injection in the cisterna magna with the intention to fill the cisterns However, a transcerebral approach can never be justified only to achieve selective injections in the cisterna magna

In examination of the cerebello-pontine cisterns a high selectivity is obtained when metrizamide is administered through a needle introduced in the subarachnoid space in Meckel's cave The route through the foramen ovale for exploration of the basal cisterns with positive contrast media has previously been proposed by JELASIC (1955) and JIMENEZ et coll (1966) using iodized oils Whether this approach is superior to the suboccipital one cannot be evaluated at this stage In patients with trigeminal neuralgia referred for injection treatment with phenol blocking of the gasserian ganglion, the same injection needle can evidently be used for a diagnostic procedure and for a subsequent therapeutic one According to our very limited experience, metrizamide cisternography carried out with one and the same needle does not interfere with the result of the phenol blocking This is the subject of an investigation in progress (HÅKANSSON & GREPE)

No objections can be raised about the transganglionic approach for cisternography and phenol blockings in patients with trigeminal neuralgia Although nothing seems to be known about possible adverse effects of transganglionic puncture, for instance symptomatic neuralgia is not inconceivable Therefore, this route should probably only be used in combination with a therapeutic puncture or possibly in case a suboccipital puncture fails or is contraindicated

In the present series the axial projection was only used following a turning manoeuvre in the patients with suboccipital injection of the contrast medium, which may explain the decrease in concentration of the medium in comparison with the situation before the patient was moved Obtaining the axial projection by hyperextending the head and neck when the patient is still in the lateral recumbent position may be assumed to improve the quality of the images

Additional information obtainable with supplementary techniques such as tomography, stereoscopy and subtraction have to be thoroughly analysed The extent to which tomography in the lateral projection furnished new information about the anatomy of the pontine angle when the superimposed petrous bones were blurred out was striking Also the stereoscopic views seemed to be of great help in analysing

superimposed structures delineated by the medium The subtraction technique offered least additional information of the supplementary techniques applied This may have been due to a less satisfactory fixation, and also to the fact that only one projection could be used for subtraction However, the potential of subtraction in this context has to be further explored

Evaluation of a compartment of the subarachnoid space requires it to be filled with contrast medium Thus a narrow compartment is easier to examine than a spacious one, the fluid of which inevitably produces a dilution of the medium and ensuing layering of contrast solutions of different concentrations With regard to the basal cisterns in the posterior fossa undue dilution may be avoided by examining the patient in the lateral recumbent position as the tentorium prevents supratentorial filling of contrast medium until the level of the notch has been reached The topographic anatomy of the skull base a priori limits the possibilities to examine the pontine cistern in the prone position if movement of medium to the supratentorial CSF pathways is to be avoided This is illustrated by the fact that unintentional undue filling of the supratentorial CSF pathways occurred in such an examination performed in the prone position (Fig 10)

Problems of identifying cranial nerve structures within the basal cisterns have been analysed by GREPE (1975) Among cranial nerves which could be identified at clinical cisternography were included the optic, oculomotor, trigeminal, facial and statoacoustic nerves The contrast obtained was, however, too low for diagnostic purposes However, much improvement in technique does not seem to be needed in order to obtain a method allowing the examination of cranial nerves within the cisterns

Clinically the tolerance to administration of metrizamide to the basal cisterns in the posterior cranial fossa seemed to be good with regard to short term effects The subjective symptoms were few and considerably less marked than those experienced at encephalography This was invariably stated by the patients who had experience of both procedures No record was made of clinical neurologic signs or symptoms attributable to the cisternal application of metrizamide Possible long term effects cannot yet be evaluated as the observation period is too short, still less than a few months

Preliminary examinations indicate that the amount of useful projections in cisternography may be increased by the use of a positive water-soluble contrast medium Hence, it has finally been possible not only to examine the structures in the cisterns in different frontal projections but in the lateral projection as well The physical properties of metrizamide in the concentration used allow filling of narrow subarachnoid spaces which have not been filled with oily contrast media A new concept of the topographic anatomy of the cisterns in the posterior fossa may be obtained The vessels running in the narrow subarachnoid spaces may now be examined to an extent that was not possible earlier

Conclusions

The present preliminary examinations of the basal cisterns in the posterior fossa, although few in number, indicate that clinical cisternography with metrizamide can be carried out safely when the amount administered is kept low and when anticonvulsive prophylaxis is given The physical properties of metrizamide in concentrations not exceeding 300 mg I/ml make selective injections preferable Hence, the suboccipital injection and, in selected cases, the transoval approach seem to be preferable to lumbar injection Due to the low surface tension and the comparatively high attenuation, information otherwise not accessible can be obtained both with regard to anatomic details and with regard to the relationship between normal and diseased structures

SUMMARY

In 11 patients the basal cisterns in the posterior cranial fossa were examined with the new water soluble compound metrizamide Promising results were obtained when the medium was administered suboccipitally or through the foramen ovale but less favourable after lumbar administration The clinical tolerance of the compound with regard to short term effects was good

ZUSAMMENFASSUNG

Bei 11 Patienten wurden die basalen Zisternen in der hinteren Fossa cranialis mit der neuen Wasser loslichen Vereinigung Metrizamide untersucht Es wurden gunstige Ergebnisse erhalten, wenn das Medium suboccipital oder durch das Foramen ovale verabfolgt wurde, weniger gunstige jedoch nach lumbaler Gabe Die klinische Toleranz war hinsichtlich kurzzeitiger Effekte gut

RÉSUMÉ

Les citernes basales de la fosse posterieure du crane ont eté examinées chez 11 malades avec le nouveau compose hydrosoluble de métrizamide Les auteurs ont obtenu des resultats encourageants quand ce moyen de contraste est injecte par voie sous-occipitale ou à travers le foramen ovale Mais apres injection lombaire les resultats sont moins favorables La tolérance clinique de ce composé a eté bonne en ce qui concerne les effets à court terme

REFERENCES

BAKER H L JR Myelographic examination of the posterior fossa with positive contrast medium Radiology 81 (1963), 791

— Cerebellopontine angle myelography J Neurosurg 36 (1972), 614

CORRALES M A technique for selective ventriculography Acta radiol Diagnosis 14 (1973), 513

DI CHIRO G An atlas of detailed normal pneumoencephalographic anatomy Charles C Thomas Publ, Springfield, Illinois 1961

DYKE C G and DAVIDOFF L M Recent advances in encephalography Radiology 22 (1934), 461
FISCHGOLD H, BONNEMAZOU A, FREDY D et METZGER J La citerne optochiasmatique et son contenu Aspects normaux J Radiol 50 (1969), 121
GASS H Pantopaque anterior basal cisternography of the posterior fossa Amer J Roentgenol 90 (1963), 1197
GONSETTE R E Metrizamide as contrast medium for myelography and ventriculography Preliminary clinical experiences Acta radiol (1973) Suppl No 335, p 346
GREPE A Anatomy of the cranial nerves in the basal cisterns A radiologic post mortem investigation Acta radiol Diagnosis 16 (1975) 17
— and WIDÉN L Neurotoxic effect of intracranial subarachnoid application of metrizamide and meglumine iocarmate An experimental investigation in dogs in neurolept analgesia Acta radiol (1973) Suppl No 335, p 102
— — Effects of cisternal application of metrizamide An experimental investigation in dogs in N_2O analgesia with and without halothane Acta radiol (1973) Suppl No 335 p 119
HÅKANSSON S and GREPE A Unpublished data
HASTINGS JAMES R The anatomy of the posterior fossa in relation to positive contrast cisternography Radiology 92 (1969), 1065
HINDMARSH T Myelography with the nonionic water soluble contrast medium metrizamide To be published in Acta radiol Diagnosis
HITSELBERGER W E and HOUSE W Acoustic neurinoma the adaptation of polytomography to the early diagnosis of acoustic tumours Amer Surg 33 (1967) 791
JELASIC F Über die rontgenologische Darstellung der basalen Zisternen mittels direkter Applikation des Kontrastols durch das Foramen ovale Nervenarzt 26 (1955) 139
JIMENEZ A P, LYONNET J and SILVA F A new diagnostic method by trans oval cisternography Acta radiol Diagnosis 5 (1966) 662
LILIEQUIST B The subarachnoid cisterns An anatomic and roentgenologic study Acta radiol (1959) Suppl No 185
MALIS L I The myelographic examination of the foramen magnum Radiology 70 (1958) 196
Metrizamide, a non ionic water soluble contrast medium Acta radiol (1973) Suppl No 335
METZGER J Le signe du chiasma de face en pneumographie hypocycloïde Rev Neurol 117 (1967), 666
REESE D F and BULL J W D Positive contrast demonstration of normal internal acoustic meatus, Meckel s cave and jugular foramen Amer J Roentgenol 100 (1967) 650
SCANLAN R L Positive contrast medium (Iophendylate) in diagnosis of acoustic neuroma Arch Otolaryng 80 (1964) 698
STITT H L, DUNBAR H S, SCHICK R W and DUNN A A Pontocerebellar cisternography Radiology 90 (1968), 942

FROM THE DEPARTMENT OF DIAGNOSTIC RADIOLOGY, AKADEMISKA SJUKHUSET, UNIVERSITY OF UPPSALA, S-750 14 UPPSALA, SWEDEN

A TOMOGRAPHIC TEST OBJECT

H F. WILBRAND

Knowledge of the maximum permissible distance between sections in tomography of objects of known size, particularly minor ones, is of practical importance In tomography of the middle and inner ear a distance of 0 5 to 1 mm is used to demonstrate details of such structures as the ossicles and the vestibular aqueduct In order to obtain optimal visual perception of very small details it is necessary that their contours lie to the greatest possible extent in the tomographic plane The theoretical tomographic plane cannot be visually perceived Owing to this restriction, the term 'layer thickness' has to be adopted The 'layer thickness' is defined as the sum of sharply reproduced geometric planes in the object up to the borderlines against visually perceived unsharpness The term 'layer thickness' is often unfortunately used in connection with tomography of composite objects and causes confusion since there is no such layer, but a relief instead The heterogeneity of the relief in the tomographic radiation image of a composite object (GLADYSZ 1966, ECKERDAL 1973) is proof of the inadequacy of the term 'layer thickness' in describing qualities of the tomogram in clinical practice The term is useful, however, for characterizing the geometric reproduction capabilities of a tomographic system, i e the tomographic equipment together with the photographic system A test phantom will reveal the mechanical stability of the tomographic equipment and permit standardized and reproduceable determination of its geometrical imaging properties It may also be used for comparison between different tomographic systems provided

Submitted for publication 7 January 1974

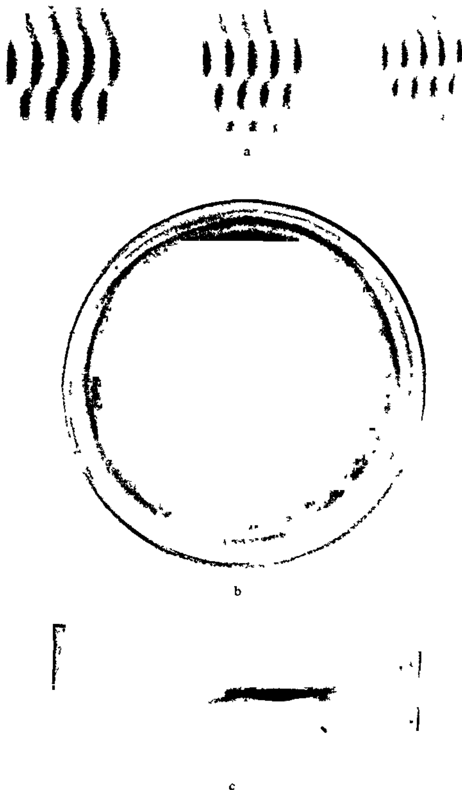


Fig 1 (For legend see opposite page)

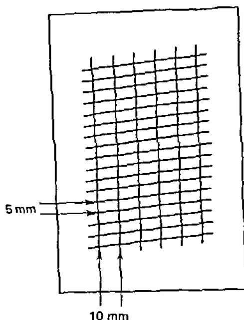


Fig 2 Arrangement of a metal ball plane in a plexiglass phantom A metal ball is placed at each junction of the furrows depicted by the dark lines

that the test series are performed on equipment functioning according to the same principles The use of a test object for comparison of tomographic equipment is superior to a clinical comparison Clinical comparison by evaluation of tomograms obtained with different angles and movements is difficult and has only limited validity

The 'layer thickness' of an object in the tomogram is estimated by assessing the borderlines of visually perceived unsharpness This involves a subjective evaluation of sharpness and unsharpness respectively The sharpness of the contour of a structure at the transition zone against perceived unsharpness governs the grade of 'permissible blurring' This is created by the spurious contours from the objects in the tomographic zone (REICHMANN 1972) and depends on the tomographic angle and the type of tomographic movement, the magnification factor and the focal spot dimension, and to a large extent on the mechanical properties of the equipment It further depends on the exposure, the nature of the film screen system and the noise

---

Fig 1 The hypocycloid tomograms of three test phantoms for estimation of layer thickness reveal the difficulties in determining measurement points in the [illegible]
cycloid tomogra [illegible]
in the center of [illegible]
cylinder Calcul [illegible]

created in it by the quality of the radiation Finally, it depends on the nature of the reproduced object (size, form, absorption and its orientation to the tomographic plane) The tomographic angle and the type of movement govern the number of absorption boundaries in the object to be struck by the radiation beam The 'layer thickness' is primarily dependent on the tomographic angle

An estimation of the 'layer thickness' is of greater importance in tomography of small than of coarser objects A simple device for measurement was developed to meet this requirement (BERGSTRÖM et coll 1971)

Estimation of the layer thickness

Mathematical calculation of the layer thickness is of theoretical interest Subjective estimation by test phantoms is applicable to the various types of equipment in *any situation Different procedures are recommended*

(a) Linear and multidirectional tomography of a lead linear grid (with a sequence of different spatial frequencies) at an inclination to the film plane corresponding to the tomographic angle The different steps are reproduced as rhomboids designating the height of the layer thickness This object is recommended by the ICRU (Fig 1 a) (STIEVE 1967)

(b) For measurement in multidirectional tomography a cylinder (7 cm in diameter and 12 cm high) with a metal wire (1 mm in diameter) arranged spirally with a distance of 1 cm between the coils is recommended by the ICRU (Fig 1 b) (STIEVE 1967)

(c) The test phantom recommended by MATTSSON (1972) for calculating the layer thickness in both linear and multidirectional tomography consists of a stellate figure of thin lead rods arranged to cover a certain range of depth with the rods placed at an angle to the base of the instrument The difference in depth between the central and peripheral parts of the rods is 15 cm at an inclination of about 20° For estimating the layer thickness it is recommended that the tomographic plane be placed halfway along the height of the instrument (Fig 1 c)

In both linear and multidirectional tomography these systems are based on a read-out of a rhomboid, the height of which represents the dimension of the layer thickness (Fig 1) It is obvious from the figure that a subjective read out is not easily possible

In order to avoid this disadvantage a phantom of metal balls (1 mm in diameter) arranged in the form of a cross in one plane was used to demonstrate both the layer thickness and the homogeneity of the tomographic plane in transverse tomography with the Mimer III (BERGSTRÖM et coll 1971) For estimating the layer thickness the metal ball phantom was placed at an angle of a few degrees with the tomographic plane This device proved to be more reliable for calculation of the layer thickness than the cylindrical test phantom with the spiral metal wire The small metal balls appeared with the same sharpness in one layer, while outside that zone their sharp-

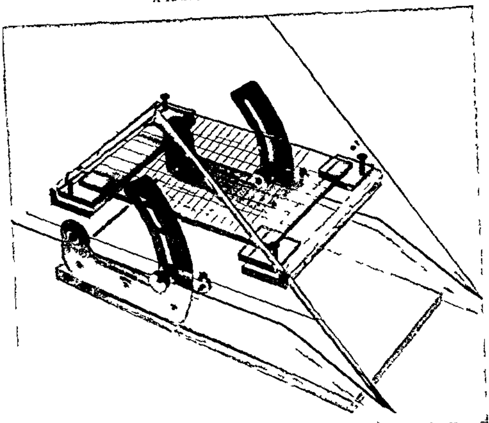


Fig. 3 Metal ball test phantom in a plexiglass stand adjustable to suitable angles with the tomographic plane

ness decreased at a varying rate At the same time the reproduction of the tomographic movement figure increased and the contrast decreased notably

In order to further improve this procedure the following test phantom was developed

Metal ball test phantom

M . .

wi

of ... to the next The metal balls covered an area of 5 cm × 8 cm (Fig 2)

A fine thread screw was inserted in each corner of the plate so as to allow the metal ball plane to be adjusted to the tomographic plane to analyse its homogeneity and to compensate for any unevenness of the object table

For measuring the layer thickness the plate was placed in a plexiglass stand adjust-

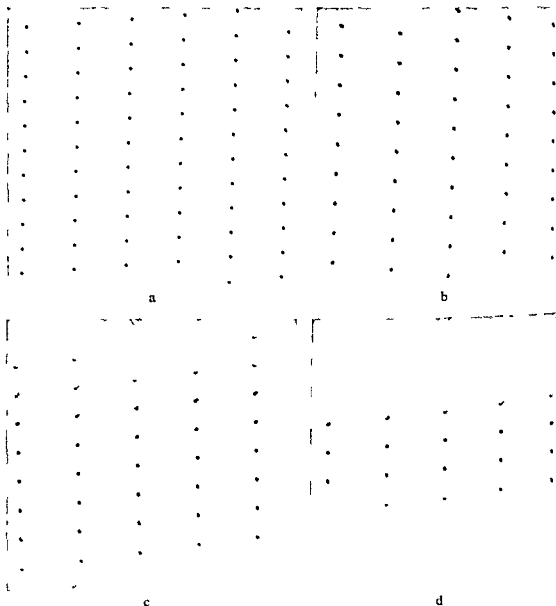


Fig 4 ...)
phic ...)
Hom ...
the to...
graphic movement figure reproduced by the metal balls outside the sharp layer and their decreasing contrast), and d) at an inclination of 8° to the tomographic plane

able to suitable inclinations to the tomographic plane (Fig 3) Measurements were performed with hypocycloid movement on the Polytome (Philips Massiot) and spiral movement on the Stratomatic (Koch & Sterzel), with the phantom at angles of 2°, 4° and 8° In the zone of sharply reproduced metal balls each ball-image was examined with a magnifying glass to establish whether its sharpness was equal to that in the central layer (Fig 4), if not, the metal ball was assigned to the transition zone

Fig 5 Calculation of layer thickness

The distance between the borderlines separating the zone of the sharply reproduced metal balls from the transition zones represented the zone of sharpness in the image, from which the layer thickness could be calculated (Fig 5)

$$\operatorname{tg}\alpha = \frac{d}{Z_0}, \qquad d = Z_0 \operatorname{tg}\alpha$$

where d = layer thickness, Z_0 = zone in the object, Z_f = zone in the film, D = focus-object distance

In the tomographic system a magnification factor (M) is included

$$\frac{\text{Zone in the film}}{\text{Zone in the object}} = M, \qquad Z_0 = \frac{Z_f}{M}$$

Thus $d = \frac{Z_f}{M} \operatorname{tg}\alpha$

or layer thickness $= \frac{\text{Zone in the film}}{\text{magnification factor}} \operatorname{tg}\alpha$

SUMMARY

Testing of the tomographic and photographic system is a prerequisite for successful reproduction of minor details particularly in tomography of the temporal bone A test phantom has been developed, consisting of a single layer of small metal balls which can be adjusted to varying inclinations to the tomographic plane It involves a simple procedure for examining the homogeneity and stability of the tomographic layer at wide movement angles and may also be used for calculating the layer thickness

ZUSAMMENFASSUNG

Prufung des Tomographiegerates einschliesslich des photographischen Systems ist eine Voraussetzung fur erfolgreiche Abbildung feinerer Details besonders bei der Tomographie des Felsenbeins Ein Testphantom bestehend aus einer Einzelschicht kleiner Metallkugelchen kann in verschiedene Neigungen zur tomographischen Ebene eingestellt werden Das Objekt eignet sich zur Untersuchung der Homogenitat und Stabilitat der tomographischen Ebene bei grossem Neigungswinkel Gleichzeitig lasst es sich zur direkten Berechnung der Schichtdicke aus dem Tomogramm verwenden

RÉSUMÉ

Il est nécessaire de tester le système tomographique et photographique pour obtenir une bonne reproduction des petits détails, en particulier dans la tomographie de l os temporal L'auteur a mis au point un fantôme test consistant en une couche unique de petites billes métalliques qui peut être orientée dans des inclinaisons variables par rapport au plan tomographique La technique d examen de l'homogénéité et de la stabilité de la couche tomographique avec des grands angles de mouvement est simple et peut aussi être utilisee pour calcula l'epaisseur de la couche de coupe

REFERENCES

BERGSTROM K, HOLMSTRÖM L, LODIN H, NYLÉN O and WILBRAND H Transverse tomography with Mimer III Acta radiol Diagnosis 11 (1971), 641

ECKERDAL O Tomography of the temporo-mandibular joint Acta radiol (1973) Suppl No 329

EDHOLM P The tomogram, its formation and content Acta radiol (1960) Suppl No 193

GLADYSZ B Rontgenschichtverfahren *In* Bildgute in der Radiologie, S 286 Symposium am 1 und 2 Oktober 1964, Herrnchiemsee Herausgegeben von F E Stieve Gustav Fischer, Stuttgart 1966

GRIESBACH R und KEMPER F Rontgenschichtverfahren Grundlagen der technischen Entwicklung und der klinischen Anwendung fur die Praxis Georg Thieme Verlag Stuttgart 1955

ICRU Methods of evaluating radiological equipment an[illegible] of the Intern Commission of radiological units and m[illegible] Measurements of the characteristics of body section [illegible] partment of Commerce, National Bureau of Standards (1963)

JENSEN J Malformations of the inner ear in deaf children A tomographic and clinical study Acta radiol (1969) Suppl No 286

MATTSSON O Formation of the tomographic image with special reference to blurring Acta radiol (1972) Suppl No 318

REICHMANN S Modified theory of the development of tomographic blurring Acta radiol Diagnosis 12 (1972) 457

— Development of spurious contours of spherical and cylindrical objects in tomography Acta radiol Diagnosis 12 (1972), 317

STIEVE F E Bevorzugte Darstellung einzelner Korperschichten *In* Handbuch der medizinischen Radiologie, S 857 Springer, Berlin, Heidelberg, New York 1957

— Über den Bildaufbau in der Tomographie bei ein- und mehrdimensionaler Verwischung Fortschr Rontgenstr 116 (1972) 253

WILBRAND H F, RASK-ANDERSEN H and GILSTRING D The vestibular aqueduct and the para vestibular canal Acta radiol Diagnosis 15 (1974), 337

FROM THE DEPARTMENT OF PHARMACOLOGY, FACULTY OF MEDICINE, UNIVERSITY OF SÃO PAULO, RIBEIRÃO PRETO, 14 100, BRAZIL

IN VITRO AND IN VIVO RELEASE OF HISTAMINE BY CONTRAST MEDIA IN THE RAT

M P LEITE, C R DE MORAES and J GARCIA LEME

Untoward reactions associated with intravascular injections of contrast media are frequently described The features of some of these reactions are similar to allergic phenomena, but not always they can be strictly attributed to allergic hypersensitivity (SANDSTRÖM 1955)

Endothelial injury following intravenous administration of contrast media to the rat (MERSEREAU & ROBERTSON 1961) and changes in vascular permeability by local application in the hamster cheek pouch (SÖRENSEN 1971) were reported A perivascular oedema was observed during the infusion of roentgenographic compounds in a bat-wing preparation (HARRINGTON & WIEDEMAN 1965)

Some reactions presented by contrast media are therefore similar to those observed by histamine injections

Histamine is not only being produced in anaphylaxis but can be released by a variety of chemical agents If radiographic compounds are included among these agents, many of their side effects referred to clinically, and many vascular alterations observed under experimental conditions might be thus explained

The histamine-releasing properties of some compounds commonly employed for radiographic diagnostics were investigated in the rat and are here reported

---

Submitted for publication 15 January 1974

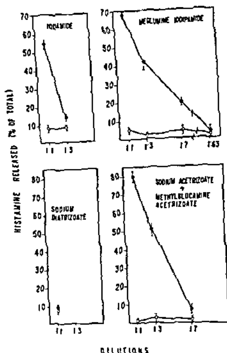


Fig. 1 Release of [illegible]

Methods

Male adult Wistar rats (250–300 g) were used

Histamine-releasing activity in vitro A procedure was employed as described by ROTHSCHILD (1965) with slight modifications From exsanguinated rats, mixed cells from the peritoneal cavity were obtained by flushing the cavity with 10 ml Krebs-Ringer solution, pH 7 3 and collecting the cells after brief centrifugation of the suspension at 500 rpm After washing, the sedimented cells were resuspended in Krebs Ringer solution The contrast media were added to 0 5 ml cell suspensions, in such volumes that various dilutions were obtained, starting from a 1 1 dilution To control samples isosmotic NaCl aqueous solutions were added instead of the agents tested The final volume of the samples was 2 ml and when necessary, it was completed with additional Krebs-Ringer solution being then incubated at 37°C for 20 minutes After centrifugation at 2000 rpm, released and bound histamine in test and control samples were immediately estimated by bioassay on the isolated, atropinized (10^{-7} g/ml) guinea pig ileum, immersed in Tyrode's solution at 37°C Non released histamine was extracted by boiling the sediment evenly resuspended in 2 ml Krebs-Ringer solution for 15 minutes Histamine release was expressed as a percentage of the total histamine content

Degranulation of mast cells in vitro Pieces of mesentery from exsanguinated ani-

Table 1

Mast cell degranulation by radiographic contrast media Results are mean ±SE of 5 experiments

	Per cent of degranulated cells by	
	Contrast media	Isosmotic saline (controls)
Sodium Diatrizoate	15 66±2 51 (P>0 5)*	13 35±2 38
Iodamide	27 25±0 41 (P<0 01)	10 35±1 71
Sodium Acetrizoate + Methyl glucamine Acetrizoate	92 63±3 01 (P<0 01)	12 57±1 81
Meglumine Iodipamide	98 09+2 56 (P<0 01)	10 67+0 85

* Student s t test by comparison with control values

mals were incubated in Krebs-Ringer phosphate buffer, pH 7 3, at 37°C for 20 minutes in the presence of contrast media or equal volume of isosmotic NaCl aqueous solutions (controls) After washing in Krebs Ringer solution, the mesentery spreads were fixed, stained and mounted as described by MOTA (1966) Approximately 300 mast cells were microscopically examined at 800 fold magnification and were considered to be affected when exhibiting methacromatically stained granules around their periphery Results were expressed as a percentage of altered mast cells

Increased vascular permeability to intradermally injected contrast media The animals were anesthetized with pentobarbitone sodium (30–40 mg/kg intraperitoneally) Evans blue in a 1% aqueous solution 20 mg/kg were intravenously administered and 5 minutes later 0 10 ml of contrast media as commercially available or following dilutions with distilled water were intradermally injected into the abdominal wall An equal volume of isosmotic NaCl aqueous solutions was injected in the opposite flank as control After 10 minutes the skin was stripped from the subcutaneous tissue, fragments containing the stained area (and corresponding controls) were cut and the accumulated dye extracted with formamide, according to REIS et coll (1971), being estimated by spectrophotometry at 600 nm Results were expressed as the amount of extravasated dye, control values being subtracted from the corresponding test values

Rat blood pressure Anesthetized animals (pentobarbitone sodium 30–40 mg/kg) receiving 2 mg/kg atropine sulfate 15 minutes before the beginning of the experiments, were used Measurement of blood pressure was performed through a polyethylene cannula inserted into one of the carotid arteries and connected to a mercury manometer with metric scale graduated from 0 to 250 mm The internal diameter of the glass tube was approximately 3 mm A stainless steel style mounted

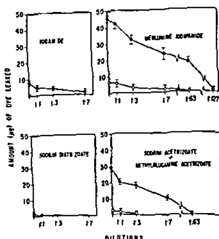


Fig 2 Dye leakage following i p injections of various dilutions (v v) of contrast media before (●) and after (○) pre treatment of the animals

14 animals Points on ordinate axis refer to results obtained with undiluted contrast injections

transversely allowed registration of pressure alterations on a smoked drum Drugs were injected into the jugular vein by means of a cannula similar to that employed for the carotid artery Results refer to the estimated hypotension areas recorded on the smoked drum These areas were measured from the base line, by means of a compensation planimeter (0 55 Nr 19/4 mm², Elphor, Munich)

Drugs used Commercially available, water-soluble organic compounds for roentgenography were employed Meglumine Iodipamide 50 %, pH 7 2–7 6 (methylglucamine salt of adipyl-bis(2,4,6-triiodo-3-carboxylanilida), (Biligrafin, Schering AG), Sodium Acetrizoate 8 55 % and Methylglucamine acetrizoate 62 62 %, pH 6 9–7 3 (sodium salt of 3 acetamido-2,4,6-triiodobenzoic acid and methylglucamine salt of 3-acetamido-2 4,6-triiodobenzoic acid), (Flupac, Johnson & Johnson), Sodium Diatrizoate 50 %, pH 6 5–7 5 (sodium salt of 3,5 diacetamido-2,4,6-triiodobenzoic acid), (Hypaque, Winthrop), Iodamine 65 %, pH 6 0–7 0 (methylglucamine salt of 3-acetylaminomethyl-5-acetamido-2,4,6 triiodobenzoic aicd), (Uromiron, Schering AG), Histamine hydrochloride (Man Research Lab), Diphenhydramine hydrochloride (Benadryl, Parke Davis), N-methyl-N-(4-(4(5)-imidazolyl)butyl)thiourea (Burimamide, Smith Kline and French), kindly supplied by Prof J W Black; atropine sulfate (Parke Davis), Evans blue (Merck AG), Formamide (Merck AG), Pentobarbitone sodium (Nembutal, Abbott)

Results

In vitro release of histamine from mast cells Various concentrations of the contrast media, starting from a 1 1 dilution were used, and, with the exception of sodium diatrizoate, were effective in releasing histamine from peritoneal mast cells in vitro Control samples, represented by isosmotic NaCl aqueous solutions, produced negligible effects (Fig 1)

Table 2

Actions of diphenhydramine (15 mg/kg) and burimamide (200 µg kg) upon the hypotensie effects of iodamide (C) and histamine (H) The contrast medium was injected as commercially available in the doses of 0 1 (C_1) 0 2 (C_2) and 0 5 ml (C_3) Histamine was given in the doses of 0 1 (H_1) 0.2 (H_2) and 0 3 µg (H_3) All drugs were intravenously injected The recorded hypotension areas were measured from the base line by means of a compensation planimeter

Exp No	Hypotensıon areas (mm²) following											
	Control doses						Doses after diphenhydramine			Doses after diphenhydramine + buramamide		
	H_1	H_2	H_3	C_1	C_2	C_3	H_2	H_3	C_3	H_2	H_3	C_3
1	100	140	—	0	20	140	0	—	40	0	—	32
2	80	100	—	0	0	100	0	—	40	0	—	20
3	8	12	20	0	100	180	0	16	100	0	0	60
4	40	80	—	0	16	60	0	—	20	0	—	0
5	60	60	—	0	60	140	0	—	28	0	—	0

Table 3

Action of diphenhydramine (15 mg/kg) and burimamide (200 µg/kg) upon the hypotensive effects of meglumine iodipamide (C) and histamine (H) The contrast medium was injected as commercially available in the doses of 0 05 (C_1) and 0 1 ml (C_2) Histamine was given in the doses of 0 1 (H_1) 0 2 (H_2) and 0 3 µg (H_3) All drugs were intravenously injected The recorded hypotension areas were measured from the base line by means of a compensation planimeter

Exp No	Hypotensıon areas (mm²) following									
	Control doses					Doses after diphenhydramine			Doses after diphenhydramine + burimamide		
	H_1	H_2	H_3	C_1	C_2	H_2	H_3	C_2	H_2	H_3	C_2
1	20	40	—	120	240	0	—	0	0	—	0
2	56	76	200	800	1 000	—	0	800	—	0	28
3	100	200	—	400	440	0	—	60	0	—	50

Degranulation of mast cells in vitro The ability to degranulate tissue mast cells in vitro is a property of most histamine releasing drugs active in the rat (ROTHSCHILD 1965) In our experiments meglumine iodipamide and the mixture of sodium acetrizoate + methylglucamine acetrizoate were seen to be potent mast cell degranulators whereas iodamide was less effective and sodium diatrizaoate ineffective Drugs as available were added to the incubation medium in the proportion of 1 1 (Table 1)

Table 4

Actions of diphenhydramine (15 mg/kg) and burimamide (200 μg/kg) upon the hypotensive effect of sodium acetrizoate + methylglucamine acetrizoate (C) and histamine (H). The contrast medium was injected as commercially available in the doses of 0.1 (C_1), 0.2 (C_2) and 0.3 ml (C_3). Histamine was given in the doses of 0.1 (H_1) and 0.2 μg (H_2). All the drugs were intravenously injected. The recorded hypotension areas were measured from the base line by means of a compensation planimeter

Exp No	Hypotension areas (mm²) following: Control doses					Doses after diphenhydramine				Doses after diphenhydramine + burimamide		
	H_1	H_2	C_1	C_2	C_3	H_1	C_1	C_2	C_3	H_2	C_2	C_3
1	60	120	—	60	120	0	—	—	140	0	—	90
2	50	160	—	130	280	0	—	—	180	0	—	140
3	20	120	40	120	360	0	—	—	160	0	—	160
4	100	180	160	200	—	0	—	200	—	0	120	—
5	10	30	10	60	—	30	10	40	—	0	40	—

Cutaneous vascular permeability following injections of contrast media. Effect of pretreatment with anti-histamines. The contrast media were intradermally injected, as commercially available or following dilutions with distilled water (v/v). No local increased vascular permeability was observed with sodium diatrizoate. Iodamide was less potent in eliciting cutaneous dye-exudation than the mixture of sodium acetrizoate + methylglucamine acetrizoate or meglumine iodipamide, which were effective even in high dilutions. The increased vascular permeability induced by these compounds was strongly inhibited by previous administration of diphenhydramine (25 mg/kg, i.p., 30 min before) (Fig. 2). In similar conditions of assay the amount of dye leaked by the action of 1 and 10 μg histamine in untreated animals was 11.98 ± 2.76 and 31.98 ± 5.61 μg respectively (mean ± SE of 5 estimations).

Blood pressure alterations observed by intravenous injections of contrast media. Effect of anti-histamines. The contrast media were intravenously injected, as commercially available, in amounts approximately equivalent to those employed in humans for radiographic purposes.

Sodium diatrizoate produced either no variation of the arterial blood pressure or a slight increase. By injecting the other three compounds tested, a drop in blood pressure was always observed. Iodamide seems to be the least potent in this respect. Intravenous injections of diphenhydramine (15 mg/kg) partially reduced the blood pressure drop which followed the injections of contrast media. When besides diphenhydramine, 200 μg/kg burimamide was infused, a complete block or a strong reduction of the effects induced by the hypotensive agents were observed (Tables 2, 3, 4). Injections of isosmotic NaCl aqueous solutions produced negligible effects.

LASSER E C, WALTERS A J and LANG J H An experimental basis for histamine release in contrast material reactions Radiology 110 (1974), 49

MERSEREAU W A and ROBERTSON H R Observations on venous endothelial injury following the injection of various radiographic contrast media in the rat J Neurosurg 18 (1961), 289

MOTA I Release of histamine from mast cells *In* Histamine and anti histaminics Hand Exptl Pharmakol XVIII/1, p 569 Edited by M Rocha e Silva Springer, Berlin 1966

REIS M L, OKINO L and ROCHA e SILVA M Comparative pharmacological actions of bradykinin and related kinins of larger molecular weights Biochem Pharmacol 20 (1971) 2935

RILEY J F and WEST G B The presence of histamine in tissue mast cells J Physiol (London) 120 (1953) 528

— — The occurrence of histamine in mast cells *In* Histamine and anti histaminics Hand Exptl Pharmakol XVIII/1, p 116 Edited by M Rocha e Silva Springer, Berlin 1966

ROCKOFF S D and BRASCH R Contrast media as histamine liberators III Histamine release and some associated hemodynamic effects during pulmonary angiography in the dog Invest Radiol 6 (1971), 110

— — KUHN C and CHRAPLYVY M Contrast media as histamine liberators I Mast cell histamine release in vitro by sodium salts of contrast media Invest Radiol 5 (1970) 503

— KUHN C and CHRAPLYVY M Contrast media as histamine liberator IV In vitro mast cell histamine release by methylglucamine salts Invest Radiol 6 (1971) 186

ROTHSCHILD A M Histamine release by bee venom phospholipase A and mellitin in the rat Brit J Pharmacol 25 (1965), 59

SANDSTRÖM C Secondary reactions from contrast media and allergy concept Acta radiol 44 (1955), 233

SÖRENSEN S E Changes in vascular permeability after local application of roentgen contrast media in the hamster cheek pouch Acta radiol Diagnosis 11 (1971) 274

FROM THE DEPARTMENTS OF SURGERY I (DIRECTOR. PROF L-E GELIN) AND II (DIRECTOR: PROF R ROMANUS) AND THE DEPARTMENTS OF DIAGNOSTIC RADIOLOGY I (DIRECTOR: PROF O BARTLEY) AND III (DIRECTOR PROF C-G HELANDER), SAHLGRENSKA SJUKHUSET, UNIVERSITY OF GOTHENBURG, S-413 45 GOTHENBURG, SWEDEN

CIRCULATORY DISTURBANCES AFTER EXPERIMENTAL FRACTURE

J SANDEGÅRD and B E ZACHRISSON

Regional blood flow is clinically difficult to evaluate immediately after limb injury Experimental investigations have demonstrated increase of blood flow to the injured extremity following different types of trauma This increase of blood flow and vasodilatation in the leg after closed tibial fracture in dogs appears early (WRAY 1964) Similar changes following extended soft tissue trauma have been observed by LIU (1968) and LEWIS & LIM (1970) The experimental fracture model used by WRAY, however, included injury to the surrounding soft tissues of an unknown degree. The genesis of the changes of regional blood flow following soft tissue injury was investigated by SANDEGÅRD et coll (1974) The lowering of peripheral vascular resistance after this type of trauma, produced by a release of the local vasoconstrictor tone, might possibly be due to the effects of vasodilator substan[illegible]

[illegible] such an alteration To elucidate this question an experimental model was designed, in which fracture was produced while keeping the

Submitted for publication 12 February 1974

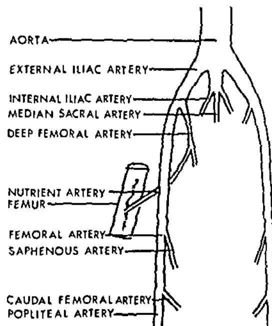


Fig 1 *Arteries in the pelvis and the hind limb of the dog*

soft tissue injury to a minimum The early effects on the regional blood flow were determined by hemodynamic methods and angiography

Material and Methods

The investigation was carried out on a total of seventeen mongrel dogs of both sexes (14 to 22 kg), anesthetized intravenously with sodium Pentobarbital in repeated small doses The dogs breathed spontaneously or were supported by mechanical ventilation Various hemodynamic determinations were made in eleven dogs, while angiography only, was performed in six dogs

For the hemodynamic measurements the vessels were dissected free, so as to isolate the blood flow to the legs by ligation of the aortic branches distal to the origin of the external iliac arteries (i e the internal iliac arteries and the median sacral artery) (Fig 1) A tourniquet was placed around each ankle to exclude the circulation of the foot with its rich arterio-venous net

Small catheters for recording of blood pressure and sampling were introduced into one carotid artery and one external jugular vein In the eleven dogs subjected to hemodynamic measurements, flow probes were placed on the external iliac arteries proximal to the deep femoral arteries The internal iliac veins were ligated to isolate the venous outflow from the legs For the measurement of venous outflow, large bore, siliconized T-tubes were introduced into the external iliac veins

Systemic arterial pressure, heart rate and arterial blood flow were monitored on a Mingograf recorder Arterial pressure was recorded by a Statham pressure transducer and heart rate was calculated from the curve Arterial blood flow was measured with an electromagnetic flow meter (Nycotron, Oslo) On the venous side the blood flow

was determined by timing of the venous effluent through the T-tubes in the external iliac veins Deviation of the venous flow was carried out by clamping of the iliac veins proximal to the T-tubes After recording of the volume, the collected venous blood was immediately reinfused

Cardiac output was measured by the dye dilution technique The dye (Cardiogreen, Beckman Instrument Co, Stockholm) was injected into the right atrium via the jugular vein and sampling was performed from the carotid artery Central venous blood was sampled for the determination of hematocrit (micro-hematocrit)

In the six dogs subjected to angiography a catheter (Bardic adult feeding tube, length 107 cm, size 2 7 mm CR Bard International Ltd, England) was introduced through the left internal iliac artery with the tip in the aorta near the origin of the external iliac arteries In these dogs the arterial pressure was recorded on a mercury manometer, by way of the carotid catheter At angiography an Elema-Schönander 35 × 35 AOT-R film changer and two tubes for stereoscopic exposures were used

Fifteen ml Isopaque Cerebral (Nyegaard & Co , Oslo) were injected manually during 1 5–3 seconds for each angiography Before the injection blood was aspirated into the syringe in order to reduce the risk of blood clot embolization from the catheter during the injection of contrast medium (Jacobsson et coll 1969) In the interval between the angiographic examinations the catheter was filled with non-heparinized saline.

Serial angiography including pelvic area and both thighs was performed in the following way 2 films/s for 5 seconds, followed by 1 film/s for 5 seconds and finally 1 film/3 s for 15 seconds

The angiographic material consisted of 21 serial angiographies performed in the six dogs Four of these were examined (1) within 15 minutes before preparation, (2) within 25 minutes after preparation, (3) 1 to 7 minutes after fracture, (4) 10 to 30 minutes after fracture In order to record later effects, two of the four dogs were examined 60 minutes after fracture, one of these also 120 minutes after fracture One dog was examined four hours and another six hours after fracture

Trauma In all dogs the fracture was made at the junction of the middle and distal thirds of one femur A 5 to 7 cm longitudinal incision was made in the skin and fascia on the anterior aspect of the thigh approximately 10 to 15 cm proximal to the knee joint By careful blunt dissection between the two parts of the sartorius muscle and division of the medial vastus muscle, the femoral diaphysis was dissected free for a length of 2 to 3 cm During this preparation care was taken to avoid bleeding and generally not more than one subcutaneous vessel had to be ligated After a period of 30 minutes the femur was divided by a pair of bone tongs, which were manipulated to produce a comminuted fracture except in two of the dogs examined angiographically in which an oscillating saw was used In the fracturing procedure care was taken not to damage the surrounding soft tissues Inspection of the wound revealed very little bleeding The wound was closed by suture of the fascia and skin After the



Fig 2 Types of fractures of the femur in the angiographic material In cases I IV the fracture was made with a pair of tongs in cases V and VI with an oscillating saw Cases I IV represent various types of comminuted fractures and V and VI transverse fractures

operative intervention of the limb, no external bleeding through the wound or swelling of the thigh was noted The fractures produced are illustrated in Fig 2

At the end of each experiment the dog was killed with an overdose of sodium Pentobarbital

Evaluation of angiography The vessels of the thighs were compared on the injured and contralateral sides In order to obtain an idea of the circulation of the legs comparisons of the legs were also made regarding (1) transit time of contrast medium between two defined levels, and (2) diameters of arteries at corresponding levels With these measurements the relative changes of the circulation in the regions defined could be estimated

The femoral artery in the dog is the continuation of the external iliac artery from the vascular lacuna in the inguinal region through the thigh About 1 to 2 cm proximal to the vascular lacuna, the deep femoral artery arises from the external iliac artery The caudal femoral artery arises from the femoral artery approximately 1 cm proximal to the entrance of the femoral artery into the gastrocnemius muscle (Fig 1) The transit time of the contrast medium in the femoral artery was defined as the time interval between the earliest filling of the external iliac artery at the origin of the deep femoral artery and the earliest filling of the caudal femoral artery The arterial filling phase of the principle nutrient arteries of the femur was evaluated by the method of GREITZ (1956) the period necessary for the artery to fill was defined as the time interval between the earliest filling of the artery in the nutrient foramen and the filling of the smallest peripheral branches of the vessel The nutrient foramen is situated at the junction of the proximal and middle thirds of the posterior surface of the femur, thus in all cases proximal to the fracture level

Measurements of the internal diameter of the arteries were performed on the films at corresponding levels only arteries well filled with contrast medium were accepted for measurements In each dog the measurements were made at equal focus film and object film distance on both the fractured and non fractured side A magnifying

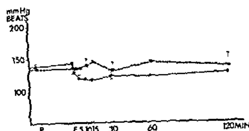


Fig 3 Systemic arterial press... (● ●) ... (■ ■) ...

... fracture level The rise of heart rate less distinct with a maximum mean value at 15 min after fracture and thereafter tended to return to the initial level

glass with a built-in scale permitting readings with a precision of 0 1 mm was used, the magnification factor was 7 The standard error of a single measurement below the inguinal region was 0 05 mm (SANDEGÅRD & ZACHRISSON 1975)

Results

Hemodynamic measurements

Before and after preparation None of the determined values changed significantly during a 30-minute period after preparation, in relation to the mean values from a control period However, the recordings of arterial and venous blood flow as well as cardiac output, displayed a tendency towards reduced values at the end of the preparation period

After fractur ...
from a mean v...
was significant ... minutes, reaching the lowest mean value 15 minutes after fracture Thereafter the pressure tended to return to the value before fracture

The heart rate (Fig 3) changed with a maximum, transient rise after 15 minutes, however, not statistically significant ($p > 0.05$) At the end of the experiment the heart rate had returned to the level before fracture

Arterial (Fig 4) and venous (Fig 5) blood flow did not change significantly ($p > 0.05$) in relation to the fracturing of the femur, nor was there any difference between the fractured and non-fractured sides

Cardiac output measurements in four dogs (Fig 5) displayed declining values throughout the experiment, with no abrupt change related to the trauma

The hematocrit did not change significantly during the experiments

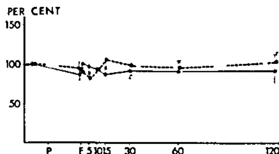


Fig 4 Iliac arterial blood flow of fractured (●—●) and non fractured (■---■) sides in 8 dogs Mean values in per cent of mean control values, as monitored on the Mingograf Standard error of the mean indicated vertically The changes on both the fractured and non fractured sides not significantly ($p > 0.05$) influenced by preparation (P) or fracture (F)

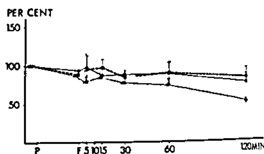


Fig 5 Venous outflow through T tube in the iliac veins in eleven dogs and cardiac output [illegible] cent of mean [illegible] paration (P) and fracture (F) no significant changes ($p > 0.05$) Cardiac output (▲ ▲) decreased continuously throughout the experiment, but not in relation to preparation (P) or fracture (F)

Angiography

Before and after preparation The contrast medium transit time of the defined segments of the femoral arteries was not affected by the preparative procedure (Fig 6) There were no differences in appearance time of contrast medium in the veins before and after preparation and no differences of venous filling on the prepared and non prepared sides The internal diameter of the femoral arteries of the four dogs subjected to the preparative procedure had decreased after preparation In two dogs a decrease of the caliber of the peripheral arteries also occurred No differences between the prepared and non-prepared sides regarding the caliber of the arteries were observed The distance between the femoral artery and the femur on the prepared side increased in one case after preparation with stretching of some branches of the caudal femoral artery (Fig 7) With this exception, no displacement of the vessels could be detected

After fracture (1) Femoral arteries The femoral arterial transit time was not affected by the fracturing procedure except in one dog, in which signs of thromboembolization were noted 60 minutes after fracture on the non-fractured side The fracture did not affect the arterial caliber except in one case In this dog the fracture was produced with an oscillating saw, a single 2 cm long segmental dilatation of the femoral artery was evident at the fracture level (Fig 8) In the middle part of the dilated vessel segment, a notching of the vessel wall, pointing to the femur was observed

The distal part of the femoral artery of the fractured side was displaced in a medial direction in all dogs In five of the six dogs this was considered to have been produced by the displacement of the distal femur fragment itself In the dog with a slight displacement of the femoral artery already after preparation (Fig 7), this displacement increased continuously during the examination

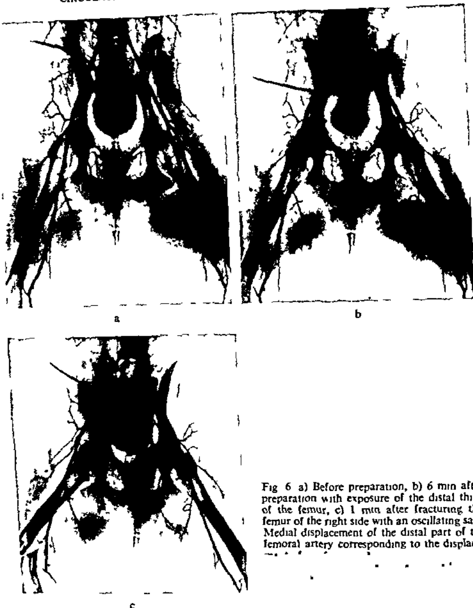


Fig 6 a) Before preparation, b) 6 min after preparation with exposure of the distal third of the femur, c) 1 min after fracturing the femur of the right side with an oscillating saw Medial displacement of the distal part of the femoral artery corresponding to the displace

(2) Peripheral arteries at the fracture level A transient dilatation of the saphenous artery occurred five minutes after fracture in one case (Fig 7 c) In another case a medial displacement of the saphenous artery was observed In all cases small arteries in the fracture region were slightly displaced, but no more than could be explained by pressure from the fracture fragments Extravasation of contrast medium was

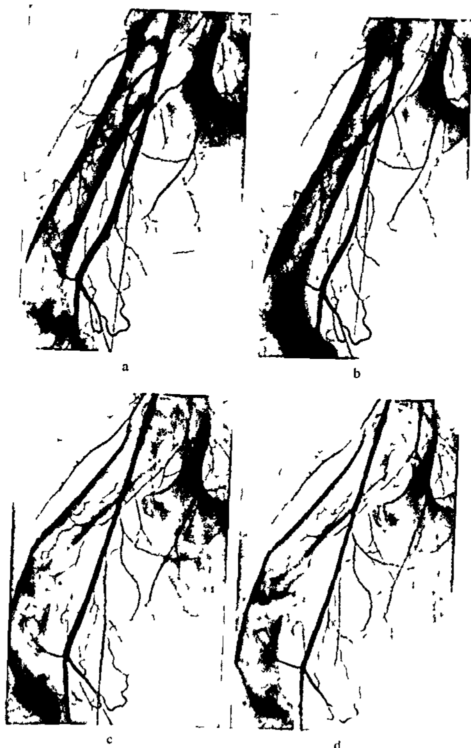


Fig 7 a) Before preparation, b) 15 minutes after preparation of the soft tissues of the distal third of the thigh with exposure of the femur c) 5 min after fracture of the femur with a pair of tongs d) dilatation of the principal nutrient and saphenous arteries evident 60 min after fracture Patchy extravasation of contrast medium in the medial part of the fracture Compared with (c) decrease of the caliber of the principal nutrient and saphenous arteries Increasing medial displacement of the distal part of the femoral artery with stretching of branches of the caudal femoral artery possibly due to hemorrhage and edema



Fig 8 Angiography 30 min after fracturing of the femur with an oscillating saw Segmental dilatation of the femoral artery at the fracture level

recorded in one case only (Fig 7 d), with slight patchy leakage near the fracture in all examinations after fracture The leakage reached a maximum after one hour, measuring 3 mm × 10 mm on the films

(3) Peripheral arteries outside the fracture level No changes of the course or of the caliber of the vessels could be detected comparing the fractured with the non fractured limb, except in the case with a continuously increasing medial displacement of the distal femoral artery on the fractured side In this case also a stretching of some branches of the caudal femoral artery appeared after preparation, which increased slightly after fracture

(4) Principal nutrient arteries of the femur Some degree of discontinuity of medullary arteries at the fracture site occurred in all cases In the two cases in which the fracture was produced by an oscillating saw, this discontinuity was total A transient dilatation of the principal nutrient arteries on the fractured side was observed five minutes after fra

... medullary branches was observed immediately afterwards In the other case the fracture was produced with a pair of tongs, the transit time of the contrast medium was not primarily affected, although it increased in the descending intramedullary branches, 60 minutes after fracture At this time also intramedullary arteries near the fracture did not fill with contrast medium, indicating occlusion of the vessels near the fracture level The nutrient artery was dilated at 4 hours after fracture in one dog, in another the descendent medullary arteries on the fractured side were not filled at 6 hours

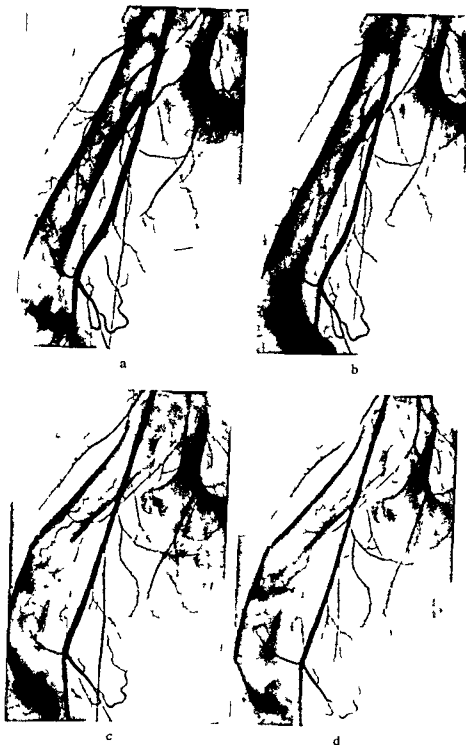


Fig 7 a) Before preparation b) 15 minutes after preparation of the soft tissues of the distal third of the thigh with exposure of the femur c) 5 min after fracture of the femur with a pair of tongs d) dilatation of the principal nutrient and saphenous arteries evident 60 min after fracture Patchy [illegible]

due to hemorrhage and edema

and distal arteries were observed after preparation and fracture, in another case a medial displacement of the saphenous artery at the fracture level These displacements were probably due to the effects of an expansive hematoma However, signs of external bleeding through the incision of the skin were not observed during the experiments, pointing to a limited degree of bleeding, as further indicated by the absence of swelling of the injured region

Contrast media are known to cause an initial reduction of flow followed by a transient increase (BOUSEN et coll 1971) The arterial phase in angiography appears in the time lag between injection and the flow increasing effect of the contrast medium even in trauma (LEWIS et coll 1975) No differences of the estimated arterial transit times between the fractured and non fractured legs could be observed, except for the thrombembolic case 60 minutes after trauma Consequently, *it is reasonable to assume that the* vascular effects of the contrast medium itself did not affect the comparison of the two sides A further support for this assumption was the close relation between the hemodynamic and the angiographic results

It is evident that the methods used for the hemodynamic measurements in the present investigation including angiography have been unable *to reveal changes* of regional blood flow in soft tissues following injury to bone, when injury to surrounding soft tissues has been kept to a minimum Thus, neither the limited injury of the soft tissues, nor the damage to the bone caused hemodynamic changes resembling *those occurring* after extensive soft tissue contusion trauma Early hemodynamic *changes* in the injured extremity above all seem to be related *to injury of the soft tissue*, and not of the bone With angiography local changes of vessels *near the fracture* could be observed as well as alteration of the intramedullary *circulation* after fracture

Conclusion The *hemodynamic* response in the traumatized extremity *is mainly related* to the soft tissue injury, not to bone injury *per se*

SUMMARY

Early hemodynamic and angiographic effects after fracture w th a m [illegible]

[illegible] in the injured extremity

ZUSAMMENFASSUNG

Frühzeitige hämodynamische und angiographische Effekte nach einer Fraktur mit einem Minimum an Weichteilschäden wurden an narkotisierten Hunden untersucht. Es wurde eine enge Beziehung zwischen den hämodynamischen und angiographischen Befunden beobachtet Die Fraktur verursachte keine Änderung der regionalen Durchblutung der Weichteile ausserhalb des Knochens der verletzten Extremität

(5) Veins Filling of the veins in the thigh region was observed in all dogs A comparison between the fractured and non-fractured limbs revealed no difference of venous filling or in appearance time of the contrast medium in the veins

Discussion

The results in the two groups investigated by hemodynamic methods and by angiography were consistent *Following fracture with a minimum of soft tissue* injury, no change of regional blood flow was observed (in eleven dogs) either in the fractured leg, or in the contralateral limb Early after fracture a transient lowering of blood pressure and an increase of heart rate were recorded These alterations cannot be explained with certainty, but may have been produced by neurogenic impulses from the fractured region Hypovolemia is less probable as a causative factor as only a limited bleeding was observed during the preparation and fracturing procedures The slow decrease of the cardiac output throughout the experiments without relation to the preparation or fracture may be the effect of experimental conditions such as anesthesia and positioning of the animals

The results of angiography were uniform in 5 of 6 dogs regarding flow, with no *differences between the fractured and the non-fractured sides in relation* to preparation and fracture In the sixth dog the examinations in the acute state revealed no change of flow on either side, in conformity with the results in the other dogs, but at 60 minutes a slight alteration occurred, possibly due to a thromboembolic complication on the non fractured side The tip of the catheter was considered to be a possible source of the thromboembolism (JACOBSSON et coll)

In spite of the absence of differences of angiographic flow in the fractured and non fractured limbs, local changes of vessels near the fracture site were observed A transient dilatation of the saphenous artery occurred in one case in the injured leg, a persistent segmental dilatation of the distal part of the femoral artery near the fracture in another animal These changes might point to local soft tissue injury producing vasodilatation However, in the case with segmental dilatation a vascular effect of vibration (BOUGHNER & ROACH 1971, LJUNG & SIVERTSSON 1972) may be discussed, as this fracture was produced by the oscillating saw

Evaluation of the effects of fracture on the circulation in the soft tissues of the fractured extremity was the main purpose of the present investigation However, apparently the angiographic method used offered information of the intramedullary circulation, with somewhat contradictory findings The principal *nutrient artery* dilated on the fractured side in some cases In addition alterations of the transit time of the contrast medium were recorded, reflecting the injury to the intramedullary tissues including the vessels These local changes of the intramedullary circulation were not related to the uniform angiographic flow of the femoral arteries

Signs of major bleeding were not present In one dog a patchy extravasation of contrast medium and a continuously increasing displacement of the femoral artery

FROM THE DEPARTMENTS OF DIAGNOSTIC RADIOLOGY, RIKSHOSPITALET AND ULLEVÅL SYKEHUS, OSLO, NORWAY

ANGIOGRAPHY IN VASCULAR INJURIES OF THE EXTREMITIES

I ENGE, T AAKHUS and A EVENSEN

The value of angiography of peripheral vascular injuries has been stressed in several reports (e g. LUMPKIN et coll 1958, SINKLER & SPENCER 1960, BELL & COCKSHOTT 1965, LOVE & BRAUN 1968, WENZ 1968, SMITH et coll 1969, GIRL 1971) Most of the series are however small, indicating that angiography is rather infrequently used The circulation in an injured limb may usually be satisfactorily evaluated clinically but a thorough knowledge of the type and site of the injury sustained to the vessels may be difficult to assess This is however of great importance for planning the operation

Angiography has been performed in 31 patients with vascular injuries of the extremities following a variety of traumas, exclusive of injuries referable to surgery or arterial catheterization, in the course of the past 13 years The different types of arterial injury were demonstrated in detail by angiography and the experiences from this material form the basis of the present report

Material and Methods The material consists of 25 males and 6 females aged between 7 and 68 years They had been exposed to the following types of trauma Gunshot (4 cases), blast (5), stabbing (6) blunt trauma with or without fracture of bone (12) luxation of shoulder joint (1), or compression by crutches or cast of plaster (3 cases) The injury was penetrating in 15 and non penetrating in 16 cases The angiography was performed within a few days after the injury in 7 cases, within 4

Submitted for publication 21 December 1973

RÉSUMÉ

Les auteurs ont etudié sur des chiens anesthesiés les effets angiographiques et hémodynamiques précoces après fracture accompagnee d'un minimum de lesions des tissus mous Ils ont trouvé une étroite relation entre les signes hemodynamiques et angiographiques La fracture ne modifie pas le débit sanguin regional dans les tissus mous autour de l'os dans le membre blesse

REFERENCES

BOIJSEN E, DAHN I and HALLBOOK T Hemodynamic effect of contrast medium in arteriography of legs Acta radiol Diagnosis 11 (1971), 295

BOUGHNER D R and ROACH M R Effect of low frequency vibration on the arterial wall Circulat Res 29 (1971), 136

GREITZ T A radiologic study of the brain circulation by rapid serial angiography of the carotid artery Acta radiol (1956) Suppl No 140

JACOBSSON B, BERGENTZ S E and LJUNGQVIST U Platelet adhesion and thrombus formation on vascular catheters in dogs Acta radiol Diagnosis 8 (1969), 221

LEWIS D H and LIM JR R C Studies on the circulatory pathophysiology of trauma I Effect of acute soft tissue injury on nutritional and non-nutritional shunt flow through the hind leg of the dog Acta orthop scand 41 (1970), 17

— — Studies on the circulatory pathophysiology of trauma II Effect of acute soft tissue injury on the passage of macroaggregated albumin (^{131}J) particles through the hind leg of the dog Acta orthop scand 41 (1970), 37

— SANDEGÅRD J, SEEMAN T and ZACHRISSON B E Effects of intra arterial injection of contrast medium on regional circulation in soft tissue trauma To be published in Acta radiol Diagnosis

LIU C T Circulatory response to muscle trauma following denervation and hemorrhage in dogs J Trauma 8 (1968), 75

LJUNG B and SIVERTSSON R The inhibitory effect of vibrations on tension development in vascular smooth muscle Acta physiol scand 85 (1972), 428

MILLER M E, CHRISTENSEN G C and EVANS H E Anatomy of the dog W B Saunders Company, Philadelphia, London 1964

RHINELANDER F W Circulation of bone *In* The biochemistry and physiology of bone Vol 2 Edited by G H Bourne Academic press, New York and London 1972

SANDEGÅRD J and ZACHRISSON B E Angiography and hemodynamic measurements in extensive soft tissue trauma to the extremity To be publishid in Acta radiol Diagnosis 16 (1975)

— NOLTE J, LEWIS D H and SEEMAN T Early hemodynamic and biochemical changes in soft tissue trauma Europ surg Res 6 (1974), 233

WRAY J B Acute changes in femoral arterial blood flow after closed tibial fracture in dogs J Bone Jt Surg 46-A (1964), 1262



Fig 3 Fig 4

Fig 3 Angiography of the arm 2 weeks after application of cast of plaster for antebrachial fracture Tapering of the arteries below the elbow (→) possibly due to compression from inflammatory edema and haematoma

Fig. 4 Angiography of the shoulder region shortly after dislocation of the shoulder joint Rupture and occlusion of the axillary artery and peripheral part of the artery filled through long collateral Extravasation of contrast medium distal to the occlusion (→)

In the 15 cases of penetrating injuries arterial occlusion was disclosed in 2 and a pseudoaneurysm in 3 cases, while an arteriovenous fistula, occasionally combined with a pseudoaneurysm, was encountered in 10 cases

Discussion

Early assessment of the circulation in an injured limb is imperative and is usually satisfactorily provided for by clinical examination However it may be difficult to evaluate the circulation in cases with extensive contusion of soft tissue, fractures of bone, deep lacerations and shock states Furthermore, in young patients collaterals may transmit arterial pulsations beyond an occlusion of a main artery and conceal the injury to the vessel

When lesions to the large vessels are difficult to exclude at clinical examination, direct demonstration of the appearances of the arteries may be urgent A preoperative knowledge of the site, extent, and type of lesion is important since the type of vascular injury may vary considerably depending upon the nature and force of the trauma Transient segmental arterial contraction, or spasm (KROH 1917), may occur





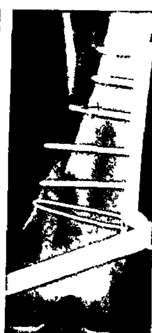


Fig 1 Fig 2

Fig 1 Angiography of the leg shortly after a blunt trauma Circumferential intimal rupture with occlusion of the popliteal artery Sharply demarcated dome shaped contour of the rolled up intima (→)

Fig 2 Angiography of both legs after surgery of femoral fractures Displacement and compression of the right popliteal artery (→), complete occlusion of the left femoral artery (→)

months in 17 and in the remainder more than a year after the trauma because of signs of persistent circulatory impairment, a bruit or pulsatile swelling

In cases of unilateral lesions the arteries of the lower limbs were examined after introduction of a catheter into the common or external iliac arteries via the femoral artery on the side of injury but in bilateral lesions the catheter was placed in the aorta and the contrast medium injected just above the bifurcation The femoral route was also usually employed in angiography of the upper extremities Depending upon the site of injury and technical conditions the tip of the catheter was placed in the aortic arch, the innominate, subclavian or axillary arteries Occasionally puncture of the brachial artery centrally to the possible site of the lesion had to be performed for proper catheter placement

Results

The injury involved the following vessels the femoral artery (9 cases), popliteal (7), axillary (4), brachial (5), tibial (2), ulnar (1), radial (1), external iliac (1) and both the ulnar and radial arteries (1 case)

Among the 16 cases with non-penetrating injuries arterial occlusion was the most frequent finding, present in 12 cases A pseudoaneurysm was the only finding in 2 and an arteriovenous fistula in another 2 cases



Fig 7a Fig 7b Fig 8

Fig. 7 Angiography of the leg 32 years after a shot gun accident a) Early arterial phase Dilated tibial arteries and early venous filling through the fistula (→) b) Late arterial phase Concentrated contrast medium in the veins delayed arterial flow distal to the fistula

Fig 8 Angiography of the thigh several years after stab wound Early venous filling through the fistula (→) Rich collateral network

Tears of the intima often give rise to thrombosis The so called circumferential intimal fracture (ELLIOT 1956) consists of a circular rupture and rolling up of the intima with subsequent thrombosis The intima is the first layer to rupture on stretching of the artery (BERGAN 1963) On exploration the artery may appear narrow and the lesion consequently be mistaken for spasm (BROIN & BIE 1966) angiography however clearly demonstrates the nature of the lesion A rupture of the intima has a characteristic dome shaped appearance (Fig 1) If secondary thrombus formation has occurred however angiography does not display this characteristic feature (Fig 2) In blunt trauma to the arteries a number of factors may contribute to the arterial occlusion Compression spasm and rupture of the intima may all probably contribute to the so called crutch thrombosis and thrombosis associated with fractures (Figs 2 3)

A complete rupture of the arterial wall passing unrecognized may result in a pseudoaneurysm particularly when only a part of the circumference is ruptured In



Fig 5 Angiography of the arm 2 years after a blunt trauma a) Early arterial phase Jet of contrast medium into a pseudoaneurysm (→) b) Late phase Retention of contrast medium outlining the pseudoaneurysm (→)

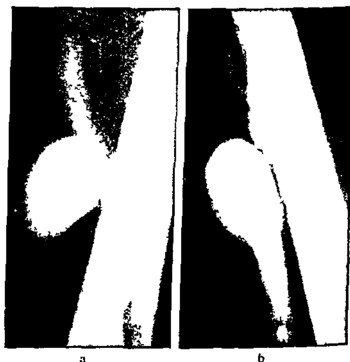


Fig 6 Angiography of the thigh a few weeks after stab wound Early venous filling through an arterio venous pseudoaneurysm a) A p view b) Lateral view

alone or be associated with all types of arterial injuries (KINMONTH 1952, LINDBOM 1957) This phenomenon is most frequently encountered in medium sized muscular arteries and may cause considerable circulatory impairment At angiography spasm usually appears as evenly outlined segments of circular constriction of varying extension Clinically the differentiation between spasm and occlusion may be impossible.

Angiographie vermag gewohnlich Typus und Umfang der Schadigung sowie das Vorkommen und den Umfang von Kollateralen nachzuweisen Deren Wert bei Fallen mit unklaren klinischen Befunden sowie deren Bedeutung fur die therapeutischen Überlegungen wird hervorgehoben

RÉSUMÉ

Presentation des résultats angiographiques dans 31 cas de lesions vasculaires des membres au cours de différents traumatismes L'angiographie met habituellement en évidence le type et la taille des lésions ainsi que la presence et l etendue des collaterales Les auteurs insistent sur son interet dans des cas où les signes cliniques sont peu nets et insistent aussi sur son importance pour les indications thérapeutiques

REFERENCES

BELL D and COCKSHOTT W P Angiography of traumatic arterio-venous fistulae Clin Radiol 16 (1965), 241

BERGAN F Traumatic intimal rupture of the popliteal artery with acute ischemia of the limb in cases with supracondylar fractures of the femur J cardiovasc Surg (Torino) 4 (1953), 300

BROIN T and BIE K Peripheral arterial occlusion following traumatic intimal rupture Acta ch r scand [illegible]

[illegible] of the arteries in World War II An [illegible]

ELLIOT J A Acute arterial occlusion An unusual cause Surgery 39 (1956), 825

FOMON J J and WARREN W D Late complications of peripheral arterial injuries Arch Surg 91 (1965), 610

GIRL J Arteriography in arterial gunshot wounds Acta radiol Diagnosis 11 (1971), 78

KINMONTH J B The physiology and relief of traumatic arterial spasm Brit Med J 1 (1952) 59

KROH F [illegible] erimentelle Studi [illegible]

LINDBOM [illegible] 47 (1957), 449

LOVE L and BRAUN T Arteriography of peripheral vascular trauma Amer J Roentgenol 102 (1968) 431

LUMPKIN M B, LOGAN W D, COUVES C M and HOWARD J M Arteriography as an aid in the diagnosis and localization of acute arterial injuries Ann Surg 147 (1958), 353

SINKLER W H and SPENCER A D The value of peripheral arteriography in assessing acute vascular injuries Arch Surg 80 (1960), 300

SMITH R F SZILAGYI E and ELLIOT J R Fracture of the long bones with arterial injury due to blunt trauma Arch Surg 99 (1969) 315

WENZ W Die Bedeutung der Angiographie fur die Traumatologie *In* Angiographie und ihre Leistungen Arbeits und Fortbildungstagung 1968, S 43 Herausgegeben von K E Loose Georg Thieme Verlag, Stuttgart 1968

ZIPERMAN H H Acute arterial injuries in the Korean War, a statistical study Ann Surg 139 (1954) 1

an early stage of rupture a poorly defined perivascular accumulation of contrast medium at the site of the rupture may be present at angiography (Fig. 4). When circulation has become established within the haematoma, a well defined saccular cavity may be demonstrated. The pulsatile arterial flow taking place into the cavity may appear as a jet of the medium (Fig. 5 a), later on pooling of medium outlines the entire cavity (Fig. 5 b). The rate of filling of the pseudoaneurysm provides a valuable suggestion of the degree of bleeding that might occur during operation. Traumatic arteriovenous fistulas may arise particularly following penetrating trauma due to the close anatomic relationship between arteries and veins in the extremities. They may be associated with a pseudoaneurysm (Fig. 6), or may represent a direct arteriovenous communication (Fig. 7). The fistula may be difficult to diagnose clinically immediately after the trauma (FOMON & WARREN 1965) but at angiography even small fistulas are likely to be revealed.

Following an arteriovenous fistula the feeding artery dilates due to increased flow, the arterial flow beyond the fistula is reduced due to a low perfusion pressure, veins are rapidly filled with more concentrated contrast medium than normally, and dilate secondary to the increased venous pressure and flow. Veins distal to the fistula fill to a variable extent, initially to the first competent valve, later varicosities may occur. Further on, a high pressure gradient past the fistula provides for a persistent incentive to collateral formation, arterial as well as venous. At later stages a rich collateral network may therefore be a common angiographic feature (Fig. 8). An active therapeutic attitude is necessary to prevent loss of the limb in major arterial injuries. The advance of vascular surgery has caused a considerable decrease in the frequency of amputation in traumatic circulatory arrest, as for instance from 49 per cent in World War II (DE BAKEY & SIMEONE 1946) to 17.9 per cent in the Korean War (ZIPERMAN 1954). Massive haemorrhage and shock may often request immediate, life saving surgery in arterial injuries; with distal ischaemia an undue delay of operation may lead to loss of the limb. Therefore it may appear that there is no time for angiography. It should be pointed out however that angiography may usually be accomplished in less than one hour and be performed in the period of observation of the patient or planning of the operation.

SUMMARY

Angiographic findings in 31 cases of vascular injuries of the extremities sustained to a variety of traumas are reported. Angiography will usually demonstrate the type and site of the lesion as well as the presence and extent of collaterals. Its value in cases with obscure clinical findings as well as its importance for the therapeutic approach is stressed.

ZUSAMMENFASSUNG

Es wird über die angiographischen Befunde bei 31 Fällen von Gefässschädigungen der Extremitäten, die durch verschiedenste Traumata hervorgerufen waren, berichtet. Die

Angiographie vermag gewohnlich Typus und Umfang der Schädigung sowie das Vorkommen und den Umfang von Kollateralen nachzuweisen Deren Wert bei Fallen mit unklaren klinischen Befunden sowie deren Bedeutung fur die therapeutischen Überlegungen wird hervorgehoben

RÉSUMÉ

[illegible] sur son interet dans des cas ou les signes cliniques sont peu nets et insistent aussi sur son importance pour les indications thérapeutiques

REFERENCES

BELL D and COCKSHOTT W P Angiography of traumatic arterio-venous fistulae Clin Radiol 16 (1965), 241

BERGAN F Traumatic intimal rupture of the popliteal artery with acute ischemia of the limb in cases with supracondylar fractures of the femur J cardiovasc Surg (Torino) 4 (1963) 300

BROWN T [illegible] traumatic intimal rupture [illegible]

DE [illegible] 'eries in World War II An [illegible]

ELLIOT J A Acute arterial occlusion An unusual cause Surgery 39 (1956) 825

FOMON J J and WARREN W D Late complications of peripheral arterial injuries Arch Surg 91 (1965), 610

GIRL J Arteriography in arterial gunshot wounds Acta radiol Diagnosis 11 (1971), 78

KINMONTH J B The physiology and relief of traumatic arterial spasm Brit Med J 1 (1952) 59

KROH F Frische Schussverletzungen der [illegible] rimentelle Studi [illegible]

LINDBOM [illegible] 47 (1957), 449

LOVE L and BRAUN T Arteriography of peripheral vascular trauma Amer J Roentgenol 102 (1968), 431

LUMPKIN M B, LOGAN W D, COUVES C M and HOWARD J M Arteriography as an aid in the diagnosis and localization of acute arterial injuries Ann Surg 147 (1958), 353

SINKLER W H and SPENCER A D The value of peripheral arteriography in assessing acute vascular injuries Arch Surg 80 (1960) 300

SMITH R F SZILAGYI E and ELLIOT J R Fracture of the long bones with arterial injury due to blunt trauma Arch Surg 99 (1969), 315

WENZ W Die Bedeutung der Angiographie fur die Traumatologie *In* Angiographie und ihre Leistungen Arbeits und Fortbildungstagung 1968, S 43 Herausgegeben von K E Loose Georg Thieme Verlag, Stuttgart 1968

ZIPERMAN H H Acute arterial injuries in the Korean War, a statistical study Ann Surg 139 (1954) 1

FROM THE DEPARTMENTS OF DIAGNOSTIC RADIOLOGY AND OF GYNECOLOGY, THE NORWEGIAN RADIUM HOSPITAL, OSLO, NORWAY

PROJECTION DIFFERENCE INDEX IN LYMPHOGRAPHIC DIAGNOSIS OF LYMPH NODE METASTASES

ALF KOLBENSTVEDT

The accuracy of lymphography in the diagnosis of lymph node metastases is still under debate Filling defects in the lymph nodes due to fibrolipomatous or inflammatory infiltration may cause differential difficulties

WILJASALO (1965) suggested that while normal lymph nodes as a rule are flat like almonds, nodes with metastatic involvement tend to be more rounded and grape-like His theory was that a globular or oval node with a more or less rounded transverse section would have practically equal transverse diameters in films taken in different projections In a normal, flat node the transverse diameters would vary *in different views (Fig 1) The influence of the geometric enlargement in* different projections was analysed by WILJASALO in phantom experiments He found that with globular lead node models the difference between the largest and the smallest diameter measured on the films was less than 20 per cent of the smallest diameter, with a flat model more than 20 per cent He introduced the term Projection Difference Index (Px %) with the following definition

$$Px\% = \frac{100(a-b)}{b}$$

where a was the maximum and b the minimum transverse diameter

In patients with primary carcinoma of the uro-genital system or rectum sigmoid

Submitted for publication 25 January 1974

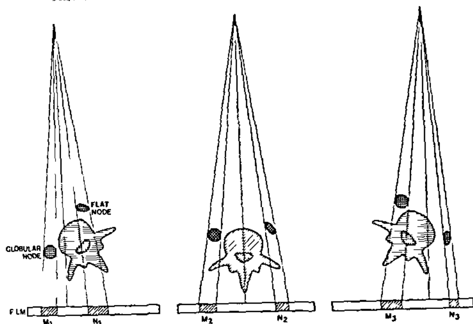


Fig 1 Projections of globular and flat lymph nodes in a p left and right oblique views The transverse diameters of the globular node (M_1 M_2 M_3) are relatively constant while those of the flat node (N_1 N_2 N_3) vary (After WILJASALO)

colon he found Px%<20 in 91 9 per cent of 62 lymph nodes presumably containing metastases histologic evidence was available in 33 nodes

WILJASALO further reported Px%>20 in 97 per cent of normal or fibrolipomatous lymph nodes in a material of 445 lymph nodes from 79 patients, 31 of whom were subjected to operation or puncture biopsy He concluded that with the Projection Difference Index it is possible to determine whether a defect of more than 0 5 cm in diameter is caused by a metastasis His statement was later supported by FISHER (1968) WIEDEMANN & SCHULZ (1972) pointed out that the smallest diameter in a flat node lying parallel to the a p film would be missed without lateral projection

This measurement method was introduced at our centre in April 1972 Certain practical problems soon emerged Firstly, the node to be measured was frequently overlapped by other nodes (particularly in lateral projection) Secondly, in lymph nodes with such large defects that only a crescent of lymphoid tissue remained there were no exact points between which measurements could be made It was thus felt that the measurements in at least one projection were often uncertain Some of the difficulties might possibly have been overcome with tomography This was considered but rejected when evidence of globular non metastatic and flat metastatic nodes were encountered (Figs 2, 3, 4) The statement that lymph nodes containing metastases larger than 0 5 cm have equal transverse diameters in all

a b

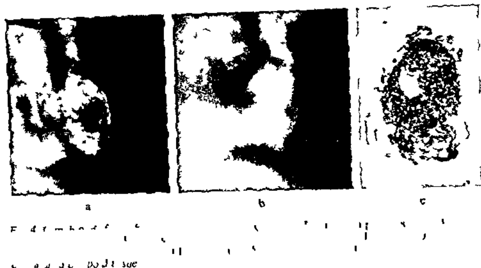
c d

Fig 2 Lymph node from the *left iliac* region a) Left anterior oblique projection The node is broad, with an evident *defect* b) The *transverse* diameter in the right anterior oblique projection is considerably *smaller* The Px % was calculated as 60 and consequently it should not contain a metastasis c) Film of the removed lymph node d) Histology (×3 5) demonstrates a metastasis



a b

Fig 3 Right iliac lymph node a) *Right anterior* oblique projection Node with large defect b) Left anterior oblique projec*tion* The transverse diameter considerably smaller Histology indicated metastasis, in spite of a Px % of 67



[illegible]

projections was therefore doubted and consequently also the value of the Projection Difference Index It was thus decided to measure lymph nodes removed by blunt dissection

Material and Methods During the period from February 1970 to March 1973 lymphography was performed in 300 patients with carcinoma of the uterine cervix, stages I and II Treatment consisted of radium insertions followed six weeks later by radical hysterectomy with pelvic lymphadenectomy An average of 30 6 lymph nodes per patient were removed The method of correlating lymphographic findings with microscopy has been dealt with previously (KOLBENSTVEDT & KNUDSEN 1974) A total of 220 removed lymph nodes were selected from 89 consecutive patients for measurements The selection criteria were as follows (1) Nodes that macroscopically appeared globular or oval with approximately equal transverse diameters in all projections (grape like) (2) nodes with possible metastases macroscopically or radiologically

Nodes with squeeze marks from the surgeon s forceps and indistinctly outlined nodes not allowing exact measurement were excluded The selected nodes were placed on envelope packed films and exposed in the following four projections (Fig 5)

1) Maximum transverse diameter parallel with film
2) Lymph node turned 60 around longitudinal axis
3) Lymph node turned 120 around longitudinal axis
4) Lymph node on edge with minimum diameter parallel to the film

When more or less flat lymph nodes were examined they were held in position by paper material FFD was 100 cm Further technical details regarding specimen radiography have been described previously (KOLBENSTVEDT & KNUDSEN) The max

Fig 5 Removed lymph node in four projections

imum and minimum transverse diameters on the films were measured and the Px% calculated After the radiologic examination the lymph nodes were without further delay prepared for histology

The selected nodes were as a rule somewhat firmer than normal No obvious change in shape due to the pressure of their own weight against the film could be observed (Fig 6), but to establish if such a change nevertheless occurred films were exposed of 20 selected lymph nodes submerged in saline immediately after removal, thus eliminating the effect of their own weight The saline was then aspirated and another film exposed with the nodes in the same position A possible shrinkage after removal was determined on films taken 5, 30 and 60 minutes later The nodes were covered by wet swabs between each exposure

Results

No differences in the diameters of the 20 lymph nodes measured submerged in saline and after aspiration of the fluid could be established and thus the pressure of their own weight did not alter the shape of the nodes The average shrinkage of the transverse diameter in one hour was less than 0 5 mm

a b c d

[illegible] - oblique projection The node has a
-fects are partly obscured by bony
verse diameter is less than half that
The flat shape is preserved In spite
ogy

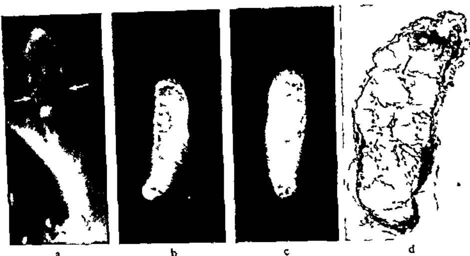


Fig 7 Lymph node from the left iliac region a) Lymph node with a large central defect The node was only clearly visible in the right anterior oblique projection b) and c) After removal films in two projections The node was almost cylindric with a Px % less than 10 d) Histology (×3 5) demonstrates a massive lipoid infiltration leaving only a rim of lymphoid tissue No evidence of metastasis

The majority of the lymph nodes were flat, with a Px % obviously greater than 20 The results of Px % calculations of the selected 220 lymph nodes are given in Table 1 No metastases were found on histologic examination in 190 nodes, of which 90 had a Px < 20 In 20 of these, defects were present which might consequently have been misinterpreted as metastases (Figs 4 7) Thus, even if the majority of the lymph nodes were flat the 89 patients on the average had 1 0 non metastatic globular or grape like lymph nodes with a Px % < 20

Of 30 lymph nodes with metastases 6 were found to be globular or grape like with the Px % < 20 The remaining 24 nodes were more or less discoid with a Px % > 20, only 1 of these metastases had a diameter smaller than 0 5 cm (Table 2) while 23 caused larger, evident defects (Figs 6, 8)

Discussion

The majority of normal lymph nodes were found to have a more or less flat shape as pointed out by Wiljasalo and by Wiljasalo & Wiljasalo (1972) A marked dis-

Table 1

Projection difference index (Px %) measured on selected removed lymph nodes

Lymph nodes	Px % 0–9 9	Px % 10–19 9	Px % 20–29 9	Px % >30	Total
Without metastases	33	57	45	55	190
With metastases	2	4	9	15	30

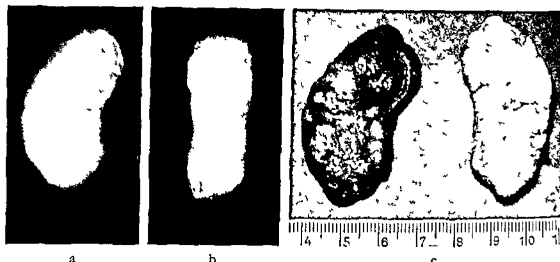


Fig 8 a) and b) Films in two projections of a removed lymph node entirely infiltrated by metastasis It is bean shaped in (a) and biconcave in (b) The Px % was about 50 c) Photograph of the totally infiltrated lymph node after sectioning into two parts

crepancy exists, however, between his Px % values of lymph nodes with metastases and those in the present material It might be said that measurements on clinical lymphographic films and on films of specimens are not directly comparable and that the Px % was originally not intended for use after removal of the nodes However, the recommended measurements are based on the assumption that lymph nodes with metastases are globular or grape like with equal transverse diameters in all projections, and the present material has indicated that this is not the case In the phantom experiments of WILJASALO the diameter of a lead globe in the pelvis varied from 37 mm in the left oblique projection to 42 mm in the a p projection Such variation due to different geometric enlargement was avoided in the present series, which gives a more correct recording of the shape and size Another possible source of error is the absence of histologic confirmation Every lymph node in the present series was subjected to histology but not in WILJASALO's series

The present material was more homogeneous than that of WILJASALO, which included patients with primary carcinomas in other pelvic organs than the uterine cervix, possibly in an advanced stage, as more than half of the lymphograms were considered to be positive The differences between the materials cannot, however,

Table 2

Size in cm of lymph node defects caused by metastases

	<0 5	0 5–0 9	1–2	>2
Px % <20	2	3	0	1
Px % >20	1	11	7	5

explain the discrepancy in the shape of metastatic lymph nodes, as both materials contain nodes with large, macroscopically evident metastases

The majority of normal lymph nodes certainly tend to be more discoid than the nodes with metastases, but an arbitrary limit at Px% 20 does not exist for either category

Conclusion

Though the overwhelming majority of normal lymph nodes were more or less flat with a Px% > 20 the patients in the present material on the average had 1 0 globular or grape like, non metastatic iliac lymph nodes with a Px% < 20 Such a node might well contain defects due to benign conditions Twenty-four of 30 removed lymph nodes with metastasis were more or less flat with a Px% > 20, which disagrees with the report of WILJASALO, who found Px% < 20 in 91 9 per cent of 62 presumably metastatic nodes from patients with carcinoma Our findings indicate that the value of the Projection Difference Index in lymphographic differential diagnosis is doubtful

SUMMARY

The Projection Difference Index (Px%) of WILJASALO for lymphographic diagnosis based on the hypothesis that normal nodes are flat while metastatic nodes are globular or grape-like was investigated in a material of 220 removed lymph nodes

The transverse diameters were measured on films exposed in four projections The metastatic lymph nodes as a rule deviated from the globular or grape like shape and doubt is therefore expressed about the diagnostic value of the Px%

ZUSAMMENFASSUNG

Der Projektions Unterschied Index (Px%) von WILJASALO fur die lymphographische Diagnose basiert auf der Hypothese, dass normale Lymphknoten flach sind während metastatische Lymphknoten rund oder traubenformig sind, was an einem Material von 220 entfernten Lymphknoten undersucht wurde Die transversalen Diameter wurden an Filmen gemessen die in vier Projektionen exponiert waren Die metastatischen Lymphknoten wichen in der Regel von einem runden oder traubenformigen Bild ab und es wird deshalb Zweifel uber den diagnostischen Wert vom Px% geäussert

RÉSUMÉ

Sur une série de 220 ganglions lymphatiques preleves l'auteur a étudié l Index de Difference suivant la Projection (Px%) de WILJASALO pour le diagnostic lymphographique base sur l'hypothése que les ganglions lymphatiques [illegible]

[illegible] ou en grappe, c est pourquoi l auteur [illegible] un doute sur l interét diagnostique du Px%

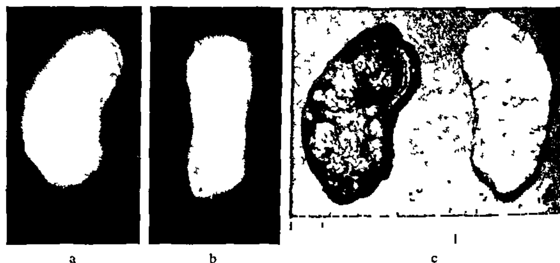


Fig 8 a) and b) Films in two projections of a removed lymph node entirely infiltrated by metastasis It is bean shaped in (a) and biconcave in (b) The Px % was about 50 c) Photograph of the totally infiltrated lymph node after sectioning into two parts

crepancy exists, however, between his Px % values of lymph nodes with metastases and those in the present material It might be said that measurements on clinical lymphographic films and on films of specimens are not directly comparable and that the Px % was originally not intended for use after removal of the nodes However, the recommended measurements are based on the assumption that lymph nodes with metastases are globular or grape like with equal transverse diameters in all projections, and the present material has indicated that this is not the case In the phantom experiments of WILJASALO the diameter of a lead globe in the pelvis varied from 37 mm in the left oblique projection to 42 mm in the a p projection Such variation due to different geometric enlargement was avoided in the present series, which gives a more correct recording of the shape and size Another possible source of error is the absence of histologic confirmation Every lymph node in the present series was subjected to histology but not in WILJASALO s series

The present material was more homogeneous than that of WILJASALO, which included patients with primary carcinomas in other pelvic organs than the uterine cervix, possibly in an advanced stage as more than half of the lymphograms were considered to be positive The differences between the materials cannot, however,

Table 2

Size in cm of lymph node defects caused by metastases

	<0 5	0 5–0 9	1 2	>2
Px % <20	2	3	0	1
Px % >20	1	11	7	5

ACTA RADIOLOGICA

OFFICIAL ORGAN OF THE RADIOLOGICAL SOCIETIES OF
DENMARK, FINLAND, NORWAY AND SWEDEN

Vol 16 Fasc 3	DIAGNOSIS	1975 May

LUMBAR MYELOGRAPHY WITH MEGLUMINE IOCARMATE AND METRIZAMIDE

TOMAS HINDMARSH

Double-blind technique has not previously been used in man to compare contrast media for use in the subarachnoid space Synthetic compounds are marketed continually and an appropriate test model is required to provide data adequate for comparison of these media The two water-soluble contrast media that at present seem to be tolerated best by the central nervous system have been compared in the present investigation The first of these is *meglumine iocarmate (Dimer-X)* which has come into wide use during the last years However, a slight but definite tendency to provoke *myoclonic* spasms has been [illegible]
GONSETTE 1971, AHLGR[illegible]
iocarmate seems to be [illegible]
lumbar myelography [illegible], a new non-ionic compound, was released for clinical trials in the middle of 1972 after having been extensively tested in laboratory animals The results suggested that the tolerance of the central nervous system [illegible]
[illegible]
[illegible] (GONSETTE 1973, HINDMARSH 1973, SKALPE *et coll.* 1973) The prospect of a medium with a toxicity low enough to permit examination

From the Departments of Neuroradiology (Director T Greitz), Thoracic Radiology (Director G Törnell) and Clinical Neurophysiology (Director L. Widén), Karolinska sjukhuset, S-104 01 Stockholm, Sweden. Submitted for publication 2 January 1974

REFERENCES

FISCHER H D Interpretation of normal and abnormal lymphograms Cancer Chemother Rep 52 (1968) 119

KOLBENSTVEDT A and KNUDSEN O A method for lymphographic and histologic correlation Experience from 300 patients treated by pelvic lymphadenectomy Gyne Oncol 2 (1974) 9

WIEDEMANN F H und SCHULZ W Der Projection Difference-Index Befunde an normalen und pathologischen Lymphadenogrammen Radiol diagn (Berl) 5 (1972) 612.

WILJASALO M Lymphographic differential diagnosis of neoplastic diseases Acta radiol (1965) Suppl No 247

— und WILJASALO S Ergebnisse mit dem Projection Difference-Index (PX%) Radiol diagn (Berl) 5 (1972) 609

the meglumine iocarmate solution had a slightly yellow tint, to hide this, brown masking tape was constantly applied to the syringe Using this somewhat elaborate procedure, the examiner could be successfully kept unaware of which medium that was used for each individual examination

Technique Examinations were performed in the forenoon on fasting patients without premedication Before myelography an EEG recording (KS group only) and a neurologic examination with special reference to the lower extremities were undertaken Lumbar puncture was made usually at the level of L2–L3 after local anaesthesia with 1 to 2 ml Xylocain 1 % The needle used for the lumbar puncture had an OD of 0 7 mm The patient was in the left lateral recumbent position and the head-end of the table was raised 10 degrees from the horizontal plane When a suitable position of the needle tip had been achieved, the CSF pressure was measured, the Queckenstedt sign was checked and 10 ml CSF was removed and sent for laboratory analysis The slow injection of contrast medium was monitored on TV The medium, which was not mixed with CSF in the syringe, was allowed to reach the level of the first lumbar vertebra as seen on an a p film with the patient still in the lateral recumbent position Films were exposed with horizontal beam direction, the patient in the left lateral, right lateral, prone, and finally erect position

The concentration used was 140 mg I/ml The physical properties of the two media in this concentration appear in Table 1 The mean dose was for metrizamide 12 7 ml (range 6–20) and for meglumine iocarmate 13 1 (range 6–19)

Following myelography the patients were kept in bed for at least 22 hours For 8 hours after the contrast injection the head-end of the bed was raised about 30 degrees and during this time the patients were under close observation After this period of time the tilt was decreased but the head-end of the bed was kept raised about 5 degrees till the next morning Written instructions accompanying each patient served to ensure that this program of after-care was carried out, with a particular warning to everybody handling the patient not to lower the head-end of the bed The next day, 22 to 26 hours after myelography, the patients were subjected to a repeat EEG recording (KS material only), another neurologic examination, a standard interview and finally also a second lumbar puncture with removal of a new specimen for laboratory analyses, and in some cases a second pressure recording

The EEG was recorded on a 16-channel apparatus using 21 electrodes arranged according to the 10–20 system Each recording had a duration of about 12 minutes The CSF pressure was measured with an open end manometer CSF laboratory analyses made on all patients were white and red cell count and protein These figures thus derive from two different laboratories Since the laboratory method and the standards were the same and since no statistical difference between the KS and HS values existed within the metrizamide and meglumine iocarmate groups respectively, it was not considered necessary to treat the two groups as separate entities Glucose analyses were made in all KS cases, chloride analyses only in 40 cases in the KS

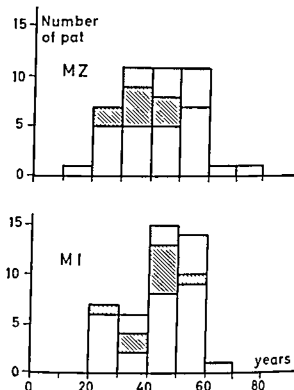


Fig 1 Sex and age distribution MZ metrizamide group MI = meglumine iocarmate group ♀, ♂ HS, ♂ KS

also of the thoracic and cervical regions prompted an extended trial Thus, the purpose of the present investigation was twofold (1) to establish a test model involving double-blind technique for comparison of myelographic contrast media, (2) to use this model for clinical comparison of the two most promising media for lumbar subarachnoid application

Material and Methods

From the clinical point of view the material was homogeneous consisting of 86 consecutive cases all presenting a history of lumbar or sacral root involvement (Fig 1) Sixty-eight patients (50 men and 18 women) were examined at Karolinska Sjukhuset and a further 18 patients (all men) were examined at Huddinge Sjukhus These fractions of the material will be referred to in the following by the letters KS and HS respectively EEG recordings were only performed in the KS material The contrast medium used in each individual case was in accordance with a code list, made up by casting lots before the start of the investigation In advance, a break of code was programmed to occur after the first 50 examinations in order to allow at this stage an evaluation of trends which might necessitate minor changes of methods or analyses Following this break the coding was resumed

The examiner was presented with a glass syringe containing 20 ml of contrast medium having been prepared in another room by assistants with access to the list and the contrast code kept under lock and key The metrizamide solution was clear,

the meglumine iocarmate solution had a slightly yellow tint, to hide this, brown masking tape was constantly applied to the syringe Using this somewhat elaborate procedure, the examiner could be successfully kept unaware of which medium that was used for each individual examination

Technique Examinations were performed in the forenoon on fasting patients without premedication Before myelography an EEG recording (KS group only) and a neurologic examination with special reference to the lower extremities were undertaken Lumbar puncture was made usually at the level of L2–L3 after local anaesthesia with 1 to 2 ml Xylocain 1 % The needle used for the lumbar puncture had an OD of 0 7 mm The patient was in the left lateral recumbent position and the head-end of the table was raised 10 degrees from the horizontal plane When a suitable position of the needle tip had been achieved, the CSF pressure was measured, the Queckenstedt test was checked and 10 ml CSF was removed and sent for laboratory analysis. The [illegible] injection of contrast medium was monitored on TV The medium, which was [illegible] mixed with CSF in the syringe, was allowed to reach the level of the first [illegible] vertebra as seen on an a p film with the patient still in the lateral recumbent [illegible] Films were exposed with horizontal beam direction, the patient in [illegible] right lateral, prone, and finally erect position

The concentration used was 140 mg I/ml The physical properties of [illegible] in this concentration appear in Table 1 The mean dose was for [illegible] (range 6–20) and for meglumine iocarmate 13 1 (range 6–19)

Following myelography the patients were kept in bed for [illegible] 8 hours after the contrast injection the head-end of the bed was [illegible] and during this time the patients were under close observation [illegible] time the tilt was decreased but the head-end of the bed was [illegible] degrees till the next morning Written instructions accompan[illegible] to ensure that this program of after-care was carried out [illegible] to everybody handling the patient not to lower the he[illegible] day, 22 to 26 hours after myelography, the patients were [illegible] recording (KS material only), another neurologic exam[illegible] and finally also a second lumbar puncture with [illegible] laboratory analyses and in some cases a second [illegible]

The EEG was recorded on a 16-channel appa[illegible] according to the 10–20 system Each recording [illegible] The CSF pressure was measured with an [illegible] analyses made on all patients were white and [illegible] thus derive from two different laborato[illegible] standards were the same and since no [illegible] values existed within the metrizamide [illegible] it was not considered necessary to [illegible] analyses were made in all KS case[illegible]

Table 1

Physical properties of the contrast media

	Viscosity at 37°C cP	Density at 37°C g/ml	Osmolality mosm/kg
Metrizamide 140 mg I/ml	1 5	1 125	260
Meglumine iocarmate 140 mg I/ml	1 7	1 159	430

material For analyses that could prove useful later, a part of each CSF specimen was always (in KS material) put away in a freezer After termination of the trial these specimens enabled determination of iodine levels (in 39 patients), quantitative paper electrophoresis in selected cases (21 patients) and a more correct estimation of protein levels *in the meglumine iocarmate group (19 patients) Remnants of meglumine* iocarmate in the CSF proved to interfere to a considerable degree with the protein analyses, made according to LOWRY (1951) In the latter 19 patients the deep-frozen specimens were analysed with a fluorometric method using the reagent Fluram (BÖHLEN et coll 1973)

Blood pressure and pulse rate were recorded at 5 min intervals during myelography and at 15 to 30 min intervals during the 8 hour period of special observation in the ward Body temperature was recorded in 20 cases of each group at 7 a m *and* 3 p m the day of myelography and the next day

The standard interview the second day was made according to a written formula Subjective symptoms were graded as follows Grade 1, the mildest degree of side effect was acknowledged only upon direct questioning of the patient as to the presence of each single symptom, e g headache, nausea, increased pain in back or in legs, numbness, twitches, difficulties to void bladder Grade 2 was defined as an affirmative answer to the general question "Did you experience any discomfort that you think *can be related to the examination?" The most relevant subjective reactions* were graded 3 and considered as such when the patient complained of a symptom spontaneously or when first greeted by the doctor with the phrase "How are you to day?"

All tabulations and interpretations of the results were made before break of code Statistical methods used were Student's *t*-test and *the* chi-square *test*

Results

Patients subjected to myelography with meglumine iocarmate are in the following referred to as MI patients and belonging to the MI group For patients who received metrizamide, the capitals MZ will be used Data obtained at second examination, 22 to 26 hours after injection of the contrast medium, are referred to as 24-hour values

Table 2

Adverse reactions during the 24 hour period after myelography

	Metrizamide		Meglumine iocarmate	
	No of patients	Per cent	No of patients	Per cent
Headache	9	21	9	21
Nausea	2 }	7	3 }	14
Vomiting	1 }		2 }	
Dizziness	5	11	6	14
Increased pain	12	28	9	21
Muscular tension	1 }		4 }	
Feeling of numbness	1 }	7	2 }	30
'Weak legs'	1 }		3 }	
Paraesthesia (late)	0 }		3 }	
Difficulties to void bladder	2		2	
Myoclonic spasms	0		2	
Epilepsy	0		1	
(Hypotension)	1		0	

During myelography adverse reactions were negligible in both groups One patient in each group complained of mild paraesthesia in the perineal region during injection of contrast medium but for no more than 10 min afterwards No other symptoms or signs occurred during myelography Blood pressure and pulse rate did not change significantly during examination with any of the media

The next morning, 22 to 26 hours after myelography, few patients spontaneously complained of symptoms On the general question from the standard formula "How do you feel to-day?", 60 per cent of all patients in both groups gave a quite indifferent answer, such as 'Alright" or "No troubles except for my usual pains" On a closer question [illegible] deni[illegible] 72 p[illegible] group and 45 5 per cent in the MI group did not reveal any symptoms at the first general question, but after a complete interview there remained only 37 2 per cent (16 patients) and 23 3 per cent (10 patients) in the MZ and MI

Table 3

Grading of headache appearing during the first 24 hours after myelography

	Grade 1	Grade 2	Grade 3	Total	Per cent
Metrizamide group	5	2	2	9	21
Meglumine iocarmate group	2	3	4	9	21

Table 4

Duration of headache appearing during the first 24 hours after myelography

	≤2 hours	2–8 hours	8–24 hours
Metrizamide group	5	2	2
Meglumine iocarmate group	2	2	5

groups respectively The overall frequency of different symptoms as reported by the patients at the interview is given in Table 2

Headache was experienced by 9 patients in each group (Table 2) When the reports of this symptom were classified according to the principles given previously a comparison tended to favour the MZ group When only duration of this symptom was considered, the tendency was the same (Tables 3, 4)

Increase of pre-existent pain in the back or leg was a common finding in both groups and using the previous classification characteristics Table 5 was constructed

Nausea and vomiting were not frequent in either group In 3 cases vomiting occurred in the morning the day after myelography but not until the patient got out of bed Mild leg symptoms, e g muscular tension, feeling of numbness, 'weak legs' and late paraesthesias, appeared in both materials Taken together these mild leg symptoms were more frequent in the MI than in the MZ group and the difference was significant on the 5 per cent level These symptoms were in all cases graded 1 or 2 except for one MZ patient, who had muscular tension and complained spontaneously None of these symptoms lasted longer than 36 hours In no one of these cases did the second neurologic examination reveal any change from the day before The late paraesthesias were similar to those mentioned before They appeared 1 to 2 hours after examination and had a duration of 2 to 6 hours Dizziness, usually combined with a feeling of a 'heavy head' or a 'hang-over', as described by the patients, had the same frequency in both groups This symptom was significantly (0 1 % level) more frequent in women than in men The incidence of headache and nausea was also more frequent in women but did not significantly differ from the incidence in male patients

Difficulties to void the bladder were reported by 2 patients in each group These difficulties were not great (grade 1), referred only to one occasion in each case and never required medical attention One MZ patient fainted in connection with the

Table 5

Grading of increased pain during the first 24 hours after myelography

	Grade 1	Grade 2	Grade 3	Total	Per cent
Metrizamide group	4	4	4	12	28
Meglumine iocarmate group	2	3	4	9	21

Table 6

EEG abnormalities before and 24 hours after myelography

	Metrizamide	Meglumine iocarmate
Total number of cases	34	34
Number of cases with abnormal EEG before myelography	9	9
Number of cases with normal EEG before and abnormal EEG after myelography	7 (1 Ep*)	4 (1 Ep*)
Number of cases with abnormal EEG before and increased abnormality after myelography	5	4 (1 Ep*)
Number of cases with no change in EEG	22	26

* Epileptogenic activity

second EEG recording However, this patient as well as all the others, displayed no hypotension during the 8 hours after myelography or at the recording 24 hours after myelography

A grand mal seizure appeared in one MI patient 23 hours after injection of the contrast medium, ceasing promptly after intravenous injection of diazepam Clonic spasms of muscles in the lower extremities occurred in 2 MI patients In one male these commenced 3 hours after injection of contrast medium and continued for about 2 hours intermittently One of these episodes was accompanied by involuntary discharge of urine The other patient, a female, reported 8 to 10 violent contractions of muscles in the gluteal regions during a period of some 30 min, occurring about 12 hours after injection Complaints from the musculoskeletal system, other than those listed, occurred in a few instances, they were identified by the patients as having been present before the examination and not related to indication for myelography Consequently these complaints were not taken into account One MZ patient with a concurrent upper respiratory tract infection, had a marked increase in temperature after myelography In the other patients recorded (19 MZ and 20 MI patients) temperature never increased more than 1°C

The second neurologic examination very seldom revealed any change compared with the first one In the vast majority of cases the author made both examinations Two MZ patients experienced a somewhat increased loss of sensibility No patient had stiffness of the neck An increase in tendon reflexes was never apparent

In the premyelographic EEG recordings minor abnormalities were present in 9 cases of each group in the form of an increased amount of diffuse slow wave activity Five of these cases in the MZ group and 4 in the MI group displayed increased abnormality at the recording 24 hours after myelography (Table 6) In 7 cases in the MZ group and in 4 in the MI group with normal premyelographic EEG, abnormalities appeared at the second recording The majority of these changes were characterized

Table 4

Duration of headache appearing during the first 24 hours after myelography

	≤2 hours	2–8 hours	8–24 hours
Metrizamide group	5	2	2
Meglumine iocarmate group	2	2	5

groups respectively The overall frequency of different symptoms as reported by the patients at the interview is given in Table 2

Headache was experienced by 9 patients in each group (Table 2) When the reports of this symptom were classified according to the principles given previously a comparison tended to favour the MZ group When only duration of this symptom was considered, the tendency was the same (Tables 3, 4)

Increase of pre-existent pain in the back or leg was a common finding in both groups and using the previous classification characteristics Table 5 was constructed

Nausea and vomiting were not frequent in either group In 3 cases vomiting occurred in the morning the day after myelography but not until the patient got out of bed Mild leg symptoms, e g muscular tension, feeling of numbness, 'weak legs' and late paraesthesias, appeared in both materials Taken together these mild leg symptoms were more frequent in the MI than in the MZ group and the difference was significant on the 5 per cent level These symptoms were in all cases graded 1 or 2 except for one MZ patient, who had muscular tension and complained spontaneously None of these symptoms lasted longer than 36 hours In no one of these cases did the second neurologic examination reveal any change from the day before The late paraesthesias were similar to those mentioned before They appeared 1 to 2 hours after examination and had a duration of 2 to 6 hours Dizziness, usually combined with a feeling of a 'heavy head' or a 'hang-over', as described by the patients, had the same frequency in both groups This symptom was significantly (0 1 % level) more frequent in women than in men The incidence of headache and nausea was also more frequent in women but did not significantly differ from the incidence in male patients

Difficulties to void the bladder were reported by 2 patients in each group These difficulties were not great (grade 1), referred only to one occasion in each case and never required medical attention One MZ patient fainted in connection with the

Table 5

Grading of increased pain during the first 24 hours after myelography

	Grade 1	Grade 2	Grade 3	Total	Per cent
Metrizamide group	4	4	4	12	28
Meglumine iocarmate group	2	3	4	9	21

Table 6

EEG abnormalities before and 24 hours after myelography

	Metrizamide	Meglumine iocarmate
Total number of cases	34	34
Number of cases with abnormal EEG before myelography	9	9
Number of cases with normal EEG before and abnormal EEG after myelography	7 (1 Ep*)	4 (1 Ep*)
Number of cases with abnormal EEG before and increased abnormality after myelography	5	4 (1 Ep*)
Number of cases with no change in EEG	22	26

* Epileptogenic activity

second EEG recording However, this patient as well as all the others, displayed no hypotension during the 8 hours after myelography or at the recording 24 hours after myelography

A grand mal seizure appeared in one MI patient 23 hours after injection of the contrast medium, ceasing promptly after intravenous injection of diazepam Clonic spasms of muscles in the lower extremities occurred in 2 MI patients In one male these commenced 3 hours after injection of contrast medium and continued for about 2 hours intermittently One of these episodes was accompanied by involuntary discharge of urine The other patient, a female, reported 8 to 10 violent contractions of muscles in the gluteal regions during a period of some 30 min, occurring about 12 hours after injection Complaints from the musculoskeletal system, other than those listed, occurred in a few instances, they were identified by the patients as having been present before the examination and not related to indication for myelography Consequently these complaints were not taken into account One MZ patient with a concurrent upper respiratory tract infection, had a marked increase in temperature after myelography In the other patients recorded (19 MZ and 20 MI patients) temperature never increased more than 1°C

The second neurologic examination very seldom revealed any change compared with the first one In the vast majority of cases the author made both examinations Two MZ patients experienced a somewhat increased loss of sensibility No patient had stiffness of the neck An increase in tendon reflexes was never apparent

In the premyelographic EEG recordings minor abnormalities were present in 9 cases of each group in the form of an increased amount of diffuse slow wave activity Five of these cases in the MZ group and 4 in the MI [illegible]

[illegible] The majority of these changes were characterized

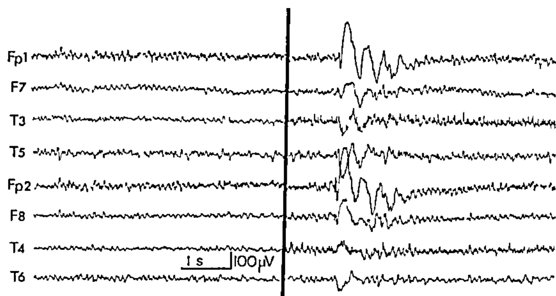


Fig 2 EEG records before (left) and 24 hours after (right) lumbar myelography with meglumine iocarmate Recordings with a Goldman average reference electrode The postmyelographic record shows a bilaterally synchronous episode with a spike and wave complex and paroxysmal slow waves

by increased slow wave activity but in 3 cases, 2 in the MI group and one in the MZ group, epileptogenic activity appeared as well (Fig 2) In the MI patients this activity (bilaterally synchronous episodes of spike and waves) was probably projected from deep structures of the brain, whereas a more focal appearance was present in the MZ case, where a few sharp waves were recorded in the temporal and parietal cortical regions in the left hemisphere

CSF white cell counts in the premyelographic specimens ranged from 0–8 cells/mm³ Three cases in each group had 24-hour cell counts that widely differed from the other counts obtained These values were 134, 168 and 1 097 cells/mm³ for the MZ patients and for the MI patients 150, 167 and 688 cells/mm³ (Table 7)

Red cell count in the CSF (Table 8) was not significantly increased in the specimens obtained at the first puncture, but after 24 hours an increase was more often encountered in both groups, suggesting a slight bleeding induced by the first puncture

With the Lowry method a significant increase in the CSF protein content was found after 24 hours in the MI group The mean increase was 40 4 (SEM 8 9) mg/100 ml, which also significantly differs from the increase in the MZ group, which was 3 7 (SEM 3 5) mg/100 ml However, in the 19 MI cases, where CSF specimens were available for a second analysis with the 'Fluram' reagent, no increase but rather a slight decrease was found in the 24-hour specimens (mean change—11 5 mg/100 ml) The 19 patients constituted a representative sample of the whole MI group with respect to protein levels The mean change in 24 hour CSF protein level obtained with the Lowry method differed significantly (1 % level) from that obtained with the 'Fluram' method

Table 7

CSF white cell count increase/mm³ 24 hours after myelography

	0	1–10	11–50	100–200	>500	Mean
Metrizamide	10	26	4	2	1	36 2
Meglumine iocarmate	14	23	3	2	1	26 3

In 2 cases with myoclonic spasms and in 3 with epileptogenic EEG changes, quantitative paper electrophoresis was made on deep-frozen CSF specimens from the first lumbar puncture In the MI group, one case with myoclonic spasms and 2 cases with epileptogenic activity in EEG had evidence of barrier damage The same analyses were made on specimens obtained from 5 patients with marked increase in 24-hour white cell count in the CSF All these had evidence of barrier damage as well Furthermore, barrier damage was verified by electrophoresis in all 11 cases (KS material) with CSF protein level ≥75 mg/100 ml (8 MZ and 3 MI cases) In these cases no meningeal reaction and no serious symptoms were apparent

CSF glucose level did not change significantly in either group (KS material), nor was there any significant change in CSF chloride content, as evidenced by analyses in 20 consecutive patients of each group

The analyses of the lumbar CSF iodine content 24 hours after myelography gave a mean of 4 94 (SEM 1 13) mg I/ml in the MI group (19 patients) and 1 44 (SEM 0 39) mg I/ml in the MZ group (20 patients) The difference between the two groups is significant on the 1 per cent level

CSF pressure was measured in 24 MZ and 26 MI patients As could be expected, a slight decrease in pressure was encountered at recording 24 hours after myelography This tendency was of the same magnitude in both groups

The diagnostic effectiveness of the two media was the same, which was also supported by the findings at operation in the 14 patients of each group who were operated upon Except for 2 MI and one MZ case, the findings at operation were consistent with the radiologic diagnosis

Table 8

CSF red cell count/mm³ before and 24 hours after myelography

	0–10	11–100	101–1 000	>1 000
Metrizamide				
0 hours	37	4	2	0
24 hours	27	8	7	1
Meglumine iocarmate				
0 hours	40	2	1	0
24 hours	27	4	10	2

Discussion

The mild paraesthesias that appeared in 2 patients during myelography were probably due to direct irritation of roots by the needle In a few cases in the MI group the same symptom appeared later, this time probably due to a direct irritative effect on the roots by the contrast medium Other mild leg symptoms, such as muscular tension, feeling of numbness and 'weak legs', were probably also due to a direct irritative effect of the contrast media The lower incidence of these symptoms in myelography with metrizamide may reflect a higher tolerance of the central nervous system to this medium GONSETTE (1973) has reported sensation of heat by injection of metrizamide This was not experienced by any patients in this material

With respect to other minor adverse reactions appearing during the first 24 hours, the two groups did not differ significantly Headache occurred in the same number of patients and the difference evidenced by the grading standard was small (Tables 3, 4) The incidence of this symptom was in fact exceptionally low in both groups Both SKALPE et coll (1973) and GONSETTE (1973) reported a much higher incidence of headache after myelography with metrizamide 37 and 67 per cent respectively They, however, used a higher concentration and brought the contrast medium above the lumbar region Furthermore, the observation time was not restricted to the 24-hour period after myelography Also with meglumine iocarmate the incidence of headache has been reported to be higher than in this material (GONSETTE 1971)

Accentuation of pre-existent back and leg pain was quite common in both groups This symptom probably had little to do with the myelography as such, but more likely was due to the confinement in bed in a fixed position

Nausea, vomiting, and dizziness as well as headache were all more common in the female patients of both groups This sex difference, which is also reported after diagnostic lumbar puncture (TOURTELOTTE et coll 1964), is of some interest since it points out the importance of an even distribution of the sexes in materials used for comparison of subjective symptoms

Symptoms indicating a more serious toxic reaction appeared in 3 MI cases 2 with myoclonic spasms and one with a grand mal seizure The doses used in the 2 myoclonus cases were 14 and 19 ml, respectively, and in the case with the grand mal seizure 16 ml These doses are fairly high The contrast level in none of these cases extended beyond the L1 vertebra However, it seems that with the dosage used, the contrast medium may later reach the spinal cord and even the cerebral cortex in a toxic concentration None of these cases had a history of epilepsy One of the patients with myoclonus had 10 years previously suffered from a luetic infection, which was properly treated and now quiescent

No change appeared in EEG in the two myoclonus cases (The grand mal case being examined at HS was not subjected to EEG recordings) The 3 cases with post-myelographic epileptogenic activity in the EEG had no clinical epileptic manifestations and no previous history of epilepsy They had only slight (grade 1 or 2) symptoms of an unspecific type

Epileptic seizures have been reported in a few cases after lumbar myelography with meglumine iocarmate (GONSETTE 1971, LUNVEN et coll 1972, among others) and in one case after cervical myelography with metrizamide (HINDMARSH et coll, to be published) This patient was on medication with a phenothiazine derivative (chlorpromazine), a drug known to lower the convulsive threshold A possible interaction between metrizamide and this drug was discussed as a cause of the seizures It is of interest that also the MZ patient, who in the present investigation had postmyelographic epileptogenic EEG abnormalities, was on medication with a phenothiazine derivative (dixyrazine) The 3 MI patients with epileptic (clinical or EEG) manifestations had no drugs of this kind

The higher incidence of the more unspecific slow wave activity in the MZ group can probably be accounted for by the lower specific weight of metrizamide (Table 1), which makes it more apt to mix with the CSF, to be more easily transported and to reach the cerebral cortex in a higher concentration than meglumine iocarmate This is further supported by the fact that the 24-hour iodine level in the lumbar CSF was significantly less in the MZ than in the MI cases Slow wave activity has also been reported by KAADA (1973), who found an incidence of 16 per cent of such findings after lumbar myelography with metrizamide in a concentration of 170 mg I/ml and also demonstrated them to be transient He considered these changes to be manifestations of a non irritative interference with the function of the brain Also GONSETTE (1973) found similar abnormalities in 15 per cent of 46 cases subjected to lumbar or thoraco-cervical myelography No correlation was found between the slow wave activity and the dose of contrast medium in the present material, nor was there any relation between EEG abnormalities and doses of analgetic drugs administered to the patients during the 24 hours after examination

The CSF cell analyses could not separate the MZ and MI groups It seems likely that the t[illegible] in m [illegible] puzz [illegible] distr[illegible] of the contrast medium It is possible that the marked meningeal cell reaction is due to an allergic phenomenon Cultivation for microorganisms proved negative The overall cell reaction otherwise was very mild with both media and well below the one induced by gas myelography with oxygen (HINDMARSH 1973) Cases with high cell reaction had only slight clinical symptoms, with the exception of the case suffering a grand mal seizure

Meglumine iocarmate interfered with the Lowry protein analysis to give too high protein values In vitro tests demonstrated that a CSF iodine level of 5 mg I/ml adds some 50 per cent to the true value obtained with the Lowry method Also metrizamide interfered with the Lowry protein analysis but far less an iodine level of 1 5 mg I/ml adds less than 1 per cent to the true value To conclude, it seems safe to state that none of the two media gives rise to an increase in protein content in the CSF during the first 24 hours after myelography

The premyelographic protein content in CSF was increased in many patients, but the level of protein did not correlate to postmyelographic symptoms or to changes in EEG recordings. No direct correlation between barrier damage, as evidenced by electrophoresis, and meningeal reaction could be established, nor between barrier damage and toxic effects from meglumine iocarmate.

Clinical aspects. Lumbar myelography should not be strictly confined to the lumbar region but should also enable examination of disorders in the cauda equina and the lower thoracic region. Hence, a positive contrast medium for myelography cannot be considered suitable unless it does allow a complete examination of the lumbar and lower thoracic regions without clinically important side effects. In this series, however, the two media were compared only at a lumbar level, since the upper limit of the contrast column was not brought above the first lumbar vertebra. The reason for this restriction was to avoid too high doses of meglumine iocarmate. Nevertheless, with the dosage used, the recommended maximum dose (5 ml of undiluted medium) often was exceeded. Because of the high dosage, observation of the patients was intensified with continuous alertness for minute symptoms.

It is obvious from the present comparison that no great differences between the two media exist when used for lumbar myelography. It seems reasonable to believe, however, that the margin of security is smaller with meglumine iocarmate when a dosage is used that enables a complete examination of the lumbar subarachnoid space. The central nervous system seems to tolerate metrizamide better than meglumine iocarmate, as reflected by the lower frequency of leg symptoms, particularly myoclonic spasms, which never appeared in the MZ group. Furthermore, the lower incidence of epileptogenic activity in the MZ group speaks in favour of this medium. The evidence of a high tolerance of the CNS to metrizamide is in agreement with the results obtained in animal experiments (Acta radiol. Suppl. No. 335, 1973).

The standardized questioning did not reveal any major difference between the two media. However, the use of this questionaire displayed the considerable difference in answers to a casual question as opposed to those obtained after a detailed and specific interrogation. An adequate evaluation of subjective symptoms cannot be made unless a standardized double-blind technique is rigidly applied. Thus, the answers must be noted and the evaluation of the complaints made without knowledge as to which medium has been administered in the individual case. Comparison of results from different centers is of limited value as far as subjective symptoms are concerned and this is true also for comparison of different media in the same clinic at different times.

Conclusion

A double-blind technique is recommended for comparison of contrast media for myelography. Metrizamide, although not completely inert, is better tolerated by the central nervous system than meglumine iocarmate and should be preferred for

lumbar myelography Metrizamide and meglumine iocarmate both rank high with regard to the quality of diagnostic information, and—provided that the iodine concentration is the same—seem to be equal in this respect

SUMMARY

Metrizamide and meglumine iocarmate (Dimer-X), which at present are the contrast media for myelography best tolerated by the central nervous system, were compared in a double-blind test comprising a total of 86 patients, all with symptoms of lumbar or sacral root involvement Symptoms appearing were recorded using a standard interview formula 24 hours after myelography EEG, routine laboratory analyses of CSF and neurologic examinations were also made In some cases CSF paper electrophoresis, CSF pressure recordings and determination of CSF iodine content were obtained

ZUSAMMENFASSUNG

[illegible]
zu [illegible]
in [illegible]
[illegible] sakralen Wurzelbeteiligung hatten, verglichen Die auftretenden Symptome wurden [illegible]
graphie [illegible]
des CSF [illegible]
Papierel[illegible], CSF Druck Registrierungen und Bestimmungen des CSF Jod Gehalts erhalten

RÉSUMÉ

L auteur a comparé par une etude en double aveugle, sur un total de 86 malades presentant tous des signes d atteinte des racines lombaires ou sacrées, le métrizamide et l'iocarmate de méglumine (Dimer X) qui sont actuellement les moyens de contraste myelographiques les mieux toleres par le système nerveux central Les symptomes ont eté notés suivant une formule d interv[illegible]
[illegible]
[illegible] en iode du LCR

REFERENCES

AHLGREN P Lumbar myelography with Dimer X IX Symposium Neuroradiologicum, Gothenburg, Aug. 1970 Book of abstracts, p 135
— Dimer-X A new contrast medium for lumbar myelography without spinal anaesthesia Acta radiol Diagnosis 13 (1972), 753
ALMÉN T Application of non ionic and ionic contrast media to the external vessel surface Effects on microcirculation in the bat wing Acta radiol (1973) Suppl No 335, p 239

BAUMGARTNER J, BRAUN J P, CARON J, CECILE J, FISCHGOLD H, GONSETTE R, HIRSCH J F, LEGRE J et METZGER J Radiculographie au Dimer-X Premiers résultats après 630 examens J Radiol Electrol 51 (1970), 557

BÖHLEN P, STEIN S, DAIRMAN W and UDENFRIEND S Fluorometric assay of proteins in the nanogram range Arch Biochem Biophys 155 (1973), 213

GONSETTE R An experimental and clinical assessment of water soluble contrast medium in neuroradiology A new medium—Dimer-X Clin Radiol 23 (1971), 49

— Biologic tolerance of the central nervous system to metrizamide Acta radiol (1973) Suppl No 335, p 25

— Metrizamide as contrast medium for myelography and ventriculography Preliminary clinical experiences Acta radiol (1973) Suppl No 335, p 346

GREPE A and WIDÉN L Neurotoxic effect of intracranial subarachnoid application of metrizamide and meglumine iocarmate An experimental investigation in dogs in neuro lept analgesia Acta radiol (1973) Suppl No 335, p 102

— — Effects of cisternal application of metrizamide An experimental investigation in dogs in N_2O analgesia with and without Halothane Acta radiol (1973) Suppl No 335, p 119

HINDMARSH T Methiodal sodium and metrizamide in lumbar myelography Acta radiol (1973) Suppl No 335, p 359

— GREPE A and WIDÉN L Metrizamide phenothiazine interaction Report of a case with seizures following myelography Acta radiol Diagnosis 16 (1975) 129

IRSTAM L Side effects of water-soluble contrast media in lumbar myelography Acta radiol Diagnosis 14 (1973), 648

KAADA B Transient EEG abnormalities following lumbar myelography with metrizamide Acta radiol (1973) Suppl No 335, p 380

LOWRY O H, ROSEBROUGH N J, FARR A L and RANDALL R J Protein measurement with the Folin phenol reagent J Biol Chem 193 (1951), 265

LUNVEN Y, DIDIER L, MAISTRE J M et ATLAN D Un accident inhabituel de la radiculo saccographie au Dimer X J Radiol Electrol 53 (1972), 72

Metrizamide, a non ionic water-soluble contrast medium Acta radiol (1973) Suppl No 335

OFTEDAL S-I and SAWHNEY B B Effect of water soluble contrast media on cortically evoked potentials in the cat Acta radiol (1973) Suppl No 335, p 133

SALVESEN S Suboccipital injection of metrizamide to anaesthetized and unanaesthetized rabbits Acta radiol (1973) Suppl No 335, p 93

SKALPE I O and TALLE K Lumbar radiculography with meglumine iocarmate (Dimer X) A clinical report with special reference to the adverse effects J Oslo City Hosp 23 (1973), 121

— TORBERGSEN T, AMUNDSEN P and PRESTHUS J Lumbar myelography with metrizamide Acta radiol (1973) Suppl No 335, p 367

TOURTELOTTE W W, HAERER A F, HELLER G L and SOMERS J E Post lumbar puncture headaches Charles C Thomas Publisher, Springfield, Illinois 1964

FROM THE DEPARTMENTS OF DIAGNOSTIC RADIOLOGY AND OTOLARYNGOLOGY, AKADEMISKA SJUKHUSET, UNIVERSITY OF UPPSALA, S-750 14 UPPSALA, SWEDEN.

MULTIDIRECTIONAL TOMOGRAPHY OF DEFECTS IN THE FACIAL CANAL

An experimental investigation

H F WILBRAND and B BERGSTRÖM

Defects in the facial canal, either natural or of pathologic origin, may endanger the facial nerve in middle ear surgery

A defect or dehiscence of the canal, when pre-existent, is caused by a developmental disturbance (BAST et coll 1956) The risk of inflammatory spread through such defects has been discussed for quite a long time The same applies to lesions of the canal due to cholesteatoma When these lesions are located to the cochlear process, the facial sinus or the lateral knee, their demonstration is of particular importance The trend in otosurgery today is not only to eliminate lesions but also to restore impaired hearing This has led to refined surgical procedures, which have necessitated more detailed demonstration of the anatomy Defects in the wall of the facial canal entail a risk of immediate or delayed facial paralysis caused by trauma to the nerve in middle ear surgery, e g radical mastoidectomy, stapedectomy, tympanoplasty, fenestration and eighth nerve section (FOWLER 1947, [illegible] NECKE 195[illegible] [illegible] HAM 195[illegible] [illegible] 1960, HE[illegible] [illegible] BEDDARD [illegible], [illegible] 1962, SCHWARZ 1962, ANSON et coll 1963.

Submitted for publication 22 February 1974



Fig 1

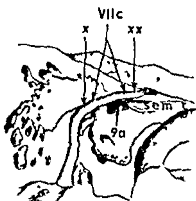


Fig 2

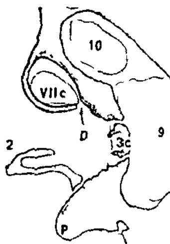


Fig 3

Fig 1 Defect of the facial canal, open to the oval window niche, probably not detectable by inspection at surgery D—defect, VIIc—facial nerve, 2b—oval window niche, 3c—stapedial footplate, 9—vestibule (Adult, 54 years old) Redrawn after photomicrograph (Anson et coll 1963)

Fig 2 Sites of natural and artificial defects in the tympanic part of the facial canal Schematic drawing VIIc—tympanic part, x—defects adjacent to the 'lateral knee', xx—defects adjacent to the cochleariform process at the anterior boundary of the oval window, 9a—oval window, sem c—semicanal for the tensor tympani muscle

Fig 3 The most common type of defect, slit like, just above the oval window not detectable on direct inspection D—defect, VIIc—tympanic segment of the facial nerve, P—promontory, 2—tympanic cavity, 3c—stapedial footplate, 9—vestibule, 10—lateral semicircular canal (Adult, 66 years old) Redrawn after photomicrograph (Dietzel 1961)

1967, Kettel 1963, 1965, Sammut 1967, Shambaugh 1967, Leonard & Alexander 1968, Baxter 1971, Schuknecht 1971) In adhesive processes and tympanosclerosis the facial nerve may be injured by inadvertent instrumentation if large defects are present

New aspects of delayed paralysis associated with middle ear surgery in cases of defective facial canal have recently been discussed by Althaus & House (1973)

Demonstration of small defects is a challenge to temporal bone tomography since the wall of the tympanic part of the canal may be very thin In the ototomographic literature the facial canal (Brunner et coll 1963, Lucarelli & Pompili 1961, 1966, de Ponteville et coll 1965, Wright et coll 1967, 1968, Vignaud et coll 1970, Brunner & Pedersen 1970, and others) there is, however (with the exception of two publications), no mentioning of the conditions which influence the demonstration of defects of the canal at tomography

Wright et coll (1967) found the tomographic disclosure of defects disappointing when compared with the operative findings and Terrahe (1972) stated that even with a well developed technique demonstration of defects is difficult Against this background experiments were undertaken to find out whether and to what extent artificially produced defects in the tympanic part of the facial canal could be demonstrated in tomography of the temporal bone

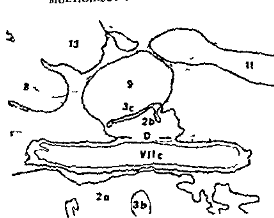


Fig 4



Fig 5

Fig. 4
Tran
2b—
13—
1967

Fig 5 Defect of the facial canal in the region below the prominence of the horizontal semicircular canal, covered only by a thin layer of mucoperiosteum The gap is nearly half of the circumference of the canal D—defect
2—tympanic cavi
vestibular aqued
fossa (Adult, 63

Anatomic remarks

In the early embryonic stages the facial canal is a mere sulcus on the primordial otic capsule Later on the sulcus is transformed to a canal by the addition of an outer wall from the second branchial arch (Reichert's cartilage), thus enclosing the nerve (VROLIK 1872, BAST & ANSON 1949, BAST et coll 1956, ANSON et coll 1963, 1967, ANSON 1965) This may persist through the first postnatal year, after which the cartilage will be replaced by bone There are reports, however, of a complete osseous tympanic wall already in the newborn (DIETZEL 1961, WILBRAND 1975) Defects of the canal are a result of disturbances of a complex developmental process and represent persistence of a foetal condition (HARPER & ANSON 1962, ANSON et coll 1963) If the closure is not completed within this early period the canal will remain defective throughout life and the defect will be covered only by mucoperiosteum (Fig 1)

Frequently the canal forms a bulging ledge above the oval window and is situated in the way of direct surgical approach to the stapes The oval window niche may be deep, thus concealing the stapes The tympanic surface of the canal may be even or irregularly rugged, it may also be thin, almost transparent In the immediate vicinity of the anterior boundary of the oval window niche the cochleariform process is located at the tympanic end of the semicanal for the tensor tympani muscle (Fig. 2)

Just below the oval window the basal turn of the cochlea forms the promontory bulging into the tympanic cavity Posteriorly the niche lies in close proximity to the tympanic sinus, where deep air cells may be present

The majority of the defects is located in the tympanic part of the facial canal above the oval window The reported frequencies vary widely (5 to 83 per cent) and depending on whether they have been observed at surgery, at gross dissection or histologically The most common type is a slit-like defect in the canal wall just above the oval window (Figs 3, 4) (GUILD 1949, DENECKE 1953, BAST et coll 1956, DIETZEL 1961, BAXTER 1971) At histology such defects have been noted but they cannot be recognized during middle ear surgery

Defects detectable in middle ear operations occur in the lateral wall of the canal or adjacent to the cochleariform process They may extend along the entire horizontal course of the canal (HOUGH 1958), the nerve being partly (DERLACKI et coll 1957) or entirely exposed (gross dissection, BEDDARD & SAUNDERS 1962) The bony wall may cover the facial nerve to only half of its width, leaving the nerve exposed in the direction of the niche (Figs 5, 6) Defects observed at surgery have been reported to be combined with other anatomic variations in several cases (HAHLBROCK 1960, HENNER 1960, KAPLAN 1960, FOWLER 1961)

The histologic appearances of defects have been illustrated in several reports (GUILD 1949, DIETZEL 1961, ANSON et coll 1967, LEONARD & ALEXANDER 1968 BAXTER 1971, ALTHAUS & HOUSE 1973) (Figs 1, 3, 4, 5, 6) The widest parts in the oval window region, measured at histology, have averaged 0 92 mm (range 0 4 to 3 08), compared with a canal diameter in this region of 0 97 mm (BAXTER 1971) BEDDARD & SAUNDERS (1962) using an operation microscope and 16 power magnification in 52 gross dissections, found defects with a mean size of 2 mm × 3 mm located above the oval window

LEONARD & ALEXANDER stated the defects in the tympanic part to be generally small, varying from 2 mm × 2 mm to 7 mm × 14 mm (width × length) and oval in shape They found the frequency to be 31 per cent, bilateral in 24 instances, in a material of 100 pairs of human temporal bones The largest defect comprised 35 per cent of the total circumference of the canal The defects always occurred in the inferior part of the canal and, when small, always involved the area near the medial wall of the middle ear The bony wall was usually extremely thin In 57 per cent of 135 temporal bone specimens, DIETZEL observed defects near the oval window, in most cases at the posterior border of the oval window niche

Fistulas from the facial canal to the lateral semicircular canal have also been reported (DENECKE 1953) Further, defects of the posterior wall of the oval window niche may be accompanied by otosclerotic invasion of the canal (ANSON et coll 1963)

It is generally considered that the defects may be regarded as a natural absence of the bony wall and not as an anomaly in a pathologic sense, unless combined with other malformations



Fig 6

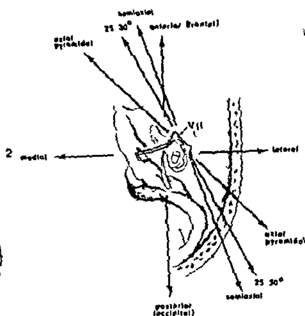


Fig 7

Fig. 6 *Large defect* of the facial canal opening to the oval window niche, the facial nerve is covered only by mucoperiosteum D—defect, P—*promontory*, VIIc—tympanic segment of the facial nerve, 2—tympanic cavity, 3c—*stapedial footplate* and head, 9—vestibule, 9b—round window (Adult, 35 years old) Redrawn after photo*micrograph* (GUILD 1949)

Fig. 7 Orientation of the facial canal in the temporal bone and corresponding tomographic projections used (dashed lines) Schematic drawing

In the mastoid part of the facial canal, defects may appear in the upper part as remnants of disturbed closure of the descending part The pneumatization of the mastoid bone *may reach the canal* and the nerve may be in contact with the mucoperiosteum lining the air cells Large cells are often found at a typical site underneath the lateral *semicircular* canal (Pogany cells) GÖRG (1935) reported that in a material of 60 *temporal* bones 10 *per cent of the total* defects in the facial canal observed histologically *were in* the mastoid part, *while in* another series 33 per cent of 294 cases were located in this *part (BAXTER 1971)* The majority occurred in the lateral wall of the canal opening *into the facial recess* In the remainder the nerve was exposed posteriorly *to the retrofacial* cells, or medially to the tympanic sinus Defects of the uppermost *mastoid part of the* canal are of equal importance in middle ear surgery to those of *the tympanic* part but only the latter part is concerned in the present investigation

The surgical anatomy of the facial canal has been described *in detail by ANSON* et coll (1963, 1967)

Material and Methods

In fresh temporal bone specimens (22) from unselected autopsy cases, a minor defect was produced on the tympanic wall of the facial canal under the otomicroscope, using the transmeatal approach Varying dimensions of the defect were obtained by using dental drills of different sizes (Fig 2) One specimen was left intact without a defect

For tomography of the isolated temporal bone specimens on the Polytome (hypocycloid movement) and on the Stratomatic (spiral movement) the bases of the specimens were embedded in flat paraffin squares These were easily adjusted to a plexi glass holder (WILBRAND et coll 1974) to facilitate reproduction of positioning The specimens were tomographed in the half axial and axial-pyramidal projections (Fig 7), the tube potential varied between 50 and 75 kV depending on the specimen and the film used The amperage and focal spot of the Polytome were 50 mA and 0 3 mm and on the Stratomatic 80 mA and 1 mm The photographic system consisted of an X-omatic cassette, a high definition screen and X-omatic regular film processed in a 1 5 min machine A corresponding series of tomographies was performed with Structurix D7 film without intensifying screens and correspondingly higher exposure (double hypocycloid movement 11 6 s) The diameters of the tomograms were 5 cm each on the Polytome and 6 cm on the Stratomatic, both in 6-seriograms

For simulating the conditions in vivo the specimens were then mounted in a skull phantom (DAHLIN et coll 1973) and tomographed in a projection intermediate between the half axial and axial-pyramidal projections (25 to 30° from the a p projection, Fig 7), the tube potentials on the Polytome were 72 to 83 kV and on the Stratomatic 70 to 77 kV The mAs value was constant

The specimens were macerated enzymatically, the tympanum was exposed by sawing and the defects then measured optically with the aid of a dissection microscope

The tomograms were evaluated at an ordinary viewing box under optimal viewing conditions (masking of the tomograms with a density of 1 7 and subdued illumination of the environment), without any image enhancing procedure

The thickness of the tympanic wall of the canal was assessed by measuring small fragments from the vicinity of the defects by means of a vernier caliper (1/100 mm)

Results

The defects in the tympanic wall of the facial canal were orientated such that their largest diameter (length) lay along the course of the canal and the smaller diameter (width) perpendicular to it The sizes of the defects ranged from 0 74 mm (width) × 0 7 mm (length) to 1 85 mm × 1 08 mm In two specimens the defect was natural, one of them measuring 0 8 mm × 3 3 mm (Fig 8), the other 1 42 mm × 2 4 mm The mean thickness of the tympanic wall was 0 12 mm (range 0 07 to 0 16 mm) in 20 temporal bones

Evaluation of the tomograms of isolated temporal bone specimens The half axial projection was more favourable than the axial-pyramidal projection for discernment of the defect (Table 1) The tomograms were viewed without knowledge of either the position or dimension of the defect Identification of the defect was doubtful in 2 and 3 of the cases in the respective projections In the tomograms of the specimen without an artificial defect no doubt existed about the bony wall of the canal

The percentages of the evident, doubtfully discerned and undiscerned defects differed only insignificantly with the two tomographic systems

The use of industrial film (Structurix D7) without intensifying screens did not have any advantage over the high definition X-omatic film and moreover gave poorer discernment of the defects in the axial pyramidal projection This film was therefore not used in spiral tomography

Evaluation of the tomograms of the temporal bone specimens mounted in phantoms Almost half the number of artificial defects were discerned with hypocycloid tomography (Table 2), whereas the percentage was somewhat smaller with spiral tomography The number of unidentified defects was relatively high with hypocycloid tomography, whereas that doubtfully discerned defects was the same as in the tomograms of isolated temporal bones With spiral tomography the percentage of doubtful defects was remarkably high, whereas this figure was halved for unidentified defects

The two natural defects appeared in both hypocycloid and spiral tomograms (Fig 8) In the temporal bone specimens without artificial defect, when mounted in the phantom, the integrity of the canal was without doubt

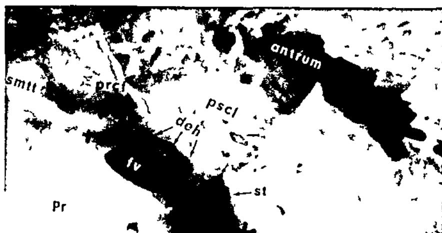
Defects less than 1 mm wide (Figs 9, 10) were identified in 7/15 of the tomograms from the Polytome and in 4/7 of those from the Stratomatic

The smallest defect in both the isolated specimen and the specimen mounted in the phantom was 0 78 mm wide and 0 8 mm long (Fig 10) and was visible in both hypocycloid and spiral tomograms

Two specimens had a defect anterior to the oval window, adjacent to the base of the cochleariform process, another specimen a defect posterior to the oval window, almost in the region of the lateral knee, these three defects were not identified spontaneously, but the first two were identifiable when their location was known

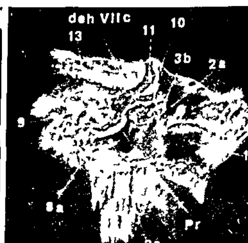
One defect (1 01 mm wide, 1 03 mm long) in a very thin wall (0 09 mm) was identified in the tomograms of the isolated specimen but not in the phantom, whereas a smaller defect (0 86 mm wide, 0 93 mm long) (Fig 9), also in a thin wall (0 10 mm), was identified in both the isolated specimen and the phantom

Table 3 gives the measurements of the smallest identified defects in hypocycloid tomograms of the phantom The defects are arranged in order of width The smallest in both the isolated and mounted specimens was 0 78 mm wide and 0 8 mm long (Fig 10), the thickness of the wall being 0 11 mm, whereas the largest undiscerned defect was 1 19 mm wide and 1 91 mm long, the thickness of the wall being 0 16 mm



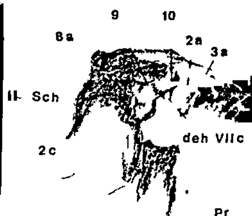
a





b





c

Fig 8 (For legend see opposite page)

Table 1

Discernment of an artificial defect in the tympanic wall of the facial canal in tomography of fresh temporal bone specimens

Projection Film	Hypocycloid tomography				Spiral tomography	
	Halfaxial		Axial pyramidal		Halfaxial	Axial pyramidal
	X omatic	Structurix D7	X-omatic	Structurix D7	X-omatic	X-omatic
Artificial defect Evident (n)	14 (67 %)	14 (67 %)	11 (52 %)	8 (38 %)	11 (74 %)	8 (53 %)
Discernment doubtful (n)	3 (14 %)	3 (14 %)	2 (10 %)	2 (10 %)	2 (13 %)	2 (13 %)
Undiscerned (n)	4 (19 %)	4 (19 %)	8 (38 %)	11 (52 %)	2 (13 %)	5 (34 %)
Total	21	21	21	21	15	15

Discussion

Defects in the wall of the tympanic part of the facial canal may be detected in tomograms provided that the wall lies at a suitable angle to the tomographic plane The canal resembles a cylinder Though its wall has irregular outlines and heterogeneous absorption, its tomographic demonstration will follow the principles for imaging a small cylinder with a short radius (EDHOLM 1960, REICHMANN 1972) In spite of the thinness of the tympanic wall there is a fairly large absorption difference between bone and air at its outer boundaries (disregarding the delicate layer of mucoperiosteum), whereas the absorption difference between bone and soft tissue at the inner surface is smaller The contours in the tomogram are depicted by those parts of the radiation beam that strike the surfaces tangentially during the tomographic movement

To increase the depth of the absorption boundaries the canal must lie at an optimum angle to the tomographic plane The contrast will be highest when the absorption boundaries are almost perpendicular to the tomographic plane The tympanic part is said to be generally orientated parallel to the long axis of the pyramid (VIGNAUD et coll 1970) Thus theoretically the tympanic wall should be best demon-

Fig. 8 a) Long defect (0 8 mm × 3 3 mm) opening in
deh—defect, Iv—oval win
of the lateral semicircular
(Adult 61 years old) b) T
defect, deh of the tympa
tympanum, 2c—hypotym
bule, 10—lateral semicirc
Pr—promontory c) Tom
in the tympanic part of th
hypotympanum, 3a—head
semicircular canal, 19—S

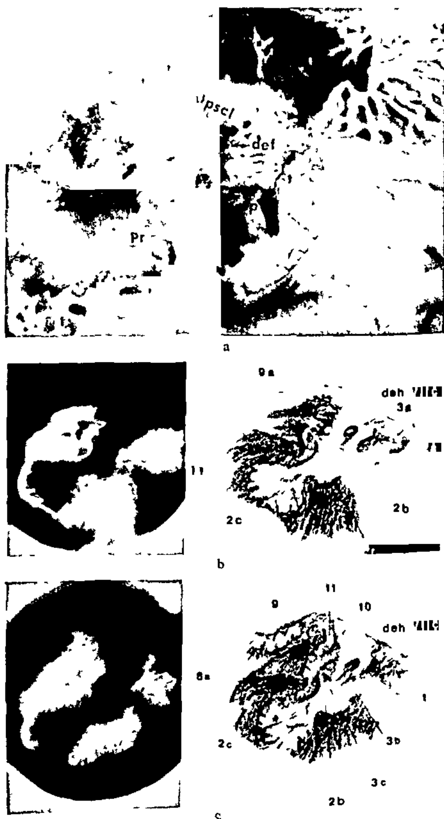


Fig 9 (For legend see opposite page)

Table 2

Discernment of an artificial defect in the tympanic wall of the facial canal in tomography of temporal bone specimens mounted in a phantom

	Hypocycloid tomography	Spiral tomography
Artificial defects		
Evident (n)	10 (48 %)	6 (40 %)
Discernment doubtful (n)	3 (14 %)	6 (40 %)
Undiscerned (n)	8 (38 %)	3 (20 %)
Total	21	15

strated in the axial pyramidal projection However, the long axis of the pyramid is not constantly at an angle of 45° to the sagittal plane of the skull (SCHÖNEMANN 1906) In the axial pyramidal projection the thin tympanic wall is well seen against the aerated tympanum (MÜNDNICH & FREY 1959, VALVASSORI 1963, ANDRÉ et coll 1968, VIGNAUD et coll 1970, and others) In the experience of many authors, however, the tympanic part of the canal is best demonstrated in the halfaxial projection (WRIGHT et coll 1967, ANDRÉ et coll 1968, BRUNNER et coll 1970, VIGNAUD et coll 1970, WILBRAND 1970, ROVSING 1971), this is in agreement with the present finding that defects are better identified in this projection (Table 1) Thus it should be possible to evaluate the bony continuity in both projections and therefore also in a projection intermediate between them (Fig 7)

In the a p projection the facial canal lies obliquely to the tomographic plane, and therefore its tympanic part is sometimes unsatisfactorily depicted

The rate of identification of defects in the wall will depend on their location Small defects adjacent to the cochleariform process (Figs 2, 8, 9, 10) may not be detected owing to the anatomic variation of this process, which may give rise to an unfavourable angle between the wall of the canal and the tomographic plane This is a disadvantage since cholesteatoma sometimes extends to that area Furthermore the

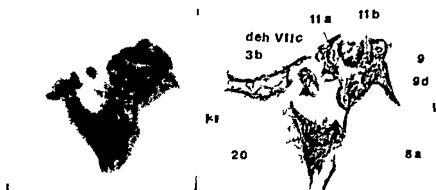
Fig 9 a) The medial wall of the tympanum from the lateral aspect [illegible] projection Defect [illegible]



a



b



c

Fig 10 (For legend see opposite page)

Table 3

Smallest defects in the tympanic part of the facial canal identified in hypocycloid tomograms of the temporal bone specimens mounted in a skull phantom (arranged according to their widths)

	Width of the defect mm	Length of the defect mm	Thickness of the lateral wall mm
1	0 78	0 8	0 11
2	0 8	3 3 (natural defect)	not destroyed
3	0 83	0 94	0 14
4	0 86	0 93	0 10
5	0 92	2 22	0 14
6	0 96	1 36	0 11
7	0 98	1 01	0 13
8	1 0	1 15	0 16

semicanal of the tensor tympani muscle not seldom has the appearance of a canal and may be mistaken for the facial canal in sections at the level of the cochlea In the present investigation two defects anterior to the oval window were small (0 74 mm × 0 77 mm and 0 98 mm × 0 78 mm) and were not detected spontaneously (Fig 2) Defects adjacent to or in the region of the 'lateral knee' may not be identified, unless they are very large, since the canal changes direction here and its wall comes into an unfavourable angle to the tomographic plane (Fig 2) Moreover, disturbing superimposition (ECKERDAL 1973) of structures of the posterior wall of the tympanum may influence the image

Cholesteatoma or abundance of granulation tissue decreases the absorption differences and renders reproduction of defects in the thin tympanic wall more difficult or makes reproduction impossible when the wall of the canal is very thin

TERRAHE (1972), mentions that a facial nerve devoid of bony covering on its course through the tympanum remains tomographically invisible, but also expresses the

Fig 10 a) The smallest artificial defect (0 78 mm × 0 8 mm) of the facial canal de[illegible]
Deep oval window niche Th[illegible]
tured. VIIc—tympanic part [illegible]
—promontory prcf—cochle[illegible]
smtt—semicanal for the tens[illegible]
[illegible]
vestibule, 9d—
canal crus ampullare 11b—
tympanica

opinion that even with a well developed technique the frequent defects in the tympanic part of the canal are concealed from identification In an attempt to assess the intactness of the wall of the facial canal WRIGHT et coll (1967) had disappointing results They applied the half axial projection and found that the canal was well demonstrated, but in only 10 per cent of the cases were they confident in stating that the canal was intact They considered that it was not intact in 39 per cent, but on subsequent operation only one of these cases had a defective canal It may be added here that defects facing the oval window niche can be concealed from direct inspection in surgery (Figs 1, 3, 4) and thus the operative report is not always reliable WRIGHT et coll used the Polytome (0 6 mm focal spot, and the tomograms were 1 mm apart), they did not state exposure or photographic system used

In the present material defects in isolated specimens were better identified with the half axial projection than with the axial-pyramidal projection, both in hypocycloid (with two different screen film systems) and spiral tomograms (Table 1) Defects in the specimens mounted in the skull phantom, however, were better discerned in tomograms with the Polytome than with the Stratomatic (Table 2) This might be due largely to the geometric unsharpness resulting from the larger focal spot (1 mm in the Stratomatic, 0 3 mm in the Polytome) and higher current, in spite of the otherwise high imaging capability of the spiral movement (STIEVE 1972, KAUFMANN et coll 1973)

The identification results for the defects in the mounted specimens may be directly applied to clinical tomography provided a satisfactory craniostasis be attained The phantom has been constructed so as to represent a more demanding tomographic situation

The mean width of the defects in the oval window region is 0 92 mm (BAXTER 1971) This corresponds to the sizes of identified defects given in Table 3 Defects of this mean width should therefore be discernible provided that the wall is not exceedingly thin and the tympanum fairly well aerated The natural defects are usually greater in length than in width, which favours their demonstration by tomography, especially when the sections are 0 5 mm apart

The smallest defect in the present material, and thus which could be tested tomographically, was 0 74 mm × 0 77 mm It seems doubtful, in view of the section thickness and the thinness of the bony wall of the canal, whether smaller defects could be demonstrated The narrow, slit-like defects adjacent to the oval window (Fig 3) cannot be expected to be visible in tomograms, mainly owing to their site and to the superimposition of spurious contours from neighbouring absorption boundaries (REICHMANN 1972, ECKERDAL 1973)

Defects of the dimensions reported by BEDDARD & SAUNDERS and the so called 'large dehiscences' of DIETZEL (with 1/3 of the canal's circumference defective) ought to be identifiable A completely defective wall presents boundaries with an absorption difference between air and soft tissue which makes reproduction more difficult A contour which does not give the impression of being skeletal is perceived

A complete but exceedingly thin wall (in these cases 0 09 mm) might be mistaken for a large defect Furthermore the largest undiscerned defect in this investigation was 1 19 mm wide and 1 91 mm long, and the thickness of the wall was 0 16 mm

The small number of specimens did not permit distinction of any statistical borderline between identified and unidentified defects, classified according to width, length and thickness of the wall Nevertheless, until more reliable statistics are available the values given in Table 3 may serve as borderline values for the three interacting factors (width and length of the defect and thickness of the wall)

The number of demonstrated defects in the mounted specimens was high compared with that of the defects in the isolated specimens In isolated specimens the percentage of discerned defects was larger with spiral (in spite of its larger focal spot) than with hypocycloid tomography The reverse held for the mounted specimens, in which the percentage of discerned defects was lower with spiral than with the hypocycloid tomography The number of specimens is too small, however, for this paradoxical finding to be explained The same was found for the number of 'doubtful identifications, which was greater with spiral tomography of mounted specimens even though no difference existed between the identification with the two types of tomography in isolated specimens

Conclusion

An attempt was made to determine to what extent defects in the tympanic part of the facial canal might be demonstrated by tomography No such experimental investigation appears to have been performed previously In a series of 21 temporal bones surgical defects were created and the fresh specimens were subsequently tomographed both in the isolated state and mounted in a skull phantom The results show that defects with dimensions of surgical interest can be revealed tomographically provided that the wall is not exceedingly thin Several other factors are decisive for demonstration of the defects, such as the anatomic location, tomographic positioning equipment and technique

Essential anatomic factors are the course of the canal, the dimension of the defect and the absorption factor of the environmental structures The half axial or an intermediate projection between this and the axial pyramidal is to be preferred In hypocycloid and spiral tomography a small focal spot size and low tube potentials (50 to 65 kV) are recommended and when feasible the use of a high definition screen film system With regard to the section thickness of the canal in both the Polytome and Stratomatic a distance between the sections of 0 5 mm is needed to guarantee overlapping of the structural details in the tomograms It is assumed that minor defects are concealed by tomographic phenomena such as spurious contours or superimposition from neighbouring structures The experience gained from these experiments is directly applicable to clinical tomography

Acknowledgements

The authors extend their thanks to Professor W. Frommhold and his staff of the Department of Diagnostic Radiology, University Hospital, Tubingen, Germany, for placing the spiral tomographic equipment at their disposal

SUMMARY

Defects on the tympanic wall of the facial canal may endanger the nerve in middle ear surgery Their preoperative tomographic demonstration is therefore valuable In an experimental investigation an attempt was made to assess the discernibility of artificial defects of different sizes by hypocycloid and spiral tomography of temporal bone specimens (both isolated and mounted in a tissue-equivalent skull phantom) The thickness of the wall was measured and its influence on the discernibility of the defects discussed

ZUSAMMENFASSUNG

Bei Mittelohroperationen kann der Fazialisnerv durch die Existenz von Dehiszenzen in der tympanalen Wandung des Fazialiskanals gefährdet sein Ihre praoperative tomographische Darstellung ist nutzlich In einer experimentellen Untersuchung wurde versucht die Darstellungsmoglichkeit kunstlicher, verschieden grosser Defekte mit hypozykloider und spiraliger Tomographie von Felsenbeinen zu ermitteln Felsenbeinpräparate wurden sowohl isoliert als auch in einem gewebeaquivalenten Schädelphantom tomographiert Die Dicke der tympanalen Wandung des Fazialiskanals wurde gemessen und ihr Einfluss auf die Darstellungsmöglichkeit der Defekte besprochen

RÉSUMÉ

Des lacunes dans la paroi tympanique du canal facial peuvent mettre ce nerf en danger au cours de la chirurgie de l'oreille moyenne C'est pourquoi leur mise en évidence tomographique préopératoire est intéressante Au cours d'une recherche expérimentale les auteurs ont essayé d'apprécier la visibilité de lacunes artificielles de différentes tailles par la tomographie hypocycloïde et spirale d'os temporaux isolés (os isolé et os monté dans un fantôme de crâne équivalent aux tissus) L'épaisseur de la paroi a été mesurée et les auteurs examinent son influence sur la visibilité des lacunes

REFERENCES

André P, Pialoux P, Poncet E, Dulac G-L et François J La tomographie en oto-rhino-laryngologie Librairie Arnette, Paris 1968

Althaus S R and House H P Delayed post-stapedectomy facial paralysis a report of 5 cases Laryngoscope 83 (1973), 1234

Anson B J. Die Embryologie und Anatomie des Fazialiskanals und des Fazialisnerven Arch Ohr-u, Nas-u Kehlk-Heilk 184 (1965), 269

— Donaldson J A, Warpeha R L and Winch T R The surgical anatomy of the ossicular muscles and facial nerve Laryngoscope 77 (1967), 1269

— HARPER D G and WARPEHA R L Surgical anatomy of the facial canal and facial nerve Ann Otol 72 (1963) 713
BAST T H and ANSON B J The temporal bone and the ear Charles C Thomas Publisher Springfield Illinois 1949
— — and RICHANY S F The development of the second branchial arch (Reichert s cartilage) facial canal and associated structures in man Quart Bull N W Univ med Sch 30 (1956) 235
BAXTER A Dehiscence of the Fallopian canal J Laryng 85 (1971) 587
BEDDARD D and SAUNDERS W H Congenital defects in the Fallopian canal Laryngoscope 72 (1962) 112
BRUNNER S and PEDERSEN C B Roentgen examination of the facial canal Acta radiol Diagnosis 10 (1970) 545
— PETERSEN Ö and STOKSTED P T
pals
CAWTH
J Laryng 71 (1957) 524
DAHLIN H NYLÉN O and WILBRAND H F Radiation dose distribution in temporal bone tomography Acta radiol Diagnosis 14 (1973) 353
DENECKE H J Die oto rhino laryngologischen Operationen Springer Verlag, Berlin Gottingen Heidelberg 1953
DERLACKI E L SHAMBAUGH G E and HARRISON W H The evolution of a stapes mobilization technique Laryngoscope 67 (1957) 420
DIETZEL K Über die Dehiszenzen des Fazialskanals Z Laryng Rhinol 40 (1961) 366
EDHOLM P The tomogram its formation and content Acta radiol (1960) Suppl No 193
ECKERDAL O Tomography of the temporo-mandibular joint Acta radiol (1973) Suppl No 329
FOWLER E P Medicine of the ear Second edition p 121 Thos Nelson & Sons New York 1947
— Variations in the temporal bone course of the facial nerve Laryngoscope 71 (1961) 937
GUILD S R Natural absence of part of the bony wall of the facial canal Laryngoscope 59 (1949) 668
GÖRG P Über Dehiszenzen des knochernen Fazialiskanals Passow Schaefer Beitr Anat Ohr 31 (1935) 483
HAHLBROCK K H Zweiteilung des N Facialis im Warzenfortsatz Arch Ohr Nas Kehlk Heilk 174
HARPER D
wall of
HENN
— an
de
HOUGH J V D Malformations and anatomical variations seen in the middle ear during operation for mobilization of the stapes Laryngoscope 68 (1958) 1337
JONGKEES L B W Über die intratemporalen Fazialislahmungen und ihre chirurgische Behandlung Z Laryng Rhinol 40 (1961) 319
KAPLAN J Congenital dehiscence of the Fallopian canal in middle ear surgery Arch. Otolaryng 72 (1960) 197
KAUFMANN H SCHMITT G und HACH G Schichtuntersuchungen mit spiralform d hypozykloidaler System
KETTEL K Repa
— Surgery of the

Acknowledgements

The authors extend their thanks to Professor W Frommhold and his staff of the Department of Diagnostic Radiology, University Hospital, Tubingen, Germany, for placing the spiral tomographic equipment at their disposal

SUMMARY

Defects on the tympanic wall of the facial canal may endanger the nerve in middle ear surgery Their preoperative tomographic demonstration is therefore valuable In an experimental investigation an attempt was made to assess the discernibility of artificial defects of different sizes by hypocycloid and spiral tomography of temporal bone specimens (both isolated and mounted in a tissue-equivalent skull phantom) The thickness of the wall was measured and its influence on the discernibility of the defects discussed

ZUSAMMENFASSUNG

Bei Mittelohroperationen kann der Fazialisnerv durch die Existenz von Dehiszenzen in der tympanalen Wandung des Fazialiskanals gefahrdet sein Ihre praoperative tomographische Darstellung ist nutzlich In einer experimentellen Untersuchung wurde versucht die Darstellungsmoglichkeit kunstlicher, verschieden grosser Defekte mit hypozykloider und spiraliger Tomographie von Felsenbeinen zu ermitteln Felsenbeinpraparate wurden sowohl isoliert als auch in einem gewebeaquivalenten Schädelphantom tomographiert Die Dicke der tympanalen Wandung des Fazialiskanals wurde gemessen und ihr Einfluss auf die Darstellungsmoglichkeit der Defekte besprochen

RÉSUMÉ

Des lacunes dans la paroi tympanique du canal facial peuvent mettre ce nerf en danger au cours de la chirurgie de l'oreille moyenne C'est pourquoi leur mise en évidence tomographique préopératoire est intéressante Au cours d'une recherche expérimentale les auteurs ont essayé d'apprécier la visibilité de lacunes artificielles de différentes tailles par la tomographie hypocycloïde et spirale d'os temporaux isolés (os isolé et os monté dans un fantôme de crâne équivalent aux tissus) L'épaisseur de la paroi a été mesurée et les auteurs examinent son influence sur la visibilité des lacunes

REFERENCES

André P, Pialoux P, Poncet E, Dulac G-L et François J La tomographie en oto-rhino-laryngologie Librairie Arnette, Paris 1968

Althaus S R and House H P Delayed post stapedectomy facial paralysis a report of 5 cases Laryngoscope 83 (1973), 1234

Anson B J Die Embryologie und Anatomie des Fazialiskanals und des Fazialisnerven Arch Ohr-u, Nas-u Kehlk-Heilk 184 (1965), 269

— Donaldson J A, Warpeha R L and Winch T R The surgical anatomy of the ossicular muscles and facial nerve Laryngoscope 77 (1967), 1269

ROM THE DEPARTMENT OF DIAGNOSTIC RADIOLOGY, REGIONSJUKHUSET, UNIVERSITY
OF LINKOPING, S 581 85 LINKOPING, SWEDEN

PATENCY OF VENTRICULO-ATRIAL SHUNT DETERMINED RADIOLOGICALLY

M RESJÖ and C RÅDBERG

Manual pumping of the valve of an intracranial shunt invariably does not provide information about the patency of the diversionary shunt Therefore other methods have been devised (ATKINSON & FOLTZ 1962, BELL 1957, 1959, BRISMAN et coll 1973, CARRINGTON 1959, DI CHIRO 1966, GO et coll 1968, JAMES et coll 1972, KAGEN et coll 1963, MIGLIORE et coll 1962, NULSEN & SPITZ 1951, SCHLESINGER et coll 1959, SILLANPÄÄ et coll 1970) These methods produce only indirect evidence or require opening or puncture of the ventricular system involving risk of leakage or infection

The method described in this report is based on the demonstration of gas in the valve during pneumography

Material and Methods

Eleven patients aged 33 months to 12 years, were examined all together 14 times One patient had a subdural shunt (Hakim), the others, a ventriculo-atrial shunt (Spitz Holter) except one in whom the tip of the intracranial catheter was found to be placed in the interhemispheric fissure instead of in the lateral ventricle

Three patients had communicating hydrocephalus, five had tumours with manifest

Submitted for publication 17 February 1974

— Surgery of the facial nerve Arch Otolaryng 81 (1965), 523

KODROS A and BUCKINGHAM R A The anatomy of the descending portion of the facial nerve Arch Otolaryng 66 (1957), 735

LEONARD J R and ALEXANDER D W Anatomic variations in the area of the oval window Arch Otolaryng 87 (1968), 48

LUCARELLI U e POMPILI G Indicazioni cliniche allo studio stratigrafico del canale del nervo faciale (In Italian) Arch ital Otol 72 (1961), 654

— — Anatomia e tecnica stratigraphice del canale del nervo facciale (In Italian) Radiol med 48 (1966), 729

MIEHLKE A Die Chirurgie des Nervus facialis Urban & Schwarzenberg Munchen und Berlin 1960

MOLLICA V Considerazioni anatomo-cliniche e patogenetiche sulle anomalie del canale di Falloppio (In Italian) Otorinolaring ital 12 (1962), 230

MUNDNICH K und FREY K -W Das Rontgenschichtbild des Ohres Georg Thieme Stuttgart 1959

DE PONTEVILLE M , PIGANIOL G et HORIOT J -C L'exploration radiologique du canal facial, technique pratique d examen Rev Laryng 86 (1965) 695

REICHMANN S Modified theory of the development of tomographic blurring Acta radiol Diagnosis 12 (1972), 457

— Development of spurious contours of spherical and cylindrical objects in tomography Acta radiol Diagnosis 12 (1972), 317

ROVSING H The semiaxial projections *In* Fundamentals of ear tomography Edited by J Jensen and H Rovsing Charles C Thomas Publisher, Springfield Illinois 1971

SAMMUT J J The middle ear in accidental deaths J Laryng 81 (1967), 37

SCHUKNECHT H F Stapedectomy Little, Brown & Comp , Boston 1971

SCHWARZ M Missbildungen des Ohres Arch Ohr -, Nas - u Kehlk -Heilk 179 (1962) 327

SCHÖNEMANN A Schlafenbein und Schadelbasis, eine anatomisch-otiatrische Studie Neue Denkschriften allgem Schweiz Gesellschaft Naturwissensch 40 (1906), 95

SHAMBAUGH S E Surgery of the ear W B Saunders Comp , Philadelphia and London 1967

STIEVE F E Über den Bildaufbau in der Tomographie bei ein- und mehrdimensionaler Verwischung Fortschr Rontgenstr 116 (1972), 253

TERRAHE K Diagnostik der Missbildungen des Ohres und des Ohrschadels Arch klin exp Ohr -, Nas - u Kehlk -Heilk 202 (1972), 85

VALVASSORI G E Laminagraphy of the ear Amer J Roentgenol 89 (1963), 1155

VIGNAUD J , BURLAMAQUI B J et AUBIN M L Étude tomographique de l'aqueduc de Fallope J Radiol Électrol 51 (1970), 127

VROLIK J A Studien over de Verbeening en de Beenderen van den Schedel der Teleostei, met Aanhangsel over de *Verbeening van het Slaapbeen der Zoogdieren* (In Dutch) Dissertation Haarlem 1872 (Cited by Gegenbaur, Morphol Jahrb 2 (1876), 435)

WILBRAND H F Facialiskanalens rontgenanatomi (In Swedish) Nord Med 84 (1970) 1314

— Multidirectional tomography of the facial canal To be published in Acta radiol Diagnosis

— RASK-ANDERSEN H and GILSTRING D The vestibular aqueduct and the para-vestibular canal An anatomic and roentgenologic investigation Acta radiol Diagnosis 15 (1974), 337

WRIGHT J W and TAYLOR C E Tomography and the facial nerve Trans Amer Acad Ophthal Otolaryng 72 (1968), 103

— — and MCKAY D C Variations in the course of the facial nerve as illustrated by tomography Laryngoscope 77 (1967), 717

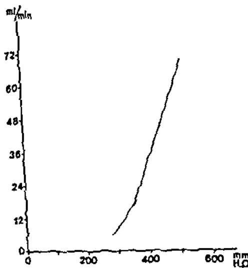


Fig. 1 Maximum amount of nitrous oxide that passed through a Spitz Holter valve (medium type) under varying pressure (in vitro)

in dogs anaesthetized with an inhalant mixture of 91 to 93 per cent nitrous oxide and 9 to 7 per cent oxygen (GREEN 1925)

The solubility of nitrous oxide in blood in man is 41 2 per cent (v/v) at 37° and 760 mm Hg (mean value) and varies but little with the haematocrit (KETY et coll 1948)

The blood can obviously hold a great deal more nitrous oxide in solution than during nitrous oxide oxygen anaesthesia, and nitrous oxide may be administered intravenously without any risk of gas embolism Intravenous injection of up to 6 ml nitrous oxide per kg body weight per min, seems to be without risk (JACOBY et coll 1948, RAGINSKY & BOURNE 1934)

The passage of nitrous oxide through a Spitz-Holter valve of medium type was analysed at different pressure gradients (Fig 1) Eight ml nitrous oxide passed per minute at a pressure of 300 mm H_2O, which is a level rarely exceeded during nitrous oxide gas encephalography in patients without increased intracranial pressure (GORDON & GREITZ 1970)

During the examinations at most 100 to 120 ml nitrous oxide was injected within 20 to 30 minutes. The reason why the amount of gas sometimes had to be large was that part of the gas probably was absorbed in the tissues

With the tip of the catheter in the ordinary position in the anterior part of a lateral ventricle the gas did not pass through the valve during the first part of the examination with the patient in the usual sitting position Such a passage only took place in the supine position, provided the catheter-shunt system was patent

Gas in the valve could then be demonstrated in the films although this was sometimes evident only following pumping of the valve To prove that there is gas inside the shunting device it is necessary to compare this film with that exposed before

or threatening obstructive hydrocephalus, two had myelomeningocele combined with hydrocephalus and one patient relapsing hygroma

Encephalography was performed under general anaesthesia according to LINDGREN's technique (1949) and mainly to demonstrate the degree of hydrocephalus and the function of the shunt The anaesthesia was induced with nitrous oxide plus halothane in addition the older children received suxamethonium before intubation Anaesthesia was maintained with 0 5 to 1 5 per cent halothane in a 50 50 or 60 40 mixture of nitrous oxide and oxygen delivered in an open or half-open system without rebreathing In order to minimize the risk of gas embolism through the ventriculo-atrial shunts (JACOBY et coll 1948, STEVENAERT et coll 1972) and increase in intracranial pressure (BERGSTRÖM et coll 1969, GORDON & GREITZ 1970, PHILIPPART & THIBAUT 1966, 1967) nitrous oxide was used as contrast medium

Carbon dioxide, which has an even somewhat higher solubility in blood than nitrous oxide (BUCHWALD 1965, STAUFFER et coll 1956), could have been used as contrast medium but as it is absorbed quickly it is difficult to obtain satisfactory encephalograms Nitrous oxide is 'an ideal contrast medium for encephalography (AIRD 1936) being neither toxic nor explosive, but, like carbon dioxide, it is absorbed rapidly when the patient is breathing air However, if the patient is breathing nitrous oxide-oxygen during the encephalography the nitrous oxide in the subarachnoid space is absorbed slowly and the encephalograms are then comparable to those obtained with air or oxygen (PHILIPPART & THIBAUT 1966 BERGSTRÖM et coll 1969)

Experiments have shown that large amounts of nitrous oxide can be safely administered intravenously (JACOBY et coll 1948) The maximum doses tolerated by animals (dogs) averaged 12 1 ml per kg body weight per min In those experiments ordinary anaesthetic nitrous oxide was used which, according to the USP standard consists of at least 95 per cent pure nitrous oxide The remaining 5 per cent is made up mainly of nitrogen JACOBY et coll (1948) suggested that the embolic phenomena which have appeared after larger doses of nitrous oxide have been caused by the nitrogen

The gas used as contrast medium in the present investigation consisted of 99 per cent pure nitrous oxide (manufacturer AGA, Sweden)

Nitrous oxide	Purity	99 %
Impurities	Air	1 %
	CO	1 ppm
	CO_2	300 ppm
	NO-NO	0 1 ppm
	H O	13 ppm

The amount of nitrous oxide in arterial blood in man during nitrous oxide oxygen anaesthesia has been reported to range from 16 to 22 per cent (v/v) with an inhalant mixture of 80 per cent nitrous oxide and 20 per cent oxygen (RAGINSKY & BOURNE 1934), and from 19 to 26 per cent in arterial and about 22 per cent in venous blood



Fig 4 a) Gas filling of valve despite disconnection and displacement of the cranial catheter b) Hakim valve filled with gas despite loss of continuity between the valve and the catheter, whose tip is situated in a subdural hygroma c) Same valve as in (b), but before being filled with gas

loss of continuity between the intracranial catheter and the valve, but nevertheless the gas passed through (Fig 4) At operation a firm sleeve of tissue around the subcutaneous part of the catheter and valve was revealed Such a channel does not collapse when the catheter is removed and may allow passage of fluid or gas at least for some time

Discussion

The present radiologic method for testing the patency of ventriculo atrial shunts has not been attended by complications Gas in the catheters and valve invariably disappeared quickly and did not disturb continued drainage function

The passage should be regarded as satisfactory if the valve fills spontaneously with gas If pumping is required to fill the valve this may be due to low intraventricular pressure but partial obstruction is more likely as the pressure is somewhat elevated by the encephalographic procedure Our experience, however, is too limited to allow an estimation of the site of the stenosis If the valve fails to fill with gas after pumping obstruction probably exists

The experiences indicate that the shunt may be functioning despite interruption of the shunting system, which to the best of our knowledge has not been demonstrated before It is also possible to demonstrate that the shunt may function even in cases when the tip of the intracranial catheter is not located in the ventricular system This does not seem to be possible with techniques based on ventricular puncture alone



Fig 2a



Fig 2b



Fig 3

Fig 2 Same Spitz Holter valve (a) before and (b) after being filled with gas

Fig 3 Area of bone with reduced attenuation of radiation near the valve This raref ed bone can be d stinguished from gas in the valve by the fact that it extends beyond the metal parts and is wider than the lumen of the valve

administration of gas (Fig 2) since the bone adjacent to the valve may have become thinner postoperatively or owing to pressure atrophy simulating gas in the valve (Fig 3)

Results

The method employed allowed demonstration of patency of the valve on one occasion when the shunt was thought to be obstructed and on seven occasions when its function clinically was uncertain On six occasions the results of the clinical and radiologic tests were consonant and demonstrated patency of the valve In one case with clinical signs of shunt obstruction relieved by drainage of the ventricles passage of gas through the valve could be demonstrated but only after repeated manual pumping

It was possible to demonstrate gas in the valve in two cases in which the tip of the intracranial catheter was not located in the lateral ventricle In one of them the catheter had intentionally been placed on the convexity of the brain in order to drain a hygroma and in the other the tip of the catheter was located in the interhemispheric fissure immediately above the most ventral part of the body of the lateral ventricle In these two cases and in a third with an intraventricular catheter, there was also

CARRINGTON K W Ventriculo-venous shunt using the Holter valve as a treatment of hydrocephalus J Mich med Soc 58 (1959) 373

DI CHIRO G and GROVE A S Evaluation of surgical and spontaneous cerebrospinal fluid shunts by isotope scanning J Neurosurg 24 (1966) 743

FOLTZ E L and SHURTLEFF D B Conversion of communicating hydrocephalus to stenosis or occlusion of the aqueduct during ventricular shunt J Neurosurg 24 (1966) 520

GO K G LAKKE J P W F and BEKS J W F A harmless method for the assessment of the patency of ventriculoatrial shunts in hydrocephalus Dev Med Child Neurol Suppl 16 (1968) 100

GORDON E and GREITZ T The effect of nitrous oxide on the cerebrospinal fluid pressure during encephalography Brit J Anaesth 42 (1970) 2

GREEN C W The distribution of nitrous oxide and oxygen in the blood of dogs during gas anesthesia Arch intern Med 35 (1925) 379

JACOBY J J GEILING E M K and LIVINGSTONE H M Intravenous nitrous oxide and experimental embolism A preliminary report Curr Res Anesth 27 (1948) 13

JAMES A E DEBLANC H J DELAND F H and MATHEWS E S Refinements in cerebro spinal fluid diversionary shunt evaluation by cisternography Amer J Roentgenol 115 (1972) 766

KAGEN A TSUCHIYA G PATTERSON V and SUGAR O Test for patency of ventriculo-vascular shunt for hydrocephalus with radioactive iodinated serum albumin J Neurosurg 20 (1963) 1025

KETY S S HARMEL M H BROOMELL H T and BELLE RHODE C The solubility of nitrous oxide in blood and brain J biol Chem 173 (1948) 487

LINDGREN E Some aspects on the technique of encephalography Acta radiol 31 (1949) 161

MIGLIORE A PAOLETTI P and VILLANI R Radioisotopic method for evaluating the patency of the Spitz Holter valve J Neurosurg 19 (1962) 605

NULSEN F E and SPITZ E B Treatment of hydrocephalus by direct shunt from ventricle to jugular vein Surg Forum 2 (1951) 399

PHILIPPART C et THIBAUT A Utilisation du N_2O au cours de l encéphalographie gazeuse Une nouvelle technique Acta anaesth belg 17 (1956) 16

— — Utilisation du protoxyde d azote en tant que moyen de contraste et d anesthesie au cours de l encephalographie gazeuse Ann Anesth franç 8 (1967) 631

RAGINSKY B B and BOURNE W Cyanosis in nitrous oxide oxygen anaesthesia in man Canad m d Ass J 30 (1934) 518

SCHLESINGER E B DEBOVES S and CHEEK W A method for the evaluation of the patency of shunts in the treatment of obstructive hydrocephalus Trans Amer neurol Ass 84 (1959) 197

SILLANPAA M TÖRMÄ T PARVINEN T and MAKELA P Ventriculocardiac shunts in hydrocephalic children testing with hippuran ^{131}J Acta paediat scand (1970) Suppl No 205 p 140

STAUFFER H M DURANT T M and OPPENHEIMER M J Gas embolism Radiology 66 (1956) 685

STEVENAERT A THIBAUT A et DEPRESSEUX J C Considérations sur les critères de régression d une hydrocéphalie communicante de l adulte Acta neurol belg 72 (1972) 406

It is easier to demonstrate gas in the valve than in the catheter, mainly due to the fact that the valve is the widest part of the system

There are, however, some disadvantages attached to the method If the subarachnoid space is to be investigated thoroughly, the examination has to be performed under inhalation of nitrous oxide Following a shunt operation occlusion of the aqueduct may occur (FOLTZ & SHURTLEFF 1966) which requires ventriculography It is also obvious from our investigation that encephalography with gases as air or oxygen in a patient with a patent ventriculovenous shunt involves a risk of gas embolism

SUMMARY

A radiologic method for assessment of the patency of ventriculo atrial shunts is described together with a safe technique for gas encephalography of patients with ventriculo atrial shunt Despite discontinuity the shunting system may be functioning

ZUSAMMENFASSUNG

Eine rontgenologische Methode um die Durchgangigkeit eines ventriculo atrialen Shunts festzustellen wird zusammen mit einer sicheren Technik zur Gas Encephalographie von Patienten mit ventriculo artrialem Shunt beschrieben Trotz Diskontinuitat kann das Shunt System funktionieren

RESUME

Les auteurs decrivent une méthode radiologique pour déterminer si les shunts ventriculo auriculaires sont ouverts et décrivent aussi une technique sans danger pour l encéphalographie gazeuse chez des malades présentant un shunt ventriculo auriculaire Le système de shunt peut fonctionner de façon discontinue

REFERENCES

AIRD R B Experimental encephalography with anesthetic gases Arch Surg 32 (1936) 193

ATKINSON J R and FOLTZ E L Intraventricular RISA as a diagnostic aid in pre and postoperative hydrocephalus J Neurosurg 19 (1962) 159

BELL R L Isotope transfer test for diagnosis of ventriculosubarachnoidal block J Neurosurg 14 (1957) 674

— Isotope transfer test in the diagnosis and treatment of hydrocephalus Int J appl Rad at 5 (1959) 89

BRISMAN R SCHNEIDER S and CARTER S Subarachnoid infusion and shu [illegible] Technical note J Neurosurg 38 (1973) 379

VON BUCHWALD W Die Verwendung schnell resorbierbarer Gase bei diagnostischen Gasinsufflationen Fortschr Rontgenstr 103 (1965) 187

to a tube potential of 26 kV from a tungsten anode, filtering 0 5 mm Al, not only the soft tissues were well depicted but also the bone structure In radiography of the shoulder joint the technique of GROS was completely unsuccessful due to the long exposure times Therefore, it is to be recommended to use a tungsten target operating at low potentials for all types of radiography of periarticular tissues

The filtering in connection with a tungsten anode tube is incompletely known KYSER (1972) presented the radiation spectrum of a combination of a tungsten anode tube with a molybdenum filter, which contained large amounts of energy below the K-absorption edge of molybdenum at 20 keV However, he did not analyse their circumstances any further Later an attempt was made to adapt the molybdenum anode to radiography of thick tissue volumes by combining the anode with other filtering materials, such as aluminium and silver (JÖTTEN et coll 1973) With the latter filters the continuous spectrum of the molybdenum anode was brought out and the K-emission lines were to some extent filtered away GAJEWSKI & HEILMANN (1971) compared the image contrast obtained with a tungsten target to that obtained with one of molybdenum under identical operating conditions A molybdenum filter (0 03 mm) was used in both cases, the tube window being made of beryllium A glass filter (0 5 mm Al) was also combined with the tungsten target Clinical radiography on non-screen film was performed but no spectrometry Their results are partly at variance with the principles of GROS, insofar as the tungsten target was claimed to yield higher contrast under certain conditions Thus the value of K-edge filtering in the examination of joints cannot be completely assessed from previous reports

An investigation of the K-edge filtering of two types of filter, molybdenum and tin, was therefore undertaken A thin object was used, since it was considered that if the filtering effect had little or no value in such a case, it would be even more useless with thicker objects Furthermore, Al filtration in this type of radiography has also been considered

Materials and Methods

The experiments were carried out by means of an ordinary diagnostic roentgen tube with a tungsten rhenium target (Siemens Bi 125 30 50 MaR) The glass window of the tube had a filtering effect equivalent to 0 5 mm Al It was operated by means of a 6-valve generator, according to the principles described by REICHMANN et coll (1974) The tube potential and tube current were recorded at the high-voltage side of the generator The leak current of the system was found to be completely insignificant The tube potential was recorded by means of an oscilloscope and seemed to oscillate at an amplitude of ± 1 kV In the following the maximal potential values are given In the main experiments the tube was operated with five types of filters, one of these without extra filtration In the other four molybdenum (0 06 mm), tin (0 11 mm), copper (0 06 mm), and aluminium (1 75 mm) were used as extra filters The thicknesses were chosen so as to give approximately the same incident dose rate at 29 kV The filters were placed next to the tube

FROM THE DEPARTMENT OF DIAGNOSTIC RADIOLOGY III (DIRECTOR C-G HELANDER)
SAHLGRENSKA SJUKHUSET, S-411 32 GOTHENBURG, SWEDEN

FILTRATION IN SOFT TISSUE RADIOGRAPHY

E DEICHGRÄBER and S REICHMANN

In mammary radiography GROS (1967) used the K-emission from a molybdenum anode in combination with a molybdenum filter This filter to some degree absorbes photons at energy levels above the K emission lines, at 17 to 19 keV (BEARDEN 1968/69) more effectively than those just below the K absorption edge

There has been some difference of opinion on the feasibility of the technique introduced by GROS (GAJEWSKI & MIKA 1968, MIKA & REISS 1968, JAEGER 1969, KYSER 1972, HACH 1972) It appears that the technique is applicable only for limited tissue thickness, the upper limit being five to six cm When this is exceeded, the filtering effect of the tissue counteracts the combined effect of the molybdenum anode and the molybdenum filter The image is in fact made up of photons within the continuous spectrum above the K-emission lines For this reason compression is strongly advised in radiography of the breast

Radiographic techniques similar to that of breast radiography have been successfully applied to periarticular tissues in different regions (FISCHER 1973 a, b, FISCHER & BRAUN 1973, REICHMANN et coll 1974, DEICHGRABER & OLSSON, to be published) The limit of the tissue thickness pertaining to the technique of GROS should be valid to periarticular tissues as well However, even in examination of such thin objects as finger joints this technique was found to be unsuitable, as too high an image contrast is obtained (REICHMANN et coll) If a radiation quality were employed, corresponding

Submitted for publication 28 May 1974

to a tube potential of 26 kV from a tungsten anode, filtering 0 5 mm Al, not only the soft tissues were well depicted but also the bone structure In radiography of the shoulder joint the technique of GROS was completely unsuccessful due to the long exposure times Therefore, it is to be recommended to use a tungsten target operating at low potentials for all types of radiography of periarticular tissues

The filtering in connection with a tungsten anode tube is incompletely known KYSER (1972) presented the radiation spectrum of a combination of a tungsten anode tube with a molybdenum filter, which contained large amounts of energy below the K absorption edge of molybdenum at 20 keV However, he did not analyse their circumstances any further Later an attempt was made to adapt the molybdenum anode to radiography of thick tissue volumes by combining the anode with other filtering materials, such as aluminium and silver (JÖTTEN et coll 1973) With the latter filters the continuous spectrum of the molybdenum anode was brought out and the K-emission lines were to some extent filtered away GAJEWSKI & HEILMANN (1971) compared the image contrast obtained with a tungsten target to that obtained with one of molybdenum under identical operating conditions A molybdenum filter (0 03 mm) was used in both cases, the tube window being made of beryllium A glass filter (0 5 mm Al) was also combined with the tungsten target Clinical radiography on non screen film was performed but no spectrometry Their results are partly at variance with the principles of GROS, insofar as the tungsten target was claimed to yield higher contrast under certain conditions Thus the value of K edge filtering in the examination of joints cannot be completely assessed from previous reports

An investigation of the K edge filtering of two types of filter, molybdenum and tin, was therefore undertaken A thin object was used, since it was considered that if the filtering effect had little or no value in such a case, it would be even more useless with thicker objects Furthermore, Al filtration in this type of radiography has also been considered

Materials and Methods

The experiments were carried out by means of an ordinary diagnostic roentgen tube with a tungsten rhenium target (Siemens Bi 125 30 50 MaR) The glass window of the tube had a filtering effect equivalent to 0 5 mm Al It was operated by means of a 6-valve generator, according to the principles described by REICHMANN et coll (1974) The tube potential and tube current were recorded at the high voltage side of the generator The leak current of the system was found to be completely insignificant The tube potential was recorded by means of an oscilloscope and seemed to oscillate at an amplitude of ±1 kV In the following the maximal potential values are given In the main experiments the tube was operated with five types of filters, one of these without extra filtration In the other four molybdenum (0 06 mm), tin (0 11 mm), copper (0 06 mm), and aluminium (1 75 mm) were used as extra filters The thicknesses were chosen so as to give approximately the same incident dose rate at 29 kV The filters were placed next to the tube

Two separate thin-walled basins containing distilled water and vegetable oil with equally high fluid levels were used as soft tissue substitute The basins were placed alternatingly in the radiation beam, the transmitted radiation intensity being measured by means of an intensimeter, type Victoreen, model 440, serial 442 The spectral sensitivity of the ionization chamber was checked against a similar instrument (Labor Prof Dr Berthold, Modell TOL/D) with a constant sensitivity within the spectrum used Control measurements displayed a standard error of ± 0.087 In order to reduce the sensitivity, the entrance opening of the instrument was shielded by a lead plate with a hole of 5 mm diameter For each tube potential and filter the intensities of transmitted radiation through oil and water, respectively, were measured and the quotient between them calculated In some experiments the incident intensity was also measured, so that the absorbed radiation dose could be calculated (incident radiation dose minus transmitted radiation dose) The intensimeter measurements were supplemented by film dosimetry in certain cases The radiation, having passed oil and water, exposed the film (Agfa-Gevaert Mamoray T 3) the exposures being made in a stepwise manner, the film was developed in a roll machine (DEICHGRÄBER et coll 1974) By means of densitometry the relative mAs-values resulting in equal film density behind oil and water, respectively, could be assessed In this way the same quotient could be calculated as was obtained from the intensimeter measurements Differences in the spectral sensitivity of the two detectors could thus be recorded to a certain degree

Two experimental series were performed In the first the effect of the K-edge absorption was tested The phantom thickness of oil and water was 3 cm and the potential was set at 24, 29, 34, and 39 kV The intensity of the incident radiation was measured without phantom inserted into the beam Transmitted radiation with strict collimation, eliminating all secondary radiation, was measured with the phantom in the beam These measurements were repeated with uncollimated radiation so as to imitate the conditions present in clinical radiography, where no secondary screening is used By subtracting the transmitted intensity obtained with collimation from that obtained without collimation, a figure of the secondary radiation intensity in relation to the primary radiation could be obtained The relative dose absorbed within the water layer of the phantom was calculated, water being considered equivalent to the major part of tissue in clinical examinations In the same way the relative heating of the anode in the different types of exposure was calculated from the exposure data a given dose transmitted by water being considered necessary for obtaining an image In this way the contrast caused by the various tube potentials and filters could be analysed together with the absorbed dose and tube load

These experiments gave evidence that K-edge filters are not useful in clinical practice under the conditions given Another series of experiments with increasing Al filtration was therefore performed The measurements were based on previous clinical experiences The soft tissue roentgen tube was mounted in a Lysholm skull table, the FFD being 70 cm Medium sensitivity industrial film (Mamoray T 3) and

Table 1

Relative radiation dose in relation to contrast of the radiation relief and tube load The contrast function implies the quotient between radiation intensities behind oil and water with a thickness of 3 cm, respectively

Filter	Tube potential											
	24 kV			29 kV			34 kV			39 kV		
	Rel dose	Intens quot	Tube load	Rel dose	Intens quot	Tube load	Rel dose	Intens quot	Tube load	Rel dose	Intens quot	Tube load
None	1 0	3 6	94	0 5	2 6	36	0 4	2 4	24	0 3	2 1	18
Mo	1 25	4 9	672	1 0	4 0	361	0 6	2 7	182	0 4	2 2	119
Sn	*0 5*	*3 3*	*504*	*0 3*	*2 1*	*134*	*0 3*	*2 0*	*86*	*0 3*	*1 8*	*70*
Cu	0 5	3 2	492	0 3	2 2	124	0 3	1 8	62	0 2	1 7	42
Al	0 5	2 7	520	0 3	2 1	133	0 2	1 8	65	0 2	1 6	43

a potential of 25 kV for thin objects, such as finger joints, 32 to 35 kV for medium-sized objects, such as elbow joint, and 40 kV for thick objects, such as the shoulder joint, have previously been demonstrated to give the best results (DEICHGRÄBER et coll 1974) Accordingly, a phantom consisting of 3 cm oil and water, respectively, was tested at 25 kV For phantom thicknesses of 5 and 7 cm the tube potentials were 32 5 and 40 kV, respectively The same measuring principle was utilized as in the first series, only collimated radiation being employed The quotient between the transmitted intensities behind oil and water, respectively, was calculated as earlier Beginning with tube filtration only (0 5 mm Al) Al-filters were added in a stepwise manner, the quotient being obtained for each step When the quotient started to decline, it was assumed that the filtering was so effective as to influence the spectral distribution of the photons reaching the recording medium The aim was to find the maximum Al-filtering which leaves the spectral distribution unaffected

Results

Measurements, series I The intensity of the secondary radiation varied slightly with tube potential, at the two lower it was 10 to 15 per cent of the primary radiation instensity, and 15 to 20 per cent at the higher potential No correlation existed between secondary radiation intensity and the spectral composition of the transmitted radiation as manifested in the intensity quotient of the primary beam recordings Thus it may be concluded that the different types of filtering should not possibly influence the amount of fogging radiation Any differences in the recordings obtained with different filters should thus be expected to be related only to the transmitted primary beam

Table I gives three types of data obtained from the measurements of the collimated radiation the relative absorbed dose, the intensity quotient obtained from the recordings with oil and water, respectively, and the tube load expressed in relative heat

Table 2

Influence of the spectral sensitivity of silver on the intensity quotient (cf Table 1) The intensimeter figures display the contrast, function of the radiation relief, the film figures indicate how these functions are modified when recorded on non screen film

Filter	Tube potential			
	24 kV		29 kV	
	Intensimeter	Film	Intensimeter	Film
None	3 6	4 4	2 6	2 1
Mo	4 9	4 6	4 0	2 7
Al	2 7	2 5	2 1	1 6

units Even though the degree of filtering varied relatively good agreement between the intensity quotient and the absorbed dose existed, a rising quotient caused the dose to increase to the same degree, regardless of how the rising quotient was obtained The action of the K-edge could be demonstrated with the two filters with the K edge absorption within the spectral range used (Mo and Sn) The influence of the molybdenum filter was at its maximum at a tube potential of 29 kV, whereas the same occurred at 34 to 39 kV for Sn The change of the quotient was less marked for the tin filter This may reflect a lesser filtering capacity of this filter than was obtained with the Mo-filter The tube load varied within wide limits even in cases with identical intensity quotients Thus concerning the effect on the radiation, it appears appropriate to choose the alternative giving the desired intensity quotient with the smallest tube load possible This would result in shorter exposure times and less motion unsharpness From this point of view no additional tube filtration proved a better alternative than any of the filters tested

The intensity quotients presented in Table 1 may, however, be misleading in one important respect As long as the recording is made on film, the best recording medium appears to be medium sensitive industrial film without intensifying screens (DEICHGRÄBER et coll 1974, 1975) Here the image is made up by the direct influence of photons on the silver bromide crystals Silver has its K-absorption edge at 25 5 keV (BEARDEN 1968/69) Thus the film should be expected to be more sensitive above this energy level than below it, the sensitivity here changing markedly and stepwise This assumption has been confirmed by analysing the spectral sensitivity of non screen film (CORNEY 1966) For this reason the intensity quotient was measured for three filtering alternatives (no filter, Mo, Al) at 24 and 29 kV, film being used as detector instead of the intensimeter These measurements did not appear to give the same precision as the intensimeter measurements, due to the fact that excessively high doses had to be used if strict collimation of the radiation was to be maintained The results are presented in Table 2, where the intensity quotient obtained with film is compared with the one obtained with the intensimeter At 24 kV no evident difference

Table 3

Effect of increasing Al filtration on the intensity quotient (cf Table 1) Pht = phantom thickness

mm Al	Tube potential		
	25 kV Pht 3 cm	32 5 kV Pht 5 cm	40 kV Pht 7 cm
0 000	3 16	3 02	2.95
0 125	3 16	2 80	2 90
0 250	3 35	2 80	2 86
0 500	3 26	2 65	2.64
0 750	3 02	2 65	2 60
1 000	2 75		2 75
1 750			2 70

was seen between the two types of recording At 29 kV the film quotient was lower in all three cases, indicating that the film was relatively more sensitive to photons of the highest energy levels The most evident decrease occurred for the molybdenum filter, so that no great difference remained between the quotients of unfiltered rays and rays having passed the molybdenum filter

Measurements, series 2 It appears from Table 3 that at 25 kV the optimum filtration (0 75 mm Al) could be readily assessed At the other two tube potentials the optimum was less well defined It was considered, however, that at 32 5 kV 0 75 mm Al should be recommended, 1 75 mm Al being optimal at 40 kV The inherent filtration of the tube (0 5 mm Al) should be added to these values The tube load and the dose are affected by these filtrations The tube load was increased about 100 per cent in all three cases but only a moderate lowering of the dose occurred In the three cases the dose reduction as compared with the case without extra filtration was 34, 33 and 44 per cent, respectively, the last value corresponding to 40 kV

Discussion

In the present experiments a tube with a glass window (filtering effect, 0 5 mm Al) was used The unspecific filtration of the window to some degree counteracted the specific effects of the K-edge filters However, the window filtration is not only a matter of window material, it also increases with use, owing to precipitations of vaporized tungsten atoms originating from the cathode (HACH 1972) In soft tissue radiography of joints high dose rates—which imply high risks of such tungsten precipitations—are mostly unavoidable A beryllium window might result in more marked K-edge filtration (GAJEWSKI & HEILMANN) The ageing of such tubes would be fairly rapid, however Furthermore, few departments can afford to have a special apparatus for soft tissue radiography of joints The same tube should be useful in

— und MIKA N Optimierung von Bildkontrast und Bildschärfe bei der Weichstrahl Mammographie Deutscher Rontgenkongress 1968, S 115

GROS CH E Méthodologie Symposium européen de radiologie mammaire J Radiol Électrol 48 (1967), 638

HACH G Betrachtungen zur optimalen Mammographie-Technik Fortschr Rontgenstr 117 (1972), 208

JAEGER H Physikalisch-technische Grundlagen zur rontgenphotographischen Abbildung von Weichteilen Rontgen-Bl 23 (1969), 323

JÖTTEN G, KYSER K and OOSTERKAMP W J X-ray source for mammography Lecture held at the International Congress of Radiology, Madrid 1973

KYSER K Rontgenspektrometrische und rontgendosimetrische Untersuchungen der Strahlenqualitaten fur Weichstrahlaufnahmen Fortschr Rontgenstr 116 (1972) 818

MIKA N und REISS K H Optimierung der Rontgenbelichtungstechnik mit Hilfe der Halbleiterspektrometrie Rontgenpraxis 21 (1968), 164

REICHMANN S, DEICHGRÄBER E, STRID K-G, HEYMAN F and STRAND T Soft tissue radiography of finger joints Acta radiol Diagnosis 15 (1974), 439

FROM THE DEPARTMENTS OF PERIODONTOLOGY AND ODONTOLOGIC ROENTGENOLOGY,
SCHOOL OF DENTISTRY, KAROLINSKA INSTITUTET, S-103 64 STOCKHOLM, SWEDEN

QUANTITATIVE LONG-TERM DETERMINATIONS OF THE ALVEOLAR BONE MINERAL MASS IN MAN BY ^{125}I ABSORPTIOMETRY

III. Effect of experimental dental plaque formation

J BERGSTRÖM and C O HENRIKSON

Dental plaque as a cause of gingivitis is well known and generally accepted Gingivitis can be induced by avoiding oral hygiene (LÖE et coll 1965) The subsequent penetration of the inflammatory process through the gingival mucosa will cause changes of the underlying supporting periodontal tissues These changes may give a resorption of the alveolar bone

A method using the isotope ^{125}I has been shown to be suitable for measuring the mineral content of thin bone in vivo (HENRIKSON 1967) and has previously been used for measurements of changes in alveolar bone following periodontal surgery (BERGSTRÖM & HENRIKSON 1970, 1974) The technique has been further developed by HENRIKSON & JULIN (1971) and the precision of the method as used under optimum operational circumstances, i e on young people with healthy periodontia and a complete dentition has been analysed by HENRIKSON & BERGSTRÖM (1974)

The aim of the present work was to induce a marginal gingivitis by allowing plaque material to accumulate on tooth surfaces for a period of three weeks and to determine

This investigation was supported by a grant from the Swedish Medical Research Council, No B-73-24X 2787-04C Submitted for publication 22 February 1974

the effect of this gingivitis, if any, on the mineral mass of the subjacent alveolar bone The data refer to measurements of the mineral mass as it is reflected in one interdental bone septum Besides, fluctuations of the labio-lingual transverse thickness of the alveolar tissues in that region were recorded

The material consists of 13 students at the Dental School, 4 female and 9 male, aged 22 to 28 years All oral hygiene measures were refrained from during a period of 20 days

Before this period dental plaque and calculus, if present, were removed in order to establish good gingival health When this was achieved (with gingival index defined as 0) two recordings of the bone mineral mass within one week were made immediately before the experiment started, 0_1 and 0_2 Following the start of the 20 day period the mineral mass of the interdental alveolar bone and transverse thickness of the alveolar process were recorded at 20 and 100 days Plaque and condition of the gingiva were recorded on days 5, 10 and 20 At the end of the period oral hygiene was reinstituted

Methods

Recording of plaque The amount of plaque present on tooth surfaces was recorded following a scale 0–3 according to the index method of SILNESS & LÖE (1964) All surfaces of all teeth were recorded

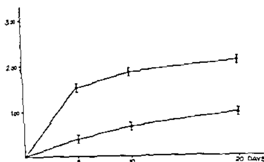
Recording of gingivitis The inflammatory changes of the marginal gingiva were classified according to the clinical index method described by LÖE & SILNESS (1963) The marginal gingiva adjacent to all surfaces of all teeth was assigned a score from 0–3

The clinical recordings were performed by the same observer (J B) throughout the observation period

Recording of bone mineral mass and of transverse thickness The apparatus used for measurements of the mineral mass of the alveolar bone has been described by HENRIKSON (1967), HENRIKSON & JULIN (1971), and in Part I of this investigation (HENRIKSON & BERGSTRÖM 1974) For analysis of the accuracy and precision of the method for bone mass measurements the reader is referred to Part I No correction for the 'shorter wave length' of the radiation was made

Results

The amount of plaque accumulated on tooth surfaces during the 20-day period appears in the Figure At the end of the period the plaque index based on all tooth surfaces for the total material was $2\ 05 \pm 0\ 33$ (M + SD) This is a significant increase ($p < 0\ 001$)



Changes in plaque index (O) and gingival index (Δ) The values are given on the ordinate as mean and standard deviation of the mean

The marginal gingivitis as recorded by the clinical index method progressed with time (Figure), and at the end of the experimental period a manifest mild gingivitis was evident, 0 92±0 37 (M±SD), which is a significant change ($p<0\,001$)

Changes of the interdental transverse thickness between the lateral incisor and canine will reflect fluctuations in tissue volume of the interdental gingiva Of the 13 subjects, 11 had an increased thickness after 20 days For the total material this increase was 0 29±0 077 mm (M±SD), which is significant ($p<0\,01$) Comparison of the thickness values at the start with those at the end of the observation period of 100 days for all individuals shows a mean difference of 0 05 mm, indicating that the swelling of the marginal interdental gingiva had disappeared

The precision of the method for determination of bone mineral mass as expressed by the replication procedure described in Part I was 0 026 mg mm $^{-2}$ (1 %) as average for all individuals throughout the observation period

The values of bone mineral mass for the total material at the start of the 20-day period are given in the Table For each individual the differences were calculated between the mean of two pre-experimental values, 0_1 and 0_2, and the values at 20 and 100 days, respectively Nine subjects out of 13 had a lower value of bone mineral mass after 20 days as compared to the pre-experimental level The differences are small, however, and not statistically significant for the group on an average ($p>0\,05$)

Discussion

Absence of oral hygiene measures will predispose to the accumulation of plaque material on tooth surfaces and, according to LÖE et coll (1965), a 3 week period is sufficient to produce gingivitis in young adults

The formation of plaque and the increasing gingivitis with time found in the present investigation was similar to that described by LÖE et coll An additional sign of gingivitis, swelling of the gingival margin, also appeared

It may be expected from long term observations in dogs that the absence of oral hygiene will cause a destruction also of the supporting periodontal tissues (GREENE & VERMILLION 1971, LINDHE et coll 1973) Evidence of reduced 'bone density' was re-

Table

Bone mineral mass in mg mm ² Differences of bone mineral mass between pre-experimental values (0) and values obtained at the end of the 20 day period as well as at day 100

Individual No	Bone mineral mass at start (0)	Bone mineral mass differences between periods		
		0–20	100–20	0–100
1	3 211	0 132	0 062	0 070
2	2 823	0 023	0 107	−0 083
3	2 590	0 004	0 035	0 039
4	3 320	0 052	−0 015	0 067
5	3 231	0 030	0 044	−0 014
6	2 685	0 122	0 092	−0 116
7	2 846	0 119	0 164	0 045
8	3 787	−0 045	0 081	−0 126
9	1 718	0 164	0 038	0 127
10	1 726	0 158	0 105	0 053
11	2 481	0 184	0 049	0 233
12	2 328	0 075	−0 092	0 168
13	1 353	−0 041	−0 011	−0 030
Mean	*2 623*	*0 0296*	*0 0254*	*−0 0025*
SD	0 707	0 1061	0 0793	0 1124
SE	0 196	0 0294	0 0220	0 0311

ported to occur after 18 months (LINDHE et coll 1973) In the present material the same method as used by LÖE and his collaborators (LÖE 1971) was extended to comprise also an examination of the marginal alveolar bone to determine by means of the sensitive ^{125}I absorptiometric technique whether a demineralization occurred accompanying early stages of gingivitis

The results of the present short-term experiment are not conclusive regarding the reaction of the alveolar bone to a 3-week period of plaque accumulation and associated gingivitis A reduction in bone mass, although not significant, was however observed at the end of the 20 day period This possible loss of alveolar bone was reestablished eighty days after the reinstitution of tooth cleansing It seems, therefore, safe to state that no permanent injury to the marginal alveolar bone follows upon a 3-week period of absent oral hygiene

The evaluation of the mineral mass was confined to one interdental region, that between the lateral incisor and canine of the upper jaw Roentgenograms and clinical

the region as regards plaque accumulating ability might be questioned The correlation between plaque index values based on all tooth surfaces and those based on surfaces of the upper front teeth during the period of observation was examined and found to be rather close The correlation coefficient on day 20 was +0 84 The plaque

formation on the buccal and proximal surfaces of the lateral incisor and canine was also examined on stereophotographs, which confirmed the close relationship to the rest of the dentition

Plaque accumulation rate and subsequent manifestation of gingivitis, as has been observed by other authors, vary between individuals, this was also true regarding the mineral mass changes However, an extension of the period of experiment seems to be desired as well as further analyses on an individual basis of the correlation between the three parameters

SUMMARY

Gingivitis was induced in young adults who refrained from all oral hygiene measures during a three week period No significant alterations concerning the mineral mass of the subjacent alveolar bone could be demonstrated.

ZUSAMMENFASSUNG

Es wurde bei jungen Personen, die sich wahrend einer 3 wochentlichen Periode aller oralen hygienischen Massnahmen enthielten, eine Gingivitis hervorgerufen Es konnten keine signifikanten Änderungen im Mineralgehalt des darunterliegenden alveolaren Knochens nachgewiesen werden

RÉSUMÉ

Une gingivite est apparue chez des adultes jeunes restés sans aucun soin d hygiène buccale pendant une période de trois semaines Il n'a pas eté possible de mettre en évidence des altérations significatives du contenu minéral de l'os alvéolaire sous-jacent

REFERENCES

BERGSTRÖM J and HENRIKSON C O Quantitative longitudinal study of alveolar bone tissue in man I Changes in alveolar bone tissue following periodontal surgery as recorded by an iodine 125 source J per odon

— — Quanti

^{125}I absorp

(1974), 48

GREENE J and VERMILLION J Oral hygiene research and implications for periodontal care J dent Res 50 (1971), 184

HENRIKSON C O Iodine 125 as a radiation source for odontological roentgenology Acta radiol (1967) Suppl No 269

— and BERGSTRÖM J Quantitative long-term determinations of the alveolar bone mineral mass in man by ^{125}I absorptiometry I Accuracy and precision of the method Acta radiol Ther Phys Biol 13 (1974), 377

— and JULIN P Iodine-125 apparatus for measuring changes in X ray transmission and the thickness of alveolar process J periodont Res 6 (1971), 152.

LINDHE, J., HAMP S.-E. and LÖE H Experimental periodontitis in the Beagle dog J periodont Res 8 (1973), 1

LOE H Human research model for the production and prevention of gingivitis J dent Res 50 (1971), 256

— and SILNESS J Periodontal disease in pregnancy I Prevalence and severity Acta odont scand 21 (1963), 533

— THEILADE E and BÖRGLUM JENSEN S Experimental gingivitis in man J Periodont 36 (1965), 177

SILNESS J and LÖE H Periodontal disease in pregnancy II Correlation between oral hygiene and periodontal condition Acta odont scand 22 (1964), 121

FROM ROENTGEN DEPARTMENT I (DIRECTOR H ARVIDSSON) AND THE PHARMACY CENTRE, STOCKHOLM COUNTY COUNCIL (DIRECTOR R BARKMAN), SODERSJUKHUSET, S-100 64 STOCKHOLM, SWEDEN

PHYSICAL CHARACTERISTICS OF BARIUM CONTRAST MEDIA AND THEIR INFLUENCE ON ROENTGEN IMAGE INFORMATION

K JEKELL, T OHLSON and J WIDEBECK

Barium sulfate was introduced as a contrast medium more than 50 years ago Since then the manufacturers have attempted to produce contrast media suitable for radiography of various parts of the gastrointestinal tract by adding various substances (EMBRING & MATTSSON 1968) The additives to the media affect the concentration of the barium sulfate and the stability and viscosity of the suspensions (BROWN 1963, BEEKMAN & BAEYENS 1971, JAMES & GODDARD 1971, 1972) The physical properties can be measured in the laboratory, but the effects on the formation of the image can be evaluated only by radiography, ordinarily in connection with examinations of patients The quality of the films is a result of radiographic technique, the patient s build of body and condition and the physiologic state of the organ being examined Thus the appearance of the films is influenced by so many factors that the part played by the contrast medium can only be evaluated with difficulty More adequate methods are thus needed and in the present work a radiographic method is described for a more objective estimation of different barium contrast media by means of a model

Submitted for publication 10 May 1974

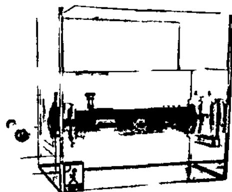


Fig. 1

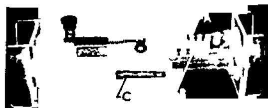


Fig. 2

Fig. 1. The model. A tube for the contrast medium within a container filled with water.

Fig. 2. The tube for the contrast medium. Two rows of seven beads with diameters of from 1 to 10 mm. On the lower surface of the tube a series of small steps each 1 mm in height. A) Upper. B) middle row of beads. C) steps.

Material and Methods

The model. A plastic model was constructed with the colon as a biologic 'prototype'. It was made of Plexiglass in two sections, an outer container filled with water and an inner horizontal tube for the contrast medium (Fig. 1). The attenuation level of the radiation of the model was equivalent to that of a heavy patient. The tube had an inner diameter of 5 cm and a volume of 500 ml. A row of seven spherical plastic beads, measuring from 1 to 10 mm in diameter, were attached to the upper surface of the tube. A similar row was located in the center of the tube on the edge of a supporting plate. At the bottom of the tube there were six descending flat surfaces resembling a staircase with one mm steps (Fig. 2). The beads and the steps were made to simulate abnormalities of the colon such as polyps and irregularities of the wall. With the model it was possible to obtain comparable films by means of which the relationship between the properties of various barium contrast media and the appearance of the films could be analysed.

The contrast media. Several barium contrast media commonly used routinely and a new product from Ferring AB not yet available on the market, here referred to as 'Ferrings', were tested (Table 1). Mixobar Colon 0.2 g/ml was used as delivered. The other media were diluted with tap water to 0.6, 1 and 2 according to the scale on Mattsson's areometer (MATTSSON 1969). Thus a number of 19 mixtures were evaluated. The contrast concentrations were the ones used for routine barium enemas with positive contrast only, i.e. not for double contrast technique.

Physical properties. The specific weight (density) of the contrast suspensions was determined in accordance with Mohr-Westphal's method (Table 1). Viscosity was measured at 37°C by Ostwald's method.

Table 1

Physical characteristics of the contrast media

Contrast medium	Areometer measurement	Specific gravity	$BaSO_4$-conc (% w/v)	Viscosity (according to Ostwald cps)
Barosperse	0 6	1 034	6 3	—*
	1	1 056	12 2	1
	2	1 118	23 2	2
Ferrings	0 6	1 036	4 9	—*
	1	1 082	9 9	1
	2	1 152	19 7	1
Micropaque	0 6	1 053	3 7	—*
	1	1 081	7 5	2
	2	1 142	15 0	2
Mixobar 1 g ml	0 6	1 051	5 0	2
	1	1 033	10 0	4
	2	1 155	20 0	12
Mixobar Colon 0 2 g ml		1 159	20 0	115
Unibaryt C	0 6	—*	—*	—*
	1	—*	12 6	—*
	2	1 146	25 8	2
Unibaryt Rektal	0 6	—*	—*	—*
	1	—*	7 1	—*
	2	1 123	14 2	2

* Due to sedimentation no measurement possible

Radiographic technique The contrast media were evaluated under standardized physical and rad olog
colon at the
mary focusing ... exposure control were used Films were exposed at 140 kV with horizontal and vertical beam direction at intervals of between 1 and 15 minutes after the filling of the tube A total of 6 films were exposed for each contrast medium In the areas observed the photographic density of the films was approximately 0 9 The model was kept at a temperature of 37 C during the experiments

The films were examined with regard to sedimentation and image information Sedimentation could be observed both in the upper and lower parts of the tube On the films exposed with horizontal beam direction sedimentation was visible as a

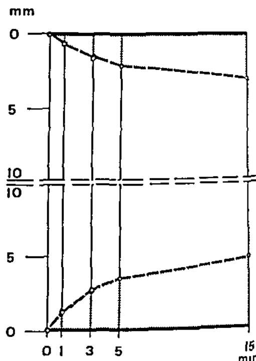


Fig. 3. Sedimentation profile. The walls of the tube are represented by the solid horizontal lines at the top and bottom of the figure. The depths of the sedimentation layers in the upper and lower part of the tube after 1, 3, 5 and 15 minutes are marked by circles connected by broken lines. These lines demonstrate the increase of thickness of the sedimentation layers during the experiment.

layer of well-delineated higher barium concentration at the bottom of the tube, while at the top a more or less contrast-free layer was observed. The increase of depth of the two layers was measured on consecutive films between 1 and 15 minutes. The progress of sedimentation was demonstrated by using a schematic figure of the tube on which the positions of the layers were marked at the various time intervals in relation to the upper and lower limits of the tube (Fig. 3). A figure was obtained, in the following called the 'sedimentation profile'. Image information was evaluated by counting the number of visible beads and steps in films exposed with vertical beam direction at intervals of 1 and 4 minutes (Fig. 4).

Results

Physical properties. The barium concentration of the contrast media appear in Table 1. A double test showed no differences in flocculation between tap water and distilled water. When calcium chloride was added to the tap water, flocculation increased markedly. The viscosity of the media varied considerably and one contrast mixture had a viscosity that was a hundredfold of others.

Sedimentation varied greatly (Fig. 5); it was only slight in a number of media and the *sedimentation* profiles are then almost completely rectangular. Other contrast mixtures displayed extreme sedimentation. In general, the effects of sedimentation were evident in the upper as well as in the lower parts of the tube after only one minute. During the following minutes the increase was slower. The intermediate layer, between the bottom sediment and the contrast-free upper layer, appeared

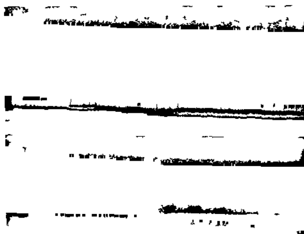


Fig 4 Roentgenograms of the contrast filled tube The upper film is exposed with horizontal beam direction and the lower with vertical The two rows of beads and the steps may be identified in both projections The arrow indicates contrast medium sediment in the lower part of the tube

homogeneous in the films with one exception in which several intermediate layers could be identified With a number of mixtures the bottom sediment had a thick and sticky concistency, and it was impossible to reestablish a homogeneous suspension even by vigorously rotating and shaking the tube

Image information varied markedly, with almost twice as many perceptible details with the most informative contrast medium as compared with the least informative (Table 2) The information available in the lower part of the tube, represented by the number of identifiable steps, was considerably greater in films exposed after four minutes than in those exposed after only one minute During this period of time, however, the number of visible details in the upper part of the tube diminished

Discussion

In radiographic evaluation of the suspension stability of a barium contrast medium it is common to take a series of films, with horizontal beam direction, of the mixture in a vessel with a rectangular cross section (HEJGAARD et coll 1956) In the present experiments, however, the sedimentation was analysed in a horizontal tube, which, like its anatomic 'prototype', had a circular cross section The effect of sedimentation was more evident in vessels with a circular cross section, and in the case of slight sedimentation, it was demonstrable only in vessels of this type (Fig 6) This is partly due to the fact that sediment from a relatively large volume of contrast medium collects on a small surface Another factor which may be of importance is the rapidity of sedimentation which may differ in vessels with slanting walls from such with vertical walls Sedimentation which occurred in the horizontal tube was demonstrated by means of sedimentation profiles, providing a detailed picture of the sedimentation characteristics of different media and making possible an analysis of the relationship between sedimentation and image information

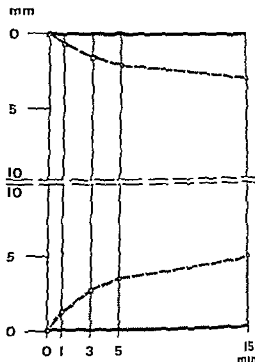


Fig 3 Sedimentation profile The walls of the tube are represented by the solid horizontal lines at the top and bottom of the figure The depths of the sedimentation layers in the upper and lower part of the tube after 1, 3, 5 and 15 minutes are marked by circles connected by broken lines These lines demonstrate the increase of thickness of the sedimentation layers during the experiment

layer of well delineated higher barium concentration at the bottom of the tube while at the top a more or less contrast-free layer was observed The increase of depth of the two layers was measured on consecutive films between 1 and 15 minutes The progress of sedimentation was demonstrated by using a schematic figure of the tube on which the positions of the layers were marked at the various time intervals in relation to the upper and lower limits of the tube (Fig 3) A figure was obtained, in the following called the 'sedimentation profile' Image information was evaluated by counting the number of visible beads and steps in films exposed with vertical beam direction at intervals of 1 and 4 minutes (Fig 4)

Results

Physical properties The barium concentration of the contrast media appear in Table 1 A double test showed no differences in flocculation between tap water and distilled water When calcium chloride was added to the tap water, flocculation increased markedly The viscosity of the media varied considerably and one contrast mixture had a viscosity that was a hundredfold of others

Sedimentation varied greatly (Fig 5), it was only slight in a number of media and the sedimentation profiles are then almost completely rectangular Other contrast mixtures displayed extreme sedimentation In general, the effects of sedimentation were evident in the upper as well as in the lower parts of the tube after only one minute During the following minutes the increase was slower The intermediate layer, between the bottom sediment and the contrast free upper layer, appeared



Fig 9 Film exposed with horizontal beam direction 3 min after beginning of routine barium enema

gives a coating of the upper wall allowing optimum information in that area In conventional barium technique, however, the best diagnostic information is obtained from the lowermost wall of the organ By taking films in different positions it is possible to demonstrate all walls of the colon

No efforts were made to evaluate how physiologic conditions such as the amount of intestinal wall mucus, variations in pH etcetera affect the diagnostic efficiency of a contrast medium The sedimentation, however, should have the same effect in the colon as in the model, i e enhance the diagnostic quality in the lowermost parts of the colon A contrast medium with sedimentation would thus seem to be preferable to a completely stable suspension, because it provides increased image information regarding the wall of the colon on which it settles This is true only provided that the sedimentation is moderate If sedimentation is very marked the barium sulfate layers rapidly towards bottom and the enema, when reaching the oral part of the colon, contains very little barium (Fig 9)

The present investigation demonstrates that differences in stability of barium suspensions are of vital importance for the radiographic quality Tests in a colon model of the type described are important for the evaluation of barium contrast media

SUMMARY

Various barium contrast media intended for radiographic examinations of the colon were analysed in a plastic model This model contained fixed test objects which could be identified and counted on the films thus providing a measure of image information obtainable



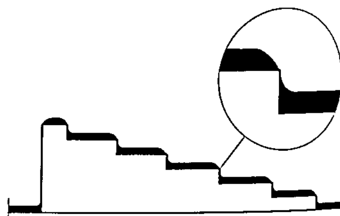


Fig. 8. Sedimentation on the steps. Film of the steps exposed with vertical beam direction (top). Drawing of the steps seen from the side (bottom).

of flocculation was demonstrated on the films, but had no relation to the image information obtained, nor did viscosity influence information.

A definite correlation, however, existed between the depth of the sediment layer in the bottom of the tube and the image information obtained from this area (Fig. 7). Increased sedimentation provided increased information from the bottom of the tube. This explains why with most of the contrast media the number of steps, which were visible, was greater after four minutes than after one minute. Even a minimal amount of sediment on the steps made it possible to recognize them clearly on the films, as sediment at the edge of the steps glided down to the steps below resulting in a greater difference in absorption at the edge of the steps (Fig. 8). Perception of the upper row of beads was obviously impaired by the top layer sedimentation and also to some degree by the sediment layer at the bottom. Thus the total image information was not related to the degree of sedimentation since the increase of information at the bottom of the tube as a result of sedimentation was counteracted by a loss of information from the upper part. When contrast media without evident sedimentation were used, the steps were more difficult to identify in the films and the image information from the lower part of the tube was poorer than with contrast media with sedimentation. On the other hand, contrast media without sedimentation provided optimum image information from the upper part of the tube.

In the colon a certain amount of gas always accumulates above the contrast medium making it difficult to obtain information of diagnostic value from the walls of the organ which are turned upward. This is true only for conventional barium examinations. Double contrast technique with higher barium concentration usually



Fig. 9 Film exposed with horizontal beam direction 3 min after beginning of routine barium enema.

gives a coating of the upper wall allowing optimum information in that area In conventional barium technique, however, the best diagnostic information is obtained from the lowermost wall of the organ By taking films in different positions it is possible to demonstrate all walls of the colon

No efforts were made to evaluate how physiologic conditions such as the amount of intestinal wall mucus, variations in pH etcetera affect the diagnostic efficiency of a contrast medium The sedimentation, however, should have the same effect in the colon as in the model, i e enhance the diagnostic quality in the lowermost parts of the colon A contrast medium with sedimentation would thus seem to be preferable to a completely stable suspension, because it provides increased image information regarding the wall of the colon on which it settles This is true only provided that the sedimentation is moderate If sedimentation is very marked the barium sulfate layers rapidly towards bottom and the enema, when reaching the oral part of the colon, contains very little barium (Fig 9)

The present investigation demonstrates that differences in stability of barium suspensions are of vital importance for the radiographic quality Tests in a colon model of the type described are important for the evaluation of barium contrast media

SUMMARY

Various barium contrast media intended for radiographic examinations of the colon were analysed in a plastic model This model contained fixed test objects which could be identified and counted on the films thus providing a measure of image information obtainable

Particular attention was paid to the marked differences in sedimentation of the various contrast media and the manner in which these affected image information.

ZUSAMMENFASSUNG

Verschiedene für röntgenologische Untersuchungen des Colon vorgesehene Barium-Kontrast-Mittel wurden in einem Kunststoffmodell analysiert. Dieses Modell enthielt feste Testobjekte, die auf den Filmen identifiziert und gerechnet werden konnten, wodurch ein Mass der zu erlangenden Bildinformation vorlag. Es wurden besonders die starken Unterschiede in der Sedimentation der Kontrastmittel und die Art, wie diese die Bildinformation beeinflussten, beachtet.

RÉSUMÉ

Différents moyens de contraste barytés destinés à l'examen radiographique du colon ont été étudiés dans un modèle en plastique. Ce modèle contenait des objets tests déterminés qui pouvaient être identifiés et comptés sur les films, donnant ainsi une mesure de l'information fournie par l'image. Les auteurs ont accordé une attention particulière aux différences marquées de sédimentation des divers moyens de contraste et à l'effet de ces différences sur l'information fournie par l'image.

REFERENCES

BEEKMAN P. et BAEYENS J.: Analyse de certains facteurs intervenant dans le résultat d'un lavement baryté et d'un examen en double contraste. J. belge Radiol. 54 (1971), 7.

BROWN G. R.: High density barium sulfate suspensions, an improved diagnostic medium. Radiology 81 (1963), 839.

EMBRING G. and MATTSSON O.: Barium contrast agents. Acta radiol. Diagnosis 7 (1968), 245.

HEJGAARD J. J., RATJEN E. und SCHULZE K.: Eine objektive Methode zur Bestimmung der Suspensionsstabilität von Bariumsuspensionen. Fortschr. Röntgenstr. 84 (1956), 349.

JAMES A. M. and GODDARD G. H.: A study of barium sulphate preparations used as X-ray opaque media. *Pharm. Acta helv. 46 (1971), 708.*

— — Barium meals. A physical chemical study of the adsorption of hydrocolloids by barium sulphate. Pharm. Acta helv. 47 (1972), 244.

MATTSSON O.: Areometer for estimating the concentration of modern barium meals. Acta radiol. Diagnosis 8 (1969), 446.

FROM THE DEPARTMENT OF DIAGNOSTIC RADIOLOGY III (DIRECTOR DOCENT CARL-GUSTAV HELANDER) SAHLGRENSKA SJUKHUSET, S-411 32 GOTHENBURG, AND THE DEPARTMENT OF PHYSICS, DIVISION IV A (DIRECTOR PROFESSOR GÖSTA BROGREN), CHALMERS UNIVERSITY OF TECHNOLOGY, S-402 20 GOTHENBURG, SWEDEN

SPECTRAL VARIATION OF THE CONVERSION FACTOR OF AN IMAGE INTENSIFIER

BO LANTZ and KARL GUSTAV STRID

One of the important characteristics of an image intensifier is the relation of the luminance of its output screen to the exposure rate of radiation at its front end. It is known that the luminance responds linearly to the exposure rate up to more than $100\ mR\ s^{-1}$ for radiation of given quality (HENNY & BECKER 1961, BOSTRÖM 1969). The International Commission on Radiological Units and Measurements (ICRU) (1962) recommends that the quotient between the output screen luminance and the input exposure rate be used as a quantity characteris[illegible] BECKER 1961, HALE et coll 1964, HOLM & MOSELEY 1964, GUYOT & DRIARD 1965, BOSTRÖM 1969). The ICRU (1962) therefore prescribes the conversion factor to be measured at a standard value of the tube voltage, viz. 85 kV, and with standard filtering, viz. 22 mm aluminium (and approx. 70 cm air). HOLM & MOSELEY, on the other hand, propose that the maximum value of the conversion factor should be specified.

Submitted for publication 9 April 1974.

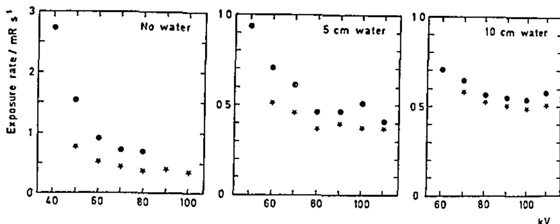


Fig 1 *The exposure rate required to produce constant video level in the absence of a Cu filter* (●) and with an 0 2 mm thick Cu filter (★)

The present report describes an investigation of the spectral variation of the response of an image intensifier employed in fluoroscopic videodensitometry (LANTZ & STRID 1973, 1975) The radiation quality was varied and the exposure rate required to produce a fixed luminance value was measured, the measurements yielding relative values for the conversion factor By the method described, the spectral response function of an image intensifier can be determined experimentally without the use of a spectrometer

The measurement object

The image intensifier, Sirecon duplex 25/15 (Siemens), has a roentgen screen with a useable area of 25 cm diameter (DENECKE & FENNER 1965) The diameter of the screen area actually projected can be varied electron-optically between 12 5 cm and 25 cm, the linear projection ratio then varying between 6 5 1 and 13 5 1 The screen phosphor consists of silver-activated zinc cadmium sulfide (60 % ZnS, 40 % CdS)

With the projection ratio 13 5 1, the conversion factor is stated to have a value greater than 70 cd m^{-2} mR^{-1} s (DENECKE & FENNER) It is reasonable to assume that the conversion factor varies as the square of the linear projection ratio In the present investigation the intensifier was used with a 12 5 cm input field, corresponding to the projection ratio 6 5 1

Experimental

The measuring system The measurements were performed by means of roentgenologic standard equipment in conjunction with a videodensitometric system and an air ionisation chamber as described previously (LANTZ & STRID 1975)

The *experimental set-up* is illustrated in Fig 1 of the article by LANTZ & STRID The distance between the tube focal spot and the intensifier input plane was 93 cm The ionisation chamber was placed centrally in the radiation field, close to the intensifier Water layers of varying thickness were placed immediately before the

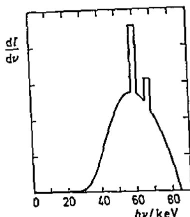


Fig 2. Spectrum calculated according to the mathe-

chamber, and copper filters were introduced close to the tube The irradiated field was confined by diaphragms to form a square 5 cm by 5 cm at the ionisation chamber

Measurements The exposure rate was measured for tube potential values ranging from 40 kV to 110 kV at 10 kV intervals, with copper filters of thickness ranging from 0 to 1 0 mm at 0 2 mm intervals and with water layers of thickness 0, 5 and 10 cm The procedures established previously (LANTZ & STRID 1975) were followed Thus, the tube current was adjusted to yield a constant value of the video level in the television chain, corresponding to constant luminance of the intensifier output screen

Results

With unfiltered radiation, the exposure rate required to produce the desired luminance value is very high in the lower potential range (Fig 1) Even slight filtering reduces the exposure rate considerably The maximum value of the conversion factor in the absence of a water layer was found to occur for tube potential values about 80 kV and with a 1 0 mm thick Cu filter

In the presence of a water layer, the maximum value of the conversion factor moves toward higher tube potential values Thus, for a 5 cm thick water layer it is situated at 80 to 90 kV and for a 10 cm thick layer around 100 kV Furthermore, it became obvious that Cu filtering increases the conversion factor of the intensifier but does not change the potential value at which the maximum appears Filtering with water, on the other hand, decreases its conversion factor

However, a plot of the exposure rate versus the tube potential (Fig 1) does not reflect the true spectral variation of the sensitivity of the image intensifier, since the tube potential alone does not determine the spectrum of the radiation entering the intensifier In order to form the base of a more adequate description, the spectrum of the filtered radiation was calculated for each of the combinations of tube potential values and filters used in the experiments The calculations followed a model which

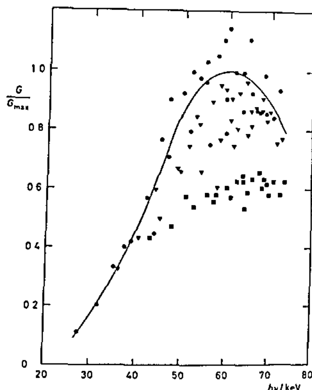


Fig 3 The spectral variation of the relative conversion factor of the Sirecon duplex 25/15 as measured with a water layer of varying thickness (● 0, ▼ 5 cm ■ 10 cm) The solid line represents the average of the measurements in the absence of water

regards the K absorption of the filters (STRID & LANTZ 1973) and yielded spectra like that in Fig 2 Moreover, for each case the 'average photon energy' was calculated as

$$h\bar{\nu} = \int h\nu I_\nu \, d\nu \, / \int I_\nu \, d\nu$$

ν being the radiation frequency, h being Planck's quantum of action and I_ν being the spectral function with respect to frequency For all measurements, finally, the reciprocal values of the exposure rate were plotted versus the corresponding $h\bar{\nu}$ values (Fig 3)

Discussion

The sensitivity of the image intensifier is low in the lower photon energy range (Fig 3), reaches a maximum at about 60 keV and then decreases toward higher photon energy values Apparently, different sensitivity functions apply to the different values of the water layer thickness However, the model used in the calculation of spectra does not regard the secondary radiation emitted by the water This radiation, which contributes to the exposure rate, falls in the soft part of the spectrum and thus does not give rise to luminance

Photons of energy lower than about 45 keV do not contribute appreciably to the output luminance of the image intensifier Photographic material, on the other hand, responds more strongly to this radiation Thus, the image intensifier appears less useful in soft-roentgen radiography However, with harder radiation, the roentgen relief will be less masked by the background due to diffusely scattered soft radiation

when an image intensifier is being used than in the case of direct photographic recording

The solid line (Fig 3) was drawn to reproduce the average reciprocal value of the exposure rate in the absence of a water layer It thus represents the relative spectral sensitivity of the image intensifier The maximum value (G_{max}) of the conversion factor appears for 60 keV photons

Conclusion

The present investigation has confirmed that the conversion factor of an image intensifier is a function of the tube potential, as pointed out by others (HENNY & BECKER 1961, HALE et coll 1964, HOLM & MOSELEY 1964, GUYOT & DRIARD 1965) The measurements have also confirmed that the conversion factor depends on the absorbing object and the filters in the radiation beam Thus, the conversion factor can be increased by Cu filtering

Moreover, by analysis of the measurement data, the spectral variation of the conversion factor of the image intensifier Sirecon duplex 25/15 has been determined The conversion factor has a maximum for photon energy values about 60 kV and drops rapidly for photons of energy below 45 keV No spectrometer was required for the determination

SUMMARY

The conversion factor of the image intensifier Sirecon duplex 25/15 was investigated by means of a videodensitometer for varying values of the tube potential and varying filtering of the radiation It was found that the conversion factor can be increased by Cu filtering By analysis of the measurement data, the spectral variation of the conversion factor was determined The conversion factor has a maximum for 60 keV photons and falls rapidly for photons of energy below 45 keV By the method described the spectral response function of an image intensifier can be determined experimentally without the use of a spectrometer

ZUSAMMENFASSUNG

Der Umrechnungsfaktor des Sirecon duplex 25/15 Bildverstarkers wurde mit Hilfe eines Videodensitometers fur verschiedene Werte der Rohrenspannung und unterschiedliche Filterung der Strahlung untersucht Es wurde festgestellt dass der [illegible]

RÉSUMÉ

Les auteurs ont étudié expérimentalement [illegible]
d image Sirecon [illegible]
potentiel du tub [illegible]

facteur de conversion peut etre augmenté par une filtration de cuivre Ils ont determine la variation spectrale du facteur de conversion par l'analyse des résultats de mesure Le facteur de conversion présente un maximum pour les photons de 60 keV et tombe rapidement pour les photons dont l'energie est inferieure a 45 keV Par la méthode decrite on peut déterminer expérimentalement sans utiliser un spectrometre la fonction de réponse spectrale d un intensificateur d'image

REFERENCES

BOSTROM U Investigation of x-ray image intensifier tubes Research Laboratory of Medical Electronics, Chalmers University of Technology, Gothenburg 1969

DENECKE R und FENNER E Die Rontgen-Bildverstarker-Rohre Sirecon duplex 25/15 Rontgen-Bl 18 (1965), 85

GUYOT L F et DRIARD B Développements recents dans le domaine des amplificateurs de luminance radiologiques Rev Techn CFTH 42 (1965), 53

HALE J, EPPERSON R D, GEORGE D L. and TRISTAN T A Physical factors in cinefluorography Amer J Roentgenol 92 (1964), 1192

HENNY G C and BECKER J A Comparison of the light output of image intensifier tubes Radiology 77 (1961), 472

HOLM T and MOSELEY R D The conversion factor for image intensifiers Radiology 82 (1964), 898

International Commission on Radiological Units and Measurements Methods of evaluating radiological equipment and materials ICRU Report 10 f (1962), National Bureau of Standards Handbook 89 (1963)

LANTZ B and STRID K-G Contrast formation in fluoroscopic videodensitometry II A comparison between theoretically computed and experimentally measured contrast Acta radiol Diagnosis 14 (1973), 625

— — Contrast formation in fluoroscopic videodensitometry III Relation between roentgen tube potential and exposure rate to produce constant video level Acta radiol Diagnosis 16 (1975), 65

STRID K-G and LANTZ B Contrast formation in fluoroscopic videodensitometry I A mathematical model for optimising contrast in radiography Acta radiol Diagnosis 14 (1973), 395

FROM THE DEPARTMENTS OF SURGERY I (DIRECTOR PROF L E GELIN) AND II (DIRECTOR PROF R ROMANUS) AND THE DEPARTMENTS OF DIAGNOSTIC RADIOLOGY I (DIRECTOR PROF O BARTLEY) AND III (DIRECTOR PROF C-G HELANDER), SAHLGRENSKA SJUKHUSET, UNIVERSITY OF GOTHENBURG, S 413 45 GOTHENBURG, SWEDEN

ANGIOGRAPHY AND HEMODYNAMIC MEASUREMENTS IN EXTENSIVE SOFT TISSUE TRAUMA TO THE EXTREMITY

J SANDEGÅRD and B E ZACHRISSON

After trauma an increase of blood flow of the extremity appears (REMINGTON et coll 1950, LIU 1968 LEWIS & LIM 1970 a, b) Different explanations for this phenomenon have been proposed BLALOCK & BRADBURN (1930) reported that following soft tissue trauma there was an increase of oxygen saturation of the venous blood draining the traumatized leg, which suggests a shunting of blood in the injured region On the other hand LEWIS & LIM (1970 b) consider the cause being an increase of capillary flow Vasodilator metabolites found in the venous blood from the injured region have been proposed as a possible explanation for the circulatory changes (SANDEGÅRD et coll 1974) A neurogenic response as the sole explanation for the changes of blood flow following trauma is less plausible as shown in experiments with contusion trauma performed after sympathectomy (LEWIS & LIM 1970 a) and denervation (LIU)

Trauma of a moderate degree to soft tissue may give local, functional disturbances of the vasomotor response, constriction or dilatation (LERICHE 1928, FOISIE 1947, KINMONTH et coll 1949, MORITZ 1954) On the other hand, a more intense trauma may result in various types of arterial injuries including aneurysm and arterio

Submitted for publication 28 March 1974

facteur de conversion peut être augmenté par une filtration de cuivre Ils ont déterminé la variation spectrale du facteur de conversion par l'analyse des résultats de mesure Le facteur de conversion présente un maximum pour les photons de 60 keV et tombe rapidement pour les photons dont l'énergie est inférieure à 45 keV Par la méthode décrite on peut déterminer expérimentalement sans utiliser un spectromètre la fonction de réponse spectrale d un intensificateur d'image

REFERENCES

BOSTRÖM U Investigation of x-ray image intensifier tubes Research Laboratory of Medical Electronics, Chalmers University of Technology, Gothenburg 1969

DENECKE R und FENNER E Die Rontgen-Bildverstärker-Rohre Sirecon duplex 25/15 Rontgen-Bl 18 (1965), 85

GUYOT L F et DRIARD B Développements recents dans le domaine des amplificateurs de luminance radiologiques Rev Techn CFTH 42 (1965), 53

HALE J, EPPERSON R D, GEORGE D L and TRISTAN T A Physical factors in cinefluorography Amer J Roentgenol 92 (1964), 1192

HENNY G C and BECKER J A Comparison of the light output of image intensifier tubes Radiology 77 (1961), 472

HOLM T and MOSELEY R D The conversion factor for image intensifiers Radiology 82 (1964), 898

International Commission on Radiological Units and Measurements Methods of evaluating radiological equipment and materials ICRU Report 10 f (1962), National Bureau of Standards Handbook 89 (1963)

LANTZ B and STRID K-G *Contrast formation in fluoroscopic videodensitometry II A* comparison between theoretically computed and experimentally measured contrast Acta radiol Diagnosis 14 (1973) 625

— — Contrast formation in fluoroscopic videodensitometry III Relation between roentgen tube potential and exposure rate to produce constant video level Acta radiol Diagnosis 16 (1975), 65

STRID K-G and LANTZ B Contrast formation in fluoroscopic videodensitometry I A mathematical model for optimising contrast in radiography Acta radiol Diagnosis 14 (1973), 395

with a padded hammer and lasted an average of 2 minutes It produced contusion of the tissues from the inguinal region to the knee, without fracture of the femur or rupture of the skin

Hemodynamic measurements of blood flow An electromagnetic flow meter (Nycotron, Oslo) was used for determination of arterial flow to the legs The flow probes were placed on both external iliac arteries proximal to the origin of the deep femoral arteries Arterial blood flow and arterial blood pressure were registered continuously on a Mingograf (Elema Schönander, Stockholm) For details of the techniques the reader is referred to a previous report (SANDEGÅRD et coll)

Angiography Central arterial blood pressure was measured by way of a mercury manometer AOT-R film changer and two tubes enabling stereoscopic exposures were used The equipment was the same as previously reported (SANDEGÅRD & ZACHRISSON) The dogs were placed supine and the films covered the thighs and pelvic region A catheter (Bardic adult feeding tube, length 107 cm, size 2 7 mm CR Bard International Ltd, England) was introduced through the left internal iliac artery with the tip placed in the aorta near the origin of the external iliac arteries In each angiography 15 ml Isopaque Cerebral (Nyegaard & Co, Oslo) were injected manually during 1 5–3 seconds The rate of exposure was 2 films/s for 10 s, followed by 1 film/s for 10 s

In five dogs the first examination was performed within 15 min before trauma, followed by examinations 1, 10, 30 and 60 min after trauma Two dogs were examined one minute after soft tissue contusion performed 45 to 60 min after fracturing of the femur with minimum soft tissue trauma In these two cases the primary aim was to analyse the effects of fracture of the femur with a minimum of soft tissue injury (SANDEGÅRD & ZACHRISSON) As the fracture did not affect the circulation of the soft tissues the dogs were included in the present material Four dogs were examined 210 to 360 min after trauma with two subsequent examinations performed within 5 to 15 min in three of the dogs In one dog a single examination was performed

At the conclusion of the experiments the animals were killed with an overdose of sodium Pentobarbital The hind limbs were dissected and the femoral arteries were cut longitudinally as well as the femoral veins The tissues were sectioned and examined macroscopically

Evaluation of the films As the evaluation principles have been described previously (SANDEGÅRD & ZACHRISSON), they are only summarized in this connection (1) transit time of contrast medium between two defined levels (GREITZ 1956) and (2) diameters of arteries at corresponding levels (ERIKSON 1965) were determined With these measurements the relative changes of the circulation in the defined regions could be estimated

All determinations of the transit time were related to the same zero level (time 0)

venous fistula (COLLINS & JACOBS 1961, SMITH et coll 1963, BRADHAM et coll 1964, *BROYN & BIE 1966, LOVE & BRAUN 1968, ADLER* et coll *1972, RICH 1973* and others)

Angiography has only rarely been used in the examination of extremity trauma in the acute state Single arteriograms were taken by WRAY (1964) in closed tibial fractures He observed vasodilatation and increase of flow to the injured extremity However, SANDEGÅRD & ZACHRISSON (1975) did not find any changes of blood flow in the soft tissues following experimental fractures performed with a *minimum* of soft tissue injury

A rapid transient increase of blood flow following intraarterial injection of water soluble contrast medium has been demonstrated (HILAL 1966, DELIUS & ERIKSON 1969, BOIJSEN et coll 1971) It has also been revealed that the arterial phase in angiography appears before the effects of the medium occur (BOIJSEN et coll) Injury to the soft tissue evidently does not change this character of flow alteration after injection of contrast medium (LEWIS et coll 1975)

Measurement of the arterial inflow to a traumatized extremity gives the total blood flow There are reasons to assume that the distribution of blood within the *traumatized region may be uneven and that the vessels might be variously affected* It was thus considered of interest to investigate whether it was possible with angiography, not only to assess the blood flow to the extremity, but also to get more detailed information of the local circulation in different areas of the traumatized region

Material and Methods

Twenty-two mongrel dogs of both sexes, weighing 14 to 26 kg were used for the experiments Eleven dogs were examined with serial angiography and in eleven dogs blood flow determinations were performed Anesthesia was provided by sodium Pentobarbital intravenously, administered in repeated small doses The trachea was *intubated and the dogs breathed spontaneously or were supported by mechanical* ventilation

The following procedures were carried out in both groups of animals

Following laparotomy the vessels near the aortic bifurcation were dissected free The aorta distal to the origin of the external iliac arteries was ligated, thus excluding the median sacral and the internal iliac arteries A tourniquet was placed around both ankles to exclude the circulation to the feet with its rich net of arterio venous anastomoses

Small polyethylene catheters for continuous registration of arterial blood pressure and for injections and sampling were introduced into one carotid artery and one jugular vein, respectively The venous catheter was kept open with a slow infusion of saline 0 9% amounting *to less than a total of 100 ml in each experiment* The arterial catheters were kept open by repeated small injections of saline No heparin was used

Extensive soft tissue trauma to one hind *leg* was performed *manually by 200 blows*

with a padded hammer and lasted an average of 2 minutes It produced contusi of the tissues from the inguinal region to the knee, without fracture of the femur rupture of the skin

Hemodynamic measurements of blood flow An electromagnetic flow meter (Nyc tron, Oslo) was used for determination of arterial flow to the legs The flow prob were placed on both external iliac arteries proximal to the origin of the deep femo arteries Arterial blood flow and arterial blood pressure were registered continuou on a Mingograf (Elema Schönander, Stockholm) For details of the techniques t reader is referred to a previous report (SANDEGÅRD et coll)

Angiography Central arterial blood pressure was measured by way of a merc manometer AOT R film changer and two tubes enabling stereoscopic exposu were used The equipment was the same as previously reported (SANDEGÅRD ZACHRISSON) The dogs were placed supine and the films covered the thighs and pel region A catheter (Bardic adult feeding tube, length 107 cm, size 2 7 mm CR Ba International Ltd, England) was introduced through the left internal iliac artery w the tip placed in the aorta near the origin of the external iliac arteries In each ang graphy 15 ml Isopaque Cerebral (Nyegaard & Co, Oslo) were injected manua during 1 5–3 seconds The rate of exposure was 2 films/s for 10 s, followed by 1 fil for 10 s

In five dogs the first examination was performed within 15 min before traur followed by examinations 1, 10, 30 and 60 min after trauma Two dogs were exami one minute after soft tissue contusion performed 45 to 60 min after fracturing of femur with minimum soft tissue trauma In these two cases the primary aim to analyse the effects of fracture of the femur with a minimum of soft tissue inj (SANDEGARD & ZACHRISSON) As the fracture did not affect the circulation of soft tissues the dogs were included in the present material Four dogs were ex ined 210 to 360 min after trauma with two subsequent examinations performed wit 5 to 15 min in three of the dogs In one dog a single examination was performed

At the conclusion of the experiments the animals were killed with an overdos sodium Pentobarbital The hind limbs were dissected and the femoral arteries v cut longitudinally as well as the femoral veins The tissues were sectioned and exami macroscopically

Evaluation of the films As the evaluation principles have been described previo (SANDEGÅRD & ZACHRISSON) they are only summarized in this connection transit time of contrast medium between two defined levels (GREITZ 1956) and diameters of arteries at corresponding levels (ERIKSON 1965) were determined V these measurements the relative changes of the circulation in the defined regions c be estimated

venous fistula (COLLINS & JACOBS 1961, SMITH et coll 1963, BRADHAM et coll 1964 BROYN & BIE 1966, LOVE & BRAUN 1968, ADLER et coll 1972, RICH 1973 and others)

Angiography has only rarely been used in the examination of extremity trauma in the acute state Single arteriograms were taken by WRAY (1964) in closed tibial fractures He observed vasodilatation and increase of flow to the injured extremity However, SANDEGÅRD & ZACHRISSON (1975) did not find any changes of blood flow in the soft tissues following experimental fractures performed with a minimum of soft tissue injury

A rapid transient increase of blood flow following intraarterial injection of water soluble contrast medium has been demonstrated (HILAL 1966, DELIUS & ERIKSON 1969, BOIJSEN et coll 1971) It has also been revealed that the arterial phase in angiography appears before the effects of the medium occur (BOIJSEN et coll) Injury to the soft tissue evidently does not change this character of flow alteration after injection of contrast medium (LEWIS et coll 1975)

Measurement of the arterial inflow to a traumatized extremity gives the total blood flow There are reasons to assume that the distribution of blood within the traumatized region may be uneven and that the vessels might be variously affected It was thus considered of interest to investigate whether it was possible with angiography, not only to assess the blood flow to the extremity, but also to get more detailed information of the local circulation in different areas of the traumatized region

Material and Methods

Twenty two mongrel dogs of both sexes, weighing 14 to 26 kg were used for the experiments Eleven dogs were examined with serial angiography and in eleven dogs blood flow determinations were performed Anesthesia was provided by sodium Pentobarbital intravenously, administered in repeated small doses The trachea was intubated and the dogs breathed spontaneously or were supported by mechanical ventilation

The following procedures were carried out in both groups of animals

Following laparotomy the vessels near the aortic bifurcation were dissected free The aorta distal to the origin of the external iliac arteries was ligated, thus excluding the median sacral and the internal iliac arteries A tourniquet was placed around both ankles to exclude the circulation to the feet with its rich net of arterio venous anastomoses

Small polyethylene catheters for continuous registration of arterial blood pressure and for injections and sampling were introduced into one carotid artery and one jugular vein, respectively The venous catheter was kept open with a slow infusion of saline 0 9 % amounting to less than a total of 100 ml in each experiment The arterial catheters were kept open by repeated small injections of saline No heparin was used

Extensive soft tissue trauma to one hind leg was performed manually by 200 blows

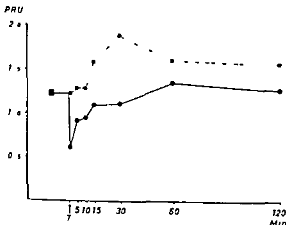


Fig 2 Mean of calculated vascular peripheral resistance (PRU) in 11 dogs of the traumatized limb (●—●) and of the non traumatized limb (■---■) On the traumatized side the trauma was followed by a marked transient reduction of PRU and thereafter a continuous increase and a tendency to normalization 60 to 120 min after the trauma On the non traumatized side PRU increased transiently following trauma with maximum values 30 min after the trauma

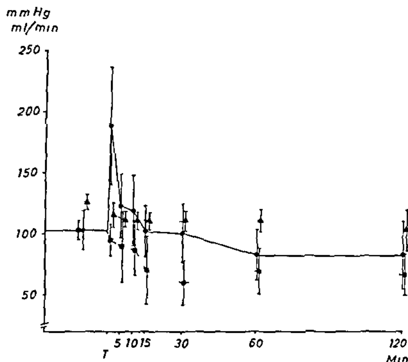
femoral arteries, of the femoral arteries at the level of the lower acetabular borders, 10 mm proximal to the origin of the saphenous arteries and 20 mm proximal to the origin of the caudal femoral artery Measurements were performed on both the injured and the intact leg with a magnifying glass with a built-in scale permitting readings within 0 1 mm The magnification factor was 7

The formula $\sqrt{\sum d_i^2/2N}$ was used to calculate the standard error of a single measurement, where the internal arterial diameter was independently measured twice (DAHLBERG 1948) The difference between two determinations was d_i and the number of duplicate measurements N The standard error of a single measurement of the iliac arteries was $\pm 0\,07$ mm (N = 51) and of the femoral arteries $\pm 0\,05$ mm (N = 185)

In addition to determinations of transit times and calibers, the course, contour and number of vessels were also considered Extravasation and transient more or less homogeneous accumulation of contrast medium was appraised Extravasation into the extravascular space will begin when the bolus reaches a leaky vessel It will persist beyond the vascular phases and be present on the final films in any given series On the other hand, accumulation of contrast medium reaching its maximum during the vascular phase and combined with early venous filling was considered as a sign of increased flow The medium has thus disappeared on the final films

Results

Hemodynamic measurements Immediately after the trauma there was a marked increase of blood flow to the traumatized leg which gradually returned to the pre-trauma level but after 60 to 120 min was lower than before the trauma (Fig 1) On the non traumatized side, the blood flow decreased continuously until 30 min after the trauma, being slightly lower than the blood flow on the traumatized side after 60 to 120 min (Fig 1)



traumatized side Five min after the trauma and thereafter blood flow on the traumatized side decreased further However it was still increased in relation to blood flow on the non traumatized side

which was chosen as the earliest observable filling of the external iliac artery at the origin of the deep femoral artery

The femoral arterial transit time was consequently defined as the time difference between the zero level and the earliest filling of the caudal femoral artery arising from the distal part of the femoral artery Arterial filling phase was denoted as the period from zero level to filling of the smallest visible peripheral arteries determined in two regions of the thigh (1) anteriorly and (2) in the adductor region In addition in these regions the time interval to the earliest filling of the veins was recorded In an analogous way the earliest filling of the distal part of the femoral vein was estimated These intervals are referred to in the text as venous appearance times

Transit times were evaluated in ten of the eleven dogs In one dog examined early after the trauma, zero level (time 0) could not be defined according to technical errors of timing This dog was, however, not excluded from the material as the angiographic appearance of the vascularity nevertheless could be analysed

The internal diameter of the arteries was measured on the films at corresponding levels and in each dog at equal focus film and object film distance Only arteries heavily filled with contrast medium at measuring levels were measured Measurements of the external iliac arteries were performed 10 mm proximal to the origin of the deep

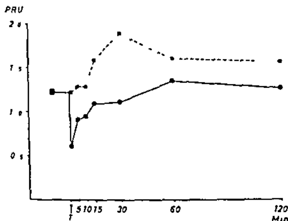


Fig 2 Mean of calculated vascular peripheral resistance (PRU) in 11 dogs of the traumatized limb (●—●) and of the non traumatized limb (■---■) On the traumatized side the trauma was followed by a marked transient reduction of PRU and thereafter a continuous increase and a tendency to normalization 60 to 120 min after the trauma On the non-traumatized side PRU increased transiently following trauma with maximum values 30 min after the trauma

femoral arteries, of the femoral arteries at the level of the lower acetabular borders, 10 mm proximal to the origin of the saphenous arteries and 20 mm proximal to the origin of the caudal femoral artery Measurements were performed on both the injured and the intact leg with a magnifying glass with a built-in scale permitting readings within 0 1 mm The magnification factor was 7

The formula $\sqrt{\sum d_i^2/2N}$ was used to calculate the standard error of a single measurement, where the internal arterial diameter was independently measured twice (DAHLBERG 1948) The difference between two determinations was d_i and the number of duplicate measurements N The standard error of a single measurement of the iliac arteries was ±0 07 mm (N = 51) and of the femoral arteries ±0 05 mm (N = 185)

In addition to determinations of transit times and calibers, the course, contour and number of vessels were also considered Extravasation and transient more or less homogeneous accumulation of contrast medium was appraised Extravasation into the extravascular space will begin when the bolus reaches a leaky vessel It will persist beyond the vascular phases and be present on the final films in any given series On the other hand, accumulation of contrast medium reaching its maximum during the vascular phase and combined with early venous filling was considered as a sign of increased flow The medium has thus disappeared on the final films

Results

Hemodynamic measurements Immediately after the trauma there was a marked increase of blood flow to the traumatized leg which gradually returned to the pre-trauma level but after 60 to 120 min was lower than before the trauma (Fig 1) On the non-traumatized side, the blood flow decreased continuously until 30 min after the trauma, being slightly lower than the blood flow on the traumatized side after 60 to 120 min (Fig 1)

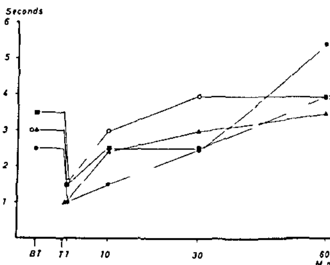


Fig 3 Femoral arterial transit time of the injured leg in 4 dogs One min after trauma (T) a marked reduction of the transit times Thereafter a gradual increase with a tendency to reach pre traumatic levels after 30 to 60 min

Arterial blood pressure fell significantly within 5 min after the trauma, and thereafter remained unchanged throughout the experiment (Fig 1)

Peripheral resistance calculated as the ratio of arterial blood pressure to blood flow, decreased markedly on the traumatized side and was unchanged on the non-traumatized side immediately after the trauma but after 5 to 15 min the peripheral resistance increased on both the traumatized and the non-traumatized sides Sixty min after the trauma the peripheral resistance was slightly higher than before trauma both on the traumatized and on the non-traumatized side (Fig 2)

Angiography (1) Femoral arterial transit time Angiography before trauma demonstrated minor differences between the two legs

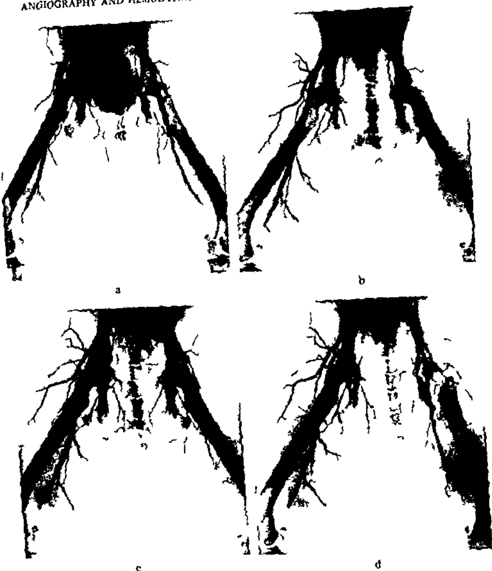
One minute after trauma the transit time on the traumatized side decreased about 50 per cent or more of the pre-trauma values, that is, there was a more rapid transit of the contrast medium through the leg (Figs 3, 4) This was even more evident in view of the slowing of the transit time in the non-traumatized leg

The transit time was increased after 10, 30 and 60 min compared with the examination one minute after trauma with a tendency to normalization after 30 min and slight prolongation after 60 min (Figs 3, 4)

On the non-traumatized side a tendency to a slight increase of transit times after trauma compared to the pre trauma value was observed In comparison with the injured side, the transit times were markedly prolonged

In the series of dogs examined 210 to 360 min after trauma, different results were obtained Thus in comparing the traumatized and non-traumatized legs no difference of transit times, occurred in one case In two cases a difference of 0 5 s was recorded, and in one case the transit time of the injured side was 1 s shorter than on the contra-lateral side

(2) Internal diameters of the external iliac and the femoral arteries One minute after trauma marked, highly significant increase of arterial diameters on the injured



F g 4 Ang ography a) before trauma (femoral arte 1 tm...
1 5 s) c) 30 m n (FA
t me refers to the r
larger arter es Obv c

s de occurred (Figs 5 6) The diameter increased 1 1 to 1 7 mm at the defined level of the external iliac arteries (Fig. 5) while the values of the femoral arteries (Fig 6) varied between 0 6 and 1 8 mm at the three measuring levels In the two dogs with prior fractures the same dilator response was observed following soft tissue trauma Other levels of the arteries (not defined in the figures) were also continuously dila

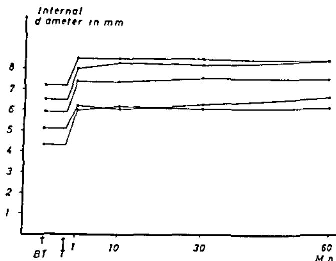


Fig 5 Internal diameters of the *external iliac artery of the injured* side in 5 dogs Measurements in 0 1 mm were performed on the films 10 mm proximal to the origin of the deep femoral artery The standard error of a single measurement was $\pm 0\ 07$ mm In all cases a persistent significant dilatation was observed following trauma

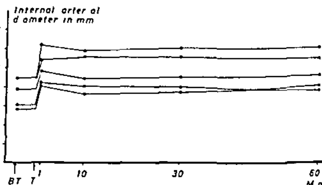


Fig 6 Internal diameters of the femoral artery of the injured leg in 5 dogs Measurements in 0 1 mm were performed on the films 10 mm proximal to the origin of the saphenous artery The standard error of a single measurement was $\pm 0\ 05$ mm In all cases a persistent significant dilatation of the femoral *artery occurred after trauma*

tated without segmental narrowing The dilatation of the arteries persisted during the experiments On the non injured side a tendency to narrowing of the calibers, compared to pre trauma values was observed

In the dogs examined 210 to 360 min after trauma significantly wider arteries occurred on the traumatized side compared to the non traumatized side

(3) Peripheral arteries of thigh Before trauma equal transit times in the two legs were recorded No abnormalities of the arteries and no homogeneous accumulation of medium were observed

One minute after trauma the arterial filling phase was about 50 per cent shorter in comparison with pre-trauma values Concomitantly larger and smaller arteries were markedly dilated leading to that previously non observable vessels could be identified, followed by a fairly homogeneous accumulation of contrast medium combined with an *early venous filling, particularly in the middle anterior thigh* and in the adductor regions (Fig 7) Some arteries developed segmental variations of caliber

In three cases a discontinuity was demonstrated in a middle sized muscular artery of the adductor region with extravasation of medium in two of the cases Smaller

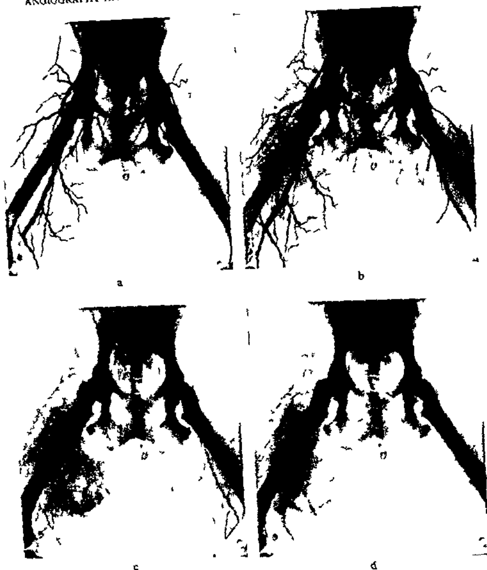


Fig 7 Angiography 1 min after *contusion trauma to the r* ...
after the earl est filling of the n ...
0) a b) Arterial phase c) End ...
medium in the traumatized are ...
leg with marked general arter. ...

avascular areas occurred at various *sites fol*lowing trauma, especially in the adductor region and slight stretching of arteries, but no major displacement

The arterial filling *phase* was prolonged 10, 30 and 60 min after *trauma and the* concentration of the *contrast medium within* peripheral arteries and the areas of

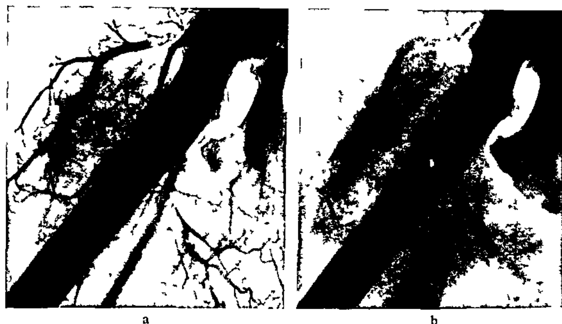


Fig 8 Angiography of contused thigh 30 min after trauma a) Arterial phase b) Venous phase. Changes of caliber of the artery close to the femur Slight, increasing extravasation of contrast medium in this region during the examination Interval between zero level and the respective films a) 6 5 s, b) 16 5 s

accumulation of medium decreased in the injured leg Accumulation of medium was not observed later than 30 min after trauma In different parts of the injured region the transit times of the smaller arteries varied The earlier observed local variations of arterial caliber (Fig 8 a) had progressed further at the end of the experiments when the avascular areas were more defined Locally, in the vicinity of these areas a discontinuity of smaller arteries was sometimes demonstrated In some arteries the medium remained for a longer period than in other arteries of the thigh They were filled also during parts of the venous phase This was especially apparent 60 min and 210 to 360 min after the trauma (Fig 9)

The peripheral arteries on the non traumatized side were somewhat less well filled, especially in examinations 1, 10 and 30 min after trauma

(4) Veins of thigh Venous appearance times decreased markedly immediately after trauma on the traumatized side, followed by a gradual increase Early venous filling constantly occurred in the areas with transient accumulation of medium On the non traumatized side a tendency to increased appearance times following trauma was observed

Some divergent observations of venous appearance times were made in four traumatized legs In two cases the venous appearance times in the adductor regions had further decreased 10 min after trauma, the estimated values being 1 s longer than the arterial filling phase of the same region Similar, but more evident findings were encountered in one case in which the appearance of venous filling of the anterior thigh was observed 2 s before the end of the arterial filling phase in the same region

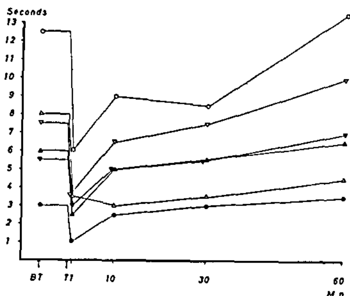


Fig 9 Angiography 225 min after trauma to the right h ob (h ...
traumatized s de (
f il ng of peripher
vessels Changes
to an increase of ... traumatized leg.

10 30 and 60 min after trauma (Figs 10 11) Early venous filling in the adductor region was also recorded 1 and 10 min after trauma in that dog in which transit times could not be recorded according to the definitions used

The filling of the veins in the contused thigh was clearly improved within 30 min after the trauma Comparisons of venous caliber with angiography before trauma were uncertain because of deficient venous filling in these examinations On the later films (210 to 360 min after trauma) the veins could not be scrutinized because of low concentration of the medium

(5) Extra...
as me...
occur ... At later examinations no increased extravasation was observed except in one dog (Fig 11 d) Extravasation appeared in soft tissues near the femur especially in the middle and proximal part and in the adductor region The source of extravasation could not be recognized with certainty except in two cases with lesions of middle sized muscular arteries of the adductor region



(6) Macroscopic examination The trauma produced a gradual swelling of the thigh and small subcutaneous patchy bleedings, but no rupture of the skin Sections of the injured leg gave evidence of edematous swelling of the muscles and patchy interstitial bleedings, especially near the femur and in the adductor regions More localized hematomas were proved in the two cases with discontinuity of muscular arteries of the adductor regions on the films combined with extravasation No macroscopic lacerations of the tissues including the fasciae were observed Longitudinal dividing of the femoral arteries and veins revealed no interruption of the vessel walls No thrombosis in the segment of the large vessels exposed to trauma was recognized

Discussion

In the present experiments a repeated trauma of the same type as used by previous authors (LIU, LEWIS & LIM SANDEGÅRD et coll) was performed evenly over the thigh avoiding laceration The experiments were carried out under uniform conditions and were adapted to previous experiments in order to be able to relate the present results to those of previous hemodynamic investigations in which the same type of trauma was used

The flow was estimated angiographically by measurements of the transit of contrast medium between two defined levels and of internal arterial diameters By repeated examinations, comparisons of the respective sides could be performed before and



Fig. 11 Angiography of the contused th gh 60 m
of venous filling Inter
18 s Commencement of
increase of blood flow
indicating lesion of sma

after trauma The evaluation of the findings was further facilitated by the possibility of contralateral comparisons The measurements of internal arterial diameters proved to be fairly exact However, the determination of transit times has weaknesses because of the intervals between the exposures and the *difficulty in defining the* head of the contrast column (KJELLBERG 1943) Objections therefore must be raised against calculation of the absolute flow based on angiography Nevertheless, there *was a positive relationship between the determinations of flow by angiography and* by electromagnetic flowmeters By the measurement of transit times and arterial diameters it was possible to define the relative changes of total blood flow to the injured region and to obtain information on the local circulatory conditions These results are in agreement with the data of GREITZ, ERIKSON, NILSON et coll (1968) from angiographic determinations of blood circulation in brain, kidneys and amputated limbs, respectively In investigations of this kind the effects of contrast medium on flow must be considered The informative period of angiography occurs in the time lag between the injection of contrast medium and the flow increasing effect (BOIJSEN et coll) As the same response also exists following soft tissue injury (LEWIS et coll), it is evident that the medium per se does not affect the results in the angiographic evaluation of relative changes of flow, based on the measurements of transit times and calibers of the vessels

A marked increase of blood flow to the traumatized region immediately after the trauma was revealed This corresponds angiographically to arterial and capillary dilatation demonstrated as marked accumulation of contrast medium By its rapid disappearance, this accumulation may be differentiated from extravasation of medium The homogeneous accumulation of medium in the traumatized area possibly indicates filling of numerous non-identifiable blood vessels suggesting increased capillary flow which was further emphasized by early venous filling This agrees with the ob*servations* of LEWIS & LIM (b) who examined the peripheral circulation in soft tissue trauma by injections of macroaggregated albumin The assumption of increased capillary flow was further suggested in the present material by the absence of true *arterio-venous shunting*

During the later parts of the experiments decreased blood flow was recorded in the traumatized extremity which contrasted to an angiographically persistent dilatation of larger *arteries including the external iliac artery This includes* vessels proximal to the trauma level However, these experiments provide no explanation for the dilatation observed up to 6 hours after trauma, but suggest at least a temporary loss of vascular tone *Possible etiologic factors might be a decrease of sympathetic* tone (LEWIS & KERSTEIN 1970), vasodilator metabolites released from the traumatized region (SANDEGÅRD et coll) or a disturbance of the contractile function of the vascular smooth muscle

The later decrease of blood flow in the traumatized region was accompanied by an inhomogeneous distribution of blood within the injured region, as shown by irregular decrease of accumulation of *medium and locally varying transit times* These local

changes of blood flow pointed to different influences on the vascular bed following trauma, with mainly impaired peripheral circulation Corresponding to the impaired flow were demonstrated absence of filling, general or segmental narrowing, discontinuity, avascular areas and extravasation of contrast medium These vascular abnormalities suggest injuries of functional (LERICHE, FOISIE, MORITZ) or organic nature viz microthrombosis (KNISELY et coll 1945, GELIN 1956) Another cause for changes of the peripheral vascularization following trauma is the possible increase of tissue pressure due to edema and bleeding On the films, extravasation of medium could generally not be referred to a specific artery suggesting that it was mostly due to capillary injury No evidence of macroscopic lacerations of the muscles was found but patchy interstitial bleedings and edema within the intact fascial spaces This supports the opinion that increased tissue pressure is at least partly responsible for the later non filling of peripheral vessel segments as in the acute state of lower leg venous thrombosis (MAY & NISSL 1967, NYLANDER 1968) The extent to which the edema and hemorrhage raise tissue pressure in skeletal muscle is not known From the work of GUYTON et coll (1971) it is known that all types of edema raise interstitial pressure and that the acute injection of fluid into tissue, can produce pressure of the order of +15 to +20 mm Hg Whether or not the elevated tissue pressure under the present experimental conditions was sufficient to cause vascular collapse remains to be investigated

In the hemodynamic measurements there was a gradual increase of calculated peripheral resistance in the later parts of the experiments This corresponded to the decreasing filling of arteries within the traumatized region at angiography The increase of peripheral resistance cannot be explained solely by morphology, since the injection of contrast medium during this period after the same type of soft tissue trauma results in a transient increase of blood flow (LEWIS et coll) This suggests that the increase of peripheral resistance is at least partly functional This is supported by the absence of homogeneous accumulation of contrast medium at a later phase which might be due to a return of vascular tone with a concomitant decrease of vascular caliber

The nature of the flow changes following soft tissue injury observed in the present material corresponds closely to the previously reported findings following the same type of trauma (LIU, LEWIS & LIM, SANDEGÅRD et coll) A similar observation was made by WRAY after experimental fractures However, it seems reasonable to assume that WRAY also produced soft tissue injury of a not unessential degree as fracture with a minimum of soft tissue injury (SANDEGÅRD & ZACHRISSON) did not cause this kind of flow increase in the soft tissues

Conclusion

Using repeated serial angiography relative changes of the blood flow may be demonstrated in the traumatized extremity as well as the local distribution of flow

Angiography also gives an appreciation of morphologic alterations following early after trauma, such as bleeding and discontinuities of vessels, and of functional disturbances The results obtained indicate that the soft tissue injury is decisive for the hemodynamic response to extremity trauma with or without injury to the bone

SUMMARY

The early circulatory changes following extensive soft tissue injury to the hind leg of the dog was examined by angiography and by measurement of blood flow by an electromagnetic flowmeter The trauma caused a marked increase of blood flow and vasodilatation in the injured extremity with or without combination of a fracture The later gradual increase of calculated vascular peripheral resistance was angiographically reflected by successively impaired flow in peripheral arteries In spite of the decrease of flow, the dilatation of the larger arteries persisted for several hours

ZUSAMMENFASSUNG

Die frühzeitigen zirkulatorischen Veränderungen nach einem umfassenden Weichteilschaden des Hinterbeines des Hundes wurden angiographisch und durch Messungen der Durchblutung mit einem elektromagnetischen Blutstrommeter untersucht Das Trauma rief einen markant erhöhten Blutstrom und eine Vasodilatation der geschädigten Extremität mit und ohne Kombination mit einer Fraktur hervor Der später nach und nach steigende, berechnete vaskuläre periphere Widerstand manifestierte sich angiographisch in einer successiv herabgesetzten Durchblutung der peripheren Arterien Trotz des herabgesetzten Blutstroms bestand die Dilatation der grösseren Arterien während einiger Stunden

RÉSUMÉ

Les modifications circulatoires precoces consécutives à un traumatisme étendu des parties molles de la patte postérieure du chien ont ete examinées par angiographie et par mesure avec un débit mètre électromagnétique du débit sanguin Le traumatisme a cause une augmentation marquée du débit sanguin et une vasodilatation du membre traumatisé aussi bien en présence qu'en l'absence d une fracture associée L'augmentation graduelle tardive de la résistance vasculaire périphérique calculée s'est traduite angiographiquement par une diminution secondaire du débit dans les artères périphériques Malgré la diminution du débit la dilatation des grosses artères a persisté pendant plusieurs heures

REFERENCES

ADLER S C, WEXLER L and CASTELLINO R. A Angiography of lower extremity soft-tissue arterio-venous fistulas J Canad Ass Radiol 23 (1972), 207

BLALOCK A and BRADBURN H Distribution of the blood in shock The oxygen content of venous blood from different localities in shock produced by hemorrhage, by histamine and by trauma Arch Surg 20 (1930), 26

BOIJSEN E DAHN I and HALLBÖÖK T Hemodynamic effect of contrast medium in arteriography of legs Acta radiol Diagnosis 11 (1971) 295
BRADHAM R R BUXTON J T and STALLWORTH J M Arterial injury of the lower extremity Surg Gynec Obstet 118 (1964) 995
BROYN T and BIE K. Peripheral arterial occlusion following traumatic intimal rupture Acta chir scand 131 (1966) 167
COLLINS H A and JACOBS J K Acute arterial injuries due to blunt trauma J Bone Jt Surg 43 A (1961) 193
DAHLBERG G Statistical methods for medical and biological students George Allen & Unwin London 1948
DELIUS W and ERIKSON U Effect of contrast medium on blood flow and blood pressure in lower extremities Amer J Roentgenol 107 (1969) 869
ERIKSON U Circulation in traumatic amputation stumps angiographical and physiological investigation Acta radiol (1965) Suppl No 238
FOISIE P S Traumatic arterial vasospasm New Engl J Med 237 (1947) 295
GELIN L E Studies in anemia of injury Acta chir scand (1956) Suppl No 210
GREITZ T A radiologic study of the brain circulation by rapid serial angiography of the carotid artery Acta radiol (1956) Suppl No 140
GUYTON A C GRANGER H J and TAYLOR A E Interstitial fluid pressure Physiol Rev 51 (1971) 527
HILAL S K Hemodynamic changes associated with the intra arterial injection of contrast media Radiology 86 (1966) 615
KINMONTH J B SIMEONE F A and PERLOW V Factors affecting the diameter of larger arteries w[illegible]
KJELLBERG S [illegible]
mitteln b[illegible]
KNISELY M [illegible]
scopic ot[illegible] blood flowing through vessels in crushed tissues Arch Surg 51 (1945) 220
LERICHE R The problem of osteo-articular diseases of vasomotor origin J Bone Jt Surg 10-B (1928) 492
LEWIS D H and KERSTEIN M D Trauma and sympathetic nerve stimulation in the dog. Europ surg Res 2 (1970) 12
— and LIM JR R C (a) Studies on the circulatory pathophysiology of trauma I Effect of acute soft tissue injury on nutritional and non nutritional shunt flow through the hind leg of the dog Acta orthop scand 41 (1970) 17
— — (b) Studies on the circulatory pathophysiology of trauma II Effect of acute soft tissue injury on the passage of macroaggregated albumin (^{131}I) particles through the hind leg of the dog Acta orthop scand 41 (1970) 37
— SANDEGÅRD J SEEMAN T and ZACHRISSON B E Effects of intraarterial injection of contrast medium on regional circulation in soft tissue trauma To be published in Acta radiol Diagnosis 16 (1975)
LIU C T Circulatory response to muscle trauma following denerva[illegible]
n dogs [illegible]
L[illegible]
M[illegible] NISSL R Zur Symptomatik der frischen Thrombose der tiefen Beinvenen Fortschr Rontgenstr 107 (1967) 262
MILLER M E CHRISTENSEN G C and EVANS H E Anatomy of the dog W B Saunders Company Philadelphia 1964

MORITZ A R The pathology of trauma Lea & Febiger, Philadelphia 1954
NILSON A E, JACOBSSON B, BERGENTZ S-E and WESTBERG G Angiography of the transplanted kidney Scand J Urol Nephrol 2 (1968), 46
NYLANDER G Phlebographic diagnosis of acute deep leg thrombosis Acta chir scand (1968) Suppl No 387, p 30
REMINGTON J W, HAMILTON W F, CADDELL H M, BOYD JR G H, WHEELER N C and PICKERING R W Vasoconstriction as a precipitating factor in traumatic shock in the dog Amer J Physiol 161 (1950), 125
RICH N M Vascular trauma Surg Clin N Amer 53 (1973), 1367
SANDEGÅRD J and ZACHRISSON B E *Circulatory disturbances after experimental fracture* Acta radiol Diagnosis 16 (1975) 181
— NOLTE J, LEWIS D H and SEEMAN T Early hemodynamic and biochemical changes *in soft tissue trauma* Europ surg Res 6 (1974), 233
SMITH R F, SZILAGY D E and PFEIFER J R Arterial trauma. Arch Surg 86 (1963), 825
WRAY J B Acute changes in femoral arterial blood flow after closed tibial fracture in dogs J Bone J Surg 46-A (1964), 1262

FROM THE DEPARTMENTS OF DIAGNOSTIC RADIOLOGY (DIRECTOR PROF G F SALTZMAN AND UROLOGY (DIRECTOR PROF L ANDERSSON), UNIVERSITY OF UMEÅ, S 901 85 UMEÅ, SWEDEN

ANGIOGRAPHY IN URINARY BLADDER TUBERCULOSIS

S O HIETALA and M DUCHEK

Angiography of tuberculosis of the urinary bladder has previously been restricted to isolated cases only one case was described by MARANTA et coll (1964) They demonstrated tortuous blood vessels in a locally thickened bladder wall No abnormality of the veins was reported LANG et coll (1966) reported 2 cases and stated that bladder tuberculosis appeared as a poorly vascularized area on angiography that could be diagnostic

NILSSON (1967) described 3 cases of bladder tuberculosis in which no evident angiographic signs existed distinguishing tuberculosis from cystitis of other genesis Common features of these 3 cases were relatively poor vascularization, slight contrast accumulation in the bladder wall and a shorter circulation time than usual Thus, the opinions as to the angiographic appearances and their diagnostic value differ and are partly contradictory This has prompted a further investigation of a larger and more uniformly examined material of tuberculosis of the urinary bladder and in addition to this, an evaluation of the possibility of utilizing angiography to differentiate tuberculous cystitis from cystitis of other aetiology as well as from tumours of the urinary bladder

Material

During the period extending from 1962 through 1973 846 pelvic angiographies were performed on the basis of different clinical indications, mainly neoplastic, in

Submitted for publication 27 September 1974

flammatory or vascular diseases of the pelvic organs Nine patients with microscopically and bacteriologically verified urinary bladder tuberculosis were extracted from this material Culture of the urine on Lowenstein-Jensen's medium plus guinea pig inoculations were performed routinely Microscopic sections were stained with haematoxylin-eosin and by the Ziehl-Neelsen method Three of these 9 cases were excluded due to technically incomplete angiography Thus, the material comprised 6 cases, briefly described in the following

Case 1 A 41-year-old male with symptoms of cystitis No serious disease or tuberculosis in family history Urography revealed a non-functioning right kidney and an expansive lesion on the right in the minor pelvis with displacement of the bladder to the left Rectal palpation disclosed a large, hard tumour encompassing the upper part of the right lobe of the prostate and the vesicle without clear demarcation superiorly A transperineal biopsy of the prostate was performed in order to eliminate cancer of the prostate A polypous tumour suggesting malignancy was demonstrated cystoscopically at the site of the right ureteral ostium A biopsy was performed, as well as angiography of the kidneys and bladder Microscopy of the excised material suggested tuberculosis In addition, positive results were obtained in a guinea-pig test A right sided nephrectomy was carried out 9 months later and microscopy of the specimen revealed advanced tuberculosis

Case 2 A 23-year-old male Family history of tuberculosis, pulmonary tuberculosis during pre school-age years Cystitis, unresponsive to conventional therapy, indicated cystoscopy which revealed extensive inflammatory changes with ulcerations in the bladder mucosa Microscopy of biopsy material as well as a Lowenstein Jensen culture and a guinea-pig test performed on urine revealed tuberculosis Bladder angiography was carried out to determine the extent of the tuberculous lesion in the pelvis

Case 3 A 52-year-old male Family history of tuberculosis The patient had previously had surgery for strangulation ileus and had been treated for cardiac incompensation Haematuria and bacteriuria prompted urography, which revealed a non-functioning left kidney with concretions that had the appearance of coral calculi The Lowenstein-Jensen culture and the guinea-pig test were both negative Radical treatment was not given because of the patient's heart disease He was admitted 11 years later with cardiac incompensation Macroscopic haematuria and raised serum creatinine values (4 5 and 8 mg/100 ml) were demonstrated at the same time At cystoscopy extensive inflammatory changes and an expansive lesion at the site of the ostium of the right ureter were demonstrated Cytology revealed inflammatory cells, and microscopy indicated tuberculosis of the bladder Bladder angiography was performed Subsequently, the Lowenstein Jensen culture and the guinea pig test were also positive.

Case 4 A 76-year-old male Right-sided hemiparesis after a crebral haemorrhage at the age of 60 A previous chest film showed healed tuberculous lesions Admitted with macroscopic haematuria and symptoms indicating hyperplasia of the prostate Received conservative treatment Cystoscopy revealed an ulceration suggesting malignancy to the left and posteriorly in the bladder Angiography of the bladder was performed Microscopy of a biopsy specimen did not reveal any malignancy A vasoresection and biopsy of an enlarged caput epididymidis on the left side were performed later Microscopy indicated tuberculosis and the diagnosis was confirmed by a bacteriologic examination of the urine

Case 5 A 57-year-old male Treated during his youth for right-sided nonspecific thoracic empyema Sought consultation in 1957 for right-sided renal colic No concretions could be demonstrated The same symptoms recurred 3 years later, at which time urography showed [illegible]

trocoagulation of recurrent papillomas was carried out on 2 different occasions Nine years after the first diagnosed papilloma a larger recurrent growth was discovered at the same site as before Urography revealed a non-functioning right kidney Angiography of the kidneys and bladder was performed Microscopy of excised biopsy material suggested tuberculosis. The diagnosis was later confirmed by a Lowenstein-Jensen culture and the guinea pig test

Case 6 A 53 year-old male No family history of tuberculosis Right-sided nephrectomy [illegible]

vesiculitis were diagnosed 19 years later Angiography of the left kidney of the bladder was performed

Angiography

After the conventional cleansing of the bowel and preoperative medication (Fenemal, phenobarbital, ACO), a catheter was introduced percutaneously into the femoral artery The position of the catheter was controlled using a small amount of contrast medium with the aid of an image intensifier and TV monitor The urinary bladder was emptied via an inserted catheter (5 3 mm) and filled slowly with carbon dioxide, as a rule 100 to 200 ml The catheter for the contrast medium was then connected to the syringe, either directly or, if 2 catheters were used, via a Y-joint The contrast medium (Urografin 60 %, diatrizoate, Schering) was injected with an automatic injector (Cisal II, Elema-Schönander) The injection time and exposure rate were recorded on a Mingograf 81 (Elema Schonander) An AOT film changer, 24 × 30 (Elema Schonander), was used The rate of exposure was 2 films per second during the first 4 seconds followed by one film per second for an additional 11 seconds

Non selective angiography with 2 catheters (3 examinations) The tip of each polythene catheters (PE 205) was passed up into the common iliac artery just above the origin of the internal iliac artery The amount of contrast medium was 50 ml The rate of injection was 15 to 20 ml per second using automatic injection

Selective angiography with 2 catheters (3 examinations) The catheterization was performed as described by NILSSON (1967) The amount of contrast medium on unilateral injection was 10 to 15 ml The rate of injection was 10 to 12 5 ml per second using automatic injection

The films were exposed with the patients supine An anterior-posterior series was first taken in all cases and then additional series in order to obtain a tangential projection on each side of the bladder wall



a



b



c



d

ous than usual

Evaluation of the films was made on the basis of the findings in a control series described previously (HASSLER & HIETALA 1973) In the arterial phase the number width and tortuosity of the arteries in the bladder wall and its immediate surroundings were assessed in the capillary phase the accumulation of contrast medium and the thickness and outer limit of the bladder wall The appearance of the veins was assessed and the circulation time determined An increase in the number of arteries was graded as moderate or marked The width of the arteries was measured at the



Fig 2 Case 4 a) Arterial phase b) capillary phase Wide and tortuous arteries (→) in the bladder wall in the arterial phase The wall (→) is well defined against the perivesical tissue and is moderately thickened—a maximum of 10 mm on the left side

widest extravesical point in the bladder artery that could be identified with certainty The width was considered to have increased if it was more than 1 5 mm The tortuosity, which refers to an increase in the length of the vessels, was estimated subjectively and increased tortuosity was graded as moderate or marked The presence of tortuous vessels of varying calibre was also recorded

In the capillary phase an increased accumulation of contrast medium in the bladder wall was graded as moderate or marked The thickness of the bladder wall was measured in the lateral convex part of the bladder If the thickness of the bladder wall ranged between 5 mm and 10 mm, this was considered as a moderate increase, as marked if the values exceeded 10 mm

The appearance of the veins was estimated subjectively in the same manner as described for the arteries The time from the filling of arteries to the filling of veins in the same bladder wall was called *the circulation* time It was considered as ordinary when it ranged between 7 and 12 seconds and as shorter than usual when under 7 seconds

Results

Arteries The number of arteries was moderately or markedly increased and they were wider than usual in most cases (Table) They exhibited increased tortuosity (*Figs 1 a b 2 a*) and in 2 cases tortuous vessels of varying calibre could be demonstrated on both sides of the bladder wall, in one of the cases also in a localized 3 cm 3 cm protrusion of soft tissue (Fig 1 a)

Or

Table 1

Angiographic findings in bladder tuberculosis

Case No	Number of arteries*	Width of arteries (mm)	Tortuosity*	Tortuous vessels of varying calibre	Accumulation of contrast medium	Thickness of bladder wall (mm)	Local protuberant mass	Veins**	Circulation time (s)
1	+	2	n	0	0	—	0	—	—
2	+ +	2	+	0	0	5–10	0	n	5 5
3	+ +	3	+	+	+	12–15	+	+	5 5
4	+ +	2	+ +	+	0	20–25	0	+	8 0
5	+	1	+	0	0	10–25	0	n	9 5
6	+	1	+	0	0	—	0	n	9 0

* n = ordinary
+ = moderate increase
+ + = marked increase
** n = ordinary venous appearance
+ = moderately widened and tortuous veins

(Fig 1 c) as well as the bladder wall itself accumulated slightly more contrast medium than the perivesical tissues

Thickness of the bladder wall It was not possible to outline the bladder wall in 2 cases (Nos 1 and 6) In one of these (No 1) also other angiographic abnormalities were slight In the other case (No 6) a Coffey type ureterostomy had been carried out and the bladder wall was partly concealed by contrast medium in the bowel In one case (No 2) the bladder wall was moderately thickened and could be well defined against the perivesical tissue (Fig 2 b) In the remaining 3 cases the bladder wall was moderately thickened and also evidently irregular Its outer limits were diffuse and it was not always possible clearly to define the bladder wall against the perivesical tissue (Fig 1 d)

Veins The venous abnormalities were generally slight In 2 cases (Nos 3 and 4) widened and tortuous veins appeared locally in the bladder wall (Fig 1 d) The concentration of contrast medium in the veins was low and in one case (No 1) the veins were not visible in the bladder wall, and consequently the circulation time could not be determined In 2 of the remaining 5 cases the circulation time was shorter than usual

Discussion

It is evident that the angiographic appearances of bladder tuberculosis in the present material were non-specific and similar to those described previously (Nilsson 1967, Hassler & Hietala 1973) in cystitis of other aetiology Thus, in the present

material it was generally possible to demonstrate hypervascularization with decidedly widened and tortuous arteries in the bladder wall This observation does not agree with the poor vascularization reported by MARANTA et coll (1964), LANG et coll (1966) and NILSSON (1967) It is probable that the different angiographic appearances only reflect different stages of activity of the tuberculous process Thus, in one of the present cases with microscopically advanced fibrosis of the bladder with contraction, only a moderate increase in the number of arteries was demonstrated

Tortuous vessels of varying calibre occurred locally in the thickened bladder wall In part these vessels had the same appearance as described in tumours of the urinary bladder In the patient with soft tissue protrusions into the bladder simultaneously with tortuous vessels of varying calibre, it would not have been possible to differentiate angiographically between a tuberculous infection and tumour of the bladder This is in accordance with previous observations (HASSLER & HIETALA) that angiographic differentiation between tumours, post irradiation conditions and non-specific bacterial cystitis, is not possible

Accumulation of the contrast medium in the capillary phase was slight even in the cases with localized thickenings of the bladder wall or soft tissue protrusions and did not deviate from those previously described (NILSSON) They were not pathognomonic of tuberculosis NILSSON considered the circulation time to be shorter than usual in tuberculosis of the urinary bladder However, in the present material the circulation time was more often of ordinary length, and the veins were not changed at all or only slightly Thus no conclusive findings were noted in the venous phase

Acknowledgement

The bacteriologic examinations were performed at the Institute of Bacteriology and the microscopic examinations at the Department of Pathology, University of Umeå

SUMMARY

tu
cu ... demonstrated in the ...
abnormalities were observed The circulation
giographic appearances were non specific An...
between tuberculous cystitis cystitis of other g...

ZUSAMMENFASSUNG

Angiographie wurde in 6 Fallen bakteriologisch und mikroskop...
kulose der Harnblase ...
kularisation d...

jedoch keine venosen Abnormalitaten zu beobachten Das angiographische Bild war somit nicht spezifisch Angiographisch ist es unmoglich, zwischen einer tuberkulosen Cystitis einer Cystitis anderer Genese oder auch einem Tumor der Blase zu unterscheiden

RÉSUMÉ

Une angiographie a été faite dans 6 cas de tuberculose de la vessie vérifiee bactériologiquement et microscopiquement Dans la majorité des cas on a pu mettre en évidence une hypervascularisation marquée, genérale ou localisee, dans la paroi vésicale à la phase artérielle mais on n'a pas observé d'anomalies veineuses Le temps de circulation n'est habituellement pas modifié Les aspects angiographiques ne sont donc pas spécifiques Angiographiquement il est impossible de faire la différence entre une cystite tuberculeuse, une cystite d'autre origine ou même une tumeur de la vessie

REFERENCES

Hassler O and Hietala S O Angiographic abnormalities in the urinary bladder wall after irradiation Part I Animal experiments Part II Clinical investigation Acta radiol (1973) Suppl No 328

Lang E K, Nourse M H, Wishard W N Jr and Mertz J H O The accuracy of preoperative staging of bladder tumors by arteriography A 5-year study J Urol 95 (1966), 363

Maranta E, Camponovo F und Del Buono M S Die Beckenangiographie Fortschr Rontgenstr 101 (1964), 229

Nilsson J Angiography in tumours of the urinary bladder Acta radiol (1967) Suppl No 263

FROM THE DEPARTMENT OF DIAGNOSTIC RADIOLOGY, UNIVERSITY HOSPITAL, INSELSPITAL, BERNE, SWITZERLAND

LYMPHOGRAPHY AS A GUIDE TO PROGNOSIS IN MALIGNANT TESTICULAR TUMOURS

W. A FUCHS and M GIROD

Lymphography has become a routine procedure in patients with malignant neoplasms of the testes Several authors have reported their findings and experience concerning the diagnostic accuracy of the method and its clinical indications The possible implications of the lymphographic results on the prognostic outlook of this malignant disease have, however, not yet been widely discussed

Material and Methods

The material consists of 130 patients with malignant neoplasms of the testes, aged 16 to 71 years (mean 34 years) and investigated between 1963 and 1972 The histologic classification was done according to DIXON & MOORE (1953) into germinal tumours (seminoma, teratocarcinoma, teratoma, embryonal carcinoma, choriocarcinoma) and non germinal tumours All patients were subjected to lymphography and inferior cavography, urography was added in about half of the cases

Evaluation of the lymphography was done according to strict diagnostic criteria A positive diagnosis was made only when solitary or multiple well demarcated filling defects of at least 10 mm diameter obliterating the marginal and intermediary sinuses in regional lymph nodes were present (Fig 1) Additional obstruction of the lymphatic

Submitted for publication 10 July 1974



Fig 1 Seminoma (patient aged 43) Large confluent well demarcated filling defects Displacement of remaining lymphatic tissue due to metastases in the left aortic lymph nodes

circulation was the other significant finding indicating malignant neoplastic involvement of the lymphatic system (Fig 2)

The first diagnostic and therapeutic measure consisted in all patients of a radical orchidectomy with extensive resection of the spermatic duct and hemiscrotectomy The irradiation technique applied was as follows Seminoma without metastatic spread to the regional lymph nodes was treated with 4 000 to 4 500 rad The portal fields included the entire regional lymphatic circulation reaching from the spermatic duct to the supraclavicular area on the side of the terminal portion of the thoracic duct In the presence of metastatic lymph node involvement the dosage was increased to 5 000 rad In embryonal carcinoma the radiation dosage was 5 000 to 5 500 rad, in teratocarcinoma 4 500 to 5 000 rad In cases of choriocarcinoma 4 500 rad was administered in addition to chemotherapy

Chemotherapy was used in nearly all cases presenting lymph node metastases as well as in a few patients with a normal lymphography Therapy programs consisting of a combination of several drugs (Vinblastine, Chlorambucil, N-Methyl-Aminopterin, Actinomycin D, Chlorambucil, N-Methyl-Aminopterin, Mithramycin, Vinblastine, Cyclophosphamide, Bleomycin, Natulan) were given and continued as long as a remission of the tumour growth was observed In case of recurrence a new combination of drugs was administered (BRUNNER 1970)

Retroperitoneal lymphadenectomy was done on 10 patients (2 seminoma, 4 embryonal carcinoma, 3 teratocarcinoma, 1 choriocarcinoma) Pulmonary metastases were excised in 2 cases

The actuarial method of BERKSON & GAGE (1950) was used to evaluate the survival rates

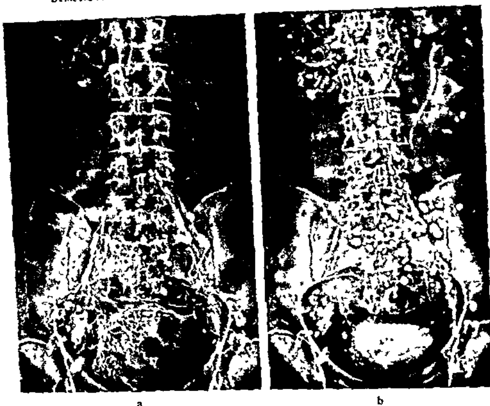


Fig 2 Teratocarcinoma (patient aged 43) Extensive metastatic involvement of the aortic and common iliac lymph nodes Obstruction of the lymphatic circulation Collaterals in the pelvic area Displacement of remaining lymphatic tissue of aortic lymph nodes a) Filling, b) storage phase

Results

The grouping of the 130 patients investigated according to the microscopic findings and the [illegible] (41 5 [illegible] Meta [illegible] present in 26 per cent of the 65 seminomas, in 42 per cent of the 26 teratocarcinomas, in 61 per cent of the embryonal carcinomas and in 6 of the 7 choriocarcinoma patients

The metastatic spread was confined in 76 per cent to the aortic lymph nodes and in 16 per cent to the aortic and iliac lymph nodes In 4 cases metastases to the supraclavicular lymph nodes and in 1 case to the mediastinal lymph nodes were detected at lymphography In 4 cases the positive lymphographic diagnosis was substantially supported by positive findings at cavography Pulmonary metastases were initially present in 16 cases, liver metastases in 1 case

The survival rates for the different groups of patients are graphically demonstrated in Figs 3 to 5

Table

	Total	Lymphography	
		Neg	Pos
Seminoma	65	47	18 (28 %)
Teratocarcinoma	26	15	11 (42 %)
Embryonal carcinoma	23	9	14 (61 %)
Choriocarcinoma	7	1	6
Teratoma	2	1	1
Non germinal tumours	6	2	4
Undefinable necrotic neoplasm	1	1	—
Total	130	76	54 (41 5 %)

In 65 patients with seminoma the 2-year survival rate was 97 per cent, the 5 year *survival rate 94 per cent for the 47 cases with negative lymphography For the 18 patients with pathologic lymphography, the 2-year and 5-year survival rates were* 87 and 69 per cent, respectively (Fig 3) In embryonal carcinoma (n = 23) the survival rate of patients with negative lymphography (n = 9) was for 2 years 78 and for 5 years *64 % Patients with positive lymphography (n = 14) had a 2-year survival rate of* 33 per cent and a 5-year survival rate of 33 per cent (Fig 4) In teratocarcinoma (n = 26) the 2-year survival rate was 86 per cent, the 5-year survival rate 86 per cent in the *15 patients with negative lymphography In 11 patients with pathologic lymphography,* the 2-year survival rate was 28 per cent, the 5 year survival rate 14 per cent (Fig 5) Of the 7 patients with choriocarcinoma only 2 lived for more than 2 years

Discussion

The results presented indicate that lymphography may provide a more differentiated prognostic outlook in the different histologic subdivisions of malignant testicular tumours The overall 5-year survival rate of testicular neoplasms is about 60 per cent (PATTON et coll 1969) It varies inversely as the metastases rate increases (DIXON & MOORE, COX 1954, NOTTER & RANUDD 1964, WINDEYER & DISCHE 1971) Furthermore, the prognosis of testicular neoplasms is also largely dependent on their histologic differentiation Consequently, a subdivision of the case material according to tumour histology and lymphographic findings is necessary The overall survival rate of 86 per cent in the 65 patients with seminoma compares favourably with the results of other series (PATTON et coll , DIXON & MOORE) The difference of about 25 per cent in the 5-year survival rate in patients with seminoma according to the negative or positive lymphographic findings is of particular interest This applies also to the high 5-year survival rate of 94 per cent in patients with negative lymphography This differentiation is even more marked in the more malignant histologic subdivisions

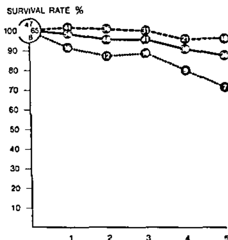


Fig 3

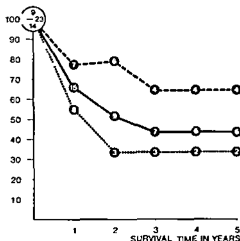


Fig 4

Fig 3 Survival rates in 65 patients with seminoma Normal lymphography 47 cases 2 year survival rate 97% 5 year survival rate 94% pathologic lymphography 18 cases 2 year survival rate 87%, 5 year survival rate 69% Figures indicate number of patients alive Total number of cases (——), negative lymphography (--) positive lymphography ( )

Fig 4
year
vival
of ca

In embryonal carcinoma the 5-year survival rate is double (64%) in cases with normal lymphography, compared to those with positive findings (33%), the 5 year overall survival rate of 45 per cent being slightly higher than that of 35 5 per cent in the series of DIXON & MOORE The greatest difference is encountered in the cases with teratocarcinoma, where the 5 year survival rate in cases with negative lymphography (86%) is six times higher than for those with positive lymphography (14%) FRIEDMAN (1966) achieved similar high survival rates of 77 per cent in 18 cases of embryonal carcinoma and teratocarcinoma without lymph node metastases These considerable differences of the survival rates reflect the different degrees of malignancy of the various microscopic tumour groups When considering the case of an individual patient it is important to realize the favourable 5 year survival rate of 94 per cent of the seminoma group with negative lymphography and of 86 per cent in cases of teratocarcinoma with negative lymphography The very low 5-year survival rate of 14 per cent in cases of teratocarcinoma with pathologic lymphography and of 33 per cent in cases of embryonal carcinoma with lymph node metastases strongly indicates the urgent need for more efficient chemotherapy in these groups

Surgical removal of the retroperitoneal lymph nodes seems to be of great importance in cases of embryonal carcinoma and teratocarcinoma with a 5 year survival rate of 64 and 86 per cent, respectively The prognostic outlook may still be substantially

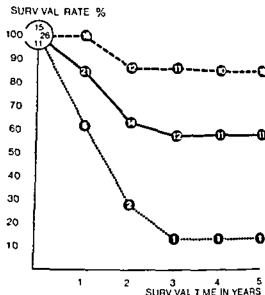


Fig 5 Survival rates in 26 patients with teratocarcinoma Normal lymphography 15 cases 2 year survival rate 86 %, 5 year survival rate 86 %, pathologic lymphography 11 cases 2-year survival rate 28 %, 5 year survival rate 14 % Figures indicate number of patients alive Total number of cases (——), negative lymphography (---), positive lymphography ( )

improved in these groups by this measure Lymphadenectomy is also indicated in cases with not too extensive unilateral malignant involvement of the regional aortic lymph nodes Preoperative irradiation seems to be of particular importance in these cases (NOTTER & RANUDD, PATTON et coll, SMITHERS & WALLACE 1962, THOMPSON et coll 1961)

The small differences between the 2-year and 5-year survival rates observed in our case material have also been reported by other working groups (DIXON & MOORE, PUGH 1962, KUROHARA et coll 1967, NOTTER & RANUDD)

The clinical value of lymphography depends upon the accuracy of its results The application of strict diagnostic criteria guarantees an accuracy rate of 85 to 90 per cent as has been demonstrated in carcinoma of the uterine cervix (FUCHS & BÖÖK-HEDERSTRÖM 1964, FUCHS & SEILER-ROSENBERG 1975) Solitary or multiple well demarcated filling defects of at least 10 mm diameter are diagnostic when obliteration of the intermediary and marginal sinuses is present Obliteration and collateral circulation are definite signs of malignant lymphatic obstruction Displacement of lymphatics and lymph nodes within the aortic area must be regarded as an indirect sign of malignant infiltration However, arteriosclerotic elongation of the abdominal aorta may lead to displacement of the lymphatic system Cavography is a compulsory investigation because the right aortic lymph node chain is demonstrated by lymphography in 40 per cent up to or below the level of L3, in 20 per cent up to L2, and only in 11 per cent as high as L1 The number of right aortic lymph nodes contrast filled by lymphography is considerably smaller than that of the two other aortic node chains (FUCHS 1969) This is in contrast to anatomic findings, which reveal the right aortic lymph node group comprising the greatest number of nodes Applying these strict diagnostic criteria, the rate of false positive diagnoses is minimal The therapist

can therefore, rely on a positive lymphography and select the appropriate therapeutic means Small malignant metastatic foci are, however, difficult to detect, because of the restricted resolution of the macroscopic method of lymphography and the great variation of lymph nodes Furthermore, some of the laterally situated regional aortic lymph nodes are not outlined by foot lymphography A negative lymphography, therefore, does not exclude malignant metastatic deposits in the regional lymph nodes of the testis This fact has to be considered when determining therapeutic options However, absence of pathologic lymphographic findings does exclude advanced malignant disease

Acknowledgements

The co-operation of the Departments of Therapeutic Radiology (Prof A Zuppinger), Urology (Prof E Zingg) and Pathology (Prof H Cottier) as well as the Division of Chemotherapy (Prof K W Brunner) is gratefully acknowledged

SUMMARY

Lymphography was performed in 130 patients with malignant neoplasm of the testes The patients were treated by irradiation supplemented by chemotherapy when lymph node metastases were present The survival rates of the various pathologic subdivisions were analyzed according to the lymphography The following 5 year survival rates were observed seminoma normal lymphography 94% pathologic lymphography 69%, teratocarcinoma normal lymphography 86% pathologic lymphography 14%, embryonal carcinoma normal lymphography 64%, pathologic lymphography 33%

ZUSAMMENFASSUNG

Eine Lymphographie wurde bei 130 Patienten mit einem malignen Neoplasma der Hoden vorgenommen Die Patienten wurden strahlenbehandelt, unterstutzt durch Chemothera pie wenn Lymphknotenmetastasen vorhanden waren Die Überlebensraten der verschie denen pathologischen Untergruppen wurden entsprechend der Lymphographie analy siert Die folgenden 5 Jahres Überlebensraten wurden beobachtet Seminom normale Lymphographie 94% pathologische Lymphographie 69%, Teratokarzinom normale Lymphographie 86% pathologische Lymphograpie 14%, Embryonales Karzinom normale Lymphographie 64% pathologische Lymphographie 33%

RÉSUMÉ

Les auteurs ont fait une lymphographie chez 130 malades [illegible]
testicule [illegible]
y avait d[illegible]
divisions [illegible]
les taux d [illegible]

pathologique 69 %, térato-carcinome lymphographie normale 86 %, lymphographie pathologique 14 %, carcinome embryonnaire lymphographie normale 64 %, lymphographie pathologique 33 %

REFERENCES

BERKSON J and GAGE R P Calculation of survival rates for cancer Proc Mayo Clin 25 (1950), 270

BRUNNER K W Prognose, Verlauf und Therapie metastasierender Hodentumoren Schweiz med Wschr 100 (1970), 1359

COX R Radiotherapy in malignant diseases of testicle and penis Brit J Urol 26 (1954) 350

DIXON F J and MOORE R A Testicular tumors A clinical pathological study Cancer 5 (1953), 427

FRIEDMAN M Testis *In* Textbook of radiotherapy Edited by G H Fletcher Lea & Febiger, Philadelphia 1966

FUCHS W A Normal anatomy *In* Lymphography of cancer Edited by W A Fuchs J W Davidson and H W Fischer Recent results in cancer research Vol 23 Springer, Berlin/Heidelberg/New York 1969

— and BOOK-HEDERSTRÖM G Lymphography in the diagnosis of metastases with special reference to the carcinoma of the uterine cervix Acta radiol diagnosis *2 (1964), 161*

— and SEILER ROSENBERG G Lymphography in carcinoma of the uterine cervix Acta radiol Diagnosis (in print)

KUROHARA S S, GEORGE F W III, DYKHUISEN R F and LEARY K L Testicular tumors Analysis of 196 cases treated at the U S Naval Hospital in San Diego Cancer 20 (1967) 1089

NOTTER G and RANUDD N E Treatment of malignant testicular tumors Report on 355 patients Acta radiol Ther Phys Biol 2 (1964), 273

PATTON J F, HEWITT C B and MALLIS N Diagnosis and treatment of tumors of testis J Amer med Ass 171 (1969), 2194

PUGH R C B Tumours of the testes Some pathological considerations Brit J Urol 34 (1962), 393

SMITHERS D W and WALLACE E N K Radiotherapy in the treatment of patients with seminomas and teratomas of the testicle Brit J Urol 34 (1962), 422

THOMPSON I M, WEAR J JR, ALMOND C, SCHEWE E J and SALA J An analytical survey of one hundred and seventy-eight testicular tumors J Urol (Baltimore) 85 (1961), 173

WINDEYER B and DISCHE S *Tumours of the male genital tract In* Encyclopedia of medical radiology Vol 14/III Springer, Berlin/Heidelberg/New York 1971

FROM THE DEPARTMENT OF MEDICAL STATISTICS AND EPIDEMIOLOGY, LONDON SCHOOL OF HYGIENE AND TROPICAL MEDICINE, LONDON, ENGLAND

RADIOLOGIC HEART VOLUME FROM 100 MM PHOTOFLUOROGRAMS

DAVID CHRISTIE

The ellipsoid approximation technique of estimating radiologic heart volume (JONSELL 1939), is widely used as part of routine clinical practice in Scandinavia. Considerable experience has been reported with standard chest radiography where the subject has had a barium swallow, less well documented is the use of miniature radiography.

This report examines the practicability of radiologic heart volume estimation from 100 mm photofluorograms taken under the circumstances of mass radiography, with unmodified apparatus and no special subject preparation.

Methods

In the [illegible] se[illegible] of [illegible] sample of these pairs of films resulted in 1 263 subjects in whom an attempt was made to calculate radiologic heart volume. The films were taken throughout by a single radiographer using a standard ODELCA-100-X111 S photofluorographic camera.

For estimation of radiologic heart volume by the ellipsoid approximation tech-

Submitted for publication 30 January 1974

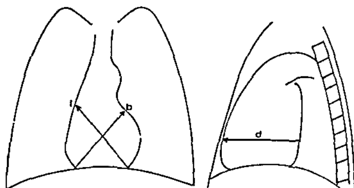


Fig 1 The long (l), broad (b) and horizontal (d) axes of the heart

nique, the following three measurements on the p a and lateral films are required (JONSELL 1939, Fig 1)

Long axis (l) The distance in mm between the left cardiophrenic junction and the junction of the right heart border with the great vessels

Broad axis (b) The distance between the junction of pulmonary conus with left heart border, and the right cardiophrenic junction

Horizontal axis (d) The greatest distance between anterior and posterior cardiac borders, on the lateral film

The formula used is as follows

$$\text{Radiologic heart volume (ml)} = l \times b \times d \left(\frac{\pi}{6} 46.52\right) \Big/ 1\,000$$

were $\pi/6$ is a constant, and 46.52 a constant to correct for magnification and subsequent reduction in size of the cardiac image (appendix), l, b and d are the long, broad and horizontal axes measured in mm

Each film was viewed on a WATSON back-illuminated 100 mm viewing box, through a 12.7 cm magnifying glass Initially it was thought that measurements could be made with a simple ruler, but it quickly became apparent that parallax error would be serious The solution adopted was to imprint upon a thin, clear, rigid sheet of plastic slightly larger than the miniature film, a centre line and several scales graduated in half-millimetres The plastic sheet could easily be moved over the surface of the film, the layout of the scales being determined by trial and error as the most appropriate

Of the 1 263 subjects, a heart volume could be computed in 1 188 (94 %) 54 subjects were rejected because of technical inadequacy of the lateral films, and a further 21 subjects because of extensive post tubercular scarring, gross kyphoscoliosis, thoracoplasty or evidence of other thoracic surgery

The optical system and correction factor For comparability of different investigations, a correction for magnification of the cardiac image is needed, in miniature radiography the situation is complicated by subsequent reduction in image size In estimations of radiologic heart volume where standard units are used, often for a given tube-film distance (1.5 M both directions), a constant correction factor of 0.42

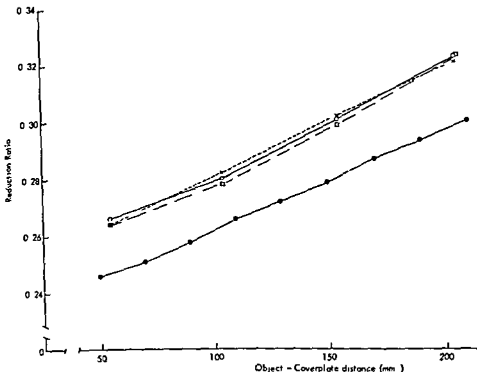


Fig 2 Reduction ratios of Odelca cameras, London and Finland, at varying object-coverplate distances The three upper curves represent three different distances within the central area of the phantom The bottom curve is from the Touru Kaisila series

is assumed (JONSELL 1939, HUMERFELDT 1963, TIBBLIN 1967) With regard to miniature radiography, TOURU KAISILA (1970) in a meticulous evaluation of the physical characteristics of Odelca cameras showed that there was marked individual variation between the optical systems of different cameras

In order that a correction factor could be calculated for the present camera, a 'phantom' was constructed This consisted of a sheet of 3 5 mm perspex measuring 43 cm 35 cm, with 3 mm diameter lead shot fixed to the surface in rows and columns exactly 2 54 cm apart With the plane of the phantom parallel to the camera coverplate, a series of films were taken at varying object-coverplate distances

The reduction ratio is the ratio of the length of an object as measured on the film (Xr) to the true length of the object (Xo) This ratio varies with the object-coverplate distance, and in Fig 2 the reduction ratio at each of four experimental object-coverplate distances is given For comparison, the reduction ratios reported by TOURU-KAISILA on a similar camera, are given These two Odelca units, one in Finland and one in London, show parallel linear change of reduction ratio with varying object-

Table

Estimates of observer variability in chest film measurements

Measurement	Mean (mm)	Variance* $\frac{E(X_1-X_2)^2}{2n}$	95 % confidence limits of single measurements	Coefficient of variation
Long axis (l)	38 86	2 182	±2 89 mm	3 8 %
Broad axis (b)	31 94	0 765	±1 72 mm	2 7 %
Horizontal axis (d)	32 54	2 340	±3 00 mm	4 7 %

* Variance of a single measurement

coverplate distances The individuality of the optical systems is evident by the difference in height of the two lines

The conclusion is drawn that correction factors vary between Odelca cameras and should be calculated for each machine The method of calculation used in the present investigation is described in the Appendix

Observer variability The observer variation inevitable with measurements made on chest films, is likely to be proportionately greater with 100 mm films than with standard size films An assessment of method error is thus an integral part of an assessment of the worth of radiologic heart volume estimation from miniature films

The long, broad and horizontal axes were measured on the first 200 pairs of films in the sample and the measurements repeated 3 weeks later after thorough mixing of the films The variance of a single measurement can be estimated from the formula

$$V(x) = \frac{E(x_1 - x_2)^2}{2n}$$

Where x_1 and x_2 are replicate measurements The variance, confidence limits of a single measurement, and coefficient of variation (standard deviation as a percentage of the mean) are set out in the Table

In a comparable investigation using miniature films, LINDGREN & ODEN (1954) reported a 1 to 2 % variation in diameter measurement These results were from a department specialising in the technique and dealt with a relatively small number of selected subjects, great care was taken over subject positioning, and all cases had a barium swallow It is likely that the observer variation of 3 to 5 % in diameter measurements found in the present report is a realistic assessment of the situation which holds in large scale surveys

'*Normal values* Initial inspection of the distribution of radiologic heart volumes revealed a solitary value of 2 500 ml, that is almost three times the mean and 500

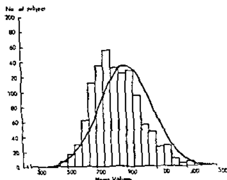


Fig. 3. Distribution of radiologic heart volume in 1 187 male subjects over age 40.

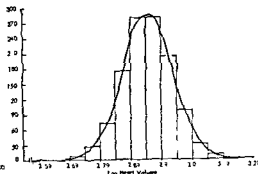


Fig. 4. Distribution of log. radiologic heart volume in 1 187 male subjects over age 40.

ml greater than the next highest recording. On reviewing this pair of films, an exceptionally large heart was present with the unmistakable contours of valvular heart disease. With exclusion of this subject, Fig. 3 gives the distribution of radiologic heart volume in a free living male population over the age of 40, unselected on any medical grounds. Mean heart volume was 898.8 ml with standard deviation of 175.4 ml. The positive skew is apparent and with logarithmic transformation of the data the distribution becomes 'bell shaped' (Fig. 4).

The usual practice in the Scandinavian literature is to adjust heart volume for body size by reporting results in terms of ml/m² body surface area, the resulting value being generally termed 'Relative heart volume'. Body surface area is calculated from height and weight according to the formula of DUBOIS (1927).

$$\text{Area (sq. metres)} = \frac{W^{0.425} \times H^{0.725} \times 71.84}{10^4}$$

Where W is weight in kg and H is height in cm. Relative heart volume was calculated for each case: the distribution had a positive skew, the mean being 464.5 ml/m², standard deviation 78.7 ml/m².

DISCUSSION

The principle that a reasonable approximation to the volume of the heart can be made from simple measurements on the chest film was first presented by ROHRER (1916). The technique was made a *practical* proposition by a group of workers at Serafimerlasarettet, Stockholm (JONSELL 1939) and is part of Scandinavian clinical practice. That the volume estimate from a p.a. and lateral film corresponds to anatomic heart size has been shown by several authors (FRIEDMAN 1951, EVANS & CARPENTER 1965). Little work has been done using miniature radiography, but TOURU KAISILA (1970) demonstrated that volume estimates of different plastic heart

ZUSAMMENFASSUNG

Es wurde das Herzvolumen bei 1 188 (94%) einer Gruppe von 1 263 zivilen mehr als 40 Jahre alten Bediensteten röntgenologisch berechnet Die Brust Filme wurden unter Bedingungen der Massen-Kleinbild Röntgenuntersuchung ohne eine individuelle Vorbereitung und mit einer nichtmodifizierten Odelca 100 mm Einheit gemacht Es wird über die Variabilität der Untersucher berichtet und 'Normalwerte' einer frei-lebenden Population gegeben Es wird eine Methode zur Berechnung eines Korrektionsfaktors für die Bildvergrösserung und die nachfolgende Verminderung in der Grösse beschrieben, und ein Anhalt dafür gegeben, dass jede Odelca Einheit einen individuellen Korrektionsfaktor aufweist

RÉSUMÉ

Le volume radiologique du coeur a pu être calculé sur 1 188 (94%) d'un échantillon de 1 263 fonctionnaires hommes âgés de plus de 40 ans Les radiographies thoraciques ont été prises dans les conditions de radiophotographie systématique sans préparation du sujet et au moyen d'une caméra Odelca 100 mm non modifiée Les auteurs présentent une estimation de la variabilité des résultats en fonction de l'observateur et donnent les 'valeurs normales' pour une population ordinaire Les auteurs décrivent une méthode de calcul d'un facteur de correction pour l'agrandissement d'image et pour la réduction ultérieure et fournissent la preuve que chaque caméra Odelca a un facteur de correction unique

REFERENCES

BJERKELUND C J The effect of long-term treatment with dicoumarol in myocardial infarction Acta med scand (1957) Suppl No 30

DUBOIS E I Basal metabolism in health and disease 2nd Ed Lea & Febiger, Philadelphia 1927

EVANS D W and CARPENTER P B Error involved in radiological heart volume determination by the ellipsoid approximation technique Brit Heart J 27 (1965), 429

FRIEDMAN C E Heart volume, myocardial volume and total capacity of the heart cavities in certain chronic diseases Acta med scand (1951) Suppl No 257

HUMERFELDT S An epidemiological study of high blood pressure Universitetsforlaget Bergen-Oslo 1963

JONSELL S A method for the determination of the heart size by teleroentgenography Acta radiol 20 (1939), 325

LINDGREN G and ODÉN S Heart volume determination in microfilms Acta radiol 42 (1954), 374

REID D D, BRETT G Z, HAMILTON P J S, JARRETT R J, KEEN H and ROSE G Cardiorespiratory disease among middle aged male civil servants Lancet 1 (1974) 469

ROHRER F Volumbestimmung von Körperhöhlen und Organen auf Orthodiagraphischem Wege Fortschr Röntgenstr 24 (1916/17), 285

TIBBLIN G High blood pressure in men aged 50—a population study of men born around 1913 Acta med scand (1967) Suppl No 470

TOURU KAISILA K Heart size determination by photofluorography Acta radiol (1970) Suppl No 295

WARIS E. K, SIITONEN L and HIMANKA E Prognosis in myocardial infarction Amer Heart J 71 (1966), 187.

ACTA RADIOLOGICA

OFFICIAL ORGAN OF THE RADIOLOGICAL SOCIETIES OF
DENMARK, FINLAND NORWAY AND SWEDEN

Vol 16	DIAGNOSIS	1975
Fasc 4		July

MYELOGRAPHY IN METASTATIC LESIONS

A HATAM, T HINDMARSH and T. GREITZ

Metastatic lesions affecting the spinal cord are generally thought to be almost exclusively extradural in their location These tumours are usually said to produce an indentation in the subarachnoid space which becomes progressively tapered towards the largest part of the tumour (Fig 1 a) LINDGREN (1954) pointed out that metastases may have varying myelographic appearances and may be difficult to distinguish from other types of tumours According to TAVERAS & WOOD (1964) the subarachnoid space may be abruptly collapsed without tapering as a result of angulation of the dural sac by a tumour, they claimed that tumours producing such changes may be intradural as well as extradural Furthermore, they state that metastatic carcinoma as a rule remains outside of the dural sac This would imply that an abrupt compression of the dura by the tumour is unusual However, in our experience this kind of myelographic appearance, suggesting intradural extension of the tumour, is not rare, in particular this is the case when the tumour appears to encircle the cord in a cuff-like fashion (Fig 1 b, c) which should correspond to the 'angulation of the dural sac' as described by TAVERAS & WOOD Hence, it was considered of interest to analyse the myelographic findings and correlate them to the

From the Department of Neuroradiology, Karolinska sjukhuset, S 104 01 Stockholm, Sweden
Submitted for publication 2 January 1974

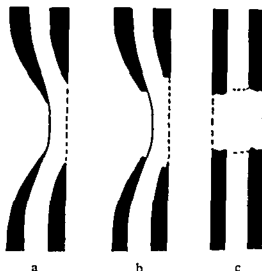


Fig 1 Schematic drawings of myelographic appearances with metastatic lesions a) Conventional concept of extradural lesion, b) and c) suggest intradural growth

findings at surgery in order to find out whether the mode of growth of the tumour could be defined by myelographic examination The possibility to establish an intradural extension of the tumour would be of clinical importance because the presence of a compression of the cord within the dura would reduce the effect of a simple laminectomy and possibly necessitate a removal of the intradural tumour On the other hand, as pointed out by TAVERAS & WOOD, a correct diagnosis may prevent unnecessary, extensive exploration, opening of the dura and trauma to the spinal cord

Material and Methods The material includes 52 patients with metastatic lesions admitted during the period 1963–1971 examined with gas myelography Only cases *in which the diagnosis was confirmed by operation or cases with an identified primary* malignant tumour were included in the material In order to evaluate technical factors influencing the myelographic appearance of metastases, 5 patients recently examined not only with gas myelography but also with a water-soluble contrast medium, Metrizamide, were included Hence, the total series consists of 57 patients examined with gas myelography The age of the patients ranged from 14 months to 79 years, with a mean of 56 years Ten patients were examined by gas myelography following suboccipital puncture according to the method of LINDGREN (1939) and 36 patients following lumbar puncture according to the technique of WESTBERG (1966) In 11 cases both suboccipital and lumbar puncture were used, these 11 patients and 23 additional patients had a complete block and 15 had a partial block to the passage of gas For various reasons films were not available in the antero posterior projection in 12 cases The account of the results and the discussion are in the following based only on the examinations of these 45 cases in which complete examination in the lateral as well as in the antero-posterior projection had been made, if not otherwise stated

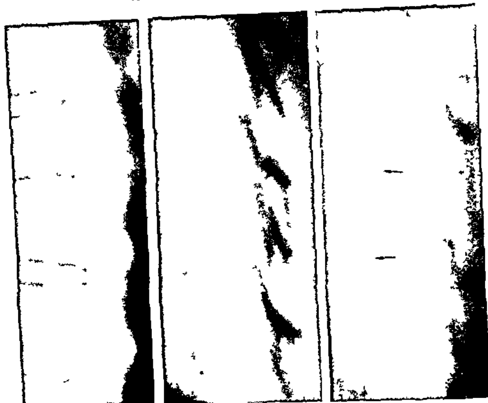


Fig 2 Fig 3a Fig 3b

Fig 2. Hand Schuller Christian disease Typical appearance of extradural lesion extending over five vertebral segments Tapering of the subarachnoid space at its upper and lower ends Spinal cord ( ) No bone destruction

Results

In addition to the generally recognized appearance with extradural tumours (Fig 1 a) an abrupt indentation of the subarachnoid space adjacent to the tumour (Fig 1 b) was also observed This latter finding proved to be consistent with purely extradural growth in several cases Such changes also occurred in one additional case of proven intradural metastasis Because these appearances bore a certain resemblance to those encountered in intradural extramedullary tumours they were classified as 'juxtamedullary' Sometimes the appearance of a lesion was different at the upper and the lower end of the tumour, being characteristic of an extradural lesion at one end and of a juxtamedullary lesion at the other In a few cases the impression in one projection of an extradural lesion was combined—in the other

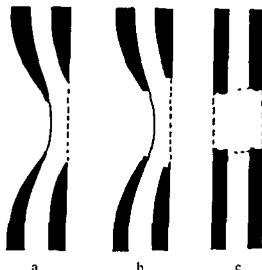


Fig 1 Schematic drawings of myelographic appearances with metastatic lesions a) Conventional concept of extradural lesion, b) and c) suggest intradural growth

findings at surgery in order to find out whether the mode of growth of the tumour could be defined by myelographic examination The possibility to establish an intradural extension of the tumour would be of clinical importance because the presence of a compression of the cord within the dura would reduce the effect of a simple laminectomy and possibly necessitate a removal of the intradural tumour On the other hand, as pointed out by TAVERAS & WOOD, a correct diagnosis may prevent unnecessary, extensive exploration, opening of the dura and trauma to the spinal cord

Material and Methods The material includes 52 patients with metastatic lesions admitted during the period 1963–1971 examined with gas myelography Only cases in which the diagnosis was confirmed by operation or cases with an identified primary malignant tumour were included in the material In order to evaluate technical factors influencing the myelographic appearance of metastases, 5 patients recently examined not only with gas myelography but also with a water-soluble contrast medium, Metrizamide, were included Hence, the total series consists of 57 patients examined with gas myelography The age of the patients ranged from 14 months to 79 years, with a mean of 56 years Ten patients were examined by gas myelography following suboccipital puncture according to the method of LINDGREN (1939) and 36 patients following lumbar puncture according to the technique of WESTBERG (1966) In 11 cases both suboccipital and lumbar puncture were used, these 11 patients and 23 additional patients had a complete block and 15 had a partial block to the passage of gas For various reasons films were not available in the antero-posterior projection in 12 cases The account of the results and the discussion are in the following based only on the examinations of these 45 cases in which complete examination in the lateral as well as in the antero-posterior projection had been made, if not otherwise stated

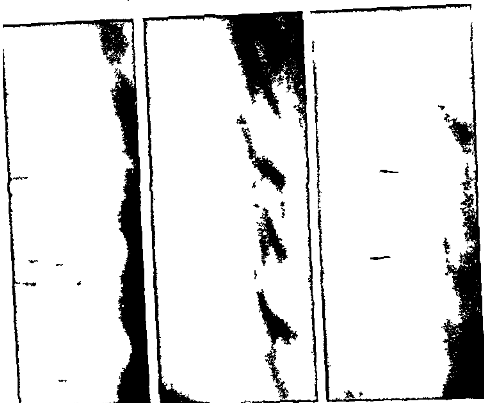


Fig 2 Hand-Schuller Christ an d sease Typ cal appearance of extradural les on extend ng over f ve vertebral segments Tapering of the subarachno d space at its upper and lower ends Sp nal cord ( ) No bone destruct on

Results

In add tion to the generally recogn zed appearance with extradural tumours (Fig 1 a) an abrupt indentation of the subarachnoid space adjacent to the tumour (F g 1 b) was also observed This latter finding proved to be consistent with purely extradural growth in several cases Such changes also occurred in one additional case of proven intradural metastasis Because these appearances bore a certain resemblance to those encountered in intradural extramedullary tumours they were class f ed as juxtamedullary Sometimes the appearance of a lesion was d fferent at the upper and the lower end of the tumour being characteristic of an extradural les on at one end and of a juxtamedullary lesion at the other In a few cases the impress on in one projection of an extradural les on was combined—in the other

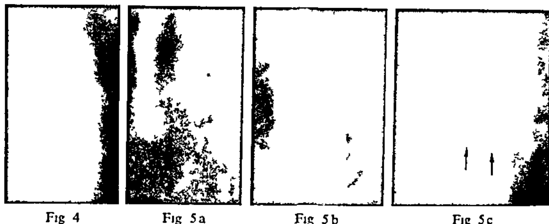


Fig 4 Fig 5a Fig 5b Fig 5c

Fig 4 Complete block with extradural metastatic lesion from a colloid carcinoma of the breast located posterior to the cord, which is pressed forward As the posterior limit of the cord and the indentation in the posterior subarachnoid space is seen, the extradural nature of the tumour is apparent

Fig 5 Poorly differentiated mucus producing carcinoma with bone destruction growing mostly anterior to the spinal cord which is displaced posteriorly at the cervicothoracic junction a) Head elevated Caudally the appearance is that of an extradural lesion, while the tumour has a cuff like border at its upper limit, anterior to as well as posterior to the spinal cord b) This cuff like appearance is preserved in the head down position which proves that it is not due to fluid accumulation at the upper end of the tumour c) The sharp anterior margin (→) is evident also in the a p projection At operation the dura was opened but no growth of tumour was found within the dural sac

projection—with a suggestion of intradural extension at one and the same end of the tumour, in both these situations the lesions were classified as extradural as well as juxtamedullary, this combination being present in 13 cases

The appearance of an extradural lesion was established in 26 tumours (Figs 2, 3, 4) In this group the lesion was combined with bone destruction in 20 cases In some cases a long indentation in the subarachnoid space was produced with or without bone destruction, in some other cases a short protrusion from a compressed vertebral body was observed

One tumour, examined only in the lateral projection with a juxtamedullary appearance, at operation was found to be a malignant melanoma located exclusively juxtamedullary It was adherent to the dura and indented the spinal cord In two cases in which the juxtamedullary appearance was evident the dura was opened but no intradural tumour was found In one of these two cases (Fig 5) the dura was also opened anteriorly and the extradural tumour was found to grow like a cuff around the dura, extending from one intervertebral foramen to the opposite one

The usual appearance of an intramedullary lesion was observed in 4 tumours, all growing within the spinal cord (Fig 6) In 7 cases a marked spindle shape of the cord existed in one projection, resembling that of an intramedullary tumour The extradural site was, however, proven in the projection perpendicular to the first one

As the myelographic appearance of a metastatic lesion may be influenced by the



Fig 6 Strictly intramedullary metastasis involving the cervical cord in a case of reticulum cell sarcoma Typical spindle shape of intramedullary tumour No alteration in the shape of the lesion indicating cystic tumour was observed

physical properties of the contrast medium used, such as its concentration, viscosity, surface tension and attenuation of radiation, the results with gas myelography from a lumbar puncture in 5 cases were compared with those obtained when a water soluble contrast medium (metrizamide) was used Films in the a p projection were not obtained at gas myelography in 3 of these cases Although this material is far too small to allow any definite conclusions as to the relative value of gas and water-soluble contrast media in myelography, some observations of interest could still be made One striking observation was the fact that the border of the spinal cord was more sharply outlined with gas In 4 instances the subarachnoid space posterior to the cord was wider and hence more easy to observe when positive contrast medium was used In all 5 cases the passage of gas was found to be completely blocked at the inferior end of the tumour In 3 cases the water soluble contrast medium passed above the tumour and in one case the extradural appearance became more evident when the upper border of the tumour was outlined (Fig 10) The extradural nature of the lesion was not clear from the lateral view in 2 cases when using gas myelography but became apparent in the a p view In one of these the extradural location of the tumour could be observed already in the lateral projection when metrizamide was used due to the more anterior location of the cord within the dural sac

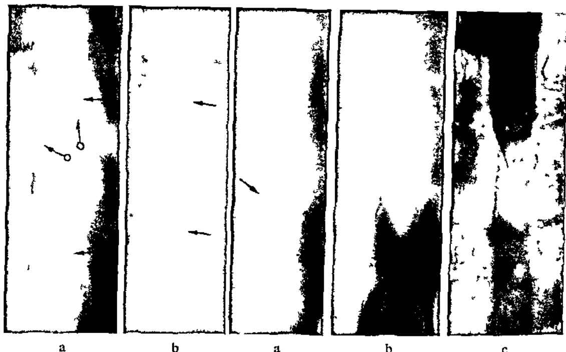


Fig 9 Extradural neurinoma without evidence of juxtamedullary component at operation The tumour caused enlargement of the intervertebral foramen and contained small calcifications (o→) in the upper pole Slight displacement of the dura to the right and anteriorly (→) over several segments giving the impression of extended extradural invasion of tumour

Fig 10 Metastasis from prostatic carcinoma a) Gas myelography Gas at the lower end of the tumour (→) but not posterior to the cord b, c) Myelography with water-soluble contrast medium which penetrates into the space posterior to the cord The borders of the spinal cord are not sharply outlined when the positive contrast medium is used The contrast medium passes above the tumour, the upper limit of which is established

was due to a true juxtamedullary mode of tumour growth in those cases not intradurally explored As mentioned, a purely intradural extramedullary location was encountered only once in this material The case illustrated in Fig 5 proves that a very sharp indentation may be produced by an extradural metastasis, and this evidently causes the juxtamedullary appearance in many cases A sharp indentation may perhaps also be explained by the fact that only a part of the tumour is seen in the subarachnoid space while the remainder is partly growing into the vertebral body and partly invaginates into the spinal cord (Fig 7) This situation can be compared to that of an acoustic neurinoma growing into the internal acoustic meatus being invaginated into the pons and only partially seen in the basal cisterns

It is obvious that fluid accumulating in a narrow space close to a tumour pole may sometimes produce a false impression of a 'tumour pole'. A similar impression may be created at tomography *if the radiation beam does not intersect the tangent* to the pole of the tumour

As mentioned previously, the spinal cord sometimes appeared broadened in one

projection, as with an intramedullary tumour, due to compression by the extramedullary tumour Difficulties in differentiating this from an intramedullary lesion sometimes resulted from the fact that in some cases the subarachnoid space posterior to the cord was not filled with gas (Figs 3, 5) This can usually be overcome by examining the patient in the prone position However, when water soluble contrast medium is used, the cord is more anteriorly located within the dural sac in the lateral recumbent position (HINDMARSH, *to be published*) and consequently the space posterior to the cord is wider and an adequate concept of the anatomy is more easily obtained The tendency of a water soluble contrast medium to penetrate into narrow spaces, such as the root sleeves, will probably facilitate an accurate evaluation of the very narrow parts of the subarachnoid space usually encountered in the vicinity of an extradural tumour Moreover, metrizamide injected in the lumbar area passed the tumour in 3 instances having a complete blockage at gas myelography (Fig 10), which suggests that the water soluble media might be useful in defining the upper limit of an expanding lesion without a second puncture As the nature of a metastatic tumour is sometimes more evident from the appearance at one pole than at the other, not only the extension but also the pathology of the lesion may then be evaluated with greater accuracy These technical and diagnostic considerations will be the subject of a later publication (HINDMARSH)

SUMMARY

The radiologic appearances at gas myelography were analysed in 57 metastatic lesions, all histologically verified or having known primary tumours Five of these cases were al

...out, and not to intradural extension

ZUSAMMENFASSUNG

Das röntgenologische Bild bei der Gas Myelographie wurde bei 57 metastatischen Veränderungen die alle histologisch verifiziert waren, oder die bekannte primäre Tumoren hatten, analysiert Fünf dieser Fälle wurden auch mit einem

RÉSUMÉ

Les auteurs ont étudié les images radiolog

Les résultats des examens radiologiques ont été comparés aux constations opératoires et à l'anatomie pathologique des tumeurs Les auteurs pensent que les signes myélographiques *simulant une tumeur juxtamédullaire sont habituellement dus à une saillie locale de la dure* mère causée par la tumeur extradurale et non à une extension intradurale

REFERENCES

ALMÉN T *Contrast agent design Some aspects on the synthesis of water soluble contrast* agents of low osmolality J theor Biol 24 (1969), 216

CHADE H O Matastasen der Wirbelsäule und des Ruckenmarkes Schweiz Arch Neurol Neurochir Psychiat 102 (1968) 257

GREENBERG A D, SCATLIFF J H, SELKER R G and MARSHALL M D Spinal cord metastasis from bronchogenic carcinoma J Neurosurg 23 (1965), 72

HENSCHEN F *In* Handbuch der speziellen pathologischen Anatomie und Histologie Springer-Verlag Berlin, Gottingen, Heidelberg 1955

HINDMARSH T Myelography with the non ionic water soluble contrast medium metrizamide To be published in Acta radiol Diagnosis

LINDGREN E On the diagnosis of tumors of the spinal cord by the aid of gas myelography Acta chir scand 82 (1939), 303

— Handbuch der Neurochirurgie Zweiter Band Rontgenologie Springer Verlag Berlin 1954

Metrizamide, a non ionic water soluble contrast medium Acta radiol (1973) Suppl No 335

NITTNER K *In* Handbuch der Neurochirurgie Band VII/2 Springer Verlag, Berlin *Heidelberg* New York 1972

PRENTICE W B, KIEFFER S A, GOLD L H A and BOURNSON R G B Myelographic characteristics of metastases to the spinal cord and cauda equina Amer J Roentgenol *118 (1973)*, 682

SMITH W T and TURNER E Solitary intramedullary carcinomatous metastasis in the spinal cord J Neurosurg 29 (1968), 648

TAVERAS J and WOOD E Diagnostic neuroradiology Williams & Wilkins Company, Baltimore 1964

VAKILI H The spinal cord Intercontinental Medical Book Corporation New York 1967

WESTBERG G Gas myelography and percutaneous puncture in the diagnosis of spinal cord cysts Acta radiol (1966) Suppl No 252

FROM THE DEPARTMENT OF DIAGNOSTIC RADIOLOGY (DIRECTOR PROF. H LODIN),
AKADEMISKA SJUKHUSET, UNIVERSITY OF UPPSALA, S-750 14 UPPSALA, SWEDEN

FIBROUS SEPTA IN THE STRAIGHT DURAL SINUS

ERIC BERGQUIST

The presence of septa in the straight sinus has received only scant attention in the literature GRAY's Anatomy (1962) states that the straight sinus is traversed by a few transverse bands Numerous septa in the dural sinuses in the region of the confluens sinuum, similar to those present in the cavernous sinus, were observed at cerebral angiography by TÖNNIS & SCHIEFER (1959)

KRAYENBUHL & YAŞARGIL (1965) reported that the straight sinus may be duplicated ('spaltförmig') but do not discuss the anatomic basis

In the course of an investigation concerning the tentorial notch (BERGQUIST 1973), one or more septa in the upper part of the straight sinus were incidentally observed and a systematic search thus seemed to be warranted

Material and Methods During routine autopsies performed at the Department of Pathology the straight sinus in 145 cases (83 men and 62 women, 30 to 93 years old) was opened after removal of the tentorium of the cerebellum and adjacent parts of the falx In 15 cases, before the tentorium was removed and the straight sinus opened, a 50% suspension of Micropaque in water was injected into the lower part of the sinus, which was exposed by removing the left half of the vault and the left cerebral hemisphere Following optimal filling of the sinus, lateral films were taken

Submitted for publication 30 August 1974

Les résultats des examens radiologiques ont été comparés aux constations opératoires et à l'anatomie pathologique des tumeurs Les auteurs pensent que les signes myélographiques simulant une tumeur juxtamedullaire sont habituellement dus a une saillie locale de la dure-mère causée par la tumeur extradurale et non à une extension intradurale

REFERENCES

ALMÉN T Contrast agent design Some aspects on the synthesis of water soluble contrast agents of low osmolality J theor Biol 24 (1969), 216

CHADE H O Matastasen der Wirbelsaule und des Ruckenmarkes Schweiz Arch Neurol Neurochir Psychiat 102 (1968), 257

GREENBERG A D, SCATLIFF J H, SELKER R G and MARSHALL M D Spinal cord metastasis from bronchogenic carcinoma J Neurosurg 23 (1965), 72

HENSCHEN F *In* Handbuch der speziellen pathologischen Anatomie und Histologie Springer-Verlag, Berlin, Gottingen, Heidelberg 1955

HINDMARSH T Myelography with the non ionic water-soluble contrast medium metrizamide To be published in Acta radiol Diagnosis

LINDGREN E On the diagnosis of tumors of the spinal cord by the aid of gas myelography Acta chir scand 82 (1939), 303

— Handbuch der Neurochirurgie Zweiter Band Rontgenologie Springer-Verlag, Berlin 1954

Metrizamide, a non-ionic water soluble contrast medium Acta radiol (1973) Suppl No 335

NITTNER K *In* Handbuch der Neurochirurgie Band VII/2 Springer-Verlag, Berlin Heidelberg-New York 1972

PRENTICE W B, KIEFFER S A, GOLD L H A and BOURNSON R G B Myelographic characteristics of metastases to the spinal cord and cauda equina Amer J Roentgenol 118 (1973), 682

SMITH W T and TURNER E Solitary intramedullary carcinomatous metastasis in the spinal cord J Neurosurg 29 (1968), 648

TAVERAS J and WOOD E Diagnostic neuroradiology Williams & Wilkins Company, Baltimore 1964

VAKILI H The spinal cord Intercontinental Medical Book Corporation, New York 1967

WESTBERG G Gas myelography and percutaneous puncture in the diagnosis of spinal cord cysts Acta radiol (1966) Suppl No 252



Fig 2



Fig 3

Fig 2 Lateral film of the straight sinus (autopsy case) Same case as in fig 1 a The septum causes a long filling defect in the upper part of the sinus, its anterior part is divided by the septum into an upper and a lower canal

Fig 3 Lateral film of the straight sinus (autopsy case) The cannula through which the contrast medium was injected is placed in the anterior upper canal and only the lower posterior part of a long septum (→) is demonstrated, giving a false impression of the width of the straight sinus

the contrast medium was injected had been placed in the anterior canal, there was only a narrow opening in the upper part of the septum and the contrast medium did not pass through it to the posterior canal Consequently, only the lower part of the septum was demonstrated on the film (Fig 3) The synechiae were not visible at radiography

Discussion

The straight sinus develops from the lower part of the sagittal venous plexus (STREETER 1918, PADGET 1957) O CONNEL (1934) reported single or multiple 'platforms' subdividing the lumen of the superior sagittal sinus into dorsal and ventral parts The longest platform was 8 cm The orifices of the superior cerebral veins joining the superior sagittal sinus were always located below any nearby platform O CONNEL was of the opinion that the platforms persist as evidence of the original plexiform character of the superior sagittal sinus

The septa in the straight sinus reported here would seem to be of the same nature as these platforms, since the straight sinus develops from the same plexus as the superior sagittal sinus In addition, the observed thread like synechiae had the same appearance as the so-called cords of Willis—strands of endothelium traversing the lumen of the superior sagittal sinus—which are also generally considered to be remnants of the sagittal plexus

Anatomically the septa, which were present in about one fifth of the cases, varied greatly in length, position and number from one subject to another, and all must be viewed as normal anatomic variants If a septum was present in the upper part of the straight sinus, however, the great vein of Galen and the major part of the inferior

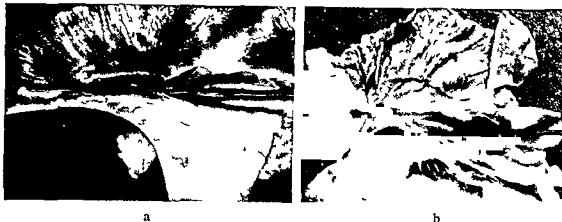


Fig 1 Septa in the upper part of the straight sinus A wire is introduced into the posterior canal

Results

Transverse septa or synechiae were found in 44 of the 145 straight sinuses (from 30 men and 14 women) Septa crossing the sinus in the transverse direction, dividing it completely or partially into an anterior and a posterior canal, were observed in 31 cases (21 per cent) A single septum was present in 28 cases, varying greatly in length (2 to 5 mm in 11 cases, 6 to 10 mm in 9, 11 to 20 mm in 5 and over 20 mm in 3 cases) In a further 3 cases two septa were present (12 and 3 mm long in each of 2 cases, and 6 and 4 mm long in the third case)

The septa (Fig 1) were found in all parts of the sinus In 5 cases the septum was situated behind the opening of the great vein of Galen into the straight sinus These septa, which varied in length between 6 and 23 mm, divided the upper part of the sinus into two canals, the great vein of Galen invariably joining the anterior one The inferior sagittal sinus mainly drained into the same canal, however, a small aperture in the upper part of the septum would seem to permit drainage to the posterior canal Proximally positioned septa separated the lacuna at the origin of the straight sinus from other parts of the sinus

Thread-like synechiae no more than 1 mm thick were found in 15 cases (10 per cent), in 4 of them the synechiae were multiple, and in addition a septum occurred in 2 cases, 7 mm and 3 mm long, respectively Like the septa, the synechiae were observed in all parts of the sinus

Septa were identified on the autopsy films in 5 of 15 examined cases In 9 of the other 10 cases no septum was found on exploration of the sinus In the remaining case a thin septum in the lower part of the straight sinus existed, this could not be identified on the film, probably because it was obscured by the fairly concentrated contrast medium

The septa appeared on the films as narrow longitudinal filling defects in the sinus (Fig 2) In one case with a long septum in the upper part of the sinus, the film gave incomplete information concerning the septum, because the cannula through which

than at the left angiography (Fig 4 b), at vertebral angiography the sinus appeared to be broad and single-channelled and seemed to contain more contrast medium than at the carotid angiographies (Fig 4 c) Various factors were probably responsible for the varying appearances It was observed at postmortem radiography that when a septum was present the straight sinus could have a two channelled appearance At the left carotid angiography in the patient, the straight sinus appeared to have two channels and the presence of a septum could therefore be considered proven The filling of the straight sinus was more complete at the vertebral angiography than at the carotid angiographies and probably obscured the septum This indicates that the septum was thin These findings may be compared with the autopsy case in which a thin septum subsequently seen on dissection, could not be identified on the films because it was obscured by the contrast medium The different appearances of the straight sinus on the left and right carotid angiograms may have been due to differing topography of the veins draining into the deep venous channels on the left and right sides, in addition the septum may have caused a deviant flow

SUMMARY

Postmortem exploration of the straight sinus supplemented in some cases by radiography revealed the presence of single or multiple septa or synechiae in the sinus in 44 of 145 cases A septum should not be mistaken for a thrombus The septa are of roentgenologic significance because of their ability to alter the appearance of the sinus from one cerebral angiography to another in one and the same patient

ZUSAMMENFASSUNG

Die postmortale Exploration des Sinus rectus in einigen Fallen durch Rontgenuntersuchungen ergänzt zeigte das Vorkommen einzelner oder multipler Septen oder Verwachsungen in den Sinus von 44 von 145 Fallen Ein Septum sollte nicht mit einem Thrombus verwechselt werden Die Septen sind wegen ihrer Fahigkeit, das Bild des Sinus von einer zerebralen Angiographie zur anderen bei ein und demselben Patienten zu ändern, von rontgenologischer Bedeutung

RÉSUMÉ

L examen postmortem du sinus droit, complete dans certains cas par la radiographie, a montré la présence de cloisons uniques ou multiples ou de synéchies dans le sinus dans 44 cas sur 145 Il ne faut pas prendre une cloison pour un thrombus, les cloisons ont un intérêt radiologique car elles peuvent modifier l aspect du sinus d une angiographie cerebrale à l autre chez un meme malade

REFERENCES

BERGQUIST E Tentorial notch and adjacent major vessels in carotid angiography Acta radiol (1973) Suppl No 327

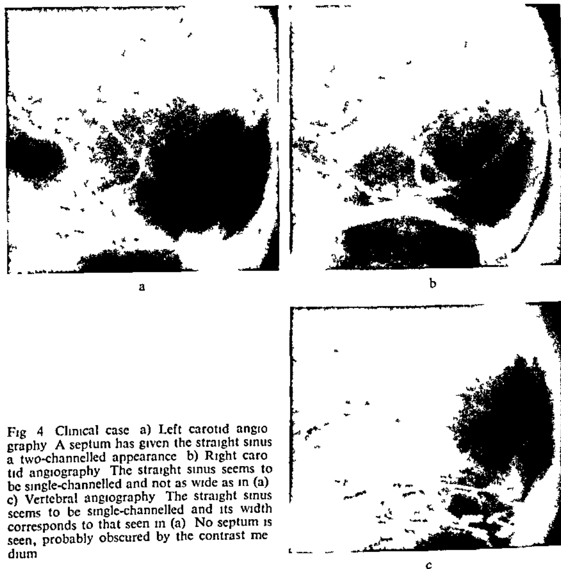


Fig 4 Clinical case a) Left carotid angiography A septum has given the straight sinus a two-channelled appearance b) Right carotid angiography The straight sinus seems to be single-channelled and not as wide as in (a) c) Vertebral angiography The straight sinus seems to be single-channelled and its width corresponds to that seen in (a) No septum is seen, probably obscured by the contrast medium

sagittal sinus invariably drained in front of the septum This may be compared with the position of the orifices of the superior cerebral veins in relation to the platforms in the superior sagittal sinus (O'CONNEL)

A septum may appear as a defect in the straight sinus filled with contrast medium, i e it may resemble a thrombus The possible presence of septa in this sinus should be borne in mind so as to avoid an erroneous diagnosis of a thrombus A blood clot, however, generally gives rise to an increase in the circulation time

Furthermore, it seems possible that in the presence of a septum the straight sinus may vary in appearance at different angiographic examinations in one and the same patient This may be illustrated by the following clinical case At carotid angiography on the left side the straight sinus had a two channelled appearance (Fig 4 a) while on the right side only the anterior canal filled, the sinus thus appearing narrower

than at the left angiography (Fig 4 b), at vertebral angiography the sinus appeared to be broad and single-channelled and seemed to contain more contrast medium than at the carotid angiographies (Fig 4 c) Various factors were probably responsible for the varying appearances It was observed at postmortem radiography that when a septum was present the straight sinus could have a two-channelled appearance At the left carotid angiography in the patient, the straight sinus appeared to have two channels and the presence of a septum could therefore be considered proven The filling of the straight sinus was more complete at the vertebral angiography than at the carotid angiographies and probably obscured the septum This indicates that the septum was thin These findings may be compared with the autopsy case in which a thin septum, subsequently seen on dissection, could not be identified on the films because it was obscured by the contrast medium The different appearances of the straight sinus on the left and right carotid angiograms may have been due to differing topography of the veins draining into the deep venous channels on the left and right sides, in addition, the septum may have caused a deviant flow

SUMMARY

Postmortem exploration of the straight sinus supplemented in some cases by radiography revealed the presence of single or multiple septa or synechiae in the sinus in 44 of 145 cases A septum should not be mistaken for a thrombus The septa are of roentgenologic significance because of their ability to alter the appearance of the sinus from one cerebral angiography to another in one and the same patient

ZUSAMMENFASSUNG

Die postmortale Exploration des Sinus rectus, in einigen Fallen durch Rontgenuntersuchungen erganzt zeigte das Vorkommen einzelner oder multipler Septen oder Verwachsungen in den Sinus von 44 von 145 Fallen Ein Septum sollte nicht mit einem Thrombus verwechselt werden Die Septen sind wegen ihrer Fahigkeit das Bild des Sinus von einer zerebralen Angiographie zur anderen bei ein und demselben Patienten zu andern, von rontgenologischer Bedeutung

RÉSUMÉ

L' [illegible]
mo [illegible]
cas [illegible]
[illegible] cloison pour un thrombus, les cloisons ont un intérêt radiologique car elles peuvent modifier l'aspect du sinus d'une angiographie cérébrale à l autre chez un meme malade

REFERENCES

BERGQUIST E. Tentorial notch and adjacent major vessels in carotid angiography Acta radiol (1973) Suppl No 327

GRAY'S ANATOMY Thirty-third Edition Longmans, Green & Co Ltd, London 1962
KRAYENBUHL H und YAŞARGIL M G Die zerebrale Angiographie Zweite Auflage Georg Thieme Verlag Stuttgart 1965
O'CONNEL J E A Some observations on the cerebral veins Brain 57 (1934) 484
PADGET D H The development of the cranial venous system in man, from the viewpoint of comparative anatomy Carnegie Inst Washington, Publ 611 Contrib to Embryol 36 (1957), 79
STREETER G L The developmental alterations in the vascular system of the brain of the human embryo Carnegie Inst Washington, Publ 271 Contrib to Embryol 8 (1918) 5
TÖNNIS W und SCHIEFER W Zirkulationsstorungen des Gehirns im Serienangiogramm Springer Verlag, Berlin-Gottingen-Heidelberg 1959

FROM THE DEPARTMENT OF DIAGNOSTIC RADIOLOGY (DIRECTOR PROF B NORDENSTRÖM), KAROLINSKA SJUKHUSET, S-104 01 STOCKHOLM, SWEDEN

BONE SCINTIGRAPHY OF FACIAL SKELETON WITH $^{99}Tc^{m}$-DIPHOSPHONATE

HANS F BERGSTEDT

Technetium has tended to supercede strontium and fluorine in recent years for diagnostic scintigraphy of tumors, metastases and inflammatory conditions of the skeleton (GALASCO & DOYLE 1972) The isotope is bound to a diphosphonate, $^{99}Tc^{m}$-DP (CASTRONOVO & CALLAHAN 1972, CASTRONOVO et coll 1973) Like calcium, it is deposited in bone tissue that is decomposing with derangement of structure Decay of $^{99}Tc^{m}$ involves the emission of gamma rays with the energy of 140 keV, which is suitable for recording with the gamma-camera

Pathologic processes are discernible on the scintigram due to the uptake of isotopes Conventional radiography and biopsy may then be confined to regions with increased uptake Sometimes scintigraphy will reveal lesions even before they can be demonstrated at radiography (GALASCO & DOYLE 1972)

The normal scintigraphic appearance of the skeleton, as well as various abnormalities have been described, but no detailed scintigraphic examination of the facial skeleton has appeared in the literature, which is the reason for the present report

Material and Methods

The scintigraphy was performed using the gamma-camera Nuclear Chicago Pho-Gamma III The photons emitted were collected by a converging collimator, giving

Submitted for publication 28 June 1974



Fig 1 Gamma-camera scintigram of facial skeleton Uptake of $^{99}Tc^m$–DP and normal distribution a) A p b) lateral projection

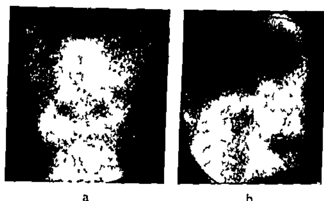


Fig 2 Solitary bone cyst of the right mandible Scintigraphy a) A p b) lateral projection

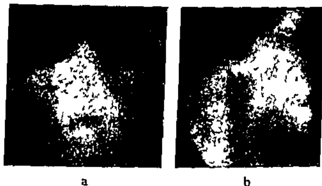


Fig 3 Carcinoma of the maxilla and ethmoidal region Scintigraphy a) A p, b) lateral projection

maximal enlargement of the region examined Scintigraphy was performed in 10 patients with no signs of abnormality in the facial skeleton (normal material) in conjunction with skeletal survey, they received 10 mCi $^{99}Tc^m$ diphosphonate intravenously 5 to 6 hours before the recording was started Four patients with roentgenologically evident pathology in this region were also examined In all cases 300 000 counts were recorded in each projection, a p and lateral projections were obtained in every case For the a p projection, the patient was in supine position with the anatomic orbito meatal base line perpendicular to the detector and the tip of the nose in the center of the detector field For the lateral projection, the sagittal plane of the patient was placed parallel to the front of the camera with the naso pharyngeal

a b c

Fig 4 Large cyst of the maxilla. a) Lateral projection b) A p projection Bone destruction of the medial and lateral walls of the right maxillary sinus c) Scintigraphy, lateral view Low activity in the center of lesion increased peripherally

region in the center The distance between the face of the patient and the front of the camera was always about 5 centimeters

Normal scintigraphy The uptake of the isotope was highest in the bone of the midface, the middle and anterior parts of the calvarium and the cervical vertebrae High activity was also recorded in the nasal region, the conchae and the maxilla, particularly evident in the a p projection, in which this region appeared as an upright triangle with its tip in the nasion (Fig 1 a) In the corresponding lateral projection the activity appeared to be rather uniformly distributed, bound posteriorly by the air space of the pharynx (Fig 1 b)

In the mandible the isotope distribution was also uniform, but less intense than in the rest of the facial skeleton The anterior part of the mandible seemed to display a somewhat higher uptake due to increase in mass, projected on the detector A certain amount of activity was present in the tongue and other soft tissues

Pathology Four patients with pathologic processes were examined, in all cases the lesion had been demonstrated at radiography The diagnoses were confirmed in postoperative histologic reports

Case 1 A 30-year-old –
mandible at the level of t
of the mandible Microsc
uptake of $^{99}Tc^{m}$ DP in t ... evident in the a p (Fig 2 a), as well as in
the lateral projection (Fig 2 b)

Case 2 A 60-year-old man in whom conventional radiography indicated a bone destroying maxillary and ethmoidal tumor Microscopy evidenced a low differentiated carcinoma of the maxilla with infiltrative growth Scintigraphy displayed an accumulation of the isotope to the region of the lesion, in the a p projection (Fig 3 a) the uptake was asymmetric, in the lateral projections there was an evident difference between the sides, with the




a b

Fig 5 a) Oblique lateral view of multilocular epithelium lined cyst of the mandible b) Scinti graphy, lateral view Increased uptake

uptake on the right side (Fig 3 b) concentrated to the basal parts of the maxilla and to the ethmoidal region

Case 3 A 50 year old man who had a soft tissue mass completely filling the right max illary sinus at radiography (Fig 4 a, b), the medial and lateral bony walls were destroyed Microscopy revealed an epithelium lined cyst without signs of malignancy On the scinti gram there was low activity in the central part of the lesion (Fig 4 c) surrounded by a rim of slightly increased activity

Case 4 A 70 year old woman had a multilocular cystic lesion involving the body of the mandible from the angulus to the midline (Fig 5 a) microscopically an epithelium lined cyst There was an increased uptake in the cystic region of the mandible with a homogeneous distribution of the isotope (Fig 5 b)

Discussion

The present report describes the scintigraphic appearances of the facial skeleton after a 10 mCi intravenous dose of $^{99}Tc^{m}$ diphosphonate, as recorded with a gamma camera The normal isotope distribution in the facial bones was fairly homogeneous Minor variations were partly due to the amount of bone and the distance to the front of the camera This distance should be less than 6 to 8 cm as the sensitivity of the camera will decrease above this distance (GALASCO)

The uptake in soft tissue is a source of disturbance, limited by performing the examination with an interval of at least 5 to 6 hours from the injection of the isotope

Four pathologic cases demonstrated increased uptake of $^{99}Tc^{m}$-DP associated with lesions, all evident on radiography To be scintigraphically distinguishable, the lesion must cause a certain amount of bone destruction

Roentgenographic evidence of bone lesions in the central parts of the jaw may not be recognized until the compact border of the jaw is eroded Therefore, bone scinti graphy may be of value for the early diagnosis of malignant as well as of other lesions in the facial skeleton

SUMMARY

Bone scintigraphy of the facial skeleton with $^{99}Tc^m$-diphosphonate using gamma-camera was performed in 10 cases without, and in 4 cases with pathologic processes A p and lateral projections were used and a converging collimator The normal distribution of the isotope in the bones of the face seemed to be uniform with minor variations Increased uptake varying in intensity was evident in the region of the lesion

ZUSAMMENFASSUNG

Die Knochen Skintigraphie des Gesicht Skeletts mit $^{99}Tc^m$ Diphosphonat unter Verwendung einer Gamma Kamera wurde bei 10 Fallen ohne und 4 Fallen mit pathologischen Prozessen ausgefuhrt Es wurden a p und laterale Projektionen und ein konvergierender Kollimator verwendet Die normale Verteilung des Isotops scheint in den Knochen des Gesichtes mit geringeren Variationen gleichformig zu sein Eine gesteigerte Aufnahme, variierend in ihrer Intensitat, war in den Abschnitten der Schadigung festzustellen

RÉSUMÉ

La scintigraphie osseuse du squelette de la face au moyen du $^{99}Tc^m$ diphosphonate avec une gamma-camera a été pratiquée dans 10 cas sans processus pathologique et dans 4 cas pathologiques L auteur a utilise les projections de face et de profil avec un collimateur convergent La distribution normale de l isotope dans les os de la face semble etre uniforme, avec des variations minimes La fixation de l isotope est augmentée de façon variable dans la région de la lesion

REFERENCES

AISENBERG M S and INMAN C L Tumors that have metastasized to the jaws Oral Surg 9 (1956) 1210

CASTRONOVO F P and CALLAHAN R J A new bone scanphosphonate J nucl Med 13 (1972) 823

— POTSAID M S and PENDERGRASS H P Effects of radiation therapy on bone lesions as measured by $^{99}Tc^m$-diphosphate J nucl Med 14 (1973) 604

COOK T J Adenocarcinoma

GALASCO C S B and DOYLE

cancer A comparison betw

FROM THE DEPARTMENTS OF RADIOLOGY AND OTORHINOLARYNGOLOGY, CENTRAL-LASARETTET, S-721 89 VÄSTERÅS, SWEDEN

DOUBLE-BARRELED HYPOPLASTIC INTERNAL AUDITORY CANAL IN UNILATERAL DEAFNESS

F CLEMENS and J SANDSTRÖM

Within a short period of time two patients with unilateral neurosensory deafness and double-barreled hypoplastic auditory canals have been observed at this hospital As only one similar well documented case has been published the following presentation seems to be justified

Case reports

Case 1 A 12-year-old girl was admitted to the children's clinic in 1970 for analysis of brief attacks of the petit mal type Deafness on the right side had been found by a physician at the age of 4 No heredity of impaired hearing was found She had not had parotitis, nor otitis Hearing on the left side was normal as well as speech development Nothing abnormal was found at inspection of ears, nose and throat The ear-drums were intact The audiogram showed extinct cochlear function on the right side and normal hearing on the left side, the nystagmogram a weak leftward spontaneous nystagmus The caloric reaction on the right side was extinct when irrigating water of 30°, 44° and 0° The left labyrinth reacted normally on caloric excitation Facial nerve functioning was normal

Radiology The internal auditory canal on the right side was separated into two canals by a dividing bony septum approximately 1 mm thick (Fig 1) The upper canal measured on the films 2 mm × 2 mm, the lower 2 mm × 3 mm The left auditory canal was normal and measured 7 mm × 8 mm No associated anomalies of the labyrinth and temporal bones could be revealed with tomography in a p and lateral projections (distance between the sections 1 mm) The temporal bones were normally aerated on both sides

Submitted for publication 22 July 1974



a



b



c



d



e

Fig. 1 Case 1 a) T...
auditory
of right s

Case 2 A 25 year old man visited the ENT clinic in 1972 w th a ...
6 months on the ...
duct on ...

... ogram showed no spontaneous or posi




a




b c




d e

tional nystagmus Caloric testing gave bilateral symmetric reactions The corneal reflex on the right was possibly weakened but otherwise nothing abnormal was found

Radiology The right internal auditory canal was separated into two canals one upper 2 mm × 3 mm wide and one lower 2 mm × 2 mm wide A longitudinal dividing bony septum was present (Fig 2) The left internal auditory canal was normal and 7 mm × 8 mm wide No other anomalies were demonstrated in the labyrinths, temporal bones or cranium Encephalography (including cerebello pontine cisterns) was normal The hypoplasia of the right internal auditory canal proved that the reduction in hearing was congenital The headache and other symptoms were considered to be due to migraine

Discussion

In both the related cases a unilateral (rightsided) double barreled hypoplastic internal auditory canal was associated with neurosensory deafness In the first case there was also an extinct vestibular function on the right side, the facial nerve was in both cases intact No further malformation was demonstrated at the otologic or radiologic examinations Radiology proved the congenital origin of the deafness and was of differential diagnostic value

A similar case has been described by EVERBERG et coll (1963), who regarded their case as unique In a 12 year old girl with rightsided deafness as the only symptom or sign, these authors found 'a unilateral atresia of the internal auditory meatus'. An otoradiologic examination including tomography demonstrated a narrow right internal auditory meatus divided into a cranial and a caudal canal, 2 and 3 mm in diameter respectively, with a bony septum in between, coursing from the vestibulum to the porus It was supposed that the internal auditory canal was occupied only by the facial nerve The description of the radiologic findings as well as the illustrations are almost identical with the appearances in the present two cases, the only difference being a slight hypoplasia of the tip of the right pyramid in the former case, not demonstrated in the present cases It is also of interest that the patient of EVERBERG et coll had a cousin with a onesided ear malformation and a deaf-mute aunt No hereditary background was revealed in the present cases Further, two illustrations, examples of congenital malformation of the temporal bone, in Monographia Otoradiologica (DULAC et coll 1973) represent probably the same kind of malformation of the internal auditory canal A dividing wall in the canal is described as a hypertrophic crista falciformis One of the patients was totally deaf

Narrowness of the internal auditory canal per se is otherwise known to occur in association with deafness TERRAHE (1972) found narrowness of the internal auditory canal most often associated with other malformations of the temporal bone (most of them thalidomide induced) but also isolated narrowness of the canal in otherwise tomographically normal inner ears Cases with a canal containing only the facial nerve have also been reported by TERRAHE Total aplasia of the internal auditory canal was associated either with an aplasia of the inner ear or with persistence of the otocyst stage LAPAYORKER et coll (1966) examined 50 children with congenital neurosensory deafness In 6 children and one of their parents there was radiologic evidence of temporal bone abnormalities, among these also unilateral or bilateral narrowness of the internal auditory canal Neither TERRAHE nor LAPAYORKER mention a double canal

JENSEN (1969) reported on tomography of the temporal bones in 62 deaf children and in a collection of 39 museum specimens He found narrowing of the internal auditory canal in cases with total or partial aplasia of the cochlea JENSEN mentioned the case described by EVERBERG et coll , apparently no such case was included in his own material

The two cases in the *present report* are *radiologically almost identical* A *double*-barreled hypoplastic internal auditory canal represents a congenital defect It seems evident that the upper canal in these cases contains the facial nerve That the lower canal may contain the intact nerve fibres from the stato-acoustic nerve is demonstrated *by the second case, in which the vestibular function* was intact The term hypoplasia of the internal auditory canal is therefore more correct than atresia

Since two cases of this rare anomaly have been observed within a short period of time at this hospital it is possible that it may not be only a curiosity, and a knowledge of its radiologic appearances may also have practical value

SUMMARY

The radiologic appearance of a double barreled hypoplastic internal auditory canal is described in two cases with unilateral congenital deafness In one of the patients the vestibular function was not affected

ZUSAMMENFASSUNG

Das rontgenologische Erscheinungsbild eines doppellaufigen hypoplastischen inneren Gehorganges wird anhand von zwei einseitig kongenital tauben Patienten beschrieben Wahrend bei dem einen Patienten auch die vestibulare Funktion erloschen war, war *sie im zweiten* Fall erhalten

RÉSUMÉ

Description dans 2 cas de surdité congénitale unilatérale d'un aspect radiologique hypoplasique en double tonnelet du conduit auditif interne Chez un de ces malades, la fonction vestibulaire n'était pas atteinte

REFERENCES

EVERBERG G, RATJEN E and SÖRENSEN H Unilateral atresia of the internal auditory meatus, confirmed by radiography Brit J Radiol 36 (1963), 568

DULAC G L, CLAUS E and BARROIS J *Monographia otoradiologica, X-ray Bulletin Spec* issue 1973, 68 Publ Agfa Gevaert

JENSEN J Malformations of the inner ear in deaf children Acta radiol (1969) Suppl No 286

LAPAYORKER M S, WOLOSHIN H J, RONIS M L and RONIS B J Temporal bone abnormalities in congenital neurosensory deafness as revealed by *plesiosectional tomo-* [illegible] 97 (1966), 125

[illegible] ildungen des Ohres und des Ohrschadels Arch klin [illegible] 202 (1972), 85

FROM THE DEPARTMENT OF OTOLARYNGOLOGY (DIRECTOR PROF S INGELSTEDT), ALLMÄNNA SJUKHUSET, S 214 01 MALMO, AND THE DEPARTMENT OF DIAGNOSTIC RADIOLOGY (DIRECTOR PROF O OLSSON), UNIVERSITY HOSPITAL, S-221 85 LUND, SWEDEN

COMPARISON BETWEEN THE AREA AND THE VOLUME OF THE AIR-FILLED EAR SPACE

LARS ANDREASSON and WIGHER MORTENSSON

It is generally accepted that chronic otitis media is more likely to occur in ears with a small mastoid cell system than in those with a larger system Opinions differ, however, as to which of the two conditions is primary The development of the mastoid air cell system has been considered to be impeded by repeated and protracted otitis during early life (WITTMAACK 1918, TUMARKIN 1957) Other authors are of the opinion that the size of the cell system is dependent mainly on genetic factors and that a small cell system may facilitate infection in the middle ear and hinder restitutio ad integrum (HEINE 1906 CHEATLE 1923, DIAMANT 1940 1952)

In chronic otitis media, the inflammatory changes affect the mucosa not only in the middle ear but also in the mastoid air cell system and in the eustachian tube This influences the tubal function and it has been proven that a correlation exists between a small cell system and poor tubal function (HOLMQUIST 1970, SIEDENTOP 1972)

Adequate function of the eustachian tube is a prerequisite for the successful restoration of hearing by surgery Preoperative testing of tubal function has also been found to be most important from a prognostic point of view (SIEDENTOP) However, HOLMQUIST found that determination of the size of the mastoid air cell system gave

Submitted for publication 15 August 1974

Table 1

Age distribution of the patients

Age	Chronic otitis media	Traumatic perforation	Total
11–20	5	1	6
21–30	20	2	22
31–40	9	3	12
41–50	15	1	16
51–60	15	2	17
61–70	5		5
Total	69	9	78

information as valuable as hearing tests and tests of tubal function in determining the conditions required for successful tympanoplasty

Previously the distribution of the mastoid air cell system has been judged mainly by conventional roentgen examination DIAMANT (1940) introduced planimetry for assessing the area of the air cell system and reported the results in a large material of healthy ears and ears with chronic otitis media

A method based on Boyle's law to determine the volume of the air-filled ear space was described by FLISBERG et coll (1963) Using this method, FLISBERG & ZSIGMOND (1965) reported that a good correlation existed between the volume of the air-filled space and its area, the latter being assessed by planimetry However, the technical performance of their method of determining volume involved some sources of error (cuff-sliding, variations in the mucosal volume) as was pointed out by INGELSTEDT et coll (1967)

To avoid these errors the method of FLISBERG et coll was modified and applied in a comparison between the volume and the area of the air-filled ear space, its clinical application in the preoperative investigation of chronic otitis media has been published previously (ANDREASSON 1973)

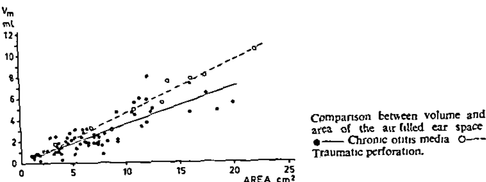
Material and Methods

The material consisted of 69 ears (65 patients) with chronic otitis media and central perforation and 9 ears (9 patients) with recent traumatic perforation of the tympanic membrane The age distribution of the patients is given in Table 1

All ears had been dry for a period of at least two months before examination, ears with signs of present infection or cholesteatoma were excluded

Assessment of the volume and area was carried out by the two authors independently of each other

Planimetry of the area of the air-filled space was carried out on films, with the



Comparison between volume and area of the air filled ear space ●—— Chronic otitis media ○--- Traumatic perforation.

temporal bone projected in Runström's projection P_{II} (35° cranially) using stereoscopy (RUNSTRÖM 1933) The same method was used by DIAMANT (1940) except that, in the present material, the area of the mastoid antrum was included in all cases The area given for each ear represents the mean value of the measurements on the two stereoscopic films and, in turn, the mean value for each of the two films represents the mean of three measurements

The roentgen examinations were performed with different magnification factors, these were assessed to be 1 11 in the examination of 58 ears and 1 15 in the examination of 20 ears

Results

The results of the comparison between the volume and the area of the air filled spaces of the ear appear in the figure

In cases with chronic otitis media the regression line was $y = 0\ 34\,x + 0\ 18$ and in cases with traumatic perforation of the tympanic membrane it was $y = 0\ 49\,x - 0\ 38$ The difference in the slope of the two lines was significant ($p < 0\ 05$) With repeated measurements of the same area, the standard deviation was 2 7 per cent of the mean value of the measurements The standard deviation of the measurements of the area of the same ear in the two stereoscopic films was calculated as 0 37 cm²

Discussion

The error on repeated measurements of the area of the air-filled ear space was similar to that reported by DIAMANT (1940)

In cases with traumatic perforation of the tympanic membrane, the area values were grouped close to the line of regression These ears were healthy before the trauma and were used as a reference group The present results of the area and volume measurements agree with those published by DIAMANT (1940), RIU et coll (1966) and INGELSTEDT et coll (1967)

Table 1

Age distribution of the patients

Age	Chronic otitis media	Traumatic perforation	Total
11–20	5	1	6
21–30	20	2	22
31–40	9	3	12
41–50	15	1	16
51–60	15	2	17
61–70	5		5
Total	69	9	78

information as valuable as hearing tests and tests of tubal function in determining the conditions required for successful tympanoplasty

Previously the distribution of the mastoid air cell system has been judged mainly by conventional roentgen examination DIAMANT (1940) introduced planimetry for assessing the area of the air cell system and reported the results in a large material of healthy ears and ears with chronic otitis media

A method based on Boyle's law to determine the volume of the air-filled ear space was described by FLISBERG et coll (1963) Using this method, FLISBERG & ZSIGMOND (1965) reported that a good correlation existed between the volume of the air-filled space and its area, the latter being assessed by planimetry However, the technical performance of their method of determining volume involved some sources of error (cuff-sliding, variations in the mucosal volume) as was pointed out by INGELSTEDT et coll (1967)

To avoid these errors the method of FLISBERG et coll was modified and applied in a comparison between the volume and the area of the air-filled ear space, its clinical application in the preoperative investigation of chronic otitis media has been published previously (ANDREASSON 1973)

Material and Methods

The material consisted of 69 ears (65 patients) with chronic otitis media and central perforation and 9 ears (9 patients) with recent traumatic perforation of the tympanic membrane The age distribution of the patients is given in Table 1

All ears had been dry for a period of at least two months before examination, ears with signs of present infection or cholesteatoma were excluded

Assessment of the volume and area was carried out by the two authors independently of each other

Planimetry of the area of the air filled space was carried out on films, with the

their results with the normal values for children of corresponding age (RUBENSOHN 1965) they found the relative retardation in the pneumatisation of the temporal bone to decrease when the infection was successfully treated They concluded that this favours the hypothesis that infection is the primary condition and causes retardation of the development of the mastoid cell system In view of the fact that adequate antibiotic therapy was not practised until the early fifties, the larger area of the mastoid air cell system reported by HOLMQUIST (1970) and the present authors may reflect the effect of more effective control of infection

As a conclusion it may be stated a significant correlation exists between the area and the volume of the air space of the healthy ear When the ear is affected by chronic otitis media, however, the area is larger in proportion to the volume This is explained by the fact that part of the cell system is filled with thickened mucous membrane

SUMMARY

The area of the air filled ear space, assessed planimetrically, was compared with the volume in cases with chronic otitis media with central perforation or recent traumatic perforation of the tympanic membrane A significant correlation between the area and volume existed In chronic otitis media the area was larger than in cases with traumatic perforation with equal volume In these cases the area does not correlate completely with the volume of the functioning air space The results favour the hypothesis that the pneumatisation of the temporal bone is affected by infection

ZUSAMMENFASSUNG

Es wurde die planimetrisch erhaltene Flache des luftgefullten Ohr Raums mit dem Volumen bei Fallen mit chronischer [illegible] traumatischen Perforation [illegible] tion der Flache zum Volu[illegible] Fallen mit traumatischer [illegible] mit gleichem Volumen In diesen Fallen sind die Flächen Bestimmungen nicht vollstandig zum Volumen des funktionellen Luftraumes zugeordnet Diese Ergebnisse mogen die Hypothese, dass die Pneumatisation des Schlafenbeins durch die Infektion beeinflusst wird, stutzen

RÉSUME

La surface de l espace rempli d air dans l oreille, mesuree par planimètrie a été comparée avec le volume dans des cas d otites chroniques moyennes avec perforation centrale du tympan ou après perforation traumatique récente du tympan Les auteurs ont trouvé une corrélation significative entre la surface et le volume Dans l otite chronique moyenne la surface était plus grande que dans les cas de perforation traumatique ayant un volume égal dans ces cas la mesure de la surface n est pas parfaitement en correlation avec le volume de l espace aérien fonctionnel Ces résultats viennent à l appui de l hypothèse que la pneumatisation de l os temporal est affectée par l infection

Table 2

Results of different investigations of the area (in cm²) of the air filled ear space assessed planimetrically

	Healthy ears		Chronic otitis media	
	Mean ± SD	Number of ears	Mean ± SD	Number of ears
Diamant (1940)	12 04 ± 0 37	328	3 81 ± 0 45	70
Flisberg & Zsigmond (1965)	12 69 ± 0 81	11	4 39 ± 0 44	41
Holmquist (1970)			6 3	124
Andreasson & Mortensson (1975) (present investigation)	12 70 ± 1 86	9	6 90 ± 0 52	69

In chronic otitis media the mastoid air cell system is partly filled with thickened mucous membrane and the trabeculae are coarse Furthermore, part of the air cell system may be shut off, thereby losing air connection with the other parts At operation obstruction at aditus ad antrum was sometimes found in cases with a mastoid cell system of small volume In determining the volume of the cell system it is in fact the functioning air volume that is measured Consequently it is reasonable to assume, and it is confirmed in this investigation, that the area of the mastoid cell system is larger in relation to the volume in cases with chronic otitis media than in the healthy ears in the reference group

The relation between area and volume differs in the present material from that reported by Flisberg & Zsigmond (1965) They found the regression coefficient to be 0 91 in the group with chronic otitis media, while in the present material it was 0 34 This may be explained partly by the fact that the method used by Flisberg & Zsigmond in measuring the volume produced values 1 ml too high, which gives a percentage effect most marked in cases with small air space volume (Andreasson 1973) In addition, the material of Flisberg & Zsigmond was heterogeneous, and besides cases with dry chronic otitis media, included cases with cholesteatoma, as well as some with healthy ears The discrepancy between the area and volume measurements in these cases may possibly be of diagnostic value, e g in cholesteatoma

The areas of the mastoid cell system reported are compared in Table 2 They agree well with the measurements in healthy ears (in the present material ears with traumatic perforation may be regarded as healthy ears) However, the results differ in cases with chronic otitis media and the mean area is largest in the two most recent reports (Table 2) The difference in magnification at the roentgen examination is not significant Diamant (1940) as well as Flisberg & Zsigmond excluded the area of the mastoid antrum when this could be clearly delineated If this is done in the present material the mean value of the area is reduced by 0 15 cm² at most Kolihová et coll (1972) reported on planimetric measurements of the mastoid air cell system in children with one or several episodes of acute middle ear infection By comparing

FROM THE DEPARTMENT OF DIAGNOSTIC RADIOLOGY, UNIVERSITY HOSPITAL, INSELSPITAL,
CH-3008 BERNE, SWITZERLAND

LYMPHOGRAPHY IN CARCINOMA OF THE UTERINE CERVIX

W. A. FUCHS and G. SEILER-ROSENBERG

Lymphography has become a routine procedure in patients with carcinoma of the uterine cervix. Several groups of authors have reported their results and experiences concerning the diagnostic accuracy of the method, its clinical indications and possible implications in the prognosis. In 1964 FUCHS & BOOK-HEDERSTRÖM presented a report on the accuracy and the clinical indications of the method based on a material of 60 patients. Comparison of these results with those of the present investigation 10 years later, covering a different case material, might yield some further information and demonstrate the advances of lymphography.

Methods and Material. A total of 158 patients with carcinoma of the uterine cervix were examined between 1963 and 1972. The ages ranged from 28 to 81 years (mean 51 years). [illegible] the [illegible] stage [illegible]. The therapy cons[illegible] [illegible] and postoperative irradiation in 81 cases and radiation therapy only in 73. Two patients were treated only by operation and two cases with advanced tumor received chemotherapy alone. The main techniques for irradiation were as follows: High kilovoltage irradiation (6 000 rad) in 131 cases, complemented with local radium therapy in 81 cases.

Submitted for publication 6 September 1973.

REFERENCES

ANDREASSON L Kronisk slemhinneotit—preoperativ bedomning (Chronic otitis media—preoperative evaluation) (In Swedish with summary in English) Malmo Sjukhus Centraltryckeri, Malmo 1973

CHEATLE A H The etiology and prevention of chronic middle ear suppuration Acta otolaryng (Stockh) 5 (1923), 283

DIAMANT M Otitis and pneumatization of the mastoid bone Acta otolaryng (Stockh) (1940) Suppl No 41

— 'Chronic otitis' a critical analysis S Karger, Basel/New York 1952

FLISBERG K and ZSIGMOND M The size of the mastoid air cell system Acta otolaryng (Stockh) 60 (1965), 23

— INGELSTEDT S and ÖRTEGREN U Clinical volume determination of the air filled ear space Acta otolaryng (Stockh) (1963) Suppl No 182

HEINE B Operationen am Ohr Second edition, p 82 S Karger, Berlin 1906

HOLMQUIST J Size of mastoid air cell system in relation to healing after myringoplasty and to Eustachian tube function Acta otolaryng (Stockh) 69 (1970), 89

INGELSTEDT S, IVARSSON A and JONSON B Mechanics of the human middle ear Acta otolaryng (Stockh) (1967) Suppl No 228

KOLIHOVÁ E, ABRAHAM J und BLÁHOVÁ O Rezidivierende Mittelohrentzundung im frühen Kindesalter und ihr Einfluss auf die Zellsystementwicklung des Schlafenbeins Radiologe 12 (1972), 62

RIU R, FLOTTES L, BOUCHE J et LE DEN R La physiologie de la trompe d'Eustache Arnette, Paris 1966

RUBENSOHN G Mastoid pneumatization in children at various ages Acta otolaryng (Stockh) 60 (1965), 11

RUNSTRÖM G A roentgenological study of acute and chronic otitis media Acta radiol (1933) Suppl No 17

SIEDENTOP K H Eustachian tube dynamics, size of the mastoid air cell system and results with tympanoplasty Otolaryng Clin N Amer 5 (1972), 33

TUMARKIN A On the nature and vicissitudes of the accessory air spaces of the middle ear J Laryngol Otol 71 (1957), 65

WITTMAACK K Über die normale und die pathologische Pneumatisation des Schlafenbeines einschliesslich ihrer Beziehungen zu den Mittelohrerkrankungen, p 125 G Fischer, Jena 1918



Fig 1 Solitary filling defect of 10 mm diameter due to metastasis within a medial external iliac lymph node of normal size in a 42 year-old patient Obliteration of the intermediary sinuses confirmed by histology

the first days of treatment and in 24 cases when a recurrence was suggested At lymphography a positive diagnosis of malignant metastatic involvement was made only when solitary or multiple well demarcated filling defects of at least 10 mm diameter in regional lymph nodes were present (Figs 1, 2) Obstruction of the lymphatic circulation was an additional finding indicating malignant involvement of the lymphatic system (Fig 3)

Results

Thirtyfive (21 per cent) of the 164 lymphographic examinations in the 158 cases were considered pathologic, 9 (5 5 per cent) possibly pathologic, and 120 (73 per cent) normal Four positive findings (10 per cent) were encountered in stage I (n = 39), 13 (19 per cent) in stage II (n = 68) and 18 (31 5 per cent) in the advanced stages III (n 44) and IV (n 7) (undetermined stage III to IV n = 6) (Table 1) In 23 lymphographies (66 per cent) the external iliac lymph nodes alone were invaded by metastases, in 5 (14 per cent) the aortic lymph nodes alone, and in 4 (11 per cent) both the iliac and aortic lymph nodes In 1 case with infiltration of the vulva the inguinal lymph nodes were involved, 2 cases had iliac and inguinal metastases, and 2 cases had microscopically confirmed metastases in obturator lymph nodes Malignant tissue was found in the supraclavicular lymph nodes in a patient with aortic lymph node involvement

The accuracy of the lymphographic diagnosis was evaluated in 135 cases, operative

Table 1

Metastases revealed by lymphography in 158 patients with carcinoma of the uterine cervix

Stage	No of cases	No of lymphographies	Primary tumour +	Primary tumour ?	Primary tumour −	Recurrence +	Recurrence ?	Recurrence −	Total +	Total ?	Total −
I	37	39	3	—	31	1	—	4	4 (10%)	—	35
II	66	68	9	3	47	4	—	5	13 (19%)	3	52
III	42	44	9	5	26	3	—	1	12 (27%)	5	27
IV	7	7	2	1	4	—	—	—	2	1	4
Undetermined (III–IV)	6	6	—	—	—	4	—	2	4	—	2
Total	158	164	23	9	108	12	—	12	35	9	120

\+ = metastases present
? = uncertain
− = no metastases

The actuarial method of BERKSON & GAGE (1950) was used to evaluate the survival rate

Altogether 164 lymphographies were carried out on 158 patients in 134 cases a combination of lymphography, cavography and urography and in 30 cases lymphography and urography In 18 cases the lymphography was conducted only unilaterally because of technical difficulties, in 6 patients it was repeated during the course of the disease In 78 cases lymphography was performed initially, in 62 cases during

Table 2

Accuracy of lymphographic diagnosis in 135 cases with carcinoma of the uterine cervix

Stage	No of lympho graphies	Correct: Operative and histologic findings	Correct: Clinical course	False positive: Histology	False positive: Clinical course	False negative: Histology	False negative: Clinical course
I	36	28	5	—	—	1	2
II	55	27	21	—	2	2	3
III	32	2	24	—	—	—	o (2 un certain)
IV	6	1	4	—	—	—	1
Undetermined (III–IV)	6	1	4	—	—	—	1
Total	135	59	58	—	2	3	13
		117 (86 7%)		2 (1 5%)		16 (11 8%)	

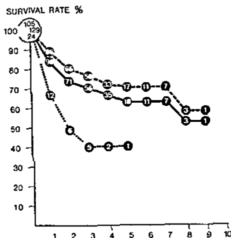


Fig 4 Survival rates of 129 patients with carcinoma of the uterine cervix all clinical stages 105 patients with negative lymphography 2 year survival rate 79 % 5 year survival rate 69 % 24 patients with pathologic lymphography 2 year survival rate 48 % 5 year survival rate 40 % Figures indicate number of patients alive Total number of cases (——) negative (---) and positive ( ) lymphography

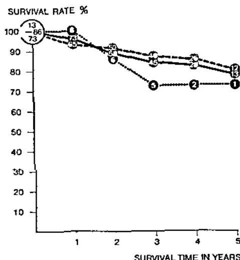


Fig 5 Survival rates of 86 patients with carcinoma of the uterine cervix stage I and II 73 patients with negative lymphography 2 year survival rate 92 % 5 year survival rate 80 %, 13 patients with positive lymphography 2 year survival rate 86 % Figures indicate number of patients alive Total number of cases (——) negative (---) and positive ( ) lymphography

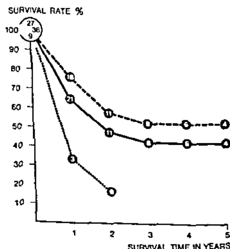


Fig 6 Survival rates of 36 patients with carcinoma of the uterine cervix, stage III 27 pa [illegible]

patients alive Total number of cases (——) negative (- -) and positive ( ) lymphography

graphy (n = 13) had a 2 year survival rate of 86 per cent (Fig 5) In stage III (n = 36) the 2 year survival rate was 58 per cent, the 5 year survival rate 52 per cent in the 27 patients with negative lymphography In 9 patients with pathologic lymphography the 2 year survival rate was 17 per cent (Fig 6) The survival rate was markedly



Fig 2



Fig 3

Fig 2 Multiple confluent filling defects within enlarged left aortic lymph nodes due to metastases in a 42-year-old patient Slight displacement of the left ureter

Fig 3 Large confluent filling defects in lymph nodes and obstruction of the lymphatic circulation in the right aortic area in a 61-year old patient No displacement of the right ureter

and histologic findings were available in 62 of these, and in 73 the clinical course of the disease was considered to confirm the evaluation Twenty-three patients had died within two years following the initial treatment and were therefore not included A correct lymphographic diagnosis was made in 87 per cent, a false positive diagnosis in 1 5 per cent, and a false negative in 12 per cent (Table 2) The overall failure rate was therefore approximately 14 per cent

In 9 cases the lymphographic diagnosis was not conclusive, and only suggestive of malignancy, in 2 cases microscopy revealed a negative result The clinical course of the disease was uneventful in 2 cases, but malignant spread was suggested in 2 cases In 3 patients the observation time was too short for evaluation

Cavography did not reveal abnormality in all the 103 cases of stages I and II In advanced stages III and IV pathology was present in about 25 per cent of the cases In one patient metastatic spread to the right aortic lymph nodes was diagnosed only by cavography

The survival rate of carcinoma of the uterine cervix was estimated in 129 patients of all clinical stages with malignant disease at first presentation (86 cases stages I and II, 36 cases stage III, 7 cases stage IV) The 2-year survival rate was 79 per cent, the 5-year survival rate 69 per cent, for the 105 cases with negative lymphography For the 24 patients with abnormal lymphography the 2-year and 5-year survival rates were 48 and 40 per cent, respectively (Fig 4) In clinical stage I and II carcinoma (n = 86) the survival rate of patients with negative lymphography (n = 73) was for two years 92 per cent and for five years 80 per cent Patients with positive lympho-

necessary for a conclusive diagnosis of lymph node metastases Obliteration and collateral circulation are definite signs of lymphatic obstruction Delayed contrast filling of lymph vessels 24 hours following injection of contrast medium is mainly due to technical factors and must not be regarded as a sign of lymphatic obstruction Increase of lymph node size or a globular shape of lymph nodes are unreliable signs of metastases Displacement of lymphatics and lymph nodes cannot be regarded as pathognomonic for malignancy, since elongation and tortuosity of the concomitant arteries frequently lead to displacement of the iliac and aortic lymphatic systems

Applying these strict diagnostic criteria the rate of false positive diagnoses is minimal It is thus possible to rely on a positive lymphography and select the appropriate therapeutic means Early metastatic involvement of lymph nodes is however difficult to detect The limited resolution of lymphography, the great variation of physiologic filling defects of the lymph nodes and the failure to demonstrate medially localized pelvic lymph nodes, often first involved, restrict the value of a negative lymphography Consequently, a negative lymphography does not exclude metastatic foci in regional lymph nodes of the uterine cervix This fact has always to be borne in mind when determining therapeutic options Absence of malignant involvement of regional lymph nodes as judged by lymphography does however exclude advanced disease

The prognostic outlook is generally better in patients with negative lymphography than in those with demonstrable malignant lymph node involvement The present results that the survival rate of patients with negative lymphography is improved by 50 per cent, compared with patients with positive lymphograms, are similar to those of DAVIDSON & VAN LIEROP Although the material is relatively small and the observation time short, it is however interesting to analyse this result when applied to the clinical stages In stages I and II positive lymphographic findings did not affect the survival rate to the same extent as in patients with stage III This fact may at least be partially attributed to the more accurate and selective therapeutic approach—surgery, irradiation, or both combined—according to the lymphographic findings

Acknowledgements

The assistance given by the Departments of Therapeutic Radiology (Prof A Zuppinger), Gynaecology and Obstetrics (Prof M Berger) and Pathology (Prof H Cottier) is gratefully acknowledged

SUMMARY

[illegible] lymphography does not alter the survival rate in clinical stages I and II, probably due to the more accurate and selective therapeutic approach induced by lymphography In stage III the 2 year survival rate of patients with negative findings is 58 per cent compared to *only* 17 per cent in case of positive lymphographic findings

lower in patients with recurrent disease Of the 24 patients concerned none survived the 2-year limit when lymphography was positive The 2-year survival rate was 36 per cent, the 5-year survival rate 9 per cent in recurrences with negative lymphography.

Discussion

The 10 per cent frequency of positive lymphographic findings in the cases of stage I carcinoma of the uterine cervix compares favourably with the results of other groups (KUNITSCH & HOLSTEN 1968, LEE et coll 1971, DAVIDSON & VAN LIEROP 1972, DOUGLAS et coll 1972) A 25 per cent frequency rate of positive lymphography in stage I has been reported by others (RÜTTIMANN 1966, GERTEIS 1967, BÉLANGER 1971) Histology of removed lymph nodes demonstrates malignant involvement in 18 8 per cent (REIFFENSTUHL 1967), ranging from 8 5 to 35 9 per cent (MITANI et coll 1962) The variation of these results may however be explained by different surgical and microscopic techniques as well as the accuracy of the clinical grading

In stage III carcinoma a frequency rate of 45 to 65 per cent of malignant involvement of the regional lymph nodes demonstrated by lymphography has been reported by many (RÜTTIMANN, GERTEIS, KUNITSCH & HOLSTEN, DOUGLAS et coll) In the present material the initial rate of 27 per cent must however be changed to 39 per cent, because in retrospect 3 out of 27 examinations have to be judged as false negatives and 2 of the uncertain cases as positives

Great discrepancies in the diagnostic accuracy of lymphography in carcinoma of the uterine cervix have been published, ranging from 50 (REIFFENSTUHL, DARGENT 1970) to 96 per cent (GERTEIS) The present failure rate of 14 per cent in this series confirms the accuracy rate of 85 per cent in the report presented ten years ago based upon *another material (FUCHS & BÖÖK-HEDERSTRÖM) Accuracy rates of the same* order have since been published by several authors (MOULONGUET-DOLERIS et coll 1961, KRITTER et coll 1962, PICARD 1962, ARVAY & PICARD 1963, VIAMONTE et coll 1963, AVERETTE et coll 1964, DOLAN 1964, FISCHER & THORNBURY 1965, CHAVANNE et coll 1967, JANISCH & WAGENBICHLER 1968, WOLFF et coll 1968, FUCHS et coll 1969, LEE et coll 1971, PIVER et coll 1971) In an extensive investigation comparing lymphography and histology of 2 456 lymph nodes in 111 operated patients, KINDERMANN et coll (1970) were able to reach an accuracy rate of 90 per cent In 1 case a false positive, in 10 cases a false negative diagnosis was made These findings are similar to the 90 per cent accuracy rate in our series of 41 cases with microscopic confirmation of the lymphographic results As a consequence, an accuracy rate of 85 to 90 per cent may be expected in lymphography of the uterine cervix when strict diagnostic criteria are applied Solitary or multiple well-demarcated filling defects with a minimal diameter *of 10 mm in regional lymph nodes are* diagnostic for metastatic foci Filling defects of smaller size do not have the same diagnostic significance In these cases additional signs of obstruction of the lymph circulation are

GERTEIS W The frequency of metastases in carcinoma of the cervix and the corpus Progress in lymphology, p 209 Thieme Verlag, Stuttgart 1967

JANISCH H und WAGENBICHLER P Lymphographie—diagnostische und therapeutische Hilfsmethoden Wien klin Wschr 80 (1968), 173

KINDERMANN G, GERTEIS W und WEISHAAR J Was leistet die Lymphographie in der Erkennung von Metastasen beim Cervixcarcinom? Geburtsh u Frauenheilk 30 (1970), 444

KRITTER H, ARVAY N, PICARD J D et MANLOT G La lymphographie dans le cancer du col uterin Ann Radiol 5 (1962), 55

KUNITSCH G und HOLSTEN D R Erfahrungsbericht uber 429 Lymphographien bei Geschwulstkranken Med Welt 4 (1968), 239

LEE K F, GREENING R, KRAMER S, HAHN G A, KURODA K, LIN S-R and KOSLOW W W The value of pelvic venography and lymphography in the clinical staging of carcinoma of the uterine cervix Amer J Roentgenol 111 (1971), 284

MITANI Y, FUJII J I, MIYAMURA M, JSHIZU S I and MATSUKADO M Lymph node metastases of carcinoma of the uterine cervix Amer J Obstet Gynec 83 (1962) 515

MOULONGUET DOLÉRIS P, ARVAY N, PICARD J D et MANLOT G La lymphographie Technique indications et resultats J Radiol Électrol 42 (1961), 281

PICARD J D La lymphographie en gynecologie Ann Chir 25 (1962), 1

PIVER M S, WALLACE S and CASTRO J R The accuracy of lymphangiography in carcinoma of the uterine cervix Amer J Roentgenol 111 (1971), 278

REIFFENSTUHL G Das Lymphknotenproblem beim Carcinoma colli uteri und die Lymphirradiatio pelvis Urban & Schwarzenberg Munchen, Berlin, Wien 1967

RÜTTIMANN A (Hrsg) Progress in Lymphology, p 225 Thieme Verlag, Stuttgart 1966, 1967

VIAMONTE M, ALTMAN D, PARKS R, BLUM E, BEVILAQUA M and RECHER L Radiographic pathologic correlation in the interpretation of lymphangioadenograms Radiology 80 (1963), 903

WOLFF J P, MARKOVITS P, GASQUET CH, GRELLET J et DABLANC H Valeur de la lymphographie dans les cancers du col uterin au stade I Rev franç Gynec 63 (1968), 169

GENERAL ASSEMBLY OF FIGO, NEW YORK Classification and staging of malignant tumors in the female pelvis Acta obstet gynec scand 50 (1971), 1

ZUSAMMENFASSUNG

Lymphographie wurde bei einer Gruppe von 158 Patienten mit einem Karzinom der *Cervix uteri* ausgeführt Die diagnostische Genauigkeits-Rate von 85% stimmt gut mit den Ergebnissen einer ähnlichen zehn Jahre zuvor vorgenommenen Untersuchung überein Eine positive Lymphographie beeinflusst nicht die Überlebensrate in den klinischen Stadien I und II, wahrscheinlich wegen des durch die Lymphographie veranlassten genaueren, selektiven therapeutischen Vorgehens Beim Stadium III betrug die 2-Jahres-Überlebensrate der Patienten mit negativen lymphographischen Befunden 58%, bei positiven nur 17%

RÉSUMÉ

Une lymphographie a été pratiquée sur une série de 158 malades atteintes de cancer du col de l'utérus Le taux d'exactitude diagnostique de 85% se compare favorablement avec les résultats d'une étude similaire faite il y a 10 ans Une lymphographie positive ne modifie pas le taux de survie aux stades cliniques I et II probablement parce que la lymphographie permet d'établir un traitement plus précis et plus sélectif Au stade III le taux de survie des malades présentant des signes lymphographiques négatifs est de 58%, en cas de lymphographie positive de 17%

REFERENCES

ARVAY N et PICARD J D La lymphographie Etude radiologique et clinique des voies lymphatiques normales et pathologiques Masson & Cie, Paris 1963

AVERETTE H E, HUDSON R C and FERGUSON J H Lymphangioadenography Applications in the study and management of gynecologic cancer Cancer 17 (1964), 1093

BÉLANGER R Les avantages de la lymphographie dans la conduite thérapeutique et dans la recherche des métastases ganglionnaires du cancer du col utérin Laval med 42 (1971), 859

BERKSON J and GAGE R P Calculation of survival rates for cancer Proc Mayo Clin 25 (1950), 270

CHAVANNE G, PELLIER D et VALATTE M La lymphographie dans les stades I et II du cancer du col utérin Étude de 150 cas opérés et vérifiés histologiquement J Radiol Électrol 48 (1967), 137

DARGENT D Place actuelle de la lymphographie dans le diagnostic d extension du cancer cervico-utérin et dans les indications thérapeutiques tirées de l'existence de cette affection Minerva ginec 22 (1970), 764

DAVIDSON J W and VAN LIEROP M J Lymphography and prognosis in carcinoma of the cervix Amer J Obstet Gynec 112 (1972) 669

[illegible] l cancer Surg Gynec Obstet 118 (1964), 1286

[illegible] BAKER J W Lymphography in carcinoma of the [illegible]

FISCHER H W and THORNBURY J R Lymphangiography in the diagnosis of malignant neoplasms Progress in clinical cancer, p 213 Grune & Stratton, New York 1965

FUCHS W A and BÖÖK-HEDERSTRÖM G Lymphography in the diagnosis of metastases with special reference to the carcinoma of the uterine cervix Acta radiol Diagnosis 2 (1964), 161

— DAVIDSON J W and FISCHER H W Lymphography in cancer Recent results in cancer research Vol 23 Springer Verlag, New York, Heidelberg, Berlin 1969



Fig 1 Craniocaudal projection of the breast Subareolar inhomogeneous tumour outlined by an indistinct capsule

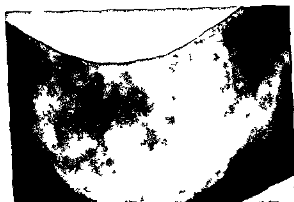


Fig 2 Craniocaudal projection Central inhomogeneous tumour surrounded by a distinct capsule

fatty tissue (Fig 3) The epithelium of the ducts was cylindrical and with a conspicuous clear-cell appearance

Case 2 A 54-year old woman had had retraction of the left nipple for a number of years and a short time bef [illegible]
matous t [illegible]
Mamm [illegible]
rounded [illegible] *capsule* was found The tumour was inhomogeneous with fatty tissue and several areas with an appearance similar to the surrounding glandular tissue There were no apparent microcalcifications

Operation An encapsulated tumour was removed Microscopically the tumour was built of fatty tissue interspersed with islands of glandular tissue The epithelial ducts were covered by a low epithelium in some places in the fatty tissue in others in a rather abundant loose connective tissue (Fig 4)

Discussion

Both patients had for a number of years had retraction of the nipple but whether this was caused by the tumour is uncertain No other symptoms were encountered, however A disproportion between the clinical and radiographic size of the tumour existed

The radiographic appearance was that of an encapsulated inhomogeneous tumour

FROM THE DEPARTMENTS OF RADIOLOGY AND PATHOLOGY, ODENSE UNIVERSITY HOSPITAL, DK-5000 ODENSE, DENMARK

ADENOLIPOMA MAMMAE

U DYREBORG and H STARKLINT

Lipoma of the breast is presumably rare The exact frequency is unknown, as it seldom produces symptoms and is seldom palpable A special type of tumour containing fatty and glandular tissue has been described by SPALDING (1945) and TEDESCHI (1948) and termed mammary adenolipoma

In the general available atlas and textbooks on radiography of the breast (EGAN 1972, GERSHON-COHEN 1970, RASMUSSEN 1969, WILLEMIN 1972) no illustrations or descriptions of mammary adenolipoma appear, but DURSO (1971) has reported one case Two cases have been encountered at this hospital within one year, however, and as mammary radiography is nowadays more frequently used it seems appropriate to draw attention to the existence of adenolipoma and its radiographic appearance

Case reports

Case 1 A 52-year-old, otherwise healthy woman had for approximately 30 years had a non symptomatic retraction of the right nipple A thickened and irregular gland was palpated but no isolated tumour

Mammary radiography (Fig 1) A 6 cm × 4 cm × 7 cm subareolar tumour surrounded by a capsule was found The tumour consisted of fat and numerous islands of strings of a tissue with the appearance of ordinary glandular tissue and without microcalcifications

Operation A well defined subareolarly located tumour was removed Macroscopically, nearly all the tumour seemed to consist of fatty tissue Microscopy revealed islands of epithelial ducts lying in a rather firm connective tissue and a few epithelial ducts lying in the

Submitted for publication 12 September 1974



Fig 1 Craniocaudal projection of the breast Subareolar inhomogeneous tumour outlined by an indistinct capsule



Fig 2 Craniocaudal projection Central inhomogeneous tumour surrounded by a distinct capsule

fatty tissue (Fig 3) The epithelium of the ducts was cylindrical and with a conspicuous 'clear-cell' appearance

Case 2 A 54-year-old woman had had retraction of the left nipple for a number of years and a short time before admission pains located to the sternum A well defined, soft, lipomatous tumour, the size of a child s fist was palpated

Mammary radiography (Fig 2) A 10 cm × 10 cm × 10 cm well-defined tumour surrounded by a thin capsule was found The tumour was inhomogeneous with fatty tissue and several areas with an appearance similar to the surrounding glandular tissue There were no apparent microcalcifications

Operation An encapsulated tumour was removed Microscopically, the tumour was built of fatty tissue interspersed with islands of glandular tissue The epithelial ducts were covered by a low epithelium, in some places in the fatty tissue, in others in a rather abundant loose connective tissue (Fig 4)

Discussion

Both patients had, for a number of years, had retraction of the nipple, but whether this was caused by the tumour is uncertain No other symptoms were encountered, however A disproportion between the clinical and radiographic size of the tumour existed

The radiographic appearance was that of an encapsulated inhomogeneous tumour

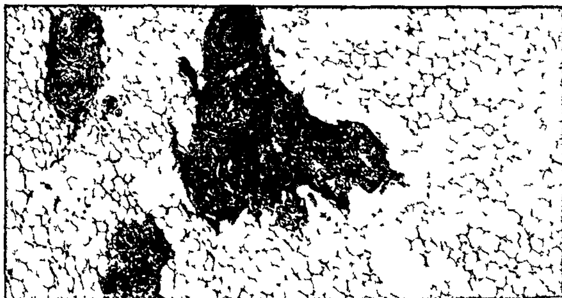


Fig 3 Same case as in fig 1 Microscopy Islands of glandular tissue containing epithelial ducts only Clear cells of the epithelium are prominent No glandular acini (Haematoxylin-eosin × 38)

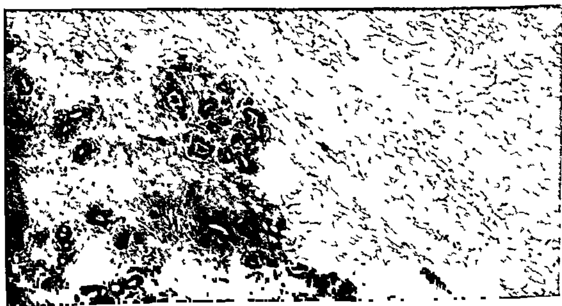


Fig 4 Same case as in fig 2 Microscopy Fibrosis of the central part In the margin of the fibrosis a juxtaposition of glandular epithelium and fat (Haematoxylin-eosin × 38)

consisting of fatty tissue and irregular areas not differing from glandular tissue as in the case reported by DURSO

The inhomogeneous appearance separates the adenolipoma from the pure lipoma and other tumours rich in fat such as galactocele or colostrolipocele, which are homogeneous Fibroadenomas and cysts are homogeneous as well, but have a higher at

tenuation of the radiation than the lipomatous ones The capsule separates adenolipoma and the other tumours mentioned from the malignant tumours

Only few cases have been published in the pathologic literature within recent decades

SPALDING (1945) reported a case of a 56-year-old woman with an encapsulated tumour, which peripherally consisted of fatty tissue with islands of glandular tissue and centrally with varying degrees of fibrosis around glandular elements This description corresponds closely to the present two cases The central fibrosis was thought to represent a differentiation or a maturation in this part of the tumour, a view shared by TEDESCHI

SPALDING considered the tumour to be a mixed tumour because of the fact that epithelial tissue was evenly spread and because no remains of interlobular loose connective tissue were found, which could have been expected if the original glandular tissue had been infiltrated with fat

In connection with a description of pure lipoma of the breast HALPERT & YOUNG (1946) classified SPALDING's adenolipoma as lipomatosis only, comparing it with fatty infiltration of the myocardium or the pancreas

TEDESCHI in his material found two tumours with an appearance similar to those presented by SPALDING but he suggested that they should be classified as remains of the embryonic breast because of the lack of glandular acini and the close relationship between epithelial ducts and fatty tissue

CUTLER (1962) and HAAGENSEN (1971) considered the tumours as an entity and of rare occurrence

The question of whether it is a lipoma infiltrating the glandular tissue or whether it is a concurrent proliferation of the two elements cannot be further elucidated from the present cases The composition of the tumour corresponds closely to the normal surroundings, a fact which may explain the discrepancy between the clinical and the radiographic finding

The diagnosis depends on the characteristic radiographic appearance Particularly, the recognition of a capsule is essential in the morphologic classification

SUMMARY

[illegible] the [illegible] the [illegible] particular tumour.

ZUSAMMENFASSUNG

Es werden zwei Falle von Brust Adenolipomen beschrieben Diese Falle und die Beschreibungen in der Literatur deuten darauf hin, dass das rontgenologische Bild charakteristisch und wichtig fur die Diagnostik und Klassifikation dieses besonderen Tumors ist



Fig 3 Same case as in fig 1 Microscopy Islands of glan only Clear cells of the epithelium are prominent No glandu

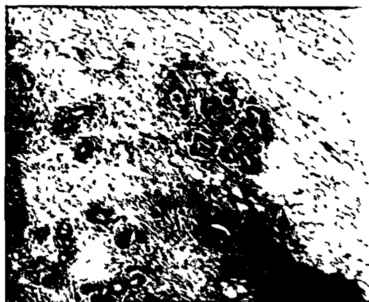


Fig 4 Same case as in fig 2 Microscopy Fibrosis of the central a juxtaposition of glandular elium and fat (Haematoxylin-

consistin fatty tissue a
in the ca rted by DUR
The inh neous appea
and other t rich in fat s
geneous Fi omas and c

tenuation of the radiation than the lipomatous ones The capsule separates adenolipoma and the other tumours mentioned from the malignant tumours

Only few cases have been published in the pathologic literature within recent decades

SPALDING (1945) reported a case of a 56-year-old woman with an encapsulated tumour, which peripherally consisted of fatty tissue with islands of glandular tissue and centrally with varying degrees of fibrosis around glandular elements This description corresponds closely to the present two cases The central fibrosis was thought to represent a differentiation or a maturation in this part of the tumour, a view shared by TEDESCHI

SPALDING considered the tumour to be a mixed tumour because of the fact that epithelial tissue was evenly spread and because no remains of interlobular loose connective tissue were found, which could have been expected if the original glandular tissue had been infiltrated with fat

In connection with a description of pure lipoma of the breast HALPERT & YOUNG (1946) classified SPALDING's adenolipoma as lipomatosis only, comparing it with fatty infiltration of the myocardium or the pancreas

TEDESCHI in his material found two tumours with an appearance similar to those presented by SPALDING but he suggested that they should be classified as remains of the embryonic breast because of the lack of glandular acini and the close relationship between epithelial ducts and fatty tissue

CUTLER (1962) and HAAGENSEN (1971) considered the tumours as an entity and of rare occurrence

The question of whether it is a lipoma infiltrating the glandular tissue or whether it is a concurrent proliferation of the two elements cannot be further elucidated from the present cases The composition of the tumour corresponds closely to the normal surroundings, a fact which may explain the discrepancy between the clinical and the radiographic finding

The diagnosis depends on the characteristic radiographic appearance Particularly, the recognition of a capsule is essential in the morphologic classification

SUMMARY

Two cases of mammary adenolipoma are presented These cases and descriptions in the literature suggest that the radiographic appearance is characteristic and important in the diagnosis and classification of this particular tumour

ZUSAMMENFASSUNG

Es werden zwei Falle von Brust Adenolipomen beschrieben Diese Falle und die Beschreibungen in der Literatur deuten darauf hin dass das rontgenologische Bild charakteristisch und wichtig fur die Diagnostik und Klassifikation dieses besonderen Tumors ist

RÉSUMÉ

Présentation de deux cas d adénolipome mammaire Ces cas et les descriptions de la littérature font penser que l'aspect radiographique est caracteristique et important pour le diagnostic et la classification de ces tumeurs particulieres

REFERENCES

CUTLER M Tumours of the breast J B Lippincott Co, Philadelphia 1962

DURSO E A Mammographic findings in adenolipoma J Amer med Ass 218 (1971) 886

EGAN R L Mammography Second edition Charles C Thomas, Springfield Illinois 1972

GERSHON COHEN J Atlas of mammography Springer-Verlag, Berlin-Heidelberg-New York 1970

HAAGENSEN C D Diseases of the breast Second edition W B Saunders, Philadelphia 1971

HALPERT B and YOUNG M O Lipoma of the mammary gland Arch Path 42 (1946) 641

RASMUSSEN T Mammografi (In Danish) Author-publisher Hjorring 1969

SPALDING J E Adenolipoma and lipoma of the breast Guy s Hosp Rep 94 (1945), 80

TEDESCHI C G Mammary lipoma Arch Path 46 (1948), 386

WILLEMIN A Les images mammographiques S Karger, Paris 1972

FROM THE DEPARTMENT OF NEURORADIOLOGY P, THE E N T DEPARTMENT AND THE DEPARTMENT OF RADIOLOGY R, THE RADIUM CENTRE, MUNICIPAL HOSPITAL, UNIVERSITY OF ÅRHUS, AND THE INSTITUTE OF PATHOLOGY, COUNTY HOSPITAL OF ÅRHUS, UNIVERSITY OF ÅRHUS, DK 8000 ÅRHUS, DENMARK

RADIOGRAPHY OF LARYNGEAL CARCINOMA

Assessment of value

J JØRGENSEN, K JØRGENSEN, O MYHRE JENSEN, J TH JENSEN, O ELBRØND and A P ANDERSEN

The value of radiographic examination of laryngeal carcinoma has always been much in dispute Therefore, an attempt was made to assess the diagnostic accuracy, to define the indications and to evaluate the significance of radiography to the T classification as well as its therapeutic consequences

Material and Methods

During the period January 1972 to May 1973 a total of 74 radiographic examinations were performed on 71 patients with 64 primary tumours and 10 [illegible]

[illegible] geal skeleton However they could not be carried out in all cases (Table 1)

Submitted for publication 20 February 1974

Table 1

Distribution of the radiographic methods used in 74 examinations

	Performed	Not performed	Technically unsatisfactory
Conventional radiography	73	1	4
Tomography	74	0	1
Cinematography	62	12	2
Low voltage radiography	56	18	0

Technique. Both at conventional radiography and linear tomography, a p and lateral views were exposed during phonation (the vowel e) and during free inspiration with high-voltage technique and using Cu filter (BEIQUE & ROTENBERG 1965, MAQUIRE 1966, HEMMINGSSON 1972, HILL 1973) Cinematography was carried out with a 35 mm camera, 24 frames/s The a p views were exposed at a potential up to 110 kV In all cases films were taken during a barium swallow

Low-voltage exposures were made to demonstrate laryngeal calcifications using a mammography apparatus and high-definition screens Laryngography was not performed although it is assumed to be superior to other methods, especially in detecting small tumours (HEMMINGSSON 1972)

On the basis of these examinations a radiographic diagnosis was made including a T classification according to the AJC and UICC rules (1972) for the TNM classification of laryngeal carcinoma (Table 2)

Indirect laryngoscopy was performed in all cases both by a radiotherapist and an otolaryngologist and direct microlaryngoscopy in cases in which it has not been performed before admission or in which its result was uncertain The clinical findings were then compared with the primary radiographic diagnosis

Primary tumours The age distribution of the 64 cases was

Years	40–49	50–59	60–69	70–79	80
No of cases	4	22	27	9	2

All tumours were epidermoid carcinomas, including 4 carcinomas *in situ*

The radiographic and clinical results are compared in Table 3 The classification of the T1 and T2 groups (52 cases) is based exclusively upon definite indirect and direct laryngoscopic findings Radiography revealed no factors that altered this classification

T1 and T2 Radiography indicated abnormality on the wrong side in 3 cases and in another 3 cases nothing abnormal was demonstrated (Table 3) All these tumours were very small and had been removed entirely or partially before admission In 3 cases only oedema was observed, possibly due to direct laryngoscopy a day or

Table 2

T-classification of 64 cases of primary carcinomas of the larynx

	Supraglottic	Glottic	Subglottic	Total
T1	4	30	0	34
T2	6	11	1	18
T3	1	6	0	7
T4	4	1	0	5
Total	15	48	1	64

two before radiography At radiography the tumours were classified in a less advanced stage than at the clinical examination in 8 cases, in one in a more advanced stage, the disagreements were small In 5 cases an incorrect report on the mobility of the cords was made at radiography

Even if radiography did not contribute to the T classification, it was of value in 3 cases Subglottic involvement was revealed in 2 cases with unsatisfactory laryngoscopy, partly because of subglottic oedema and partly because of papillomatosis In one case radiography disclosed that an intumescence in the plica ventricularis was caused by a multicystic process, possibly an internal laryngocele

T3 and T4 In these 12 cases the T classification was based upon laryngoscopy as well as radiography

In 3 cases the tumours were radiographically classified in a less advanced stage than at the clinical examination In 2 cases direct laryngoscopy could not be carried out due to heart disease and laryngeal stenosis The extent of the tumour was revealed at radiography which demonstrated that the tumour did not extend into the subglottis In one case of a very extensive tumour its distal extent could not be determined with certainty at laryngoscopy because of the narrow space and haemorrhage Radiography revealed that the tumour extended down to the uppermost part of the trachea In 2 cases destruction of the calcified cartilage was demonstrated on films exposed with low potential indicating deep growth (T4) Thus, in the T3 and T4 groups radiography was of decisive importance in the classification in 5 out of 12 cases

Recurrences Ten patients were admitted for treatment of recurrences; total laryngectomy was performed in eight and partial laryngectomy in two The operative specimens were examined macro- and microscopically. In all cases the extent of the tumour was accurately recorded

Rad...

th [illegible]

[illegible] direct laryngo-

Table 3

Comparison between radiographic and clinical staging in 64 primary carcinomas of the larynx

Radiography	Clinical stage			
	T1	T2	T3	T4
Complete agreement	21	8	5	4
Wrong lateralisation	3			
Normal appearances	3			
Oedema	1	2		
Radiographic staging less advanced than clinical	3	5	2	1
Radiographic staging more advanced than clinical	1			
Radiographic staging more advanced than clinical and incorrect information about mobility of the true cords	1			
Wrong lateralisation and incorrect information about mobility of the true cords	1			
Incorrect information about the mobility of the true cords	0	3		
Total	34	18	7	5

scopy with biopsy of the tumour had been performed on the preceding day, in another case of a small recurrence radiography was inaccurate

Laryngoscopy was misleading in 3 cases, whereas radiography was correct as later confirmed at pathology

In the first case subglottic involvement was not found at direct laryngoscopy and in the second case a tumour ulceration on the posterior aspect of the epiglottis was not observed In the third case direct laryngoscopy indicated recurrence, although biopsy had been negative Radiography before the laryngoscopy revealed only oedema Total laryngectomy was performed despite the negative biopsy as the patient had respiratory difficulties and severe pain At pathologic examination of the laryngeal specimen no malignancy was found, only severe oedema

Discussion

This analysis of 64 primary cases of laryngeal carcinoma has indicated that in more than 75 per cent of the material radiography did not contribute to the diagnosis With the radiographic methods used it was impossible precisely to establish the sub- or supraglottic extent of small tumours Thus, routine radiography is not indicated for the large group of primary laryngeal carcinomas of stages T1 and T2 Radiography is indicated if direct laryngoscopy is not feasible but other diagnostic procedures, such as e g transconioscopy (MÅRTENSSON 1967, SORENSEN 1970) may also be indicated in such cases Only relatively extensive sub- or supraglottic involvement can be demonstrated at radiography However this may be of significance for radiation therapy in selecting the size of the field of irradiation and the direction

of the rays On the other hand, radiography is of essential importance in classifying the T3 and T4 cases It should be emphasized, in particular, that the demonstration of destruction of cartilage by low-voltage exposures may transfer a case from the T3 to the T4 group This may have therapeutic consequences, i e. leading to combined irradiation and surgery (GOLDMAN et coll 1972)

Radiography was of value in the 10 recurrences Thus, radiography is always indicated in cases of recurrent tumours before operation to establish the distal extent of the tumour.

Low voltage films were only taken in 3 of the 10 recurrences It is evident that this technique gives information about deep infiltration which otherwise hardly can be obtained by radiographic methods. A prerequisite is that the cartilage to some extent is calcified, however, this is generally the case at the age when malignant tumours usually appear

SUMMARY

The value of various radiographic methods (except laryngography) in laryngeal carcinoma was assessed in a material of 71 patients Radiography proved of no value in T1 and T2 tumours if a satisfactory clinical examination could be performed but gave valuable information in recurrences as well as in T3 and T4 cases

ZUSAMMENFASSUNG

Der Wert verschiedener röntgenolog ...
phi ...
Ro ...
stel ... klinische Untersuchung vorgenommen werden konnte, gab jedoch wertvolle Informationen bei Recidiven sowie bei T3 und T4 Fällen

RÉSUMÉ

La valeur de différentes méthodes radiographiques (a l'exception de la laryngographie) dans le cancer du larynx a été étudiée sur une série de 71 patients La radiographie s'est montrée sans intérêt dans les tumeurs T1 et T2 quand on a pu faire un examen clinique satisfaisant, mais a donné des renseigenements utiles dans les recidives ainsi que dans les cas T3 et T4

REFERENCES

AJC American Joint Committee on Cancer Staging and End Results Reporting Clinical Staging System for Car ...
BEIQUE R A and ROTH ...
kilovoltage radiogra ... actical approach to high-
GAJEWSKI H und GER ...
Stuttgart 23 (1970), ... Radiologische Technik

GOLDMAN J L, ZAK F G, ROFFMAN J D and BIRKEN E A High dosage preoperative radiation and surgery for carcinoma of the larynx and laryngopharynx Ann Otol 81 (1972), 488

HEMMINGSSON A Roentgenologic examination of the larynx Acta radiol Diagnosis 12 (1972), 433

— Roentgenologic methods in examination of the larynx Acta radiol Diagnosis 12 (1972) 673

— and LUNDQVIST H Optimum photon energy in ordinary radiography of the larynx Acta radiol Diagnosis 12 (1972), 305

— JUNG B and LUNDQVIST H Soft tissue intensification in frontal roentgenography of the larynx Acta radiol Diagnosis 12 (1972), 593

HILL B J Radiology of the larynx Otolaryng Clin N Amer 6 (1973), 549

MAQUIRE G H *The larynx Simplified radiological examination using heavy filtration* and high voltage Radiology 87 (1966), 102

MÅRTENSSON B Transconioscopy A method for improvement of endolaryngeal diagnosis Pract oto rhino laryng 29 (1967) 217

OLOFSSON J, RENOUF J H P and VAN NOSTRAND A W P Laryngeal carcinoma Correlation of roentgenography and histopathology Amer J Roentgenol 117 (1973) 526

SORENSEN H Transconioscopy in laryngeal carcinoma Arch Otolaryng 92 (1970) 28

UICC Union Internationale Contre le Cancer, Geneva 1972

FROM THE DEPARTMENTS OF SURGERY I (DIRECTOR PROF L.-E GELIN) AND II (DIRECTOR PROF R ROMANUS) AND THE DEPARTMENTS OF DIAGNOSTIC RADIOLOGY I (DIRECTOR PROF O BARTLEY) AND III (DIRECTOR PROF C G HELANDER), SAHLGRENSKA SJUKHUSET, UNIVERSITY OF GOTHENBURG, S-413 45 GOTHENBURG, SWEDEN

EFFECTS OF INTRAARTERIAL INJECTION OF CONTRAST MEDIUM ON REGIONAL CIRCULATION IN SOFT TISSUE TRAUMA

D H LEWIS, J SANDEGÅRD, T SEEMAN and B E ZACHRISSON

The injection of water soluble contrast media into peripheral arteries causes an immediate vasodilatation This decrease in regional peripheral resistance results in an increase in regional blood flow (LINDGREN & TÖRNELL 1958, SAKO 1963, HILAL 1966, DELIUS & ERIKSON 1969, BOIJSEN et coll 1971) This immediate effect of contrast medium is trans[illegible] and [illegible] of the vasc[illegible] et coll (19[illegible] while MOT[illegible] & L[illegible] (1970) were unable to reveal such an effect

In addition to the flow increasing effect, the contrast medium has toxic properties on the microcirculation, resulting in injury to the endothelium, to the vascular smooth muscle and to the cellular elements of the blood, sometimes resulting in thrombus formation (WIEDEMAN 1963, ALMÉN & WIEDEMAN 1968, BRÅNEMARK et coll [illegible]

Tr[illegible] increase of blooc[illegible] (L[illegible], LEWIS & LIM 1970) In order to

Submitted for publication 28 March 1974

Table 1

Arterial flow in relation to end of injection of contrast medium determined in five dogs examined before and after the trauma Time in seconds

	Before	1 minute	10 minutes	30 minutes	60 minutes	120 minutes	180 minutes
Traumatized side							
Onset of flow increase	5 8 (4 0–8 0)	3 7 (2 0–5 0)	5 8 (5 5–7 0)	5 7 (5 0–6 5)	6 0 (2 8–8 0)	6 5 (6 0–8 0)	4 6 (4 0–5 0)
Maximum of flow	23 4 (16–41)	11 2 (10–15)	16 4 (15–18)	16 4 (15–19)	18 9 (15–24)	20 5 (17–25)	19 0 (17–22)
Maximum flow in per cent of preinjection value	*586* (202–760)	*238* (157–314)	*311* (217–433)	*350* (212–590)	*429* (207–895)	*424* (380–455)	*311* (224–365)
Duration of flow increase	112 (80–140)	109 (75–120)	129 (85–180)	133 (75–180)	116 (70–140)	124 (85–180)	136 (90–180)
Non traumatized side							
Onset of flow increase	5 7 (4 0–8 0)	6 3 (5 0–8 0)	7 9 (7 0–10 0)	7 6 (6 5–9 0)	7 7 (7 0–9 0)	7 2 (6 0–9 0)	4 7 (4 0–5 0)
Maximum of flow	22 4 (16–24)	23 0 (20–25)	24 0 (18–27)	21 7 (17–26)	23 0 (22–24)	23 5 (20–26)	20 3 (17–25)
Maximum flow in per cent of preinjection value	*502* (190–724)	*423* (334–500)	*635* (150–1 150)	*565* (144–1 130)	*501* (180–975)	*527* (164–1 125)	*320* (129 550)
Duration of flow increase	112 (80–140)	97 (75 120)	113 (70–180)	106 (75 120)	99 (70–130)	104 (85–120)	106 (90–120)
Delay of non traumatized flow maximum in relation to traumatized		11 8	7 6	5 3	4 1	3 0	1 2

Evaluation of Angiography On the films, determinations of transit time of contrast medium were made between two defined levels (GREITZ 1956) In all estimations the zero level (time 0) on the film was chosen as the earliest visible filling of the external iliac artery at the origin of the deep femoral artery The transit time of medium in the femoral artery was thus defined as the time interval between zero level and the earliest filling of the caudal femoral artery The time interval between zero level and the earliest filling of peripheral arteries was estimated in two regions of the thigh, anteriorly and in the adductor region (arterial filling phases) In these regions the time interval necessary for the earliest filling of the veins was demonstrated in a similar way (Table 2) *A more detailed report on the angiographic results in* soft tissue trauma is given by SANDEGÅRD & ZACHRISSON (1975 b)

Table 2

Transit time of contrast medium in seconds estimated on films in four dogs before and after contusion trauma

	Before trauma	1 minute	10 minutes	30 minutes	60 minutes
Traumatized side					
Femoral artery	3.0 (2.5–3.5)	1.3 (1.0–1.5)	2.6 (2.5–3.0)	3.0 (2.5–4.0)	4.3 (3.5–5.5)
Arterial filling phase	5.9 (5.5–6.0)	3.3 (3.0–3.5)	5.0 (4.5–5.5)	6.0 (5.0–7.0)	7.8 (6.0–11.0)
Earliest venous filling	10.0 (7.5–11.5)	4.4 (3.5–6.5)	5.5 (4.5–6.5)	7.2 (5.5–8.0)	9.5 (7.0–14.0)
Non traumatized side					
Femoral artery	3.0 (2.0–3.5)	3.9 (3.0–5.5)	4.3 (4.0–4.5)	4.1 (2.5–6.0)	4.0 (3.5–4.5)
Arterial filling phase	6.4 (5.5–7.0)	7.8 (5.0–11.5)	6.9 (6.0–7.5)	7.8 (7.0–9.0)	6.3 (6.0–6.5)
Earliest venous filling	10.0 (7.5–11.5)	11.5 (7.0–14.5)	13.1 (11.0–15.0)	13.4 (10.5–18.0)	11.5 (7.5–15.0)

Results

Before trauma In the three dogs in which simultaneous hemodynamic registration and angiography was performed, the following results were obtained The end of each injection was followed by a biphasic flow response consisting of either no change or an initial decrease, generally not exceeding 10 per cent of the pre injection value This phase lasted an average of 4 to 6 s and was followed by a marked transient increase of flow, reaching its maximum at a mean 22 to 23 s after end of injection (Fig 1, Table 1) The flow increasing effect of the contrast medium was no longer seen approximately 110 to 120 s after end of injection The medium also caused a transient minor lowering of arterial pressure, being lowest slightly before the maximum flow increase Before trauma the onset and magnitude of this flow increase appeared in a uniform way in the two limbs (Figs 1, 2) Relating the flow changes to the timing of the films, revealed that the filling of the peripheral arteries appeared before the flow increasing effect of the contrast medium An increase of flow was registered when the medium on the films had reached the veins The maximum increase of flow occurred when hardly any contrast medium was observed in the arteries The same flow response was registered in all animals in which blood flow measurements were performed

The two groups examined before trauma were compared In the first group, with flow measurements only, the period between the injection and the flow increasing effect of contrast medium was determined In the second group, with angiography

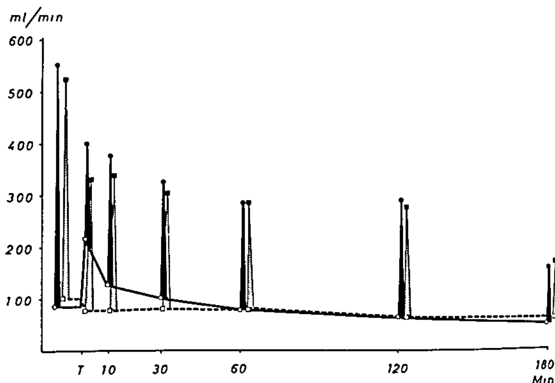


Fig 2 Mean arterial blood flow before and at different intervals following contusion trauma (T) in the traumatized O—O and non traumatized □---□ leg The filled symbols give the transient increase of flow following injection of contrast medium (Traumatized side = black bars and non traumatized side = hatched bars) Following the trauma this response to contrast medium is transiently reduced on the traumatized side

only, the periods between injection and the different angiographic phases were determined It appeared that the period of informative arterial phase was shorter than the period between injection and the flow increasing effect of the contrast medium

Thus, the results in these two separate series were identical to those obtained in the animals with simultaneous angiography and flow measurements The changes of arterial flow in relation to the injection of contrast medium are presented in Table 1 and the transit time on the films in Table 2

After trauma One minute after trauma the blood flow on the traumatized side was slightly more than double the pre-trauma values (Fig 2) The injection of contrast medium at this phase caused a further increase of blood flow amounting to approximately 240 per cent of values immediately before the injection (Table 1) The relative flow increasing effect of the medium was thus less than before trauma The duration of the flow increasing effect was only slightly shortened as compared to the pre-trauma value Following trauma the blood flow on the non-traumatized side was slightly lower than before The injection of contrast medium on this side caused an increase of blood flow, amounting to approximately 420 per cent of the

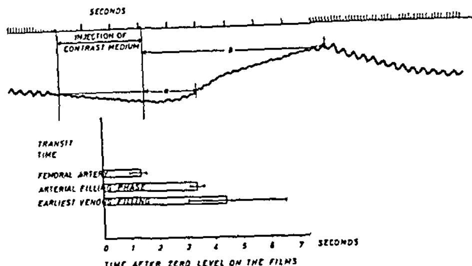


Fig 3 Recording of arterial flow with the earliest onset of flow change following contrast medium injection 1 min after trauma Below the registration of transit time in four dogs (mean ⊓ and range ⊢⊣) The zero level on the [illegible] 12 seconds later The informative arterial phases on the films occur within the first phase (a)

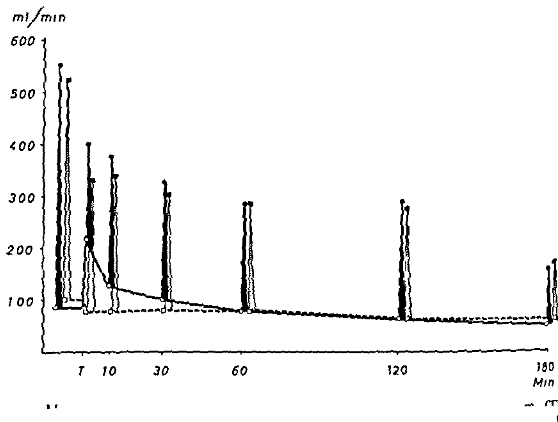
values immediately before injection The duration of the flow increase was slightly reduced compared with the pre trauma value

The flow increase following injection of contrast medium appeared approximately 12 seconds earlier on the traumatized side than on the non-traumatized side (Table 1)

In the dogs in which angiography only was performed, a marked decrease of transit time, indicating increase of blood flow was registered 1 min after trauma (Table 2)

Comparison of these dogs with those in which flow measurements only were performed revealed at this phase a close agreement with the findings in the dogs with simultaneous angiography and blood flow measurements after compression trauma Thus also at this phase the flow-increasing effect of medium appeared mainly after the arterial filling phase (Fig 3)

In examinations 10, 30, 60, 120 and 180 min after trauma, the blood flow on the traumatized side gradually decreased compared with 1 minute after trauma and approached the values registered on the non-traumatized side The injection of contrast medium caused successively increasing responses on the traumatized side, whereas on the non-traumatized side the responses were essentially unchanged compared with the values obtained 1 min after trauma (Fig 2) Corresponding to the flow increase after medium injection, the calculated peripheral resistance of the



only, the periods between injection and the different angiographic phases were determined It appeared that the period of informative arterial phase was shorter than the period between injection and the flow increasing effect of the contrast medium

Thus, the results in these two separate series were identical to those obtained in the animals with simultaneous angiography and flow measurements The changes of arterial flow in relation to the injection of contrast medium are presented in Table 1 and the transit time on the films in Table 2

After trauma One minute after trauma the blood flow on the traumatized side was slightly more than double the pre trauma values (Fig 2) The injection of contrast medium at this phase caused a further increase of blood flow amounting to approximately 240 per cent of values immediately before the injection (Table 1) The relative flow increasing effect of the medium was thus less than before trauma The duration of the flow increasing effect was only slightly shortened as compared to the pre trauma value Following trauma the blood flow on the non traumatized side was slightly lower than before The injection of contrast medium on this side caused an increase of blood flow, amounting to approximately 420 per cent of the

clinically and experimentally, a transient flow increasing effect (BOIJSEN et coll) and a low toxicity (SÖRENSEN) Injection of this medium was followed by hemodynamic changes resulting in a biphasic response, as previously reported (MARSHALL & SHEPHERD 1959, SAKO, BOIJSEN et coll) The initial and slight decrease of arterial blood flow might be related to increased viscosity of the blood by the injected medium (SAKO BOIJSEN et coll)

In the second phase following the injection the arterial blood flow was at a maximum 5 to 6 times greater than the blood flow immediately before injection The exclusion of the rich arterio-venous net of the foot by a tourniquet at the ankle meant that the injection was made into a vascular bed mainly within skeletal muscles The maximum blood flow in those muscles is much more than 5 to 6 times resting values (MELLANDER & JOHANSSON 1968) It thus appears that the injection of contrast medium caused a submaximal increase of blood flow

The mechanisms behind the vasodilating effect of contrast medium have been discussed Considering the magnitude of the effect the site of this action is in all certainty on the arterioles and the capillaries Regarding the transit of medium on the films and the registered blood flow it is apparent that the increase of blood flow started after the contrast column had passed the larger arteries and reached the peripheral ones The flow gradually increased when contrast medium appeared in the veins with maximum effect when the medium had left the arteries It appears that the effect of contrast medium on smooth muscle cells of the small blood vessels must be extremely rapid as the time of onset very nearly paralleled the shortening of medium transit time on the films in the high flow state immediately after the trauma This relationship between transit time of medium on the films and observed changes of flow on the curves was not affected by the trauma The acceleration of medium on the films was accompanied by a more rapid onset of the flow increasing effect by contrast medium on the traumatized side in comparison to the non traumatized side The appearance of the maximum increase of arterial blood flow at about half the time after end of injection immediately after trauma in comparison to the pre-trauma injections, corresponded to the finding at angiography of a reduction of medium transit time to about fifty per cent of that before trauma

The uniform flow response following contrast medium injection before and at different time intervals after the trauma suggests a similar involvement of the dilator mechanism(s) These mechanisms seem thus not to be influenced by those factors which determine the peripheral vascular resistance following the soft tissue trauma

In addition to the direct effect on the vascular smooth muscles it has been suggested that the osmotic characteristics of the contrast medium may cause a shift of fluid from the extravascular to the intravascular space Following trauma the injured tissues increase in volume which to a great extent consists of edema and hemorrhage It may be suggested that even in an edematous tissue the immediate effect of contrast medium is dominated by the direct action on the vascular smooth muscles It is, however evident that the later progressive increase of peripheral resistance in the

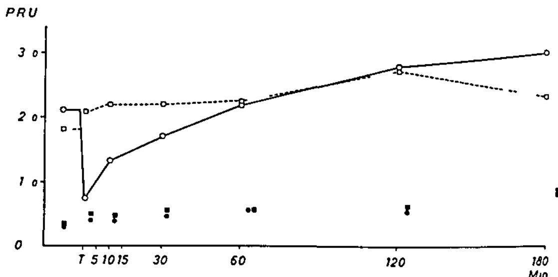


Fig 4 Calculated peripheral resistance (PRU) before and at different intervals following trauma (T) on one hind limb The filled symbols represent mean values of PRU during the transient flow increase following injection of contrast medium ○ traumatized side ● traumatized side, dilator response by contrast medium □ non traumatized side ■ non traumatized side, dilator response by contrast medium

two legs revealed no difference, whether the injection was done before, 1 min after trauma or later (Fig 4)

The dogs with angiography only demonstrated successively increasing transit time on the traumatized side and essentially unchanged or slightly increased values on the non-traumatized side (Table 2) In the later examinations the transit time retained the above-mentioned relationship to the transient changes of flow following injection

The injection of contrast medium caused a transient lowering of arterial pressure and an unchanged or slightly elevated heart rate, appearing slightly before the maximum flow increase, reproduced to the same degree before as well as after the trauma

Discussion

Angiography may contribute considerably to an understanding of the hemodynamic conditions and vascular reactions following soft tissue trauma However, the objection may be raised that most contrast media have a vasodilator effect, that may influence the angiographic flow determination It may be questioned whether the vascular bed of a traumatized region possesses more or less sensitivity to this effect Moreover, a cumulative effect of repeated injections of medium has been discussed (MOTTRAM & LYNCH, LINDGREN et coll) and the local toxicity on the microcirculation must be considered (ALMÉN & WIEDEMAN, SÖRENSEN) There is evidence that these effects are related to the composition of the medium The contrast medium used in the present experiments methylglucamine metrizoate (Isopaque Cerebral), has, both

dynamiques et par angiographie Les modifications du débit après injection de ce moyen de contraste ont été confrontées aux films La phase artérielle intéressante apparaît au cours du delai compris entre l injection et l'effet d'augmentation du débit par le moyen de contraste aussi bien avant qu'après traumatisme Les auteurs n'ont pas constaté de signes d effets cumulatifs

REFERENCES

ALMEN T and WIEDEMAN M P Application of contrast media to the external surface of the vasculature Invest Radiol 3 (1968), 151

BOIJSEN E, DAHN I and HALLBÖÖK T Hemodynamic effect of contrast medium in arteriography of legs Acta radiol Diagnosis 11 (1971), 295

BRÅNEMARK P-I, JACOBSSON B and SÖRENSEN S E Microvascular effects of topically applied contrast media Acta radiol Diagnosis 8 (1969), 547

COFI M N and LASTER E C ...

DE ...

GELIN L E Studies in anemia of injury Acta chir scand (1956) Suppl No 210

GREITZ T A radiologic study of the brain circulation by rapid serial angiography of the carotid artery Acta Radiol (1956) Suppl No 140

HILAL S K Hemodynamic changes associated with the intra arterial injection of contrast media Radiology 86 (1966), 615

KNISELY M H, ELIOT T S and BLOCH E H Sludged blood in traumatic shock I Microscopic observations of the precipitation and agglutination of blood flowing through vessels in crushed tissues Arch Surg 51 (1945), 220

LEWIS D H and LIM JR R C Studies on the circulatory pathophysiology of trauma I Effect of acute soft tissue injury on nutritional and non nutritional shunt flow through the hind leg of the dog Acta orthop scand 41 (1970), 17

— — Studies on the circulatory pathophysiology of trauma II Effect of acute soft tissue injury on the passage of macroaggregated albumin (^{131}I) particles through the hind leg of the dog Acta orthop scand 41 (1970), 37

LINDGREN P and TÖRNELL G Blood circulation during and after peripheral arteriography Experimental study of the effects of Triurol (sodium azetrizoate) and Hypaque (sodium diatrizoate) Acta radiol 49 (1958), 425

— SALTZMAN G-F and TORNELL G Vascular effects of metrizoate compounds, Isopaque Na and Isopaque Na/Ca/Mg Acta radiol (1967) Suppl No 270, p 44

LIU C T Circulation response to muscle trauma following ... in dogs ...

MARSHALL ... flow thr...

MELLANDER ... in the ...

... and AKER U T Contrast media as histamine liberators VI Arterial plasma histamine and hemodynamic responses following angiocardiography in man with 75 per cent Hypaque Invest Radiol 7 (1972), 403

SAKO Y Hemodynamic changes during arteriography J Amer med Ass 183 (1963), 121

traumatized region cannot solely be explained by mechanical factors determined by the edema or bleeding

The immediate effect of contrast medium on the regional blood flow in the vascular bed of a traumatized region is transient The long term effects of injection of medium in the present model are difficult to evaluate However, in this respect there are similarities between the effects of contrast media and trauma Injury to the endothelial lining may be caused by a bolus of contrast medium injected intraarterially (WIEDEMAN), while microthrombi may be formed following trauma (GELIN 1956 KNISELY et coll 1945) The release or activation of vasodilator substances has been demonstrated following contrast medium injection and trauma (COEL & LASSER 1971, ROCKOFF & AKER 1972, SANDEGÅRD et coll 1974) *The present investigation* has, however, not given any evidence that these effects of medium, even in repeated injections, changed the circulatory response to the trauma It seems reasonable therefore to assume that the repeated injection of medium produced transient effects but did not alter the experimental conditions to any appreciable degree With this background and in consideration of the fact that the vasodilator response of contrast medium is registered on the flow curve markedly later than the informative arterial phase, it seems justified to evaluate circulatory changes in traumatized regions by angiography

SUMMARY

The effects of repeated intraarterial injections of methylglucamine metrizoate on regional circulation were registered in soft tissue trauma to the dog hind leg The circulatory disturbances were determined by hemodynamic measurements and by angiography The changes of flow following injection of the contrast medium were related to the films The informative arterial phase appeared in the time lag between injection and the flow increasing effect of the contrast medium both before and after trauma No evidence of a cumulative effect was recorded

ZUSAMMENFASSUNG

Die Wirkungen wiederholter intraarterieller Injektionen von Methylglucamin Metrizoat auf die regionale Zirkulation bei einem Weichteil Trauma des Hinterbeins des Hundes wurden registriert Die Zirkulationsveranderungen wurden durch hamodynamische Messungen und Angiographie bestimmt Die Änderungen der Durchblutung nach Injektion des Kontrastmittels waren den Filmen zugeordnet Die informative arterielle Phase liegt in der Zeitverzogerung zwischen Injektion und dem Zirkulations steigerndem Effekt des Kontrastmittels sowohl vor als and nach dem Trauma Es fanden sich keine Zeichen eines kumulativen Effekts

RESUMÉ

Les auteurs ont observe les effets d injections intraartérielles répétées de métrizoate de méthylglucamine sur la circulation régionale dans les traumatismes des parties molles de la patte postérieure du chien Les troubles circulatoires ont été étudiés par des mesures hemo

FROM NIUVANNIEMI HOSPITAL (DIRECTOR: H. P. A. HAKOLA), AND THE UNIVERSITY CENTRAL HOSPITAL (DIRECTOR: O. CASTRÉN), SF-70210 KUOPIO, FINLAND

BONE MINERAL CONTENT IN HEREDITARY POLYCYSTIC OSTEODYSPLASIA ASSOCIATED WITH PROGRESSIVE DEMENTIA

H. P. A. HAKOLA and P. KARJALAINEN

Eight cases of a formerly unknown disease of the skeleton and the nervous system

[illegible]

..., 1973, 1974). More or less well delineated cysts containing partly decomposed fatty tissue and lipid membranes occur in the bones of the extremities. Degenerative lesions of the blood vessels within the cavities may also be observed. The structure of the bone tissue outside the cysts appeared without abnormality. The cysts were first ascertained about the age of twenty in some cases and may slowly progress. Symptoms and signs from the nervous system begin during the fourth decade of life, incapacitate the patient in a few years and lead to death around the age of 40. Pathologic examination of the brain was performed in three cases in which a general diffuse atrophy of the white matter was observed macroscopically as well ...

[illegible]

..., whereas the magnesium and hydroxyproline contents were at the upper normal limits. During the terminal phase of the disease the diurnal urinary excretion of calcium, phosphorus and hydroxyproline was below normal

Submitted for publication 6 May 1974

SANDEGÅRD J and ZACHRISSON B E (a) Circulatory disturbances after experimental fracture Acta radiol Diagnosis 16 (1975), 181
— — (b) Angiography and hemodynamic measurements in extensive soft tissue trauma to the extremity Acta radiol Diagnosis 16 (1975), 279
— — SEEMAN T and LEWIS D H Angiographic study of soft tissue trauma Abstract presented at the 7th Congress of the European Society for Experimental Surgery, Amsterdam 1972
— NOLTE J, LEWIS D H and SEEMAN T Early hemodynamic and biochemical changes in soft tissue trauma Europ surg Res 6 (1974), 233
SÖRENSEN S E Changes in vascular permeability after local application of roentgen contrast media in the hamster cheek pouch Acta radiol Diagnosis 11 (1971), 274
— ASANO M Effects of water soluble contrast media on the microcirculation in peripheral nerves Registration of flow by microphotoelectric plethysmography Acta radiol Diagnosis 11 (1971), 402
WIEDEMAN M P Vascular and intravascular responses to various contrast media Angiology 14 (1963), 107
WRAY J B Acute changes in femoral arterial blood flow after closed tibial fracture in dogs J Bone Jt Surg 46-A (1964) 1262
ZACHRISSON B E Angiografi vid mekaniska mjukdelsskador (In Swedish) Thesis, Gothenburg 1974



Fig 1 Case 3 Left hand and wrist Cavities in both ends of phalanges and partly also in the diaphyseal medulla The distal ends of the metacarpals, radius and ulna as well as the carpal bones are cystic Measuring site indicated by a line

cm from the distal end of the left radius and of cortical bone at a point between the middle and distal thirds of the left radius and ulna by means of the ^{241}Am gamma ray attenuation method At the site of measurement in the distal radius, Cases 2, 3 and 7 had a cyst and Cases 2 and 7, in addition, old fractures The mineral content per unit length of bone (g/cm) was computed from the formula (KARJALAINEN 1973)

$$\gamma = K \frac{\Delta x \cdot \varrho_m}{\mu_m \varrho_m - \mu_s \varrho_s} \sum_{i=1}^{n} \ln \frac{I_0}{I_1}$$

where Δx (selected as 0 1 cm) = the interval over which the values of $\ln I_0/I_1$ are summated, ϱ_m (2 70 g/cm^3) = the microscopic density of bone —

... and soft tissue,

... rate that has penetrated through water and soft tissue and I_1 = photon fluence rate that has penetrated the bone

Table 1

Radiographically detected cysts in the upper extremities of the patients (the cases are numbered as in HAKOLA et coll 1974) D = right, S = left, ( ) = mineral changes, — = no changes

Case No	Sex	Age years	Upper extremities					
			Phalanges	Metacarpals	Carpals	Radius	Ulna	Humerus
1	M	35	DS	DS	DS	—	—	—
2	F	35	DS	DS	DS	DS	—	DS
3	M	41	DS	DS	DS	DS	DS	DS
7	F	35	DS	DS	DS	DS	DS	—
8	F	33	DS	DS	DS	—	—	—

Table 2

Cysts in the lower extremities of the patients in Table 1

Case No	Lower extremities						
	Phalanges	Metatarsals	Tarsals	Fibula	Tibia	Patella	Femur
1	DS	DS	DS	DS	DS	DS	DS
2	DS	DS	DS	DS	DS	—	DS
3	DS	DS	DS	DS	DS	DS	DS
7	DS	DS	DS	DS	(DS)	(DS)	DS
8	DS	DS	DS	DS	—	—	—

Electrophoresis has shown that the relative value of alpha globulin in both serum and spinal fluid has been raised (HAKOLA 1972) No specific metabolic disorder has been found

Material and Methods

All five typical cases still alive were examined, two men and three women, aged 31 to 41 years The diagnosis has been ascertained by biopsy in all cases Cyst formations were present in the short bones of the extremities and, predominantly in the distal ends, in the long bones (Tables 1, 2, Fig 1), most marked in the oldest patient and slightest in the youngest No cystic degeneration was observed in the diaphyses of radius or ulna in any of the patients At the time of examination, all five were incapacitated for work because of dementia, and Cases 2 and 3 had, moreover, lost ability for locomotion The symptoms and signs from the nervous system were mildest in the youngest case (No 8)

The measurements of the mineral content of spongy bone were made about 1 5

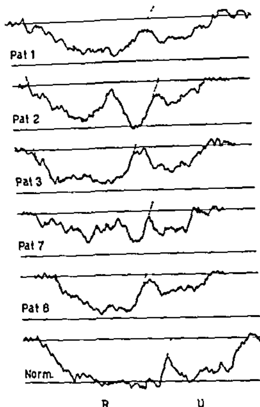


Fig 2 The radiation attenuation for the left distal radius of five patients of the series and one healthy control Estimated from the films Cases 3 and 7 had an extensive area of cystic degeneration in the measuring site in Case 2 a single cavity in the radius was evident whereas no cystic degeneration was detectable radiographically in Cases 1 and 8

Results

The mineral content per unit length of bone and the mean bone mineral density values for the distal radius and for the midshaft radius and ulna are given in Table 3, where the comparative values used and the significance of the differences appear Differences in mineral content per unit length of bone depend mainly on the size of the bone and are therefore not considered The gamma ray attenuation curves for the distal radius of both patients and a healthy control appear in Fig 2

In Case 8 the ^{85}Sr vertebral uptake was significantly lower (1 960 counts/2 min) than normal (3 260 $\pm$ 520 counts/2 min), in Cases 1 and 7 it was normal (3 570 and 3 250 counts/2 min, respectively), in Cases 2 and 3 it was significantly raised (5 650 and 5 760 counts/2 min, respectively) In the last mentioned two cases the uptake in the knees was significantly asymmetric (the left/right ratio being 1 20 and 1 25 respectively) whereas in the other three cases it was symmetric

Neither the ^{85}Sr scanning of the bones nor the gamma camera scintigraphy revealed any exceptional 'hot or 'cold uptake areas

Table 3

Mineral content per unit length of bone (g/cm) and mean bone mineral density (g/cm³) values for the left upper extremity λ_1 and ϱ_1 = distal radius, λ_2 and ϱ_2 = midshaft radius, λ_3 and ϱ_3 = midshaft ulna P = patients, N = the value for a healthy population

Case No	Sex	Age	λ_1		ϱ_1		λ_2		ϱ_2		λ_3		ϱ_3	
			P	N	P	N	P	N	P	N	P	N	P	N
1	M	35	1 42	1 76	0 223	0 326	1 04	1 63	0 76	0 94	0 97	1 28	1 18	1 29
2	F	35	1 29	1 20	0 235	0 280	0 88	1 11	0 75	0 90	0 64	0 95	0 85	1 34
3	M	41	1 21	1 72	0 295	0 316	1 30	1 58	0 77	0 92	1 04	1 25	1 17	1 26
7	F	35	1 00	1 20	0 220	0 280	1 01	1 11	0 62	0 90	0 98	0 95	0 82	1 34
8	F	33	0 82	1 23	0 307	0 282	0 85	1 22	1 04	0 91	0 68	0 96	1 18	1 35
Mean			1 15	1 42	0 256	0 298	1 02	1 33	0 79	0 91	0 86	1 08	1 04	1 32
±SD			0 24	0 29	0 042	0 022	0 18	0 26	0 15	0 02	0 19	0 17	0 19	0 04
t			2 633		2 047		3 846		1 845		3 367		2 920	
p <			0 06		0 11		0 02		0 14		0 03		0 04	
			(not sign)		*(not sign)*		*(sign)*		*(not sign)*		*(sign)*		*(sign)*	

$$K = 1 + a\ \exp\left(-\frac{b}{A}\sum_{i=1}^{n}\ln\frac{I_0}{I_1}\right)$$

where a = 5 42, b = 4 95 cm², A (0 47 (d² + 1)) = the cross-sectional area of the bone at the measuring site and d = the diameter of distal radius The mean bone mineral density (g/cm³) of the distal radius is $\varrho = K\lambda/A$

In the forearm, K = 1, and the cross-sectional area of the bone was determined from the formula $A = \pi/4\ (d_2^2 - d_1^2)$, where d_2 and d_1 were respectively the outer and the inner diameter of the radius or the ulna, as determined from roentgen films

The values for the patients were compared with normal values (the t-test, paired comparison) taken from the regression line for the left upper extremity corresponding to the patient's age The regression was calculated for the range 30 to 80 years and included 104 individuals (ALHAVA & KARJALAINEN 1973)

Each patient was also given 50 μCi ^{85}Sr intravenously as a chloride A week after the injection the vertebral uptake was determined employing the measuring technique and the principles of evaluation of results described by ANTTONEN et coll (1973) The uptake in the knees was also measured

In one case (No 1) ^{85}Sr scanning of hands, knees, legs and spine was carried out In another case (No 8) gamma camera examination was performed employing $^{99}Tc^{m}$ labelled polyphosphate

metabolic disorder of the bone, in the sense that no deviating uptake values were observed However the significance of the observations must be considered uncertain as they failed to reveal the cysts demonstrated at roentgen examination

The findings reported here do not indicate a storage disorder of the bone This possibility seems unlikely from the pathologic examinations as well

SUMMARY

Measurements of the bone mineral content were made in five patients with a disease characterized by progressive dementia and lipomembranous polycystic osteodysplasia Decreased bone mineral density (g/cm²) was observed not only in the region of cysts in the

ıtake was

.ervations

ZUSAMMENFASSUNG

Es wurden Messungen des Mineral Gehalts der Knochen bei funf Patienten vorgenommen deren Erkrankungsbild durch eine fortschreitende Demens und eine l pomembranose

Gehalt wurde

Diaphyse des

ı dem jungsten

normal bei zwei und erhoht bei zwei anderen Die Befunde sind mit der Hypothese einer generellen metabolischen Storung der Knochen vereinbar

RESUME

Des mesures de la teneur minérale de l os ont éte faites chez 5 malades atteints d une maladie caracterisee *par une demence* progressive et une osteodysplasie polykystique lipomembraneuse On a observe une diminution de la teneur minérale non seulement dans la region des kystes dans la partie distale du radius mais aussi dans les diaphyses du radius et du cubitus La fixation vertébrale du ^{85}*Sr a ete basse chez le plus* jeune malade normale chez 2 malades et elevee chez 2 autres Ces observations sont compatibles avec l hypothese d un trouble metabolique general de l os

REFERENCES

ALHAVA E M and KARJALAINEN P The mineral content and mineral density of bone of the forearms in healthy persons measured by Am 241 gamma ray attenuation method Ann clin Res 5 (1973) 238

ANTTONEN V M KARJALAINEN P RAUNIO H and HOLOPAINEN T Uptake of radioactive Sr 85 by the spine in patients with untreated and treated hyperthyroidism Ann clin Res 5 (1973) 223

HAKOLA H P A Neuropsychiatric and genetic aspects of a new hereditary disease characterized by progressive dementia and lipomembranous polycystic osteodysplasia Acta psychiat scand Suppl 232 (1972)

Discussion

As was to be expected, in cases where a cyst existed at the measuring site, low attenuation of radiation was observed (Fig 2) Surprisingly, however, in Case 1, where no cyst existed at this site, the mean bone mineral density (g/cm³) of the distal radius was also evidently decreased Moreover, it was found that in all five patients this bone mineral density of the diaphyseal cortical bone was also below normal value, and in the same proportion as that of the spongy bone This decrease was fairly uniform from case to case and was statistically significant in the diaphyses of the ulna A general decrease of the mean bone mineral density could be considered to result from disuse atrophy In such cases, however, this is known to occur first in the region of spongy bone, where the metabolic rate is higher (JOHNSTON 1968) Another possibility is a hereditary enzyme defect disturbing the metabolism of the bone tissue *and leading to a general decrease in mineral content and loss of bone tissue* The development of cysts in spongy bone alone could then be explained by assuming that the disorder first causes rarefaction of the spongy bone, also roentgenologically demonstrable (HAKOLA 1972, HAKOLA et coll 1974, JÄRVI et coll, to be published), in the most severe cases leading to a total absence of bone tissue, i e a cyst, which apart from fatty tissue contains only decomposition products Cortical bone, because of its large amount of mineral compounds or for other reasons would be structurally more resistant The microscopic appearances of the structure of the bone tissue peripheral to the cysts being normal (JÄRVI 1970) speak to some extent against this hypothesis

The measurements of the bone mineral content reveal the amount of calcium apatite but do not permit conclusions as to which of the bone components is primarily affected by the disorder nor the connection between the bone lesion and the injury to the nervous system The intake of calcium, the regulation of the calcium content of the blood and the output of calcium seem to be normal (HAKOLA 1972) The decrease in the excretion of calcium, inorganic phosphate and hydroxyproline observed during the terminal phase of the disease may reflect a decrease in the metabolizing bone tissue The conflicting findings concerning the strontium uptake in the spine may be due to a compensatory phenomenon regulating the calcium content of the blood in the youngest patient the amount of calcium set free from the decomposing bone tissue was so large that the calcium turnover in the remaining bone tissue was decelerated With the loss of bone the metabolic rate of the remaining bone tissue will accelerate, so as to keep the calcium content of blood unchanged and at the end stage of the disease the rate will rise above the normal level The increased values of the strontium uptake in the spine are also incompatible with the presence of disuse atrophy The asymmetry of the uptake in the knees, observed in two patients, may be caused by a slight difference in size of the cysts

The findings yielded by the Sr scanning and the $^{99}Tc^{m}$ polyphosphate scintigraphy, performed on one patient each, were also compatible with the hypothesis of a general

FROM DEPARTMENT III OF DIAGNOSTIC RADIOLOGY (DIRECTOR C-G HELANDER), SAHLGRENSKA SJUKHUSET, S-411 32 GOTHENBURG, AND THE ORTHOPEDIC CLINIC (DIRECTOR B OLSSON), VASA SJUKHUS, S-411 33 GOTHENBURG, SWEDEN

SOFT TISSUE RADIOGRAPHY IN PAINFUL SHOULDER

E DEICHGRÄBER and B OLSSON

Specialized soft tissue radiography of joints of the extremities was introduced by F

c

soft tissues of the periarticular regions were demonstrated in greater detail than is possible with conventional techniques No systematic description of soft tissue abnormalities in or adjacent to the joints has as yet appeared, however

The shoulder region, with its great vulnerability to wear and tear, is particularly prone to degenerative and inflammatory changes (OLSSON 1953, MOSELEY 1969, BATEMAN 1972) Radiography has long constituted an integral part of the evaluation of shoulder diseases Many reports on bone changes and soft tissue calcifications have been published OLSSON found a high correlation between 'tubercular irregularities' and tendon and rotator cuff ruptures, KAMIETH (1965) BAUER (1969), and LEACH & GREGG (1970) described calcific deposits in tendons and bursae, but while LEACH & GREGG considered the presence of calcifications a sign of actual shoulder disease, the two former authors stated that calcifications may also be

The topography of the fatty layer adjacent to the subdeltoid fascia has been de-

Submitted for publication 28 May 1974

— JÄRVI O H and SOURANDER P. Osteodysplasia polycystica hereditaria combined with sclerosing leukoencephalopathy A new entity of dementia praesenilis group Acta neurol scand Suppl 42 (1970)
— — — A new type of hereditary dementia Generalized demyelination and lipomembranous polycystic osteodysplasia International Congress Series, No 296, p 62 Excerpta Medica, Amsterdam 1973
— — LAUTTAMUS L L, SOLONEN K A, SOURANDER B J P and VILPPULA A H Polycystic osteodysplasia associated with progressive dementia—a new hereditary disease Duodecim 90 (1974), 106
JÄRVI O H A new entity of phacomatosis, a Bone lesions (Hereditary angionecrotic polycystic osteodysplasia) Acta path microbiol scand (1970) Suppl No 215, p 27
— LAUTTAMUS L L and SOLONEN K A Membranous reticulin dysplasia of bones Probably a new disease entity (Only title) *In* Proc of the 14th Scandinav Congr of Path and Microbiol, p 51 Universitetsforlaget, Oslo 1964
— HAKOLA H P A and SOURANDER P To be published
— — LAUTTAMUS L L, SOLONEN K A and VILPPULA A H Cystic capillary necrotic osteodysplasia A systemic bone disease probably caused by arteriolar and capillary necroses Relations to brain affections Abstracts Seventh International Congress of International Academy of Pathology, p 291 State University of Milan 1968
JOHNSTON JR C C Measurement of bone mass in the radius Conf-680211 (1968), 283
KARJALAINEN P A method for determination of the mineral content and mineral density of the distal radius using gamma ray attenuation Ann clin Res 5 (1973), 231
SOURANDER P A new entity of phakomatosis, b Brain lesions (Sclerosing encephalopathy) Acta path microbiol scand (1970), Suppl No 215, p 44

Table 2

Distribution of the radiographic findings in the different clinical groups

	n	Blurring and displacement	No abnormality	Blurring only (B)	Displacement only (D)	Calcific deposits (C)	C+D	C+B	C+B+D
Cervical pain only	24	3	9	—	—	12	—	2	1
Peritendinitis with cervical pain	10	8	1	4	—	1	1	3	—
Peritendinitis only	40	29	8	6	1	3	1	20	1
Miscellaneous									
Uncertain peritendinitis	7	4	1	—	—	2	—	3	1
Trauma with or without peritendinitis	7	5	—	4	—	2	—	—	1
Frozen shoulder	9	—	4	—	—	5	—	—	—
Rheumatic disease	2	2	—	—	—	—	1	1	—
Doubtful clinical findings	9	1	5	1	—	3	—	—	—
Total	108	52	28	15	1	28	3	29	4

of molybdenum filtered radiation generated on a molybdenum target, was tested at the outset of the experiments The tube was built into a compact apparatus for mammary radiography (Siemens Mammomat), but in spite of a short FFD (45 cm) the tube could not generate sufficient radiation, and the method had to be discarded

The clinical material consisted of 102 patients, 33 men and 69 women, selected from the orthopedic out patient department Six had both shoulders examined, making up a total of 108 examinations Efforts were made to select a group of patients with signs of only peritendinitis and as a reference group patients with only radiating pain considered to be of cervical origin They were examined within a few days after their first visit to the hospital The course of the disease made certain corrections necessary, as the pains in a shoulder might have been covered by a slight cervical pain, or vice versa Miscellaneous and doubtful cases thus were brought together in one group In the latter group are also included the contralateral shoulder of some cases as well as some obviously malingering patients

The majority of the patients were in the late middle age (Table 1), which is in agreement with the observation that soft tissue changes in the shoulder region increase with age (MOSELEY, BATEMAN, STEINBROCKER 1967)

The films were evaluated by two radiologists, 61 cases being inspected twice, with an adverse result in 5 cases The parameters were recorded, blurring and displacement of the fatty layer being classed as signs of peritendinitis, whereas calcifications

Table 1

Age distribution of the clinical material

Age groups	20–29	30–39	40–49	50–59	60–69	>70
No of cases	2	3	15	43	30	9

scribed by LANZ & WACHSMUTH (1959) and LEB (1961) LEB stated that in all cases of peritendinitis and subacromial bursitis this fatty layer tends to be blurred or invisible but made no mention of his clinical material His radiographic technique consisted of overexposing and underdeveloping the film No data were published on tube potential, type of film, intensifying screens, secondary screening, etc

The purpose of the present work was to develop a technique for radiography of the soft tissues of the shoulder joint, to test its clinical value, as well as to describe the roentgen appearances of peritendinitis of the shoulder The hypothesis was based on the assumption that inflammatory reactions of tendons and bursae cause the surrounding tissues to become oedematous, thus reducing the differences in attenuation capacity between them For the subacromial region this means that the subdeltoid fatty layer should become blurred or invisible on the films in cases of peritendinitis and bursitis, regardless of whether calcifications can be demonstrated or not

Material and Methods

The technique was worked out in a series of preliminary experiments not included in the present clinical material A medium sensitive industrial film (Agfa-Gevaert Mamoray T 3) was preferred due to its low mottle level in relation to its sensitivity It was developed in a roll machine (DEICHGRÄBER et coll 1974) An attempt was made to use intensifying screens in order to reduce exposure time and patient dose, but this proved unsatisfactory and had to be abandoned, as reported separately (DEICHGRÄBER et coll 1975) The target of the tube was made of tungsten-rhenium The tube had a low inherent filtration (0 5 mm Al) and no additional filtration was used It was mounted on a Lysholm skull table with FFD 70 cm The tube potential had to be set at 40 kV to keep the exposure time at acceptable values By means of a pinhole camera the size of the focus was determined at 40 kV, 400 mA to be 1 2 mm × 2 2 mm (nominal size 1 mm × 1 mm) This fairly large focus did not lead to disturbing unsharpness, the object-to-film distance being as short as possible No secondary screening was employed The incident dose was measured to be 0 4 to 0 5 rad/exposure Two a p projections were taken of the shoulder, one with the arm rotated inwards, the other with outward rotation, to demonstrate the tissues adjacent to the greater and lesser tubercles of the humerus, respectively The condition of the often elderly patients rigid from shoulder pain did not allow other projections to be used

The method of soft tissue radiography developed by GROS (1967), implying the use

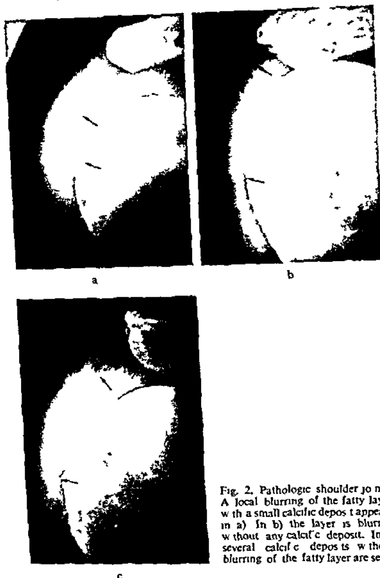


Fig. 2. Pathologic shoulder joints. A local blurring of the fatty layer with a small calcific deposit appears in a) In b) the layer is blurred without any calcific deposit. In c) several calcific deposits without blurring of the fatty layer are seen

The same applies to the category no abnormality In cases with a definite clinical peritendinitis (n=50) blurring or displacement of the fatty layer was common (37) being the only radiographic *abnormality in* 11 of these cases Most common were blurring and calcification (23 out *of 50 cases*) Frozen shoulder occurred in 9 cases none of them displaying soft tissue abnormality Calcifications were not significantly more frequent in the group with *definite* peritendinitis than in the one with brachialgia ($\chi^2 = 0.04$) Soft tissue abnormalities were significantly more common in the group

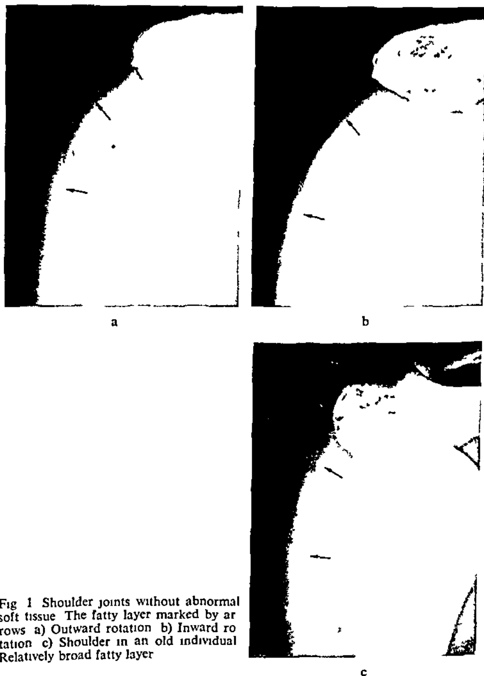


Fig 1 Shoulder joints without abnormal soft tissue The fatty layer marked by arrows a) Outward rotation b) Inward rotation c) Shoulder in an old individual Relatively broad fatty layer

alone were not A χ^2 test was used to find out the correlation, if any, between the findings and clinical symptoms and signs The level of significance was set at 5 per cent

Results

Table 2 gives a survey of observed radiologic abnormalities in relation to clinical signs Calcific deposits appear in all clinical groups without any evident preference

tissue volume of the shoulder No compression can be employed to reduce thickness in the same way as in mammary radiography The exposure time is of great importance and motion unsharpness was the greatest obstacle to good image quality Tubes with a greater load capacity would provide a welcome improvement of the technique

A clinical differentiation between pains originating from the shoulder region and radiating pains from cervical lesions may be difficult except in cases with acute peritendinitis The vast majority of cases in the present material presented themselves with subacute disorder, thus cases in which auxiliary procedures are desirable

As a reference group patients with radiating pain, brachialgia, were used instead of 'healthy' individuals, the reason being the ubiquity of pathologic changes in the rotator cuff of middle aged persons regardless of symptoms (OLSSON) Moreover, the problem is actually one of differentiating between peritendinitis and brachialgia rather than between peritendinitis and no disease Since the radiographic method was tested in such cases where the two types of pain primarily could not be easily differentiated clinically the grouping of the patients had to be revised when the course of the disease and the results of the treatment were at hand Thus, the statistical evaluation may be open to some discussion, and its results should not be overestimated However, it may at least indicate that further trial of the radiographic technique used is motivated The projections to be recommended may be reconsidered A rather large number of the present cases with peritendinitis did not display any inflammatory abnormalities This may be due to the fact that the projections used demonstrated only a limited area of the soft tissues adjacent to the tubercular region Smaller areas of blurring may have escaped detection The further testing of the method must thus include a consideration of which projections are to be preferred for an evaluation of the best results

SUMMARY

Specialized soft tissue radiography was applied to the shoulder region to differentiate between shoulder peritendinitis and radiating cervical pain The technique is presented, together with the results of a clinical trial Local inflammation was demonstrable even in the absence of calcific deposits

ZUSAMMENFASSUNG

Eine spe
wend
Schr
zusammen mit den Ergebnissen eines klinischen Versuchs werden gegeben Lokale Inflammationen waren auch in Abwesenheit von Kalkablagerungen nachzuweisen

RESUMÉ

La radiographie spécialisée
faire le diagnostic differ
Les auteurs presentent l
sible de mettre en évider

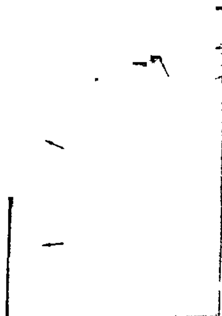


Fig 3 Lateral displacement of the fatty layer The distance between the layer and the greater tubercle is increased

with only peritendinitis, as compared with the cases with cervical pain ($\chi^2=21.60$) If the peritendinitis group was extended to comprise cases with peritendinitis and brachialgia, the statistical significance remained unchanged ($\chi^2=24.70$)

Radiology In cases with brachialgia the fatty layer on the lateral aspect of the tubercular region was thin, well demarcated and visible in the entire length of its course from the lateral part of the lower surface of the acromion passing in a gentle curve the tubercular region at a distance of 1 to 2 mm Usually it could be traced well beyond the tubercular region, curving towards the humeral shaft (Fig 1) The fatty layer broadened with age (Fig 1 c)

In the presence of peritendinitis or bursitis the fatty layer was indistinct or invisible The degree of blurring did not seem to indicate the severity of the inflammatory process, as in some cases of exquisitely tender bursitis the blurring was only slight In the majority of cases (Fig 2 a) the fatty layer was invisible over a distance of 0.5 to 1 cm close to the most protruding part of the greater tubercle A case without calcifications but with blurring of the fatty layer appears in Fig 2 b, another one with calcifications but without blurring in Fig 2 c

Displacement of the fatty layer was only rarely encountered but if so it was stretched over a distended bursa, i e its distance to the greater tubercle was increased (Fig 3) If the displaced layer was associated with blurring its recognition was more difficult

Discussion

The technique arrived at is based on the use of a medium sensitive industrial film with a high silver content and a tube with a tungsten target The use of a tube with a molybdenum target has not been successful in shoulder examinations due to the large

OM THE DEPARTMENT OF DIAGNOSTIC RADIOLOGY (DIRECTOR PROF E BOIJSEN), UNIVERSITY OF LUND, MALMÖ ALLMÄNNA SJUKHUS, S-21 401 MALMÖ, SWEDEN

ARTERIAL COLLATERALS IN INTRAHEPATIC ARTERIAL OCCLUSION

H PETTERSSON

Arterial collateral circulation to the liver has been thoroughly described both in man (BENGMARK & ROSENGREN 1970, BOIJSEN et coll 1971, DUX et coll 1966, MICHELS 1955 1966, NEBESAR et coll 1969, PLENGVANIT et coll 1972, REUTER 1966, REDMAN & REUTER 1970, WIRTANEN & KAUDE 1973) and animals (FARKOUH et coll 1970, KAMAN 1967) In man different collateral pathways have been observed, all reported to originate from sources outside the liver or in the liver hilum In this report, two cases are described where peripherally located intrahepatic collaterals developed

Case 1 A woman, 69 years old was operated upon for gallbladder carcinoma The resected tumor had a diameter of 10 cm Five months later she was readmitted because of jaundice Angiography was performed with simultaneous injections into the celiac and superior mesenteric arteries (Fig 1) Widespread malignant involvement of the liver was observed, most extensive in the ventrocranial segment A branch of the ventrocranial segmental artery was occluded The part of the branch distal to the occlusion received its blood supply from a collateral, arising in the dorsocaudal segment On operation, even palliative measures were impossible The autopsy revealed widespread malignancy in the liver with intrahepatic cholestasis The intrahepatic arteries were not examined in detail

Case 2 (Previously reported by BOIJSEN et coll 1971) A female, 14 years old, had a trauma towards the upper part of the abdomen as the result of a bicycle accident She was admitted 5 days later, with increasing pain below the right costal arch As hepatic rupture

Submitted for publica 18 november 1974

REFERENCES

BATEMAN J E *The shoulder and neck W B Saunders Company, Philadelphia, London* & Toronto 1972

BAUER R Differentialdiagnose und Therapie der Periarthritis humero scapularis Arch orthop Unfall Chir 65 (1969), 13

DEICHGRÄBER E, REICHMANN S and BURÉN M Film quality in mammary radiography Acta radiol Diagnosis 15 (1974), 93

— — and STRID K G Intensifying screens in soft tissue radiography Acta radiol Diagnosis 16 (1975), 54

FISCHER E und BRAUN J Neue diagnostische Moglichkeiten an den Extremitaten durch Weichstrahlaufnahmen mit Mammographiegeraten Electromedica 3 (1973), 90

GROS CH E Méthodologie Symposium Europeen de Radiologie Mammaire J Radiol Électrol 48 (1967), 638

KAMIETH H Die Periarthritis humeroscapularis im Rontgenbild der Schulter Arch orthop Unfall Chir 58 (1965), 191

LANZ T und WACHSMUTH W Praktische Anatomie Ed 2 vol I/3 Arm Springer-Verlag Berlin 1959

LEACH R E and GREGG T P Preoperative evaluation of the painful shoulder Surg Clin N Amer 50 (1970) 603

LEB A Der rontgendiagnostische Beitrag zur Diagnose der Periarthrose und unspezifischen *Periarthritis Wien klin Wschr 73 (1961), 141*

MOSELEY H F Shoulder lesions Third edition E & S Livingstone Ltd Edinburgh and London 1969

OLSSON O Degenerative changes of the shoulder joint and their connection with shoulder pain Acta chir scand (1953) Suppl No 181

REICHMANN S, DEICHGRABER E, STRID K-G, HEYMANN F and STRAND T Soft tissue radiology of finger joints Acta radiol Diagnosis 15 (1974) 439

STEINBROCKER O The painful shoulder *In* Arthritis and allied conditions p 1233 Ed J L Hollander Lea & Febiger, Philadelphia 1967



Fig. 2. Case 2. Celiac angiography ... artery is occluded (→) segmental artery distal to ... after accident The collat... is larger

1966) After ligation of the proper hepatic artery and total dearterialization of the liver a rapid development of collaterals usually occurs, most often via the phreni coabdominal and sub and intercostal arteries, but occasionally also via gastroduodenal branches, inferior pancreaticoduodenal splenic, and left gastric arteries (BENGMARK & ROSENGREN 1970 PLENGVANIT et coll 1972, REDMAN & REUTER 1970) If the occlusion is present in the left or right hepatic artery, collaterals may develop within the liver hilum (REDMAN & REUTER) All these pathways consist of preformed interarterial anastomoses that open and become wider and all come from sources outside the liver or in the liver hilum The segmental branches of the hepatic artery are said to be end arteries without the possibility of developing collaterals between each other (MICHELS 1966) However, collaterals have been described connecting the middle and left hepatic arteries in the fissure between the quadrate and the left lateral segments (NEBESAR et coll 1969) After ligation of subsegmental arteries in pigs intrahepatic collaterals have been described (KAMAN 1967), which seemed to consist of preformed interarterial anastomoses

In case 1, a fairly wide collateral artery had its origin in the dorsocaudal segment and supplied a part of the ventrocranial segment The collateral was situated in the

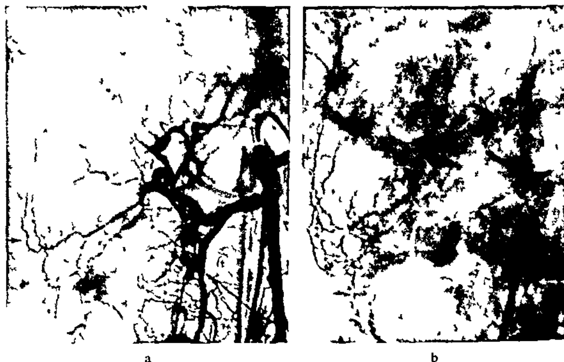


Fig 1 Case 1 Simultaneous injection into the celiac and superior mesenteric arteries a) Early and b) late arterial phase A collateral artery (→) arising in the dorsocaudal segment is connected with the distal part of a branch of the ventrocranial segmental artery (↔) The proximal part of that branch is occluded though the site of occlusion is not identifiable

was possible celiac angiography was performed (Fig 2 a) An abrupt occlusion of an intrahepatic arterial branch of the ventrocranial segment of the liver was observed The artery distal to the occlusion received its blood via collaterals arising from branches of the middle hepatic artery No connections existed between these collaterals and the inferior phrenic artery In the same region extravasation occurred and the liver was slightly displaced medially by a hematoma The patient was treated conservatively At repeat angiography 2 weeks later the described collaterals persisted and the hematoma had increased in size (Fig 2 b) The conservative treatment was confirmed After a month the collaterals had the same appearance but the hematoma had diminished

Discussion

MICHELS (1955) demonstrated 26 possible arterial collateral pathways to the liver However ten of these were anatomic variations of the hepatic arteries Among the others were described pathways over the greater omentum the lesser omentum the pancreas and over arteries outside the celiac blood supply A scheme of the possible hepatic collaterals is given in Fig 3 The type of collateral circulation depends mainly on the site of the occlusion Thus if the celiac or common hepatic arteries are occluded the liver will be supplied via the pancreaticoduodenal arcades and the gastroduodenal artery (DUX et coll 1966 MICHELS 1955 1966 REUTER

obviously passed over this fissure and appeared to be a connection within the liver capsule between the most peripheral branches of the middle hepatic artery and the ventrocranial segmental artery, respectively This rapid development of collaterals in the periphery may indicate that preformed anastomoses between the different lobes actually exist in the human liver capsule

SUMMARY

Two cases are reported where intrahepatic peripheral arterial collaterals were angiographically observed In one case the collateral artery connected the subsegmental arteries of the dorso-caudal and ventro-cranial segments in the other collateral circulation existed between the ventro-cranial segmental artery and the middle hepatic artery Thus the segmental arteries of the liver are not always end arteries A schematic drawing of the hitherto angiographically confirmed collaterals is given

ZUSAMMENFASSUNG

Es wird uber zwei Falle berichtet bei denen angiographisch intrahepatische periphere arterielle Kollateralen beobachtet wurden In dem einen der Fälle verband die Kollateral arterie die Subsegmentarterien der dorso-caudalen und ventro kranialen Segmente, bei dem anderen Fall bestand eine Kollaterale Zirkulation zwischen der ventro-kranialen Segmentarterie und der mittleren Arteria hepatica Die Segmentarterien der Leber sind somit *nicht immer End Arterien* Es wird eine schematische Zeichnung der bislang angiographisch nachgewiesenen Kollateralen gegeben

RESUMÉ

Presentation de deux cas ou l auteur a observé angiographiquement des collaterales arterielles peripheriques intra hepatiques Dans un cas l artère collatérale connectait les arteres sous-segmentaires des segments postéro-inférieur et antéro-supérieur Dans l autre cas il existait une circulation collaterale entre l artère segmentaire antéro-supérieure et l artere hépatique moyenne Ainsi les artères segmentaires du foie ne sont pas toujours des arteres terminales L auteur donne un dessin schematique des collatérales confirmees angiographiquement jusqu a maintenant

REFERENCES

BENGMARK S and D
liver aft
BOIJSEN E
11 (197
DUX A BUCHELER E und THURN P Der arterielle Kollateralkreislauf der Leber Fortschr Rontgenstr 105 1966) 1
FARKOUH E F DANIEL A M and MACLEAN L D The effect of collateral circulation on survival in liver ischemia J surg Res 11 (1971) 130

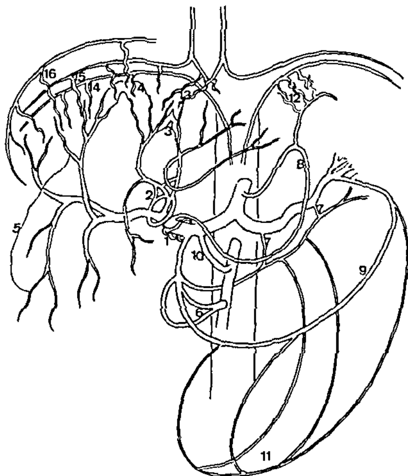


Fig 3 Scheme of hepatic collaterals angiographically demonstrated (Anatomic variations of the origin of the hepatic arteries excluded) Collaterals connecting branches of the hepatic artery 1 Vasa vasorum around the hepatic artery, portal vein and biliary duct 2 Collaterals within the liver hilum, between the main hepatic arteries 3 Small collaterals in the fissure between the left [illegible]

arteries 9 From the left to the right gastroepiploic arteries 10 Arc of Buhler 11 Arc of Barkow Collaterals arising from arteries outside the splanchnic region 12 Cardioesophageal arteries, [illegible] from the ensiform [illegible] 14 Collaterals [illegible] Collaterals from [illegible] terals from the

anterolateral part of the liver Thus, this collateral should be a peripheral, partly capsular connection between different segments in the right liver lobe

In the literature, no arteries are reported to cross the fissure between the right and left lobes of the liver except at the liver hilum In case 2, however, the collaterals

FROM THE DEPARTMENT OF DIAGNOSTIC RADIOLOGY III (DIRECTOR DOCENT C.-G. HELANDER), SAHLGRENSKA SJUKHUSET, S 411 32 GOTHENBURG, AND THE RESEARCH LABORATORY OF MEDICAL ELECTRONICS (DIRECTOR PROF. H. WALLMAN), CHALMERS UNIVERSITY OF TECHNOLOGY, S-402 20 GOTHENBURG, SWEDEN

SPEED OF RESPONSE OF A 50 HZ AND A 250 HZ TV SYSTEM

BO LANTZ and BENGT LINDBERG

By injecting contrast medium containing iodine into the circulation and measuring the absorption changes by videodensitometry caused by the medium when passing a selected area of a blood vessel, it is possible to evaluate the flow in absolute units (RUTISHAUSER et coll. 1967) or relative units (LANTZ 1974). The accuracy of the results strongly depends on two parameters: the dispersion and inertia of the contrast medium injected in the circulation, and the speed of response of the detecting system (image intensifier tube—TV camera—videodensitometer).

The television systems used in clinical radiology today work at the image rate of 50 (Europe) and 60 (USA) per second. Recently a Plumbicon television system working at a rate of 250 images per second has been developed by LINDBERG (1972) in order to improve the speed of response in video kymography. The purpose of this investigation has been to com-
the ordi
second

250 Hz TV system. The modified TV system, developed and described by LINDBERG, has an image rate of 250 per second and a horizontal scanning time of 32 μs

Submitted for publication 19 February 1974

KAMAN J Eine Studie uber die Plasticitat des arteriellen Strombettes der Schweinslebei nach teilweiser oder vollstandiger Unterbindung der Arteria hepatica Gegenbaurs morph J 110 (1967), 390

MICHELS N A Blood supply and anatomy of the upper abdominal organs Lippincott and Co, Philadelphia 1955, pp 302–324

— Newer anatomy of the kidney and its blood supply and collateral circulation Amer J Surg 112 (1966), 337

NEBESAR R A, KORNBLITH P L, POLLARD J J and MICHELS N A Celiac and superior mesenteric arteries A correlation of angiograms and dissections Little, Brown and Co, Boston 1969, p 166

PLENGVANIT U, CHEARANAI O, SINDHVANANDA K, DAMRONGSAK D, SASIPRAPA T and VIRANUVATTI V Collateral arterial blood supply of the liver after hepatic artery ligation angiographic study of twenty patients Ann Surg 175 (1972), 105

REUTER S Development of collateral vessels in an acute occlusion of the common hepatic artery Amer J Roentgenol 97 (1966), 473

REDMAN H and REUTER S Arterial collaterals in the liver hilus Radiology 94 (1970) 575

WIRTANEN G and KAUDE J *Inferior phrenic artery collateralization in hepatic artery* occlusion Amer J Roentgenol 117 (1973), 615

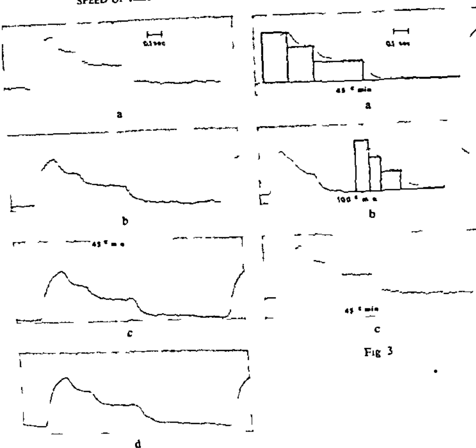


Fig 2

Fig 3

Fig 2 The ... with ... filte ...

Fig. a b V ... 50 H ... low p ... (c)

Because of the synchronizing procedure, video recorders usually accept only incoming video signals with 50 Hz vertical synchronizing pulses The 250 Hz system does not provide locking of the drum revolution to the incoming signal while recording and 250 Hz control track pulses do not yield locking during playback

The recorder chosen for this project, the Bell & Howell type 2910 EDEX, permits phase locking the drum revolution to mains frequency during recording, and records mains frequency control pulses on the control track This allows a signal not including 50 Hz vertical synchronizing pulses to be recorded and played back

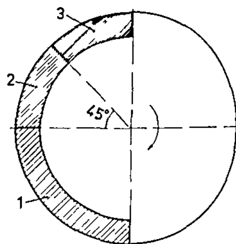


Fig 1 The motor ' the radiation bean thicknesses attache mm (2) and 0 4 ı constant speed the relations between the exposure times of the different copper layers are 1 1 2, and the extinction (exponential) being 3 2 1 Thus the relations between the integrated areas estimated from the extinction time' curve of the different copper fields have the proportions 3 2 2 when registered by a videodensitometer

The horizontal resolution in that system is measured to be 225 lines per image height and vertical resolution to be 120 lines In the 250 Hz system special demands are made upon the video tape recorder In a recorder used with an ordinary 50 Hz TV system, the drum rotation is synchronized to the video signal so that the drum makes one revolution per vertical synchronizing pulse, i e 50 revolutions per second During recording the drum revolution is phase locked to the vertical synchronizing pulses of the incoming video signal The vertical synchronizing pulses are also recorded on a special track, the control track, of the tape These control track pulses are used during playback to control the drum revolution so that the head will scan the video track properly

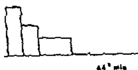
Table 1

Roentgen television, and recording equipment

	Vidicon 50 Hz	Plumbicon 50 Hz	Plumbicon 250 Hz
Roentgen generator	Triplex Angiomatic 1023/2CE Elema Schonander	Maximus 100 Philips	Triplex Optimatic 1003 Elema Schonander
Roentgen ray tube	Bi 150/30/50 R Siemens	XF 2050/00 Philips	P150/30/50 Siemens
Image intensifier tube	Sirecon 25/15 Siemens	XG 5018/00 Philips	XG 3000/00 Philips
TV-camera tube	Videomed I Siemens	XG 7107/00 *Philips*	Multi purpose *LDH 0151* Philips
Video tape recorder	OD X40 Oude Delft	OD X40 Oude Delft	2910 Edex Bell & Howell
Video densitometor	Model 'Chalmers'	Model Chalmers	Model Chalmers'



a



b

c

Fig 5 Videodensitometric registration of the rotating disk in the Plumbicon 250 Hz ...

The speed of the rotation could be increased up to about 110 'cardiac cycles' per minute (c/min)

A multi channel strip chart recorder (Mingograf 800, Siemens-Elema) served the purpose of recording the densitometer output

Results

Vidicon 50 Hz system In order to smooth the registrations, the integrator was followed by different low pass filters Three filters could be used alternatively 60 Hz 40 Hz or 20 Hz

The filters did not change the amplitudes of the pulse profiles (Fig 2) In Fig 2 a (no low pass filter) the registration of each field can be seen as a short horizontal line lasting 0 02 s

When the rotation of the disk in the radiation beam was increased from 45 c/min to 100 c/min (Fig 3) the densitometer output signal did not reach the correct maximum amplitude because of the inertia of the system and a flattening of the curve occurred

Plumbicon 50 Hz system The corresponding examinations for this TV system are illustrated in Fig 4, where the disk was rotating with the speed of 44, 92 and 97 c/min The correct maximum amplitude was not reached for an event lasting 0 08 s (Fig 4 a)

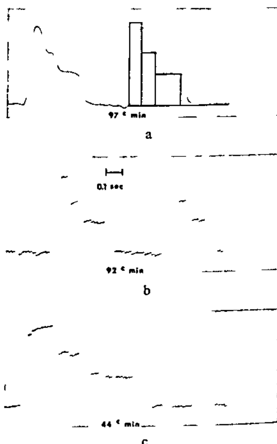


Fıg 4 Vıdeodensıtometrıc registratıon of the rotatıng dısk ın the Plumbıcon 50 Hz system
vıthout
not be

As the vertıcal synchronızıng pulses of the 250 Hz system are phase locked to the maıns frequency, the drum revolutıon and the 250 Hz vertıcal pulses are ınterlocked In one drum revolutıon there are fıve TV ımages ınstead of the usual half ımage

Materıal and Method

Three dıfferent televısıon systems were compared ın conjunctıon wıth the same vıdeodensıtometer, permıttıng measurements ın a 50 Hz TV system as well as ın a 250 Hz TV system (Table 1) The hıgh ımage rate TV system ıs well adapted to vıdeodensıtometry

The measurements were performed ın fluoroscopy wıth fıxed kV (60) and mA (0 1) A small generator wındow was placed ın the center of a well lımıted small radıatıon fıeld (3 cm × 4 cm) where a rotatıng dısk was operatıng (Fıg 1) At the margın of the cırcular alumınıum dısk, copper layers of dıfferent thıcknesses were attached (0 1, 0 2 and 0 4 mm), whıch durıng a certaın tıme were ıntroduced ın the radıatıon beam when the dısk was rotatıng The aım of the rotatıng dısk was to sımulate changes of the concentratıon of a contrast medıum wıthın a cardıac cycle

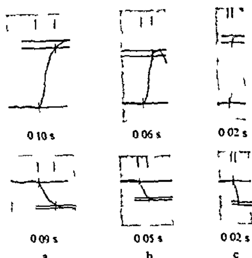


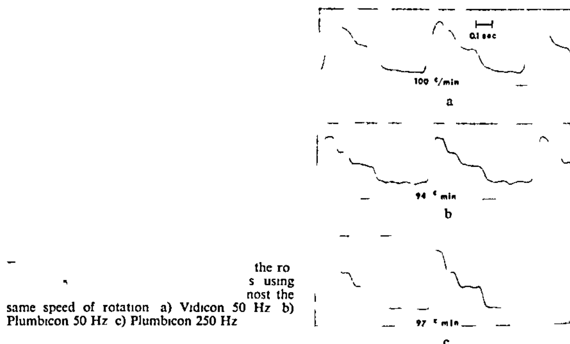
Fig 7 Videodensitometric registration of fall times (upper curves) and rise times (lower curves) of the three different television systems a) Vidicon 50 Hz, b) Plumbicon 50 Hz, c) Plumbicon 250 Hz.

system was developed by LINDBERG This very fast television system with a high speed of response is well fitted to improve the response in videodensitometry During the last ten years extensive investigations have been carried out in order to measure blood flow by videodensitometric methods in connection with angiography (HEINTZEN 1971, RUTISHAUSER et coll 1970, SMITH et coll 1971) The method is based on the principle of measuring extinction variations arising when an iodine contrast medium passes through a selected region of the circulation By measuring the velocity of the contrast bolus or the total integrated contrast area it is possible to estimate the mean flow However, if the flow profile, i e , the flow in systole respectively

Table 2

Expected and measured videodensogram of the different television systems at different speed of rotation of the disk The densogram represents the integrated area (time × density) measured by planimetry

	Disk speed c/min	
	44–45	97–100
Copper thickness of the disk (expon values)	3 2 1	3 2 1
Exposure time of the copper fields	1 1 2	1 1 2
Expected densogram (time × density)	15 10 10	15 10 10
Vidicon 50 Hz	10 12 13	9 12 14
Plumbicon 50 Hz	13 11 11	9 13 13
Plumbicon 250 Hz	13 11 11	13 11 11



the ro
s using
nost the
same speed of rotation a) Vidicon 50 Hz b) Plumbicon 50 Hz c) Plumbicon 250 Hz

Plumbicon 250 Hz system The registrations with this system were performed at the speed of the rotating disk of 64, 86 and 109 c/min (Fig 5) Also with very high speed (Fig 5 a), the correct maximum amplitude was reached even though the duration of the event was not more that 0 07 s When no low pass filter was used (Fig 5 c) a recording signal was delivered every 0 004 s The low pass filter used (20 Hz) increased the inertia of the system (compare the curves in Fig 5 b and c)

The speed of response A comparison of the speed of response of the three investigated television systems is illustrated in Fig 6, where the duration of the different copper fields of the rotating disk in the radiation beam was almost the same Obviously the Plumbicon 50 Hz system registers the events of the rotating disk better than the Vidicon 50 Hz system Also it is evident that the Plumbicon 250 Hz system is superior to the Plumbicon 50 Hz system This depends on the different speeds of response, which can be estimated from fall and rise times (Fig 7) These are defined as the time between 10 and 90 per cent of full deflection The fall of the signal occurs towards the black level of the videosignal and the rise of the signals occurs towards light The fall times and the rise times were longer for the Vidicon 50 Hz system in comparison with the Plumbicon 50 Hz system (Fig 7) Also was noted the very short fall and rise times for the Plumbicon 250 Hz system, only 0 02 s in comparison with 0 10 s fall time and 0 09 s rise time for the Vidicon 50 Hz system

Discussion and Conclusions

To provide higher time resolution in video kymography in order to demonstrate rapid changes of the movement of the heart contour, a 250 Hz Plumbicon television

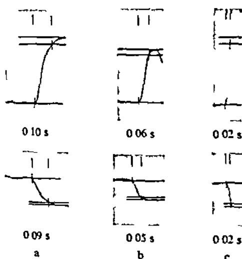


Fig. 7 Videodensitometric registration of fall times (upper curves) and rise times (lower curves) of the three different television systems a) Vidicon 50 Hz, b) Plumbicon 50 Hz, c) Plumbicon 250 Hz

system was developed by LINDBERG This very fast television system with a high speed of response is well fitted to improve the response in videodensitometry During the last ten years extensive investigations have been carried out in order to measure blood flow by videodensitometric methods in connection with angiography (HEINTZEN 1971, RUTISHAUSER et coll 1970, SMITH et coll 1971) The method is based on the principle of measuring extinction variations arising when an iodine contrast medium passes through a selected region of the circulation By measuring the velocity of the contrast bolus or the total integrated contrast area it is possible to estimate the mean flow However, if the flow profile, i e , the flow in systole respectively

Table 2

Expected and measured videodensogram of the different television systems at different speed of rotation of the disk The densogram represents the integrated area (time × density) measured by planimetry

	Disk speed c/min	
	44–45	97 100
Copper thickness of the disk (expon values)	3 2 1	3 2 1
Exposure time of the copper fields	1 1 2	1 1 2
Expected densogram (time × density)	15 10 10	15 10 10
Vidicon 50 Hz	10 12 13	9 12 14
Plumbicon 50 Hz	13 11 11	9 13 13
Plumbicon 250 Hz	13 11 11	13 11 11

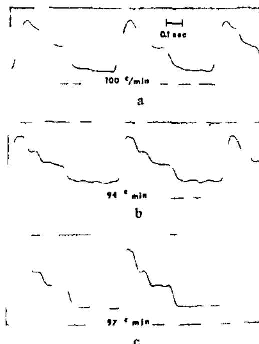


Fig 6 Videodensitometric registration of the rotating disk in the three television systems, using the same low pass filter (20 Hz) and almost the same speed of rotation a) Vidicon 50 Hz, b) Plumbicon 50 Hz, c) Plumbicon 250 Hz

Plumbicon 250 Hz system The registrations with this system were performed at the speed of the rotating disk of 64, 86 and 109 c/min (Fig 5) Also with very high speed (Fig 5 a), the correct maximum amplitude was reached even though the duration of the event was not more that 0 07 s When no low pass filter was used (Fig 5 c) a recording signal was delivered every 0 004 s The low pass filter used (20 Hz) increased the inertia of the system (compare the curves in Fig 5 b and c)

The speed of response A comparison of the speed of response of the three investigated television systems is illustrated in Fig 6, where the duration of the different copper fields of the rotating disk in the radiation beam was almost the same Obviously the Plumbicon 50 Hz system registers the events of the rotating disk better than the Vidicon 50 Hz system Also it is evident that the Plumbicon 250 Hz system is superior to the Plumbicon 50 Hz system This depends on the different speeds of response, which can be estimated from fall and rise times (Fig 7) These are defined as the time between 10 and 90 per cent of full deflection The fall of the signal occurs towards the black level of the videosignal and the rise of the signals occurs towards light The fall times and the rise times were longer for the Vidicon 50 Hz system in comparison with the Plumbicon 50 Hz system (Fig 7) Also was noted the very short fall and rise times for the Plumbicon 250 Hz system, only 0 02 s in comparison with 0 10 s fall time and 0 09 s rise time for the Vidicon 50 Hz system

Discussion and Conclusions

To provide higher time resolution in video kymography in order to demonstrate rapid changes of the movement of the heart contour, a 250 Hz Plumbicon television

crepancy between the true value and the densitometer output signal in the 50 Hz Vidicon system is illustrated in Fig 8

When measuring the pulse profile within intact circulation, the results are also dependent on the inertia of the contrast medium, the mixture conditions, the pressure injection profile and so on A discussion of these parameters, however, is beyond the scope of this report.

SUMMARY

The speed of response of a newly developed 250 Hz high image rate Plumbicon television system was compared with the ordinary 50 Hz Vidicon and Plumbicon television systems The high time resolution of the 250 Hz system, almost five times that of the 50 Hz Vidicon and three times that of the 50 Hz Plumbicon system, makes it well adapted for videodensitometry particularly if the velocity of the contrast bolus or the pulse profile within the circulation are to be evaluated

ZUSAMMENFASSUNG

Die Geschwindigkeit der Antwort eines neu entwickelten 250 Hz Plumbicon Fernsehsystems mit hoher Bildgeschwindigkeit wurde mit den normalen 50 Hz Vidicon und Plumbicon Fernsehsystemen verglichen Die hohe Zeitauflosung des 250 Hz Systems, beinahe funf mal hoher als die des 50 Hz Vidicon und drei mal hoher als die des Plumbicon Systems, macht dieses gut geeignet fur die Bildverstärkerdensitometrie, besonders wenn die Geschwindigkeit der Kontrast Ansammlung oder das Puls Profil in der Zirkulation festgestellt werden soll

RÉSUMÉ

La rapidite de reponse d un système de television Plumbicon à grande vitesse d image de 250 Hz recemment mis au point a été comparée avec les [illegible]

[illegible] pulsation dans la circulation

REFERENCES

HEINTZEN P (editor) Roentgen-, cine- and video dens[illegible] [illegible]ntals and applica-tions [illegible]

LAN[illegible] [illegible]ttgart 1971

[illegible] [illegible]rement of

LIN[illegible]

Report [illegible] Technical

Gothenburg 1972 [illegible] School of Electrical Engineering,

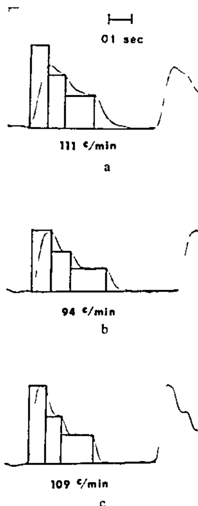


Fig 8 Videodensitometric registration of the rotating disk in the three different television systems The 'true densitometric registrations are marked in the curves to facilitate comparison of the inertia of the different systems a) Vidicon 50 Hz, b) Plumbicon 50 Hz, c) Plumbicon 250 Hz

diastole, is to be determined by videodensitometry, a fast television system with high time resolution is needed The ordinary 50 and 60 Hz systems are too slow to give a true picture of the flow alterations within one cardiac cycle Very rapid changes like the systolic peak flow cannot at all be registered by the 50 Hz Vidicon system The long fall times observed in the Vidicon system are mainly due to the lag in the reset process (discharge lag) of the Vidicon camera tube The rise-times vary slightly with the target potential, while increasing target brightness leads, as expected, to a certain reduction of the rise time The fall time is moreover strongly dependent on both the target potential and the brightness as pointed out by STRINDEHAG (1961) The Plumbicon 50 Hz system is faster but has an inertia three times the 250 Hz Plumbicon system The limiting factor of the 50 Hz Plumbicon system is the image rate The Plumbicon itself is sufficiently fast to register very quick illumination variations To obtain the full benefit of the high speed of response of the Plumbicon, the 250 Hz image rate system must be used

Table 2 gives the 'pulse profile' at different speeds of the rotating disk The dis-

ACTA RADIOLOGICA

OFFICIAL ORGAN OF THE RADIOLOGICAL SOCIETIES OF
DENMARK, FINLAND, NORWAY AND SWEDEN

Vol 16
Fasc 5

DIAGNOSIS

1975
September

MYELOGRAPHY WITH THE NON-IONIC WATER-SOLUBLE CONTRAST MEDIUM METRIZAMIDE

TOMAS HINDMARSH

The use of water-soluble contrast media for myelography has up till now been restricted to the lumbar region of the subarachnoid space Recent advances in chemical synthesis, however, have provided a medium, metrizamide, which seems promising for use also in other parts of the subarachnoid space Animal experiments (Acta radiol Suppl No 335, 1973) and preliminary clinical experiences (HINDMARSH 1973, GONSETTE 1973, SKALPE et coll 1973) have indicated that the toxicity of this medium is very low Apart from toxicity, water soluble media raise specific technical problems when used for examination of the spinal subarachnoid space The purpose of this report is to review some of these problems

Material and Methods The material consisted of a consecutive series of 45 patients (28 males and 17 females) with a mean age of 51 2 years (range 19 to 78), examined with myelography above the lumbar level from May, 1973 to March, 1974 With the exception of one patient with a subarachnoid haemorrhage all patients had a history of loss of sensibility or muscular dysfunction indicating spinal cord or root involvement In 14 cases the symptoms and signs were considered to be

From the Department of Neuroradiology (Director T Greitz), Karolinska sjukhuset, S-104 01 Stockholm, Sweden

Submitted for publication 5 April 1974

RUTISHAUSER W, SIMON H, STUCKY J, SCHAD N, NOSEDA G and WELLAUER J: Evaluation of roentgen densitometry for flow measurement in models and in intact circulation Circulation 36 (1967), 951

— BUSSMANN W, NOSEDA G, MEYER W and WELLAUER J Blood flow measurement through single coronary arteries by roentgen densitometry I A comparison of flow measured by radiologic technique applicable in the intact organism and by electromagnetic flowmeter Amer J Roentgenol 109 (1970), 12

— NOSEDA G, BUSSMANN W and PRETER B Blood flow measurement through single coronary arteries by roentgen densitometry II Right coronary artery flow in conscious man Amer J Roentgenol 109 (1970), 21

SMITH H, FRYE R, DAVIS G, DANIELSON G, PLUTH J, WALLACE R, STURM R and WOOD E Measurement of flow in aorta-coronary saphenous vein grafts by roentgen videodensitometry Circulation 44 (1971), 107

— — DONALD D, DAVIS G, PLUTH J, STURM R and WOOD E Roentgen videodensitometric measurement of coronary blood flow Proc Mayo Clin 46 (1971), 800

STRINDEHAG O Optimized performance of the vidicon Chalmers University of Technology, Division of Tele Technique, Gothenburg 1961

started with injection of oxygen and at the finding of a complete spinal block at the tumour site, the examination was continued with metrizamide The gas myelography was always performed by lumbar puncture and the technique of WESTBERG (1966) was used The injection of the positive contrast medium was always made by the lumbar route usually at the level L2-L3 With 4 exceptions the patients were given diazepam 5 mg intravenously before myelography and most of them at 4 hour intervals during the following 24 hours

Metrizamide—chemically a glucose amide—is a non ionic compound with a molecular weight of 789 1, containing three iodine atoms The substance is only available as a freeze-dried crystallinic powder which before use is dissolved in a bicarbonate buffer solution in the amount needed to obtain the suitable concentration In 4 cases the concentration used was 140 mg I/ml, in 14 170 mg I/ml, in 16 200 mg I/ml, and in 11 cases 300 mg I/ml The mean dose calculated as the amount of iodine was 2 56 g (range 0 9–5 1 g), which corresponds to 15 ml of an isotonic solution

Physical properties Metrizamide forms molecular solutions in water and does not dissociate into anions and cations Owing to this fact solutions of this medium are of comparably low osmolality A concentration of 170 mg I/ml, sufficient for many purposes, is isotonic with the CSF (Fig 1) The highest concentration used in this material was 300 mg I/ml, which corresponds to an osmolality of 0 484 mol/kg

Due to the iodine content solutions of water-soluble contrast media in concentrations used in radiologic practice, have a density that exceeds that of normal CSF, which varies from 1 005 to 1 009 g/ml (SUNDERMAN & BOERNER 1950) Metrizamide has a density of 1 184 at a concentration of 170 mg I/ml and 1 329 at 300 mg I/ml (Fig 1) The high density is responsible for the initial layering of the contrast medium The layering phenomenon must be appreciated and can be made an advantage in examination of a selected region by positioning the patient in such a way that this region constitutes the lowermost part of the subarachnoid space When the medium is directed to an area distant from the injection site mixing with the CSF takes place Hence, the longer the distance from the injection site, the higher the concentration to be used 140 to 170 mg I/ml for examination of the lumbar region, 300 mg I/ml for the cervical region

The density of any clinically useful water soluble contrast medium also exceeds that of the spinal cord, as exemplified during examination of the thoracic region When metrizamide in a concentration of 200 *mg I/ml* was first injected with the patient in the lateral recumbent position, the cord became elevated as if floating on the contrast medium this being merely due to the space occupying effect of the medium (Fig 8) However, when the patient was *turned to* the supine position, the spinal cord returned to the midline position and stayed there irrespective of further changes in the patient s position because by *this time* the contrast had been almost fully mixed with the CSF, and the spinal cord was floating in a fluid with a density

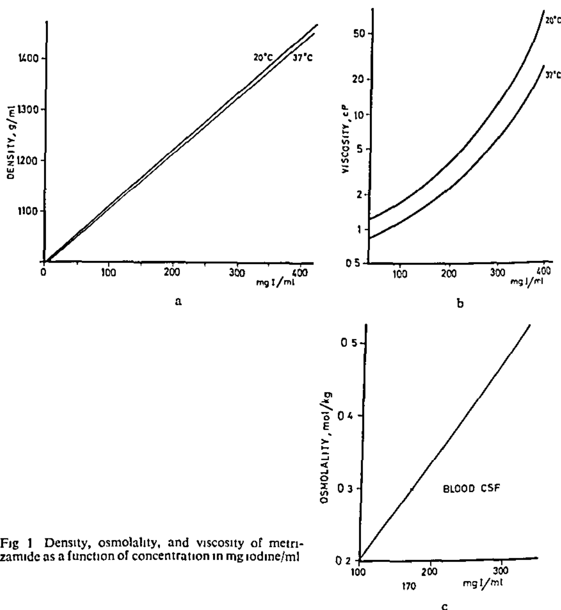


Fig 1 Density, osmolality, and viscosity of metrizamide as a function of concentration in mg iodine/ml

caused by protrusion of disks, osteophytes on vertebral bodies or on articular facets Extradural expansive lesions were revealed in 7 cases, juxtamedullary tumour (4 meningiomas and 1 neurinoma) in 5, and intramedullary tumour in 6 cases One case of syringomyelia was found One fracture dislocation (of a vertebral body), one dislocation from spondylolisthesis and a severe kyphosis of the thoracic region were the probable causes of presented clinical symptoms and signs in 3 other cases One patient had an arteriovenous malformation In a further 8 patients the myelography did not reveal any pathology to account for symptoms Twenty-two patients were also examined with gas myelography In 7 of these cases, all with tumours with rapid onset or a fast deterioration of neurologic symptoms and signs, the examination

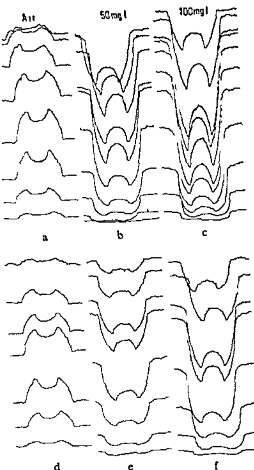


Fig 3 Densitometry tracings of test films obtained from the plastic phantom in Fig 2 a, b, c) Exposed with 80 kV, d, e, f) with 140 kV Optimum exposure data in a) 78 mAs, 0 32 s, b) 165 mAs 0 8 s, c) 420 mAs, 3 2 s, d) 16 mAs, 0 08 s, e) 16 mAs, 0 08 s, f) 26 mAs, 0 16 s

A fairly high viscosity of the contrast medium may in some instances be an advantage as it makes the medium more dirigible However, available high viscosity media have a high surface tension, which brings about a decreased capacity of these media to penetrate into narrow spaces and consequently lessens their diagnostic potential It is evident that water-soluble contrast media are superior to oily media in providing detailed information of small structures and narrow spaces, such as nerve roots and root pockets (Fig 10) In this respect they also excel gaseous media However, the spinal cord itself is often not as well delineated with water soluble medium as with gas (Fig 11) One explanation for this may be that fairly long exposure times are required

The exposure data to be used are determined by the attenuation properties of iodine solutions Densitometry on test films of a plastic phantom of the spinal cord and the surrounding subarachnoid space (Fig 2) demonstrated that, with optimum exposure data, iodine solutions (50 mg I/ml and 100 mg I/ml) were superior to gases in produc-

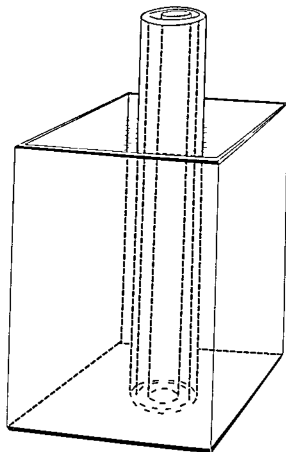
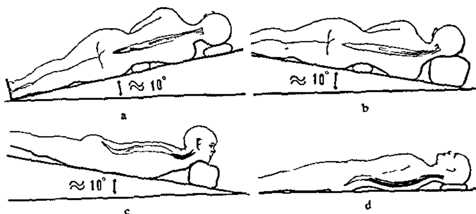


Fig 2 Plastic phantom used for test film series Central rod (diameter 10 mm) represents spinal cord, the surrounding space (diameter 20 mm) represents sub arachnoid space The phantom is immersed in a water basin with a thickness of 10 cm in the beam direction

close to that of normal CSF In the sagittal plane the thoracic part of the spinal cord always had a rather anterior location and remained there irrespective of the positioning of the patient (Fig 9) Hence, the posterior subarachnoid space in all cases was well filled with medium At gas myelography on the other hand, the cord is usually posteriorly located in the thoracic segment In the 22 cases examined with both media the retromedullary space in the thoracic region was not filled with gas in 15 instances Most of these cases were examined in the lateral recumbent position with vertical beam and not in the prone position However, JIROUT (1969), who systematically employs the prone position of the patient, reports adequate filling of the posterior subarachnoid space in only 50 per cent of 117 cases with a normal thoracic vertebral canal The anterior location at metrizamide myelography is probably the true one under physiologic conditions as in patients with a slow elimination of medium, the cord had the same position after 24 to 48 hours when complete mixing of the contrast medium with the CSF had taken place Except for the displacement induced by the contrast medium when first injected, it seems unlikely that the medium induces unphysiologic displacements This is more common when gaseous media are used



these requirements In lumbar myelography, where the contrast medium is brought to the level of the L1 vertebra, diagnostic films can be obtained for several hours after the injection, provided that the patient remains in a half sitting position (Fig 12 c) In the thoracic region films with adequate information can be obtained for up to 2 hours, if escape of medium to the cervical region and the head is kept to a minimum (Fig 12 b) In the cervical region, however, it is not possible to prevent dilution and transport of medium to the basal cisterns, which brings out time as an essential factor (Fig 12 a) The early appearance of contrast medium in the basal cisterns after myelography of the cervical region can be evidenced by use of computer tomography (CT scanning) shortly after myelography (Fig 13) It would appear that elimination of the medium takes place mainly over the convexity of the brain and probably to a minor degree in the spinal subarachnoid space When the CSF circulation is impaired, e g by partial block, contrast medium may be radiologically demonstrated inferior to the lesion up to 48 hours after injection In patients without signs of impediment of the CSF circulation, the medium can no longer be demonstrated in the spinal subarachnoid space after 24 hours In 10 patients without block, 24 hour CSF specimens were analysed for iodine content This gave a mean of 3 mg I/ml (range 0 2–6 0) The mean dose of contrast medium in these cases was 2 79 g I In another patient with a relative block to the passage of contrast, the iodine content was 23 6 mg/ml (dose at myelography 2 4 g I), which also indicates that spinal subarachnoid absorption of the medium is low

Adverse reactions A complication indicative of a serious toxic effect appeared in one patient who was under treatment with chlorpromazine, which is known to lower the

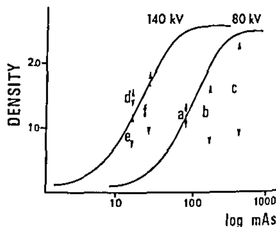
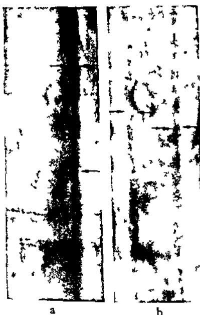


Fig 4 Film density curves for the 140 kV and 80 kV exposures in the test films The span of density variations obtained by optimum exposure in each series is demonstrated Films indicated by letters as in Fig 3

ing differences in absorption This capacity was greatest lateral to the cord in the subarachnoid space alone and increased with increasing concentration of the iodine solution From the densitometry curves (Fig 3) and the corresponding film density graphs (Fig 4) it is, furthermore, apparent that the range of absorption differences produced by iodine at optimum exposure has a much greater span in the linear part of the film density curve than the range of absorption differences in an optimum exposure using gas This means that with iodine it is more difficult to adapt the exposure data for optimum recording of all parts of the phantom, and this also implies long exposure times In practice it often proves difficult to obtain optimum conditions in all parts of a film exposed at myelography with a positive medium, where bony structures are superimposed on the contrast medium in the subarachnoid space and where the medium is often unevenly distributed due to anatomic conditions or to layering Often the cord is sharply outlined at one border and unsharp at the other border in the same film In lateral films of the lumbar area and the thoracocervical junction it often proves necessary to increase the tube potential to the level of 90 kV or sometimes 100 kV to reduce exposure times enough to avoid blurring by motion High kilovoltage may be used in combination with media of high concentration but is not recommended since this would lessen the attainable range of absorption differences (Fig 3 f) to a range close to that obtained with gas This would also necessitate higher radiation doses than gas myelography As has been stated gas produces much smaller differences in absorption than iodine solutions However, with high kilovoltage technique, preferable in that it avoids obscuration by osseous structures, the exposures are very short, radiation doses are not too high and blurring due to motion is negligible

Elimination of the contrast medium To allow complete examinations of the subarachnoid space the contrast medium should be eliminated at a suitable rate, slow enough to provide time for survey films, detailed scrutiny of possible lesions and repeat films, but not as slow as to cause problems with after-care Metrizamide fulfils



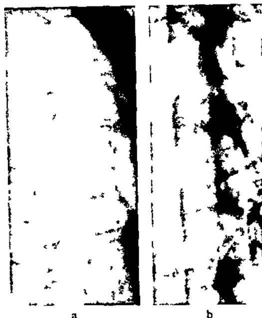


Fig 8 Fig 9

Fig. 8 a) Film obtained with horizontal beam direction demonstrating initial layering of the water-soluble medium and displacement of the cord to the right (upper side) b) Later stage of examination Contrast med um almost completely mixed with CSF midline position of the cord

Fig 9 Typical position of the spinal cord in the lateral projection in the upper thoracic segment Myelography with a) gas and b) metrizamide Both films exposed with vertical beam direction

tumour) had a slight and transient increase of leg paresis All symptoms and signs were of a mild character and usually passed within the first 24 hours after examination and never lasted longer than 48 hours

As in lumbar myelography (HINDMARSH 1975) the meningeal reaction, as evidenced by increase in CSF white cell count usually was very small Twenty seven patients were repunctured 22 to 26 hours after examination Twenty of these had none or very slight increase (less than 10 cells/mm³) Seven cases, 4 of which had complete or partial block had increase in white cell count ranging from 75 to 1 035 cells/mm³ No direct correlation existed between spinal block and 24 hour white cell count in these few cases

Technical considerations The ideal equipment for myelography with water soluble contrast media should allow a rotation of 360° about the longitudinal axis of the patient and should also incorporate the standard myelographic requirements of a +90° to −30° tilting table An image intensifier-TV system is necessary to make use of the layering effect to its greatest advantage Moreover, facilities for taking films with both vertical and horizontal beam directions are required

An equipment that fulfils the abovementioned requirements was the UGX apparatus manufactured by Muller, but no longer on the market (Fig 6) The patient is fully

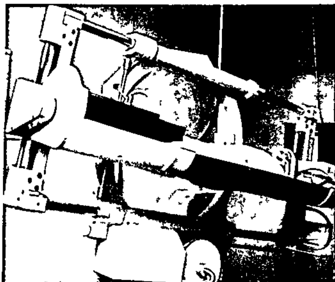
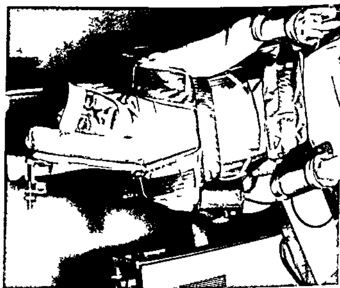


Fig 6 The UGX apparatus has facilities for full somersault movement and allows, in addition, 360 rotation about the longitudinal axis of the table Any position of the patient is possible Firm attachment of the patient is offered by the curved table



a



b

Fig 7 Elema rotating chair table (RCT III) equipped with head rest, hip rest and extra braces (a) providing proper support to the patient in the lateral decubitus position (b)

seizure threshold This patient, who had no premedication with diazepam, had two grand mal seizures A report of this case is given separately (HINDMARSH et coll 1975), where evidence is presented suggesting interaction between metrizamide and phenothiazine derivatives In no other case has any serious complication appeared Excluding 8 patients who were operated upon directly after myelography, the frequency of different symptoms was for headache 29 per cent, nausea 16 per cent, dizziness 14 per cent, and increase of preexisting pain 27 per cent Two patients (one suffering from arteriovenous malformation, the other from an intramedullary

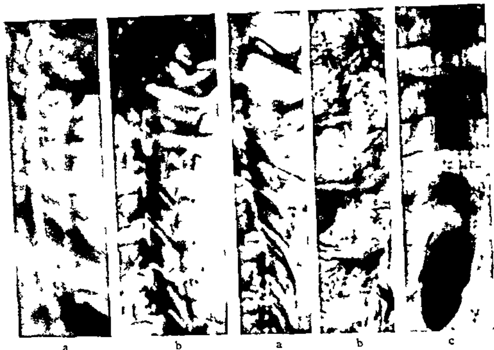


Fig 11 Fig 12

Fig 11 Same patient examined with myelography a) with gas and b) metrizamide With gas (140 kV) the delineation of the cord is better than with metrizamide (70 kV)

Fig 12 Three different patients examined 2 hours after injection of metrizamide in a concentration of 170 mg I/ml Dose in a) 12 ml in b) 16 ml and in c) 15 ml

head rests However, if the root pockets are to be examined on both sides using the layering technique it is necessary to raise the patient to the sitting position between examination of the two sides This is the consequence of the limited rotation and usually implies the necessity of introducing more contrast medium in order to outline the roots of the second side Nevertheless, the RCT III Mimer combination has been used particularly for the cervical region, where detailed films of the rootlets may be obtained For complete routine myelography, however, it was found that an ordinary remote-control tilting table was more advantageous

The procedure employed in the majority of examinations in the present material was as follows The patient was positioned in the lateral decubitus position with the head end of the tilting table elevated 10° (Fig 5 a) The puncture was performed usually at the L2–L3 level with a needle (OD 0 7 mm) connected to a glass syringe with a plastic tube (length 15–20 cm) The injection of contrast medium was monitored on the TV screen and when the medium reached the first lumbar vertebra three films were exposed with horizontal beam the first with the patient slightly rotated forward the second in the prone position, the third with the patient on the other side again slightly rotated forward (Fig 14) If the lumbar region only is to be

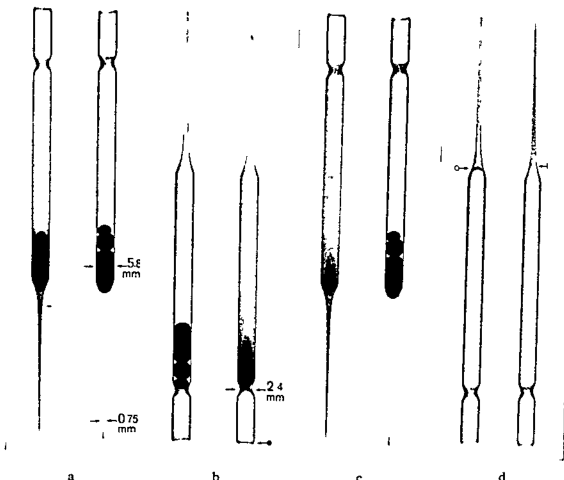


Fig 10 Two glass pipets filled with CSF, to one 1/2 ml of metrizamide 300 mg I/ml has been added and to the other 1/2 ml of an oily medium with the same iodine concentration (Pantopaque) a)

have been emptied by gentle injection of air Fluid lingers above an oil film at (o→) and at (↦) in the metrizamide containing pipet

extended and firmly attached to a table with curved side supports in either lateral decubitus position The lumbar puncture needle may remain in place during the whole examination without risk of displacement or trauma However, modifications to incorporate a cassette holder are needed An alternative equipment is a rotating chair, such as Elema RCT III (Fig 7) in combination with a Mimer The chair allows, in addition to 360° rotation about the transverse axis, 200° rotation about an axis perpendicular to the seat, i e the longitudinal axis of the patient, as long as the chair is not converted to the flat table position Unfortunately, this set-up cannot readily be used for complete myelography in its present form because of the small margin of movement of the U-arm around the chair It is true that all parts of the spinal canal in a patient of ordinary size can be examined using additional braces, hip and

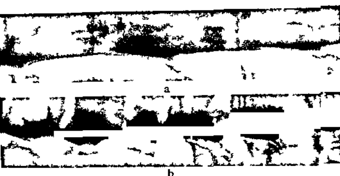


Fig 15



Fig 16

Fig 15 Roots and root sleeves on left side demonstrated with the layering techn que using horizontal beam d rection and metrizam de ?00 mg I/ml a) D10–D1? b) C4–C8

Fig 16 Tomograph c cut demonstrating rootlets (→) C6 and C7

a b c

Fig 17

a b

F g 18

Fig 17 Survey f lms exposed at the end of the examination a b) Lateral f lms of normal case c) A p f lm of a tumour cyst in the conus reg on

F g 18 P

a) Gas m

not demo

space f lle

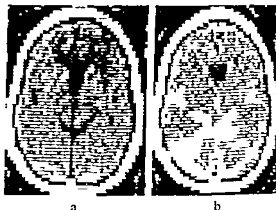


Fig 13 Computer tomography a) before and b) 3 hours after myelography with 16 ml metrizamide in a concentration of 200 mg I/ml Tomographic section above and parallel to the supraorbitomeatal line In (b) contrast medium is demonstrated infra- as well as *supratentorially*

examined straight and oblique films exposed in the upright position after withdrawal of the needle may conclude the examination At this stage it is possible to examine the spine and the lumbar subarachnoid space in various conditions regarding motion, strain, etc, if desirable However, it is not often that a myelography is strictly confined to the lumbar region, as it is generally accepted that a lumbar myelography should also include the lower thoracic region

For examinations also of other parts of the spinal subarachnoid space, the needle must be kept in position With the patient still in the lateral position, the contrast medium was made to flow in the cephalic direction by gently lowering the head-end of the table Intracranial escape of the medium was prevented by placing the head on a firm 10 to 15 cm thick pillow (Fig 5 b) A p films were exposed of the roots and root pockets in the thoracic region (Fig 15 a) and then the tilt was increased until these structures were outlined also in the cervical region (Fig 15 b) The needle



Fig 14 ... lateral films of the ... zontal ... from disk hernia in the subarachnoid space on the left side with flattening of the L5 root

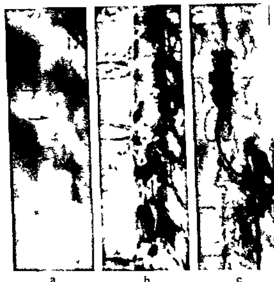


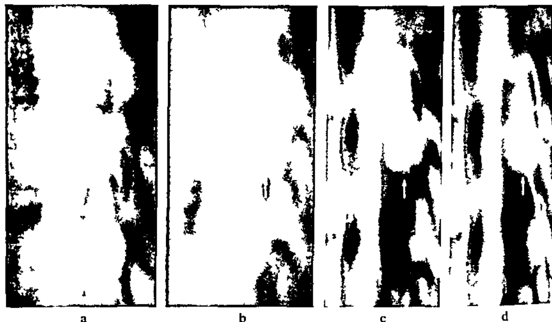
Fig 20 Arteriovenous malformation with maximum extension at the level of D 10 a) Gas myelography demonstrates minor irregularities in the anterior border of the cord (→) b) Myelography with metrizamide gives a better concept of the nature and extent of the lesion c) Spinal angiography

a specific level, this should be examined in the first place If the cervical roots are of paramount interest, contrast medium should be directed to the cervical region initially, with the patient in the lateral position on the symptomatic side, and the head deflected upwards as described

The amount of contrast medium should be related to the clinical signs and symptoms, as well as to the extent of the myelography For example, a complete block could be demonstrated with only a few ml of medium, while for the lumbar region 10 ml were usually sufficient, this amount also being adequate if the examination is extended to the lower thoracic region For the thoraco cervical region 10 to 15 ml were required, but if a thorough detailed examination of all parts of the spinal subarachnoid space was performed then 20 ml or more were required if the space was wide All figures given refer to a concentration of 170 mg I/ml If a higher concentration is used the volume should be decreased proportionately

Comparison between myelography with metrizamide and myelography with other media No direct comparison with oily media has been possible, since oily media have not been adopted for clinical use in this country, but the results obtained in the 22 cases examined with both gas and water-soluble medium have been compared

In 3 cases with extradural metastasis, the medium passed readily the lesion, which, however, caused a complete block to the passage of gas In 4 other cases (2 extradural metastases and 2 intramedullary tumours) obstruction was complete to both media The narrowed space adjacent to the tumour was, however, usually better outlined with metrizamide and the constant filling of the retromedullary space was an advantage Filling of this space easily gave a conclusive diagnosis in a case of severe atrophy of the spinal cord ... secondary to kyphosis (Fig 18) The posterior dura



— elia with a cyst
olume variations

was then withdrawn unless the roots and root pockets of the other side also were to be demonstrated The patient was again placed prone (Fig 5 c), care being taken to keep the head as high as necessary and a p films of the cervical region were exposed If tomography was applied even the rootlets in the cervical region were usually well identified (Fig 16) In other regions, tomography did not provide much information that could not be gained from conventional films From the prone position the patient was placed on the side not yet examined, as before with the head deflected upwards A general survey could be obtained directly but detailed information of the roots of the second side required further injection of medium At this stage the needle could be withdrawn in all cases Lateral survey films were then obtained (Fig 17 a b) before the patient was eventually placed supine (Fig 5 d) the table now coming to the horizontal position and survey a p films were exposed as required These final films usually provided an excellent demonstration of the spinal cord and the cauda equina (Fig 17 c) possibly supplemented by oblique a p views If only complementary films of the lower thoracic region are wanted in connection with a lumbar examination a reduced program may be applied

Throughout the entire examination the head was consistently kept at a higher level than the cervical region Because of the quick mixing with the CSF taking place in this region contrast medium nevertheless filled completely the cervical subarachnoid space to the foramen magnum Details were lost in the later phases however, due to the concentrated medium being successively more diluted by the CSF for every new position Consequently when clinical signs and symptoms indicate

Metrizamide, a non ionic water-soluble contrast medium Acta radiol (1973) Suppl No 335

PEACHER W G and ROBERTSON R C. L Pantopaque myelography Results, comparison of contrast media, and spinal fluid reaction J Neurosurg 2 (1945), 220

SKALPE I O, TORBERGSEN T, AMUNDSEN P and PRESTHUS J Lumbar myelography with metrizamide Acta radiol (1973) Suppl No 335, p 367

SUNDERMAN F W and BOERNER F Normal values in clinical medicine Saunders, Philadelphia 1950, p 315

TARLOV I M Pantopaque meningitis disclosed at operation J Amer med Ass 129 (1945), 1014

WESTBERG G Gas myelography and percutaneous puncture in the diagnosis of spinal cord cysts Acta radiol (1966) Suppl No 252

ZUSAMMENFASSUNG

Es werden die technischen Probleme bei der Myelographie mit einem wasserloslichen Kontrastmittel, Metrizamide, analysiert und eine verwendete Technik zur Untersuchung des gesamten spinalen subarachnoidalen Raums beschrieben Die Wahl zwischen einem gas- oder wasser-loslichen Kontrastmittel zur Myelographie wird ebenfalls diskutiert

RÉSUMÉ

L'auteur étudie les problèmes techniques de la myélographie avec un moyen de contraste hydrosoluble, le métrizamide, et décrit une technique utilisée pour l'examen de totalite de l'espace sous-arachnoïdien rachidien Il examine aussi le choix du moyen de contraste gazeux ou hydrosoluble pour la myélographie

REFERENCES

BERGERON R T, RUMBAUGH C L, FANG H and CRAVIOTO H Experimental pantopaque arachnoiditis in the monkey Radiology 99 (1971), 95

CLARK R G, MILHORAT T H, STANLEY W C and DI CHIRO G Experimental pantopaque ventriculography J Neurosurg 34 (1971), 387

DAVIES F L Effect of unabsorbed radiographic contrast media on the central nervous system Lancet 2 (1956), 747

ERICKSON T C and VAN BAAREN H J Late meningeal reaction to ethyl iodophenylundecylate used in myelography J Amer med Ass 153 (1953) 636

FERRY D J, GOODING R, STANDEFER J C and WIESE G M *Effect of pantopaque myelo*graphy on cerebrospinal fluid fractions J Neurosurg 38 (1973), 167

GONSETTE R E Metrizamide as contrast medium for myelography and ventriculography Preliminary clinical experiences Acta radiol (1973) Suppl No 335 p 346

HINDMARSH T Methiodal sodium and metrizamide in lumbar myelography Acta radiol (1973) Suppl No 335, p 359

— Lumbar myelography with meglumine iocarmate and metrizamide Acta radiol Diagnosis 16 (1975) 209

— GREPE A and WIDÉN L Metrizamide-phenothiazine interaction Report of a case with seizures following myelography Acta radiol Diagnosis 16 (1975) 129

HOWLAND W J and CURRY J L Experimental studies of pantopaque arachnoiditis Radiology 87 (1966), 253

— — Pantopaque arachnoiditis Acta radiol Diagnosis 5 (1966), 1032

HURTEAU E F, BAIRD W C and SINCLAIR E Arachnoiditis following the use of iodized oil J Bone Jt Surg 36 (1954), 393

JMIELINSKI B L et CHMIELEWSKI J M Arachnoidite adhésive intrarachidienne à la suite de myélographies à l'ethiodane (pantopaque) J Radiol Electrol 52 (1971), 31

JAK [illegible] the side effects of myelo [illegible]

JIROUT J [illegible] Springfield, Illinois 1969, p 59

MASON M S and RAAF J Complications of pantopaque myelography J Neurosurg 19 (1962), 302

The present investigation deals with the use of pre- and postoperative tomography in reconstructive surgery of the ossicular chain

In middle ear surgery the intention is usually to reconstruct the sound transmitting mechanism directly after cleaning measures have been undertaken If this is not feasible, it may be done in a second stage operation Preservation or reconstruction of the bony external acoustic meatus is essential for the anatomic and functional result

In cases with a previous radical mastoidectomy the bony meatus can be reconstructed with cortical bone autograft The operation cavity in the present series of operations was usually obliterated with bone chips and muscle tissue

There are two fundamental types of ossicular reconstruction with auto- or homotransplants, based on the primary defect (Fig 1)

(1) In the first type of procedure (the A type), the stapes is intact The lesion is often located to the long process of the incus (Fig 1 a) The gap between the stapes and the malleus or the drum can be bridged with the body of the incus—incus transposition (Fig 1 b)—or by using a boot shaped transplant prepared from an incudal auto or homograft or from cortical bone (Fig 1 c)

(2) In the second type of procedure (the B type), only the stapedial footplate remains (Fig 1 d), and the columella (cortical bone) acquires a boomerang like shape with its long, gracile wing resting on the footplate and its wider shaft attached to the reconstructed tympanic membrane—myringoplasty (Fig 1 e) This type is often combined with extensive reconstruction of parts of the osseous external meatus after previous radical mastoidectomy (Fig 1 d, e, f, g)

The present investigation is limited to the tomographic appearances of reconstructed middle ears with osseous transplants The intention is to elucidate the possibilities of tomography to provide information in pre- and postoperative examination of patients with middle ear diseases

Material and Methods

Experience was gained from 65 selected, operated cases from the period 1967 to 1970 The patients were primarily examined by conventional roentgenography and also underwent preoperative and postoperative tomography with the Polytome in some of the five routine projections, the true lateral, antero posterior, halfaxial, axial pyramidal and Stenvers' projections (MUNDNICH & FREY 1959, JENSEN & ROVSING 1971) Exposure data 55–75 kV, 50 mA, 11 6 s (double hypocycloid movement) 0 3 mm focal spot, magnification factor 1 3 The radiographic system consisted of universal film (processed in a 3 5 min Pakorol machine) and high definition screens (Siemens Rubin) The tomograms (4- or 6-seriograms, each tomogram 5 cm in diameter) were evaluated in an ordinary viewing box with a mask with a density of 1 5–1 8 The tomograms were harmonized by means of an electro mechanical dodger (courtesy Rikets Allmänna Kartverk, Geographical Survey Office of Sweden, Stockholm)

FROM THE DEPARTMENT OF DIAGNOSTIC RADIOLOGY, AKADEMISKA SJUKHUSET, UNIVERSITY OF UPPSALA, S-750 14 UPPSALA, AND THE DEPARTMENT OF OTOLARYNGOLOGY, REGIONSJUKHUSET, UNIVERSITY OF LINKÖPING, S-581 85 LINKÖPING, SWEDEN

MULTIDIRECTIONAL TOMOGRAPHY IN RECONSTRUCTIVE MIDDLE EAR SURGERY

H F WILBRAND and L EKVALL

The planning and prognosis of reconstructive surgery of the middle ear require detailed information about the functional and anatomic status of the tympanic cavity and mastoid cells This is also of particular importance in the occasional occurrence of secondary postoperative hearing impairment Clinical and audiologic data extended by a detailed roentgenographic evaluation afford the best possibility of arriving at a reliable diagnosis

Tomography has proved its usefulness in the demonstration of the ossicles (BRUNNER et coll 1961, DULAC 1961, FREY 1964, WRIGHT et coll 1969, SANDSTRÖM & WILBRAND 1971, JENSEN et coll 1973) Conventional roentgenography of the temporal bone, even with a variety of special positioning, is unable to provide similar information The tomographic appearance of various pathologic conditions which give reason for surgical reconstruction of the ossicular chain has been described extensively in otoradiologic literature (AGAZZI et coll 1958, MÜNDNICH & FREY 1959, VALVASSORI 1963, 1965, 1967 PORTMANN & GUILLEN 1967, ANDRÉ et coll 1968, JENSEN & ROVSING 1971)

LANGFELDT (1960, 1963) reported on tomography of the middle ear in columella operations (HALL & RYTZNER 1957, 1959)

Submitted for publication 11 January 1974

a b c

d e f

F g 1 Defects in the oss cular cha n and correspond ng



g

Preoperat ve tomography yields essential information in

(1) *Chronic otitis* The condition of the mastoid cells and their septa the extent of destruction and of the a r content of the cells and of the tympanic space can be evaluated in detail The extent of destruction of the indiv dual ossicles can be established In *cl olesteatoma* destruction of the bony septa in the epitympanum and

Abbreviations used in the figures (they correspond to those applied by K H Frey, J Jensen, H Roising and K Terrahe)

1	external acoustic meatus
2	tympanic cavity
2 a	epitympanic recess
2 b	mesotympanic cavity
2 c	hypotympanic recess
3 a	malleus
3 b	incus
3 c	stapes
5	mastoid process
VII	facial canal
VII a	facial canal, labyrinthine part
VII b	facial canal, 1st bend
VII c	facial canal, tympanic part
VII d	facial canal, 'lateral knee', 2nd bend
VII e	facial canal mastoid part
VII f	sty omastoid foramen
8	cochlea
8 a	cochlea, basal turn
9	vestibulum
9 a	oval window
9 b	round window
10	lateral semicircular canal
11	superior semicircular canal
11 a	superior semicircular canal, ampullary region

12	posterior semicircular canal
12 a	posterior semicircular canal ampullary region
13	internal acoustic meatus
17	temporal squama
18	sigmoid sinus
19	jugular fossa
20	tympanic temporal bone
22	mandible
23	zygomatic process
28 e p	pyramidal eminence
B Tr	bone transplant (bone chips or cortical transplants
C m	mastoid cells
C Sk	canal skin
C tr	cortical transplant
Col	columella
F	fascial tissue
f c m	middle cranial fossa
f c p	posterior cranial fossa
M T	muscle tissue
Op	operation defect
Op C	operation cavity
Pr	promontorium

The indication for postoperative tomography after reconstructive procedures for chronic otitis was to establish the appearance and position of the osseous auto- or homotransplant or in some cases to find an explanation for failure of hearing improvement or a secondary hearing reduction

Roentgenography

Conventional roentgenography The evaluation of the temporal bone on these films is restricted to an appraisal of the air cells, the range of pneumatization (distance between the sigmoid sinus and the posterior wall of the external auditory meatus and the peri-labyrinthine pneumatization) as well as changes of an inflammatory, cholesteatomatous, or other nature Conventional roentgenography allows a survey of the middle ear and inner ear structures, but finer details such as alterations for example in the ossicular chain, the optic capsule and the facial canal or the boundaries of the jugular fossa cannot be satisfactorily demonstrated Such structural details may be demonstrated however, by multidirectional tomography (hypocloid, spiral)

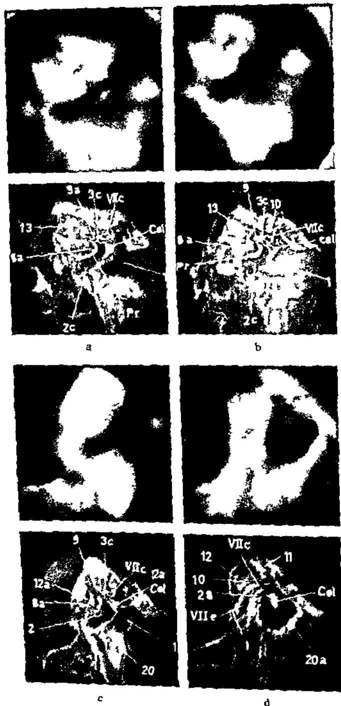


Fig 3 (For legend see opposite page)

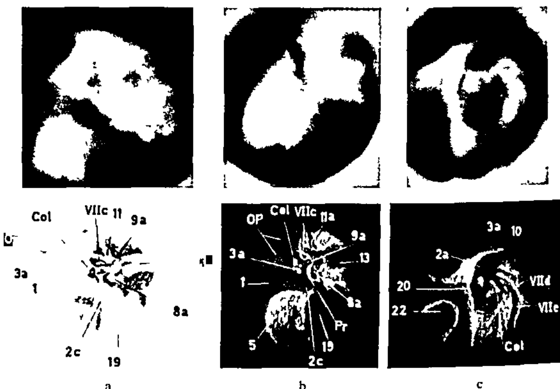


Fig 2 A-type reconstruction (incus transposition) a) A p projection The remainder of the incus ... the peri-

space c) Lateral projection Appearance of the transposed incus in relation to the lateral aspect of the facial canal

aditus ad antrum can be revealed In extensive cholesteatoma tegmental erosions may be detected, as well as destructions in the otic capsule (labyrinthine fistula)

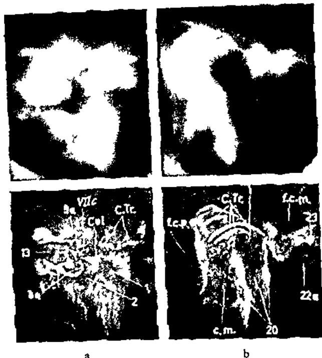
Preoperative knowledge of spontaneous or pathologic defects of the facial canal increases the safety of the surgical procedure

(2) *Trauma* It is essential that the dislocations in the ossicular chain (luxation) and the detailed course of fractures be outlined In traumatic facial palsies the appearance of the facial canal must be established

(3) *Malformations* of the middle ear The extent and configuration of the air spaces as well as of the osseous atresia of the external acoustic meatus and the shape of the ossicular chain need to be clearly revealed

... shows a bevelled section of ...

eminence



F g 5 Ro me [illegible]

[illegible] external meatus

footplate of the stapes (Figs 4 5) The appearance of the external meatus reconstructed by bone transplants is best demonstrated in the true lateral *projection*

(3) In cases of unattained hearing improvement or recurrence of hearing impairment the same projections will be used By tomography, dislocation or abnormal inclination of the columella may be detected A case of secondary hearing impairment is illustrated in Fig. 6 Tomography revealed that the columella was abnormally located in relation to the boundaries of the oval window and to the tympanic part of the facial canal thus possibly fixed to this structure This conclusion was confirmed at reoperation

Such complications may be more often expected in a B type than in an A type operation In the latter detachment of the columella from the stapes head might be expected Another mechanical cause of postoperative hearing loss detected by tomography in one case is penetration of the columella through the stapedial foot plate (Fig 7) Defective postoperative aeration of the middle ear is another cause of hearing impairment discernible tomographically

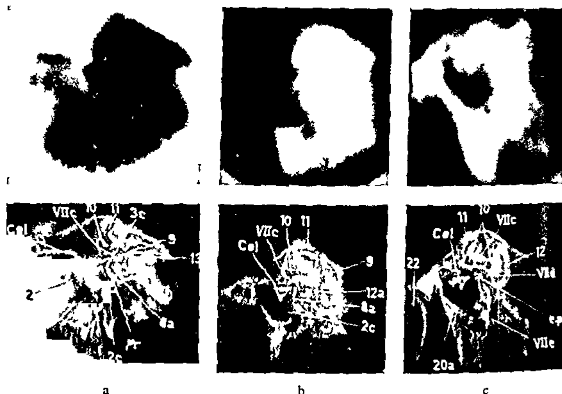


Fig. 4. Boomerang shaped B columella inserted in the middle ear in order to restore hearing. a) *Halfaxial projection.* The boomerang-columella is seen resting with its tip on the stapedial footplate and its free position in the aerated tympanic space. Small defect of the tympanic part of the facial canal. b) Axial-pyramidal projection. c) Lateral projection. The inclination of the B columella is seen to be free from contact with its bony surrounding (the tympanic part of the facial canal and the pyramidal eminence of the posterior tympanic wall).

In malformation as well as in acquired pathologic conditions information concerning the oval and round windows is important in planning of the operation. The facial canal has to be outlined since its course may be abnormal.

Postoperative tomography. The main interest is concentrated on the long term appearance and position of the bony transplants in the middle ear.

(1) In an A type reconstruction using the incus transposition method the ossicular situation is demonstrated in the a.p., halfaxial and lateral projections (Fig. 2).

In the present version a boot-like A transplant (Fig. 1 c) is well demonstrated in the a.p. view and even more favourably in the halfaxial or axial-pyramidal as well as in the true lateral projection (Fig. 3).

(2) The boomerang-shaped columella (B type) (Fig. 1 e) will be used after previous radical mastoidectomy in cases in which the external meatus often also has to be reconstructed (Fig. 1 d, e, f, g). The halfaxial and true lateral projections usually give the best information but may be complemented by the axial-pyramidal and a.p. projections for judging the site of the columella, the tip of which is located on the

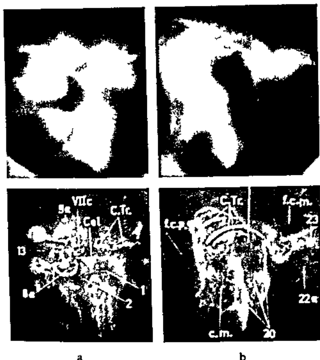


Fig 5 Boomerang shaped columella of cortical bone inserted in a previously radically operated ear a) In the halfaxial projection the gracile tip of the columella is placed in the center of the stapedial footplate b) Lateral projection (tomographic plane lateral to the tympanic space) bony reconstruction of the upper and posterior part of the external meatus

footplate of the stapes (Figs 4, 5) The appearance of the external meatus reconstructed by bone transplants is best demonstrated in the true lateral projection

(3) In cases of unattained hearing improvement or recurrence of hearing impairment the same projections will be used By tomography, dislocation or abnormal inclination of the columella may be detected A case of secondary hearing impairment is illustrated in Fig 6 Tomography revealed that the columella was abnormally located in relation to the boundaries of the oval window, and to the tympanic part of the facial canal thus possibly fixed to this structure This conclusion was confirmed at reoperation

Such complications may be more often expected in a B type than in an A type operation In the latter, detachment of the columella from the stapes head might be expected Another mechanical cause of postoperative hearing loss detected by tomography in one case is penetration of the columella through the stapedial footplate (Fig 7) Defective postoperative aeration of the middle ear is another cause of hearing impairment discernible tomographically

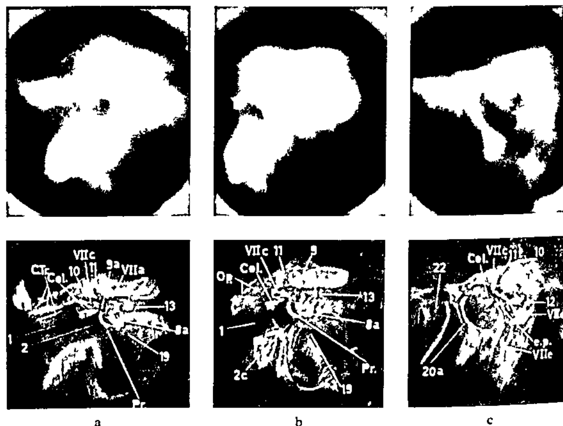


Fig 6 Dislocation of a B-columella causing postoperative hearing loss a) A p projection High position of the columella in the oval window b) Halfaxial projection Dislocated columella tip at the footplate and the intimate relationship of the columella with the tympanic part of the facial canal c) Lateral projection tomogram at the level of the oval window

Discussion

Preoperative middle ear tomography is extensively discussed in the literature The positioning is guided by the clinical demands for information and is dependent upon the results of the previous clinical examination There is always a request for detailed information about the ossicular chain, which is best demonstrated in the halfaxial, axial pyramidal and sometimes in Stenvers projection but the true lateral projection must always be applied in preoperative tomography Many authors consider that for a preoperative analysis, the a p and the lateral projections give sufficient information (LANGFELDT 1960, 1963, BRUNNER 1964, FREY 1965, 1967, VALVASSORI 1967, WRIGHT et coll 1969, HULSE et coll 1972, JENSEN 1973)

The halfaxial projection (DANIC et coll 1965, VIGNAUD et coll 1965) however, is to be preferred together with the true lateral projection in the appraisal of the long process of the incus and the incudo stapedial joint

All these projections combined give essential information about the presence of the stapes and the dimension of the oval window together with the tympanic part of the facial canal Further, the dimensions and the aeration of the tympanum,

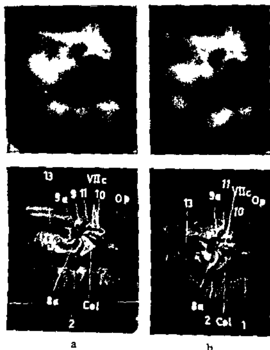


Fig 7 Penetration of the B columella through the stapedial footplate causing a postoperative secondary hearing loss of the purely conductive type a) A p projection The situation is not fully demonstrable b) Halfaxial projection The tip of the columella is seen to penetrate through the boundaries of the oval window into the vestibule Inclination of the boomerang-shaped columella medially and downwards towards the hypotympanic space

the attic and the mastoid and the peri labyrinthine cells can be appraised The other parts of the facial canal as well as the appearance of the external acoustic meatus and the protympanic space might also be examined Information concerning the existence of gaps in the tegmen and the posterior wall of the mastoid cavity, as well as of defects of the facial canal and otic capsule, are necessary in order not to vulnerate structures deprived of their osseous protection in the procedure of deepithelializing the cavity and the middle ear before reconstruction Defects in the bony wall may be detected down to dimensions of 1 mm and less, provided that they are located at a favourable angle to the tomographic plane Small tegmental defects may remain undetected but can be regarded as unessential The jugular fossa and the carotid canal in some cases have a very thin bony wall or might even lack an osseous wall against the tympanum

Otosclerotic changes in the oval window or in its direct neighbourhood can be recognized preoperatively In cases of middle ear malformation the outline of the facial canal is of cardinal importance In these respects clinical examinations give no information and even with an excellent technique such conditions cannot be demonstrated adequately by conventional radiography Minor defects are often not observed in a single tomographic projection, however, and the use of at least two projections is therefore needed

Before reconstruction in cases previously operated upon (radical mastoidectomy)

(Fig 1 d, e, f, g) the temporal bone is examined for information of possible residual cells and of the osseous continuity of the tegmen

Postoperative tomography in columella operations with bone grafts has not been discussed in the literature since the report of LANGFELDT The halfaxial view combined with the true lateral may be sufficient for the information required, in some cases complemented with the axial pyramidal or the axial projection, the latter causes discomfort to the patient, however

In an A or a B type reconstruction, the halfaxial projection is preferred to the a p because of the good discernment of the topographic relationship of the transplant to its environment

In successful reconstruction, attention is paid to the long term appearance of the transplant Since small cavities in ossicles are discernible in tomograms (SANDSTRÖM & WILBRAND 1971), it may be expected that long-term changes in the osseous transplant can be detected A great risk of resorption or fixation of the cortical bone columella has been reported (STEINBACH 1972, PULEC & SHEEHY 1973) but this does not correspond to the experience of KLEY & DRAF (1965) or EKVALL (1973)

Postoperative hearing impairment or unattained hearing improvement without clinically evident cause may be explained by tomography A secondary hearing loss may be due to malposition of the B type columella tip on the stapedial footplate Undue inclination of the graft, contact of the graft with environmental structures, or penetration of the columella through the footplate may comprise other mechanical causes Also minute penetrations may be disclosed when the tomographic plane is at a right angle to the plane of the oval window and the footplate

Viewing conditions are of special importance in evaluation of the tomograms as we are concerned here with visual perception of fine structural details, the image contrast of which lies at a low level of the characteristic curve Any dazzling effect should be avoided

SUMMARY

The tomographic demonstration of essential structural details before reconstructive middle ear surgery with osseous auto and homografts is described and the preoperative information requirements are briefly discussed The tomographic appearance of the different types of reconstruction is presented The halfaxial and true lateral projections are to be preferred, if necessary complemented by the axial pyramidal projection Tomography may disclose obvious morphologic causes of absence of postoperative hearing improvement or secondary hearing impairment

ZUSAMMENFASSUNG

Die tomographische Darstellung wichtiger Detailstrukturen vor einer rekonstruktiven Operation des Mittelohres mit knochernen Auto- und Homotransplantaten wird beschrieben

Gleichzeitig wird die Frage des präoperativen Informationsbedurfnisses erortert Das

[illegible]

vorliegende morphologische Ursachen einer postoperativ nicht eingetretenen Gehorverbesserung oder eine sekundaren Gehorverschlechterung geklart werden

RÉSUMÉ

Les auteurs decrivent la mise en evidence tomographique de détails structuraux essentiels avant *la chirurgie reconstructrice de l'oreille moyenne par des auto-* et des homogreffes osseuses, et ils examinent brievement quelles sont les informations preopératoires necessaires Ils presentent les aspects tomographiques des differents types de reconstruction Il faut prefer [illegible]
l incid [illegible]
evider [illegible]
diminution secondaire de l acuite auditive

REFERENCES

AGAZZI C, COVA P L e SENALDI M Semeiotica stratigrafica dell osso temporale (In Italian) Relazione al XVI raduno del gruppo Alta Italia della Soc Ital Otolaringologica, Milano 1958

ANDRÉ P, PIALOUX P, PONSET E, DULAC G-L et FRANCOIS J La tomographie en otorhino laryngologie Librairie Arnette, Paris 1968

BRUNNER S Radiological examination of temporal bone in infants and children Radiology 82 (1964), 401

— PETERSEN Ø and STOKSTED P Tomography of the auditory ossicles Acta radiol 56 (1961), 20

DANIC J, VIGNAUD J, SUDAKA J et LICHTENBERG R Visibilite radiographique de l'etrier et de la fenêtre ovale Interet dans l'otospongiose Ann Oto laryng (Paris) 82 (1965), 681

DULAC G-L Incidences analytiques dans la tomographie des osselets de l'oreille moyenne J Radiol Électrol 42 (1961), 85

EKVALL L Total middle ear reconstruction Acta Oto-laryng (Stockh) 75 (1973), 279

FREY K W Die Tomographie zur Diagnostik der Gehorknochelchen Rontgen Bl 12 (1964) 527

— Die Tomographie zur Diagnostik der kleinen Ohrmissbildungen Missbildungen der Gehorknochelchen bei offenem Gehorgang und vorhandenem Trommelfell Rontgen-Bl 18 (1965), 346

— Die Tomographie bei Luxationen und Frakturen der Gehorknochelchen Z Laryng Rhinol 46 (1967), 765

HALL A and RYTZNER C Stapedectomy and autotrans[illegible]
[illegible]

— — [illegible]

HULSI [illegible]
D [illegible]

JENSEN J and ROVSING H Fundamentals of ear tomography Charles C Thomas Publisher Springfield Illinois 1971
— and THOMSEN J Dislocation of the incus The reliability of tomography Arch Ohr Nas u Kehlk Heilk 204 (1973) 143
KLEY W und DRAF W Histologische Untersuchungen uber autotransplantierte Gehor knochelchen und Knochenstuckchen im Mittelohr beim Menschen Acta oto-laryng (Stockh) 59 (1965) 593
LANGFELDT B Tomography in the middle ear in columella operations Acta radiol 53 (1960) 129
— Tomography in the middle ear in sound transmission disturbances Acta radiol Diagnosis 1 (1963) 133
MUNDNICH K und FREY K W Das Rontgenschichtbild des Ohres Georg Thieme Stutt gart 1959
PORTMANN M et GUILLEN G Radiodiagnostic en otologie Masson & Cie Paris 1967
PULEC J L and SHEEHY J L Tympanoplasty ossicular chain reconstruction Laryngo-scope *(St Louis) 83 (1973) 448*
SANDSTROM B and WILBRAND H F Anatomic cause for intraossicular cavities in temporal bone tomography Acta radiol Diagnosis 11 (1971) 225
STEINBACH E Vergleichende Untersuchungen an Gehorknochelchen und Knochentrans plantaten beim Kaninchen und Menschen Habilationsschrift Tubingen 1972
VALVASSORI G E Laminagraphy of the ear Amer J Roentgenol 89 (1963) 1155
— Otosclerosis a new challenge to roentgenology Amer J Roentgenol 94 (1965) 566
— Tomography of the temporal bone *In* Surgery of the ear p 137 W B Saunders Com pany Philadelphia and London 1967
VIGNAUD J DANIC J LICHTENBERG R et SUDAKA J Nouvelles recherches en radiootologie I Radiographie de l étrier II Aspect tomographique de la fenetre ovale dans l oto-spongiose J Radiol Électrol 46 (1965) 129
WRIGHT W TAYLOR C E and BIZAL J A Tomography and the vulnerable incus Ann Oto laryng 78 (1969) 263

ROM THE DEPARTMENT OF DIAGNOSTIC RADIOLOGY II (ACTING DIRECTOR ASS PROFESSOR
LAS ROSENGREN) AND THE DEPARTMENT OF CLINICAL NEUROPHYSIOLOGY (DIRECTOR
PROFESSOR INGEMAR PETERSEN), SAHLGRENSKA SJUKHUSET, S-413 45 GOTHENBURG,
SWEDEN

SIDE EFFECTS AFTER LUMBAR MYELOGRAPHY WITH DIMEGLUMINE IOCARMATE (DIMER-X)

Further experiences

LARS IRSTAM and ULLA SELLDEN

In recent years new water-soluble contrast media, particularly dimeglumine iocarmate (Dimer X) have increasingly replaced methiodal sodium in lumbar myelography The side effects of Dimer-X have been reported as relatively few and mild (BAUMGARTNER et coll 1970, BRABAND et coll 1971, DANZIGER & BLOCH 1973, IRSTAM 1973, SKALPE & TALLE 1973) Moreover, its use is rarely followed by adhesive arachnoiditis (IRSTAM & ROSENCRANTZ 1973, 1974, IRSTAM et coll 1974)

In guinea pigs Dimer X administered subarachnoidally has scarcely any irritative effect on the spinal cord or brain Vasodilatation, oedema and inflammatory reactions may occur, but they regress and disappear almost completely within 48 hours (GONSETTE 1971) In rabbit experiments PRAESTHOLM (1971) found the adverse effects of Dimer-X to be less severe than those of other media, though nerve root degenera-

Submitted for publication 6 June 1974

tion was observed in one animal 6 weeks after myelography with Dimer-X This medium has been shown to be less epileptogenic in animal experiments than any other water-soluble contrast medium used in routine clinical work (GONSETTE 1971)

In man, however, Dimer-X has not infrequently caused fibrillations of the legs or clonic convlulsions, which in one case proved fatal (GUERBET 1974) It should, however, be mentioned that most severe convulsions have been caused by large doses, occasionally several times the maximum recommended dose (GUERBET)

The risk of clonic convulsions increases when the contrast medium comes into contact with the medullary cone during myelography (AHLGREN 1969, 1972, IRSTAM 1973) Such contact must thus be prevented both during the examination and the after-care of the patient

The epileptogenic effect of a contrast medium may be assessed from the behaviour of animals after intracerebral injection of the medium, after application over the cerebral hemispheres or after direct application to the cortex GONSETTE and LUNDERVOLD have, however, revealed that the epileptogenicity of a contrast medium is reflected better by EEG The effect of cortical subarachnoid application of Dimer-X in guinea pigs (GONSETTE) and in rabbits (LUNDERVOLD) has been reported to be much weaker than that of meglumine iothalamate (Conray 60) and of methiodal sodium (GONSETTE 1971)

Only 3 reports on EEG in man following myelography with Dimer-X have been found in the literature The earliest sign of incipient convulsions elicited by Conray 60 or Dimer-X is the appearance of spikes in EEG recordings made 1 to 3 hours after myelography (GONSETTE 1971) Such manifestations can be suppressed immediately by intravenous administration of 10 mg of diazepam IRSTAM (1973) reported that no such spikes had occurred in a few cases where the medium had accidentally come into contact with the medullary cone, however, these patients had been premedicated with diazepam which might have inhibited such activities

In 1973 DE GRAAF & KAYED reported on a 14-year-old boy examined on one occasion with Conray 60 and 18 months later with Dimer-X Within one hour of administration of Conray 60 generalized tonic convulsions occurred Simultaneous EEG revealed generalized theta and paroxysmal delta activity with focal sharp waves in the right fronto-temporal region Moderate diffuse theta but no paroxysmal activity was demonstrated the following day, while EEG 3 weeks later was normal At the second examination, then with Dimer-X, the patient had no seizures, but 1 and 2 5 hours after the injection of the medium theta-delta activity and 'sharp components were recorded, 24 hours after the myelography the EEG was normal

In 1973 IRSTAM reported on immediate side effects seen in the first 300 of a total of 682 lumbar myelographies In that series, however, EEG was performed in only a few of the patients It was therefore thought legitimate to try to find out (1) whether myelography with Dimer-X produces electroencephalographic changes and, if so, to ascertain their character and appearance time and (2) to find out whether any correlations exist between immediate side effects and EEG-abnormalities, if any

Material and Methods

The material consisted of 89 patients (52 men and 37 women) None had a history of epilepsy, severe alcoholism or iodine allergy, i e conditions contraindicating myelography with any water soluble contrast medium One woman was examined twice, at the first examination almost all the medium was injected subdurally, at the second, subarachnoidally On both occasions the woman was kept under close observation after the examination and both examinations are included in the material Immediately before myelography the patients were premedicated with diazepam (Valium) intravenously in a dose of usually 5 mg, but occasionally 7 5 to 10 mg depending on weight, age and the clinical effect of the drug In order to reduce the risk of respiratory complications in the event of general anaesthesia being necessary during or after the examination, the patients were instructed to refrain from eating or drinking for at least 4 hours before the examination

The subarachnoid space was punctured at the level of L2–L3 or L3–L4 with a Stenstrom needle, OD 1 0 mm Five ml of Dimer-X was diluted in 2 ml of spinal fluid (200 mg I/ml) This mixture was injected slowly with the patient in the lateral position and with the head end of the examination couch elevated about 15°, usually the whole amount of the mixture was injected Films were exposed with the patient in the lateral and prone positions and with the beam horizontal Both sides of the patient were always examined on the same occasion Passage of the contrast medium up into contact with the medullary cone, i e above the lower border of the first lumbar vertebra, was always attempted to be avoided In some cases films were obtained also with the patient standing After myelography, the patients rested in bed with the trunk and the head raised about 30° for 6 to 8 hours, and afterwards horizontal for a further 18 hours All patients spent at least 6 hours in the intensive care unit immediately after myelography They were carefully observed for at least 3 days mostly up to one week, for untoward reactions

EEG was performed with a 16-channel electroencephalograph The 10–20 electrode system of the International Federation was used with longitudinal and transverse bipolar derivations Hyperventilation was used only in connection with recording before myelography Recordings were made in all cases except 6 before, in all cases 3 hours after, and in 21 cases also 24 hours after myelography The EEG recordings were analysed according to customary visual technique For definitions of normal and pathologic findings, reference is made to articles by SELLDEN (1964), EEG-OLOFSSON et coll (1971) and PETERSEN & EEG OLOFSSON (1971)

Results

The immediate side effects appearing during or after lumbar myelography fall into three groups, depending on the part of the nervous system irritated by the contrast medium (IRSTAM 1973) (1) Hyperexcitation (clonic convulsions/fibrillations,

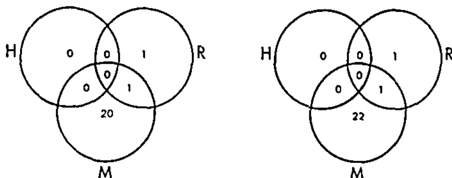


Fig 1 Immediate side effects in the present material of 90 cases Left absolute figures, Right relative figures (per cent) H = hyperexcitation, R = radicular signs, M = meningeal irritation

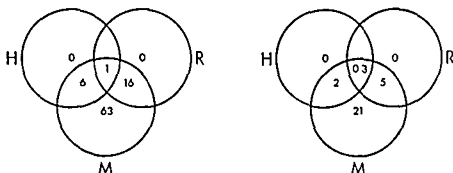


Fig 2 Immediate side effects in earlier published series of 300 Dimer-X myelographies (IRSTAM 1973) Left absolute figures, Right relative figures (per cent) H = hyperexcitation, R = radicular signs M = meningeal irritation

epileptic convulsions), (2) radicular reaction (hyperalgesia, pain in the abdomen, retention of urine) and (3) meningeal irritation (cephalgia, nausea, rise in temperature with or without meningitis, fall in blood pressure)

In the present material these side effects appeared at 22 (24.4 %) of the 90 myelographies The distribution among the various groups is presented in Fig 1, which might be compared with the results obtained in the previous material (Fig 2) Immediate side effects were equally common in the two series except that no instance of hyperexcitation was noted in the present series

Twenty cases presented signs of meningeal irritation, with mild to moderate headache The headache usually began within 3 to 6 hours after myelography and disappeared within 24 to 72 hours None of the patients had the severe type of headache, i e intense and lasting for 1 week or more In one case moderate headache was accompanied by mild stiffness of the neck for 24 hours No other signs of meningism were present Re-puncture for examination of the CSF was not performed In another case mild headache was accompanied by retention of the urine for 24 hours That patient had a large disc herniation which could explain the retention In a

Table

Age and sex distribution of patients with EEG before myelography

	Age				
	≤20	21 35	36–50	51–65	≥66
Males	2	11	23	11	0
Females	0	6	19*	11	1

* One of the patients of this group was examined twice and registered as two cases

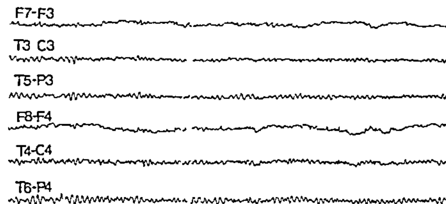
further case, the lumbo sciatic pain in both thighs increased for about 24 hours after myelography, but no other side effects occurred

EEG before myelography was usually made the day before the myelography The age , and sex distribution of these patients appears in the Table Eleven (13 %) of 84 patients presented abnormalities before myelography In 10 of these the EEG was slightly abnormal with some increase in low frequency activity within the theta range Equivocal and sporadic sharp wave potentials appeared in one female The remaining patient had a moderate increase in low frequency activity No focal or paroxysmal activities were ever seen

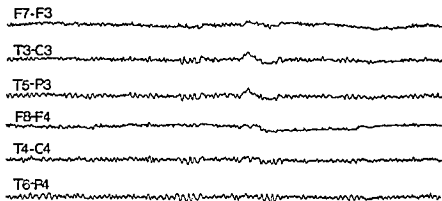
EEG after myelography The EEG was not altered in 78 (93 %) of the 84 cases who had been examined electroencephalographically before myelography This number includes 69 of the patients with a normal EEG, the above mentioned patient with a moderate increase in low frequency activity, and 8 with slightly abnormal EEG Myelography had thus no effect on the EEG in these patients

Certain alterations were encountered in the EEG recordings made 3 hours after myelography in 6 cases, 4 with primarily normal EEG and 2 with primarily abnormal findings Two of the 4 cases with a primarily normal EEG had a slight increase of theta activity, most certainly due to drowsiness following medication with diazepam A more marked increase of low frequency activity including some 2 Hz waves occurred in one case Episodes of slow waves appeared bilaterally, evidently more on the left side Slight drowsiness was noted now and then throughout the recording At the 24 hour EEG drowsiness occurred to the same extent, but slow activity was markedly reduced and no delta activity was observed (Fig 3) The 4th case presented a typical 6 Hz spike and wave pattern ('phantom spike waves', WALTER 1950) This activity usually appears during drowsiness This was evident in the 3 hour EEG (after 5 mg of diazepam), but not in the recording before the myelography or in the third recording 24 hours after the myelography, when the EEG was normal

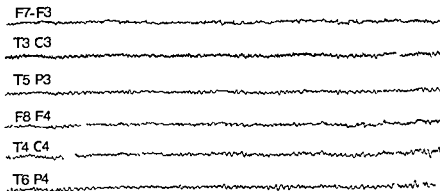
One of the 2 patients with primarily abnormal findings at the first examination had a slight increase in low frequency activity within the theta range as well as some



a

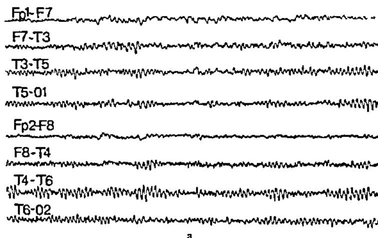


b



c

Fig 3 a) Normal EEG before myelography b) Discharge of low frequency
fter myelo
hours after



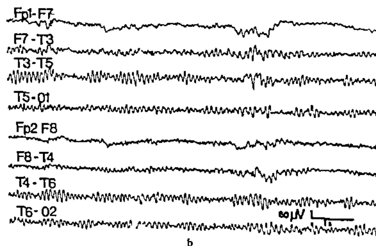
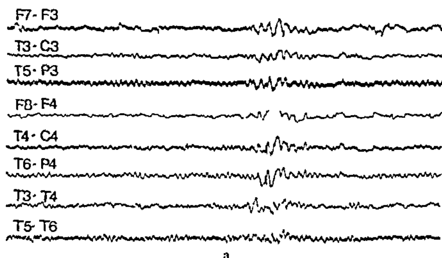
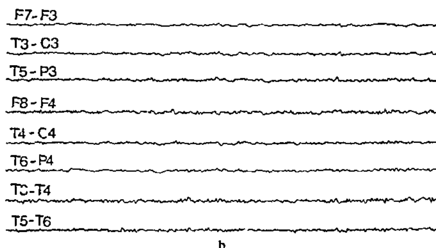


Fig 4 a) Pre ... al ... l

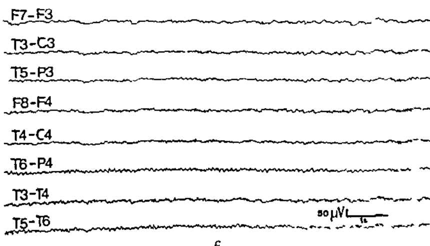
equivocal paroxysmal activity bilaterally (a few sharp wavelike potentials) No equivocal paroxysmal activity was seen at the 3 hour control, possibly owing to medication with diazepam The remaining *patient* who primarily had a slight increase in low frequency activity in the left fronto-temporal region presented further episodes of theta activity ... first and the seco ... Judging from the (Figs 3, 4), but h ... the others, might have been influenced to some extent by the ... Thus two patients Dimer-X myelography as such, *even* though drowsiness caused by diazepam cannot be excluded as a possible contributory factor



a



b



c

Fig 5 a) Paroxysmal discharge including spike potentials 3 hours after myelography and 5 mg of diazepam i v b, c) Normal EEG 24 hours and 6 days, respectively, after myelography *Certain drowsiness at all occasions*

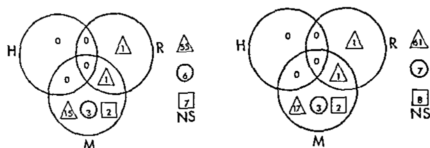


Fig. 6 Immediate side effects in absolute and relative figures in correlation to EEG findings 3 hours after lumbar myelography with Dimer X Left absolute figures, Right relative figures (per cent) H = hyperexcitation R = radicular signs M = meningeal ir-

had not been performed

In 6 cases EEG was not performed before the myelography, but first 3 hours afterwards In 2 of the cases EEG was normal, one had a normal EEG also 48 hours after myelography Three cases presented slight increase of low frequency activity diffusely and bilaterally, probably mainly due to drowsiness One patient was re-examined 48 hours later, no relevant differences were observed The remaining case presented a few short symmetric episodes of 4–5 Hz spike and wave activity (100–

cases EEG was performed 3 and 24 hours after the myelography In none

wave activity Similar findings were also common in the recording made 24 hours after myelography

EEG abnormalities versus immediate side effects Patients with alterations in the EEG obtained 3 hours after myelography were evenly distributed among those patients with and without immediate adverse reactions (Fig 6) Those with EEG alterations reported mild to moderate headache, lasting for about 24 hours No other clinical signs of irritation of the CNS were evident in these cases

Discussion

Apart from the exclusion of patients with a history of epilepsy, the present material was unselected To avoid undue overburdening of the staff, EEG before myelo-

graphy was omitted in 6 cases and only 21 patients, all belonging to the latter part of the material, were examined 24 hours after myelography These 21 patients included all but 3 of those in whom abnormalities had been found in the recordings made before or 3 hours after myelography

EEG abnormalities occur in at least 5 to 15 per cent of all apparently healthy persons (SELLDEN 1964) Such abnormalities may thus be expected also in a certain percentage of the present material The frequency of EEG abnormalities before myelography in the present series, was what could be expected from the age and sex distribution of the material The hospital records of these patients contained no notes suggesting a lesion of the CNS

Medication with diazepam provokes drowsiness, and drowsiness per se increases low frequency activity and usually accentuates any existing abnormality Such medication in connection with myelography sometimes made it difficult to evaluate the differences between recordings before and 3 hours after myelography Certain types of spike activity appear mainly in association with drowsiness, e g in the above mentioned cases with 6 Hz spike activity This activity may therefore not be directly ascribed to the myelography with Dimer-X, it did not appear in the initial recording and may be explained by the fact that drowsiness was manifest at the second EEG, but not at the first

Two patients (Figs 3, 4) exhibited EEG-changes presumably due to Dimer-X In one of them low frequency activity increased without any associated significant EEG-signs of drowsiness, in the other, fairly marked discharges of low frequency activity were recorded at 3 hours, but not at 24 hours, after the administration of Dimer-X The drowsiness reflected in the EEG was equal on both occasions, the EEG effects were comparatively mild

One of the patients, not examined before myelography, exhibited the same degree of drowsiness 3 hours and 24 hours after myelography, but spike activity was seen only in the recording made at 3 hours after Dimer-X, suggesting a causal relationship between the EEG abnormality and the myelography Such paroxysmal discharges (spikes) are considered as prodromes of incipient convulsions (GONSETTE) Large doses of diazepam were therefore given immediately, and no eclampsia occurred

AHLGREN (1972) holds the opinion that premedication with diazepam is useless in the prophylaxis of seizures and that the anti eclampsia effect of this drug is brief, and the effect, if any, is that it prevents the alarming prodromes until the sudden onset of seizures Instead of diazepam, AHLGREN recommends promethazine It is however, known that the half-life of the elimination of diazepam is 21 to 37 hours (KAPLAN et coll 1973) and that some anticonvulsive effect of the drug and its metabolites is maintained at least during this period If diazepam is to ward off eclampsia, it must be given in doses larger than those in the present material According to our experience of previous series, 5 mg of diazepam given intravenously does not mask any clinical prodromes of seizures Many patients require premedication owing to anxiety and pain, and, in our opinion, diazepam is quite satisfactory for this purpose

HINDMARSH et coll (1975) have suggested that interaction between the new contrast medium metrizamide and phenothiazine might produce seizures This implies that certain drugs are capable of lowering the convulsive threshold This increases the risk of using a potentially epileptogenic drug at myelography Antihistamines with a sedative effect, 3 cyclic antidepressive drugs as well as analeptic drugs are known to have a lowering effect on the convulsive threshold (JARVIK 1970, MARTIN et coll 1971)

Until more is known about these potential risks, such drugs should be avoided in connection with myelography with water-soluble media None of the mentioned *drugs had been used in the patients in the present investigation*

It has been stressed by AHLGREN (1969, 1972) and IRSTAM (1973) that contact between the medullary cone and the medium increases the risk of later convulsions In the series of IRSTAM, 7 cases of clonic convulsions occurred in the material of 300 myelographies performed with Dimer-X In all these cases the medium had reached the medulla during examination No measures had been taken to prevent eclampsia in those cases except premedication of diazepam 5 mg intravenously In the latter third of those series and in a further 382 myelographies with Dimer-X, including those of the present series, no complicating convulsions or fibrillations of the legs occurred If the contrast medium reached too high in the subarachnoid space, preventive steps were immediately taken, i e administration of large and repeated doses of diazepam and in some cases repuncture and withdrawal of CSF containing Dimer X

In at least 10 patients of the present material, the contrast medium had possibly reached the cone on some occasion during the examination, in a further 8 such contact during the examination might have been more prolonged In none was found any correlation between the duration of contact and later appearance of EEG-abnormalities or immediate side effects In 4 cases massive contact occurred between the contrast medium and the medullary cone In 2 of these cases further doses of diazepam (5 to 10 mg) were given intravenously, repuncture was performed and CSF and contrast medium were withdrawn In the remaining 2 cases only large doses of diazepam were administered In one of the repunctured cases, 6 Hz spike activity was observed in the 3 hour recording In none of the other cases were any EEG abnormalities recorded No adverse reactions were observed in any of these cases

The case with paroxysmal discharges (spikes) occurred in a patient in whom some of the contrast medium had reached the upper border of L2 No contact occurred between the medium and the medullary cone during the examination Large doses of diazepam were given as soon as the paroxysmal discharges were discovered in the EEG At this stage—3 to 4 hours after the myelography—repuncture was considered meaningless No side effects were accounted for

Experience with cisternography indicates that labelled albumin passes within 3 hours from the site of l…
geminal cisterns as…
evenly distributed…
…ITO 1966, HARBERT 1971)

DI CHIRO also stated that the rate of ascent of the isotope varies considerably with the volume of fluid injected Only a few reports are available on the distribution and transport of Dimer-X within the subarachnoid space However, HAMMER (1973) has reported that labelled Dimer-X behaves in the same manner as the labelled albumin, with similar transport times Some of the medium is known to be resorbed locally in the most caudal part of the subarachnoid space (GUERBET 1974) Thus, the medium reaching the brain is far less concentrated than that in the cul-de-sac

All these observations imply that the level of the contrast medium should be kept as low as possible and that the amount of Dimer-X should be individualized and kept as small as possible, i e just enough to obtain a satisfactory survey of the three most caudal lumbar discs It has been shown by HINDMARSH (1975) that large doses of Dimer-X markedly increase the frequency of hyperexcitation But his patients were not premedicated and several had received a contrast dose larger than the recommended maximum dose Thus, there is a reason to propose that the recommended maximum dose of 5 ml of Dimer-X should never be exceeded in routine clinical work

It is difficult to explain the mechanism of clonic convulsions/fibrillations of the muscles of the legs and sometimes of the erector trunci muscles The site where these seizures are elicited is unknown The trigger area might be spinal or located in the brain stem or the cortex Diazepam given intravenously arrests such disorders and might thus serve as an indirect tracer of the trigger zone of Dimer X However, diazepam acts at a spinal, cortical and subcortical level and no conclusion can be drawn from the action of this drug

It is obvious that the medium has some irritating effects at a spinal level, as indicated by a few cases with increased tendon reflexes of the legs 1 to 3 hours after myelography These findings have not been closely analysed in the present material, but will be the subject of further investigations Eclampsias encountered always start in the legs, and if they spread, they do so cranially Furthermore, the seizures appear 1 5 to 4 hours after the administration of the contrast medium The EEG abnormalities in the present material appeared 3 hours after myelography No paroxysmal changes were recorded 24 hours after myelography and the low frequency activities were always equally or less evident at the 24 hour control Thus, no additional findings have been recorded 24 hours after myelography—when the concentration of the medium reaching the cortex was probably highest This suggests that the trigger area of eclampsias, elicited by Dimer-X is located mainly in the brain stem, possibly in combination with a spinal trigger

The EEG abnormalities recorded 3 hours after lumbar myelography with Dimer-X were evenly distributed among patients with and without side effects In this material, previous lesions of the CNS reflected by EEG abnormalities appeared not to be a site of lessened resistance to Dimer-X when used in patients premedicated with diazepam This was true both from an electroencephalographic and a clinical point of view

SUMMARY

Lumbar myelography with dimeglumine iocarmate was performed in 90 cases premedicated with diazepam (Valium) EEG was performed before, as well as 3 and 24 hours after myelography The use of diazepam interfered to some extent with the interpretation of the EEG In 3 cases EEG abnormalities occurred 3 hours after myelography, most probably ascribable to Dimer X No further changes were found in the 24-hour recording Immediate side effects were few and mild and seizures did not appear The EEG abnormalities were equally distributed among patients with and without side effects

ZUSAMMENFASSUNG

Lumbale Myelographie mit Dimeglumin Iocarmat wurde bei 90 Patienten, die mit Diazepam (Valium) vorbehandelt waren vorgenommen Ein EEG wurde zuvor als auch 3 bis 24 Stunden nach der
rungen auf, die sehr
rungen waren bei d
waren gering und Kr
den Patienten mit und ohne Nebeneffekte verteilt

RÉSUMÉ

Une myelographie lombaire par iocarmate dimeglumine a eté faite chez 90 malades premediqués par le diazepam (Valium) Un electroencephalogramme a eté fait avant, 3 heures apres et 24 heures apres la myelographie L'administration de diazepam a gené dans une certaine mesure l'interpretation de l'E E G Dans 3 cas, des anomalies electroencephalographiques sont apparues 3 heures apres la saccoradiculographie, tres probablement attribuables au Dimer X On n'a pas constate de modification ultérieure sur l'enregistrement fait au bout de 24 heures Il y a eu peu d'effets secondaires immediats et ils ont ete benins et il n s a pas eu de crise convulsive Les anomalies E E G étaient distribuees de façon egale chez les malades qui avaient des effets secondaires et chez ceux qui n'en avaient pas

REFERENCES

AHLGREN P Lumbale Myelographie mit Conray Meglumin 282 Fortschr Rontgenstr 111 (1969), 270

— Dimer-X A new contrast medium for lumbar myelography without spinal anaesthesia Acta radiol Diagnosis 13 (1972), 753

BAUMGARTNER J, BRAUN J P, CARON J, CECILE J, FISCHGOLD H, GONSETTE R, HIRSCH J F, LEGRÉ J et METZGER J Radiculographie au Dimer-X Premier résultats apres 630 examens J Radiol Electrol 51 (1970), 557

BRABAND H, WENKER H, GROTH W, KOSTADINOW G, CIARKOWSKI J und LESSMAN H D Klinische Prufung eines neuen wasserloslichen Kontrastmittels zur lumbosakralen M

DANZ
Cl r X in lumbar radiculography

DE GRAAF A S and KAYED K S Epileptic seizures and EEG changes after radiculography with meglumine iothalamate (Conray) and meglumine iocarmate (Dimer-X) Psychiat Neurol Neurochir 76 (1973), 77

DI CHIRO G Observations on the circulation of the cerebrospinal fluid Acta radiol Diagnosis 5 (1966), 988
EEG-OLOFSSON O, PETERSÉN I and SELLDÉN U The development of the electroencephalogram in normal children from the age of 1 through 15 years Paroxysmal activity Neuropadiatrie 4 (1971), 375
GONSETTE R An experimental and clinical assessment of water-soluble contrast medium *in neuroradiology A new medium—Dimer-X Clin* Radiol 22 *(1971), 44*
GUERBET M Personal communication 1974
HAMMER B Clinical experimental investigations on the lumbosacral myelography Read at the 4th Congress of the European Society of Neuroradiology, Frankfurt/Main, Sept 1973
HARBERT J Radionuclide cisternography Sem nucl Med 1 (1971), 90
HINDMARSH T Lumbar myelography with meglumine iocarmate and matrizamide Acta radiol Diagnosis 16 (1975), 209
— GREPE A and WIDÉN L Metrizamide—phenothiazine interaction Report of a case with seizures following myelography Acta radiol Diagnosis 16 (1975), 129
IRSTAM L Side effects of water-soluble contrast media in lumbar myelography Acta radiol Diagnosis 14 (1973), 647
— and ROSENCRANTZ M Water-soluble contrast media and adhesive arachnoiditis I Reinvestigation of nonoperated cases Acta radiol Diagnosis 14 (1973) 497
— — Water-soluble contrast media and adhesive arachnoiditis II Reinvestigation of operated cases Acta radiol Diagnosis 15 (1974), 1
— SUNDSTRÖM R and SIGSTEDT B Lumbar myelography and adhesive arachnoiditis Acta radiol Diagnosis 15 (1974), 356
JARVIK M E Drugs used in the treatment of psychiatric disorders In The pharmacological basis of therapeutics, ed by L S Goodman and A Gilman, 4th ed, The Macmillan Co, USA 1970
KAPLAN S A, JACK M L, ALEXANDER K and WEINFELD R E Pharmacokinetic profile of diazepam in man following single intravenous and oral and chronic oral administrations J pharm Sci 62 (1973), 1789
LUNDERVOLD A Unpublished data (Quoted by GONSETTE)
MARTIN E W, ALEXANDER S I, HASSAN W E Jr and FARAGE D J Hazards of medication J B Lippincott Co, Philadelphia 1971, p 359
PETERSÉN I and EEG-OLOFSSON O The development of the electroencepalohgram in normal children from the age of 1 through 15 years Nonparoxysmal activity Neuropadiatrie 3 (1971), 247
PRAESTHOLM J Dyreeksperimentelle undersøgelser med vandopløslige kontraststoffer til myelografi (In Danish) Nord Med 86 (1971), 1214
SELLDÉN U Electroencephalographic activation with megimide in normal subjects Acta neurol scand (1964) Suppl No 12
SKALPE I O and TALLE K Lumbar radiculography with meglumine iocarmate (Dimer X) J Oslo Cy Hosp 23 (1973), 121
WALTER U G Normal rhythms—their development, distribution and significance *In* Electroencephalography First ed Edited by D Hill and G Parr Mac Donald & Co Ltd, London 1950

OM THE DEPARTMENTS OF DIAGNOSTIC RADIOLOGY AND DERMATOLOGY, UNIVERSITY CENTRAL HOSPITAL, SF 00170 HELSINKI, FINLAND

PSORIATIC LESION OF THE STERNAL SYNCHONDROSIS

M KORMANO, J KARVONEN and A LASSUS

Psoriatic arthritis occurs predominantly in the hands and feet and appears as a destructive lesion in the interphalangeal joints gradually resulting in ankylosis (AVILA et coll 1960) Other joints more or less frequently involved are the temporo mandibular joints (LUNDBERG & ERICSON 1967), shoulders, knees and ankles (PETERSON & SILBIGER 1967, MCEWEN et coll 1971) Spondylitis is reported to occur in 10 to 50 per cent of patients with psoriatic arthritis (WRIGHT 1961, BAKER et coll 1963, PETERSON & SILBIGER, JAJIC 1968, MCEWEN et coll, MOLIN 1973, KILLEBREW et coll 1973)

The synchondrosis between the manubrium and body of the sternum has been reported to be involved in 58 to 70 per cent of patients with rheumatoid arthritis (DILSEN et coll 1962, KORMANO 1970, LAITINEN et coll 1970), mostly to a mild degree Higher frequency (up to 87 per cent) and more severe involvement has been described in ankylosing spondylitis (SOLOWAY & GARDNER 1951, SAVILL 1951, DILSEN et coll) A high incidence of spondylitis in association with psoriatic arthritis has also been reported (MCEWEN et coll, KILLEBREW et coll) Inflammatory lesion of the synchondrosis has been reported in 68 per cent of patients with psoriatic spondylitis by MCEWEN et coll Except for these authors, possible involvement in patients with psoriatic arthropathy with or without spondylitis has not received attention This fact as well as occasional observations of inflammatory lesion at the sternal angle initiated the investigation presented in this report

Submitted for publication 8 November 1974

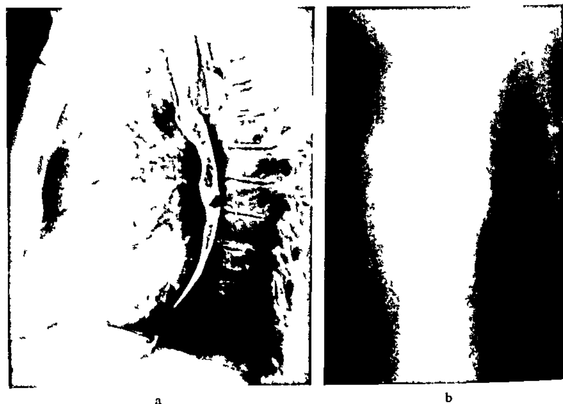


Fig 1 a) Lateral projection of the chest of a patient with a 16 year history of psoriatic arthritis in the hands and feet Sternal pain a year earlier Abnormal sternal synchondrosis b) Detail of (a)

Material and Methods

The material consisted of 30 patients (16 men 14 women aged 24 to 75 years) with psoriatic arthropathy Two of the patients had psoriasis pustulosa, one psoriasis erythrodermia and one psoriasis inversa, while the remaining patients had a typical psoriasis vulgaris All patients fulfilled the clinical criteria of definite psoriatic arthritis except one, who was omitted from the series due to a positive Latex fixation test All other patients were serologically negative The onset and course of arthralgia was closely related to the development of the skin lesion The presence of psoriatic arthropathy was based on radiography of the hands and feet

The appearance of the sternum on a lateral chest film was assessed and tomography performed in p a projection The abnormalities found were classified into four groups as follows,

Group I Decalcified, unsharp bony margins of the synchondrosis with sub chondral erosion with or without reactive bone formation

Group II More marked erosion with irregular bony margins

Group III Widening of the space between the manubrium and sternal body and more extensive bone formation

Group IV Complete synostosis



Fig 2 Fig 3

Fig 2 Tomography of a normal sternum and sternal synchondrosis

Fig 3 Tomography of a sternal synchondrosis with extensive arthritic destruction and reactive bone formation

Tomography of the sternum was performed in 10 subjects (aged 30 to 80 years) without symptoms of arthropathy In addition, 400 unselected chest films of patients from the Dermatology Clinic were surveyed to elucidate the frequency of major sternal abnormalities in dermatologic patients in general

Results

The normal synchondrosis (Fig 2) has slightly undulating well defined bony margins in young individuals In older persons bone appositions around the bony margins of the synchondrosis are common Previously LAITINEN et coll have reported that slight abnormalities, similar to those in group I may appear in a routine patient material This was also encountered in the present material Among the 400 unselected cases 18 presented abnormalities suggestive of erosion, while bony synostosis was observed in 26 cases This figure is a minimum figure as no special examination was performed

Roentgenologic criteria of psoriatic arthropathy of hands was demonstrated in 19 of the 29 patients The remaining cases had either no (4 cases) or only slight and non typical abnormalities not allowing definite roentgenologic diagnosis of psoriatic arthritis Among the 29 patients bone erosion in the sternal synchondrosis occurred in 18 (Figs 1, 3) synostosis in 4 cases

No correlation was found between the frequency of erosion and the age of the patient However, evident correlation existed between the frequency of erosion and

Table

Clinical and roentgenologic data of 29 patients with psoriasis and seronegative polyarthritis

Duration of joint involvement	No of patients	Roentgenologically peripheral psoriatic arthritis	Radiography of sternal synchondrosis					Duration of skin lesion (years)
			Erosion				Synostosis IV	
			I	II	III	Total		
< 5 years	11	5	2	1	1	4	1	7 1
> 5 years	18	14	4	2	5	11	3	21 2
Total	29	19	6	3	6	15	4	15 8

the duration of arthritic symptoms in the hands or feet (Table) In patients with a history of less than 5 years arthritis in the hands or feet were found in 55 per cent, with a longer history in 78 per cent In the group with a history longer than 5 years lesion of the synchondrosis (excluding synostosis) was found in 61 per cent of all cases and in 71 per cent of the subjects with typical hand or feet arthritis

Twelve patients had either past or present sternal pain In some cases the sternal angle was also tender to palpation Two of the patients with ankylosis reported a period of pain at the time of onset of the arthropathy Erosions were observed in 7 of the 12 patients with pain but only in 2 without a history of pain

The radiographic abnormalities were closely correlated to hand and foot involvement Among the 10 cases without arthropathy in the hands and feet slight erosion of the bony margins of the synchondrosis was observed in 2 cases only, 2 patients had ankylosis without a history of pain

Discussion

It is obvious that involvement of the synchondrosis between the manubrium and the sternal body is closely related to the existence of psoriatic arthropathy There was no evidence of primary, solitary involvement of the synchondrosis in any of the cases, although some patients experienced sternal pain as early as the first appearance of pains in finger or toe joints Both the inflammatory lesions of the spine and of the sternum develop during a severe or long history of psoriatic joint affection The abnormalities visible on the lateral chest film are relatively infrequent, tomography being mandatory for early diagnosis Sternal involvement in psoriatic patients seems to occur at a frequency similar to what is reported in ankylosing spondylitis (SAVILL, SOLOWAY & GARDNER, DILSEN et coll) The percentage given by MCEWEN et coll in patients with psoriatic spondylitis is of the same order Similar sternal involvement also occurs in patients with peripheral polyarthritis without spondylitis (LAITINEN et coll)

Ankylosis was more common in the present material than in the unselected material. Two patients with bony synostosis reported a period of sternal pain many years previously, concomitantly with joint symptoms, which indicates that fusion may be secondary to arthritic destruction, as has been suggested by SOLOWAY & GARDNER and SAVILL in ankylosing spondylitis.

A good correlation existed between the history of sternal pain and the roentgenologic sternal abnormalities. Sternal pain spontaneously reported even in a patient with arthritic symptoms may be erroneously interpreted as cardiac pains, especially because lesions of the synchondrosis are frequently overlooked on routine chest films. Sternal pains in a psoriatic patient is always an indication for tomography of the sternum. The oblique projections of the sternum often used are unreliable for certain diagnosis. Even a single tomographic section at the depth of about 1.5 to 2.5 cm with the patient supine demonstrates in most cases the entire sternum.

SUMMARY

Radiography of the synchondrosis between the manubrium and the sternal body was performed in 29 patients with clinically certain psoriatic arthropathy. Tomography proved necessary for a detailed analysis. Erosive inflammatory lesions were detected in 18 cases, in 61 per cent of cases with a history of more than 5 years and in 71 per cent of cases with typical hand and feet arthropathy. It is concluded that the sternum is frequently involved in cases with roentgenologically typical psoriatic arthropathy.

ZUSAMMENFASSUNG

Röntgenuntersuchung der Synchondrose zwischen dem Manubrium und dem Korpus des Sternum wurde bei 29 Patienten mit klinisch gesicherter psoriatischer Arthropathie vorgenommen. Tomographie erwies sich für eine detaillierte Analyse als notwendig. Errosive inflammatorische Veränderungen wurden in 18 Fällen gefunden und in 61 % der Fälle mit einer Vorgeschichte von mehr als 5 Jahren sowie in 71 % der Fälle mit typischen Hand- und Fuss-Arthropathien. Es wird geschlossen, dass das Sternum häufig bei Fällen mit röntgenologisch typischer psoriatischer Arthropathie mit betroffen ist.

RÉSUME

Les auteurs ont fait une radiographie de la synchondrose entre le man...
du sternum che...
tomographie
lésions érosiv...
... dans 61 % des cas évoluant depuis plus de 5 ans et dans 71 % des cas présentant une arthropathie typique des mains et des pieds. Ils concluent que le sternum est fréquemment atteint dans les cas où il y a une arthropathie psoriasique radiologiquement typique.

Table

Clinical and roentgenologic data of 29 patients with psoriasis and seronegative polyarthritis

Duration of joint involvement	No of patients	Roentgenologically peripheral psoriatic arthritis	Radiography of sternal synchondrosis					Duration of skin lesion (years)
			Erosion				Synostosis IV	
			I	II	III	Total		
< 5 years	11	5	2	1	1	4	1	7 1
> 5 years	18	14	4	2	5	11	3	21 2
Total	29	19	6	3	6	15	4	15 8

the duration of arthritic symptoms in the hands or feet (Table) In patients with a history of less than 5 years arthritis in the hands or feet were found in 55 per cent, with a longer history in 78 per cent In the group with a history longer than 5 years lesion of the synchondrosis (excluding synostosis) was found in 61 per cent of all cases and in 71 per cent of the subjects with typical hand or feet arthritis

Twelve patients had either past or present sternal pain In some cases the sternal angle was also tender to palpation Two of the patients with ankylosis reported a period of pain at the time of onset of the arthropathy Erosions were observed in 7 of the 12 patients with pain but only in 2 without a history of pain

The radiographic abnormalities were closely correlated to hand and foot involvement Among the 10 cases without arthropathy in the hands and feet slight erosion of the bony margins of the synchondrosis was observed in 2 cases only, 2 patients had ankylosis without a history of pain

Discussion

It is obvious that involvement of the synchondrosis between the manubrium and the sternal body is closely related to the existence of psoriatic arthropathy There was no evidence of primary, solitary involvement of the synchondrosis in any of the cases, although some patients experienced sternal pain as early as the first appearance of pains in finger or toe joints Both the inflammatory lesions of the spine and of the sternum develop during a severe or long history of psoriatic joint affection The abnormalities visible on the lateral chest film are relatively infrequent tomography being mandatory for early diagnosis Sternal involvement in psoriatic patients seems to occur at a frequency similar to what is reported in ankylosing spondylitis (SAVILL, SOLOWAY & GARDNER, DILSEN et coll) The percentage given by MCEWEN et coll in patients with psoriatic spondylitis is of the same order Similar sternal involvement also occurs in patients with peripheral polyarthritis without spondylitis (LAITINEN et coll)

FROM THE DEPARTMENT OF DIAGNOSTIC RADIOLOGY (DIRECTOR PROF G -F SALTZMAN),
UMEÅ UNIVERSITY, S 901 85 UMEÅ, SWEDEN

ANGIOGRAPHY IN EPIDEMIC NEPHROPATHY

Bo Lundström

Epidemic nephropathy (nephropathia epidemica) is an acute, benign nephritic disease causing transient uraemia of varying degrees The first cases were reported from Northern Sweden in 1934 (Myhrman, Zetterholm) In the course of time the disease has also been reported from other parts of Sweden (Hällqvist 1949, Myhrman 1957, Fjellström 1960, Ornstein & Söderhjelm 1965), as well as from Norway (Knutrud 1949, Muri 1950), Denmark (Hansen 1958) and Yugoslavia (Radosević & Mohacek 1954) During the Second World War an epidemic resulted in over 1 000 cases among German soldiers in Northern Finland (Stuhlfauth 1943, Hortling 1946) A material of 380 cases of epidemic nephropathy in Finland was published by Lahdevirta (1971)

The clinical symptoms and signs are well documented, well known and characteristic The microscop[illegible]
of a la[illegible]
no rep[illegible]
angiog[illegible]
course [illegible] Although being an acute inflammatory lesion, causing oliguric renal insufficiency, the angiographic appearances are markedly different from what is commonly considered to be characteristic of renal lesions giving rise to acute oliguric uraemia

Submitted for publication 18 July 1973

REFERENCES

AVILA R, PUGH D G, SLOCUMB C H and WINKELMAN R K Psoriatic arthritis A roentgenological study Radiology 75 (1960), 691

BAKER H, GOLDING D N and THOMPSON M Psoriasis and arthritis Ann intern Med 58 (1963), 909

DILSEN N, MCEWEN C, POPPEL M, GERSH W, DITATA D and CARMEL PH A comparative roentgenological study of rheumatoid arthritis and rheumatoid (ankylosing) spondylitis Arthritis Rheum 5 (1962), 341

JAJIĆ J Radiological changes in the sacro iliac joints and spine of patients with psoriatic arthritis and psoriasis Ann rheum Dis 27 (1968), 1

KILLEBREW K, GOLD R H and SHOLKOFF S D Psoriatic spondylitis *Radiology* 108 (1973), 9

KORMANO M A microradiographic and histological study of the manubrio sternal joint in rheumatoid arthritis Acta rheum scand 16 (1970), 47

LAITINEN H, SAKSANEN S and SUORANTA H Involvement of the manubrio sternal articulation in rheumatoid arthritis Acta rheum scand 16 (1970), 40

LUNDBERG M and ERICSON S Changes in the temporomandibular joint in psoriasis arthropathica Acta derm-venereol 47 (1967), 354

MCEWEN C, DITATA D, LINGG C, PORINI A, GOOD A and RANKIN T Ancylosing spondylitis and spondylitis accompanying ulcerative colitis, regional enteritis, psoriasis and Reiter's disease Arthritis Rheum 14 (1971) 291

MOLIN L Psoriasis Acta derm-venereol 53 (1973) Suppl No 72

PETERSON JR C C and SILIBIGER M L Reiter's syndrome and psoriatic arthritis Their roentgen spectra and some interesting similarities Amer J Roentgenol 101 (1967), 860

SAVILL D L The manubrio-sternal joint in ankylosing spondylitis J Bone Jt Surg 33B (1951), 56

SOLOWAY J and GARDNER C Involvement of the manubriosternal joint in Marie Strumpell disease Amer J *Roentgenol 65 (1951), 749*

WRIGHT V Psoriatic arthritis A comparative radiographic study of rheumatoid arthritis and arthritis associated with psoriasis Ann rheum Dis 20 (1961) 123

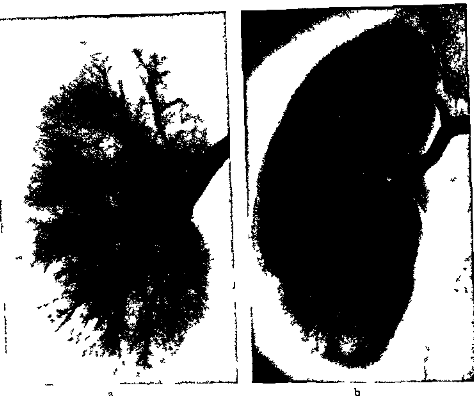


Fig 2 Nephroangiography a) Epidemic nephropathy b) normal kidney The kidney is moderately enlarged and the cortex is thickened The peripheral arterial branches are dilated and the arcuate arteries divide at an acute angle giving the kidney a striated appearance

oedema and distended tubules in the cortex with low epithelium i e on the whole, fairly moderate changes

Material

Selective nephroangiography was performed in altogether 40 patients during or after the disease The diagnosis was based on the clinical course, laboratory data and as a rule renal biopsy and microscopy The majority of the patients had out

Table 1

Age and sex distribution

Years	Men	Women
0–20	5	2
21 30	11	
31–40	8	3
4?	5	1
Total	29	6

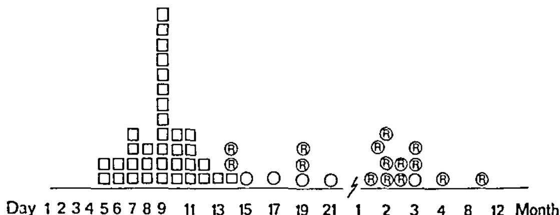


Fig 1 Time of nephroangiography in relation to day of onset of disease □ during disease ○ recovered patient, R repeat angiography

Clinical features are characteristic comprising 3 phases following each other fairly distinctly in time The onset is sudden, influenza-like, with high temperature, pain in the back and abdomen and headache combined with nausea and vomiting After 4 to 5 days a renal lesion phase begins with massive proteinuria and varying degrees of renal injury As a rule, there is considerable oliguria, in isolated instances anuria, and a rise of serum creatinine to 3 to 10 mg/100 ml During this phase the majority of patients are often in a very bad condition Recovery generally begins on the 8th to 10th day Oliguria is replaced by polyuria and the proteinuria diminishes As a rule, the symptoms and signs have more or less disappeared 2 weeks after the onset of the disease The concentrating power of the kidneys may be reduced a few weeks, but renal function is always restored The prognosis is good Only one case of death has been reported (LÄHDEVIRTA) The cause of the disease is unknown but some pathogen is assumed to be transmitted by small rodents The frequency of the disease is uncertain Many cases are probably not diagnosed About a dozen cases a year appear in Umeå and are distributed all over the year with a certain over-representation during November to January Epidemic nephropathy occurs endemically and mainly affects adult males with out dour occupations The vast majority of cases have been reported from the Scandinavian countries, and because of this it has sometimes been referred to as epidemic nephropathy of Scandinavia However, it is to be assumed that the disease should exist throughout the subarctic region, i e Iceland Greenland, Northern Asia and on the North American continent Haemorrhagic fever with renal syndrome has been suggested to be a closely related condition On the other hand, this is a more malignant nephritis, occurring, among other places, in the Far East where it caused hundreds of fatalities among American soldiers during the Korean war (ANDREW 1953, FROEB & MCDOWELL 1954, DODGE et coll 1956)

The microscopic appearances of the kidney in the acute phase consist of slight increase in inflammatory cells in the glomeruli, more or less evident interstitial

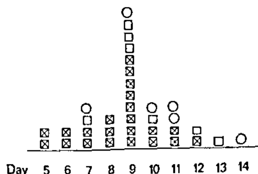


Fig 4 Angiographic abnormalities in relation to time after onset of disease ☒ evident signs ☐ suggestive signs ○ no abnormality of epidemic nephropathy

Methods

Percutaneous selective nephroangiography was performed bilaterally Ten ml Urografin 60 % were injected by an automatic injector operated at a pressure of 3 5 kg/cm², the injection time was 1 0 to 1 1 s The exposure rate was 2 films/s during the first 4 seconds, followed by 1 film/s during another 3 seconds and a final film after an additional 2 seconds ECG, injection and exposure data were recorded on a polygraph Premedication was given in the majority of cases in the form of pethidine chloride 25 mg and vasopressin 5 to 15 units (in order to eliminate bowel gas) In 10 cases no premedication was administered Renal biopsies were performed in connection with angiography in all but 2 patients (JUNGHAGEN et coll 1968)

Results

Size of kidney and diameter of renal artery In the acute phase all kidneys were enlarged, the cortex was thicker than usual and the trunk of the renal artery was slightly dilated A comparison with the condition at repeat angiography is given in Table 2

In the majority of cases examined during the period of the 5th to 14th day after the onset of the disease, the intrarenal arterial branches were dilated All arteries were widened but most evidently the peripheral ones Together with the renal enlargement and a thickened cortex this gave the kidneys a characteristic, striated appearance in the late arterial phase The arcuate arteries were stretched and, as a re-

Table 3

Relation between diuresis, typical changes and rapid circulation

	Rapid circulation	Evident change
Anuria	2/2	2/2
Oliguria	5/11	11/11
Polyuria	3/22	16/22



Fig 3 Epidemic nephropathy Patient examined a) 9, b) 16 and c) 40 days after onset of disease The kidney decreases in size progressively In a) the arteries are dilated and the interlobular arteries are filled

door occupations or interests Three of them were related mother, father and son Angiography was performed in 5 of the patients after recovery, i e more than 3 weeks after the onset of the disease and in 35 during the course of the disease The age and sex distributions for the latter are presented in Table 1

The time at which nephroangiography was carried out in relation to the day of the onset of the disease appears in Fig 1 In the 35 patients examined during the disease, the angiography was performed on the 5th to 14th day, usually on the 9th day Repeat angiography was carried out in 14 patients from 14 days to 10 months after the onset of the disease, in one on the 12th and 19th day as well as after 7 weeks Urography was performed in most of the patients without repeat angiography at varying times after recovery Twenty had uraemia at the time of the examination with serum creatinine exceeding 5 mg/100 ml, 2 had anuria and 11 oliguria No patient was dialysed

Table 2

Comparison between the morphology at nephroangiography in acute phase and after recovery (14 cases)

	Primary angiography		Repeat angiography		Decrease
	Mean	Range	Mean	Range	Mean
Kidney length (cm)	15 4	(16 7–12 5)	14 0	(15 5–11 0)	1 4
width (cm)	8 0	(8 7–6 8)	6 6	(8 0–5 0)	1 4
Renal art diam (mm)	9 1	(8 0–10 0)	7 2	(5 0–8 0)	1 9
Renal cortical width (mm)	9 0	(8 0–10 0)	6 8	(5 0–8 0)	2 2

All 13 patients with anuria or oliguria had typical angiographic appearances of the kidneys, the 6 normal were all in the polyuric phase

Renal blood flow In 10 cases contrast filling of the renal vein occurred already in the arterial phase (Fig 5), 9 of these had evident, and 1 possible changes

The renal blood flow was measured in 5 of the cases by a dye dilution technique (LINGÅRDH et coll 1975) In the acute phase only slight reduction of the renal blood flow was demonstrated which had returned to normal after recovery All cases had oliguria and uraemia at the time of the first examination

The arterial wash out time was normal in these 5 cases as well as in all the others

Discussion

Acute oliguric renal insufficiency may be encountered in a variety of pathologic conditions, including, inter alia, acute glomerulonephritis, lower nephron nephrosis after nephrotoxins, rejection of the transplanted kidney, haemolysis and sepsis The experience of angiography in acute renal failure is fairly comprehensive, previous observations have indicated that the angiographic appearances are nonspecific and similar regardless of the underlying disease The kidneys are enlarged and the cortex is thickened The arcuate arteries and above all the interlobular arteries are difficult, if not impossible, to observe The circulation and arterial wash out times are frequently prolonged A marked reduction of the cortical circulation exists which has been demonstrated by nephroangiography as well as by renal blood flow measurements employing the xenon wash out method (HOLLENBERG et coll 1968, 1970) A diffuse, homogeneous reduction of renal cortical perfusion representing a final common pathway in acute oliguric renal failure regardless of aetiology has been suggested by HOLLENBERG et coll (1969)

By contrast, entirely different appearances are obviously encountered in epidemic nephropathy The 13 cases examined in the anuric or oliguric phase all presented a dilatation of the renal artery as well as of intrarenal branches, including the cortical arteries In 7 of these cases the circulation time was also rapid, contrast medium could be observed in the renal vein already in the late arterial phase, most likely due to increased cortical blood flow Although a reduced blood flow through the cortical vessels may restrict the volume of the glomerular filtrate, it is evident that oliguria and anuria also may occur in a well preserved and even increased, cortical circulation The late arterial phase in a case of acute, anuric glomerulonephritis has been compared with that in epidemic nephropathy with anuria (Fig 6) In both conditions the kidneys are large and the cortex thick In glomerulonephritis the intrarenal blood vessels are narrow and separated and taper subcortically with no visible filling of the arcuate or the cortical vessels The arterial wash-out time is prolonged, as is the circulation time The difference to the condition of epidemic nephropathy is obvious In principle, the same differences exist between epidemic nephropathy and lower nephron nephrosis

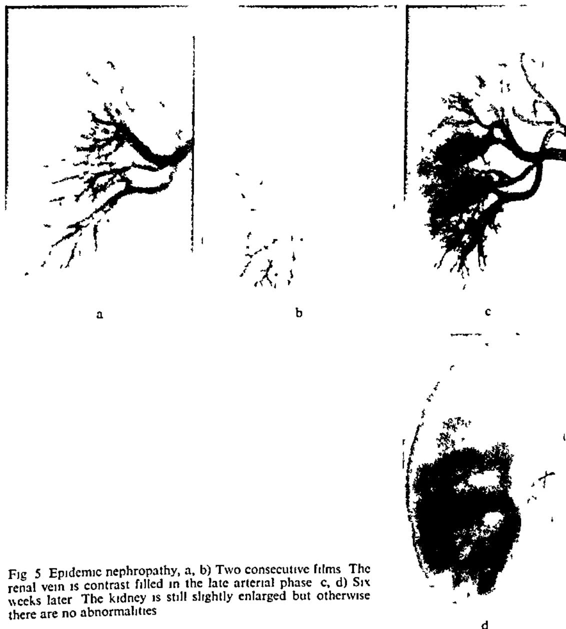


Fig 5 Epidemic nephropathy, a, b) Two consecutive films The renal vein is contrast filled in the late arterial phase c, d) Six weeks later The kidney is still slightly enlarged but otherwise there are no abnormalities

sult, did not form a distinct boundary of the cortex but appeared to continue straight out into the cortical interlobular arteries As a consequence, the dilated peripheral arterial branches seemed to be arrayed in palisade fashion (Fig 2)

The abnormalities were more or less evident and have been graded as evident (Fig 2) and as possible (Fig 3 a) Of the 35 patients examined during the disease 22 presented evident, and 7 possible abnormalities, while 6 were normal, except that the kidneys were somewhat enlarged (Fig 4) The changes were always bilateral, but sometimes more evident in one of the kidneys They were never encountered after the 13th day following the onset of the disease

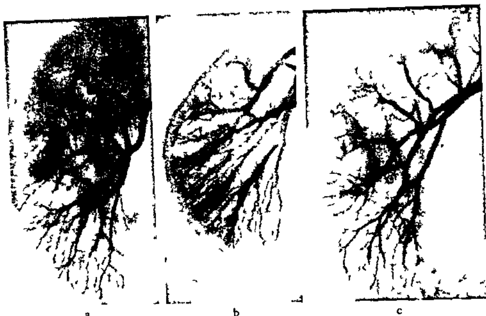


Fig. 7 a) Epidemic nephropathy b) Slight pyelonephritis c) Subchronic glomerulonephritis In a) the peripheral arteries give the kidney a striated palisade like appearance The cortical arteries are also filled in b) but branch off at right angles from the arcuate arteries in c) the peripheral circulation is markedly reduced

graphy the diameter of the renal artery had diminished, as well as the size of the kidney and the thickness of the renal cortex in all cases of epidemic nephropathy However, the kidneys were still larger than usual at the latest angiographies but the kidneys had always returned to normal size at subsequent urography

In a healthy kidney the arcuate arteries divide at right angles and run parallel to the renal surface The interlobular arteries branch off from the arcuate arteries at right angles to the surface They are about 300 μ in diameter and can normally be observed if high image quality is obtained As a result of the fact that the kidney is enlarged and the cortex thickened in epidemic nephropathy the arcuate arteries divide at a more acute angle and the interlobular arteries, which are dilated, continue straight out towards the renal surf...

a characteristic, striated appearan...

when vasodilator drugs are used

WOOD et coll 1969, DANFORD 197... Since the cortex then is not thickened, the angle of the division of the arcuate arteries is not changed The differences in the appearance of the cortical and subcortical arteries in epidemic nephropathy, in slight pyelonephritis (clinical and microscopic diagnosis after renal biopsy) and in subchronic glomerulonephrit...

The ...

orrhagi... raises the question whether similar angiographic

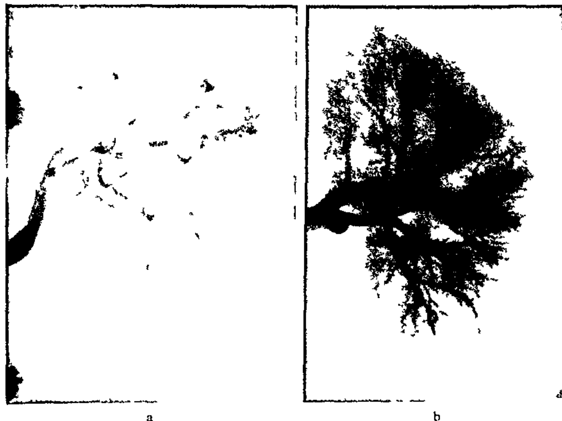


Fig 6 a) Acute glomerulonephritis with anuria b) Epidemic nephropathy In both cases the kidney is large and the cortex thick In a) the peripheral intrarenal arteries are contracted while dilated in b)

The blood flow was slightly reduced in the acute phase in the 5 cases in which measurements were performed using the dye dilution technique (LINGÅRDH et coll) Rapid circulation was not revealed in any of these cases, however

Like the clinical features of the disease, three distinct angiographic phases may be distinguished The 5th day after the onset of the disease was the earliest time nephro angiography was carried out Vasodilatation could be observed from the 5th through the 13th day in 29 cases out of 35 (Fig 4) The 6 cases without vasodilatation had already entered the polyuric phase However, 16 of 22 patients in the polyuric phase also presented changes typical of epidemic nephropathy

In one case angiography was performed on the 9th, 16th and 40th day after the onset of the disease (Fig 3) The size of the kidney had decreased at the later examinations, as had the diameters of both the main stem of the renal artery and the peripheral branches There may be some doubt about the diagnosis at the first angiography In cases of acute oliguric insufficiency due to another lesion than epidemic nephropathy reduced circulation of varying degree occurs In epidemic nephropathy a certain cortical accumulation of contrast medium may be observed in the nephrographic phase, which is not the case in other conditions At repeat angio-

ment à ce qu on supposait l insuffisance rénale oligurique aiguë peut aussi se produire dans des cas ou il y a une vasodilatation peripherique L aspect angiographique de la néphropathie ... alement net dans les phases oligurique et anuri

REFERENCES

ANDREW R. Epidemic hemorrhagic fever 40 cases from Korea Brit med J 1 (1953), 1063

DANFORD R The effect of glucagon on renal hemodynamics and renal arteriography Amer J Roentgenol 108 (1970) 665

DODGE H J GRIFFIN H E GAULD R L and KIM Y S Epidemic hemorrhagic fever in a Korean farm population Epidemiologic observations during 1954 Amer J Hyg 63 (1956) 38

FJELLSTRÖM K E Nephropathia epidemica in Uppland Acta med scand 167 (1960), 111

FREED T A HAGER H and VINIK M Effects of intraarterial acetyl-choline on renal arteriography in normal humans Amer J Roentgenol 104 (1968) 312

FROEB H F and McDOWELL M E Renal function in epidemic hemorrhagic fever Amer J Med 16 (1954) 671

HALLQVIST B Sporadiskt fall av nephropathia epidemica (In Swedish) Svenska Lak Tidn 46 (1949) 985

HANSEN E Atypisk akut nephritis (In Danish) Ugeskr Laeg 120 (1958) 908

HOLLENBERG N K EPSTEIN M BASCH R I and MERRILL J P No Man s Land of the renal vasculature An arteriographic and hemodynamic assessment of the interlobar and arcuate arteries in essential and accelerated hypertension Amer J Med 47 (1969) 845

— ADAMS D F OKEN D E ABRAMS H L and MERRILL J P Acute renal failure due to nephrotoxins Renal hemodynamic and angiographic studies in man New Engl J Med 282 (1970) 1329

— EPSTEIN M ROSEN S M BASCH R I OKEN D E and MERRILL J P Acute oliguric renal failure in man evidence for preferential renal cortical ischemia Medicine 47 (1968) 455

HORTLING H En epidemi av faltfeber (?) i finska Lappland (In Swedish) Nord Med 30 (1946) 1001

JUNGHAGEN P LINDQVIST B MICHAELSSON G and NYSTROM K Percutaneous renal biopsy on uraemic patients aided by selective arterial angiography and roentgen television Acta med scand 184 (1968) 141

KNUTRUD O Nephropathia epidemia (In Norwegian) T norske Laegeforen 69 (1949), 259

KUHLBACK B FORTELIUS P and TALLGREN L G Renal histopathology in a case of nephropathia epidemica Myhrman A study of successive biopsies Acta path microbiol scand 60 (1964) 323

LAHDEVIRTA J Nephropathia epidemica in Finland A clinical histological and epidemiological study Ann clin Res 3 (1971) Suppl No 8

LINGÅRDH G LUNDSTRÖM B and NYSTRÖM K Renal blood flow in acute epidemic nephritis Scand J Urol Nephrol 9 (1975) 57

MURI J Nephropathia epidemica (In Norwegian) Nord Med 43 (1950) 290

appearances may be encountered in this latter disease No report on nephroangiography in this disease seems to have been published, however

The underlying mechanisms that cause acute renal failure are not fully understood Since previous reports have suggested a reduced cortical blood flow as a common denominator, an active, functional vasomotor preglomerular spasm has been considered probable Such a mechanism may exist also in epidemic nephropathy but if so in an earlier stage than the present nephroangiographies have been performed The vasodilatation demonstrated angiographically, could then be regarded as reactive hyperaemia Another explanation could be that vasodilatation in fact also occurs in early stages in other diseases causing acute renal failure, although angiography seldom has been performed at these stages However, until cases have been examined in such an earlier stage, the findings reported here must be looked upon as evidence suggesting that epidemic nephropathy is a renal disease involving acute renal failure with angiographic changes of an entirely different kind than those described hitherto in other lesions presenting this symptom

SUMMARY

Nephroangiography has been performed in 35 patients with epidemic nephropathy during the course of the renal lesion phase In addition to enlarged kidney with thickened cortex, generalized renal vasodilatation was demonstrated in the majority of the cases, frequently combined with rapid circulation Thus, contrary to previous assumptions, acute oliguric renal insufficiency may also occur in cases with peripheral renal vasodilatation The angiographic appearance of epidemic nephropathy was characteristic and most evident in the oliguric and anuric phases Nephroangiography in acute oliguric renal failure may thus be of value for the differential diagnosis and thereby influence the clinical management of the patient

ZUSAMMENFASSUNG

Es wurde eine Nephroangiographie bei 35 Patienten mit epidemischer Nephropathie im Verlauf der Phase der Nierenschadigung vorgenommen Zusatzlich zu einer Nierenvergrosserung mit verbreiterter Cortex wurde eine generalisierte renale Vasodilatation in der Mehrzahl der Falle, haufig verbunden mit einer raschen Zirkulation, gefunden Somit kann auch, im Gegensatz zu fruheren Annahmen, eine akute oliguramische Niereninsuffiziens bei Fallen mit peripherer renaler Vasodilatation vorkommen Das angiographische Bild der epidemischen Nephropathie war wahrend der oliguramischen und anuramischen Phasen charakteristisch und am meisten ausgepragt Die Nephroangiographie bei einem akuten oliguramischen Nierenversagen kann somit bei der Differentialdiagnose von Wert sein und dadurch die klinische Behandlung des Patienten beeinflussen

RÉSUME

L'auteur a fait une nephro angiographie chez 35 malades atteints de néphropathie epidémique au cours de la phase de lesion rénale Outre l'augmentation de dimensions du rein avec épaississement du cortex il a mis en evidence une vaso dilatation rénale généralisé dans la majorité des cas, fréquemment associee avec une circulation rapide Ainsi contraire-

Six of the dogs were examined before trauma, 1 to 3, 10, 30, 60 and 90 min after the trauma, in one dog only 330 and 350 min afterwards

After angiography the wound cavity was filled with barium as a contrast medium to demonstrate the wound cavity in detail and single films were exposed

Trauma The weapon used was a smooth bore gun with a caliber of 6 2 mm The gun was fixed to a tripod and fired electrically The distance from the muzzle to the skin was approximately 60 cm A spherical steel bullet 6 mm in diameter and weighing 0 86 g was used The entrance velocity of the projectile was measured electrically and the exit velocity after passage through the leg was estimated by the number of soft wall boards the missile penetrated The thickness of the injured thigh was measured before the shot In this series only 1000 m/s was used as the impact velocity The amount of energy released to the extremity was calculated from the formula kinetic energy $= \frac{\text{mass} \times \text{velocity}^2}{2}$ (FRENCH & CALLENDER) The average kinetic energy released in the tissue of the traumatized leg was approximately 225 joule corresponding to about 50 per cent of the impact kinetic energy The missile was aimed at the medial aspect of the thigh so that the projectile traversed only skin and muscles and at a distance from the large vessels without hitting them, as judged from angiography and macroscopic examination after the experiment The direction of the wound channel was nearly parallel to that of the central radiation beam

At the end of the experiment the dogs were killed with an overdose of sodium Pentobarbital The tissues were then sectioned and examined macroscopically

Evaluation of the films The same principles were used as in previous reports (SANDEGÅRD & ZACHRISSON 1975 a, b) Determinations were made of (1) transit time of contrast medium between two defined levels (GREITZ 1956), and (2) diameters of arteries at corresponding levels (ERIKSON 1965)

In the determination of transit times the same zero level (time 0) was chosen on the film in the respective series as the earliest observable filling of the external iliac artery at the origin of the deep femoral artery The transit time of the contrast medium in the femoral arteries was defined as the difference between zero level (time 0) and the time of earliest filling of the caudal femoral artery (arising from the distal part of the femoral artery) In an analogous way, the earliest filling of veins in the adductor regions and the earliest filling of the distal part of the femoral veins were estimated These intervals are also referred to in the text as venous appearance times

Measurements of the internal diameter of the arteries were performed on the films at corresponding levels with a magnifying glass with a built in scale permitting reading to 0 1 mm The magnification factor was 7 The standard error of a single measurement of the external iliac artery was $\pm 0\,07$ mm and of the femoral artery $\pm 0\,05$ mm (SANDEGÅRD & ZACHRISSON 1975 b)

The course, contour and number of the vessels were scrutinized on the films The appearance of transient homogeneous accumulation of contrast medium during the vascular phase was considered as well as the presence of extravasation of contrast

clusions regarding the early circulatory disturbances within the traumatized region Furthermore, angiography of the subsequent complications after missile wounding (SHUMACKER & CARTER 1946, BERK 1963, PATMAN et coll 1964, BELL & COCKSHOTT 1965, TREIMAN et coll 1966, KYLLÖNEN 1966, SALETTA & FREEARK 1968, GIRL 1971) does not reflect the immediate hemodynamic conditions as the angiographic examinations were performed hours to days after the injury

The subject of this report is the early circulatory conditions following high velocity missile wounding of soft tissue

Material and Methods

The material consists of seventeen mongrel dogs of both sexes (14–24 kg) anesthetized intravenously with sodium Pentobarbital in repeated small doses The trachea was intubated and respiration was supported by mechanical ventilation Ten of the dogs were used for hemodynamic measurements and seven dogs for serial angiography

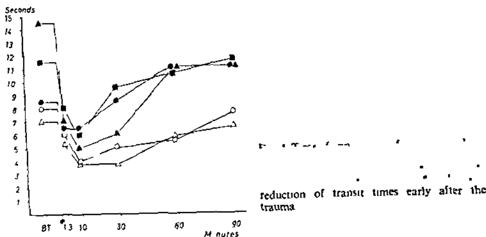
In both groups the following procedures were performed

Through a lower midline abdominal incision the vessels near the aortic bifurcation were dissected free The aorta distal to the origin of the external iliac arteries was ligated thus excluding the internal iliac arteries and the median sacral artery, so as to isolate the blood flow to the limbs The circulation of the foot with its rich net of arterio-venous anastomoses was excluded by a tourniquet placed around each ankle *Small polyethylene catheters for infusion and blood pressure recording* were introduced into one carotid artery and one external jugular vein All the catheters were kept open by repeated small injections of saline

Special procedures of the hemodynamic measurements

Arterial blood flow was measured continuously with an electromagnetic flow meter (Nycotron, Oslo) with the flow probes placed on the external iliac arteries proximal to the deep femoral artery Heart rate, arterial blood flow and arterial blood pressure (Statham Pressure Transducer) were registered continuously on a Mingograf (Elema Schonander)

For the angiography a catheter (Bardic adult feeding tube, length 107 cm, size 2 7 mm, CR Bard International Ltd, England) was introduced through the left internal iliac artery with the tip placed in the aorta near the origin of the external iliac arteries The dogs were held in the supine position and serial angiography was performed with the apparatus (Elema Schonander 35 × 35 AOT-R film changer and two stereoscopic tubes) and technique described previously (SANDEGÅRD & ZACHRISSON 1975 a) The angiography method used, enabled exposure of both thighs and the pelvic region simultaneously The contrast medium (Isopaque Cerebral, Nyegaard & Co, Oslo) was injected manually in a volume of 15 ml during 1 5 to 3 s In six dogs the rate of exposures was as follows 2 films/s for 10 seconds, followed by 1 film/s for 10 seconds, in one case 4 films/s for 4 seconds followed by 2 films/s for 4 seconds and finally 1 film/s for 6 seconds



reduction of transit times early after the trauma

medium The vascular phase was defined as the period of intravascular appearance of contrast medium When all contrast medium had disappeared in later films, the homogeneous accumulation of contrast medium during the vascular phase was judged to be mainly in vessels too small to be defined separately Extravasation of contrast medium was said to be present when medium appeared in the extravascular space during and after the vascular phase

Results

Hemodynamic measurements of blood flow revealed an increase of flow to the injured extremity during the first 30 min after the impact (Fig 1) The flow increase started with a peak flow of up to 200 per cent of the pre-trauma value immediately after the shot The flow peak subsided within the first minute after the trauma and was followed by a more moderate increase of the blood flow

Arterial blood pressure and heart rate fell slightly within the first 5 min after the shot, but then returned towards control and remained at a fairly constant level throughout the experiment Peripheral vascular resistance (PRU) calculated as the ratio of blood pressure to blood flow revealed a marked decrease on the traumatized side immediately after the shot, corresponding to the flow peak Thereafter PRU increased but was significantly decreased in comparison with pre trauma values 30 min after the injury and then tended to normalize A fairly marked transient increase of PRU occurred on the non traumatized side within the first 15 min after the shot and was equal to pre trauma level and the values of the traumatized side after 60 min (Fig 2)

Angiography The entrance of the wound channel was placed at the medial aspect of the hind leg corresponding to the adductor tract The centre of the wound cavity following passage of the missile was mostly marked by localized areas of gas measuring 1 5 cm × 2 cm on the films In all animals gas was recognized in streaks, outlining

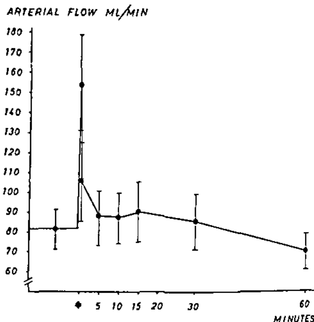


Fig 1 Arterial blood flow in ml/min ± SE measured in the iliac artery of the traumatized leg before during and at repeated intervals following missile injury (*) to the thigh

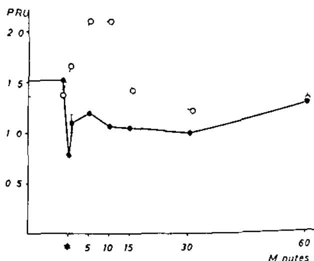


Fig 2 Peripheral vascular resistance

● ●

non traumatized o---o legs before and after missile injury (*)

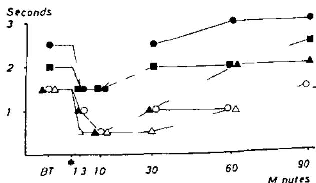


Fig 3 Transit time of contrast medium in the femoral artery of the missile injured leg in five dogs measured on the films BT – examination before trauma (*) Immediate marked reduction of transit times after the trauma

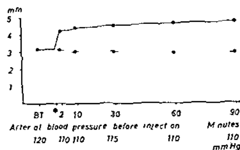


Fig 6 Internal diameter of the femoral arteries measured on the films 10 mm proximal [illegible] measuring level after shot Slight reduction of arterial diameter in the non injured leg

and of the distal femoral vein (Figs 4, 5) revealed the same tendency as on the arterial side with a marked shortening of transit time of the medium 1 to 10 min after the impact The values tended to normalize about 60 to 90 min after the trauma The changes of flow emanated mainly from the region in which scattered gas was observed Outside this region the vascular bed was evidently not affected by the trauma On the non traumatized side the transit time tended to increase or was fairly unchanged

Significant increase of the internal diameter of the femoral arteries of the traumatized leg was found in those four animals in whom the distance from the arterial wall to the approximate centre of the permanent cavity was less then 3 cm (Table) This dilatation persisted during the experiments even up to 90 min (Fig 6) On the contralateral side no localized change of diameter related to missile wounding was observed in any of the animals and the calibers tended to decrease throughout the experiments

A small avascular zone occurred around the periphery of the wound channel Surrounding this area the arteries were markedly dilated during 1 to 10 min after the trauma, in addition to an important accumulation of contrast medium, followed by an early venous filling (Fig 7) Some of the dilated arteries close to the wound channel also revealed segmental narrowing (Fig 8) Concomitant with these findings the muscular arteries supplying the injured area were dilated up to their origin

The homogeneous accumulation of contrast medium in the vascular phase gradually decreased in the examinations later than 10 min after trauma, and did not exist later than 60 min after the gunshot, the area tended to decrease from the periphery towards

Table

Distance in mm between the centre of the permanent cavity and the femoral artery measured on the films in seven dogs + denotes dilatation of the femoral artery after missile wounding, − denotes absence of dilatation

Dog No	1	2	3	4	5	6	7
Distance in mm from the centre of wound channel perpendicular to the femoral artery	18	20	24	25	30	35	40
Presence of dilatation of the femoral artery	+	+	+	+	−		−

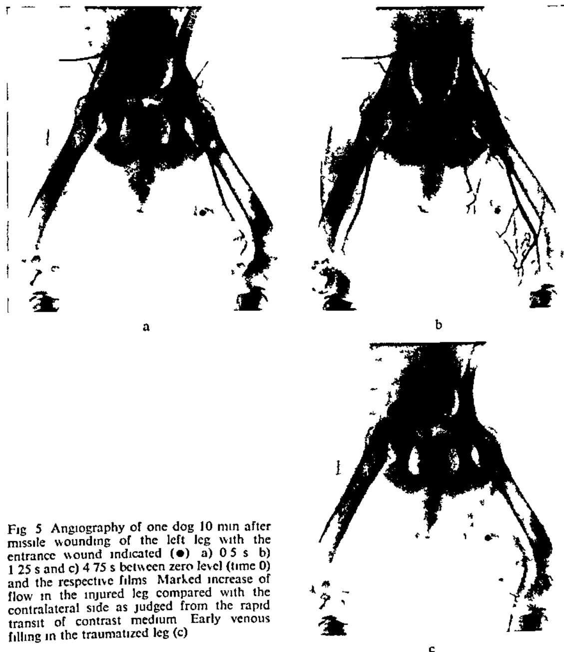


Fig 5 Angiography of one dog 10 min after missile wounding of the left leg with the entrance wound indicated (●) a) 0 5 s b) 1 25 s and c) 4 75 s between zero level (time 0) and the respective films Marked increase of flow in the injured leg compared with the contralateral side as judged from the rapid transit of contrast medium Early venous filling in the traumatized leg (c)

fascial spaces up to 8 to 10 cm from the wound channel Small accumulations of scattered gas also occurred in the tissues surrounding the wound channel indicating intramuscular spreading

Femoral arterial transit times decreased markedly on the traumatized side and at 1 to 10 min after the impact, the estimated periods amounted to about half of the pre trauma levels Thereafter the transit times increased and were normalized or slightly elevated 60 to 90 min after injury in comparison with pre trauma values (Fig 3)

The venous appearance time of the adductor region close to the permanent cavity,

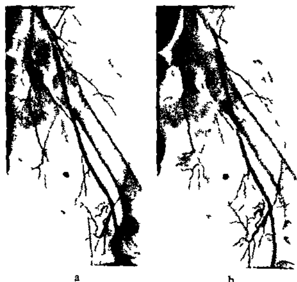


Fig 8 Stereoscopic films of the missile wounded leg of one dog 2 min after impact with marking of the entrance wound (•) Arterial phase a) 1 5 s and b) 1 75 s between zero level (time 0) and the respective films In the centre of the wound tract no arteries are filled The injured region is outlined by curved displacement of arteries and within this region scattered gas Segmental narrowing of the saphenous artery

the vascular disturbances were most evident in the area surrounding the central avascular zone and diminished towards the periphery

Macroscopic examination At the end of the experiments the wound regions were dissected The macroscopic findings were similar in all animals The spaces between the fasciae were opened up by the injury 8 to 10 cm in both directions from the wound channel The muscle tissue had a mushy brown appearance with scattered interstitial hemorrhages in an area up to 5 cm from the permanent cavity In no case could any macroscopic injury to large vessels or bone be ascertained

Discussion

In order to obtain reproducible experimental conditions a spherical bullet of defined mass and velocity was used Both bone fracture and laceration of major arteries were avoided As the influence on the blood flow from the rich net of arterio venous anastomoses in the paw was excluded the flow values reflect mainly the flow in the muscle tissue and to some extent bone

An immediate marked increase of flow appeared in the first minute after the gun shot It might be suggested that this peak flow, which corresponds to an immediate decrease in regional vascular resistance could be caused by the shock wave of pressure from the missile (Harvey et coll 1962) producing a sudden loss or inhibition of vasoconstrictor tone and a reduction in the mechanical facilitation of precapillary tone After this phase the flow values declined to a level of more moderate flow increase normalized within 60 minutes Calculation of peripheral resistance revealed a transient lowering parallel to this flow increase The normalization of the values

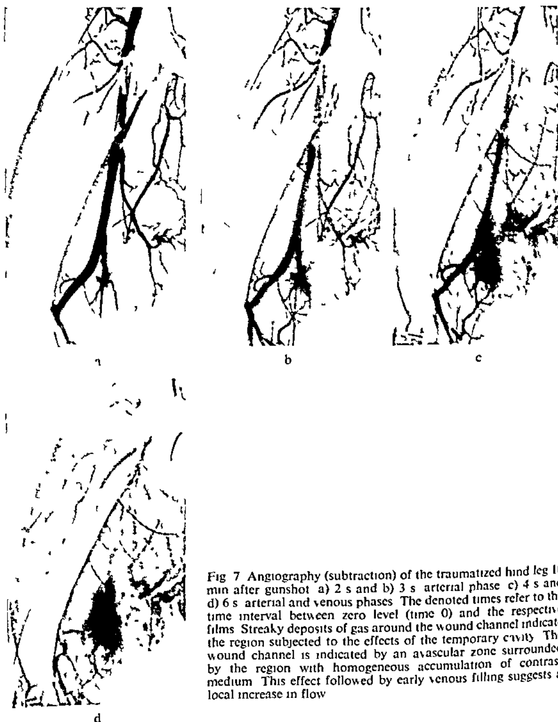


Fig 7 Angiography (subtraction) of the traumatized hind leg 10 min after gunshot a) 2 s and b) 3 s arterial phase c) 4 s and d) 6 s arterial and venous phases The denoted times refer to the time interval between zero level (time 0) and the respective films Streaky deposits of gas around the wound channel indicate the region subjected to the effects of the temporary cavity The wound channel is indicated by an avascular zone surrounded by the region with homogeneous accumulation of contrast medium This effect followed by early venous filling suggests a local increase in flow

the wound channel Coexisting with the decrease, localized successively increasing changes of the smaller arteries occurred, in the form of decreasing caliber and segmentally more marked constriction accompanied by impaired venous filling Displacement of vessels and discontinuity of the arteries close to the permanent cavity were observed as well as extravasation of contrast medium to a minor degree In general,

increased flow, i e the transient homogeneous accumulation of contrast medium followed by an early venous filling

The vascular alterations of the traumatized region surrounding the central avascular zone had the same appearances as those following extensive soft tissue contusion trauma, in which transient hyperemia of the injured region with progressive vascular abnormalities was encountered (SANDEGÅRD & ZACHRISSON 1975 b) Thus, apart from the destructive effect of the missile, the present angiographic and hemodynamic results indicate a mechanism of contusion caused by the rapidly expanding temporary cavity These observations agree with the opinion of AMATO et coll, who have proposed that a high velocity missile produces blunt contusion effects in the tissues

In conformity with the vascular alterations in soft tissue contusion trauma (SANDEGÅRD & ZACHRISSON 1975 b), persistent dilatation of major arteries during the present experiments was revealed Thus, in those cases in which the distance between the femoral artery and the estimated centre of the permanent cavity was less than 3 cm, a persistent dilatation of the artery occurred after gunshot This suggests a loss of vascular tone or a disturbance of the contractile function of the vascular smooth muscle due to the trauma It is difficult to evaluate the hemodynamic significance of this dilatation, but it is apparent that the flow changes and the dilatation are not parallel phenomena

In comparing the angiographic findings with the macroscopic examination of the wound region, an agreement was evident between the extension of the macroscopic findings and of the severe angiographic abnormalities such as disruption, extravasation of contrast medium, major changes of caliber and marked displacement However, in regions more distant from the wound channel, it was evident that the border line of vascular changes in the films appeared partly in macroscopically non-affected tissues This fact indicates that angiography is decisive in the determination of the extent of the traumatized region in the acute phase after high velocity missile injury

Since constriction of the femoral arteries was not observed, it appears advisable in clinical practice not to make the diagnosis of arterial spasm in the immediate posttraumatic phase without performing angiography or exploration of the artery

SUMMARY

The early circulatory changes following high velocity missile wounding to soft tissue of an extremity were analysed by hemodynamic methods and serial angiography The extent of the tissue injury and the functional disturbances were mapped out and the time-course of the alterations in blood flow was registered Possible mechanisms for the observed abnormalities are discussed

ZUSAMMENFASSUNG

Die fruhzeitigen Zirkulationsveranderungen nach einer Verwundung der Weichteile einer Extremitat durch ein Geschoss mit hoher Geschwindigkeit wurden mit haemodynamischen Methoden und durch Film Angiographie untersucht Der Grad der Gewebe

within 60 min pointed to at least a partial recovery of vascular tone The observed changes of flow and peripheral resistance following the initial peak flow after the gunshot are similar to the flow changes described in extensive soft tissue trauma (LIU 1968, LEWIS & LIM 1970) The effect of vasodilator substances released from injured region was considered as one possible cause of the increase of blood flow following soft tissue trauma (SANDEGÅRD et coll 1975) It might be assumed that a similar mechanism applies to missile wounding of soft tissue The increase of blood flow in missile wounding was, however, not as marked as that found in extensive soft tissue trauma (SANDEGÅRD et coll) Although the kinetic energy transferred by the high velocity spherical bullet was high, the macroscopic examination revealed that the injury was confined anatomically to a rather limited part of the thigh In the more extensive soft tissue injury (SANDEGÅRD et coll) presumably a larger capillary bed was involved than in the missile wound This observation may suggest that the differences in the extent of the engaged capillary areas may explain the variations in lowering of vascular resistance following missile wounding and soft tissue contusion trauma, respectively On the non-traumatized side the blood flow decreased moderately after missile wounding pointing to a redistribution of flow to the injured extremity

In the series of dogs examined with angiography it was of importance to consider the possible effects of the contrast medium itself on the circulation in the investigated area LEWIS et coll (1975) have pointed out that, even in the traumatized soft tissue of the extremity, the informative arterial phase on the films appears in the time lag between the injection and the flow-increasing effect of the contrast medium They found no evidence that repeated injections of medium altered the experimental conditions to any appreciable degree Moreover, comparison of flow in the traumatized extremity by hemodynamic methods and angiography have revealed similar results (SANDEGÅRD & ZACHRISSON 1975 a, b)

The observed marked peak flow within the first minute after the gunshot registered hemodynamically, could not be demonstrated at angiography, as these examinations were not performed until 1 to 3 min after the injury The more constant flow increase following the initial peak flow corresponded to the markedly decreased femoral arterial transit time and venous appearance time on the traumatized side at angiography The transit time mainly regained pre-trauma level 60 to 90 min after trauma, concomitant with the normalization of blood flow Thus, a concordance between the hemodynamic and angiographic flow measurements existed, which suggests the possibility of using angiography in the evaluation of the distribution of flow in the missile injured leg

The findings of gas and vascular abnormalities mainly within the same regions enabled a fairly exact delimitation on the films of the region affected by the transferred kinetic energy Serious injury to the circulation was registered close to the wound channel, diminishing towards the periphery, indicating a decreasing influence of the missile In addition to these morphologic changes, there were signs pointing to an

Effect of acute soft tissue injury on nutritional and non nutritional shunt flow through the hind leg of the dog Acta orthop scand 41 (1970) 17
— — Studies on the circulatory pathophysiology of trauma II Effects of acute soft tissue injury on the passage of macroaggregated Albumin (^{131}I) particles through the hind leg of the dog Acta orthop scand 41 (1970) 37
— SANDEGÅRD J SEEMAN T and ZACHRISSON B E Effects of intraarterial injection of contrast medium on regional circulat on in soft tissue trauma Acta radiol Diagnosis 16 (1975) 373
LIU C T Circulatory response to muscle trauma following denervation and hemorrhage in dogs J Trauma 8 (1968) 75
MENDELSON J A and GLOVER J L Sphere and shell fragment wounds of soft tissues Experimental study J Trauma 7 (1967) 889
PATMAN R D POULOS E and SHIRES G T The management of civilian arterial injuries Surg Gynec Obstet 118 (1964) 725
RICH N M
— MANTON \ vascular injuries in
SALETTA J D and FREEARK R J The partially severed artery Arch Surg 97 (1968) 198
SANDEGARD J and ZACHRISSON B E (a) Circulatory disturbances after experimental fracture Acta radiol Diagnosis 16 (1975) 181
— — (b) Angiography and hemodynamic measurements in extensive soft tissue trauma to the extremity Acta radiol D agnosis 16 (1975) 279
— NOLTE J LEWIS D H and SEEMAN T Early hemodynamic and biochemical changes in soft tissue trauma Europ surg Res 6 (1974) 233
SHUMACKER JR H B and CARTER K L Arterio venous fistulas and arterial aneurysms
TR trauma A fifteen year study
WILSON L B D spersion of bullet energy in relation to wound effects Mil Surg 49 (1921) 241

schadigung und die funktionelle Storung wurden festgestellt und der Zeitverlauf der Veranderungen der Durchblutung untersucht Mogliche Mechanismen der beobachteten Veranderungen werden besprochen

RESUMÉ

Les modifications circulatoires precoces consécutives à une blessure des tissus mous d'un membre part un projectile a haute vitesse ont éte étudiees par des methodes hemodynamiques et par angiographies en série Les auteurs ont dessine l étendue des lesions tissulaires et des troubles fonctionnels et ont note l evolution en fonction du temps des modifications du debit sanguin Ils examinent les mécanismes possibles qui sont à l origine des modifications observees

REFERENCES

AMATO J J and RICH N M Temporary cavity effects in blood vessel injury by high velocity missiles J cardiovasc Surg 13 (1972), 147

— — BILLY L J, GRUBER R P and LAWSON N S High velocity arterial injury a study of the mechanism of injury J Trauma 11 (1971) 412

— BILLY L J, GRUBER R P, LAWSON N S, ARSENAL E and RICH N M Vascular injuries Arch Surg 101 (1970), 167

BELL D and COCKSHOTT P W Angiography of traumatic arterio venous fistulae Clin Radiol 16 (1965) 241

BERK M E *Arteriography in peripheral trauma Clin Radiol 14 (1963) 235*

BLACK A N, BURNS B D and ZUCKERMAN S *An experimental* study of the wounding mechanism of high velocity missiles Brit med J 2 (1941), 872

DEMUTH JR W E Bullet velocity and design as determinants of wounding capability An experimental study J Trauma 6 (1966) 222

— Bullet velocity as applied to military rifle wounding capacity J Trauma 9 (1969) 27

ERIKSON U Circulation in traumatic amputation stumps An angiographical and physiological investigation Acta radiol (1965) Suppl No 238

FRENCH R W and CALLENDER G R Ballistic characteristics of wounding agents *In* Wound ballistics, chapter II Edited by J B Coates and J C Beyer Office of the surgeon general department of the army Washington D C 1962

GIRL J Arteriography in arterial gunshot wounds Acta radiol Diagnosis 11 (1971) 78

GREITZ T A radiologic study of the brain circulation by rapid serial angiography of the

[illegible] W O Mechanism of wounding

— MCMILLEN J H, BUTLER E G and PUCKETT W O Mechanism of wounding *In* Wound ballistics, chapter III Edited by J B Coates and J C Beyer Office of the surgeon general department of the army Washington D C 1962

HORSLEY V The destructive effects of projectiles Proc roy Inst Great Brit 14 (1894), 228

KRAUSS M Studies in wound ballistics Temporary cavity effects in soft tissues Mil Med 120 (1957), 221

KYLLONEN K E J Traumatic arterial lesions Acta chir scand (1966) Suppl No 356 B

LEWIS D H and LIM JR R C Studies on the circulatory pathophysiology of trauma I

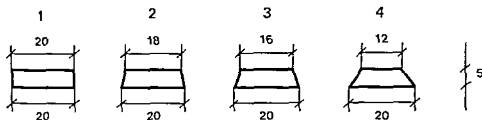


Fig 1 Drawings of the cylindrical objects 1 to 4 The dimensions are given in mm

Fig 2 Films of a) the chest b) the test objects 1 to 4 and c) their superposition A F in (a) label the lung areas

FROM THE DEPARTMENT OF DIAGNOSTIC RADIOLOGY (DIRECTOR, PROF H LODIN) AND RADIATION PHYSICS (DIRECTOR J CEDERLUND), AKADEMISKA SJUKHUSET, S-750 14 UPPSALA, SWEDEN

PERCEPTION OF SIMULATED LESIONS IN THE LUNG

ANDERS HEMMINGSSON, BO JUNG and TORSTEN LÖNNERHOLM

The detection of a lesion in a roentgenogram depends on the photographic density difference across the outline of the object, the characteristics of the object's border zone and the adjacent structures The observer's experience, capacity and mental condition and the viewing conditions also affect the detectability Changes in one or more of these factors thus influence the detectability of a lesion in a roentgenogram

Normal pulmonary structures, for example, introduce a high frequency pattern in chest films, which may mask the outline of pulmonary lesions (TUDDENHAM 1957, 1963) This explains why lesions are overlooked in a substantial fraction of clinical examinations (e g GARLAND 1950, NEWELL & GARNEAU 1951, TUDDENHAM 1962, SHEA & ZISKIN 1972)

The spatial frequency spectrum of roentgenograms has been analysed by several authors (ROSSMAN & MOSELEY 1969, KUNDEL et coll 1972, HEMMINGSSON et coll 1972) The modulation transfer function of the human eye has a maximum at a certain spatial frequency (HEMMINGSSON et coll 1972) SHEA et coll (1970) have suggested that there may be an optimum viewing distance for chest films At this ideal distance the spatial frequencies of the natural structures in the film should be too high for the human eye, whereas the spatial frequencies characteristic of the outline of pulmonary lesions should be close to the optimum

Submitted for publication 29 April 1974

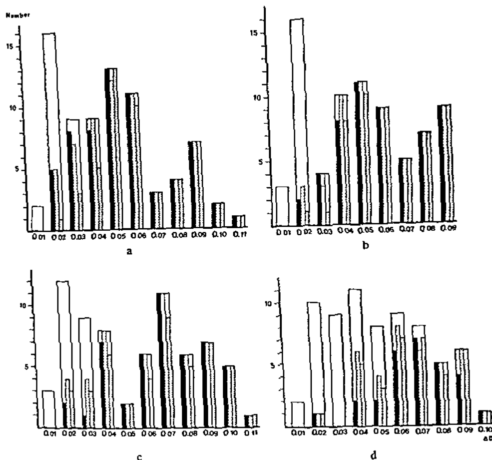


Fig 3 Distributions of presented and detected objects with respect to density difference, ΔD Open columns represent presented objects filled columns objects detected at 0 3 m (■), 1 0 (□) and 3 0 m (□) a) Object 1 (n = 77), b) object 2 (n = 74) c) object 3 (n = 70) and d) object 4 (n = 69)

When the object films were superposed on a chest film copy, no more than one object was present in any of the six lung areas A–F, and none was present outside these areas (Fig 2 b, c) The distance between the objects was always greater than 4 cm and each object was present as many times in the upper as in the middle and basal lung areas

The photographic density was measured (Quantalog TDA 100, Mac Beth, aperture 1 mm) in 6 40 points, evenly spaced over the six lung areas in one chest film copy, and inside and immediately outside the images of the objects in all object films At least four points on both sides of the object were measured

The gradient zones in one of the object films containing all four objects were recorded by microdensitometry with a modified spectrophotometer (Shimadzu) with a slit aperture of 0 2 mm × 2 mm

Table 1

Density (optical density units) in the six lung areas (A to F) of one chest film copy

Lung area	Mean	Range	Standard deviation
A	1.53	1.15–1.73	0.15
B	1.53	1.10–1.80	0.19
C	1.21	0.62–1.56	0.26
D	1.49	1.25–1.68	0.12
E	1.41	0.91–1.70	0.23
F	0.84	0.40–1.32	0.26

The perceptibility of pulmonary lesions is also strongly related to the minimum photographic density difference rendering an object detectable. This minimum difference has been reported for ideal experimental conditions (JACOBSON & STUART MACKAY 1958, KANAMORI 1966, JOHNS & CUNNINGHAM 1971) and has been applied in theoretical considerations concerning 'optimum' techniques for some roentgenologic procedures (HENRIKSON 1967, HEMMINGSSON & LUNDQVIST 1972).

In this report a model is presented for investigating the detectability of simulated pulmonary lesions under different experimental conditions. The model was applied in an investigation of the relation between viewing distance and the detection rate of certain defined lesions in chest films. An estimate was also obtained of the smallest density difference rendering a pulmonary structure visible under various experimental conditions simulating clinical situations.

Material

Thirty full size copies of a normal p.a. chest film of a 72-year-old woman were made on gradient 1:1, positive duplicating film (RP/DX-omat, Kodak) with an automatic copier (BXR MK II, Bluray Inc.) and a 90 s automatic processor (RP-X-omat Processor, Kodak). The original was recorded with 140 kV, 1 mm added iron filter, FFD 150 cm and focus size 1.2 mm × 1.2 mm, between intensifying screens (Saphir, Siemens) on a 35 cm × 35 cm film (Curix RP 1L, Agfa Gevaert). The film was processed automatically in 90 s (Pakorol, Agfa Gevaert).

Another set of films was obtained of one cylindrical and three conical objects of methylmethacrylate (base diameter 20 mm, thickness 5 mm, Fig. 1) on the same type of film and with the same type of intensifying screens. The exposure factors were 40 kV, 400 mA, FFD 200 cm, and the focus size 0.6 mm × 0.6 mm. No grid was used. The films were processed automatically in 90 s (Pakorol).

The four objects were placed directly on the cassette and were distributed in 30 different groups containing 0 to 4 objects. Each group was exposed for 10, 13, 16, 20 and 25 ms, yielding a total of 150 object films.

Table 2

Viewing time at the three distances

No of films	Viewing distance (m)	Viewing time (s)		
		Mean	Standard deviation	Standard error of the mean
150	0 3	15 9	3 8	0 3
150	1 0	17 8	5 4	0 4
150	3 0	19 8	3 8	0 3

across the borderline, ΔD, i e

$$P = \frac{1}{\sqrt{2\pi}} \int_{-\infty}^{(\Delta D - \mu)/\sigma} \exp\left(-\tfrac{1}{2}t^2\right) dt$$

The parameters μ and σ were estimated by weighted least squares techniques and their standard errors by correlation matrix inversion

In some cases the adequacy of the equation was tested by χ^2 tests No statistical reason for rejecting the detection probability hypothesis was found The observations were grouped according to density difference, with a class interval of 0 01 The parameter μ is the density difference yielding a 50 per cent detection probability and $\mu \pm \sigma$ the density difference yielding a 50 ± 34 per cent detection probability

Results

One chest film copy, one film of the test objects and one superposition of the two films are illustrated in Fig 2 The mean photographic density was similar (1 2–1 5) in five of the six lung areas and somewhat lower (0 8) in the remaining area (Table 1)

The density difference between object and background varied from 0 01 to 0 11 in the object films The background density varied between 0 2 and 0 4

The density gradients across the borders of the three tapered objects were found to be close copies of the tapered objects themselves i e a linear decrease in density across a distance close to 1 0 2 0 and 4 0 mm, respectively For the straight cylinder the gradient was also linear but had a width of 0 8 mm due to geometric distortion

The detectability of the objects appears in Figs 3 and 4 as a function of their density differences across the border The detectabilities of the three objects with the sharpest gradients (objects 1 2 and 3) did not differ significantly from one another for any of the three viewing distances. Object 4 was significantly more difficult to observe at all three distances Object 1 was best detected at 0 3 m, and objects 2 and 3 at 1 0 m although their detectability at 0 3 m was not significantly poorer Object 4 was better detected at 1 0 and 3 0 m than at 0 3 m The viewing time increased with the viewing distance (Table 2)

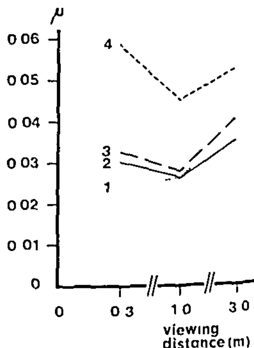


Fig 4 Density differences μ yielding a 50% detection probability for objects 1 to 4 viewed at distances of 0 3, 1 0 and 3 0 m.

Method

Thirty superposed pairs of lung and object films were placed on a viewing box (Rolloskop, Siemens-Elema) by one of the authors with radiologic training He also acted as supervisor during the viewing of the films This was carried out by the other author with radiologic experience The room was dark except for the light from the viewing box, on which areas not occupied by film pairs were covered with overexposed films The viewer knew the general set-up of the experiments and was asked to tell whether or not a ⌀ 2 cm object was present in each of the six lung areas in each film pair The viewing time was not restricted but was noted by the supervisor The 30 pairs were viewed at distances of 0 3, 1 0 and 3 0 m In total, 5 sets of 30 pairs were viewed at each of the three distances The sequence of the pairs in the sets was unknown to the viewer The different object films were randomly distributed between the sets The sets were viewed one per day at about the same hour of the day in order to reduce the influence from variability in the observer's performance

The viewing of the film pairs resulted in very few false positives (10/1800) Probit analysis (BEYER 1968) was therefore considered a more adequate technique for data reduction than the receiver's operating characteristics (GOODENOUGH et coll 1974)

The material was split into groups according to viewing distance and object tapering The detectability, P (number of detected objects divided by number of presented objects), in the groups was considered to be a function of the density difference

The visibility of objects with a wide gradient zone was less than that of objects with a narrow zone Similar results have been reported by MORGAN (1966), SHEA et coll (1970) KUNDEL et coll (1972) This indicates that image enhancement of structures with a wide gradient zone such as pulmonary lesions might be of value

All objects were detected best at 1 0 m, except object 1, which had the best detectability at 0 3 m This is in keeping with the fact that chest films of reduced size have good diagnostic accuracy (GARLAND 1950) It would also suggest that chest films should be viewed at several distances in order to achieve optimum diagnostic accuracy for lesions with different characteristics

The longer viewing time per film at longer distances was ascribed by the viewer to distraction from adjacent films

Conclusions

The model applied here with direct positive copies of chest films superposed on films of well defined objects should be relevant for perception analyses Objects with ⌀ 20 mm should have a density difference of 0 025 to 0 060 in order to be detectable on chest films In theoretical investigations of object visibility considerably smaller density difference values have been applied

The smallest visible photographic density difference is also a function of viewing distance and characteristics of object border and adjacent structures This suggests that the optimum viewing distance varies for different pulmonary lesions

SUMMARY

The detectability of 20 mm disk shaped objects on a normal chest film was investigated at viewing distances of 0 3 1 0 and 3 0 m Objects with a tapered border were found to be best perceived at longer distances The photographic density difference between object and background yielding a 50% detection probability was found to increase from 0 025 to 0 060 when the outer gradient zone of the object increased from 0 8 to 4 0 mm

ZUSAMMENFASSUNG

Die Auffindbarkeit von ⌀ 20 mm scheibenformigen Gegenstanden bei normalen Thoraxfilmen wurde bei Abbildungsabstanden von 0 3 1 0 und 3 0 m untersucht Gegenstande mit einer sich verschmalenden Kante wurden am besten bei weiten Abstanden dargestellt Die photographischen Dichte Unterschiede zwischen dem Gegenstand und dem Hintergrund bei einer 50%igen Wahrscheinlichkeit fur deren Entdeckung stieg von 0 025 auf 0 060 wenn die äussere Gradienten Zone des Gegenstandes von 0 8 auf 4 0 mm anstieg

RESUMÉ

Les auteurs ont étudie la visibilite d objets en forme de disque d un diamètre de 20 mm sur une radiographie normale du thorax à des distances d examen de 0 3 1 et 3 m Ils ont constaté que les objets à contours effiles sont mieux préçus à de plus grandes distances Ils

Table 3

Estimates of μ and σ from the probit analysis. μ is the density difference yielding a detection probability of 50 %. The detection probability increases from 16 to 84 % in the density difference interval $\mu-\sigma$ to $\mu+\sigma$. The standard errors of μ and σ were found to be in the ranges 0.003 to 0.006 and 0.002 to 0.008, respectively.

Object number	Viewing distance (m)	μ	σ
1	0.3	0.024	0.012
	1.0	0.026	0.014
	3.0	0.039	0.014
2	0.3	0.030	0.010
	1.0	0.026	0.006
	3.0	0.035	0.010
3	0.3	0.033	0.010
	1.0	0.027	0.011
	3.0	0.040	0.031
4	0.3	0.059	0.026
	1.0	0.045	0.026
	3.0	0.053	0.024

The density differences rendering the four objects visible with 50 per cent probability are given in Table 3.

Discussion

When the object films were viewed without an overlying chest film a photographic density difference of about 0.01 rendered the objects visible. This agrees well with the reports of JACOBSON & STUART MACKAY (1958), KANAMORI (1966), JOHNS & CUNNINGHAM (1971). These values have been applied in theoretical analyses of optimum radiation energy for object demonstration (HENRIKSON 1967, HEMMINGSSON & LUNDQVIST 1972).

The fact that the smallest density difference rendering the most easily perceived object detectable with 50 per cent probability was 0.025 when the chest film was superposed indicates that the effect of disturbing structures in the films may have been underestimated in the theoretical investigations (HENRIKSON, HEMMINGSSON & LUNDQVIST). The inevitable increase in background density introduced by the object films should influence the minimum detectable density difference. Data given by KANAMORI suggest this influence being small in the present case and further reduced by the concomitant decrease in the detectability of disturbing image structures. The present results of smallest detectable density differences are in good accordance with those reported by REVESZ & HAAS (1972) for the demonstration of pulmonary lesions in films transmitted by video techniques.

FROM THE DEPARTMENT OF DIAGNOSTIC RADIOLOGY III (DIRECTOR DOCENT C-G HELANDER), SAHLGRENSKA SJUKHUSET, S-411 32 GOTHENBURG, SWEDEN

RELATIVE FLOW MEASURED BY ROENTGEN VIDEODENSITOMETRY IN HYDRODYNAMIC MODEL

BO LANTZ

The use of roentgen, cine or videodensitometry for blood flow measurements in single arteries has been reported frequently during the last few years (HEINTZEN et coll, RUTISHAUSER et coll, WOOD et coll) The method facilitates measurement of flow in any unbranched vessel outlined clearly by angiography in intact, conscious man without the insertion of a sensing device (RUTISHAUSER 1971) This technique for measurement of flow utilizes the movement of radiation absorbing indicators within a vessel For calculation of flow by this method it is necessary to know the volume of the segment of the circulation in which the flow is to be measured, together with the mean transit time from a pair of indicator dilution curves recorded at the [illegible] stream [illegible]

[illegible] outlines the vessel dimensions (length and internal diameter) Comparison of the two dilution curves obtained from two different sites of a vessel can be done after calibration of the densitometer output at the sites of the measurements or by cross-correlation techniques (ROSEN & SILVERMAN 1973)

Despite the good results reported with this method, the direct measurements of the dimensions of the vessel are a large source of errors For example, an error of

Submitted for publication 16 April 1974

ont constaté que la difference de densité photographique entre l'objet et le fond donnant une probabilité de détection de 50 % augmente de 0,025 à 0,060 quand la zone externe de gradient de l'objet augmente de 0,8 à 4 mm

REFERENCES

BEYER W H Handbook of tables for probability and statistics Second edition The Chemical Rubber Co , Ohio, 1968

GARLAND L H On the reliability of roentgen survey procedures Amer J Roentgenol 44 (1950), 32

GOODENOUGH D J , ROSSMANN K and LUSTED L B Radiographic applications of receiver *operating characteristic (ROC) curves Radiology 110 (1974), 89*

HEMMINGSSON A and LUNDQVIST H Optimum photon energy in ordinary radiography of the larynx Acta radiol Diagnosis 12 (1972), 305

— JUNG B and LUNDQVIST H Soft tissue intensification in frontal roentgenography of the larynx Acta radiol Diagnosis 12 (1972), 593

HENRIKSON C O Iodine 125 as a radiation source for odontological roentgenology Acta radiol (1967) Suppl No 269

JACOBSON B and STUART MACKAY R Radiological contrast enhancing methods Advanc biol med Phys 6 (1958), 201

JOHNS H E and CUNNINGHAM J R The physics of radiology Third edition Charles C Thomas Publisher, Springfield, Illinois 1971

KANAMORI H Determination of optimum film density range for roentgenograms from visual effects Acta radiol Diagnosis 4 (1966), 463

KUNDEL H L , REVESZ G , ZISKIN M C and SHEA F J The image and its influence on quantitative radiological data Invest Radiol 7 (1972) 187

MORGAN R H Visual perception in fluoroscopy and radiography Annual oration in memory of John D Reeves, Jr, M D 1924–1964 Radiology 86 (1966), 403

NEWELL R R and GARNEAU R The threshold visibility of pulmonary shadows Radiology 56 (1951), 409

REVESZ G and HAAS C A television display of radiographic images with superimposed simulated lesions Radiology 102 (1972), 197

ROSSMAN K and MOSELEY R D Measurement of the input to radiographic imaging systems Radiology 92 (1969) 265

SHEA F J and ZISKIN M C Visual system transfer function and optimal viewing distance for radiologists Invest Radiol 7 (1972), 147

— REVESZ G , ZISKIN M C and KUNDEL H L Correlation of the frequency spectrum of a pulmonary nodule with observer detection rate Radiology 95 (1970) 443

TUDDENHAM W J The visual physiology of roentgen diagnosis Amer J Roentgenol 78 (1957), 116

— Visual search image organization and reader error in roentgen diagnosis Studies of the psychophysiology of roentgen image perception Memorial fund lecture Radiology 78 (1962) 694

— Problems of perception in chest roentgenology Facts and fallacies Radiol Clin N Amer 1 (1963) 277

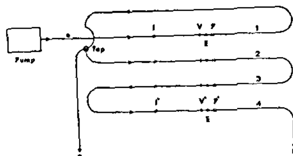


Fig. 2. Pipe system with one ma n o tlet, b, and a s de [illegible]

I^1 to V^1 60 cm
I^1 to V^2 370 cm
I^1 to V^3 540 cm
I^1 to V^4 = 750 cm
I^2 to V^2 = 50 cm
I^3 to V^3 = 50 cm
I^4 to V^4 = 50 cm

model experiments However, some basic principles about flow in general can only be evaluated in a stable hydrodynamic model where different parameters can be examined one by one, by changing the standard conditions of the model

Set up for hydrodynamic flow measurements

The hydrodynamic model for analysing the dispersion of injected contrast medium and propagation of the bolus throughout a pulsative flow system is illustrated in F [illegible]

The hydrodynamic system was arranged for non recirculating pulsative flow where the temperature of the fluid was regulated by a thermostat (1) before entering a cistern with a constant fluid level (2) The flow through the main pipe (4) was delivered by a pulsative pump (3) Varying amounts of fluid could be directed through the side pipe (5), and the peripheral resistance in the system could be altered at the end of the pipes (6, 7) The absolute amount of flow per unit time was measured volumetrically (8, 9) Contrast medium was injected into the main flow through catheters with occluded tip and side holes by pressure injectors (10, 11) The main pipe (4) passed through the radiation beam between the roentgen tube (12) and the image intensifier (15) along with copper f [illegible] urements were [illegible] and recorded o [illegible] illustrated in th [illegible] the oscilloscope (18) the latter controlling the optimal level of the video signal

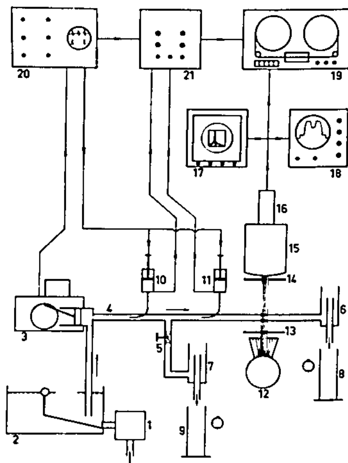


Fig ... electronic
equip ... cistern 3
Pulsa ... resistance
8 anc ... tion filter
14 D ... tube 18
Oscil

1 mm in measuring the diameter of a vessel with actual diameter of 4 mm will give an error in the area and flow estimates in the range of 44 to 56 per cent

The aim of the present work is to present another approach to measuring peripheral flow by roentgen videodensitometry, not in absolute but in relative units By injecting contrast media at two different sites of a circulatory system and comparing the dilution curves at one cross section of a vessel distally to the injection sites, the flows at the sites of the two injections may be estimated The dimensions of the vessel at the site of measurement do not have to be taken into consideration

In the present investigation, flow measurements have been made by a logarithmated videodensitometer in a hydrodynamic model to determine some basic properties of the behaviour of injected contrast media in pulsative flow, fundamental for the understanding of estimating relative flow It is always a simplification and often highly precarious to draw conclusions about hemodynamics out of hydrodynamic

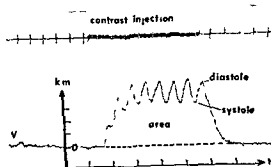


Fig 4 Videodensitometric recording at a cross section of the main pipe just distally to the injection site where 40 ml Isopaque Cerebral was injected. The amplitudes of the densitometer output correspond to the mass, *m*, of the contrast medium in the sampling area during the time Δt

within a distance of 1 5 cm close to the tip of the catheter also ensured good mixing of the injected medium with the fluid

Isopaque cerebral, 280 mg iodine/ml (Nyegaard), was used as contrast medium The measurements were performed at 20–22°C where the viscosity of the medium is 6 9 centipoise according to the manufacturer

Two pressure injectors were used, Cisal II and Gidlund, both manufactured by Elema Schonander, during experiments with only one pressure injector Cisal II only The stated delivery according to the dial of the two injectors agreed well with measurements in open vessels Since the catheters were filled with contrast medium before connecting them to the injectors, no account had to be taken of the volume of medium within the catheters Impulses from a switch attached to the crank web of the pump, simulating the R wave of the ECG, were fed to a heart-phase correlator (Nycotron) for the automatic start of injection

Roentgen equipment and device for storing of information The investigation was carried out with standard roentgenologic equipment (Apparatus Triplex Angiomatic 1023-2 CE, Elema-Schönander, Tube Bi 150/30/50 R, Siemens, Image Intensifier Tube Sirecon 25/15, Siemens, Vidicon Television Chain, Videomed I, Siemens, Videotape recorder deOude Delft, OD-X 40)

The image information, signals from the pulsating pump and from the pressure injections were all stored on video tape The videotape recorder had only one audio channel For that reason, the signals from the pump (transmitted through the heart-phase correlator) and the injectors were both multiplexed on a frequency modulator before entering the audio channel of the recorder

Equipment for recording and replaying of information After the experiments the stored information on the tape could be replayed multiple times (Fig 3) From the tape recorder (1) the signals from the audio channel of the tape were transmitted over the FM demodulator (6) to a multi-channel strip-chart recorder (Mingograf 800, Elema Schonander) marked (7) in the figure The image information of the tape was transmitted to the videodensitometer (2) which measured the density changes in a

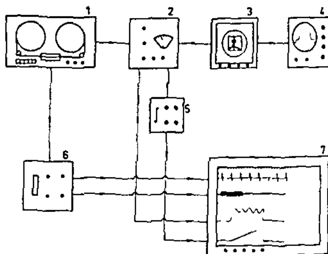


Fig 3 Equipment for recording and replaying of information 1 Video tape recorder 2 Videodensitometer 3 Television display tube 4 Oscilloscope 5 Integrator 6 FM demodulator 7 Multichannel strip-chart recorder

Signals from the cyclic movement of the pump were transmitted to a heart-phase correlator (20) triggering the pressure injectors These signals, together with the signals from the injectors were transmitted to the audio channel of the tape over a frequency modulator (21) Thus during the investigations, all the information was stored on the videotape

The hydrodynamic system A dosing pump (DT-300/10, Wretman & Soner, capacity of 3 500–8 000 ml/min) was used The pump had double ball valves on both suction and discharge The discharge was controlled by adjusting the stroke length by a screw on the crank web The pump, operating at a constant rate of 106 strokes per minute, gave a constant delivery directly proportional to the stroke length independent of discharge pressure The outlet of the pump was connected to transparent elastic pipe (Montecatini Edison) with outer and inner diameters of 12 and 10 mm and a length of approximately 15 m (Fig 2) A tap was placed about 3 m from the pump to permit an arbitrary amount of fluid to leave the main pipe through a side pipe At different distances from the pump, four different catheters with side holes and occluded tip were inserted into the flow representing different injection sites (I^{1-4})

Just distally to the radiation field (videodensitometric measurement points V^{1-4}), electromagnetic cannular flow transducers (E^{1-4}) (Biotronex BL310) were attached as well as intravascular pressure transducers (P^{1-4}) (Statham) The absolute amounts of flow in the main pipe and the side pipe were estimated volumetrically by repeated sampling of the outlet for 5 minutes

Pressure injections of iodine contrast medium Grey Kifa catheters with four side holes and occluded tip were inserted into the flow system through the pipe wall with the tip opposite to the flow at different sites of the model This arrangement was done in order to decrease the extension of the contrast bolus The four side holes, spread

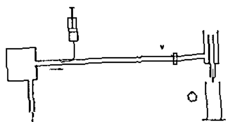


Fig 5 Model arrangement in experimental series 1

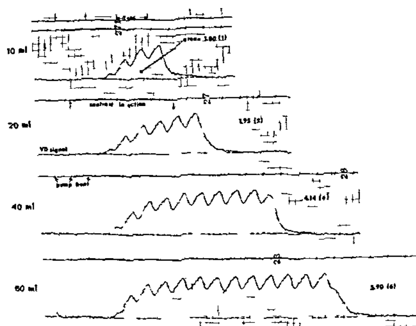


Fig. 6 Videodensitometric recordings obtained at the same site 60 cm distally to pressure injections of 10 20 40 and 60 ml Isopaque Cerebral The integrated area had the proportions 1 00 1 95 4 14 and 5 90 respectively (see numbers next to the corresponding curves)

The integrated area A will then be

$$A = k \int_0^t m \mathrm{d}t \tag{2}$$

Integration of the videodensogram Integration was performed by planimetry using the mean value of three repeated measurements The results were controlled with an electronic integrator, but disturbances of the integrator output occasionally made its results unreliable In some cases the integral was calculated by weighing the cut out curves on a micro balance but that method was time consuming and no more reliable than planimetry

selected area of the image The signals representing the mass time curves from the videodensitometer output were integrated by an electronic integrator (5) (GRANDIN & HARTIKAINEN) The output of the integrator was presented on the stripchart recorder together with the output of the videodensitometer Zero position of the integrator occurred automatically when the signal was below the value where the integration started The magnitude of the integration was represented by the vertical change of the integrator curve The television monitor (3) was used for placing the electronic window in proper position over the area of interest The oscilloscope (4) was used to control the video signal

Recording technique and measurements of the densitometer output

The videodensitometer was logarithmated in order to get a linear response of density changes in the object in the radiation field (STRID & LANTZ 1973, LANTZ & STRID 1973) The measurements were carried out with a fine-focus tube with a rhenium anticathode and an image intensifier with 15 cm entrance screen diameter during fluoroscopy with constant potential and current (usually 70 kV and 0 9 mA) The radiation was filtered only by 0 6 mm Cu The four main loops of the pipe system were arranged parallel and 5 mm apart in the center of a radiation field of about 2 cm × 6 cm Thus, the flow in four loops was video taped at the same time and in the same field The luminance of the Vidicon was adjusted before the measurement by means of the cathode-ray oscilloscope to yield optimal black and white levels in the video signal

During replaying of the tape recording the size of the sampling window of the videodensitometer was a constant rectangle, corresponding to an area in the object plane of 5 mm × 15 mm By moving the densitometer window to cover each of the main loops at a time (V^1–V^4), it was possible to compare the dilution curves and the flow profile at different distances from the injection site

Videodensogram A videodensitometric recording is illustrated in Fig 4 during dynamic conditions in the flow model with the densitometer window placed over a cross section of the main pipe just distally to the injection point where 40 ml Isopaque Cerebral had been injected The amplitude of the densitometer output, V, can be written (LANTZ & STRID)

$$V = km, \tag{1}$$

where m is the total mass of contrast medium within the sample volume The constant, k, accounts for dependence on the effective mass extinction coefficient, the conversion factor of the image intensifier, the transfer function of the television system, the intensity of incident radiation, and the gains of the densitometer and chart recorder

The recording of the densitometer output, i e , the videodensogram, represents the mass time curve of the iodine medium passing the measurement site

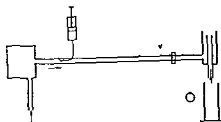


Fig. 5 Model arrangement in experimental series 1

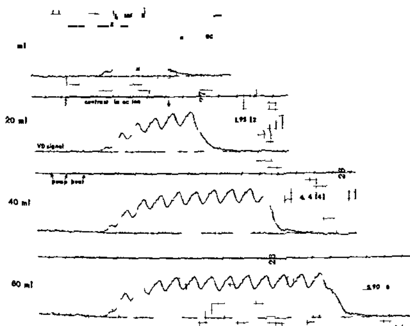


Fig. 6 Videodensitometric recordings obtained at the same site 60 cm distally to pressure injections of 10 20 40 and 60 ml Isopaque Cerebral The integrated area had the proportions 1.00 1.95 4.14 and 5.90 respectively (see numbers next to the corresponding curves)

The integrated area A will then be

$$A = k \int_0^t m \mathrm{d}t \tag{2}$$

Integration of the videodensogram Integration was performed by planimetry using the mean value of three repeated measurements The results were controlled with an electronic integrator but disturbances of the integrator output occasionally made its results unreliable In some cases the integral was calculated by weighing the cut out curves on a micro balance but that method was time consuming and no more reliable than planimetry

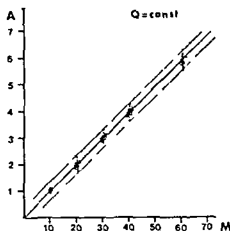


Fig 7

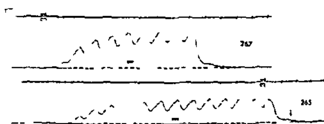


Fig 8

Fig 7 Comparison of the amount of injected contrast medium and the integrated densitometric area $y = -0.04 + 0.10x$ is the equation for the linear regression line, $\hat{\sigma}_{y.x}$ is the unbiased standard error (SE) of estimate of y on x, n is [illegible] correlation coefficient The dashed lines represent [illegible] from the regression line is equal to 2 [illegible]

Fig 8 Sixty ml of contrast medium injected in the same flow with different speeds No significant difference was noted between the integrated area for fast speed (top, 267) and slow (bottom, 265)

Results

In order to empirically establish the relationship between the integrated area, A, the constant pulsative flow, Q (volume/unit of time), and the total amount of injected contrast medium, M, seven series of experiments were performed on the hydrodynamic model

(1) *Integrated area, A, as a function of the injected amount of contrast medium, M* Different amounts (10, 20, 30, 40 and 60 ml) of the medium were injected through the catheter and the densitometric measurements were made at a constant distance from the injection site (Fig 5) Since no side pipe was connected between injection and measurement sites, the flow was equal at the two points and the total injected amount of medium, M, also passed the measurement site Fig 6 demonstrates the records from one series and the reproducibility of 103 measurements is illustrated in Fig 7 As could be expected, the integrated area was directly proportional to the injected amount of medium ($r = 0.9957$) A stable pulsative flow was established throughout the pipe system before injection was performed

Thus

$$A = \lambda M, \quad (3)$$

λ being a constant

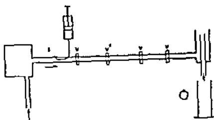


Fig 9

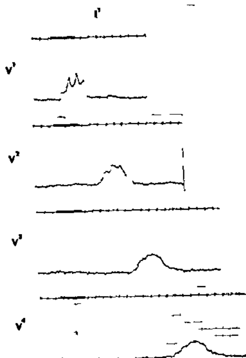


Fig 10

Fig 9 Model arrangement in experimental series 3

Fig 10 …

observed

(2) *Integrated area A, in relation to speed of injection* By using the same procedure as described, but altering the speed of injection for the same amount of medium, it was established that the speed of injection did not alter the measured area Recordings from pressure injections of different speeds are illustrated in Fig 8 Two series ($n=15$) were compared after injecting the same amount of contrast medium at two different speeds, maintaining constant flow in the pipe system No significant alteration of the integrated areas was obtained ($t_{29}=0.0082$, $p>0.10$)

(3) *Distance between injection and measuring site* A constant pulsative flow was established throughout the pipe system One series of injections was performed (n 16) at the same site By replaying the tape and moving the videodensitometer window videodensograms could be obtained at the distance of 60, 370, 540 and 750 cm respectively from the injection site (Fig 9) Recordings from one of the measurements are illustrated in Fig 10 Comparison of the integrated areas *A* obtained at a distance of 60 cm and 750 cm from injection point revealed no significant difference (t_{30} 0.0402, $p>0.10$)

(4) *Diameter of the pipe at the site of the injection* Two series were made ($n=16$) by injecting the same amount of contrast medium in pipes with a diameter of 10 mm

Fig 11 Model arrangement in experimental series 4

Fig 12 Model arrangement in experimental series 5

a

b

and 20 mm respectively (Fig 11) Comparison of the two series did not show any significant difference (t_{30} – 0 0070, p≫0 10)

(5) *Integrated area, A, as a function of the flow, Q at the site of injection* A constant pulsative flow was established throughout the pipe system (Fig 12) With the tap

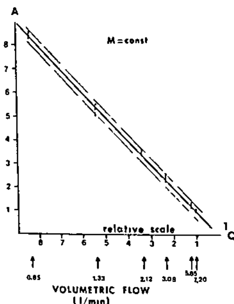


Fig 14 A comparison of the relationship between the flow (Q) and the integrated area (A) after injection of the same amount of contrast medium The horizontal axis is labelled in reciprocal flow units (1/Q) relative to the maximum flow (7 2 l min) used during the procedure $y = 0\ 04 + 0\ 98x$ $\sigma_{y,x} = 0\ 12$ $n = 24$ $r(\log Q/A) = -0\ 9989$ $r(1/Q, A) = 0\ 9989$ (For other symbols in the figure, see Fig 7)

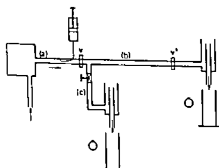


Fig 15 Model arrangement in experimental series 6

open for outlet through the side pipe, the flow could be altered at the measuring site Injections of the same amount of medium by the injector distally to the side pipe into different flows in the main pipe, are illustrated in Fig 13 Forty four measurements were made in flows of the main pipe ranging from 0 85 l/min to 7 2 l/min The results, graphically presented in Fig 14, show that the integrated area, A, is inversely proportional to the flow, Q

$$A = k\frac{1}{Q} \tag{4}$$

Q being the mean flow in the pipe at the site of the contrast injection

(6) *Outlet of contrast medium between injection and measurement sites* By injecting contrast medium proximally to the side pipe, the dilution curves were measured be-

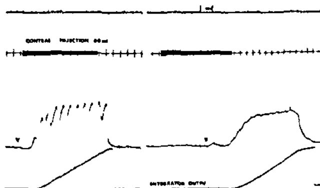


Fig 16 Videodensitometric recordings in a cross section of the main pipe a) before and b) after outlet of about 50 % of the mixture contrast medium fluid through the side pipe Distance between measurement points was 690 cm

fore and after the outlet for varying amounts of contrast mixed flow (Fig 15) Two series (n = 16) were compared No significant difference in measured area, A, between the two series was obtained ($t_{30} = 0\ 2384$, $p > 0\ 10$) Recordings from the experiments are illustrated in Fig 16 Thus the integrated area, A, is a function of flow and the mixing of contrast medium and fluid at the site of injection and is not dependent on the absolute amount of medium passing the measurement site Combining equations (3) and (4) gives

$$A = k \frac{M}{Q} \tag{5}$$

The integrated area, A, is thus directly proportional to the amount of medium, M, and inversely proportional to the flow, Q, at the site of injection The videodensogram, measured over a certain cross-section of a pipe, does not depend on the distance from the injection points or the speed of injection, nor does the size of the cross section of the pipe at the injection point alter the integrated area

(7) *Relative flow* If two different injections are made with known amounts of medium at two different locations of a flow system and the measurement is performed at the same site distally to the injection points (Fig 17), the flows in the two locations can be compared and the relative flow estimated as indicated below With

$$A^1 = k \times \frac{M^1}{Q^1} \quad \text{and} \quad A^2 = k \times \frac{M^2}{Q^2},$$

the relative areas expressed in terms of flows are

$$\frac{A^1}{A^2} = \frac{M^1 \times Q^2}{M^2 \times Q^1}$$

and relative flows, in terms of areas are

$$\frac{Q^1}{Q^2} = \frac{M^1 \times A^2}{M^2 \times A^1} \tag{6}$$

Relative flow measured by videodensitometric and volumetric methods is compared in Fig 18 Volumes of contrast medium ranging from 10 to 60 ml were injected at

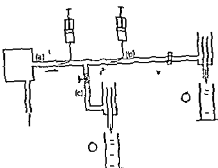
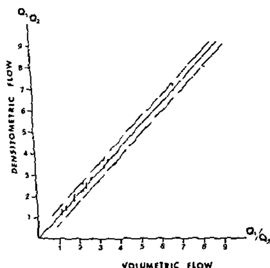


Fig 17 Model arrangement in experimental series 7



[illegible]

the same [illegible]
rang[illegible]
to b[illegible] accurate (r = 0 9971) Recordings from a series of the measurements are illustrated in Fig 19 (c, d) Relative flow can be measured after injection in two different pipe locations at two different times or at the same time If the distance between the injection points is short, the two injected boli can mix By repeating the two injections and changing the injected amount of contrast medium at one point, a correct estimation can still be obtained (Fig 19 a, b)

Discussion and Conclusions

The present series of experiments showed a very simple relationship between the integrated densitometric area, the amount of injected contrast medium and the flow

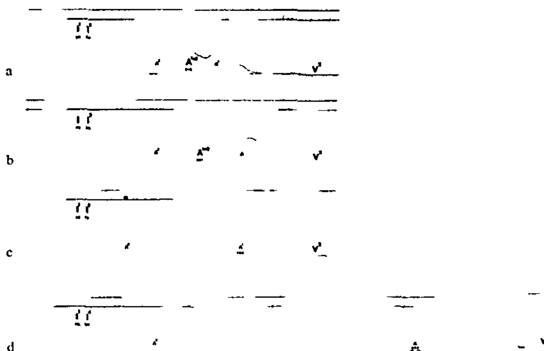


Fig 19 Estimation of relative flow by injection of two boli at the same time but into two different ... site distally in the ... were mixed at the ... mount of contrast ... an error of 0 6% ... at I^2 the two bol ... d measuring at V^4 ... on with volumetric ... min

$$A(A^1 + A^2) = \frac{M^1}{Q} + \frac{M^2}{Q^2} \qquad A_{diff} = \frac{M_{diff}}{Q} \qquad A_b \quad A_a = \frac{M_b^1 \quad M_a}{Q}$$

			error (%)
	2 701	(measured)	
Q^1	2 718	a b	0 6
Q^2	2 722	c	0 8
	2 721	d	0 7

at the site of the injection On condition that the measurements are performed at one site of a circulatory system where the background density is constant the results are highly accurate No calibration of the detector system is required nor are any direct measurements of the segment of the vessel on film or on television image which would be needed when estimating flow in absolute units by videodensitometry (RUTISHAUSER 1971 ROSEN & SILBERSTEIN 1973)

It is important to emphasize that the videodensogram is a linear mass time curve measuring the temporal rate of change of contrast medium mass and in that way differs from the indicator dilution curve which measures the temporal rate of change of concentration Neither of these methods measures the absolute amount of contrast

medium passing the sampling area The videodensitometer registers the amount of medium in the cross-section as a function of time This is well illustrated in the experiments presented in series 6, where different amounts of medium passing the two sampling sites give the same integrated videodensogram

By estimating relative flow with the presented method, it is also important that the measurements are performed at the same site if repeated injections are made If the background density or the mean cross-section area at the measurement site is changed, a correlation between the two sites must be performed by calibration of the densitometer output

The measurements revealed that the injected contrast bolus was propagated throughout the entire pipe system with almost the same speed as the fluid However, the pulsative profile gradually disappeared with increasing distance from the site of the injection (Figs 10, 16) A slight spreading out of the bolus was observed at great distances from the injection point

The necessary conditions for obtaining a useful and accurate measurement of relative flow are as follows

(a) After injection at two different circulation sites, the densitometric measurement should be performed at the same site without changing any conditions concerning the constant, k, (see explanation to equation 1),

(b) The background density during the densitometric recording must be unchanged,

(c) Oscilloscopic control of the video signals is necessary so that the maximal extinction caused by the contrast medium at the sampling site will not exceed the range of linearity of the densitometer or reach the dark current level of the video signal,

(d) The mean flow in the pipe or vessel should be constant and not change in the time interval between injection and measurement

(e) Good mixing of the contrast medium with the flow at the site of the injection, is necessary

SUMMARY

The behaviour of injected iodine contrast m[illegible]
was recorded on videotape in televi[illegible]
metry By a simple relationship be[illegible]
injected contrast medium, and the flow at the site of the injection, it was possible to compare the flow in two different cross sections of the circulatory system with high accuracy

ZUSAMMENFASSUNG

Das Verhalten injizierten Jod-Kontrastmittels in ein pulsierendes hydrodynamisches Modell wurde bei der Bildverstarkerdurchleuchtung auf einem Verstärkertape registriert und durch Rontgenverstärker-Densiotometrie gemessen Aus einer einfachen Beziehung zwischen dem integrierten densitometrischen Gebiet, der Menge des injizierten Kontrast

mittels und dem Fluss an der Stelle der Injektion war es moglich, die Durchstromung an zwei verschiedenen Querschnitten des Zirkulationssystems mit hoher Genauigkeit zu ver gleichen

RÉSUMÉ

Le comportement d un moyen de contraste iodé injecté dans un modèle hydrodynamique pulsatile a ete enregistré sur magnétoscope en radioscopie télevisee et a eté mesure par videodensitometrie roentgen Grâce à une simple relation entre la surface densitométrique integrée, la quantité de moyen de contraste injectée et le debit au lieu de l injection, il a ete possible de comparer le débit dans deux sections transversales differentes du système circulatoire avec une grande precision

REFERENCES

BURSCH J, JOHS R, KIRBACH H, SCHNURER C and HEINTZEN P Accuracy of videodensitometric flow measurement *In* Roentgen-, cine- and videodensitometry Fundamentals and applications for blood flow and heart volume determination Edited by P H Heintzen Georg Thieme Verlag, Stuttgart, 1971

HEINTZEN P, BURSCH J, OSYPKA P und MOLDENHAUER K Rontgenologische Kontrast mittelmessungen zur Untersuchung der Herz- und Kreislauffunktion Elektromedizin 12 (1967), 82 und 145

— OSYPKA P and BURSCH J New techniques for functional studies in radiology and cardiology Ann Radiol 12 (1969), 425

LANTZ B and STRID K G Contrast formation in fluoroscopic videodensitometry II A comparison between theoretically computed and experimentally measured contrast Acta radiol Diagnosis 14 (1973), 625

ROSEN L and SILVERMAN R Videodensitometric measurements of blood flow using cross correlation techniques Radiology 109 (1973), 305

RUTISHAUSER W Kreislaufanalyse mittels Rontgendensitometrie *Verlag Hans Huber*, Bern, 1969

— Application of roentgen densitometry to blood flow measurement in models animals and in intact conscious man *In* Roentgen-, cine- and videodensitometry Fundamentals *and applications for blood flow and heart volume determination* Edited by P H Heintzen Georg Thieme Verlag, Stuttgart, 1971

— NOSEDA G, BUSSMANN W D and PRETER B Blood flow measurement through single coronary arteries by roentgen densitometry II Right coronary artery flow in conscious man Amer J Roentgenol 109 (1970), 21

— BUSSMANN W D, NOSEDA G, MEIER W and WELLAUER J Blood flow measurement through single coronary arteries by roentgen densitometry I A comparison of flow measured by a radiologic technique applicable in the intact organism and by electro [illegible]

— [illegible] roentgen [illegible] Circula-

SMITH H, FRYE R, DAVIS G, DANIELSON G, PLUTH J, WALLACE R, STURM R and WOOD [illegible] of flow in aorta-coronary saphenous vein grafts by roentgen videodensi[illegible]

— — [illegible] WOOD E Roentgen videodensito

metric measurement of coronary blood flow Determination from simultaneous indicator-dilution curves at selected sites in the coronary circulation and in coronary artery-saphenous vein grafts Mayo Clin Proc 46 (1971), 800

STRID K-G and LANTZ B Contrast formation in fluoroscopic videodensitometry I A mathematical model for optimising contrast in radiography Acta radiol Diagnosis 14 (1973), 395

WOOD E H and STURM R E Use of videometry and electronic data processing for hemo dynamic investigations by angiographic techniques *In* Pathophysiology of congenital heart disease Edited by P H Adams H J C Swan and V E Hall University of California Press, Los Angeles, 1970

— — and SANDERS J J Data processing in cardiovascular physiology with particular reference to roentgen videodensitometry Mayo Clin Proc 39 (1964) 849

FROM THE DEPARTMENT OF DIAGNOSTIC RADIOLOGY III (DIRECTOR C G HELANDER), SAHLGRENSKA SJUKHUSET, S 411 32 GOTHENBURG, SWEDEN

INFLUENCE OF SECONDARY RADIATION ON IMAGE QUALITY

K SELIN, E DEICHGRABER and S REICHMANN

Secondary radiation is generally considered to have a detrimental influence on image quality owing to its creating a background fog in the image, this in turn leading to reduction of contrast It might appear possible to calculate the amount of contrast reduction from the intensities of primary and secondary radiation so as to determine the exact influence of the latter However, such calculations do not give true information It has been known for some years that different recording media may be affected in different ways by the same amount of secondary radiation KOSSEL (1967 a) reported that in xeroradiography with selenium plates the effects of secondary radiation was much less detrimental than in radiography with film The Rank Xerox Corporation generally recommends that xeroradiography of the skull and extremities should be performed at 120 kV without any type of secondary screening a technique that gives so much secondary radiation as to make film radiography pointless The present report will suggest a possible mechanism underlying the difference between the two types of recording medium

Experiments

Initially xeroradiographic selenium plates (Rank Xerox Ltd) were compared with an industrial non screen film with nearly the same sensitivity, Agfa Gevaert Mamoray

Submitted for publication 20 December 1974

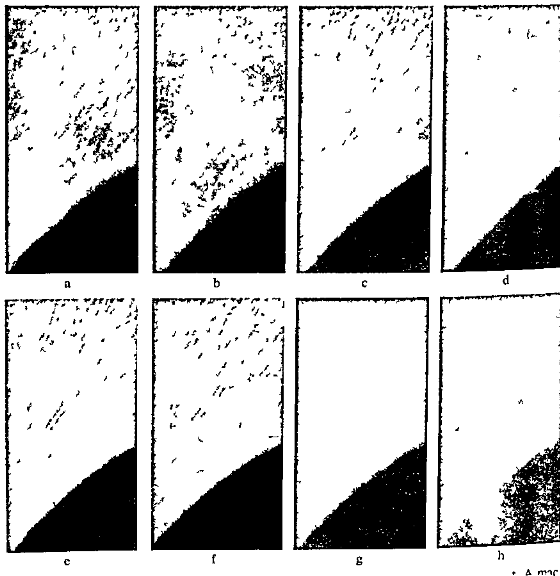
T 3 processed as described by DEICHGRÄBER et coll (1974) Two phantoms were depicted, containing nylon wires of the same dimensions, ranging from 0 25 to 1 0 mm immersed in vegetable oil The oil layer was 3 cm in one phantom and 7 cm in the other On the tube side of the phantoms a small piece of lead screened off the primary radiation so that the fogging appearing in the corresponding film area would reflect the amount of secondary radiation generated within the oil The signals created by the wires within the oil were very weak, for this reason the initial comparison was made at a tube potential of 26 kV and a total filtration of 0 5 mm Al Different mAs settings were tried so that both film and xerox plate were optimally exposed No secondary screening existed

As was expected, the thick phantom gave rise to a higher intensity of secondary radiation In the film images 4 wires (minimum 0 35 mm) were perceptible in the thin phantom while 3 wires only (minimum 0 5 mm) were visible in the thick one In the xeroradiographic images all 5 wires (minimum 0 25 mm) were discernible in both phantoms The finest wire was just barely perceptible in both images so that the impression was obtained that the difference in secondary radiation was unimportant in xeroradiography

As a second step the tube potential was increased Recording in both media was performed at 33 and 40 kV The film recordings at 40 kV were considerably impaired as compared with 26 kV so that 3 wires (minimum 0 5 mm) and 2 wires (minimum 0 75 mm) could be detected in the two phantoms In the xeroradiographic images 4 wires were perceptible in both phantoms (minimum 0 35 mm) For the latter medium the tube potential was further increased to 60, 80 and 110 kV The 60 kV xeroradiographic image of the thin phantom was considered to give the same information as did the 26 kV radiographic film For the thick phantom the 80 kV xeroradiographic image corresponded to the 26 kV roentgenogram

The test described apparently confirmed the view that secondary radiation exerts much less influence in xeroradiography than in direct film radiography It might be assumed that the peculiar edge contrast enhancement function of the xerox medium would explain the difference (SCHERTEL et coll 1974) Since signal appearance or non appearance in an image is rarely a matter of absolute contrasts but rather of the signal noise ratio, an attempt was made to find out if secondary radiation also has varying effects on different films developed to identical contrast

The Mamoray T 3 film was compared with Agfa-Gevaert Curix RP 1 film Both were exposed without intensifying screens and were developed to identical contrast, as checked by means of a small step-wedge included in each image Since directly exposed films tend to give a certain average number of developable silver halide grains for each roentgen photon absorbed (CHRISTENSEN et coll 1972), identical contrasts were obtained in both films by means of standard machine development Thus neither of the films was unfavourably developed to adapt its contrast to that of the other The silver content of the Mamoray film is about 2 5 times that of the Curix (data from the manufacturer) This implies that the Mamoray film will absorb



a b c d

e f g h

• A mac

is then better neutralised in e tha but
and b, and the same amount of ned
not in h owing to the larger nun
to the same density to facilitate printing and inspection

more photons from a given roentgen dose The grain size of this film is considerably smaller, as checked in a microscope For this reason the sensitivity of the films differed but little, the dose given to the Mamoray film was 80 per cent of that given to the Curix A further difference concerns the total number of silver halide grains

Since there is more silver in smaller grains in the Mamoray film, there is thus a considerable difference to the advantage of this film

The phantoms used in the first experiment could not be employed, since they were too poorly depicted on the Curix film even at low tube potentials Instead a macerated femur surrounded by air was used Tube potential was 120 kV, filtration 1 2 mm Cu, there being no secondary screening The object could be expected to give rise to slight secondary radiation only The femur was positioned in such a way that the film could be placed above or below without the femur being moved First, one image on each film was obtained without any measures being taken to introduce secondary radiation (Fig 1 a, b) There was a clear difference in image quality, the Mamoray film yielding more information Close inspection revealed a more granular background in the Curix film, apparently reflecting a higher level of quantum mottle This mottle was to be expected since the larger grains of this film will make use of a low number of roentgen photons

The second step implied the introduction of fogging radiation (Fig 1 c, d) The original roentgen dose was split into two equal fractions, the film being placed on the tube side of the object during one of the two exposures Thus, a condition of equal amounts of primary and secondary radiation was simulated With this technique two films of each kind were exposed A considerable impairment of image quality ensued for both film types By mere inspection it could not be decided whether the loss of information was greater in the one or the other of the films However, when the two films of each kind were exactly superimposed on each other, the decision was easy (Fig 1 e, f) In the Mamoray film the original image quality was practically restored, whereas in the Curix film this was not the case The latter film thus lost proportionally more of its information from a given dose of fogging radiation

When two films were used and superimposed on each other the same number of primary roentgen photons were absorbed as in the original image, where no secondary radiation was added As a final step, one image on each film was obtained in which the primary roentgen dose was the same as in the original image (i e Fig 1 a, b), on top of this dose an equal amount of fogging radiation was added (Fig 1 g, h) The density thus became higher in these images than in the other ones In the Mamoray film, again, an image was obtained where the loss of information was small In the Curix film there was evident loss of information

Discussion

The number of silver halide grains per unit area differed in the two films in the last series of experiments, the Mamoray film having more grains than the Curix film If either of these films is struck only by image forming primary radiation—as in the first type of exposure—all grains will participate in the formation of the image If secondary radiation is added in such a way that the total number of photons

remains unchanged, the information content of the image must suffer from the loss of informative primary photons. One might expect that if the number of image-forming photons could be restored to the original level, the same information would be obtained even in the presence of secondary radiation, the number of primary photons determining the amount of information. However, this was demonstrated to be wrong, especially as regards the Curix film (Fig. 1 b, f, h). Since the contrasts of Figs. 1 b and f were the same, the contrast can be disregarded. Instead, it appears that the limited number of grains may be the important factor.

Let it be assumed that the total number of unexposed silver halide grains does not greatly exceed the quantity necessary for an image of ordinary density. The very high silver prices and the urge towards short processing times make this assumption realistic for the Curix film, which is designed for 90 s development. Since the number of available grains is small, the primary and secondary photons will in fact compete, so that if a primary photon 'comes first' to a certain grain the blackening in this point will reflect the attenuation properties of the object. If the secondary photon is absorbed before the primary one, the grain in question will be unavailable for image formation. Thus, the secondary radiation may be expected to reduce the number of silver halide grains which may form the image. If the total number of grains is many times greater than is necessary for a properly exposed image, this reduction will be relatively harmless. There will still remain grains enough for the image, the competition between primary and secondary photons then being low. This state was approached in the Mamoray film, where so many grains were present as to allow the secondary radiation to be added to the primary without large losses of information (Fig. 1 g).

The primary radiation is unevenly distributed over the film surface, in correspondence with the attenuation differences of the object forming the diagnostic signals. The secondary radiation may be considered evenly distributed. This means that competition between the two kinds of radiation varies from point to point of the image. Where primary radiation intensity is low—i.e. in the bright areas of the image—the secondary radiation will determine the image density far more *than in the* dark areas. If the number of grains had been practically unlimited, the effect of secondary radiation would have been a uniform increase in the density of the image. Such uniform densities are harmless since they may be easily compensated for by increased illumination. However, common experience indicates that increased illumination seldom eliminates the influence of secondary radiation. The varying competition that makes the influence of the secondary radiation predominate in bright image areas, *in fact makes the secondary radiation constitute* an 'anti-signal' especially adapted to remove or reduce the desired image information. This anti-signal function can only be reduced by increasing the available number of silver halide grains to amounts far exceeding that required for proper blackening.

Only films exposed to direct roentgen irradiation have been discussed. In screen-film radiography the situation is more complex. Here the number of crystals in the

screens may be of the same importance as the number of silver halide grains Furthermore, a silver halide grain is not made developable by the influence of one light photon (CHRISTENSEN et coll 1972) and so primary and secondary photons may even cooperate in making many grains developable The unsharpness introduced by the screens makes it difficult to observe directly what effects result from the different kinds of radiation Experiments of the same kind as in Fig 1 were carried out, using intensifying screens, but many factors could not be changed separately, so that their influence could not be established The amount of silver halide grains could not be varied within wide limits, keeping the sensitivity constant, the number of screen crystals could not be changed without using different brands of screens with different unsharpness and mottle characteristics etc This does not imply that the same type of photon competition for a limited number of receptors—be it screen crystals, silver halide grains, or both—does not occur in screen film radiography The fact that increased illumination cannot eliminate the influence of secondary radiation in clinical roentgenograms, regardless of mean image density, makes it probable that competition and anti signal formation may be in operation in screen film radiography

Electroradiographic recording media appear to be of importance in many clinical examinations within a decade (BOAG 1973, JOHNS et coll 1974) The Rank Xerox selenium plates are already commerically available and similar techniques, using compressed xenon gas instead of selenium, may offer a solution to the troublesome sensitivity problem of traditional xeroadiography (JOHNS et coll) Since the sensitivity of selenium plates is low, a good deal of the current interest in xeroradiography has concerned soft tissue radiography notably of the breast (GOULD et coll 1960, RUZICKA et coll 1965, KOSSEL 1967 b, O MARA et coll 1967, WOLFE 1968, BOAG et coll 1972, FISCHEDICK & EVERS 1973), where films of low sensitivity are commonly used In the phantom experiments presented here the selenium plates were compared with a non screen film which was previously found to be the best with respect to sensitivity and silver content for breast radiography (DEICHGRÄBER et coll 1974) The present results indicate that even if the Mamoray film is far less affected by secondary radiation than the Curix film, the selenium plates are still markedly more independent in this respect, making higher tube potentials useful

In the amorphous selenium of a xeroradiographic plate the interaction between a roentgen photon and the absorbing matter concerns only one selenium atom This atom changes into a state of two 'carriers' a positive hole and a negative electron (BOAG 1973) These carriers will contribute to a local reduction of the electrostatic charge applied over the selenium layer before the exposure This charge is large in relation to the eliminating capacity of one pair of carriers resulting from one photon The fact that one roentgen photon exerts a limited influence on the total charge is reflected in the wide exposure latitude of the xerox plate

The latent image of the xerox plate—i e the electrostatic charge pattern existing before powder development—is very similar to such non screen films as are mini-

mally influenced by secondary radiation, for instance the Mamoray film used in the present experiments The similarity consists in an overcapacity, having the effect that the number of roentgen photons forming an ordinary image is far from exhausting the total capacity for reception and storage of information Thus, it seems probable that competition between primary and secondary photons will be minimal in the xerox plate It is proposed that such a low level of competition explains the remarkable ability of the xerox plate to resist the detrimental effects of secondary radiation

In passing it should be noted that the number of powder grains used in the electrostatic development is not to be compared with the number of silver halide grains in the film The reason for this lies in the contrast levelling and edge contrast enhancement of the xerox plate The powder grains only indicate the location of abrupt charge changes in the latent electrostatic image

When the limit of the storage capacity of a recording medium is being approached, different roentgen photons may be expected to compete for the remaining receptor units Competition between primary and secondary photons exists, but it appears equally plausible that primary photons will compete with each other In another report (SELIN & REICHMANN to be published) it will be demonstrated that this mechanism may be operative in screen-film radiography This type of competition will, to an especially high degree, impair the recording of weak signals having a high spatial frequency The ability of the xerox plate to record this type os signal at much higher tube potentials than can be used even with non-screen industrial film probably reflects a low level of competition not only between primary and secondary photons but also between different primary photons

The generally accepted way of describing the functional capacity of a recording medium is based on the 'modulation transfer function' (MTF) For this function to be valid the response of the recording medium should be linear, since it is only under such conditions that a Fourier analysis is accurate The anti-signal function of secondary radiation implies a significant non-linearity of those recording media where the number of receptors is low As far as we know, the influence of secondary radiation on the MTF has never been tested Instead, this function has been determined in systems completely free from fogging radiation (MORGAN et coll 1964, ROSSMANN & LUBBERTS 1966, ROSSMANN 1969) It appears desirable that complementary MTF determinations be made with different amounts of fogging radiation in order to analyse the recording properties under more realistic conditions If a markedly non-linear response is then obtained, the degree of non-linearity may be used as an index of the degree of photon competition If the response for a certain type of recording medium is clearly non-linear when increasing amounts of fogging radiation are added, it should be realized that the modulation transfer function is, in that case, useless

Acknowledgement

This investigation was supported by a grant from the Swedish Society of Medical Radiology

SUMMARY

On the basis of observations concerning non screen films and xerox plates a theory is proposed as to how the image quality is impaired by secondary radiation The theory includes an explanation of why xerox plates and industrial roentgen films of a high silver content are less affected by secondary radiation than conventional roentgen films

ZUSAMMENFASSUNG

Auf Grund von Beobachtungen an nicht-Schirm-Filmen und Xerox-Filmen wird eine Theorie aufgestellt, wie die Bildqualität durch Sekundär-Strahlung beeinträchtigt wird Diese Theorie umfasst eine Erklärung, warum Xerox-Filme und industrielle Röntgenfilme mit hohem Silbergehalt weniger von Sekundär-Strahlung beeinflusst werden als konventionelle Röntgenfilme

RÉSUMÉ

En se basant sur des observations concernant les films sans écran et les plaques xerox, les auteurs proposent une théorie expliquant comment le rayonnement secondaire diminue la qualité de l'image Cette théorie explique pourquoi les plaques xérox et les films radiographiques industriels ayant une forte teneur en argent sont moins affectés par le rayonnement secondaire que les films radiographiques ordinaires

REFERENCES

BOAG J W Xeroradiography Phys in Med Biol 18 (1973), 3

— STACEY B and DAVIS R Xerographic recording of mammograms Brit J Radiol 45 (1972), 633

troduction to the physics of

in mammary radiography

FISCHEDICK O und EVERS R Möglichkeiten und Grenzen der Xeroradiographie der Brust Ein vorläufiger Überblick Fortschr Röntgenstr 119 (1973) 389

GOULD H

breas

JOHNS H

of el

KOSSEL

— (b) radiographie — ein Verfahren zur Bilderzeugung in der Röntgendiagnostik Acta radiol

MORGAN R

charact

O'MARA R

mamm

ROSSMANN line spread-function and modulation transfer function Tools for the study of imaging systems Radiology 93 (1969), 257

mally influenced by secondary radiation, for instance the Mamoray film used in the present experiments. The similarity consists in an overcapacity, having the effect that the number of roentgen photons forming an ordinary image is far from exhausting the total capacity for reception and storage of information. Thus, it seems probable that competition between primary and secondary photons will be minimal in the xerox plate. It is proposed that such a low level of competition explains the remarkable ability of the xerox plate to resist the detrimental effects of secondary radiation.

In passing it should be noted that the number of powder grains used in the electrostatic development is not to be compared with the number of silver halide grains in the film. The reason for this lies in the contrast levelling and edge contrast enhancement of the xerox plate. The powder grains only indicate the location of abrupt charge changes in the latent electrostatic image.

When the limit of the storage capacity of a recording medium is being approached, different roentgen photons may be expected to compete for the remaining receptor units. Competition between primary and secondary photons exists, but it appears equally plausible that primary photons will compete with each other. In another report (SELIN & REICHMANN to be published) it will be demonstrated that this mechanism may be operative in screen-film radiography. This type of competition will, to an especially high degree, impair the recording of weak signals having a high spatial frequency. The ability of the xerox plate to record this type os signal at much higher tube potentials than can be used even with non-screen industrial film probably reflects a low level of competition not only between primary and secondary photons but also between different primary photons.

The generally accepted way of describing the functional capacity of a recording medium is based on the 'modulation transfer function' (MTF). For this function to be valid the response of the recording medium should be linear, since it is only under such conditions that a Fourier analysis is accurate. The anti-signal function of secondary radiation implies a significant non-linearity of those recording media where the number of receptors is low. As far as we know, the influence of secondary radiation on the MTF has never been tested. Instead, this function has been determined in systems completely free from fogging radiation (MORGAN et coll. 1964, ROSSMANN & LUBBERTS 1966, ROSSMANN 1969). It appears desirable that complementary MTF determinations be made with different amounts of fogging radiation in order to analyse the recording properties under more realistic conditions. If a markedly non linear response is then obtained, the degree of non-linearity may be used as an index of the degree of photon competition. If the response for a certain type of recording medium is clearly non linear when increasing amounts of fogging radiation are added, it should be realized that the modulation transfer function is, in that case, useless.

Acknowledgement

This investigation was supported by a grant from the Swedish Society of Medical Radiology.

SUMMARY

On the basis of observations concerning non screen films and xerox plates a theory is proposed as to how the image quality is impaired by secondary radiation The theory includes an explanation of why xerox plates and industrial roentgen films of a high silver content are less affected by secondary radiation than conventional roentgen films

ZUSAMMENFASSUNG

Auf Grund von Beobachtungen an nicht-Schirm-Filmen und Xerox-Filmen wird eine Theorie aufgestellt, wie die Bildqualität durch Sekundär-Strahlung beeinträchtigt wird Diese Theorie umfasst eine Erklarung, warum Xerox-Filme und industrielle Rontgenfilme mit hohem Silbergehalt weniger von Sekundar-Strahlung beeinflusst werden als konventionelle Rontgenfilme

RÉSUMÉ

En se basant sur des observations concernant les films sans écran et les plaques xérox, les auteurs proposent une théorie expliquant comment le rayonnement secondaire diminue la qualite de l image Cette théorie explique pourquoi les plaques xérox et les films radiographiques industriels ayant une forte teneur en argent sont moins affectes par le rayonnement secondaire que les films radiographiques ordinaires

REFERENCES

BOAG J W Xeroradiography Phys in Med Biol 18 (1973), 3

— STACEY B and DAVIS R Xerographic recording of mammograms Brit J Radiol 45 (1972), 633

CHRISTENSEN E E, CURRY III T S and NUNNALLY J An introduction to the physics of diagnostic radiology Lea and Febiger, Philadelphia 1972

DE[illegible]

A[illegible]

FISC[illegible]

E[illegible]

GOU[illegible] , SANCHEZ-UBEDA R and PEREZ J Xeroradiography of the breast Amer J Roentgenol 84 (1960), 220

JOHNS H E FENSTER A , PLEWES D , BOAG J W and [illegible]

[illegible]

KO[illegible]

— [illegible]

MO[illegible]

[illegible]

O'M[illegible]

[illegible]

ROS[illegible]

[illegible]

— and LUBBERTS G. Some characteristics of the line spread function and modulation transfer function of medical radiographic films and screen film systems. Radiology 86 (1966), 235.

RUZICKA F. F., KAUFMAN L., SHAPIRO G., PEREZ J. V. and GROSSI C. E.: Xeromammography and film mammography. A comparative study. Radiology 85 (1965), 260.

SCHERTEL L., zum WINKEL K., MOTZKUS F. und KRASKA H.: Die Xeroradiographie des Schädels. Fortschr. Röntgenstr. 121 (1974), 541.

SELIN K. and REICHMANN S.: High density failure of radiographic films. To be published in Acta radiol. Diagnosis.

WOLFE J. N.: Xerography of the breast. Radiology 91 (1968), 231.

FROM THE SECTION FOR MAXILLO-FACIAL ROENTGENOLOGY, DEPARTMENT OF RADIOLOGY
CENTRALLASARETTET, S-961 19 BODEN, SWEDEN.

LAYER FORMATION IN NARROW BEAM ROTATION RADIOGRAPHY

ULF WELANDER

Narrow beam rotation radiography has been described as a modified form of tomography (DUHAMEL 1954, 1957, HUDSON et coll 1957, PAATERO 1949, 1954, SOILA 1961, TAMMISALO 1964, TAMMISALO & NIEMINEN 1964) The concept of tomography has also been adapted by the ICRU (1962) in the classification of rotation narrow beam methods This classification is only valid if the term tomography is applied in its most wide sense denoting any layer forming radiographic imaging system A restricted use of the definitions of tomography excludes narrow beam rotation radiography (EDHOLM 1960, WELANDER 1974) It has been demonstrated that the panoramic image is essentially the result of a specific projection technique, and that the layer forming effect, i e the blurring, is a side effect (NYSTRÖM & WELANDER 1971, 1972, SJÖBLOM et coll, to be published, SÄMFORS & WELANDER 1974, WELANDER 1974, WELANDER & NYSTRÖM 1971) For an optimum use of rotation narrow beam radiography a full understanding of its working principle is necessary, i e a detailed knowledge of the layer formation and the defining facts

Submitted for publication 29 November 1974

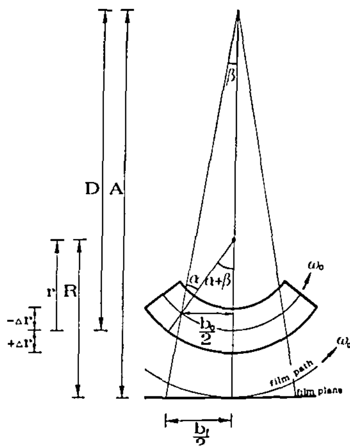


Fig 1 Symbols of essential parameters in rotation narrow beam radiography

Layer formation

Definitions (See Figs 1, 2, 3)

A	= distance tube target to film
D	= distance tube target to object
r	= distance from the rotation centre of the beam to the sharply depicted plane in the object, object projection radius
Δr	= positive or negative increment to the object projection radius
R	= radius of the film path radius of stationary film
ω_0	= angular velocity of the beam
ω_d	= angular velocity of the film
$\omega_0 - \omega_d$	= angular velocity of the film in relation to the beam
b_0	= width of the beam in the object at the object projection radius, r
b_f	= width of the beam at the film
x	= length of the projection of an object point on the film path, or on the stationary film

Fig 2 Schematic drawing of the exposure of a point P, in the object by means of a rotating narrow beam The film is stationary Two positions, I and II, are represented between which a continuous movement takes place An image of the object point is successively drawn on the film The length of the point's projection on the film is the distance x

U_x – length of the projection of an object point on the moving film, length of point spread function, characteristic blurring of rotation narrow beam methods

M magnification factor of a central projection where the rotation centre of a narrow beam serves as a functional focus

M resultant magnification factor when above mentioned central projection is combined with a moving film

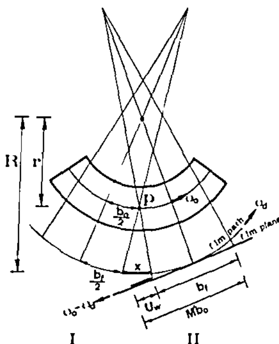
α rotation angle of the object in relation to the marginal rays of the beam, index Δr denotes the rotation angle at a distance Δr, from the object plane coinciding with the object projection radius, 2α = angle of total object rotation

β – angle of the beam/2 at the tube target

$\alpha+\beta$ rotation angle of the object in relation to the central ray of the beam, $2(\alpha+\beta)$ angle of total object rotation

In the following mathematical calculations a model of rotation narrow beam radiography is used It is assumed that the tube target is a point source of negligible size The curvature of the object within the beam is considered to be negligible (TAMMISALO & NIEMINEN 1964) The term 'object point' refers to a small object detail of negligible size The length of the projection of an object point on the film is considered to be equal to the length of the point spread function (ROSSMANN 1969) Further, it is assumed that it is satisfactory for the purpose of this report to consider the blurring to be the length of the point spread function, excluding the energy distribution

positions, I and II, are represented between which a continuous movement takes place An imaginary image of the object point is successively drawn along the film path When recorded on the film the length of the point's projection on the film path is changed depending on the ratio between the angular velocity of the film in relation to the beam ($\omega_0 - \omega_d$), and the angular velocity of the beam, ω_0



Mathematical analysis

Deduction The exposure of an image of an object point by means of a rotating narrow beam may be explained as follows

The case where both the object and the film are stationary and only the beam moves may be considered first (Fig 2), it is pre-supposed that the film is placed in a circular plane at a constant distance from the object While the beam passes the object an object point will first be projected on the film by one of the marginal rays (Fig 2, position I) Then, the point will be successively projected on the film by all the rays in one plane of the beam until it is projected on the film by the other marginal ray (Fig 2, position II) The projection of the object point by the different rays of the beam will not hit the same point on the film but will be successively displaced Thus, the object point will be depicted on the film as a line If the length of this line, i e the length of the point's projection on the film, is x, then it is found from proportionality that

$$\frac{x + b_f}{b_0} = \frac{R}{r} \qquad x = \frac{Rb_0}{r} - b_f \tag{1}$$

Considering that the object point may be situated at different distances from the object plane coinciding with the object projection radius, r, the following equation

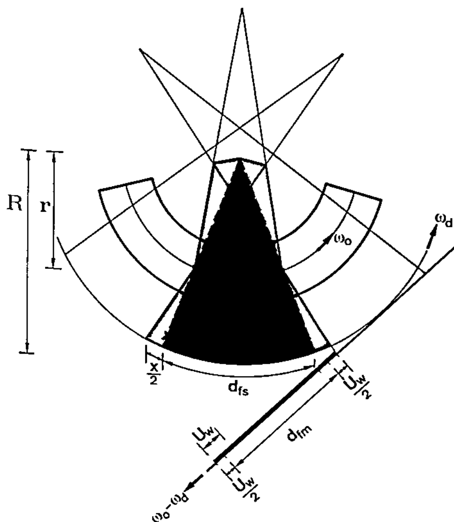


Fig 4 Schematic drawing of the projection of a distance in the object by mean[illegible]
beam. Three positions during the [illegible]
object is projected on the fil[illegible]
rotation centre of the b[illegible]

will be obtained

$$x = \frac{Rb_0'}{(r+\Delta r)} - b_f \tag{2}$$

where $b_0 = b_0(1+\Delta r)/D$ because the width of the divergent beam varies at different distances, Δr, from the object projection radius

It should be observed that $R/(r+\Delta r)$ in equation (2) expresses the magnification factor, M, in a central projection which has the rotation centre of the beam as an imaginary functional focus (Fig 4), R is the focus to film distance, and $(r+\Delta r)$ is the focus to object distance

Thus

$$x = Mb_0' - b_f \tag{3}$$

No layer will be formed when the film is stationary but the blurring of an object point will increase successively from the film towards the rotation centre proportional to the width of the beam and to the magnification factor

The introduction of a moving film in the technique described creates rotation narrow beam radiography (Figs 3, 4) Using the mathematical model deduced by WELANDER (1974) an expression of the characteristic blurring, U_w, of rotation narrow beam radiography may be written

$$U_w = \left| \frac{R(\omega_0 \quad \omega_\delta)b_0}{(r+\Delta r)\omega_0} - b_f \right| \tag{4}$$

and the magnification factor, M , in the geometrical projection of narrow beam rotation radiography (Fig 4) is expressed by

$$M = \frac{R(\omega_0 - \omega_\delta)}{(r+\Delta r)\omega_0} \tag{5}$$

Thus, by substitution equation (4) may be summarized

$$U_w = |M\, b_0' - b_f| \tag{6}$$

$M = f(\Delta r)$ and $U_w = f(\Delta r)$ calculated from equations (5) and (6), respectively (cf Fig 5)

A comparison between Figs 2 and 3 and between the corresponding equations, (2) (3) and (4) (6), respectively, shows that the moving film alters the magnification factor in the central projection caused by the rotation narrow beam The magnification factor is changed directly in proportion to the ratio between the angular velocity of the f[illegible]
$\omega_\delta)\,\omega_0$. Howe[illegible]
basic princip[illegible] [illegible]thod, i e the projection technique utilizing the rotation centre of the beam as a functional focus, remains the same when the stationary film is exchanged with a moving film

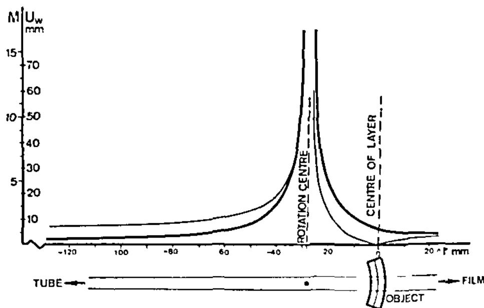


Fig 5 The magnification factor, M′, and the length of the point spread function, U_w, as functions of Δr in a section of the object, the sagittal plane A layer is formed

An object point will be recorded on the film as an image point, $U_w = 0$, when

$$M'b_0 = b_f$$

which means that no blurring will occur in a plane in the object where

$$M' = \frac{b_f}{b_0} = \frac{A}{D} = \frac{R(\omega_0 - \omega_a)}{r\omega_0}$$

Thus, the film may be programmed to follow during the exposure the projection of object points in one selected plane in the object Outside this plane blurring occurs, i e a layer is formed

The length of the point spread function outside the sharply depicted plane is directly proportional to the width of the beam, and there will be no blurring and no layer formation when b_0 and $b_f \to 0$ From this observation it follows that the primary cause of the blurring, and consequently the primary cause of the layer formation is the width of the beam The length of the point spread function is also highly dependent on the magnification factor The specific behaviour of the nonlinear magnification of the central projection, *which is typical of rotation* narrow beam radiography (Fig 5), is the significant cause of the characteristic properties of the layer The variation of the width of the beam at different depths in the object, expressed by the factor $(1+\Delta r/D)$, has a minor effect on the blurring in the layer formation

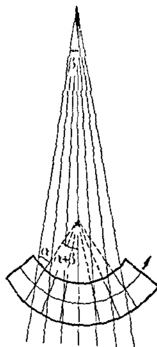


Fig 6 When an object rotates in relation to a roentgen beam a radius in the object will successively change its angle to the rays of the beam The angle of this rotation may be defined as the angle in relation to the marginal rays, α, or as the angle in relation to the central ray, $(\alpha - \beta)$, respectively It is not necessary for the description and explanation of narrow beam rotation radiography to interpret the object rotation angle as an exposure angle in the tomographic sense

The length of the projection of an object point on the film is dependent on the geometrical magnification of the image Therefore, it should be correct to define a total or absolute value of the blurring, U_w, but also a relative value, U_w/M'

For a full understanding of the panoramic image it is not satisfactory only to analyse the layer formation at the jaws Fig 5 demonstrates the magnification factor, M, and the length of the point spread function, U_w, as functions of Δr in a section of the total object It is evident that towards the rotation centre the magnification factor is so considerable that the magnification itself would eliminate from the image structures overlapping the jaws even if there were no blurring as when b_θ and $b_r \rightarrow 0$ This is not a real tomographic effect but rather an effect of an extremely short focus to object distance

Object rotation angle—exposure angle Rotation narrow beam radiography has been compared to tomography because of the layer formation, and also because the object rotates in relation to the beam during the exposure (Fig 6) This rotation movement gives seemingly an effect of a tomographic angle, or exposure angle, as defined by EDHOLM (1960) and ICRU (1962)

The object rotation may be defined as the rotation angle in relation to the marginal rays of the beam, $2\gamma_{\Delta r}$, or the rotation angle in relation to the central ray of the beam

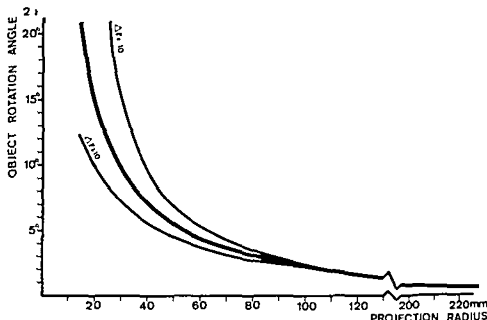


Fig 7 The object rotation angle is a function of the object projection radius, r, and varies continually in the longitudinal direction of the object Additionally, it is a function of (r + Δr) and therefore it also varies in the transverse direction at different depths in the object A = 482 6 mm, D = 406 4 mm, b_f = 6 35 mm (mean size of elliptical path in the Panelipse)

which is $2(\alpha_{\Delta r}+\beta)$, if the angle of the beam at the tube target is 2β (Figs 1, 6) These angles are defined by

$$\tan\beta=\frac{b_f}{2A},\quad \sin\alpha_{\Delta r}\quad \frac{\sin\beta(D-r)}{(r+\Delta r)},\quad \sin(\alpha_{\Delta r}+\beta)=\frac{b_0'}{2(r+\Delta r)}$$

The object rotation in relation to the marginal rays, 2α f(r), is exemplified in Fig 7 With the addition of a constant, 2β, which is very small, the angle of the object rotation in relation to the central ray will give the same function as in Fig 7 The object rotation angle varies with the object projection radius, and also with an increment given to the object projection radius This latter variation, $2\alpha_{\Delta r}=f(r+\Delta r)$, appears in Fig 7 for Δr = 10 mm and Δr = 10 mm Thus, the rotation of the object in relation to the beam varies in all parts and in all depths in the object, and an exposure angle, or a mean exposure angle, is not possible to define in rotation narrow beam methods An introduction of the object rotation angle in a mathematical analysis of the layer formation will lead to the following expression

$$U_w=\left|2M'\sin(\alpha_{\Delta r}+\beta)(r+\Delta r)-b_f\right| \tag{7}$$

But $2\sin(\alpha_{\Delta r}+\beta)(r+\Delta r)=b_0'$, thus, in equation (7) the angle of the object rotation is not an independent factor but a parameter of the beam width within the object It is not necessary for the explanation of narrow beam rotation radiography to consider the object rotation angle as an exposure angle in the tomographic sense

Discussion

The basic work that started the development of rotation narrow beam radiography was presented by PAATERO (1949, 1954) However, the possibility of using a rotating narrow beam to obtain special roentgenologic projections had been suggested previously by VALLEBONA (1930) and HECKMANN (1939) Under the term segmentography VLORINEN (1957, 1959) presented a rotation narrow beam method utilizing a conventional equipment for linear tomography for the exposure An analysis of VLORINEN s method shows that it is identical with rotation narrow beam radiography

In the first method presented by PAATERO (1949) the film was stationary The method was presented as a form of tomography but it is not layer forming, however It is distinctly a projection technique (cf Figs 2, 4) and DUHAMEL proved (1954) that it is not related to tomography Later on, PAATERO (1954) introduced the moving film and thereby he presented the method which in this report is defined as narrow beam rotation radiography (Figs 3, 4) This method also was presented as a form of tomography However, DUHAMEL (1957) claimed that it is a method where a continuous series of image fragments are exposed side by side, each fragment being a tomogram in which the width is equal to the width of the beam DUHAMEL (1954, 1957), HUDSON et coll (1957), SOILA (1961), TAMMISALO (1964) and TAMMISALO & NIEMINEN (1964), have described rotation narrow beam radiography mathematically, and many authors have described the method empirically, among them VAN AKEN (1973), ANDO (1971), BARTON (1970), BLACKMAN (1956, 1964), BRUEGGEMANN (1967), BUCHMANN (1974), EDGE & CHAMPION (1972), GRABER (1965, 1966) JUNG (1965), KUMPULA (1961) MANSON-HING (1971), PASLER (1973), and PHILLIPS (1967) The tomographic approach has been generally accepted by these authors

A more complete understanding of the working principle of rotation narrow beam methods was introduced by DUHAMEL Indirectly he pointed out the importance of the specific projection technique of these methods, a factor which has been further analysed in reports by NYSTRÖM & WELANDER (1971, 1972), SJÖBLOM et coll (to be published), SAMFORS & WELANDER (1974), WELANDER (1974), and WELANDER & NYSTRÖM (1971). In the present report a complementary analysis of the layer formation is presented, and the result clearly indicates that the generally accepted concept of tomography which has dominated the view of rotation narrow beam radiography may be questioned

It may possibly be claimed that it is satisfactory for practical clinical purposes to classify narrow beam rotation radiography as a form of tomography This wide definition has the disadvantage, however, that it might confuse the fact that narrow beam rotation radiography is similar to conventional tomography in only one respect, in that a layer is formed, but is different from tomography with respect to the basic principle and to the generation of the layer formation The tomographic approach to the theory of narrow beam rotation radiography is not necessary for the description and understanding of the working principle Instead, it might draw the

attention away from the simple basic *principle, the utilization of a specific projection* technique The layer formation, or the tomographic effect, is, furthermore, a side effect in narrow beam rotation radiography Theoretically, a panoramic image may be exposed with the aid of a roentgen beam of negligible width, in this case there will be no blurring and no layer formation The magnification factor, which is considerable towards the rotation centre of the beam and independent of the beam width, would still act in the elimination of structures overlapping the primary object, in this particular case the jaws It is also important to stress that the jaws are anatomically a layer, and the narrow beam rotation methods should preferably give *images of this anatomic layer without blurring Visible effects of the layer formation* within the jaws only have a negative effect on the image This means that the layer formation should be regarded as a secondary effect, or a side effect, at the exposure of the panoramic image

Narrow beam rotation radiography is today in wide use in odontologic radiology It has many advantages but also draw-backs A primary objective in the future development of this radiographic system should be to optimize its use For this purpose it is necessary to draw up a theory of the working principle which is as complete and reliable as possible

Acknowledgements

The author wishes to express his sincere thanks to Professor Paul Edholm, Department of Diagnostic Radiology, Regionsjukhuset, Linköping for constructive advice and suggestions and also to Tekn lic Goran Wickman, Department of Radiation Physics Umeå University, Umeå, for friendly assistance

SUMMARY

The layer formation in rotation narrow beam radiography is analysed mathematically It is shown that the blurring, and consequently the layer formation, is due primarily to the width of the beam, no blurring and no layer formation occur if the beam is of negligible width The blurring is significantly affected by the magnification factor in the specific central projection typical of narrow beam rotation methods where the rotation centre serves as an imaginary focus

ZUSAMMENFASSUNG

Es wird die Schichtbildung bei der Rotations-Radiographie mit einem feinem Strahlenbundel mathematisch analysiert Es wird gezeigt dass die Unscharfe und somit die Schichtbildung, primar von der Weite des Strahls abhangt, keine Verzerrung und keine Schichtbildung tritt auf, wenn der Strahl eine zu vernachlassigende Weite hat Die Verzerrung wird signifikant durch den Vergrosserungsfaktor bei der spezifischen centralen Projektion, die typisch fur die Rotations-Methode mit einem feinem Strahl ist wobei das Rotationszentrum als imaginarer Fokus dient, beeinflusst

RÉSUMÉ

L'auteur analyse mathématiquement la formation de la couche de coupe dans la radiographie rotatoire avec faisceau etroit Il montre que l'effacement et par conséquent la formation de la couche de coupe est du principalement à la largeur du faisceau On n'obtient pas d'effacement ni de formation de couche de coupe si le faisceau a une largeur négligeable L'effacement est modifié de façon importante par le facteur d'agrandissement dans la projection centrale spécifique qui est typique des méthodes à faisceaux étroits ou le centre de rotation sert de foyer fonctionnel imaginaire

REFERENCES

VAN AKEN J Panoramic X ray equipment J Amer dent Ass 86 (1973), 1050

ANDO S Orthopantomography It's principle and technique Department of Radiology, Nihon University, School of Dentistry, Tokyo 1971

BARTON E J The orthopantomograph development and application Aust dent J 15 (1970), 151

[illegible]

[illegible] Evaluation of the Panorex unit Oral Surg 24 (1967), 348

BUCHMANN F Die Prinzipien des Dental-Tomograph Rontgenstrahlen 31 (1974), 24

DUHAMEL J Les procedes de radiographie en coupe non rigoureux Sci Industr photogr 25 (1954), 129

— Sur la correspondance entre les espaces image et objet dans les procédes de radiographie en coupe par faisceau diaphragme Sci Industr photogr 28 (1957), 225

EDGE M B B and [illegible]

[illegible]

GRAB[illegible] [illegible] panoramic radiography in dentistry J Canad dent Ass 31 (1965), 158

— Panoramic radiography [illegible]

HECKMANN K D[illegible] durch eine neue Aufnahmetechnik F

HUDSON D C KUMPULA J W and DICKSON G A panoramic X-ray dental machine U S armed Forces med J 8 (1957), 46

ICRU Methods of evaluating radiological equipment and materials Report 10f 1962 National Bureau of Standards Handbook 89 Washington, D C 1963

JUNG T Les procedes de radiographie panoramique en stomatologie Rev belge Med dent 20 (1965) 165

KUMPULA J W Present status of panoramic roentgenography J Amer dent Ass 63 (1961) 194

MANSON HING L R Advances in dental pantomography the GE-3000 Oral Surg 31 (1971) 430

NYSTRÖM O and WELANDER U Image producing geometry and tomography in roentgenologic narrow beam methods Svensk tandläk T 64 (1971), 64

— A new theory on the image producing elements in pantomographic methods Dento-Maxillo-Fac Radiol 1 (1972) 3

PAATERO Y V A new tomographical method for radiographic curved outer surfaces Acta radiol 32 (1949) 177

— Pantomography in theory and use Acta radiol 41 (1954), 321
PASLER F A Orthopantomographie in der zahnarztlichen Praxis Schweiz Mschr Zahn heilk 83 (1973), 1163
PHILLIPS J E Principles and function of the orthopantomograph Oral Surg 24 (1967) 41
ROSSMANN K Point spread function, line spread function, and modulation transfer function Tools for the study of imaging systems Radiology 93 (1969), 257
SÄMFORS K -A and WELANDER U Angle distortion in narrow beam rotation radiography Acta radiol Diagnosis 15 (1974), 570
— — Area distortion in narrow beam rotation radiography Acta radiol Diagnosis 15 (1974), 650
SJÖBLOM A, SÄMFORS K -A and WELANDER U Form distortion in narrow beam rotation radiography To be published in Acta radiol Diagnosis
SOILA P General theory of narrow beam rotating tomography Acta radiol 55 (1961) 458
TAMMISALO E H The dimensional reproduction of the image layer in orthopantomography Suom Hammaslääk Toim 60 (1964) 2
— Determination of the form of the image layer and calculation of its location within the object in conventional and simultaneous orthopantomography Suom Hammaslaak Toim 60 (1964) 14
— and NIEMINEN T The thickness of the image layer in orthopantomography Suom Hammaslaak Toim 60 (1964), 119
VALLEBONA A Una modalità di tecnica per la dissociazione radiografia delle omre applicata allo studio del cranio (In Italian) Radiol med 17 (1930), 1090
VUORINEN P Segmental roentgenography by means of a standard tomographic device Acta radiol 48 (1957), 181
— The roentgenographic slit methods A survey and analysis of procedures based on the use of a narrow bundle of roentgen rays (scanography) Acta radiol (1959) Suppl No 177
WELANDER U A mathematical model of narrow beam rotation methods Acta radiol Diagnosis 15 (1974) 305
— and NYSTRÖM O A new approach to the theory of pantomographic methods Svensk tandlak T 64 (1971) 173

FROM ROENTGEN DEPARTMENT I, (DIRECTOR: H. ARVIDSSON), SÖDERSJUKHUSET, S-100 64 STOCKHOLM, SWEDEN

INJECTION DEVICE FOR PHARMACO-ANGIOGRAPHY

K. JEKELL, S. JOHNSSON and S. SANDQVIST

Angiographic diagnosis of tumours was improved when vasoactive agents, injected before the contrast medium, were introduced into clinical practice. ABRAMS suggested the use of epinephrine in angiography (ABRAMS et coll. 1962). More recently increased accuracy was achieved in angiographic diagnosis of kidney tumours by using angiotensin (EKELUND et coll. 1972). The effects of vasoactive agents are well-known from animal experiments and considerable experience of pharmaco-angiographic examinations has been accumulated (EKELUND & LUNDERQUIST 1974). Still, however, there is no unanimous opinion about the value of pharmaco-angiography as a routine method. The diverging results reported are to some extent attributed to insufficient standardization of the injection technique. The usual procedure of pharmaco-angiography is the following: after selective catheterization of the organ to be examined the vasoactive agent is injected by hand through the catheter immediately before administration of the contrast medium with a pressure injector. This approach does not allow standardization of timing and delivery rate of the drug. In order to obtain a predetermined and reproducible injection technique, a syringe has been constructed for injection of pharmacologic agents. In the following this syringe will be called the 'pharma-injector'.

The pharma-injector is designed to perform precision injections of small volumes of drug solutions at comparatively slow rates and is connected with a standard pressure injector for contrast medium. Together they form a mobile, compact device

Submitted for publication 23 October 1974.

60 %) was varied between 2 and 30 s. Although the pharma-injector may be used in high precision routine angiography, the device is particularly suitable for serial examinations requiring identical techniques. The use of the pharma-injector in combination with a punch-card programme unit permits adaption of the examination technique to various research projects. Automatic control of the injection in pharmaco-angiography gives a possibility to analyse the time-factor of the pharmacologic effects within various vascular areas, thus enabling an optimum use of vasoactive agents in roentgen diagnosis.

SUMMARY

A device for injections of vasoactive agents at angiography connected with an injector for contrast medium and a film changer is described. It enables the examination to be performed according to predetermined data with a high degree of reproducibility. It lends itself particularly to experimental investigations of pharmacologic effects within various vascular areas.

ZUSAMMENFASSUNG

Es wird eine Anordnung zur Injektion von vasoaktiven Substanzen bei der Angiographie verbunden mit einem Injektor für das Kontrastmittel und einem Filmwechsler beschrieben. Diese ermöglicht es, die Untersuchung entsprechend vorzubestimmter Daten mit einem hohen Grad von Reproduzierbarkeit auszuführen. Sie eignet sich besonders für experimentelle Untersuchungen von pharmakologischen Effekten innerhalb verschiedener Gefässabschnitte.

RÉSUMÉ

Description d'un dispositif pour l'injection au cours de l'angiographie d'agents vasoactifs, connecté avec l'injecteur de moyen de contraste et le changeur de films. Il permet de faire l'examen suivant un plan prédéterminé avec un haut degré de reproductibilité. Il se prête particulièrement aux recherches expérimentales d'effets pharmacologiques dans différents territoires vasculaires.

REFERENCES

[illegible]

[illegible] (1974), 533

— GÖTHLIN J. and LUNDERQUIST A.: Diagnostic improvement with angiotensin in renal angiography. Radiology 105 (1972), 33.

ACTA RADIOLOGICA

OFFICIAL ORGAN OF THE RADIOLOGICAL SOCIETIES OF
DENMARK, FINLAND, NORWAY AND SWEDEN

Vol 16
Fasc 6

DIAGNOSIS

1975
November

THREE-DIMENSIONAL RECONSTRUCTION OF THE HUMAN HEART BY VIDEO TECHNIQUE

B LANTZ, B LINDBERG and J HUEBEL

The attenuation of roentgen radiation by different structures constitutes the basis for the formation of the image recorded on film or at fluoroscopy By measuring (digitizing) the density variations of the image point by point along one cross section of the object in the radiation beam and by storing this 'attenuation profile' of the object projected in different angles, it would be possible to reconstruct a two-dimensional image of that cross section by computer

This well known physical property of the radiation has been successfully utilized in practice by the EMI scanner (AMBROSE 1973, HOUNSFIELD 1973) which proved the possibility of two dimensional reconstruction of the human anatomy by means of a pencil beam transradiating the object The impact of that development on neuro radiology is well documented

The need for reconstruction of the heart anatomy throughout the cardiac cycle in health and disease is even greater Compared to non moving organs like the human brain the vital function of the heart is linked with motion and the horizontal scan

From the Department of Diagnostic Radiology III (Director [illegible]
grenska sjukhuset S-411 32 Gothenburg Swec[illegible]
(Director Professor P Palmer) University of Ca[illegible]
more Laboratory Electronics Engineering Dep[illegible]
more Calif 94550 U S A Submitted for publica[illegible] 10 June 1975

time of the first generation CT scanners (more than one second) is too long to reproduce events within the cardiac cycle The third dimension of the object (defined as the sum of multiple cross sections) necessary for three-dimensional reconstruction can only be obtained if multiple cross sections covering the whole anatomic extent of the object are recorded in the same temporal sequence This cannot by any means be done by the EMI scanner or any similar scanner on the market using roentgen radiation

By using the television image of a moving object projected in different angles at the same temporal sequence, the third dimension of the object is achieved by the scanning television camera dissecting the image in multiple horizontal cross sections at a very high speed (60 interlaced frames/s, 64 μs horizontal scan time, US Commercial Television System) A cone beam must be used to cover the whole anatomic extent of the object This may decrease the spatial resolution at the entrance of the image intensifier because of scattering, but the temporal resolution would make it possible to reconstruct the beating heart several times within one cardiac cycle

Essentially two ways of approaching three dimensional reconstruction of the beating heart exist (1) Simultaneous recording of 'attenuation profiles' of the object in different projections by means of multiple cone beam sources and detector array assemblies, and (2) data collection from different projections at corresponding times at different cardiac cycles when rotating one fluoroscopic system and the patient relative to each other

The first method requires the use of many fluoroscopic systems each aligned geometrically, calibrated for identical system gain and synchronized in time Each fluoroscopic system then provides data for one projection angle and the number of projections is fixed by the equipment designed Any attempt though to collect multiple projection data simultaneously can lead to serious radiation scatter problems with each fluoroscopic system sensitive to scattered radiation from the other fluoroscopic systems Therefore, the generators might be activated sequentially rather than simultaneously with sequencing time dictated by the data collection rate (the frame time or filter time for each TV system) This sequencing could result in considerable time between the first and last projection with the resultant loss in temporal resolution or it would lead to the second method of collecting data from different projections at corresponding times at different cardiac cycles If it is assumed that the cardiac cycle is repetitive or that similar cardiac cycles from a large set of irregular cycles can be selected, it is possible to collect the necessary multiple projection data by choosing corresponding times in different cardiac cycles The data can then be collected with one fluoroscopic system by rotating the patient and the radiation beam relative to each other Those frames from the TV system are then selected which are sufficiently close in time to the desired cardiac state This latter system has been tried by ROBB et coll (1974) at the Mayo Clinic They have demonstrated the accuracy of the technique on test objects and isolated working canine left ventricle at different phases of the cardiac cycle

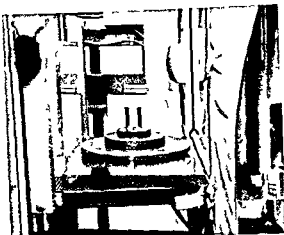


Fig 1 A Plexiglas cube in the center of the rotating device in the radiation beam between the tube (left) and the image intensifier tube (right)

The aim of the present investigation was to analyse if it is possible to use an ordinary clinical roentgen-television chain for collection of image data underlying reconstruction of the beating heart, if the spatial resolution is sufficient for evaluating major tissue structures like the cardiac chambers in intact man, and if the temporal resolution is improved by speeding up the frame rate of the television chain without losing valuable information

Different objects were placed in a cone beam from an ordinary roentgen tube The television images of the object obtained from different known angles by rotating the object in the radiation beam were stored in real time and digitized for reconstruction by computer

Measurement system

The experimental series were performed with standard fluoroscopic equipment (Diagnos 70, Philips) Lindberg's synchronization unit was adapted to the television camera tube giving 250 full frames a second (LINDBERG 1972) In the center of the radiation beam close to the input of the image intensifier a device was placed where different objects could be rotated around the axis in different known angles (Fig 1) In each angle examined 16 horizontal lines each containing 64 image points were digitized in real time and stored on magnetic tape for further processing When a student was examined, a rotating chair was used and the chest was in upright position No attempts were made to optimize the contrast function by filters, grids or by other means (LANTZ & STRID 1973, 1975 a, b, STRID & LANTZ 1973) The recordings were made in continuous fluoroscopy with stabilized constant kV and mA (LANTZ 1974) The experimental series were performed on Plexiglas phantoms of different design as well as on skull and dead human heart Different focal distances and electron optics (12 5 cm and 23 cm (5" and 9") input diameter of the image intensifier) were tried

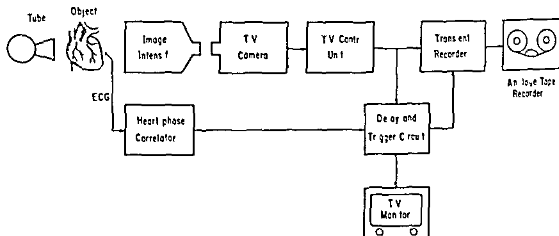


Fig 2 Recording procedure

Roentgen television system The recording procedure is illustrated by the experimental setup in Fig 2 From an ordinary tube with a focal spot of 0 6 mm roentgen radiation was emitted as a cone beam transradiating the object After attenuation of the radiation by the object, the attenuation relief was transmitted to the image intensifier to produce a visible image of the object on the target of the television camera (Plumbicon) In order to increase the scan rate of the television camera a special high image rate TV system was used (LANTZ & LINDBERG 1975, LINDBERG 1972) Compared to a standard European TV system the image rate was five times higher giving twice the horizontal scanning speed The frame rate was 250 full frames/s without interlace and the vertical scanning time was 4 ms and the number of lines in the field was 125

The transient recorder (*Biomation 802*) The fast analog video information was digitized in real time and stored in the memory of the instrument The recorder used had a memory of 1 024 eight-bit words The A/D conversion was carried out with a speed of one conversion every 0 5 μs, i e, the maximum time for storing input signals During this time 16 TV-lines of 32 μs duration were stored ($16 \times 32 = 512$) In order to utilize the whole memory of the transient recorder 64 samples were picked up from each line and A/D converted The 64 eight-bit words were stored from each of 16 lines in digital form in real-time ($64 \times 16 = 1\,024$)

The digitized data were stored on digital tape in a format compatible with Lawrence Livermore Laboratory computer facility

Delay and trigger circuits As only 16 TV-lines could be stored at each recording, it was important to know which 16 lines of the 125 available lines were stored A special delay circuit was constructed for this purpose When the present number of horizontal pulses had passed, the delay circuit gave a trigger pulse to the transient recorder and the next 16 lines were recorded

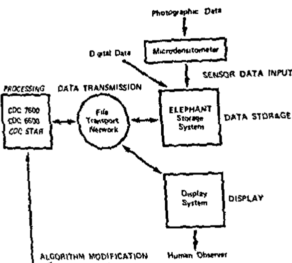


Fig 3 System data flow

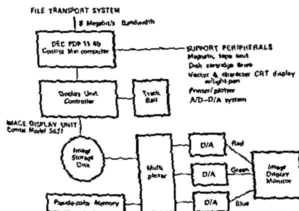


Fig 4 Image display system configuration

All recordings of a particular image included exactly the same 16 lines and no attempt was made to record the remaining 109 lines to get a full image The interest was directed only towards the part of the object falling within the 16 lines

The heart phase correlator When an object like the heart is examined it is important to know in what phase of the motion the object is recorded All recordings underlying the reconstruction of one cross section must be carried out in the same heart phase By means of a heart phase correlator it is possible to trigger the transient recorder at any phase of the heart cycle under conditions of exact reproducibility of the cardiac cycles The output pulse was fed to the delay and trigger circuits and acted as a gate for the horizontal pulse counter By using two heart phase correlators each of them could be adjusted to give an output pulse at different parts of the cardiac cycles like end systole and end-diastole

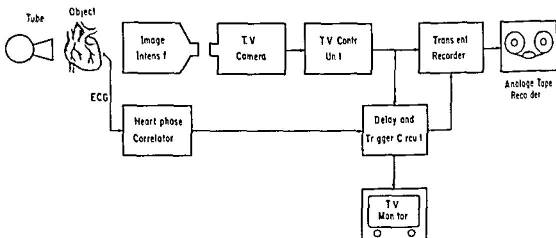


Fig 2 Recording procedure

Roentgen television system The recording procedure is illustrated by the experimental setup in Fig 2 From an ordinary tube with a focal spot of 0 6 mm roentgen radiation was emitted as a cone beam transradiating the object After attenuation of the radiation by the object, the attenuation relief was transmitted to the image intensifier to produce a visible image of the object on the target of the television camera (Plumbicon) In order to increase the scan rate of the television camera a special high image rate TV system was used (LANTZ & LINDBERG 1975, LINDBERG 1972) Compared to a standard European TV system the image rate was five times higher giving twice the horizontal scanning speed The frame rate was 250 full frames/s without interlace and the vertical scanning time was 4 ms and the number of lines in the field was 125

The transient recorder (*Biomation 802*) The fast analog video information was digitized in real time and stored in the memory of the instrument The recorder used had a memory of 1 024 eight-bit words The A/D conversion was carried out with a speed of one conversion every 0 5 μs, i e , the maximum time for storing input signals During this time 16 TV-lines of 32 μs duration were stored ($16 \times 32 = 512$) In order to utilize the whole memory of the transient recorder 64 samples were picked up from each line and A/D converted The 64 eight bit words were stored from each of 16 lines in digital form in real time ($64 \times 16 = 1\ 024$)

The digitized data were stored on digital tape in a format compatible with Lawrence Livermore Laboratory computer facility

Delay and trigger circuits As only 16 TV-lines could be stored at each recording, it was important to know which 16 lines of the 125 available lines were stored A special delay circuit was constructed for this purpose When the present number of horizontal pulses had passed, the delay circuit gave a trigger pulse to the transient recorder and the next 16 lines were recorded



Fig. 5 The image processing research laboratory at the University of California's Lawrence Livermore Laboratory In the back from left to right two nine track tape units are seen, the Comtal image display system, two discs for storing programs and a PDP 11/40 computer which is used to control the system The operator is sitting at a teletype where he is controlling the information flow within the system and displaying the images



Fig 6 Plexiglas cylinder with a central septum in the center of the rotating device.

Data processing system

The digitized data were processed on the system shown schematically in Fig 3 This system combines a large computing capability with a sophisticated digital display system to form a powerful and versatile data processing and image enhancement system (EKSTROM 1974) The user can address this system in a timesharing mode with a teletype which is often located in his office

The display system in the lower right part of Fig 3 is illustrated in greater detail in Fig 4 and photographically in Fig 5 This system is designed around a Comtal model 5631 image display unit and a Corac color display monitor It is capable of displaying a 512 × 512 image in 64 levels of gray or pseudo color or of displaying three separate images as a true color image

The PDP 11/40 minicomputer (Fig 4) controls the flow of data within the display system Although it is involved in all interactions with the display system only two of its functions will be mentioned here

In the pseudo-color mode each of the 64 intensity levels is displayed as a particular prechosen color A carefully selected coloring scheme can often bring out detail in an image not obvious in the gray image The PDP 11/40 can assign any of several pre-programmed pseudo color schemes to an image or it can accept an assignment from the user Once an assignment has been made the PDP 11/40 can rotate the 64 colors within the assignment so that each color is assigned to progressively higher or lower intensity values As the assignment is rotated the image may be viewed on the monitor The rotation can then be stopped at any point which is thought to give a more detailed image

The track ball is a device which operates through the PDP 11/40 allowing the user to move a lighted spot around on the image to indicate a particular point This device allows obtaining intensity information from selected points within the image, but more importantly, it allows information on precise locations and dimensions of areas of interest within an image

Although it may be desirable to ultimately reconstruct the data on a much less complex system than the one used, the LLL system is an ideal tool on which to develop and evaluate reconstruction methods before investing in dedicated less expensive but less versatile processing systems

Image reconstruction

The SNARK (ROWLAND 1972) routines were adapted to run on the Lawrence Livermore's CDC 7600 computers In addition to the standard reconstruction modes available in SNARK, an extended field capability based on the suggestions of CROWTHER & KLUG (1974) and possibly on the suggestions of OPPENHEIM (1974) were also included

Basically the extended field iterative reconstruction technique (EFIRT) reconstructs a larger than normal region The area outside the normal reconstruction region, called

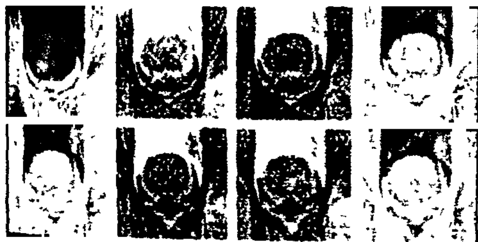


Fig. 9 A sequence of cross sectional reconstructions from a skull phantom Cranial-caudal direction from upper left to lower right Center 64 × 64 field from a 92 × 92 extended field reconstruction Unconstrained ART algorithm Ninety projections between the angles of 180 and 360 with 2° increments between projections

the extended reconstruction region, forms a field into which the noise and inconsistencies can propagate Although this extended field technique increases the number of unknown, (the number of unknowns is often doubled) and thereby makes the system even more undetermined, the reconstructed image was found to be better (subjectively by us and objectively by CROWTHER & KLUG) and to converge after only two or three iterations

CROWTHER & KLUG padded the projection data with zero's so that any projection rays which intersect the extended reconstruction region but not the normal reconstruction region are given a projection value of zero This is equivalent to assuming the extended field region contains only zero mean noise We have dropped this assumption to allow for objects which may be in the extended field and which consequently appear in some projections but not others Therefore, only those rays were reconstructed which intersect the original field but they were reconstructed over their entire path both within the original field and within the extended field It was not intended with this technique to reconstruct objects which appear in only a few projections, that is objects in the extended field, but it is hoped to minimize the effect of extended field objects within the normal reconstruction region

Results

All the recordings underlying the reconstruction in the present report have been performed with a horizontal linear scan time of 32 μs at a frame rate of 250 per second





Fig 7 Reconstructions of two Plexiglas models with air on the left and water on the right

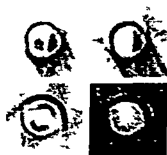




Fig 8 The same data as in Fig 7 Digital technique to enhance the contrast of the image The Plexiglas cube in water (lower right) is better recognized compared to Fig 7

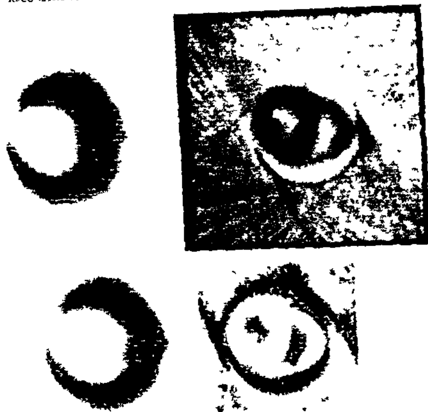


Fig 12 Four different reconstructions of one cross-sect[illegible]

Skull phantom A sequence of cross sectional reconstructions from a skull phantom appears in Fig 9 where each image represents the cross section of every other line in the field The reconstructions were made from 90 projections between the angles of 180° and 360° with 2° increments between projections The nose is directed down on the images On the last two images in the lower right corner, foramen magnum can be observed in the middle of the images as a dark spot

Human heart specimen A 3 cm thick transverse cross section through the ventricles of a human heart was used The photograph (Fig 10) and the xeroradiogram (Fig 11) demonstrate to the left the hypertrophic left ventricular wall and in the midline the septum The right ventricle to the right has a thinner wall In the left ventricle cavity papillary muscles are seen, especially in the left lower corner Four different reconstructions of one cross section of the heart muscle are given in Fig 12 These



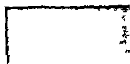
Fig 10 Three cm thick transverse cross section through the ventricles of a human heart



Fig 11 Xeroradiography of the heart sample in Fig 10

Plexiglas models Cylinders of Plexiglas (diameter 6 5 cm, wall thickness 0 5 cm) were placed on the rotating device in the center of the radiation beam (Fig 6) One cylinder contained a central septum (0 5 cm) and another cylinder contained a Plexiglas cube (2 9 cm × 2 9 cm) In the first case the empty space to the right of the septum was partly filled with water In the second case the cylinder was partly filled with water surrounding the cube By recording the image of the phantom over an area covering the same cylinder with and without water it was possible to obtain cross sections for comparison on the same image (1/250 s) Reconstructions of the Plexiglas models are seen in Fig 7 where each image represents just one cross section (one horizontal TV line) reconstructed from 65 projections between the angles of 0° and 128° in 2° increments The dark circular area in the center of the image is the Plexiglas cylinder The septum and the cube within the cylinder are well seen when surrounded by air but are more difficult to recognize when surrounded by water

In Fig 8 digital technique to enhance the contrast of the image has been used so that the distinction between the water and the Plexiglas becomes more clear



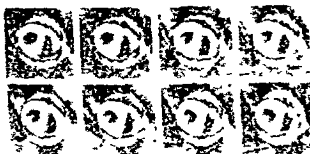


Fig 13 A sequence of cross sections (every other line) of the heart muscle in Fig 10 Each of the images is the center 64 64 field of 92 × 92 extended field reconstruction Unconstrained ART technique Seventy two projections between 0 and 360 in 5 increments 5" (12 5 cm) input

reconstructions were formed from projections between 0° and 360° in 5° increments The projection data consisted of 64 points per projection Approximately 40 of these points were across the heart itself The reconstructions on the left were formed by using the back projection technique, the reconstructions on the right were formed with the ART unconstrained technique The upper images were reconstructed on an extended field which was 92 × 92 The lower images were reconstructed in the normal manner on a 64 × 64 field In Fig 13 a sequence of cross sections of the heart model is illustrated Each of these images is the center 64 × 64 field of a 92 × 92 extended field reconstruction The angles in increments are the same as in Fig 12 The dark area in the center is the heart with septum clearly visible as a cord across the heart The white region which surrounds the heart is the fluor which extends beyond the heart The air within the heart chambers is represented by a lighter area If the papillary muscle in the left corner and the irregularity of the right ventricle wall are compared with the appearances of the specimen in Figs 10 and 11, the extended field reconstruction evidently has sharper and better defined boundaries

Human heart in vivo A student was sitting in the upright position on a chair in the radiation beam close to the image intensifier (23 cm, 9") with the arms stretched and the hands grabbing a pole above his head In continuous fluoroscopy the recordings were made in end-systole and end-diastole triggered by two heart phase correlators Twenty-one different angles were obtained by rotating the chair manually in 5° increments The thoracic spine was not covering the heart in any of the 21 projections The student was breathing normally during the recordings Because of the upright position with the stretched arms movement of the thoracic wall was minimal during respiration The 16 horizontal lines digitized from the heart image covered about 2 cm of the heart in the vertical plane In Fig 14 the reconstructed end systolic and end-diastolic images of the heart are displayed alternately Reconstruction of 7 cross sections in end-systole and end-diastole is illustrated in Fig 15 The cross sections are obtained at a fairly proximal level of the heart The upper row in Fig 15 represents the end-systolic recordings and the lower row represents the end-diastolic recordings Each of these images is the center 64 × 64 field of a 92 × 92 extended field reconstruction They were formed with the ART unconstrained technique The heart appears as a dark area in the center of a bright diamond shaped fluor field (Fig 16) The upper part of the left ventricle appears as a round bright spot in the center of the image and a brighter area below probably represents the right atrium The poor spatial resolution together with the linear artefacts outside the heart may be explained by the poor precision in obtaining angles during the recording performed by manual rotation of the patient

Discussion and Conclusion

Compared to a mechanical scanning system like the EMI scanner the video system gives multiple cross sections of the object adding the third dimension It also



Fig. 14 Display of the end systolic and end-diastolic images of the heart alternatively in 21 different projections



Fig. 15 Reconstruction of seven cross-sections in end-systole (upper row) and end-diastole (lower row) The anterior chest wall to the right

has the great advantage of a very short linear scan time required to record and reconstruct the anatomy of an organ at different phases of its motion like the beating heart and the breathing lungs

Reconstruction of Plexiglas phantoms, organic material and beating human heart was made by digitizing television images obtained from standard equipment working at a high frame rate Although the spatial resolution was limited by the memory of the A/D converter in this particular experiment, the results seem to be quite adequate for evaluation of gross structures like the boundaries of the ventricle walls of the heart without enhancement by contrast medium It has only been able to use 64 image points along each horizontal line, i e, between two horizontal synchronization pulses of the video signal As the heart only occupied a part of the radiation beam, the horizontal resolution was not more than 25 image elements with the 9" (23 cm) image intensifier input and about 40 with the 5" (12 5 cm) intensifier (compared to 180 elements by the EMI scanner)

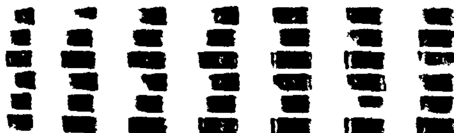


Fig. 14 Display of the end systolic and end-diastolic images of the heart alternatively in 21 different projections

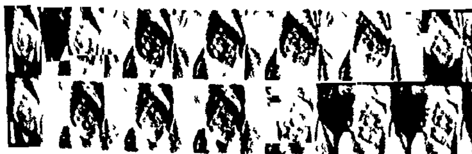


Fig. 15 Reconstruction of seven cross sections in end-systole (upper row) and end-diastole (lower row) The anterior chest wall to the right

has the great advantage of a very short linear scan time required to record and reconstruct the anatomy of an organ at different phases of its motion like the beating heart and the breathing lungs

Reconstruction of Plexiglas phantoms organic material and beating human heart was made by digitizing television images obtained from standard equipment working at a high frame rate Although the spatial resolution was limited by the memory of the A/D converter in this particular experiment, the results seem to be quite adequate for evaluation of gross structures like the boundaries of the ventricle walls of the heart without enhancement by contrast medium It has only been able to use 64 image points along each horizontal line i e, between two horizontal synchronization pulses of the video signal As the heart only occupied a part of the radiation beam the horizontal resolution was not more than 25 image elements with the 9" (23 cm) image intensifier input and about 40 with the 5" (12 5 cm) intensifier (compared to 180 elements by the EMI scanner)



a b

Fig 16 Magnification of one cross sectional reconstruction of the human heart in vivo in a) end systole and b) end diastole

With proper storing in real time of the image information recorded from different angles, it would be possible to obtain a much higher spatial resolution in the system consequently getting a more detailed reconstruction

The aim of the present investigation was to evaluate the capacity of the 250 Hz television system and test standard fluoroscopic equipment for three dimensional reconstruction It is believed that the higher frame rate would increase the temporal resolution considerably which is needed for a proper reconstruction of the beating heart By triggering the recordings by ECG at different angles in the same phase of the cardiac cycle, the prerequisites for a successful three dimensional reconstruction of the beating heart are met with

The amount of angles required to make a full three dimensional reconstruction with given resolution of the object is still unknown Considering the heart, the different angles recorded must be taken in the same temporal sequence with exact reproducibility of the cardiac cycles This can easily be done in animals where the heart beat and the respiration can be monitored In patients these parameters may vary during the recording procedure However, if sufficient amount of equal cardiac cycles are obtained during the recording procedure it is possible to reconstruct the heart even if the heart rate is irregular

Acknowledgement

We wish to express our sincere thanks to Docent Carl-Gustaf Helander, Director of the Department of Diagnostic Radiology III, University of Gothenburg, Sweden, for his advice and encouraging support of this project performed in his laboratories

We also thank Dr C John Tupper, Professor and Dean of the Medical School, University of California, Davis, who sponsored the whole project by grant

SUMMARY

Three dimensional reconstruction of different plastic phantoms, organic material and beating human heart was achieved by utilizing a standard roentgen television system In continuous stabilized fluoroscopy the television images of the object obtained from different projections were digitized in real time and computerized for reconstruction Despite a cone beam being used, the spatial resolution seems to be quite adequate for evaluation of gross anatomic structures like the cardiac walls without enhancement by contrast medium.

ZUSAMMENFASSUNG

Eine drei-dimensionale Rekonstruktion verschiedenen Plastik-Phantome, organischen Materials und des schlagenden menschlichen Herzens wurden unter Verwendung eines Standard Rontgen-Fernseh-Systems vorgenommen Bei kontinuierlicher stabilisierter Durchleuchtung wurden die Fernseh-Bilder vom Objekt, die in verschiedenen Projektionen erhalten worden waren, in der wirklichen Zeit digitalisiert und zur Rekonstruktion Computer-behandelt Obwohl ein konisches Strahlenbundel verwendet wurde, scheint die räumliche Auflosung zur Feststellung der groben anatomischen Strukturen wir die der Herzwände vollständig adäquat, ohne Anwendung von Kontrastmittel, zu sein

RÉSUMÉ

Les auteurs ont fait au moyen d' [illegible] pour l'étude de structures anatomiques volumineuses telles que les parois cardiaques, sans renforcement du contraste

REFERENCES

AMBROSE J Computerized transverse axial scanning (tomography) Part 2 Clinical application Brit J Radiol 46 (1973), 1023

CROWTHER R A and KLUG A Three dimensional image reconstruction on an extended field—a fast, stable algorithm Nature 251 (1974), 490

EKSTROM M P Digital image processing at Lawrence Livermore Laboratory, Part I Diagnostic radiology applications IEEE Computer Society Computer 7 (1974), 72

HOUNSFIELD G N Computerized transverse axial scanning (tomography) Part I Description of the system Brit J Radiol 46 (1973) 1016

LANTZ B *A methodologic investigation of roentgen videodensitometric measurement of relative flow* University of California Press Davis 1974

— and LINDBERG B Speed of response of a 50 Hz and a 250 Hz TV system Acta radiol Diagnosis 16 (1975) 407

— and STRID K G Contrast formation in fluoroscopic videodensitometry II A comparison between theoretically computed and experimentally measured contrast Acta radiol Diagnosis 14 (1973) 625

— — (a) Contrast formation in fluoroscopic videodensitometry III Relation between roentgen tube potential and exposure rate to produce constant video level Acta radiol Diagnosis 16 (1975) 65

— — (b) Spectral variation of the conversion factor of an image intensifier Acta radiol Diagnosis 16 (1975) 273

LINDBERG B Videokymography—an improved method for electrokymography Technical Report No *18* Chalmers University of Technology School of Electrical Engineering Gothenburg 1972

OPPENHEIM B E More accurate algorithms for iterative three dimensional reconstruction IEEE Transactions on Nuclear Science NS 21 (1974)

ROBB R A GREENLEAF J F RITMAN E L JOHNSON S A SJOSTRAND J D HERMAN G T and WOOD E H Three dimensional visualization of the intact thorax and contents A technique for cross sectional reconstruction from multiplanar X ray views Computers Biomed Res 7 (1974) 395

ROWLAND S W SNARK—a picture reconstruction framework M S project Department of Computer Science State University of New York at Buffalo Departmental Report 51-72 (1972) 47

STRID K G and LANTZ B Contrast formation in fluoroscopic videodensitometry I A mathematical model for optimising contrast in radiography Acta radiol Diagnosis 14 (1973) 395

FROM THE DEPARTMENT OF DIAGNOSTIC RADIOLOGY (DIRECTOR PROF U RUDHE), HUDDINGE SJUKHUS, S 141 86 HUDDINGE, AND THE DIVISION OF MAXILLO-FACIAL ROENTGENOLOGY (DIRECTOR DOCENT U WELANDER), DEPARTMENT OF RADIOLOGY, CENTRALLASARETTET, S 961 19 BODEN, SWEDEN

PHOTOGRAPHIC SUBTRACTION

I Theory of the subtraction image

CH HÅRDSTEDT and U WELANDER

The subtraction procedure was introduced by ZIEDSES DES PLANTES (1934), but remained more or less unknown for several decades, being used only to a limited extent It was not adopted as a routine method until after rapid serial angiography had been developed (SJÖGREN & FREDZELL 1953, GREITZ 1956)

Subtraction can be carried out with black and white techniques using photographic (ZIEDSES DES PLANTES 1934 1961, HANAFEE & STOUT 1962, LEVICK & MITCHELL 1962 VEZINA & MCRAE 1962, HORENSTEIN et coll 1964) or electronic methods (HOLMAN & BULLARD 1963 OOSTERKAMP 1966), or by means of color addition using photographic optical or electronic procedures (DJINDJIAN 1964, FREY & NORMAN 1965, WISE & GANSON 1965, SCHWARZ 1966, OOSTERKAMP et coll 1966, DECKER et coll 1967 GROH & HAENDLE 1968)

Whatever method is applied the purpose of the subtraction procedure is to eliminate disturbing image noise in order to facilitate the detection and perception of diagnostically significant information The prerequisite for the use of subtraction is that the information obtained represents the difference between two roentgen images which are identical *in other respects* One of the images will then contain both the desired and the undesired information, or image noise and the other contains the

Submitted for publication 4 December 1974

noise alone and can thus be used for elimination of the noise from the image containing the diagnostic information.

The essential requirements for a satisfactory subtraction procedure were set forth by ZIEDSES DES PLANTES, the original films should be printed within the 'straight' part of the characteristic curve of the masking film, this film should have a contrast corresponding to $\gamma = 1$, and the final subtraction image should have higher contrast, or $\gamma > 1$

The aim of this report is to define as exactly as possible, with the aid of physical parameters, the theoretic prerequisites of an optimum subtraction technique.

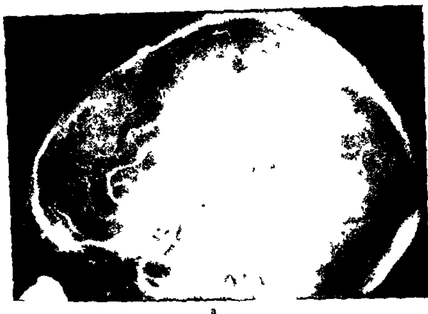
The subtraction image

The optimum angiographic subtraction image contains as regards the blood vessels filled with contrast medium all the information present in the original image while other information in the original, the image noise, has been eliminated The following conditions are valid for such an image

All structures in the image except the vessels must have as small density variations as possible *The medium-filled vessels stand out against the background of subtracted* structural details A positive subtraction image is to be preferred, in the positive image all the information regarding the vessels is present because it is exposed to a density above the background density Should the subtraction image be a negative the vessels would have a lower density than the background, this would entail a risk that part of the information regarding the vessels could be lost in a too low density range, especially in an image of low overall density

In order to ensure optimum conditions for detection and perception of small vessels and of vessels of low contrast the background in the subtraction image should have the density at which the eye's ability to distinguish the lowest perceptible contrast in ordinary viewing light is utilized to the full RÖHLER (1967) points out that the intensity of ordinary viewing light in roentgen diagnostic work allows contrast to be viewed at an optimum up to a density of 1 It was found by WIDENMANN et coll (1962) that an average film density of 0 7 above fog level was most suitable regarding both the characteristic film curve and the ordinary types of viewing light Thus, it seems to be preferable to expose subtraction images to a density of about 1

The contrast in the subtraction image should be high If the contrast is too low the smallest vessels and those with low contrast cannot be distinguished Conversely, if the contrast is too high the density in the image will be irregular and mottled a *noise* arises which lowers the information level (DE BELDER 1972) With the conditions prevailing at routine angiography, the contrast in the subtraction image should at least correspond to a γ value above 1 5 The upper limit of the γ-value cannot be defined but it should be as high as possible with retention of even density in the background of subtracted structures



a



b

Fig 1 a) Original Medichrome film b) Reproduction of a subtraction image that meets the requirements for an optimum subtraction The skeletal background has a density of 1 1 ± 0 05 in the original and the contrast corresponds to 1 5 γ 2

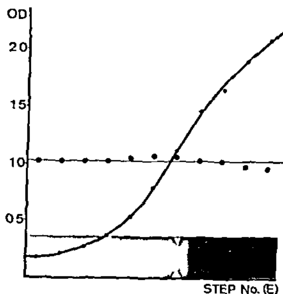


Fig 2 Experimental subtraction of a step wedge When the subtraction procedure is optimized densities from fog level to 2 can be equalized satisfactorily in the subtraction image the equalized densities exhibit a low peak due to the S shaped form of the characteristic curve of the masking film (Medichrome original film masking film GO23p Agfa Gevaert subtraction film N33p Agfa Gevaert)

The subtraction image should reproduce all structures in the original which are not subtracted down to a size corresponding at least to 3 lines/mm, a value close to the borderline at which the modulation transfer function approaches zero for both the film screen system (ROSSMAN 1964, RÖHLER 1967) and the eye at ordinary viewing distance (ORHALG 1971)

A subtraction image with the properties described can be produced only if the original and masking films meet certain requirements

The original films Optimum subtraction of the image noise in a series of roentgen films requires identical projections, in addition the exposure factors and film-screen combinations must be the same, so that both contrast and density in the images will be identical

In photographic subtraction, total contrast equalization of all densities from fog level to maximum density cannot be achieved All structures to be subtracted should cover a density range which corresponds to the straight part of the characteristic curve of the masking film The structures should therefore be exposed so that the maximum density difference within these structures is about 1 5 to 1 8, the adequate range being dependent on the properties of the masking film used

The smaller the density differences between the structures to be subtracted the better is the equalization of the contrast in the final subtraction image Thus, for technical reasons, the original image should have low contrast As this has a negative effect on both detection and perception of the diagnostic information, the original films should be exposed using the tube potential that provides for optimum absorption of the radiation by the contrast medium used With the iodinated media, this means a tube potential of about 70 kV

The mask The ideal masking film should reproduce the densities of the original in reverse, but with the contrast retained All structural details to be subtracted must be exposed within the straight part of the characteristic film curve with an average density in the middle of this straight part, usually of about 1 The exposure should give a lowest density of at least 0 25 above fog level within structures that are to be subtracted

Application A simple, routine method for the production of subtraction images has been worked out on the basis of these criteria (HÅRDSTEDT et coll 1976) A subtraction image that within practical limits meets the necessary requirements is illustrated in Fig 1 It was prepared with Medichrome original film (DE BELDER & BOLLEN 1972) The subtracted structures have a density of 1 1 $\pm$ 0 05, measured with a McBeth densitometer, within the areas where the blood vessels are depicted, the γ-value corresponds to 1 5 $< \gamma <$ 2

Some variation of the density of the subtracted structural details must be accepted in the subtraction image Due to the S-shaped form of the characteristic curve of the masking film, present even in the so-called straight part, it is in practice im-

36–753841

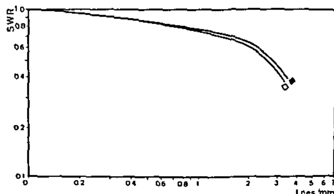


Fig 3 Square wave response (SWR) for an original Medichrome image before (■) and after (□) subtraction The difference between the functions is <4 %, down to 3 lines/mm The resolution and contrast in the original have been transferred almost unchanged to the subtraction image

possible to achieve a total equalization of contrast by the subtraction technique This is valid also when the original and the mask have optimum properties With an optimum subtraction procedure, the variation in density of subtracted structures is small, however, and in the ideal case it varies symmetrically in the subtraction image around the density that corresponds to that in the masking film of about 1 (Fig 2)

In order to analyse the reproduction of contrast and resolution in the subtraction image the square wave response has been calculated for the subtraction technique used (Fig 3) It turns out that structural details in the original image can be transferred to the subtraction image, with the contrast retained almost completely, down to a frequency close to 3 lines/mm This means that the technique used is optimal

Discussion

The purpose of using subtraction in connection with angiography is to demonstrate the blood vessels free of superimposed disturbing image noise without loss of diagnostically relevant information concerning the vessels Thus, photographic principles have to be applied in such a way that optimum appearance of the vessels will be achieved in the subtraction image

It is not possible, in practice, to prevent some decrease in resolution in the prints during the procedure of subtraction The reduction of the information present in the original image, measured with the square wave response (Fig 3), is however surprisingly small, the difference between the functions for a Medichrome image before and after subtraction is less than 4 per cent, down to 3 lines/mm This means that the technique used provides subtraction images with high resolution and satisfactory reproduction of contrast, in accordance with the criteria described for optimum subtraction The square wave response was calculated under laboratory conditions, using a linear grid It is probable however that in routine work the result might come out less satisfactorily owing among other things to difficulties when adjusting the original film to the mask

The subtraction technique usually is described as a method for eliminating the

skeletal structures in the film It would however seem more appropriate to apply the term image noise to the structural details that contain no diagnostic information A desire to eliminate the image of the bones is perhaps the reason why subtraction images are often prepared with too low density This results in a failure to obtain optimum diagnostic information regarding the blood vessels The disturbing effect of the image noise is eliminated when the contrasts within it are equalized The background of subtracted structural details can then be given a sufficient exposure to provide for the diagnostic information present in the subtraction image to appear with a density satisfactory for detection and perception

An optimum subtraction technique is a prerequisite for further treatment of the films for instance the preparation of multicolor combination images (WELANDER 1969 EKLUND et coll 1973, SCHAMPI & WELANDER 1973)

SUMMARY

The purpose of subtraction of angiographic images is to demonstrate the vessels free of superimposed disturbing image noise With the aid of physical film parameters the theoretic basis for an optimum subtraction technique is presented

ZUSAMMENFASSUNG

Die Absicht der Subtraktion von angiographischen Bildern ist die Gefasse frei von uber lagerten storenden Bild Gerauschen darzustellen Mit Hilfe physikalischer Film Parameter wird die theoretische Basis fur eine optimale Subtraktions Technik gegeben

RESUME

Le but de la soustraction d images angiographiques est de mettre en évidence les vaisseaux sans superposition d image genante Les auteurs présentent la base théorique d une technique optimale de soustraction fondée sur les paramètres physiques du film

REFERENCES

DE BELDER M Quantenrauschen Kornigkeit und Detailerkennbarkeit Rontgenblätter 25 (1972) 322

— and BOLLEN R Medichrome a new X ray film yielding more detail X ray Bulletin (1972) No 18 3

DECKER K LINCKE H O und OOSTERKAMP W J Die Beurteilung von Rontgenbildern und ihre Erleichterung durch Farbsubtraktion S 78 Deutscher Rontgenkongress Baden Baden 1967

DJINDJIAN R L angiographie en couleurs en neuroradiologie (Une méthode nouvelle de soustraction en couleurs) Atlas Radiol clin 72 (1964) 1

EKLUND S, JEVBRATT L, SCHAMPI B and WELANDER U The diazo method A simplified method of preparing multicolor combination images for use in roentgen diagnosis Acta radiol Diagnosis 14 (1973), 33
FREY H S and NORMAN A Radiographic subtraction by color addition Radiology 84 (1965), 123
GREITZ T A radiologic study of the brain circulation by rapid serial angiography of the carotid artery Acta radiol (1956) Suppl No 140
GROH F und HAENDLE J Harmonisierung und Farbsubtraktion Electromedica 3 (1968) 73
HANAFEE W and STOUT P Subtraction technic Radiology 79 (1962), 658
HOLMAN C B and BULLARD F D The application of closed circuit television in diagnostic roentgenology Proc Mayo Clin 38 (1963), 67
HORENSTEIN R, LUNDH A and SJOGREN S E The subtraction method Acta radiol Diagnosis 2 (1964), 264
HÅRDSTEDT CH, RUNDELIUS B and WELANDER U Photographic subtraction II Technical aspects and method To be published in Acta radiol Diagnosis 17 (1976)
LEVICK R and MITCHELL J Simplified method of subtraction and its application to renal aortography Brit J Radiol 35 (1962), 843
OOSTERKAMP W J Progress in recording the radiographic image Medica mundi 11 (1966) 118
— VAN T HOF A P M und SCHREN W J L Rontgenfarbbilder neue Moglichkeiten der Subtraktion durch Fernsehtechnik, S 168 Deutscher Rontgenkongress, Berlin 1966
— — and TEUNISSEN P G A L New methods of television display of roentgenological information in black and-white and in color J Soc Motion Pict Telev Engrs 77 (1968), 1290
ORHAUG T Bilder, bildinformation bildbearbetning (In Swedish) FOA 2 report A 2538 51 FOA Repro, Stockholm 1971
ROSSMAN K Measurement of the modulation transfer function of radiographic systems containing fluorescent screens Phys in Med Biol 9 (1964), 551
ROHLER R Physiologische Probleme der Betrachtung des Rontgenbildes Rontgenblatter 20 (1967), 79
SCHAMPI B and WELANDER U Important sources of artefacts in multicolor angiographic combination images Acta radiol Diagnosis 14 (1973) 177
SCHWARZ G S Subtraction radiography by means of additive color Radiography 87 (1966), 445
SJOGREN S E and FREDZELL G Apparatus for serial angiography Acta radiol 40 (1953), 361
VEZINA J L and MCRAE D L A simple method of subtraction radiography J Canad Ass Radiol 13 (1962), 123
WELANDER U Multicolor combination images in subtraction angiography A new photographic method and its applications Acta radiol (1969) Suppl No 290
WIDENMANN L, WEMBER M und SCHOTT O Untersuchungen uber den Einfluss des Strahlenreliefs auf die mittlere Filmschwarzung — eine bei Belichtungsautomaten auftretende Fragestellung Rontgenblatter 15 (1962), 97
WISE R E and GANSON J Subtraction of radiographic images by color addition Lahey Clin Bull 14 (1965), 131
ZIEDSES DES PLANTES B G Planigrafie en subtractie (In Dutch) Kemink en Zoon Utrecht 1934
— Subtraktion Thieme Verlag, Stuttgart 1961

FROM THE SECTION FOR MAXILLO-FACIAL ROENTGENOLOGY, DEPARTMENT OF RADIOLOGY, CENTRALLASARETTET, S-961 19, BODEN, SWEDEN

FORM DISTORTION IN NARROW BEAM ROTATION RADIOGRAPHY

ANDERS SJOBLOM, KJELL-ARNE SÄMFORS and ULF WELANDER

In panoramic images obtained with the aid of narrow beam rotation radiography distortion effects specific for this imaging system occur Outside the centre of an object plane, which is depicted without blurring and distortion, different magnification factors are valid in the horizontal and vertical directions The combined effect of the different horizontal and vertical dimensions in the panoramic image give rise to distortion of the angles by which obliquely positioned structural details are depicted in the image The disproportionality between the height and length measurements of the image also affects the magnification of an area SÄMFORS & WELANDER (1974) have explained the geometrical cause and calculated mathematically these distortion effects, denominated as angle and area distortion An additional consequence of the specific projection geometry of narrow beam rotation radiography is distortion of the morphology of the object, form distortion

Distortion phenomena in panoramic images have been described *empirically* (UPDEGRAVE 1966, LANGLAND & SIPPY 1968) and analysed experimentally by measurements made in the horizontal and vertical planes (KITE et coll 1962, VON SCHOPF 1966, ZACH et coll 1969, HEDIN 1971, ROWSE 1971, SELLE & SCHNEUZER 1972, MCIVER et coll 1973) The dimensional reproduction of the image layer was described by TAMMISALO (1964), but his mathematical expression for the horizontal

Submitted for publication 29 November 1974

dimension is not valid outside the centre of the object plane which is depicted distortion free

In the present report the form distortion is calculated mathematically using simple geometrical ground forms as models The reliability of the mathematical calculations was tested experimentally

The mathematical expressions used in the following were deduced in previous works by WELANDER (1974) and SÄMFORS & WELANDER (1974)

Form distortion

Definitions (See Fig 1)

h_0 = vertical distance in the object
h_f = length of the distance h_0 projected on the film
d_0 = horizontal distance in the object
d_f = length of the distance d_0 projected on the film
r = distance from rotation centre of the beam to the centre of the object plane depicted without blurring, 'object projection radius'
Δr = positive or negative increment given to the object projection radius, r
R = film radius
ω_0 = angular velocity of the beam
ω_f = angular velocity of the film
D = distance tube target to object
A = distance tube target to film

Geometrical models The square, the rhomb, the equilateral triangle, and the circle were chosen as the geometrical ground forms in the analysis of the form distortion In the horizontal plane the length dimension in the image of these geometrical figures may be calculated from

$$d_f = \frac{d_0 R \omega_f}{(r+\Delta r)\omega_0} \tag{1}$$

In rotation narrow beam methods that plane in the object is depicted without blurring, where the equation $R\omega_f/r\omega_0 = A/D$ is valid Therefore the equation above may be simplified by substitution

$$d_f = \frac{d_0 r A}{D(r+\Delta r)} \tag{2}$$

In the vertical plane the height dimensions in the image of the geometrical figures may be calculated from

$$h_f = \frac{h_0 A}{(D+\Delta r)} \tag{3}$$

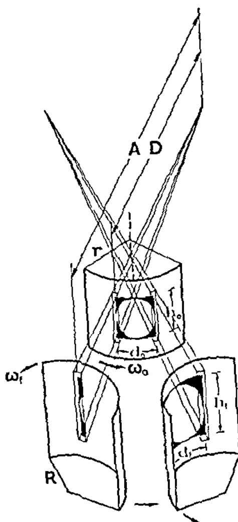


Fig 1 The principle of rotation narrow beam radiography A square object detail with an inscribed circle is exposed Between the two positions I and II a continuous movement takes place

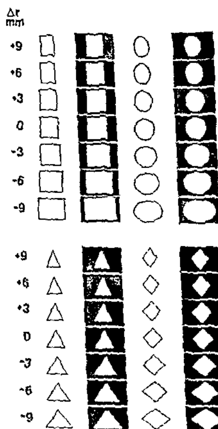


Fig 2 Form distortion of the square, the circle, the equilateral triangle, and the rhomb when placed in different positions in relation to the object plane, successive displacement 3 mm Orthopantomograph 3, frontal rotation centre, r – 28 mm Calculated form distortion to the left, experimentally exposed images to the right The latter seem to be wider in the horizontal plane than the calculated forms This effect is due to the blurring outside the sharply depicted object plane Measured at the centre of the blurred zone the experimentally exposed images are in total agreement with the calculated forms

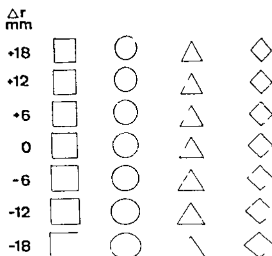
The length and the height of the geometrical ground forms chosen are the same, $d_0 = h_0$, with the exception of the equilateral triangle where

$$h_0 = \frac{d_0}{2}\sqrt{3} \tag{4}$$

The distortion of the square, the rhomb, and the equilateral triangle may be calculated directly from the length and height measurements The distortion of the circle is however more complicated but may be calculated from the following expression

$$y = \pm\frac{h_r}{2}\sqrt{1 - \frac{x^2}{\left(\frac{d_r}{2}\right)^2}} \tag{5}$$

which is deduced using the equation of the ellipse of which the circle is a special case



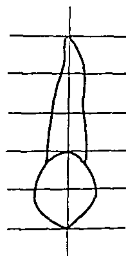


Fig 3   Fig 4

Fig 3 Calculated form distortion of the square, the circle, the equilateral triangle, and the rhomb when placed in different positions in relation to the object plane, successive displacement 6 mm Orthopantomograph 3, lateral rotation centre, r 96 mm

Fig 4 Measurements made on a tooth to calculate the form distortion of relevant structural details

With the values for the object projection radii and for the target to object and target to film distances that apply in the Orthopantomograph 3, the distortion of the four geometrical ground forms is illustrated in Figs 2 and 3 Control measurements in images of the four geometrical forms exposed in the Orthopantomograph were consistent with the calculated measurements, in Fig 2 the experimentally exposed images appear parallel to the mathematical calculation of the form distortion

Teeth The distortion of a frontal tooth, a canine, and a molar were calculated to determine the effect of the form distortion on structural details relevant in a panoramic image The vertical length of the teeth was measured and a series of horizontal measurements were performed (Fig 4) From these data the expected form in images of the teeth was calculated for different positions of the teeth towards the rotation centre and towards the film The teeth were then exposed in the Orthopantomograph when placed in corresponding positions, and the distances in the images measured, the calculated forms of the teeth and the experimentally exposed images were consistent and appear side by side in Fig 5

Characteristics When the position of the object coincides with the object plane depicted without blurring the image is magnified but not distorted Distortion occurs when the object is placed outside the sharply depicted plane When the object is positioned towards the rotation centre the magnification increases, slightly in the vertical direction but markedly in the horizontal direction, when the object is positioned towards the film the magnification decreases, slightly in the vertical direction but markedly in the horizontal direction The resultant effect of this discrepancy is

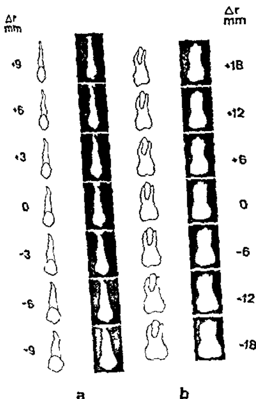


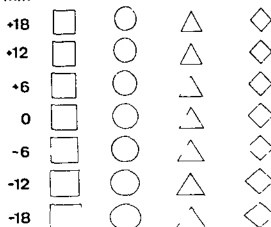
Fig 5 Form distortion of teeth Calculated form distortion to the left, experimentally exposed images to the right a) canine, Orthopantomograph 3, frontal rotation centre, r = 28 mm, successive displacement 3 mm. b) molar, Orthopantomograph 3, lateral rotation centre, r = 92 mm successive displacement 6 mm

that the square appears in the image as a *rectangle* with its long side horizontally when positioned towards the *rotation centre*, and its long side vertically when positioned towards *the film* The circle appears as an ellipse, when positioned towards the rotation centre its long axis is horizontal, and when positioned towards the film its long axis is vertical The *equilateral triangle* appears as an isosceles triangle, when positioned towards the *rotation centre its top angle is* $>60°$, and when positioned towards the film its *top angle is* $<60°$ The rhomb *is depicted in* such a way that *it* will have a long axis horizontally when *positioned towards* the rotation centre, and a long axis vertically when positioned towards *the film*

The most apparent *effect of the form* distortion on the teeth is the variation in the width

Discussion

The specific type of distortion occurring *in narrow* beam rotation methods is due to their special geometrical projection *technique* In the vertical plane the magnification of the image is dependent on a *central* projection which has the tube target as



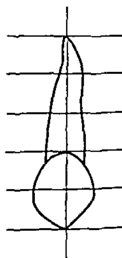


Fig 3   Fig 4

Fig 3 Calculated form distortion of the square the circle, the equilateral triangle and the rhomb when placed in different positions in relation to the object plane, successive displacement 6 mm Orthopantomograph 3 lateral rotation centre, r 96 mm

Fig 4 Measurements made on a tooth to calculate the form distortion of relevant structural details

With the values for the object projection radii and for the target to object and target to film distances that apply in the Orthopantomograph 3, the distortion of the four geometrical ground forms is illustrated in Figs 2 and 3 Control measurements in images of the four geometrical forms exposed in the Orthopantomograph were consistent with the calculated measurements, in Fig 2 the experimentally exposed images appear parallel to the mathematical calculation of the form distortion

Teeth The distortion of a frontal tooth, a canine, and a molar were calculated to determine the effect of the form distortion on structural details relevant in a panoramic image The vertical length of the teeth was measured and a series of horizontal measurements were performed (Fig 4) From these data the expected form in images of the teeth was calculated for different positions of the teeth towards the rotation centre and towards the film The teeth were then exposed in the Orthopantomograph when placed in corresponding positions, and the distances in the images measured, the calculated forms of the teeth and the experimentally exposed images were consistent and appear side by side in Fig 5

Characteristics When the position of the object coincides with the object plane depicted without blurring the image is magnified but not distorted Distortion occurs when the object is placed outside the sharply depicted plane When the object is positioned towards the rotation centre the magnification increases, slightly in the vertical direction but markedly in the horizontal direction, when the object is positioned towards the film the magnification decreases, slightly in the vertical direction but markedly in the horizontal direction The resultant effect of this discrepancy is

utilise comme modeles le carre, le cercle, le losange et le triangle équilateral Ils analysent et decrivent les caracteristiques générales de la distorsion de forme dans la radiographie rotatoire avec faisceau étroit

REFERENCES

HEDIN M Distorsionsforandringar av tander och tandgrupper i ortopantomogram (In Swedish) Svensk Tandlak T 64 (1971), 63

KITE O W SWANSON L T, LEVIN S and BRADBURY E Radiation and image distortion in the Panorex X ray unit Oral Surg 15 (1962), 1201

LANGLAND O E and SIPPY B S Anatomic structures as visualized on the orthopantomogram Oral Surg 26 (1968), 475

McIVER F T, BROGAN D R and LYMAN G E Effect of head positioning upon the width of mandibular tooth images on panoramic radiographs Oral Surg 35 (1973), 698

ROWSE C W Notes on interpretation of the orthopantomogram Brit dent J 130 (1971), 425

SELLE G und SCHNEUZER B Interpretation des Orthopantomogrammes—metrische und qualitative Untersuchungen Schweiz Mschr Zahnheilk 82 (1972), 1153

VON SCHOPF P Langen und Winkelmessungen am Orthopantomogram Fortschr Kiefer-orthop 27 (1966 [illegible]

— — Area distortion in narrow beam rotation radiography Acta radiol Diagnosis 15 (1974) 650

TAMMISALO E H The dimensional reproduction of the image layer in orthopantomography Suom Hammaslaak Toim 60 (1964), 2

UPDEGRAVE W J The role of panoramic radiography in diagnosis Oral Surg 22 (1966), 49

WELANDER U A mathematical model of narrow beam rotation methods Acta radiol Diagnosis 15 (1974), 305

— Layer formation in narrow beam rotation radiography Acta radiol Diagnosis 16 (1975) 529

ZACH G A, LANGLAND O E and SIPPY B S The use of the orthopantomograph in longitudinal studies Angle Orthodont 39 (1969), 42

the focus Thus, starting from the centre of the object plane, or image layer, the magnification factor increases towards the tube target, and decreases towards the film, the magnification factor in the vertical plane is a linear function In the horizontal plane, i e the rotation plane, the magnification is dependent on a central projection which is specific for narrow beam rotation radiography where the rotation centre of the beam serves as an imaginary functional focus (WELANDER 1974 1975) The magnification factor in this central projection increases from the object plane towards the rotation centre of the beam and decreases towards the film the magnification factor in the horizontal plane is a non linear function The variation *of the magnification factor in the vertical plane is small but it is marked in the horizontal plane* The combined effect of the different magnification factors of the two central projections mentioned gives rise to the characteristic distortion effects of narrow beam rotation radiography

The distortion is most marked when the object projection radius is small or the distance between the object and the centre of the sharply and without distortion depicted object plane is great The form distortion in the panoramic image may be considerable when the object position does not coincide with the centre of the object plane, especially when the object projection radius is small as in the frontal region (Figs 2, 5 a) The form distortion is less in the lateral parts of the image (Figs 3, 5 b)

It is of great importance to be aware of the distortion effects in the panoramic image when analysing a roentgen image To avoid an unnecessarily large image distortion the patient should always be placed carefully in the correct position at the exposure Assessments of the morphology should be made with some caution on the basis of the panoramic image, and this is especially true for the frontal region

SUMMARY

The distortion of morphologic object elements form distortion at the exposure of a panoramic image has been determined mathematically and experimentally As models the square the circle, the rhomb and the equilateral triangle were used *The general characteristics* of the form distortion in narrow beam rotation radiography are analysed and described

ZUSAMMENFASSUNG

Die Verzerrung morphologischer Objekt Elemente wurde mathematisch und experimentell bei der Exposition eines Panorama Films bestimmt Als Modelle wurden das Quadrat der Zirkel der Rhombus und der aquilaterale Triangel verwendet Die generellen Charakteristika der Form Verzerrung bei der Fein Strahl Rotations Radiographie wird analysiert und beschrieben

RESUME

Les auteurs ont determiné experimentalement et mathématiquement la distorsion d éléments morphologiques de l objet au cours de la prise d une image panoramique Ils ont



Fig 1 Detail of shoulder joint with massive calcification of the subdeltoid bursa a) Negative b) positive development A bright halo exists around the calcification in (b) which is not present in (a)

plate to record the oedematous blurring of a fatty layer has not been fully analysed The xerox plate tends to display contours alone so that the surroundings on both sides of the contour differ but little in blackening. This effect is called edge contrast enhancement The diagnostic information inherent in an inflammatory blurring of fat tissue rarely gives rise to contours, and so it appeared justified to compare the xerox technique with that of DEICHGRABER & OLSSON (1975) replacing the film by the plate

Experiments

Preliminary experiments were carried out in order to develop a technique that could be systematically compared with the industrial film technique Plates manufactured by the Rank Xerox corp were used (system 125) The electrostatic loading before exposure can be set at four levels The highest loading (D) was empirically found to be recommendable The development can be performed in a negative and a positive fashion, the former giving rise to bright image [illegible]

[illegible] xerox plate always has a bright and a dark component side by side The bright component was broader, appearing as a sort of halo With negative development (Fig 1 a) the halo deriving from high absorbing

FROM THE DEPARTMENT OF DIAGNOSTIC RADIOLOGY III (DIRECTOR C-G HELANDER),
SAHLGRENSKA SJUKHUSET, S-411 32 GOTHENBURG, SWEDEN

SOFT TISSUE XERORADIOGRAPHY OF THE SHOULDER JOINT

S REICHMANN, K ÅSTRAND, E DEICHGRABER and B OLSSON

Originally it was LEB (1961) who suggested that peritendinitis of the shoulder could be demonstrated by means of soft tissue films However, he did not refine his technique, nor did he publish any figures concerning the reliability of the method DEICHGRÄBER & OLSSON (1975) presented a technique arrived at by means of systematic experiments When this technique was used in patients with shoulder pains, the presence of soft tissue oedema and displacement of the deltoid muscle were found to correspond with clinical signs of peritendinits Industrial non screen film of medium sensitivity and with a high silver content was used, as such a film was found to be superior for soft tissue radiography by DEICHGRABER et coll (1974) A later attempt to use screen-film combinations of higher sensitivity in order to reduce the radiation dose to the patient failed, the image quality was too much impaired (DEICHGRABER et coll 1975) Likewise, K-edge filtering in combination with a tungsten target tube did not give any dose reduction (DEICHGRABER & REICHMANN 1975) Aluminium filtration, on the other hand, reduced the incident dose to the patient to about 60 per cent without affecting image contrast Unfortunately, this filtration led to such increase in the exposure times as to be of dubious value

Reports indicating the xeroradiographic medium to be useful in soft tissue radiography have appeared (WOLFE 1968, BOAG et coll 1972) but the ability of the xerox

Submitted for publication 3 April 1975

(8 males 14 females, aged 14 to 86 years) with pains in the shoulder region In one subject both shoulders were examined thus, the material consisted of 23 joints, 13 right sided With each technique two a p views were obtained, one with the shoulder joint in internal and one in external rotation The patients had to be repositioned when the recording medium was changed Thus, the film and xerox views were not quite identical Still, it was possible to determine whether the two different examinations would give the same diagnosis

Corresponding results were obtained with the two methods except in one case where the films gave evidence of a strictly localized blurring of the subdeltoid fatty layer, not detected in the xerox plate Slight projection differences might have caused this effect, since small blurrings were otherwise detectable in the xerox plates as well A normal and a blurred fatty layer are demonstrated in Fig 2 In the whole material a blurring was noted in 14 joints

The film technique has been found to give an average dose of 0 42 rad per image By means of an ionization chamber the relative dose was measured for the xerox technique The average dose was found to be 0 16 rad per image, the reduction being 0 26 rad per image in absolute figures, i e a reduction of 62 per cent

Discussion

The experiences gained indicate that xeroradiography makes possible soft tissue examinations of the shoulder at a lower dose level and with less tube load than any good film technique availabe today The reliability of the xerox method appears to be the same as that of the film technique by the method of DEICHGRABER & OLSSON No loss of quality occurred despite the dose reduction

The lowered tube load of xeroradiography means an important advantage With the film technique used, a total filtration of 2 25 mm Al was to be preferred as it gave a marked dose reduction without lowering the image contrast (DEICHGRÄBER & REICHMANN) However, this filtration tended to make the exposure times too long, why the lower filtration of 0 5 mm Al had to be accepted An important part of the dose reduction obtained with the xerox plate is due to the increased filtration This filtration (2 mm Al) is standard in conventional roentgen tubes, which means that no other special equipment is required than the xerox plates and their loading and developing machines

SUMMARY

Soft tissue xeroradiography of the shoulder joint has been compared with a film technique arrived at previously The xerox plates gave a lo[illegible]
loss of information The film technique requir[illegible]
glass window (~0 5 mm Al) while the xerox [illegible]

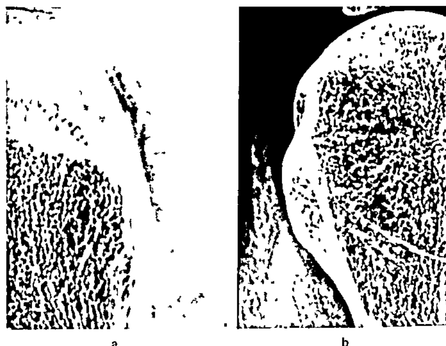


Fig 2 Xeroradiography a) Shoulder joint without abnormality and b) with extensive blurring of the fatty layer The subdeltoid fatty layer (→) is only partly visible in (b) due to the presence of inflammatory oedema

structures was superimposed upon these structures and not the tissues surrounding them, as was the case with positive development (Fig 1 b) Similar observations have been made with respect to osteosynthesis materials by FRIEDMANN et coll (1974) Thus negative development was found preferable

It is well known that the xerox plate tolerates higher tube potentials and higher levels of secondary radiation than film (SCHERTEL et coll 1974, SELIN et coll 1975) A phantom consisting of nylon wires of different dimensions in a 7 cm layer of vegetable oil was used to find out the appropriate tube potential Agfa-Gevaert Mamoray T 3 industrial film was exposed with 40 kV tungsten target and 0 5 mm Al total filtration and the xerox plates with potentials between 40 and 110 kV A tube potential of 110 kV appeared to give similar visibility of the wires on xerox plates as 40 kV on industrial films However, a lower potential was chosen for the definite testing for two reasons Initial clinical examinations indicated that the demonstration of fat tissue blurring would require softer radiation with the xerox plate than was suggested by the phantom experiments, where only sharp contours were recorded. Secondly, previous experience (DEICHGRABER & OLSSON) had suggested that although the signal/noise ratio in the film technique was acceptable, a certain improvement was still to be desired Thus, a final potential of 60 kV was arrived at This was combined with 2 mm Al as total filtration

The final comparison between the two techniques was carried out in 22 patients

FROM THE DEPARTMENTS OF NEUROLOGY AND DIAGNOSTIC RADIOLOGY, UNIVERSITY HOSPITAL, S-221 85 LUND, SWEDEN

CEREBRAL DISTRIBUTION OF CONTRAST MEDIUM AND PARADOXICAL LOCATION OF LESIONS OF THE BLOOD-BRAIN BARRIER IN THE RABBIT

P G JEPPSSON and T. OLIN

The neurotoxicity of contrast media has for many years been analysed by injection of media into the internal carotid artery of the rabbit Resultant lesions of the blood-brain barrier have been demonstrated by staining the brain parenchyma with trypan blue dye Such investigations have revealed that the lesion produced by contrast medium is sometimes most evident within the supply areas of the non-injected arteries (BROMAN & OLSSON 1948, 1949, JEPPSSON 1962, JEPPSSON & OLIN 1970)

Various explanations have been put forward BROMAN & OLSSON (1948) suggested that the cause was an embolus formed by the precipitation of contrast medium in the injection needle In their report of 1949, however, they regarded a herniation of the injected hemisphere as a more likely explanation JEPPSSON (1962) considered a retrograde filling of the carotid artery on the non-injected side or of the vertebral arteries as a possible explanation JEPPSSON & OLIN (1970) observed that paradoxical location of the lesion was more common with contrast media containing sodium

Serial magnification angiography should provide the means to record the course of the contrast medium through the vascular territories of the brain; a contrast medium with high sodium content, Isopaque 60 %, was used in our experiments since

Supported by grant from the Swedish Medical Research Board, Proj No B73-14X-605-07B
(P G J is now at the Department of Neurology, Centrallasarettet, S 291 85 Kristianstad, Sweden)
Submitted for publication 18 December 1973

ZUSAMMENFASSUNG

Die Weichgewebe-Xeroradiographie des Schultergelenks wurde mit einer zuvor ausgearbeiteten Film-Technik verglichen Die Xerox-Filme gaben dem Patienten eine niedrigere Strahlen-Dosis ohne Verlust von Information Die Film Technik verlangt eine Tungsten Schussziel Rohre mit einem besonders dunnen Glas-Fenster (≈0,5 mm Al), wahrend bei der Xeroxtechnik Standard-Rohren verwendet werden konnen

RÉSUMÉ

Les auteurs ont comparé la xéroradiographie des tissus mous de l articulation de l epaule avec une technique utilisant un film qu'ils avaient mise au point préalablement Les plaques xerox permettent de diminuer la dose de radiation au malade sans perte d information La technique avec film nécessite un tube a anode en tungstène avec une fenetre de verre très fin (≈0,5 mm Al), alors que la technique xerox peut être utilisée avec des tubes ordinaires

REFERENCES

BOAG J W, STACEY B and DAVIS R Xerographic recording of mammograms Brit J Radiol 45 (1972) 633

DEICHGRÄBER E and OLSSON B Soft tissue radiography in painful shoulder Acta radiol Diagnosis 16 (1975), 393

— and REICHMANN S Filtration in soft tissue radiography Acta radiol Diagnosis 16 (1975), 248

— — and BURÉN M Film quality in mammary radiography Acta radiol Diagnosis 15 (1974), 93

— — and STRID K-G Intensifying screens in soft tissue radiography Acta radiol Diagnosis 16 (1975), 54

FRIEDMANN G, MODDER U und TISMER R Xeroradiographische Befunde bei osteosynthetisch versorgten Frakturen Rontgen Bl 27 (1974), 586

LEB A Der rontgendiagnostische Beitrag zur Diagnose der Periarthrose und unspezifischen Periarthritis Wien klin Wschr 73 (1961) 141

SCHERTEL L, ZUM WINKEL K und SOULIER W Xeroradiographische Urographie und Cholezysto Cholangiographie Rontgen-Bl 27 (1974), 575

SELIN K, DEICHGRÄBER E and REICHMANN S Influence of secondary radiation on image quality Acta radiol Diagnosis 16 (1975), 520

WOLFE J N Xerography of the breast Radiology 91 (1968) 231

increase, then a decrease Slight bradycardia or no change at all of the pulse rate was registered The application time on the injected side varied from 13 0 to 18 0 seconds In the other hemisphere and in the basilar artery it varied between 6 5 and 13 5 seconds The lesion to the blood-brain barrier was most evident in the area supplied from the basilar artery, but in one experiment the non injected hemisphere was most injured In all animals the slightest lesions were on the injected side, and in one animal there was no injury at all on the injected side The areas with the most prominent lesions usually had the shortest application times

Series 2 (Fig 2) 5 animals Injection into the internal carotid artery at a rate of 0 089 ml/s during 15 seconds, i.e 1 32 ml of contrast medium The common carotid artery was ligated caudally A biphasic response of the blood pressure usually occurred during the injection The pulse was virtually unchanged The application time on the injected side varied from 13 0 to 18 0 seconds, in the other hemisphere between 9 0 and 14 0 seconds and in the area supplied by the basilar artery between 9 0 and 17 0 seconds The lesion of the blood–brain barrier was most evident in the area supplied by the basilar artery in two animals The injected hemisphere was most injured in one animal and the non injected hemisphere in another animal Finally, a lesion involved the whole brain of one animal In one of the animals no lesion at all was revealed in the injected hemisphere There was no consistent relation between the application time and the degree of severity of the lesion of the blood–brain barrier

Series 3 (Fig 3) 5 animals Injection into the internal carotid artery at a rate of 0 051 ml/s during 15 seconds, i e 0 76 ml of contrast medium The common carotid artery was ligated caudally The blood pressure usually fell slightly during the injection The pulse rate varied only slightly The application time in the injected hemisphere was 13 0 to 14 0 seconds In three experiments no contrast medium at all reached the other territories In the two remaining experiments the application time was 8 0 to 13 0 seconds in the non injected hemisphere In one of these experiments no contrast medium reached the basilar artery but in the other an application time of 12 0 seconds appeared within this area The lesion to the blood–brain barrier was most prominent in the injected hemisphere in all five experiments Minor lesions were revealed in the other areas although there was no visible application of contrast medium in two of these animals

Series 4 (Fig 4) 5 animals Injection into the internal carotid artery at a rate of 0 089 ml/s during 15 seconds i e 1 32 ml of contrast medium No ligation of the common carotid artery The blood pressure decreased during the injection in four animals and a biphasic response was registered in one Slight bradycardia sometimes appeared The application time in the injected hemisphere varied from 14 0 to 21 0 seconds but was intermittent in two animals and complete in one of these animals during only 4 0 seconds Partial filling of the other hemisphere was registered during 11 0 seconds in one animal No application of contrast medium was seen in territories outside the injected side in the remaining animals The lesion to the blood–

it had produced a paradoxical lesion of the blood-brain barrier in more than 50 per cent in a previous investigation (JEPPSSON & OLIN 1970)

Material and Methods

Thirty-seven rabbits were examined under general anaesthesia, obtained with intravenous sodium pentobarbitone (Mebumalnatrium, NFN, ACO, Sweden) Artificial respiration was given The arterial blood pressure was monitored electromanometrically through a catheter in the right femoral artery The left common carotid artery was exposed and the external carotid artery ligated Any anonymously arising occipital artery was ligated when present The common carotid artery was ligated caudally and cannulated The right carotid artery was exposed instead in one of the experimental series and the external branch ligated In these animals the right common carotid artery was catheterized with a catheter from the femoral artery Small amounts of Thorotrast aided during fluoroscopy to check the vascular anatomy Contrast medium, sodium metrizoate 60 % (Isopaque 350, Nyegaard, Norway= sodium metrizoate 528 mg/ml, calcium metrizoate 28 mg/ml, magnesium metrizoate 20 mg/ml, meglumine metrizoate 30 mg/ml), was injected with a constant rate infusion machine set to deliver 0 156, 0 089 and 0 051 ml/s during 15 seconds The injected volumes were 2 14, 1 32, and 0 76 ml, respectively In order to analyse the effect of a mixture of blood and contrast medium on the blood-brain barrier two further series of experiments were designed The infusion rate was set at 0 156 and 0 051 ml/s, respectively, and the injection was made intermittently with a cycle of about 3 4 seconds divided equally between injection and delay The injected volumes were 2 14 and 0 76 ml, respectively The distribution of the contrast medium to the cerebral vessels was registered in submentovertical projection

Roentgen technique 0 1 mm focal spot, direct fourfold magnification, 2 0 mAs, 0 04 s and 90 kV, high definition screens (Rubin, Siemens)

The time during which various vascular territories were filled with contrast medium (application time) was judged from the films The blood pressure, the exposures and the injection of contrast medium were recorded on a polygraph (Mingograf 800, Elema-Siemens, Sweden) The body temperature of the animal was kept at normal levels Lesions of the blood-brain barrier were registered by trypan blue administered as described by JEPPSSON & OLIN (1970)

Results

Seven animals were discarded due to damage to the internal carotid artery during the operative procedure and seven animals died during the infusion of trypan blue

Series 1 (Fig 1) 8 animals Injection into the internal carotid artery at a rate of 0 156 ml/s during 15 seconds, i e 2 14 ml of contrast medium The common carotid artery was ligated caudally A biphasic blood pressure reaction was noted first an

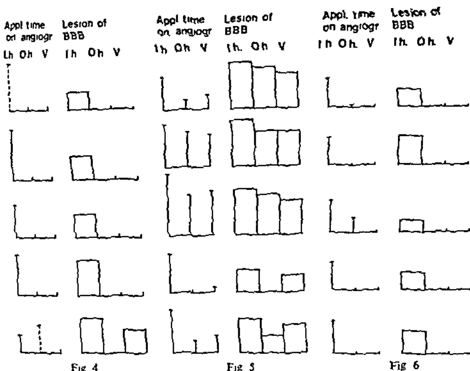


Fig 4 Fig 5 Fig 6

Fig 4 Injection into the internal carotid artery No ligation caudally Injection rate 0 09 ml/s Volume 1 32 ml

Fig 5 Intermittent injection into the internal carotid artery, ligated caudally Active injection rate 0 156 ml s Volume 2,14 ml

Fig. 6 Intermittent injection into the internal carotid artery, ligated caudally Active injection rate 0 051 ml s Volume 0 76 ml

to the blood-brain barrier The lesion, however, was marked even in the other areas

Series 6 (Fig 6) 5 animals Intermittent injection into the internal carotid artery during 30 seconds at a rate of 0 051 ml/s The actual injection time totalled 15 seconds, i e 0 76 ml contrast medium were given The common carotid artery was ligated caudally The blood pressure fell or rose moderately The pulse usually fell slightly. The application time was intermittent and amounted to 13 0 seconds in the injected hemisphere Application occurred in the opposite hemisphere in only two animals Lesion to the blood-brain barrier was registered in the injected hemisphere only

Comparison of lesions at intermittent and continuous injections

The brains exposed to intermittent injections were ranked according to JEPPSSON (1962) and compared with those from continuous injections, series 1 against 5 and series 3 against 6 The results of the ranking were tested statistically according to the Mann Whitney U-test There was no significant difference, i e the brains were no more in ured by ntermittent than by continuous injections

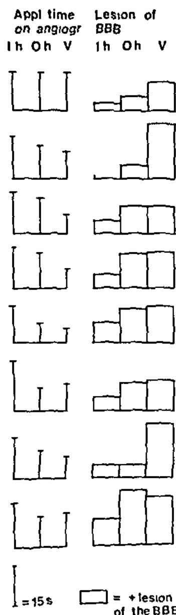


Fig 1

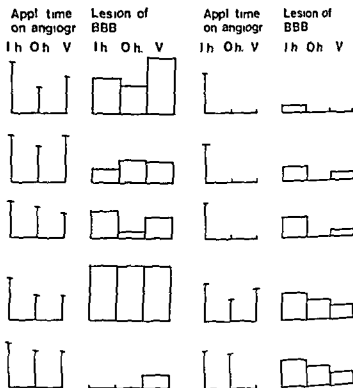


Fig 2 Fig 3

Fig 1 Injection into the internal carotid artery ligated caudally Injection rate 0 156 ml/s Volume 2 14 ml Injected hemisphere (I h) other hemisphere (O h) and areas supplied from the vertebral arteries (V) The lesion of the blood brain barrier was rated from 0 to + + + + 0 no staining + slight staining + + definite staining + + + intense staining + + + staining with stasis

Fig 2 Injection into the internal carotid artery ligated caudally Injection rate 0 089 ml/s Volume 1 32 ml

Fig 3 Injection into the internal carotid artery ligated caudally Injection rate 0 051 ml/s Volume 0 76 ml

brain barrier was confined to the injected hemisphere in all animals but in one animal the vertebral area was also injured No lesion occurred in the other hemisphere

Series 5 (Fig 5) 5 animals Intermittent injection into the internal carotid artery at a rate of 0 156 ml/s during 30 seconds The actual injection time totalled 15 seconds, *i e* 2 14 ml of contrast medium were given The common carotid artery was ligated caudally The blood pressure usually rose by 20 to 150 mm Hg The pulse rate was virtually unchanged The application time was to a certain degree intermittent In the injected hemisphere it summed up to a mean of 19 0 seconds, in the other hemisphere it was 8 0 seconds and in the basilar artery 10 0 seconds The injected area had the longest application time and exhibited the most evident lesion

filling of the contralateral carotid artery and of the vertebral arteries to be responsible for the appearance of paradoxical lesions This opinion was founded on the discovery of JEPPSSON & OLIN (1960) that a retrograde filling of the non-injected internal carotid artery and the vertebral arteries occurred at high injection rates The present investigation revealed that none of the explanations given were correct

Previous authors have emphasized that at a given concentration of contrast medium the degree of severity of the lesion to the blood-brain barrier depends upon the application time Serial films of satisfactory quality have previously been difficult to obtain in small animals Modern technique employing a small focal spot and direct fourfold magnification make such angiograms relatively simple to obtain At high rates of injection (0 089 to 0 156 ml/s) into the carotid artery (ligated caudally) the application time was as a rule shorter in the basilar artery and the contralateral medial cerebral artery as compared to that of the ipsilateral artery The lesion to the blood-brain barrier was nevertheless usually more marked in the areas with the shorter application time At low injection rate, and when there was a free flow of blood around the catheter in the carotid artery, the application time was longest in the ipsilateral hemisphere as was the lesion to the blood-brain barrier When the injection was made intermittently the lesion was most severe in the injected hemisphere even at high injection rates The concentration of the injected contrast medium has not been varied in these experiments It might therefore have been expected that the most injured areas would have been those with the longest application times As this was not the case, it must be concluded that a factor other than the application time is at work At present the nature of this factor can only be subject to speculation One possible explanation is that a mixture of blood and contrast medium may be more injuring than the contrast medium alone It must also be borne in mind that the contrast medium used is vasoactive However, no spasm or vasodilatation was observed on the films

In this context it may be mentioned that READ & MEYER (1960) observed a transitory red cell agglutination at arteriography with concentrated contrast media It has also been shown that such media cause haemolysis (SCHMID 1970) Whether these or other factors are at work in producing paradoxical lesions to the blood-brain barrier must be elucidated by further investigations

SUMMARY

in

in

the lesion to the blood-brain barrier was predominantly located to the brain area supplied by the contralateral carotid artery or the vertebral arteries It was shown by serial angiography that the application time was shorter within the vascular territory of the paradoxical lesion The results may imply that a mixture of blood and contrast medium is more vulnerable to the blood-brain barrier than contrast medium alone

Microscopy of the brains revealed blue staining of the walls of the vessels and diffuse staining of the parenchyma Occasionally staining of the nuclei of parenchymal cells was observed

Application time on the film compared with the localization of the lesion to the blood-brain barrier

When the carotid artery was ligated caudally and the injection rate was 0 156 and 0 089 ml/s the application time was longest on the injected side The lesion of the blood-brain barrier was most severe in the other areas of the brain in 11 out of 13 animals When the injection rate decreased to 0 051 ml/s the application time was still longest on the injected side In only two of these experiments contrast medium appeared in cerebral arteries in other parts of the brain The lesion of the blood-brain barrier was most marked on the injected side In order to investigate the effect of the ligation of the common carotid artery on the distribution of the lesion to the blood-brain barrier, the fourth series of experiments was performed, in which the common carotid was not ligated and the injection rate was 0 089 ml/s The application time was longest on the injected side and contrast medium appeared in the cerebral arteries of the other hemisphere only in one experiment The lesion to the blood-brain barrier was confined to the injected hemisphere in all animals although in one animal the area supplied by the vertebral arteries was also injured

When the injection was intermittent, at a rate of 0 156 ml/s during the injection period, the injected area had the longest application time and demonstrated the most evident lesion At intermittent injections, 0 051 ml/s, the lesion was confined to the injected hemisphere and a short application outside this area appeared in only two cases

Thus, at high injection rates and when the common carotid artery was ligated caudally, the severity of the lesion to the blood brain barrier was usually inversely related to the application time At a low injection rate the lesion to the blood-brain barrier was usually directly related to the application time This was also the case at a higher injection rate when the common carotid artery was not ligated caudally Following intermittent injections at high rates the inverse relationship between application time and the degree of severity of the lesion as demonstrated at continuous administration of the medium was not registered At low intermittent injection rates lesions were found only in the injected hemisphere

Discussion

Lesion to the blood-brain barrier in areas of the brain not vascularized by the artery injected with contrast medium has previously been described (BROMAN & OLSSON 1948, 1949, JEPPSSON 1962, JEPPSSON & OLIN 1970) BROMAN & OLSSON thought it was due to an embolus (precipitate) formed in the injection cannula or to herniation of the brain in the burr hole JEPPSSON (1962) considered the retrograde

FROM THE DEPARTMENTS OF OTOLARYNGOLOGY AND OF NEURORADIOLOGY, KAROLINSKA SJUKHUSET, S-104 01, STOCKHOLM, SWEDEN

OBJECTIVE SYMMETRY DETECTOR METHOD FOR GAMMAENCEPHALOGRAPHY

IV Investigation of brain tumours

M LIND

The physical characteristics of the symmetry detector method for gammaencephalography and the normal ranges of the measuring parameters have previously been described (LARSSON et coll 1975, LIND et coll 1975) Objective and semiautomatic classification of cases as normal or abnormal have been obtained by the method, which is simple and inexpensive (LIND & LARSSON 1975) The possible advantages of the method compared to conventional brain scanning, gamma camera examinations and gammaencephalography according to PLANIOL (1966), MUNDIGER & ASAI (1967) and MUNDIGER & OSTERTAG (1971) have also been discussed (LARSSON et coll LIND et coll, LIND & LARSSON) The purpose of this report is to evaluate the clinical application of the method

Material

Group I consists of 29 cases without symptoms or signs of brain lesion They have been used as a reference group and are presented in a previous report (LIND et coll)

The basic pathologic material consists of patients admitted to the Neurologic

Submitted for publication 15 January 1974

ZUSAMMENFASSUNG

Die Veranderungen der Blut-Hirn-Schranke wurden an Kaninchen nach konstanten oder intermittenten Injektionen von Natrium Metrizoat in die Arteria carotis interna mit unterschiedlicher Injektionsgeschwindigkeit untersucht Unter bestimmten experimentellen Bedingungen waren die Schadigungen der Blut-Hirn Schranke vorwiegend auf den Gehirnteil konzentriert, der durch die kollaterale Arteria carotis oder die Vertebralarterien versorgt wird Es wird durch Filmangiographie gezeigt, dass die Applikationszeit innerhalb des Gefassgebietes mit paradoxaler Schadigung kurzer war Die Ergebnisse konnen darauf hinweisen, dass eine Mischung von Blut und Kontrastmittel starker schädigend auf die Blut-Hirn-Schranke wirkt als Kontrastmittel alleine

RÉSUMÉ

Les auteurs ont étudié les perturbations de la barriere hémato-encéphalique sur des lapins après injections constantes ou intermittentes de metrizoate de sodium dans l artère carotide interne avec différentes vitesses d'injection Dans certaines conditions expérimentales la lésion de la barrière hemato encéphalique a été localisée de façon predominante sur la *région cérébrale irriguée par l'artère carotide controlaterale ou par les arteres* vertébrales L'angiographie en série a montré que le temps de sejour du moyen de contraste était plus court dans le territoire vasculaire de la lesion paradoxale Ces résultats peuvent impliquer qu'un mélange de sang et de moyen de contraste est plus agressif pour la barrière hemato encéphalique que le moyen de contraste seul

REFERENCES

BROMAN T and OLSSON O The tolerance of cerebral blood vessels to a contrast medium of the Diodrast group Acta radiol *30 (1948), 326*

— — Experimental study of contrast media for cerebral angiography with reference to possible injurious effects on the cerebral blood vessels Acta radiol 31 (1949) 321

JEPPSSON P G Studies on the blood-brain barrier in hypothermia Acta neurol scand 38 (1962) Suppl No 160

— and OLIN T Cerebral angiography in the rabbit Lunds Univ Årsskrift NF avd 2, 56, No 14 (1960)

— — Neurotoxicity of roentgen contrast media Study of the blood brain barrier in the rabbit following selective injection of contrast media into the internal carotid artery Acta radiol Diagnosis 10 (1970), 17

READ R C and MEYER M The role of red cell agglutination on arteriographic complications Surg Forum 10 (1960), 472

SCHMID H W Untersuchungen der Toxizitat der physikalisch chemischen Eigenschaften und der hamolytischen Aktivitat von trijodierten Rontgenkontrastmittel Salzen in *wässrigen* Losungen ETH, Zurich (1970), Cilag-Chemie AG Schaffhausen Pharmaceutische Abteilung Pharm Acta Helv 46 (1971) 134, 210, 298

Table 2

Classification boundaries for obtained SD_{max} considering the whole skull or a selected subdivision of the skull

Class	Regarded as	Criterion value (SD_{max}) Whole skull	Selected subdivision of the skull
I	Definitely normal	0–3 0 SD	0–2 5 SD
II	Probably normal	3 0–3 5 SD	2 5–3 0 SD
III	Probably abnormal	3 5–4 0 SD	3 0–3 5 SD
IV	Definitely abnormal	4 0–∞ SD	3 5–∞ SD

doubtful, the diagnosis being unsure because of contradictory or incomplete information Initially 3 of these 5 patients were thought to have an intracranial neoplasm because of epileptic attacks and intracerebral expansive non-vascular lesions as demonstrated by cerebral angiography However, tissue specimens taken at operation demonstrated glial hyperplasia and slight inflammatory reaction with plasma cells and lymphocytes Clinically, these three uncertain cases were finally regarded as having focal encephalitis

Group III contained 2 patients with probable intracranial neoplasm, the possibility of neoplasm was regarded as higher than 50 per cent, but less than 95 per cent These patients were not operated upon, nor was biopsy performed

Group IV consisted of 37 patients with certain intracranial neoplasm A 35 patients with positive histology B 2 patients without histology

Group V contained 8 patients, definitely without intracranial neoplasm, but with some other organic brain lesion Six patients had cerebrovascular lesions (one of these an arteriovenous malformation), one with parietal porencephaly and one with chronic meningitis caused by Cryptococcus neoformans (Table 1)

Thirty-eight of the 66 patients had a radiologically demonstrated intracranial expansive lesion, which was later examined histologically They were divided into 5 groups, based on the final diagnosis

Group A 3 patients, focal encephalitis, glial hyperplasia
Group B 4 patients, astrocytoma grade I–II
Group C 16 patients, astrocytoma grade III–IV
Group D 4 patients, brain metastasis
Group E 11 patients meningioma

Method

All cases were examined by the symmetry detector method with the clinical routine previously described (LIND et coll , LIND & LARSSON) Most cases were measured twice, measurement I starting about 30 min, and measurement II about 120 min after the injection of 10 mCi $^{99}Tc^{m}O_4$ intravenously For practical reasons some

Table 1

All cases of group V (definitely not neoplasm but some other organic brain lesion)

Diagnosis	SD_{max} in measurement		Diagnosis based on
	I	II	
Infarction (right parietal region) 2 months old	6 0	—	Clinical findings Stenosis of right *int carotid art*
Infarction (left parietal region) 1 month old	10 3	13 6	Clinical findings Stenosis of left int carotid art
Intracerebral haemorrhage (left hemisphere) 3 months old	3 3	6 0	Clinical findings Expanding lesion in left hemisphere
Subarachnoid haemorrhage 27 years old	4 5	—	Clinical findings No expanding lesion
Cerebrovascular disease (left parietal area)	2 5	3 0	Clinical findings Cortical vein occlusion
Art ven malformation (parietal, central structures)	—	7 6	Angiography
Porencephaly (right parietal area)	3 3	2 6	Exploration
Chronic meningitis (Cryptococcus neoformans)	2	< 2	Cytology of CST

Clinics during 16 months 1972–1973 with possible intracranial neoplasm Some patients were excluded due to

(1) Practical reasons, such as restricted technical assistance, (2) a bad general condition, (3) previous craniotomy or radiation therapy of the skull, or (4) a tentative diagnosis of acoustic neurinoma or pituitary tumour

The remaining patients constituted the pathologic material of 66 cases, no other selection principles than those mentioned were applied The 66 patients were examined clinically and neuroradiologically In 38 cases histology of the expansive lesion was performed by one and the same pathologist The classification proposed by RINGERTZ (1950) was used The following groups, II–V, represent a clinical summary made by a neurosurgeon without knowledge of the measuring results obtained from the symmetry detector method

Group II consists of 19 patients without probable intracranial neoplasm If the risk of having an intracranial neoplasm was regarded less than 50 per cent, the patient was placed in this group (except cases belonging to group V), which for instance consisted of patients with possible cerebrovascular disease Five of these 19 cases were

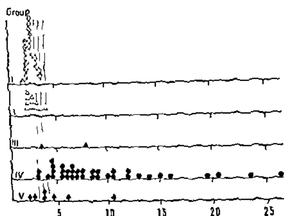


Fig 1 SD_{max} in measurement I of groups I–V Group I = reference, II = intracranial neoplasm not probable III = intracranial neoplasm probable, IV = intracranial neoplasm certain, V = definitely not intracranial neoplasm, but some other organic brain lesion

taking only the clinically possible pathologic area into consideration (Table 2) (LIND & LARSSON)

The difference between lesions with high SD_{max} (hot) and low SD_{max} (cold) was used to obtain differential diagnosis between cases with proven intracranial expansive lesions The accuracy of this differential diagnosis was estimated by comparing the criteria values of groups A–E A differential diagnosis by use of the time dependent change of $^{99}Tc^{m}O_4$ accumulation was also pursued The maximum deviation in number of SD in any of the position ratio-(r_c), sum (S_c) and difference-(D), parameters of measurement II was subtracted from the corresponding value of measurement I Those patients were excluded, in whom the region of interest did not display any SD-value of the chosen parameters above 4 0 in either measurement (LIND et coll, LIND & LARSSON)

Results

Measurement I Separation of cases with abnormal from cases with normal $^{99}Tc^{m}O_4$ distribution in the head was obtained from the SD_{max} of measurement I or II SD_{max} obtained at measurement I in group I–V were plotted in a diagram (Fig 1)

None of the 29 reference patients in group I had SD_{max} above 4 0 SD Only 2 of 29 cases had SD_{max} above 3 5 SD and 4 of 29 cases above 3 0 SD The 19 cases in group II (intracranial neoplasm not probable) had SD_{max} between <2 and 6 9 SD The 2 patients of group III (intracranial neoplasm probable) had SD_{max} of 3 4 and 8 8 SD, respectively Thirty-four of 36 patients in group IV (intracranial neoplasm certain), examined by measurement I, had SD_{max} above 4 0 SD and 2 patients had values between 3 0 and 3 5 SD, which corresponded to a diagnostic accuracy of about 94 per cent SD_{max} was generally high compared to the normal range, and could be as high as 26 4 SD Hence group IV was clearly separated from the normal range by measurement I Border-line cases are presented in Table 3 Seven patients of group V (definitely not neoplasm, but some other organic brain lesion), examined by meas-

Table 3

Nine cases from group IV with a SD_{max} lower than 5 0 SD in measurement I or II

Diagnosis	SD_{max} in measurement			Remark
	I	II	I + II	
Astrocytoma II (left parietal area)	4 5	6 5	6 5	
Meningioma (subfrontal, close to the skull base)	3 2	3 1	3 2	
Astrocytoma I (right temporal area)	4 0	5 3	5 3	
Astrocytoma III (right parietal area)	4 6	3 3	4 6	
Metastasis from colon cancer (left parietal area)	4 3	5 5	5 5	
Meningioma (close to the brain stem)	5 8	4 9	5 8	
Astrocytoma II (right parietal area)	3 1	4 2	4 2	
Small meningioma of left cerebellopontine angle, involving the jugular foramen	7 7	3 4	7 7	Large areas of the left hemisphere had higher values than the right side in measurement I
Astrocytoma II (left frontal area)	4 4	6 1	6 1	
No of cases not definitely abnormal	2	3	1	
Number of cases with SD_{max} below 5 0 SD	7	5	3	

patients were only measured once, either by measurement I or II The digital data obtained were automatically punched on paper tape and later computed by a PDP-8 computer (4K memory) The results of measurements I and II were related to corresponding normal ranges obtained from the reference group previously described The maximum deviation from the normal mean value in any of 208 parameters was calculated in numbers of SD (SD_{max}) and used as a criterion (LIND et coll , LIND & LARSSON)

The $^{99}Tc^mO_4$ distribution in the skull was classified as normal or abnormal using the criterion values given previously (LIND et coll , LIND & LARSSON)

Distributions primarily not classified as definitely abnormal, were reclassified



Fig 3 SD_{max} of the evaluation of the combination of measurement I and II Group I = reference, IV intracranial neoplasm certain

of the clinically possible region, is indicated in Fig 4, which also gives the corresponding classification of the reference group Cases of group IV were also classified (measurement I and II regarded separately) considering only that region of the skull which was of clinical interest (Fig 5) (LIND & LARSSON) It was evident that additional information used to select one region of interest increased the possibility of separating pathologic cases from the normal range, since the classification borders could be lowered by 0 5 SD, as demonstrated previously (LIND & LARSSON)

The mean value of the largest SD_{max} obtained from the combination of measurement I and II of group I (reference) was 2 7 $\pm$ 0 5 SD, which was about 0 2 SD higher than the corresponding mean values of SD_{max} in measurement I and measurement II calculated separately The classification borders of this combination of measurement I and II were therefore increased by 0 2 SD (LIND et coll , LIND & LARSSON)

The number of patients in group IV (neoplasm certain) having values around the classification borders was smaller in the combined measurements than in measurement I or measurement II taken separately Hence, the separation of group IV from group I was almost equal in measurement I and II, but somewhat better if both measurements were combined (Figs 1 to 3, Table 3)

Separation of hot and cold expansive lesions (measurement I) The values of SD_{max} obtained were differently distributed in groups A–E (Fig 6)

Evidently no difference between group C (astrocytoma III–IV), D (metastasis) and E (meningioma) existed These groups had SD_{max} above 5 0 SD with three exceptions (Table 3)

However in measurement I all patients of group B (astrocytoma I–II) had values lower than 4 5 SD and were thus separated from groups C–E but also from the normal range Group A (focal encephalitis, glial hyperplasia) had SD_{max} lower than 3 0 SD thus well within the normal range (Fig 6) In measurement II group B was less well separated from group C (Table 3)

Separation of cases with intracranial expansive lesions with increasing values from those with decreasing ones All 15 patients in group B and C (astrocytoma) examined in this respect had positive differences between measurement I and II, indicating an increasing accumulation of $^{99}Tc^{m}O_4$ in the pathologic region (Fig 7)

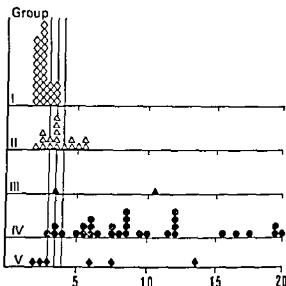


Fig 2 SD_{max} in measurement II of groups I–V Group I = reference, II = intracranial neoplasm not possible, III = intracranial neoplasm probable, IV = intracranial neoplasm certain, V = definitely not intracranial neoplasm, but some other organic brain lesion

urement I, had SD_{max} <2 to 10 3 SD The values obtained and the final diagnosis are given in Table 1

Measurement II SD_{max} obtained in group I–V in measurement II are plotted in a diagram (Fig 2) None of the 26 reference patients in group I, examined by measurement II, had values above 4 0 SD Two had values between 3 5 and 4 0 SD and another 2 had values between 3 0 and 3 5 SD The 17 patients in group II, examined by measurement II, had SD_{max} between 2 0 and 5 5 SD The 2 patients of group III had SD_{max} 3 3 and 10 7 SD Twenty-eight of the 31 patients of group IV, examined by measurement II, had SD_{max} above 4 0 and 3 of these 31 cases had SD_{max} between 3 0 and 3 5 SD, which corresponded to a diagnostic accuracy of about 90 per cent, thus this group of intracranial neoplasms was also well separated from the normal range by the second measurement Cases with values around the classification borders are presented in Table 3 The 6 cases of group V, examined by measurement II, had SD_{max} between 2 and 13 6 SD (Table 1)

Combination of measurement I and measurement II The highest SD_{max} of measurement I or measurement II, considered together, were plotted (Fig 3) for group I (reference) and group IV (neoplasm certain) None of the 26 reference cases of group I, examined by both measurement I and II, had values above 4 2 SD, none had values between 3 7 and 4 2 SD, 5 had values between 3 2 and 3 7 SD (Fig 3) Twenty nine of the 30 patients of group IV (neoplasm certain), examined by both measurement I and II, had values of 4 2 or higher, and 1 had a value = 3 2 SD, which corresponds to a diagnostic accuracy of about 97 per cent (Fig 3, Table 3)

Classification of results from group I and group IV The classification of measuring results of group IV (measurement I and II regarded separately) without knowledge

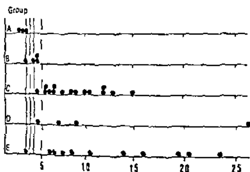


Fig 6 Differentiation of groups A, B, C, D and E by use of the SD_{max} of measurement I A = focal encephalitis, glial hyperplasia, B astrocytoma I-II, C astrocytoma III IV, D = metastasis, E = meningioma

distributions This was regarded as important, because the need of an experienced examiner could thus be avoided and the symmetry detector method would be of use even outside large medical centres (SCHIEFER 1972, MUNDIGER & OSTERTAG, PLANIOL, MUNDIGER & ASAI, DOWSETT & PERRY 1970, DOWSETT 1972, POPHAM et coll 1970, MALLARD 1966)

Digital results are necessary for objective evaluation of the isotope distribution in the skull and its correlation to different pathologic conditions Time-dependent changes of the distributions and follow-up investigations are easier to perform and evaluate when digital results are available (ASHKENAZY & CRAWLEY 1953, HANDA et coll 1969, 1971, TAKEDA 1970, QUINN 1971, SAUER 1972, HIRSCHBIEGEL & SCHWIEGER 1970)

The patient remains in one and the same supine position during the measuring procedure, which must be regarded as simple and short However, in a small number of patients uncontrolled movements of the head made the examination difficult and in exceptional cases impossible

The radiation hazards seem to be acceptable Ten mCi $^{99}Tc^{m}O_4$ is reported to deliver a whole-body dose of about 0 1 rad and after premedication by 0 4 g $KClO_4$ a critical organ dose of about 1 rad (colon, kidney, salivary glands) (SMITH 1965, Swedish National Institute of Radiation Protection 1969)

The results obtained were drawn on a diagram and could be presented a few minutes after end of examination The classification of the results could be performed by a supervised technician

Knowledge of the diagnosis did not influence the analysis of the results, as this was made objectively and semiautomatically (LIND & LARSSON) For practical reasons, no measurement was performed after measurement II, in spite of the fact that measurements at for instance 6 or 12 hours after the injection might give valuable information, especially when compared to an early measurement However, late measurements are more difficult to organize, and are thus not suitable for screening purposes (GATES et coll 1971, RAMSEY & QUINN 1972, TAUXE & THORSEN 1969)

The material presented was strongly selected The selection of cases in the reference group I has been discussed previously. All pathologic cases were initially selected for

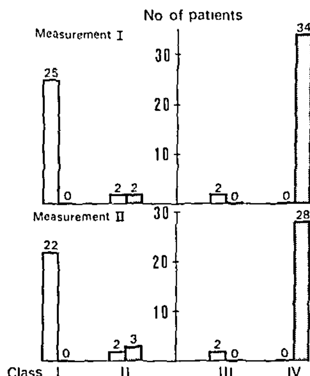


Fig 4

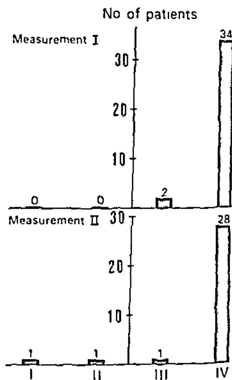


Fig 5

Fig 4 Objective classification according to Table 2 of measuring results obtained from the reference group I (dotted) and group IV (intracranial neoplasm certain black) in measurement I and II

Fig 5 Objective classification according to Table 2 of measuring results obtained from group IV (intracranial neoplasm certain) considering only the region of clinical interest (measurement I and II)

All 9 cases in group E (meningioma) had negative differences, indicating a decrease of accumulated activity in the pathologic region (Fig 7) Two patients with brain metastasis had a positive difference and one had a negative difference

Hence the time dependent change of parameter values separated the group of meningiomas from the group of astrocytomas ($p < 0.01$) However, the number of cases available was too small to permit a definitive evaluation of the possibility of separating different tumour groups

Discussion

The normally stable and symmetric isotope distribution in the skull has generally not influenced the design of commonly used examination systems Equipment specifically designed for brain examinations may increase the diagnostic accuracy and besides be less complicated and expensive

Because the evaluation parameters of the symmetry detector method were defined and of limited number it has been possible to define a strictly objective diagnostic criterion with fixed classification boundaries between normal and abnormal $^{99}Tc^{m}O_4$

the diagnostic accuracy enhanced (LIND & LARSSON), (2) a decreased $^{99}Tc^{m}O_4$ concentration in that region contradicts the existence of an intracranial neoplasm (YOUNG & ROCKETT)

Separation of pathologic and normal cases The pathologic values deviated considerably from the values of the reference group I and were often about 2 to 5 times higher than the maximum value of this group Almost all intracranial neoplasms (group IV) should consequently have been detected even if the examination had been performed when the tumour was smaller The diagnostic accuracy obtained in group IV (about 90 to 97 per cent) is high and compares favourably with other results published If clinical information was used, and only the possible region taken into consideration, all 36 patients with intracranial neoplasm (group IV) examined by measurement I were classified as probably or definitely abnormal Using measurement II, 29 to 31 cases were classified in the same way (PAOLETTI et coll , YOUNG & ROCKETT, MUNDIGER & OSTERTAG, PLANIOL, BURROWS)

Four patients in group IV (intracranial neoplasm) had SD_{max} less than 4 0 either in measurement I or measurement II Hence, in these cases, without knowledge of the clinical signs the $^{99}Tc^{m}O_4$-distribution in the skull was not classified as definitely abnormal in both measurements (Table 3) Two of these 4 patients had meningiomas, one small subfrontal meningioma in the midline and one in the left cerebello pontine angle partly involving the jugular foramen In this last case the results of measurement I but not to the same extent of measurement II indicated an increased amount of $^{99}Tc^{m}O_4$ in large parts of the left hemisphere This might possibly be explained by circulatory disturbances of the left side, caused by partial occlusion of the left jugular foramen Out of the other 2 cases 1 had an astrocytoma grade II, and 1 an astrocytoma grade III, both in the right parietal region (Table 3) Thus 2 of 4 uncertain cases were explained by a localization close to the skull base and 1 by the relatively high differentiation of the tumour The existence of a low differentiated intracerebral tumour or metastasis could thus almost be excluded by the symmetry detector method if the measuring results were within the normal range (YOUNG & ROCKETT)

Considering the overall diagnostic accuracy, there was no significant difference between measurement I and II However, the meningiomas had the highest values in measurement I and the astrocytomas in measurement II (Fig 7) Therefore evaluation of the combination of measurement I and II resulted in a higher diagnostic accuracy in this material (Fig 3) The gain was small and hardly motivates two measurements in clinical screening (RAMSEY & QUINN, GATES et coll , HIRSCHBIEGEL & SCHWIEGER, TAUXE & THORSEN, HANDA et coll 1971)

The SD_{max} of group II diverged from those of the reference group, but most cases were not classified as definitely abnormal The clinical diagnosis was uncertain and it was thus pointless to correlate the results obtained to clinical findings Three patients were diagnosed as focal encephalitis with reactive glial hyperplasia The diagnosis was based on clinical information and histology However, the specimens

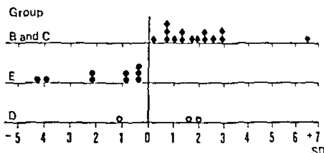


Fig 7 Difference between measure- [illegible] ence B and C = astrocytoma I–IV, D = metastasis, E = meningioma

possible intracranial neoplasm Large neoplasms may therefore be over-represented compared to a common neurologic screening material On the other hand, patients in poor condition were excluded Many patients were excluded because of lack of technical assistance, which rendered it impossible to perform the examination before the planned day of operation Some patients were excluded because of previous operation or radiation therapy, which might affect the isotope distribution in the skull Cases with acoustic neurinomas or pituitary tumours were excluded because these tumours generally present with characteristic clinical symptoms initially separating them from other intracranial neoplasms and directing the diagnostic efforts towards the pontine angle and the sella region (DE LAND & WAGNER 1969, JOHNSON 1970, BAUM & ROTHBALLER 1972, BAUM et coll 1972, OTTO et coll 1972, KINNMAN 1973)

Many authors report a diagnostic accuracy for brain scanning methods of between 70 and 90 per cent, but the materials were selected in different ways and the selection is evidently important in considering the diagnostic accuracy The relative number of false positive cases is generally not reported although it must be regarded as most important in the evaluation of the capacity of a screening method to separate pathologic from normal cases (PLANIOL, MUNDIGER & ASAI, YOUNG & ROCKETT 1972, PAOLETTI et coll 1969, BURROWS 1972)

The subjective evaluation of the scanning image generally has been made with a varying and unreported knowledge of the clinical findings and the results from other examinations Clinical information in addition to the basic information of the method has thus been involved in the evaluation of results If the amount of additional information is not taken into account in the presentation of results obtained, it is impossible to know to what degree the level of diagnostic accuracy claimed depends on information added from other sources It is thus impossible to compare the diagnostic accuracy of different methods used in different materials without knowledge of the selection of patients or the degree of clinical influence on the evaluation of results In practice screening is generally made with a restricted amount of clinical information (PAOLETTI et coll , YOUNG & ROCKETT, MUNDIGER & OSTERTAG, PLANIOL) Using the symmetry method, added clinical information may be exploited in two ways (1) By taking into consideration only that region of the brain that possibly harbours a lesion, the classification boundaries can be lowered by 0 5 SD and hence

$^{99}Tc^{m}O_4$ The general conclusion may be drawn, that it is possible to obtain high diagnostic accuracy and differential diagnosis in spite of low spatial resolution and simplicity of gammaencephalographic methods

Acknowledgements

Histologic examinations performed at the Department of Tumour Pathology, Karolinska Sjukhuset, by Prof G Moberger, as proposed by N Ringertz (1950) and clinical classification made by D Forster, FRCS, Department of Neurosurgery, Karolinska Sjukhuset are gratefully acknowledged

SUMMARY

Sixty-six cases with possible brain tumour were objectively classified as having normal or abnormal $^{99}Tc^{m}O_4$ distribution in the skull recorded by the symmetry detector method for gammaencephalography The diagnostic accuracy in 37 confirmed tumour cases was about 95 per cent Astrocytomas I II were separated from astrocytomas III–IV by the *degree of abnormality*, and meningiomas were separated from astrocytomas by diverging *time-dependent* changes in the pathologic isotope accumulation The high diagnostic accuracy *was obtained* in spite of low spatial resolution and simplicity of the method The careful *choice of evaluation* parameters and the restriction of their normal variance were necessary *and effective* in optimizing the method

ZUSAMMENFASSUNG

Sechsundsechzig Patienten mit Verdacht auf *einen* [illegible]
oder nicht normal mit Hilfe der $^{99}Tc^{m}O_4$ Verteilung in [illegible]
Detektor Methode zur Gammaencephalographie fest [illegible]
nostische Genauigkeit bei 37 nachgewiesenen *Hirntumor Fällen war etwa 95%* Astrocytome I II wurden von Astrocytomen III–IV durch *den Grad der* Abweichung getrennt, Meningiome wurden von Astrocytomen durch *unterschiedliche* [illegible]

[illegible] Methode zu *optimieren*

RÉSUMÉ

Soixante-six malades pouvant être *atteints de tumeur* cérébrale ont été classés objectivement comme ayant une distribution normale *ou anormale de* $^{99}Tc^{m}O_4$ dans le crâne au moyen de la méthode de détecteur de *symétrie pour* [illegible]
diagnostic dans 37 cas confirmés de [illegible]
I II ont été séparés des astrocytomes [illegible]

taken at operation might have been unrepresentative and thus cause a wrong diagnosis Therefore it was of interest that all three patients had SD_{max} below 3 0 in measurement I and below 4 0 *in measurement II*, thus separating them from the astrocytoma I–II group as well as the astrocytoma III–IV and meningioma groups (Fig 6)

The SD_{max} of group V varied between <2 and 13 6 The number of cases in this group was too small to allow any conclusions to be drawn (Table 1)

Differential diagnosis of expansive lesions The quantitative results permitted objective separation of cases with large SD_{max} from cases with small SD_{max} The astrocytomas grade I–II and lesions in group A (focal encephalitis, glial hyperplasia) were found to have small SD_{max} and diverge from the astrocytomas grade III–IV, from the metastases and from meningiomas which generally had large SD_{max} Hence, this separation should be of value in arriving at a differential diagnosis and in judging the prognosis and deciding the therapy of the patient However, there were only a few cases in the group of astrocytomas grade I–II, and a low SD_{max} might be explained by either a low accumulation of $^{99}Tc^{m}O_4$ or by a geometrically disadvantageous localization of the accumulation (LARSSON et coll , LARSSON & LIND) The separation was better made by measurement I than by measurement II (ZEIDLER et coll , HIRSCHBIEGEL & SCHWIEGER)

The quantitative results permitted estimation of time-dependent changes of the accumulation of $^{99}Tc^{m}O_4$ in pathologic regions The central mean value (Cmv) was regarded as the most stable reference value and thus best suited for comparison Only cases with pathologically high values (above 4 0 SD) in one or both measurements were considered, because otherwise time-dependent changes could not safely be referred to the pathologic lesion Even small differences in collimator positioning might change the values of position ratios (r_c) considerably and furthermore the intra-individual variation of the method is small but not neglectable (LIND et coll , LARSSON & LIND) However, the meningiomas which had a decreasing accumulation of $^{99}Tc^{m}O_4$ could be separated with a high degree of accuracy from the astrocytomas, all of which had increasing accumulation of $^{99}Tc^{m}O_4$ The decreasing accumulation in the meningiomas might be explained by circulatory disturbances in and around the tumours (ASHKENAZY & CRAWLEY, HANDA et coll 1969, 1971, HIRSCHBIEGEL & SCHWIEGER)

Conclusion

High diagnostic accuracy (above 90 per cent) regarding brain tumours was obtained by the objective and semiautomatic symmetry detector method for gammaencephalography A group of astrocytomas *I–II was separated from a group of astro*cytomas III–IV, from a group of meningiomas and from a group of brain metastases by the size of SD_{max}, and the groups of astrocytomas were separated from the group of meningiomas by the temporal change of the pathologic *accumulation of*

MUNDINGER F und ASAI A Ergebnisse der digitalen Gammaencephalographie bei Hirntumoren, Vergleich von Wismut[206], Quecksilber[203]—Neohydrin und Technetium[99m] Arch Psychiat Nervenkr 210 (1967), 297

— und OSTERTAG Ch Radio-Isotope in der neurologisch-neurochirurgischen Diagnostik, Hippokrates 42 (1971), 135

OTTO H, FIEBACH O, SAUER J, BETTAG W, LÖHR E and STRÖTGEN M W Cerebral scintigraphy in relation to roentgenological methods for detection of tumours situated in the sellar region and the posterior fossa Neuroradiology 4 (1972), 30

PAOLETTI P, VILLANI R, FRIGENI G and MASSAROTTI M Four years of experience in scanning brain lesions Minerva neurochir 13 (1969), 212

PLANIOL T Gamma-encephalography after ten years of utilization in neurosurgery Progr neurol Surg 1 (1966), 93

POPHAM M G, BULL J W, D and EMERY E W Interpretation of brain scans by computer analysis Brit J Radiol 43 (1970), 835

QUINN J L III Serial brain scans in glioblastoma multiforme Radiology 101 (1971), 367

RAMSEY R G and QUINN J L III Comparison of accuracy between initial and delayed ^{99m}Tc pertechn...

RINGE

SAUTER . . 116 (1972) 179

SCHIEFER W Fruhdiagnose raumfordernder Prozesse im Schädelinneren Dtsch med Wschr 23 (1972), 551

SMITH E M Internal dose calculation for ^{99m}Tc J nucl Med 6 (1965), 231

TAKEDA K Differential diagnosis of intracranial lesions by Tc-99 m brain scintigram Nippon Acta radiol 30 (1970), 124

TAUXE W N and THORSEN H C Cerebrovascular permeability studies in cerebral neoplasms and vascular lesions optimal dose to scan interval for pertechnetate brain scanning J nucl Med 10 (1969), 34

YOUNG R L and ROCKETT J F The brain scan as a routine screening procedure Sth med J 65 (1972), 65

ZEIDLER U, SUMMER K, BRUNNGRABER C V, KOTTKE S und HUNDESHAGEN H Untersuchungen zur pathophysiologischen Grundlage der Hirnszintigraphie mit ^{99m}Tc Pertechnetat Arch Psychiat Nervenkr 213 (1970), 200

éte séparés des astrocytomes par des differences de la fixation pathologique de l isotope en fonction du temps Cette grande précision diagnostique a eté obtenue malgré la faible résolution spatiale et la simplicité de cette méthode Le choix judicieux des paramètres d évaluation et la limitation de leur variance normale ont été nécessaires et efficaces pour améliorer la methode

REFERENCES

ASHKENAZY M and CRAWLEY J W The value of serial studies of cerebrovascular permeability with radioactive iodinated serum albumin and the scintillation counter, particularly *in the detection of neurosurgical lesions* Amer J Surg *19 (1953) 155*

BAUM S and ROTHBALLER A B The site of accumulation of Tc^{99m} sodium pertechnetate in a human brain tumor (acoustic neuroma) Amer J Roentgenol 114 (1972), 781

— — SHIFFMAN F and GIROLAMO R F Brain scanning in the diagnosis of acoustic neuromas J Neurosurg 36 (1972), 141

BURROWS E H The clinical utility of brain scanning in nuclear medicine *In* Progress in nuclear medicine Vol 1, p 287 Edited by E J Potchen & V R McCready S Karger, Basel 1973

DELAND F H and WAGNER H N Brain scanning as a diagnostic aid in the detection of eighth nerve tumours Radiology 92 (1969), 571

DOWSETT D J A quantitative analytical display programme (QUAD) designed for radio isotope brain scans Comput Biol Med 2 (1972), 27

— and PERRY B J A comparative statistical analysis of brain scans using a digital computer Brit J Radiol 43 (1970), 617

GATES G F, DORE E K and TAPLIN G V Interval brain scanning with sodium pertechnetate Tc^{99m} for tumor detectability J Amer med Ass 215 (1971), 85

HANDA J, HANDA H, HAMAMOTO K, TORIZUKA K and KOUSAKA T Sequential brain imaging as an aid in understanding disease etiology Seminars in nuclear medicine 1 (1971), 56

— NABESHIMA S, HANDA H, HAMAMOTO K, KOUSAKA T and TORIZUKA K Serial brain scanning with technetium 99m and scintillation camera Amer J Roentgenol *106 (1969)* 708

HIRSCHBIEGEL H und SCHWIEGER G Verlaufsmessungen der Einlagerung von Technetium *99m in Hirntumoren im Hinblick auf ihre artdiagnostische Bedeutung* Strahlentherapie 140 (1970) 499

JOHNSON E W Auditory test results in 268 cases of confirmed retrocochlear lesions Int Audiol 9 (1970), 15

KINNMAN J E G Acromegaly and ultrastructural analysis of 51 adenomas and a clinical study in 80 patients treated by transanthro—sphenoidal operation Dissertation Stockholm 1973

LARSSON S, LIND M and SODERBORG B *Objective symmetry detector method* for gammaencephalography I Physical characteristics Acta radiol Ther Phys Biol 14 (1975) 63

LIND M and LARSSON S Objective symmetry detector method for gammaencephalography III *Diagnosis* of abnormal $^{99}Tc^{m}O_4$ distribution in the skull Acta radiol Ther Phys Biol 14 (1975) 273

— — and SODERBORG B Objective symmetry detector method for gammaencephalography II Normal range Acta radiol Ther Phys Biol 14 (1975), 145

MALLARD J R Medical radioisotope visualization (A review of "scanning") *Int J appl* Radiat Isotopes 17 (1966), 205

This is substantiated by several reports during the sixties, especially concerning accidental administration of such particles during cerebral angiography The histologic effect of embolization following angiography has been recorded by several authors Thus, SILBERMAN et coll (1960) published a report on five cases, having identified at autopsy cotton fiber granulomas following cerebral angiography There is considerable evidence, according to these authors, that the embolism may have been an accessory cause of death in three of the cases CHASON et coll (1963) reported on cotton fiber emboli in routine autopsies of patients who had underwent carotid angiography GARVAN & GUNNER presented histologic evidence of small granulomas and bast fragments located within and close to the smallest arteries in an occipital lobe, resected because of an arterio-venous malformation Similar fibers had previously been identified in saline administered to the patient during preoperative carotid angiography Cotton fiber embolization during angiography was also reported by ADAMS et coll (1965) They described four cases, one following percutaneous carotid angiography and the others as sequelae of selective nephroangiography Relatively large renal infarcts were encountered Animal experiments seemed to prove that cotton fiber contamination probably could occur during flushing of catheters

Intraarterial injections are routinely and extensively used in diagnostic radiology and it is natural that particular attention has been paid to small particle embolization There is, however, very scant information on the inadvertent contamination of contrast media with glass particles on opening the ampoules (DUQUESNEL et coll 1973, SANDELL & ERNEROT 1968), and particularly concerning the possible harmful effect of the injection of such particles Also relatively few reports on the histologic reaction following glass embolization have appeared

In an investigation of the factors involved in the aetiology of atherosclerosis BYERS & FRIEDMAN (1966) induced lipidization, calcification and cellular infiltration from inclusion of glass particles into the intima of medium sized and small vessels of animals SCHULTZ et coll (1965) also used small particles of glass as one of the agents in producing experimental vascular abnormalities In some cases they succeeded in provoking proliferation of the intima of small vessels as well as extensive para-arterial and intramural cellular infiltration In several instances lesions were produced only after repeated injections of glass particles

DUQUESNEL et coll investigating filtrates of contrast media from routinely opened glass ampoules found a remarkable amount of microscopically identifiable particles of glass mixed with other particles such as cotton fiber in nine out of ten samples examined

This report and that of SANDELL & ERNEROT indicate that [illegible]

[illegible] routine opening of glass ampoules, and to what extent, (2) if particles of other origin may be identified as well, and (3) if

FROM THE DEPARTMENT OF RADIOLOGY, THE INSTITUTE OF PATHOLOGY AND THE INSTITUTE FOR EXPERIMENTAL SURGICAL RESEARCH, RIKSHOSPITALET, OSLO, NORWAY

GLASS FRAGMENTS AND OTHER PARTICLES CONTAMINATNG CONTRAST MEDIA

A. Brekkan, P. E. Lexow and G. Woxholt

Inadvertent admixture of particulate matter to fluids for intravascular use is well known and has been discussed in many reports, especially during the past decade (Garvan & Gunner 1964, Groves 1973, Irstam 1972). The 1973 edition of the British Pharmacopoeia specifies the following limits for particle contamination of parenteral fluids. The mean counts of particles per 1 ml should not exceed 1000 equal to or greater than 2 μm, and 100 or equal to or greater than 5 μm.

Garvan & Gunner (1964) examined a number of parenteral fluids from U.S.A., Europe, Australia and the Philippines and found large amounts of various size in all samples but three. These three were specially packed: one was dispensed in a plastic container, the others were closed with specially laquer prepared rubber bungs. The particles were mostly considered to derive from the bungs, consisting of rubber, diverse chemical matter, cotton fibers and other substances. Particles were present in sizes from 1 to 500 μm, the most remarkable being those of cellulose fibers from cotton, jute and hemp. Only few authors specifically mention glass particles from ampoules as a source of contamination. Sandell & Ernerot (1968) investigated the effect of membrane filtration for the elimination of glass particles from ampoules and demonstrated on microphotographs that glass contamination does occur when the tip is broken off the ampoule. Within diagnostic radiology attention has long been focused upon the risk attending intravascular injection of foreign particles

Submitted for publication 8 August 1974

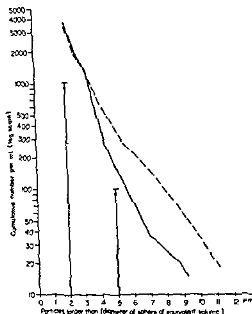


Fig 2 Results of counting of particles shed from two brands of 20 ml disposable plastic syringes, *one filling B P standard for particle contents of intravenous fluids is indicated by arrows Total particle volume* (ppm) background of test fluid 0 013, ——*producer A* 0 094, – – – – *producer* B 0 165

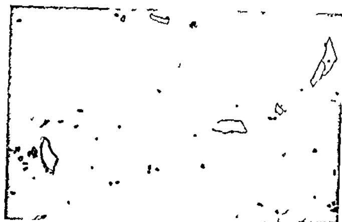
from disposable plastic syringes, and (3) embolization of canine kidneys with glass fragments at selective catheterization of the renal arteries

Eighty-one ampoules with contrast medium were routinely opened by sawing and breaking the neck of the ampoule Using 21 gauge needles, the contrast medium was then aspirated into 20 ml disposable plastic syringes of a widely used type which had been flushed once with particle free distilled water before the aspiration. The contrast medium then had to pass through a membrane filter, Nucleopore, which is supposed to retain all particles exceeding 5 µm in diameter The filter was placed on slides and specially prepared using chloroforme as solvent, thus dissolving the filter stroma as well as any contaminating plastic particles The slides were then

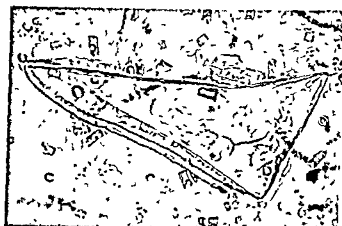
Table

Occurrence of glass fragments on microscopy of filtrates from routinely opened contrast medium ampoules

Ampoules per filter	No of filters	Total No of ampoules	Evident glass particles	Probable glass particles	No glass particles
1	3	3	2	1	—
2	14	28	7	4	3
5	10	50	6	3	1
Total	27	81	15	8	4



a



b

Fig 1 Microscopy Fragments of glass from contrast medium ampoules a) × 80 b) Largest single fragment observed, length 175 μm × 400

particles of glass may be observed in the vessels or tissues following intraarterial contrast injection, e g into the renal arteries

Preliminary experiments were undertaken to detect possible errors caused by 'back-ground' particles in flushing fluid used or laboratory contamination of other sources. Disposable plastic syringes were examined, several particles of various sizes which on polarization microscopy had properties similar to plastic were observed This observation raised the question if the widely used disposable plastic syringes contribute significantly to the contamination of soluble contrast media with alien particles

Methods

The experiments were designed to review the following matters (1) Demonstration of glass particles from contrast solutions from routinely opened glass ampoules on microscopy, (2) determination of the amount and size of particles administered



Fig 5 Dilated tubules arranged in narrow rays (Hematoxylin Azophloxine Saffron × 35)



Fig 3 Section of kidney from a dog 7 days after intraarterial ground glass embolization Intraarterial glass fragments (→) with intima proliferation (↔) and periarterial mononuclear infiltration (Hematoxylin-Azophloxine-Saffron × 80)



Fig 4 Section from kidney from a dog 7 days after intraarterial injection of ground glass suspension and repeated angiography Fibrin deposits and adhesion of part of glomerular tuft (Hematoxylin-Azophloxine-Saffron × 270)

microscoped with and without polarized light, independently by the three present authors

Flushing fluid (distilled water) from the disposable syringes was filtered in the same way, the filters being microscoped without the special preparation mentioned. Flushing fluid from syringes (Isotone) was subjected to a quantitative analysis using the Coulter counting principle, based on the measurement of electric resistance in a thin capillary vessel (GROVES 1973) The number and volume of particles were registered with great exactness, regardless of the shape of the particles

In the animal experiments four dogs, weighing 18 to 22 kg were used Glass particles were produced by crushing ampoule-glass, which after washing in saline were centrifuged and ultimately exposed to a filter holding back particles exceeding 70 μm in diameter. The particles passing this filter were then dispersed in the contrast medium After transfemoral catheterization selective nephroangiography was performed using 3 ml contrast medium (Isopaque Cerebral) immediately followed by the injection of 3 ml of the described suspension Selective angiography of the contralateral kidney was then carried out in the same session In one animal the glass particles were substituted by plastic fragments scraped from a disposable syringe, in other respects the procedures were identical

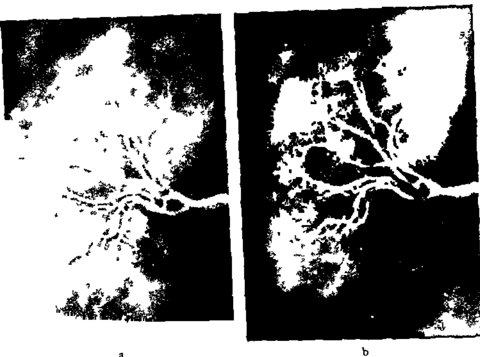


Fig 6 Selective nephroangiography in a dog (the same as in Fig 4) a) Before b) 1 week after embolization with glass particles Occlusions and irregularities of subsegmental and arcuate arteries particularly evident in middle and caudal parts

After one week bilateral selective angiography was performed followed by the removal of the kidneys for microscopy Each animal was thus considered its own control concerning pre and post embolization angiographic and histologic evaluation

Results

Ampoules from two different manufacturers were used in the test, in total 81 (Table) The results of the examination of the filtrates were recorded as positive or negative if the observers were unanimous if one of them was uncertain the findings were recorded as probably positive No attempt was made to quantify the amount of glass fragments however consistently there were only few, one to three particles to be found on each filter The sizes of the observed particles ranged between 10 and 35 μm except one which measured approximately 175 μm (Fig 1) Repeated counts of particles shed from plastic syringes were also made The results of electronic counting from two brands of disposable syringes are graphically presented in Fig 2 Comparison is made with back ground contamination of flushing fluid, and the tolerance limits for parenteral fluids according to the British Pharmacopoeia (1973), are indicated by arrows The results indicate that there is a difference in the size of

(Fig 5) Since this coincides with the proliferation of the intima and foreign particles in the interlobular arteries (Fig 3) it seems reasonable to assume that the injury to the tubules is caused by impaired circulation in the interlobular arteries or—less likely—in the smaller vessels, the vasa recta or the capillaries of the glomeruli Similar lesion of tubules occurs particularly in the first convoluted tubules in a variety of clinical conditions from the third day following onset of disease or injury (BULL 1953)

At angiography performed one week after embolization occlusion of subsegmental and arcuate branches of the arteries were the most evident lesion as well as an overall reduction in the caliber of the intrarenal vessels (Figs 6, 7) This reduction in caliber is considered to be reactive in nature and was observed in specimens with marked glomerular abnormalities

SUMMARY

Microscopy of filtrates made from contrast media of routinely opened glass ampoules substantiates previous assumptions that small fragments of glass may enter into the [illegible]

[illegible] to injectable fluids on usage of disposable syringes

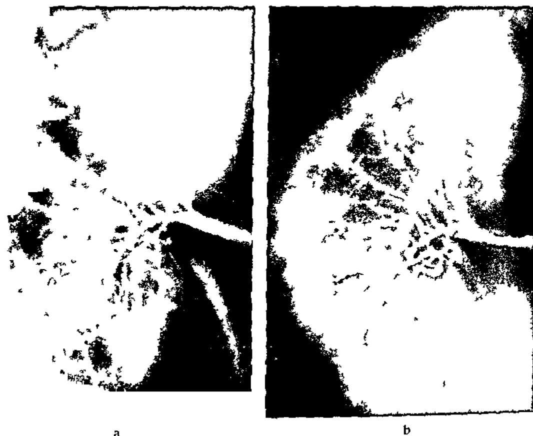
ZUSAMMENFASSUNG

Die Mikroskopie von Filtraten [illegible]
pullen bestätigte frühere Annahme [illegible]
Mittel in beträchtlicher Frequen[illegible]
intraarterieller *Injektion* des Mittels embolische Veränderungen [illegible]

[illegible] Verwendung von Eingangs Plast Spritzen zugefügt werden

RÉSUME

La microscopie de filtrats de moyen de contraste provenant d ampoules en verre ouvertes selon la technique habituelle confirme les hypothèses préalables d'après lesquelles des petits fragments de verre peuvent pénétrer dans l ampoule et dans le moyen de contraste avec une fréquence considérable Ces fragments de verre peuvent causer des lésions emboliques au cours des injections intra artérielles du moyen de contraste, ces lesions cependant sont histologiquement non spécifiques consistant en une prolifération de [illegible]
granulomes associés avec une dilatation de [illegible]
nombre important de particules de plastique [illegible]
quand on utilise des seringues en plastique à [illegible]



a b

Fig 7 Selective nephroangiography in a dog (the same as in Fig 3) a) Before b) 1 week after embolization Reduction in caliber of all intrarenal arteries with increased tortuosity particularly in peripheral subsegmental branches Evident occlusions not visible

particles shed by the two brands of syringes this is valid particularly for particles with mean diameter exceeding 6 μm

Histology of the kidneys one week after the first injection demonstrated intimal proliferation and occasional foreign particles especially lodged in the interlobular arteries and present only on the side where large numbers of particles had been injected (Fig 3) In addition minute lesions in the glomeruli with formation of red hyaline thrombus like material in the capillaries were found both in the kidney exposed to emboli and its control (Fig 4) Since this glomerular abnormality was present in both kidneys it may have been caused by the angiography per se and should not be considered an effect of the particles added experimentally Whether it should be ascribed to the chemical or physical properties of the contrast medium or to the angiographic procedure is uncertain but it is known that selective angiography may produce abnormalities in the kidneys (EDLING et coll 1959, EDLING & OVENFORS 1964)

Degenerated and dilated tubules in the cortex arranged in narrow rays in a haphazard manner were evident in kidneys exposed to a large number of particles

FROM THE DEPARTMENT OF DIAGNOSTIC RADIOLOGY (DIRECTOR PROF OLLE OLSSON), UNIVERSITY HOSPITAL, S 221 85 LUND, SWEDEN, AND DEPARTMENT OF RADIOLOGY (DIRECTOR PROF SHINJI TAKAHASHI), MEDICAL SCHOOL, NAGOYA UNIVERSITY, NAGOYA, JAPAN

EFFECTS OF VASOPRESSIN IN EXPERIMENTAL NEPHROANGIOGRAPHY

JAN GÖTHLIN, SADAYUKI SAKUMA and TAKEO ISHIGAKI

Nephroangiography is well established and yields valuable information in kidney lesions but small abnormalities may be difficult or impossible to detect The radiating arteries, the afferent and efferent vessels and the glomeruli are not angiographically demonstrable and early abnormalities may be located in these structures Vasopressin could possibly be used to improve diagnosis Eight fold direct magnification was used to enhance the demonstration of the effects of vasopressin in rabbit kidneys

Material and Methods

Thirteen white Japanese land rabbits weighing about 4 5 kg were used General anaesthesia was maintained at a fairly constant level by intravenous administration of sodium penthobarbitone For selective angiography green Cook PERT-4 N catheters

Submitted for publication 25 July 1974

REFERENCES

ADAMS D F, OLIN T B and KOSEK J Cotton fiber embolization during angiography Radiology 84 (1965), 678

British Pharmacopoeia, 1973 Edition, Appendix XVI C A 123, London 1973

BULL G M and DIBLE J H Renal function *In* Recent advances in pathology 6th edition, p 273 Edited by G Hadfield Churchill, London 1953

BYERS S O and FRIEDMAN M Lipidization induced by bone and glass fragments within an arterial plaque Brit J exp Path 47 (1966), 405

CHASON J L, LANDERS J W and SWANSON R E Cotton fiber embolism A frequent complication of cerebral angiography Neurology 13 (1963), 558

DUQUESNEL J, POUILLAUDE J M, FROMENT J C et PAPILLON D De la présence de fragments de verre dans les opacifiants vasculaires J Radiol Electrol 54 (1973), 297

EDLING N P G and OVENFORS C O Risks in selective renal catheterization and arteriography Acta radiol Diagnosis 2 (1964), 241

— — Intentional embolism in selective renal arteriography An experimental study in dogs Acta radiol Diagnosis 2 (1964), 316

— HELANDER C G, PERSSON F and ÅSHEIM Å Renal function after selective renal angiography An experimental study in dogs Acta radiol 51 (1959), 161

GARVAN J M and GUNNER B W The harmful effect of particles in intravenous fluids Med J Austr 51 (1964), 1

GROVES M J Parenteral products Heineman Medical Books, London 1973

HURST D A Particles in intravenous fluids Lancet 2 (1965), 181

IRSTAM L Frammande kroppar i parenterala losningar (In Swedish) Farm Rev 71 (1972), 333

SANDELL E and ERNEROT L Membrane filtration during administration for elimination of glass particles from ampoules Acta pharm suecica 5 (1968), 111

SCHULTZ F H, VOLKHEIMER G und JOHN H Experimentelle Gefassveranderungen durch mechanische Reize Dtsch Gesundh -Wes 20 (1965), 1122

SILBERMAN J, CRAVIOTO H and FEIGIN I Foreign body emboli following cerebral angiography Arch Neurol 3 (1960), 711

(ID/OD 0 86/1 37 mm) were used The tip of the catheter was drawn out and hooked about 80 degrees The catheter was introduced into the vascular system via a cut down in the right groin The tip was positioned in either the right or the left renal artery during fluoroscopy At every examination 2 ml of contrast medium, meglumine metrizoate (Angiografin, Schering, West Germany), was injected by hand in about 2 seconds Serial angiography with exposure every 2 second was performed using a cassette changer (hand driven, specially designed for the purpose) The tube (Toshiba M 5118 BX /DRX-89 A/ – 6059) with a 0 05 mm focal spot was located underneath the examination table The film focus distance was 106 cm and the distance between the focus and the center of the kidney was 15 cm ± 0 5 cm Exposure data were 120 kV, 3 mA, 0 1-0 2 s Intensifying screens of medium speed (Kyokko MS) and Kodak Royal Blue film were used Compression of the tissues above the kidneys was obtained with a plastic plate The magnification ratio was 7 1 to 8 1

In each rabbit synthetic arginine vasopressin (Vasopressinum INN, Ferring, Sweden) was injected in doses of 0 01, 0 1 and 1 0 IU, administered via the arterial catheter 60 seconds before angiography In 11 rabbits control series were obtained at varying intervals after the doses of 0 01 and 0 1 IU of the drug in order to check that the circulation returned to normal before testing the next dose

Results

In the control series the interlobular arteries could always be demonstrated and the glomeruli were well defined (Fig 1 a) Afferent and efferent arterioles, however, could only be traced on a few films at the juxtamedullary glomeruli The size of the glomeruli on the films varied between 1 2 and 1 8 mm The cortical veins and the collecting veins were demonstrated No venous anastomoses could be observed The border between the cortex and the medulla was well defined and the juxtamedullary glomeruli were easy to single out

The results after administration of vasopressin are summarized in the Table The concentration of the contrast medium in the main renal vein and in the intrarenal veins and especially in the cortex increased No anastomoses were observed The size of the glomeruli was unchanged but the number decreased, more marked with higher doses of vasopressin At the dose of 0 01 IU the outer part of the cortex was not filled with contrast medium and after 1 0 IU only the juxtamedullary glomeruli (Fig 1 c) The concentration of contrast medium in the glomeruli increased after all doses of vasopressin tested In the cortical veins also an increased concentration of medium occurred after 0 01 and 0 1 IU, but a decrease after 1 0 IU With the latter dose only some veins were demonstrated and the identified ones contained no contrast medium in the outer part (Fig 2 c) The width of the main renal vein and the collecting veins increased as well as the intravenous concentration of the contrast medium but the width of the cortical veins was unchanged



a

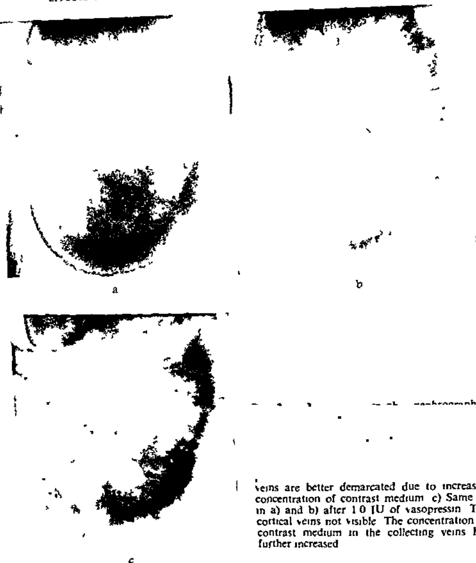


b



c

Fig 1 a) Nephroangiography arterial phase at eight fold direct roentgenographic magnification The glomeruli are seen all through the cortex All films reproduced in about half the size b) Same as in a) after injection of 0 1 IU of vasopressin into the renal artery The glomeruli in the outer part of the cortex are not well filled with contrast medium c) Same as in a) and b) after injection of 1 0 IU of vasopressin Only juxtamedullary glomeruli are filled with contrast medium The concentration of contrast medium in the arteries is increased



veins are better demarcated due to increased concentration of contrast medium c) Same as in a) and b) after 1 0 IU of vasopressin The cortical veins not visible The concentration of contrast medium in the collecting veins has further increased

pressin intravenously administered at selective nephroangiography in dogs have been reported by NYLANDER (1967) An increased width and tortuosity of the renal arteries was found and they could be traced further distally than in controls The subcortical and collecting veins were well demonstrated and the main renal vein dilated and with increased concentration of contrast medium The size of the kidney was also increased The present results are in accordance with those previously described except for the unchanged size of the kidney and the unchanged width of the arteries in this material

Table

The results of different doses of arginine vasopressin in the vascularity of the kidney. The appearances on the films after 0.01, 0.1 and 1.0 IU of arginine vasopressin injected into the renal artery. 0 = no change compared with control, + = increase compared with control, − = decrease compared with control. The number of + and − indicate the magnitude of the change

	0.01 IU	0.1 IU	1.0 IU
Arteries			
Width of main renal artery	0	0	0
Width of interlobar arteries	0	0	0
Concentration of contrast medium	(+)	+	+ +
Cortex			
Thickness	0	0	0
Number of visible glomeruli	−	− −	− − −
Size of visible glomeruli	0	0	0
Distribution of visible glomeruli	Outer cortex −	Most cortex − −	Only juxtam gl +
Concentration of medium in visible glomeruli	+	+	+ +
Size of kidney	0	0	0
Veins			
Width of main renal vein	(+)	+	+ +
Width of collecting veins	(+)	+	+ +
Concentration of medium in main renal vein	(+)	+	+ +
Concentration of medium in collecting veins	(+)	+	+ +
Width of cortical veins	−	−	−
Concentration of medium in cortical veins	+	+ +	−

Discussion

At conventional angiography it is possible to demonstrate abnormalities of the larger renal arteries and veins and of the size and shape of the kidney and its cortex. However, the conventional technique is not sufficient for the smaller structures.

With eight-fold direct magnification using a small focus it is possible to demonstrate the interlobular and sometimes the cortical arteries, the glomeruli and the cortical veins in a rabbit kidney. Photographic enlargement was not satisfactory in the present material (Fig. 3). The prerequisites for angiography with direct magnification and a small focus have previously been discussed by SAKUMA et coll. (1969). Its application in angiography of dog kidneys at four-fold magnification was reported by KANEKO (1966). The demonstration of the glomeruli was not satisfactory and only a few could be seen. This may be explained by the long exposure times needed due to the low output of the tube.

Anastomosing veins (GRAVES 1956) were not observed. They are probably not functioning during normal conditions (GÖTHLIN & OLIN 1973). The effects of vaso-

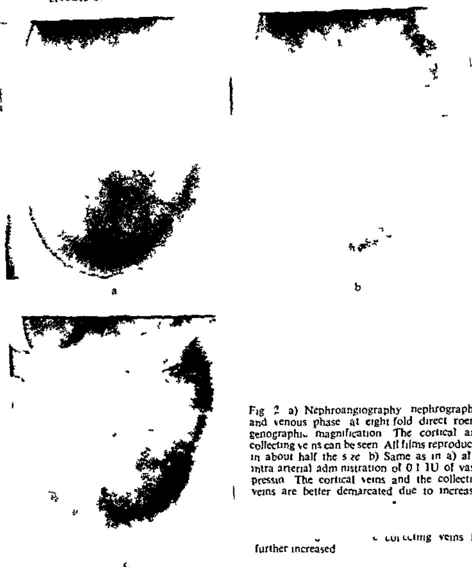


Fig 2 a) Nephroangiography nephrographic and venous phase at eight fold direct roentgenographic magnification The cortical and collecting veins can be seen All films reproduced in about half the size b) Same as in a) after intra arterial administration of 0 1 IU of vasopressin The cortical veins and the collecting veins are better demarcated due to increased

... collecting veins has further increased

pressin intravenously administered at selective nephroangiography in dogs have been reported by NYLANDER (1967) An increased width and tortuosity of the renal arteries was found and they could be traced further distally than in controls The subcortical and collecting veins were well demonstrated and the main renal vein dilated and with increased concentration of contrast medium The size of the kidney was also increased The present results are in accordance with those previously described except for the unchanged size of the kidney and the unchanged width of the arteries in this material



Fig 3 Same kidney as in Fig 2 at three-fold photographic enlargement using a 0 6 mm focal spot Glomeruli and smaller vessels not visible

BARER (1963) and BERDE (1965) demonstrated in animals that when using vasopressin the renal blood flow and the urinary flow increased without demonstrable pressor activity. ARONSEN & NYLANDER (1964) reported that an intravenous injection of 20 IU vasopressin 5 min before lumbar aortography caused an increase in the proportion of the contrast medium distributed to the kidneys and improved the nephrographic phase Since a rise in the systemic blood pressure was registered, the findings were assumed to result from vasopressin lowering the resistance of the renal vascularity relative to that in the systemic one ERIKSSON (1972) using isotope labelled microspheres in dogs found that vasopressin in doses of 0 75 and 6 75 mIU per kg bodyweight per min administered during a 10-minute period did not influence the blood flow to the kidneys. Using a dye-dilution technique EKELUND et coll (1972) reported on the effects of 0 05 IU of arginine vasopressin administered intraarterially

in a rabbit kidney with an intravenous fistula The total blood flow increased 10 per cent while the shunt flow decreased 20 per cent and the renal parenchymatous flow increased 30 per cent The mean transit time decreased slightly In man doses of 0 05 and 0 1 IU of arginine vasopressin shortens the appearance time considerably despite reduced flow (GÖTHLIN) CARTER & GÖTHLIN (1970) reported faster filling and greater concentration of contrast medium of the uterine vein in pregnant rabbits after the administration of 0 02 IU of vasopressin despite reduction in number of demonstrated smaller uterine and placental arteries, attributing the findings to shunting

In the present material a decreased number of glomeruli was visible at angiography after vasopressin After 1 0 IU only the juxtamedullary glomeruli could be identified The cortical veins were poorly seen but the concentration of medium in the larger renal veins increased, indicating that medium passed the juxtamedullary shunts into the draining veins The increased concentration of the medium within the renal arteries may be due to decreased amounts of medium passing through the glomeruli, decreased mean transit time and few glomeruli open

From previous reports and from the present material it may be assumed that the flow through the kidney after 0 01 to 0 1 IU of vasopressin increased despite the shutting off of a number of glomeruli and that it may be due to shunting, possibly in the juxtamedullary shunts.

The distribution of the glomeruli is an interesting feature The most peripherally localized glomeruli are affected by the lowest dose of vasopressin which could imply that the longer efferent or afferent vessels are the most easily affected In allotransplanted dog kidneys DEMPSTER (1971) reported that vasopressin in a dose of 1 0 IU caused renal afferent vasoconstriction and underperfusion of the outer cortex He stated that the juxtamedullary glomeruli, their afferent arterioles and corresponding vasae recta may absorb a part of the total renal blood flow to the cortex if an increased cortical resistance exists peripherally Juxtamedullary glomeruli in the rabbit kidney constitute 15 per cent of the about 200 000 glomeruli (HEGGIE 1947) and may with an increased rate of flow, contain the whole normal glomerular capillary blood volume It may explain the increased concentration of contrast medium in the veins after the administration of vasopressin as the medium easily may pass faster through the unaffected glomeruli and, in part, pass the juxtamedullary shunts This opinion is also supported by TRUETA et coll (1947, rabbit experiments) and by WAKIM et coll (1942 dogs) How this is accomplished by the effect of vasopressin is, however, not clear

Using tubes with higher output the technique may be improved, making it possible to demonstrate human glomeruli accurately It should be possible to detect abnormalities of the small vessels, especially in the cortical arteries and veins and in the glomeruli at an early stage resulting in an earlier diagnosis and an earlier therapy Renal biopsy might thus be less necessary

Recently, the use of vasopressin at nephroangiography in man has been started and it has already been found that the concentration of contrast medium in arteries and veins was improved (GÖTHLIN)

SUMMARY

Nephroangiography was performed in 13 rabbits using eight fold magnification with a 0 05 mm focus After arginine vasopressin in doses of 0 01 to 1 0 IU the glomeruli were well demonstrated as well as the subcortical arteries and veins and the concentration of contrast medium in arteries and veins increased At increasing doses of vasopressin the glomeruli were shut off to an increasing degree beginning at the outer part of the cortex At 1 0 IU only the juxtamedullary glomeruli functioned

ZUSAMMENFASSUNG

Nierenangiographie wurde bei 13 Kaninchen unter Verwendung einer achtfachen Ver grosserung mit einem 0 05 mm Fokus vorgenommen Nach Arginin Vasopressin in Dosen von 0 01 bis 1 0 IU stellten sich die Glomeruli sowie die subcorticalen Arterien und Venen gut dar und die Konzentration des Kontrastmittels in den Arterien und Venen stieg an Bei steigenden Dosen von Vasopressin wurden die Glomeruli in zunehmenden Masse ab geschaltet mit Beginn im ausseren Teil der Cortex Bei 1 0 IU waren lediglich die juxta medullaren Glomeruli in Funktion

RESUME

Une néphroangiographie a été pratiquée sur 13 lapins en utilisant un grossissement de 8 fois avec un foyer de 0 05 mm Après administration de vasopressine arginine aux doses de 0 01 à 1 0 IU les glomérules sont bien mis en evidence ainsi que les arteres sous corticales et les veines et la concentration du moyen de contraste dans les veines et dans les arteres est augmentée A des doses plus fortes de vasopressine les glomérules sont exclus dans une mesure croissante et leur exclusion commence dans la partie externe du cortex A 1 0 IU seuls les glomérules juxtamédullaires fonctionnent

REFERENCES

ARONSEN K F and NYLANDER G Angiographic studies of the action of vasopressin in the dog A preliminary report Vasc Dis 1 (1964) 127

BARER G R The action of vasopressin a vasopressin analogue (PLV$_2$) oxytocin angiotensin bradykinin and theophylline ethylene diamine on renal blood flow in the anaesthetized cat J Physiol 169 (1963) 62

BERDE B Some observations on the circulatory effects of oxytocin vasopressin and similar polypeptides *In* Advances in oxytocin research p 11 Pergamon Press London 1965

CARTER A M and GÖTHLIN J Effects of angiotensin oxytocin and vasopressin on placental circulation An angiographic study in rabbits Invest Radiol 5 (1970) 86

DEMPSTER W J The nature of experimental secondset kidney transplant rejection 2 The mimicking of the haemodynamic upset by pharmacological and other means Brit J exp Path 52 (1971) 172

EKELUND L GÖTHLIN J and *OLIN T Arteriovenous fistulae in rabbit kidney studied by* dye dilution technique and by angiography Scand J Urol Nephrol 6 (1972) 84

ERIKSSON B F Effect of vasopressin on the distribution of cardiac output in the early phase of haemorrhagic shock in the anaesthetized dog Acta chir scand 138 (1972), 119

GOTHLIN J To be published

— and OLIN T Dye dilution technique with nephroangiography for the determination of renal blood flow and related parameters Acta radiol Diagnosis 14 (1973) 113

GRAVES F T The anatomy of the intrarenal arteries in health and disease Brit J Surg 43 (1956) 606

HEGGIE J F Lesser circulation of the kidney Lancet 1 (1947), 385

KANEKO M Angiography in four timed magnification applied to the kidney of the human living body (English summary) Nippon Acta radiol 26 (1966), 55

NYLANDER G Vascular response to vasopressin as reflected in angiography Acta radiol (1967) *Suppl No 266*

SAKUMA S, IKEDA H, AYAKAWA Y, TANAKA Y and TAKAHASHI S Angiography with direct four fold magnification Invest Radiol 4 (1969), 310

TRUETA J, BARCLAY A, DANIEL P, FRANKLIN K and PRICHARD M Renal pathology in the light of recent neurovascular studies Lancet 2 (1946), 237

— BARCLAY A, DANIEL P, FRANKLIN K and PRICHARD M Studies of the renal circulation Blackwell Scientific Publications Oxford 1947

WAKIM K HERRICK J, BALDES E and MANN F The effect of pitressin on renal circulation and urine secretion J Lab clin Med 27 (1942), 1013

FROM THE DEPARTMENTS OF MEDICAL PHYSICS (DIRECTOR P-E ÅSARD), DANDERYDS SJUKHUS, S-182 03 DANDERYD, AND DIAGNOSTIC RADIOLOGY (DIRECTOR ULF RUDHE), HUDDINGE UNIVERSITY HOSPITAL, S-141 86 HUDDINGE, SWEDEN

^{75}SE-METHIONINE UPTAKE IN THE PANCREAS

An experimental investigation in mice

ROLF LEWANDER

Scintigraphy with ^{75}Se-methionine is a commonly used method for the examination of the morphology and function of the pancreas BLAU & BENDER (1962) stressed the importance of stimulation of enzyme synthesis in the gland for the test They recommended a meal of high protein content followed by administration of Cecekin (secretin + pancreozymin + cholecystokinin) one hour before the injection of the isotope A similar procedure was used by SODEE (1964) although the meal contained almost pure protein in addition glutamine acid hydrochloride was given parenterally 15 min before the isotope In later experiments in dogs he re evaluated the significance of the meal and felt it to be of no particular advantage In addition to a 'high protein breakfast', RODRIGUEZ-ANTUNEZ (1964) advocated the use of morphine in order to provoke spasm of the sphincter of Oddi to impede the release of the digestive enzymes labelled by the isotope TABERN et coll (1965) observed that this procedure was often followed by nausea and vomiting and instead used a slow intravenous infusion of Aminosol KUPIC & KASENTER (1969) demonstrated that an increased uptake in the dog was produced by injection of ^{75}Se methionine in the celiac artery Similar selective intra arterial administration of secretin and pancreozymin had an additive effect on the isotope uptake, possibly due to increase of blood flow through

Submitted for publication 30 October 1974

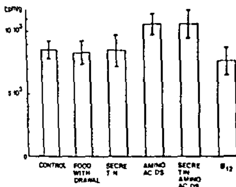


Fig. 1 Average ^{75}Se methionine activity in counts per minute per gram of pancreas ± SD

the gland and stimulation of secretion of digestive enzymes STEINBERG (1971) referring to results compiled by SHAPIRO & SCHLENK (1965), stated that repeat injections of vitamin B_{12} produced an increase in pancreatic isotope uptake

Most of the clinical reports on the improvement of scanning of the pancreas lack control series experiments aimed at objective assessment of the value of the procedures are few and generally concern single isolated attempts at increasing the rate of uptake The present investigation in mice was designed to elucidate the effects of different measures on the pancreatic uptake of ^{75}Se methionine, particularly in relation to that in adjacent organs

Material and Methods The experimental population consisted of 60 male mice weighing 14 to 24 g distributed at random into 6 groups of 10 each Ten μCi ^{75}Se methionine were administered intravenously to all of them The compounds used in addition to ^{75}Se methionine are presented in the Table Intravenous injection of

Table

The compounds used in addition to ^{75}Se methionine

Group		No of mice
I	^{75}Se methionine 1 hour after a standard meal with 20% protein (control group)	10
II	^{75}Se methionine after 12 hours food withdrawal	10
III	^{75}Se methionine and secretin	10
IV	^{75}Se methionine and amino acids (Aminosol)*	10
V	^{75}Se methionine and secretin amino acids (Aminosol)*	10
VI	^{75}Se methionine and vitamin B_{12} (24 and 2 hours before sampling)	10

* 100 ml Aminosol contains 0 4 g of Lysine 0 05 g of Tryptophane 0 1 g of each Methionine and Phenylalanine 0 6 g of Leucine 0 2 g of Isoleucine 0 16 g of Valine 0 3 g of Arginine 0 2 g of Glycine 0 3 g of Cysteine and about 0 7 g of other free amino acids and 0 2 g of Tripeptides

FROM THE DEPARTMENTS OF MEDICAL PHYSICS (DIRECTOR P-E ÅSARD), DANDERYDS SJUKHUS, S-182 03 DANDERYD, AND DIAGNOSTIC RADIOLOGY (DIRECTOR ULF RUDHE), HUDDINGE UNIVERSITY HOSPITAL, S 141 86 HUDDINGE, SWEDEN

^{75}SE-METHIONINE UPTAKE IN THE PANCREAS

An experimental investigation in mice

ROLF LEWANDER

Scintigraphy with ^{75}Se-methionine is a commonly used method for the examination of the morphology and function of the pancreas BLAU & BENDER (1962) stressed the importance of stimulation of enzyme synthesis in the gland for the test They recommended a meal of high protein content followed by administration of Cecekin (secretin + pancreozymin + cholecystokinin) one hour before the injection of the isotope A similar procedure was used by SODEE (1964), although the meal contained almost pure protein, in addition glutamine acid hydrochloride was given parenterally 15 min before the isotope In later experiments in dogs he re evaluated the significance of the meal and felt it to be of no particular advantage In addition to a 'high protein breakfast', RODRIGUEZ-ANTUNEZ (1964) advocated the use of morphine in order to provoke spasm of the sphincter of Oddi to impede the release of the digestive enzymes labelled by the isotope TABERN et coll (1965) observed that this procedure was often followed by nausea and vomiting and instead used a slow intravenous infusion of Aminosol KUPIC & KASENTER (1969) demonstrated that an increased uptake in the dog was produced by injection of ^{75}Se methionine in the celiac artery Similar selective intra arterial administration of secretin and pancreozymin had an additive effect on the isotope uptake, possibly due to increase of blood flow through

Submitted for publication 30 October 1974

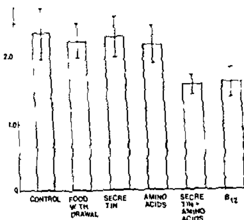


Fig 3 *Average ratio of* ^{75}Se methionine activity per gram of pancreas to that in liver $\pm$SD

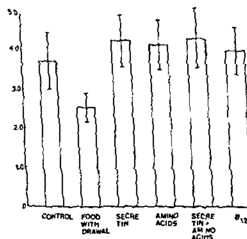


Fig. 4 Average ratio of ^{75}Se methionine activity per gram of pancreas to that in stomach + gut $\pm$SD

significant difference ($p<0.001$) was present also between the groups given amino acid and the control group when calculated as a ratio of uptake in pancreas and blood ($9.54+0.91$, 9.29 ± 0.82 and 7.46 ± 0.79, Fig 2) The remaining groups did not differ significantly from the control group

There was no evidence that injection of amino acids alone had any effect on the ratio of isotope activities of the pancreas and liver, however, this ratio was significantly decreased ($p<0.001$) for the groups Secretin + amino acids and vitamin B_{12}, respectively The ratios were 1.53 ± 0.13, 1.58 ± 0.22 and for the control group 2.34 ± 0.38 (Fig 3)

In the group maintained on 12-hour food withdrawal the ratio per gram of pancreas and gastro-intestinal tract was significantly decreased ($p<0.001$) when compared

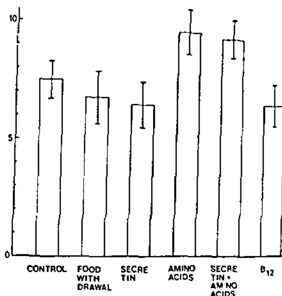


Fig 2 Average ratio of [75]Se methionine activity per gram of pancreas to that in blood ±SD

Secretin and Aminosol took part immediately following that of [75]Se-methionine while vitamin B_{12} was injected intramuscularly 24 and 2 hours before administration of the radioisotope The doses used were the following Secretin 0 15 IU, Aminosol 0 05 ml and vitamin B_{12} 0 3 μg × 2 The animals were killed 1 hour after administration of the [75]Se-methionine, preliminary experiments having revealed that the maximum uptake in the pancreas was obtained 45 to 60 min following the injection of the isotope Whole body radiation activity was measured with a scintillation detector equipped with a collimator especially designed for mice The pancreas, liver, spleen, stomach and gut were dissected free and a blood sample was taken from the inferior vena cava The activity of the organs, blood sample and a known standard were measured in a well detector and the organs and the remainder of the mouse were weighed After subtraction of the background radiation the net activity was calculated and expressed as counts per min/g tissue (cpm/g) Since the relative distribution of the isotope between the pancreas and its adjacent organs should provide more pertinent information than the absolute pancreatic uptake, the main part of the results will be presented as cpm/g—pancreas related to cpm/g—liver, -blood, -gastrointestinal tract, -spleen and -whole body This would eliminate errors due to incomplete injection and variation in the size of the mice

Results

The isotope uptake in pancreas per gram of tissue was increased significantly following administration of amino acids ($p < 0 01$), both with and without secretin (10 367±1 095 and 10 454±796 cpm/g) The other groups including that of administration of secretin did not differ significantly from the control (Fig 1) A

known that the effect of secretin on blood flow and secretion is far from organ specific it is hypothesized that the combination of the substances given might preferentially stimulate the synthesis of proteins in the liver

Vitamin B_{12} did not enhance the pancreatic uptake It is true that vitamin B_{12} mediates the transmission of methyl groups in the synthesis of methionine (SHAPIRO & SCHLENK 1965) but this effect would hardly influence the synthesis of enzymes if an excess of methionine is available

Withdrawal of food favoured the uptake in the gastrointestinal tract at the expense of that in the pancreas BLAU & MANSKE (1961), experimenting with starving dogs and comparing the activities of the pancreas and liver, recorded an increase in the liver This observation had no counterpart in the present material There is reason to believe that restriction of the food intake is of no advantage and may actually be detrimental to clinical pancreatic scintigraphy

It is concluded that the isotope uptake in the pancreas of mice is influenced by several factors Among these, the most significant is that intravenous infusion of amino acids increases the rate of isotope accumulation in the pancreas, both absolutely and relatively to the amount present in blood

A clinical investigation based on the effects recorded in the experimental series is presently being carried out, the patients serving as their own controls

SUMMARY

Measurements of the uptake of ^{75}Se methionine in the abdominal visceral organs of mice indicate that amino acids (Aminosol) significantly increase the accumulation of the isotope in pancreas Similarly a beneficial effect is observed on the distribution of activity between pancreas and blood while withdrawal of food adversely affects the uptake in the pancreas and gastro-intestinal tract

ZUSAMMENFASSUNG

Messungen der Aufnahme von ^{75}Se Methionin in den abdominalen visceralen Organen [illegible] beeinflusst

RÉSUMÉ

Les mesures de fixation de la ^{75}Se méthionine dans les viscères abdominaux de souris montrent que les acides aminés (Aminosol) augmentent notablement l accumulation de cet isotope dans le pancréas De même ils ont un effet bénéfique sur la distribution de l activité entre le pancéas et le sang alors que le jeûne au contraire affecte la fixation dans le pancréas et le tube digestif

with the control group and the other groups as well (2 53±0 36 and 3 72±0 73 (*Fig* 4)

No significant difference was registered between the uptake ratios of pancreas and spleen in the various groups

Discussion

Although scintigraphy with ⁷⁵Se-methionine is an established method for examination of the pancreas, there are several attendant problems The most important is the one fact that occasionally the uptake in the normal pancreas may be low and produce a mottled scintigraphic appearance (KING et coll 1966) The difficulty in distinguishing between various pathologic processes exhibiting a more or less uniform scintigraphic image is another disadvantage Even with the aid of computer, enhancement appraisal of the scintigrams basically remains subjective This adversely affects any comparison of clinical investigations Experiments on animals should afford a better means of standardization, due to access to homogeneous biologic material, adequate supervision of the food intake, meticulous recording of the isotope uptake and the ability to refer the activities to the weight of the organs A substantial disadvantage is that the results obtained in animal experiments cannot be transferred directly to conditions prevailing in clinical medicine because of possible differences in protein metabolism in the two species

Improvement of pancreatic scintigraphy would presuppose an increase of the isotope uptake in the gland per se and also in relation to adjacent organs, or a combination of both mechanisms Theoretically the metabolism of proteins in the pancreas may be accelerated by providing an increased amount of precursors essential for protein synthesis (amino acids) or administration of drugs capable of inducing a similar but lesser increase in adjacent organs The alternative procedure of inhibiting the synthesis in these organs would seem to impose even greater difficulties from a technical point of view and might prove deleterious to cellular function Therefore it was discarded

The results demonstrate that the rate of the protein synthesis in the pancreas is stimulated by infusion of amino acids following the injection of ⁷⁵Se methionine This finding is in agreement with that of TABERN et coll (1965) The pancreatic uptake is increased relative to the amount of isotope present in blood which would result in a reduction of background radiation

Secretin failed to exert any significant influence on the uptake in the pancreas or on the relative distribution of the isotope between pancreas and liver, a result diverging from that recorded by KUPIC & KASENTER in dogs Whether this discrepancy should be ascribed to the selective intra-arterial injection of the secretin in the dogs or factors specific to the species cannot be determined The reason why the combined injection of secretin and amino acids raised the uptake of the isotope in the liver compared to that in the pancreas is difficult to explain However, it is

FROM THE DEPARTMENT OF DIAGNOSTIC RADIOLOGY (DIRECTOR PROF O OLSSON)
UNIVERSITY HOSPITAL, S 221 85 LUND, SWEDEN

ANGIOGRAPHY IN DISEASE OF THE PERIPANCREATIC LYMPH NODES

ULF TYLÉN

The vascular abnormalities caused by pancreatitis and pancreatic carcinoma are well documented in the literature (REUTER et coll 1969, BOOKSTEIN et coll 1969, TYLÉN & ARNESJO 1973, TYLEN 1973, among others) their nature, however, is not very well understood It appears that true involvement of the vascular wall by the inflammatory or malignant process only seldom occurs (LUNDERQUIST 1965, HOWARD & NEDWICH 1971, MARIONS et coll 1974) and that the changes in the vessel wall mainly develop as a reaction on perivascular disease Angiographic appearances similar to those caused by pancreatitis and pancreatic carcinoma therefore may be anticipated also in other diseases in the peripancreatic area This fact may cause considerable differential diagnostic difficulties

The following patients with disease of the peripancreatic lymph nodes are reported to stress the fact that vascular abnormalities demonstrated by angiography often are unspecific

Material and Methods Angiography was performed in 6 patients with malignant lymphoma 3 of whom had reticulum cell sarcoma, and in 2 patients with metastatic involvement of the peripancreatic lymph nodes from prostatic carcinoma and seminoma of the testis respectively The diagnoses were in all the patients verified by microscopy of specimens obtained by operation or post mortem Angiography of

Submitted for publication 7 October 1974

REFERENCES

BLAU M and BENDER M Se[75]-selenomethionine for visualization of the pancreas by isotope scanning Radiology 78 (1962), 794

— and MANSKE R The pancreas specificity of Se[75]-selenomethionine Nucl Med 2 (1961), 102

KING E R, SHARPE A, GRUBB W, BROCK J S and GREENBERG L A study of the morphology of the normal pancreas using Se[75]-methionine photoscanning Amer J Roentgenol 96 (1966), 657

KUPIC E and KASENTER A Experimental pancreatic scanning Preliminary results using intra-arterial [75]Se-seleno methionine and hormone stimulation Radiology 93 (1969), 1376

MELMED R N, AGNEW J E and BOUCHER I A D The normal and abnormal pancreatic scan Quart J Med 37 (1968), 607

RODRIGUEZ-ANTUNEZ A Pancreatic scanning with selenium [75]-methionine, utilizing morphine to enhance contrast A preliminary report Cleveland Clin Quart 31 (1964), 213

SHAPIRO S K and SCHLENK F Transmethylation and methionine biosynthesis Symposium The University of Chicago Press, Chicago, London 1965

SODEE B Radioisotope scanning of the pancreas with seleno-methionine (Se[75]) Radiology 83 (1964), 910

STEINBERG S Personal communication The Society of Nuclear Medicine, 18th annual meeting Los Angeles 1971

TABERN D L, KEARNEY J and DOLBOW A The use of intravenous amino acids in the visualization of the pancreas with seleno 75 methionine Nucl Med 6 (1965), 762



Fig 2 Reticulum cell sarcoma in a woman aged 36 a) Irregular stenosis of splenic artery Irregular arteries to pancreatic tail b) Compression of the splenic vein (→)

in 2 patients (Fig 5) The displacement appeared caused by an avascular expansive lesion The superior mesenteric artery was displaced ventrally in one of the patients (Fig 5 b) Abnormalities of the pancreatic vascularity were not evident The portal vein was stenosed in one patient and the splenic vein in one (Fig 4 b)

The metastases from a seminoma to the lymph nodes around the pancreas caused displacement of the gastroduodenal artery and the pancreatic arcades The enlarged lymph nodes also compressed the portal vein Stenosis of arteries around the pancreas was not displayed neither was tumour vascularity encountered The patient with metastases to peripancreatic lymph nodes from prostatic carcinoma had complete stenosis of the coeliac artery and a long smooth stenosis of the common hepatic artery The pancreatic arcades were dilated and tortuous but this was considered due to collateral circulation from the superior mesenteric artery to the coeliac artery The large veins were not involved

In the entire series of 8 patients displacement of the kidney pelvis or the ureter by the enlarged lymph glands was observed in 4

Discussion

Reticulum cell sarcoma of the small intestine is reported not to give vascular abnormalities (BOIJSEN & REUTER 1966, LUNDERQUIST et coll 1971) Reticulum cell sarcoma with retroperitoneal localization, on the other hand, may give encasement

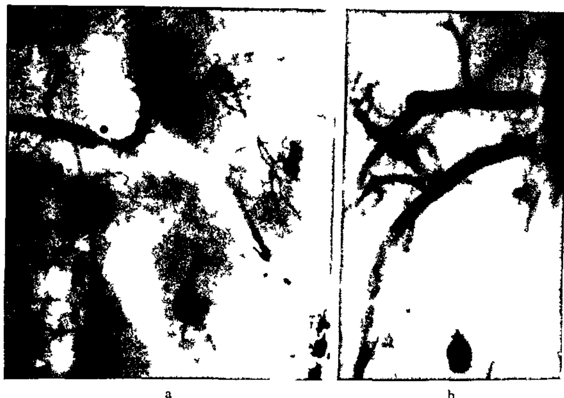


Fig 1 Reticulum cell sarcoma in a woman aged 74 a) Irregular stenos s of splen c artery Small arteries to the tail of the pancreas tortuous and irregular Lateral d splacement of left k dney pel is and ureter b) Lateral v ew Main stem of superior mesenter c artery pushed anter orly

the coeliac and superior mesenteric arteries was performed in all cases in antero posterior and right posterior oblique projections in three patients lateral views were obtained as well

Results

All the patients with reticulum cell sarcoma displayed stenosis of the splenic artery The outline of the stenosis was irregular in 2 patients (Figs 1 2) while in the third it was more smooth (Fig 3) The small arteries to the tail of the pancreas were tor tuous and irregular and the vascularity of the tail was rich in all 3 patients Tumour vessels were however not demonstrated The splenic vein was occluded in one patient and severely stenosed in 2 (Figs 2 b 3 b) Displacement of the pancreatic arteries was not observed but the main stem of the superior mesenteric artery was displaced ventrally in those patients in whom also a lateral view was obtained (Fig 1 b)

Irregular stenosis of arteries was not demonstrated in the 3 patients with malig nant lymphoma other than reticulum cell sarcoma Slight smooth rather long tapering stenosis however was evident in the splenic and hepatic arteries in 2 patients (Fig 4) The gastroduodenal artery and the pancreatic arcades were displaced and stretched



a

b

Fig. 4 Man aged 48



a



b

Fig 3 Reticulum cell sarcoma in a woman aged 67 a) Smooth stenosis of splenic artery out to the hilum of the spleen Hypervascularity of the tail of the pancreas b) Stenosis of splenic vein (→)

of arteries and tumour vessels (BRON & SHERMAN 1967, LAMARQUE et coll 1970) In our patients with peripancreatic reticulum cell sarcoma irregular stenosis of arteries similar to encasement caused by pancreatic carcinoma was demonstrated (Figs 1, 2) The part of the pancreas close to the growth was richly vascularized and the vessels markedly irregular Neovascularity, however, was not demonstrated

Pancreatic carcinomas are usually not rich in vessels, they are mainly avascular although on high quality films scanty tumour vessels often may be demonstrated This discrepancy, arterial encasement and rich vascularity, may give an indication of the diagnosis of reticulum cell sarcoma Venous compression or occlusion may be caused by both conditions Since the therapy of choice in reticulum cell sarcoma often differs from that in pancreatic carcinoma the preoperative establishment of a definitive pathologic diagnosis of reticulum cell sarcoma is needed A cytologic diagnosis may be provided by percutaneous transperitoneal fine needle biopsy directed by the findings at angiography This procedure is easily performed without risk at the same time as angiography (TYLEN et coll)

Malignant lymphoma of other type than reticulum cell sarcoma, for example lymphosarcoma in the peripancreatic area were in our patients of low vascularity acting mainly as expansive lesions displacing arteries and obstructing veins This is in accordance with the findings by others although a scanty hypervascularity may be displayed by selective injection of lumbar arteries (BRON & SHERMAN, KAHN 1971, LOWMAN et coll 1972, LEVIN et coll 1973) In some of our patients slight smooth tapering arterial stenosis was moreover evident

Metastasis to lymph nodes around the pancreas may cause encasement of arteries

sent series was not demonstrated in a series of 21 patients with pancreatic pseudocyst (TYLÉN & ARNESJÖ) Several findings therefore may point at a diagnosis of peripancreatic lymph node disease but the ultimate diagnosis has to be provided by other means for example percutaneous fine needle biopsy

SUMMARY

Angiography was performed in 8 patients with peripancreatic lymph node disease The findings were similar to those caused by pancreatitis and pancreatic carcinoma The angiographic characteristics of the diseases, respectively, are discussed

ZUSAMMENFASSUNG

Angiographie wurde bei 8 Patienten mit peripankreatischen Lymphknotenerkrankung
gerufen durch eine Pankreatitis und ein
Charakteristika der verschiedenen Er-

RÉSUMÉ

Une angiographie a éte faite à 8 malades presentant une affection des ganglions lymphatiques péripancreatiques Les résultats ont eté semblables à ceux qu'on observe dans la pancreatite et dans le cancer du pancréas L'auteur examine les caractéristiques angiographiques de ces différentes affections

REFERENCES

BOIJSEN E and REUTER S R Mesenteric angiography in the evaluation of inflammatory and neoplastic disease of the intestine Radiology 87 (1966) 1028

BOOKSTEIN J J, REUTER S R and MARTEL W Angiographic evaluation of pancreatic carcinoma Radiology 93 (1969), 757

BRON K M and SHERMAN L Arteriography in evaluating retroperitoneal mass lesions N Y J Med 67 (1967), 1875

HOWARD J M and NEDWICH A Correlations of the histologic observations and operative findings in patients with chronic pancreatitis Surg Gynec. Obstet 132 (1971), 387

KAHN P C Retroperitoneal angiography in adults *In* Angiography Second Edition Edited by H L Abrams Little, Brown & Co Boston 1971

LAMARQUE J L, GINESTIE J F, COMBES C. et SÉNAC J P Les difficultes du diagnostic arteriographique des tumeurs rétropéritonéales vraies de l'adulte J Radiol 51 (1970) 625

LEVIN D C WATSON R C and BALTAXE H A Arteriography of retroperitoneal masses Radiology 108 (1973) 543

LOWMAN R M GRNJA V, PECK D R, OSBORN D and LOVE L The angiographic patterns of the primary retroperitoneal tumors Radiology 104 (1972), 259

LUNDERQUIST A Angiography in carcinoma of the pancreas Acta radiol (1965) Suppl No 235



Fig 5 Man aged 62 with extradural metastas s from lymphosarcoma and abdom nal tumour Transperitoneal percutaneous fine needle biopsy Mal gnant lymphoma a) Displacement of gastroduodenal artery and pancreatic arcades Lateral displacement of left kidney pelvis b) Lateral vie v Anterior d splacement of superior mesenteric artery

similar to that caused by pancreatic carcinoma (BRON & SHERMAN REUTER et coll 1970) In our 2 patients however irregular encasement was not demonstrated only evidence of an avascular expansive lesion i e displacement of arteries and venous compression One of the patients moreover presented smooth stenosis of the hepatic artery The demonstration of tumour vessels or hypervascularity was not to be expected in our patients since the vascular appearances of metastatic lesions generally follow that of the primary tumour thus metastases from renal carcinoma are highly vascular but those from adeno carcinoma avascular Differential diagnostic difficulties in the first place will arise between lymphosarcoma metastatic lesions of low vascularity and pancreatitis Changes of intrapancreatic arteries consisting of alternating narrowings and dilatations are characteristic of pancreatitis although not present in every case The absence of such changes in lymphoma and metastatic lesions may be of help in the differentiation but it still may be impossible to rule out pancreatic pseudocyst which is also avascular The way the enlarged lymph nodes displaces surrounding structures may be different from that caused by pancreatitis with or without pseudocyst Ventral displacement of the main stem of the superior mesenteric artery which passes dorsal to the pancreatic gland thus seldom is caused by inflammatory enlargement of the pancreas and lateral displacement of the kidney pelvis or ureter which was demonstrated in half of our patients in the pre

FROM THE DEPARTMENTS OF DIAGNOSTIC RADIOLOGY III (DIRECTOR C-G HELANDER) AND PATHOLOGY III (DIRECTOR L ANGERVALL), SAHLGRENSKA SJUKHUSET, S-411 32 GOTHENBURG, SWEDEN

UROTHELIAL RENAL PELVIC TUMOURS IN PHENACETIN ABUSERS

E DEICHGRÄBER and S JOHANSSON

Urography and ascending pyelography may be used for diagnosis of renal pelvic tumours (OLSSON 1962) However, small tumours as well as tumours obstructing the urinary passage often require additional diagnostic procedures Direct transcutaneous pyelography (WICKBOM 1954) and double contrast methods have been advocated (CHRISTENSEN 1970, EIE & SANDER 1971) Different opinions exist as to the value of angiography only small series have been reported (BOIJSEN & FOLIN 1961, LAGERGREN & LJUNGQVIST 1965, MITTY et coll 1969)

BECKER (1969) reported on 5 patients with renal pelvic carcinoma without hydronephrosis in which the tumour could not be diagnosed by means of urography The reason was either vessel obstruction or tumour destruction of the kidney parenchyma to such an extent as to prevent excretion of the contrast medium

In a material of 75 cases of renal pelvic tumours a multivariate analysis has been performed in order to assess the dependence of the 5 year survival on different morphologic and clinical factors (JOHANSSON et coll, to be published) The extent of the tumour was the best predictor for prognosis but structure and grade also exerted some influence

A strong correlation was found between the radiographic appearances and the

Submitted for publication 25 June 1974

– LUNDERQUIST A HOLMDAHL H son K and CLEMENS F Selective superior mesenteric arteriography in reticulum cell sarcoma of the small bowel Radiology 98 (1971) 113
MARIONS O TORNBERG B och WIECHEL K L Kärlanatomin vid resekabel peri ampullär cancer In Swedish Opusc med (1974) Suppl No 32 p 51
REUTER S R REDMAN H C and JOSEPH R R Angiographic findings in pancreatitis Amer J Roentgenol 107 (1969) 56
– — and BOOKSTEIN J J Differential problems in the angiographic diagnosis of carcinoma of the pancreas Radiology 96 (1970) 93
TYLÉN U Accuracy of angiography in the diagnosis of carcinoma of the pancreas Acta radiol Diagnosis 14 (1973) 449
– and ARNESJÖ B Angiographic evaluation of inflammatory disease of the pancreas Acta radiol Diagnosis 14 (1973) 215
– — LINDBERG L G LUNDERQUIST A and ÅKERMAN M Percutaneous biopsy of pancreatic carcinoma guided by angiography To be published in Surg Gynec Obstet



Fig 1 Papillary non infiltrating renal pelvic tumour



Fig. 2 Central solid infiltrating renal pelvic tumour

formed in 23 patients the films were available in 20 cases retrograde pyelography was performed in 22 patients all films were available Seventeen patients had been subjected to urography and retrograde pyelography

The tumours were classified according to surface appearance base thickness and possible infiltration The surface might appear villous lobated or nodular and smooth the malignancy hypothetically increasing in that order Where mixed forms appeared the more malignant of the components was used to classify the entire

Table 1

Serum creatinine values in 25 patients with urothelial renal pelvis tumours

	Serum creatinine				
	<1 2	1 3–2 0	2 1–4 0	4 1–8 0	>8 0
Number of patients	4	13	4	3	1

histologic grade of bladder tumours (NILSSON et coll, to be published) The examination method used was pneumocystography and the histologic grading of BERGKVIST et coll (1965) was applied The radiologically villous tumours were all found to be well differentiated (grading 1–2) as were papillomas with a thin stalk (grade 1–2), a wide tumour base indicated low differentiation (grade 3–4) These facts initiated an attempt to classify preoperatively urothelial renal pelvic tumours by means of radiography

Material and Methods

The present series comprised 25 patients with urothelial tumours of the renal pelvis Eight of the patients were males and 17 females The mean age was 58 years and the range 44 to 79 years The majority of the patients had been treated at this hospital, the others at different hospitals all over Sweden All the patients had been operated upon, nephrectomy (19 cases), partial resection of the renal pelvis and the kidney (5 cases) and nephropyelostomy including incisional biopsy (1 case) All the patients had been abusers of phenacetin containing analgesics and had previously been subjected to an investigation concerning the relationship between urothelial renal pelvic tumour and abuse of phenacetin (JOHANSSON et coll 1974) Kidney function was estimated from the serum creatinine concentration (Table 1)

Microscopy All the surgical specimens were fixed in formalin solution 10% Sections of 5 μ were stained with hematoxylin-van Gieson and with hematoxylin-eosin and all examined by one of the authors (S J) The following factors were recorded malignancy grade, tumour infiltration, tumour structure, and renal papillary necrosis Each tumour was graded as described for urothelial tumours of the bladder (BERGKVIST et coll) the basis for classification being the deviation of cell appearance from normal transitional cell epithelium Entirely or almost entirely papillary tumours were classified as papillary, entirely solid and non papillary as solid and mixed tumours as papillary and solid (Figs 1, 2)

Radiography The preoperative examination of the urinary tract—urography, retrograde or antegrade pyelography—was reviewed by one of the authors (E D), who was ignorant of the microscopic grading of the tumours Urography was per-



Fig 6



Fig 7



Fig 8

Fig 6 Ascending pyelography Solid renal pelvic tumour Infiltrative growth evident from the involvement of the pelvic contours

Fig 7 Ascending pyelography Relatively small pelvic tumour with a nodular surface and broad base Infiltrative growth has led to pelvic deformation

Fig 8 Ascending pyelography Relatively small renal pelvic tumour (→) with smooth surface and broad base

Results

Radiography A villous tumour surface displayed itself by means of delicate strands of contrast medium at the site of the tumour (Figs 3, 4), a nodular surface was coarser and more irregular (Figs 5, 7) A smooth surface appears in Fig 8 A thin tumour base is illustrated in Fig 4 and a typical wide base in Fig 7 Infiltration was most evident in cases like those in Figs 6 and 7 In the former the infiltration was detected due to poor demarcation of the tumour, in the latter case the renal pelvis was also deformed

Table 3

Correlation between the radiologic appearances of the tumour base and the microscopic malignancy grade

Tumour base	Microscopic grade		
	2	3	4
Thin	3	3	0
Intermediate	0	3	0
Wide	2	5	9
Total	5	11	9



Fig 3



Fig 4



Fig 5

Fig 3 Ascending pyelography Papillary tumour similar to the one in Fig 1 Fine strands of con trast medium (between arrows) indicate a villous tumour surface

Fig 4 Ascending pyelography Non infiltrating papillary thin based renal pelvic tumour Villous surface (→)

Fig 5 Urography Same type of tumour as in Fig 2 Extensive displacement of the calyx groups Tumour surface nodular

tumour, this also being the case if multiple tumours were encountered The tumour base was estimated in relation to the maximum width of the tumour, a narrower base was classified as thin, one of the same width as the tumour as intermediate, and one broader than the tumour as wide The term infiltration implies that the normal, smooth outline of the renal pelvis had been distorted or replaced by an irregular, serrated margin In 3 patients the films could not be used for evaluation of infiltration, since only a small part of the tumour was visible

Table 2

Correlation between the radiologic appearances of the tumour surface and the microscopic malignancy grade

Tumour surface	Microscopic grade		
	2	3	4
Villous	4	3	0
Nodular	1	7	3
Smooth	0	1	6
Total	5	11	9

are easily accessible to diagnostic and therapeutic procedures Cystoscopy with biopsy, exfoliative cytology and cystography are well-established methods Particularly double-contrast cystography (BARTLEY & HELANDER 1960) is of value, allowing optimum demonstration of the entire tumour. A good correlation was found between the radiologic appearance at pneumocystography and the microscopic classification of the tumour (NILSSON et coll) and a similar correlation was found in the present material of tumours of the renal pelvis, although the location and impaired kidney function made diagnosis more difficult However, radiologic estimation of tumour infiltration appears to be somewhat more uncertain in the renal pelvis than in the bladder

A good conformity between cytology and microscopy of urothelial tumours of the upper urinary tract was demonstrated by ERIKSSON & JOHANSSON (to be published) Cytology of voided bladder urine was performed by means of a filter technique Thus, radiography and cytology combined may allow an even more certain estimation of morphologic factors determining the malignancy of renal pelvic tumours, which may be of importance for planning the operative treatment

SUMMARY

The appearances of renal pelvic tumours at urography and pyelography in 25 phenacetin abusers were correlated with the microscopy of operative specimens Radiography was found to contribute to the preoperative assessment of malignancy grade

ZUSAMMENFASSUNG

Das Bild von Nierenbeckentumoren bei der Urographie und der Pyelographie wurde bei 25 Phenacetin Missbrauchern zum mikroskopischen Bild der Operationspräparate korreliert Die Rontgenuntersuchung trug zur präoperativen Bestimmung des Malignitätsgrades bei

RÉSUMÉ

Les aspects urographique et pyelographique de tumeurs du bassinet rénal chez 25 sujets ayant abusé de la phénacetine ont été compares avec l'examen microscopique des pièces opératoires Les auteurs ont constaté que la radiographie contribue à la determination préopératoire du grade de malignite

REFERENCES

BARTLEY O and HELANDER C -G Double-contrast cystography in tumours of the urinary bladder Acta radiol 54 (1960), 161

BECKER J A Transitional cell carcinoma of the renal pelvis Cases of non-visualization on excretory urography J Urol 101 (1969), 280

Table 4

Correlation between radiographic and microscopic tumour infiltration

Infiltrative growth of the tumour	No of cases
Microscopic and radiologic	8
Microscopic only	4
Radiologic only	1
Neither histologic nor radiologic	9
Total	22

Correlation with microscopy The appearances of the tumour surface are compared with the histologic malignancy grades in Table 2 The results agree with the primary hypothesis implying that the malignancy grade would be lowest for villous and highest for smooth tumours, nodular tumours holding an intermediate position The same tendency was found when the appearance of the tumour surface were compared with the microscopic tumour structure Likewise, a wide tumour base seemed to indicate a high malignancy grade (Table 3)

Infiltration could be demonstrated microscopically only in tumours of malignancy grades 3 and 4 (Table 4) Conformity was found in 17 of 22 cases Among the 5 cases with non-conformity 4 tumours infiltrated to only a small degree without radiologic evidence

Renal papillary necrosis In all the 25 patients evaluation of the renal papillae was possible In 6 patients no material was available from the papillae for microscopy but papillary necrosis was demonstrated radiographically Neither microscopically nor radiographically papillary necrosis could be demonstrated in 2 patients, *their renal function* being normal (serum creatinine < 1 2 mg/100 ml) All the remaining patients but 2 had a reduced renal function (serum creatinine 1 2 mg/ml)

Discussion

The epithelium covering the calyces, renal pelvis, ureter and bladder, the so-called urothelium, is believed to derive from the same embryologic structure (MELICOW 1945) It appears identical throughout the urinary tract with local variation only in its thickness This fact may justify the use of a common morphologic classification of all urothelial tumours regardless of their location The grading system of BERGKVIST et coll has proved to correlate well with prognosis in urothelial bladder tumours (BERGKVIST et coll) as well as in renal pelvic tumours (JOHANSSON et coll , to be published)

The most common site of urothelial tumours is the bladder where the tumours

are easily accessible to diagnostic and therapeutic procedures. Cystoscopy with biopsy, exfoliative cytology and cystography are well established methods. Particularly double-contrast cystography (BARTLEY & HELANDER 1960) is of value, allowing optimum demonstration of the entire tumour. A good correlation was found between the radiologic appearance at pneumocystography and the microscopic classification of the tumour (NILSSON et coll.) and a similar correlation was found in the present material of tumours of the renal pelvis, although the location and impaired kidney function made diagnosis more difficult. However, radiologic estimation of tumour infiltration appears to be somewhat more uncertain in the renal pelvis than in the bladder.

A good conformity between cytology and microscopy of urothelial tumours of the upper urinary tract was demonstrated by ERIKSSON & JOHANSSON (to be published). Cytology of voided bladder urine was performed by means of a filter technique. Thus radiography and cytology combined may allow an even more certain estimation of morphologic factors determining the malignancy of renal pelvic tumours, which may be of importance for planning the operative treatment.

SUMMARY

The appearances of renal pelvic tumours at urography and pyelography in 25 phenacetin abusers were correlated with the microscopy of operative specimens. Radiography was found to contribute to the preoperative assessment of malignancy grade.

ZUSAMMENFASSUNG

Das Bild von Nierenbeckentumoren bei der Urographie und der Pyelographie wurde bei 25 Phenacetin Missbrauchern zum mikroskopischen Bild der Operationspräparate korreliert. Die Röntgenuntersuchung trug zur präoperativen Bestimmung des Malignitätsgrades bei.

RÉSUMÉ

Les aspects urographique et pyélographique de tumeurs du bassinet rénal chez 25 sujets ayant abusé de la phénacétine ont été comparés avec l'examen microscopique des pièces opératoires. Les auteurs ont constaté que la radiographie contribue à la détermination préopératoire du grade de malignité.

REFERENCES

BARTLEY O. and HELANDER C. G.: Double-contrast cystography in tumours of the urinary bladder. Acta radiol. 54 (1960), 161.

BECKER J. A.: Transitional cell carcinoma of the renal pelvis. Cases of non visualization on excretory urography. J. Urol. 101 (1969), 280.

BERGKVIST A, LJUNGQVIST A and MOBERGER G Classification of bladder tumors based upon the cellular pattern Preliminary report of a clinical-pathological study with a minimum follow up of eight years Acta chir scand 130 (1965), 371

BOIJSEN E and FOLIN J Angiography in carcinoma of the renal pelvis Acta radiol 56 (1961), 81

CHRISTIANSEN J Retrograde pyelography with double contrast Acta chir scand 136 (1970), 435

EIF H and SANDER S The diagnosis of tumor in the renal pelvis Scand J Urol Nephrol 5 (1971), 45

ERIKSSON O and JOHANSSON S Urothelial neoplasms of the upper urinary tract To be published in Acta cytol

JOHANSSON S, ANGERVALL L, BENGTSSON U and WAHLQVIST L Uroepithelial tumors of the renal pelvis associated with abuse of phenacetin-containing analgesics Cancer 33 (1974), 743

— — — — A clinico pathologic and progostic study of epithelial tumors of the renal pelvis To be published in Cancer

LAGERGREN C and LJUNGQVIST A The arterial vasculature of renal pelvic carcinomas Acta chir scand 130 (1965), 321

MELICOW M M Tumor of the urinary drainage tract Urothelial tumors J Urol 54 (1945), 186

MITTY H A, MURRAY G B and FELLER M Infiltrating carcinoma of the renal pelvis Radiology 92 (1969), 994

NILSSON A E, WIKLUND L-G och ANGERVALL L Jämförelse mellan blåstumörers makroskopiska utseende vid pneumocystografi och histologiska malignitetsgrad (In Swedish) To be published

OLSSON O Handbuch der Urologie V/I Diagnostic Radiology, Springer Verlag Berlin (1962), 200

WICKBOM I Pyelography after direct puncture of the renal pelvis Acta radiol 41 (1954), 505

FROM THE DEPARTMENTS OF DIAGNOSTIC RADIOLOGY (DIRECTOR PROF G F SALTZMAN), MEDICINE (DIRECTOR PROF N TÖRNBLOM) AND PATHOLOGY (DIRECTOR PROF F BERGMAN) UNIVERSITY OF UMEÅ, S 901 85 UMEÅ, SWEDEN

NEPHROANGIOGRAPHY IN WEGENER'S GRANULOMATOSIS

A comparison with panarteritis nodosa

B LUNDSTRÖM B LINDQVIST, H SÖDERBERGH, Th WENTZEL and G HALLMANS

Wegener s granulomatosis belongs to the group of necrotizing vasculitis and is often difficult to distinguish from other diseases within this group A clear description of the disease as a distinct clinical and pathologic entity was given by WEGENER (1936) on the basis of 3 cases with granulomatous inflammatory conditions of the upper respiratory tract generalized arteritis and focal granulomatous glomerulonephritis Clinically the disease is characterized by sudden rise of temperature [illegible]

[illegible] an average of about 11 months of pulmonary or renal insufficiency (KUNTZ et coll 1967) Immunosuppressive treatment has prolonged survival in some cases while steroid treatment has not been very successful (BOURNONCLE et coll 1967 HOLLANDER & MANNING 1967, KAPLAN et coll 1968, BERGLUND et coll 1972 RAITT 1971, FAUCI & WOLFF 1973)

Panarteritis nodosa as well as Wegener s granulomatosis may produce widespread vasculitis and renal disease Medium sized arteries are predominantly involved especially at their bifurcation in classical panarteritis, and smaller arteries and veins

Submitted for publication 27 November 1974

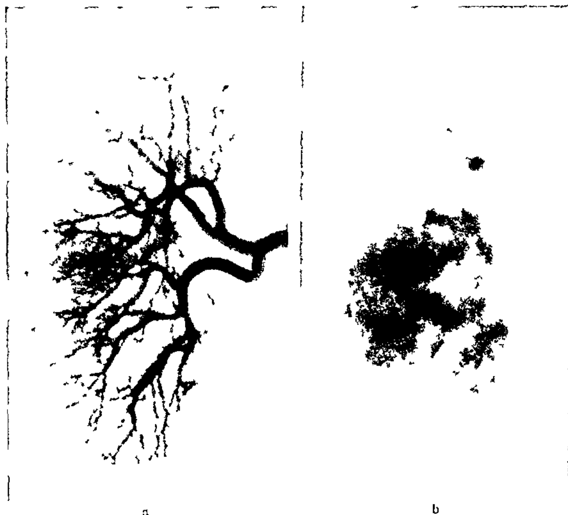


Fig 1 Ca ... phro graphic p ... ntrast filling of

in Wegener s granulomatosis (ZEEK et coll 1948, ZEEK 1952, 1953) An involvement of glomeruli and small vessels is considered to occur primarily in the so called microscopic form of panarteritis nodosa, also called hypersensitivity angiitis, which is clinically characterized by a rapid course with death due to uraemia (DAWSON et coll 1948, PIRANI & MANALIGOD 1966, MEADOWS 1973) Necrotizing granulomas are not a feature in panarteritis, hypertension is common however, contrary to what is the case in Wegener s granulomatosis (FAHEY et coll 1954) Reports on angiography in necrotizing vasculitis are rare, they deal predominantly with vasculitis associated with drug abuse (HALPERN & CITRON 1971, HALPERN 1972) The angiographic appearances of panarteritis nodosa are well documented however Small multiple aneurysms, particularly in the kidneys are generally considered almost pathognomonic of this disease (BRON et coll 1965, FLEMING & STERN 1965, EFSEN & LORENZEN 1968, DORNFELD et coll 1971, ESSINGER & BONARD 1971)



Fig 2. Case 1 A glomerulus with fibrinoid necrosis and infiltration of polymorphonuclear neutrofils H E × 180

No report on nephroangiography in Wegener's granulomatosis seems to have been published and only a few on other organs for instance the brain (LILIEQUIST & LINK 1968) This has indicated the present report on the clinical course and the nephroangiographic appearances in 6 cases 3 of Wegener's granulomatosis and 3 of panarteritis nodosa

Case reports

Case 1 A 5[illegible]
but dete[illegible]
persistin[illegible]
leucocyt[illegible] ...ocytosis *but no eosinophilia* While in hospital joint and muscle pains developed along with proteinuria haematuria and oliguria and after 2 weeks anuria Dialysis was started *On a chest film* *homogeneous* fairly well demarcated infiltrates of different sizes were observ*ed in both lungs* *He* was treated with azathioprine heparin and extracorporeal blood irradiation *and after 3 weeks of* anuria urinary production returned No improvement was noted *clinically* however and the patient died 3 months after onset of the disease

Nephroangiography was performed in the oliguric phase *The* kidneys were moderately enlarged and the cortex was thicker than usual The renal artery and [illegible]
down to [illegible]
sions [illegible]
cortex [illegible] (Fig 1)

Microscopy Renal biopsy revealed interstitial inflammation located mostly periglomerularly and severe glomerular lesions w[illegible]
of the capillary walls and lumina *capsular a*[illegible]
Thickening of the walls of the arterioles with [illegible]

Autopsy 6 weeks later Marked *interstitial* inflammation with necrosis abscess formation



Fig 3 Case 2 Wegener's granulomatosis In the vicinity of the right hilum large fairly homogeneous and well demarcated infiltrates Fluid in right pleura

and granulomatous features in the cortex, in some glomeruli necrosis, in others segmental hyalinization, some appeared normal Medium sized and small arteries and arterioles were normal

Comment The clinical course and the microscopic appearance was compatible with Wegener's granulomatosis The radiologic lesions were of such a type as may occur in any acute oliguric renal insufficiency (HOLLENBERG et coll 1968)

Case 2 A 19-year-old man with a high temperature, cough and muscular pains was treated with antimicrobic drugs without any effect He gradually deteriorated He had haematuria, proteinuria and after 3 weeks oliguria The blood pressure was 120/40, ESR 155 mm He had leucocytosis and thrombocytosis but no eosinophilia Chest film Large, homogeneous, fairly well demarcated infiltrates near the left hilum (Fig 3) Dialysis was started He was treated with azathioprine, heparin and extracorporeal blood irradiation and after 3 weeks of total anuria diuresis returned Serum creatinine decreased to 3 mg/100 ml serum, the muscular pains diminished as well as the radiologic lung lesions The patient developed agranulocytosis and sepsis, however, and died 3 months after onset of the disease

Nephroangiography The first examination was made at the beginning of the anuric period The kidneys were large and swollen the intra renal arteries thin and separated The arcuate arteries were barely filled and no demarcation of the cortex could be observed The arterial wash out time was prolonged

At repeat angiography 6 weeks later, when diuresis had returned, the kidneys had diminished in size and the cortex was of ordinary thickness (6 mm) The intrarenal arteries were still separated and no accumulation of contrast medium in the cortex occurred No aneurysms or obliteration of vessels at any of the examinations (Fig 4)

Microscopy Renal biopsy performed in connection with the first angiography, severe necrotizing inflammation with fibrin precipitates and capsular proliferations in all glomeruli, interstitially periglomerular infiltration of lymphocytes and plasma cells Accumulation of inflammatory cells in the wall of one small artery branch

Autopsy (24 days after the second angiography) Regression of the acute inflammatory changes was observed and hyalinization of glomeruli Arteries and arterioles were normal Multiple areas of infarction in the lungs and the spleen

Comment Symptoms and signs as well as microscopy were typical of Wegener s granulo-

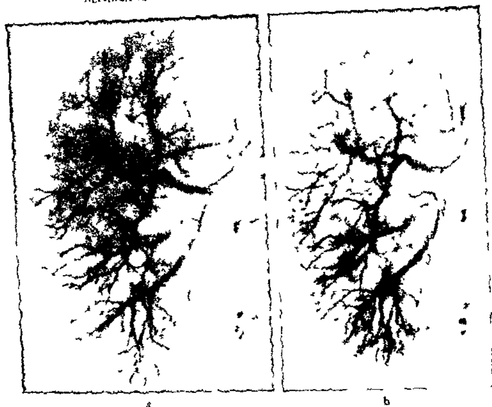


Fig 4 Case 2 ...
angiography
spl t apart Th
and the corte

matosis The angiographic appearances were similar to those seen in subacute subchronic glomerulonephritis (EKELUND et coll 1973)

Case 3 A 36-year-old man with nasal congestion since the age of ...
of high tempera...
cyto
ml s ... chest film Large infiltrates in both lung
A biopsy specimen from the nasal mucosa revealed necrotizing granulomas and vasculit with fibrinoid necrosis He was treated with prednisolone and azathioprine and improve and his pulmonary lesions regressed A year later, once again nasal congestion and hea ache and infiltrates in both lungs on chest films The serum creatinine had increased to ... mg/100 ml serum The prednisolone was discontinued and ...
phospham...

The ...
conditi... occurred but his serum creatinine rema at a level of ... to 8 mg/100 ml serum

Nephroangiography The kidneys were of normal size The cortex was thin measur 3 mm no contrast accumulation in the nephrographic phase The interlobar and arc

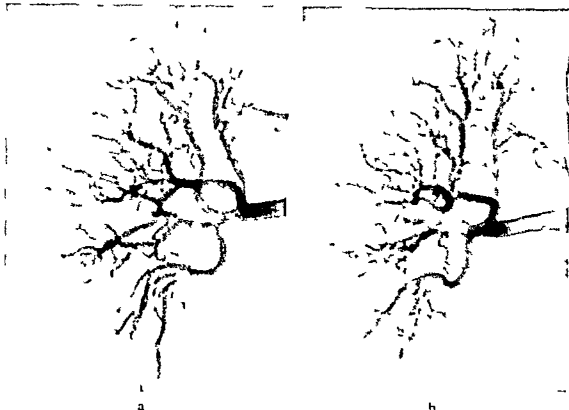


Fig 5 Case 3 Wegener s granulomatos s a) Arterial phase a p vie v b) same kidney obl que view Kidney of normal size but the cortex thin 3 mm The intrarenal arteries irregular espec ally subcortically No aneurysms only bending of the arteries The cortical vessels not vis ble

arteries were irregular especially subcortically The interlobular arteries were not visible the arterial wash out time somewhat prolonged No aneurysms or occlusions (Fig 5)

Microscopy of the renal biopsy material Most glomeruli more or less hyalinized with out obvious intraglomerular necrosis Interstitially located infiltrates of inflammatory cells both mononuclear cells and neutrophilic granulocytes frequently arranged around a small vessel with non specific necrosis in the wall No inflammatory changes in one medium sized artery

Comment The duration of the disease is somewhat uncertain in this case Kidney involve ment was noted 1½ years before nephroangiography was performed Symptoms laboratory data microscopy of specimens from the nasal mucosa and kidney were typical of a rather mild form of Wegener s granulomatosis or Wegener s granulomatosis in remission Whether or not the recovery was due to the treatment is an open question The angiographic appear ances were similar to those occurring in subchronic glomerulonephritis (EKELUND *et coll*)

Case 4 A 56 year old woman with mild arthritis since 7 years presented with increased joint pain exanthema a high temperature rhinitis and conjunctivitis She was treated with penicil n *but deteriorated* Haematuria occurred and decreasing diuresis later anuria The ...ed
blood
with
tion without any lasting effect Diuresis [illegible]
onset of the disease

Nephroangiography in the anuric phase The kidneys were somewhat larger than nor

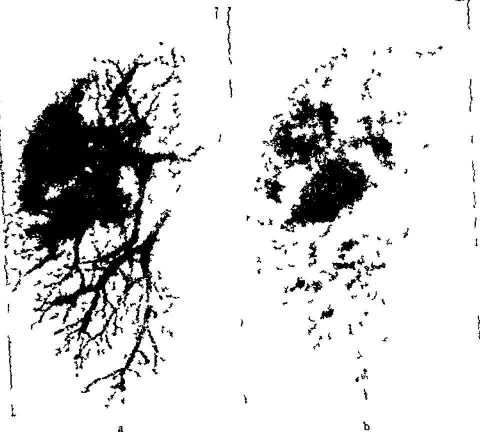


Fig 6 Case 4 Panarter tis nodosa m croscop c form Blurred intrarenal arteries Lumen variations and occlus ons In the *nephrographic phase the whole* kidney has a mottled appearance No de marcat on of the cortex

mal Most of the intrarenal arteries had blurred outlines In some vessels lumen variations and occlusions were observed but *no aneurysms* The cortex was somewhat thicker than usual In the nephrographic *phase the kidneys had* a mottled appearance without demarcation of the cortex or the *columnae Bertini* The circulation time and arterial wash out time were normal (Fig 6)

Microscopy renal biopsy *Fibrinoid necrosis* in glomeruli capsular proliferations and wide-spread intra and periglomerular infiltration of inflammatory cells mostly neutrophilic granulocytes In the arterioles *and larger vessels marked* ... d

... as in the

... wide-spread *recent infarcts* with papillary necrosis in the marrow Vascular les ons were observed also in the spleen ...

liver skin

Commer

but others ... e rapid progress was



Fig 7 Case 4 Panarteritis nodosa, microscopic form Microscopy Artery with fibrinoid

not typical of panarteritis but the course of the disease as well as the microscopy of the kidney are consistent with the microscopic form or hypersensitivity angiitis Radiologic abnormalities of a type occurring in any vasculitis existed and corresponded with those described following drug abuse (HALPERN & CITRON 1971)

Case 5 A 33-year-old man with proteinuria in 1959 and periods of sinusitis and bronchial asthma since 1965 Six months later he developed high temperature, cough, joint pains, haematuria and oliguria On admission leucocytosis was found along with eosinophilia The blood pressure was 200/120 The serum creatinine was 13 mg/100 ml serum and nephroangiography was performed during this phase He was treated with hydrocortisone, actinomycin C and azathioprine and improved After a few weeks the serum creatinine fell to less than 3 mg/100 ml, the joint pains disappeared and the patient became afebrile Five months later there was a new relapse into haematuria, oliguria and rapidly progressing uraemia, and dialysis was begun He died 3 weeks after a renal transplantation

Nephroangiography The kidneys were of normal size A few fairly small, irregular intrarenal arterial aneurysms of various size located in the branchings of the interlobar arteries were demonstrated The cortical arteries were barely filled The cortex was a little thicker than normal without demarcation in the nephrographic phase (Fig 8)

Microscopy In the left kidney, at the kidney transplantation, most of the glomeruli were completely or partly hyalinized, some with capsular adhesions and epithelial crescent formations In the arterioles and small arteries marked endothelial proliferation occasionally obstructing the vessels Thickening of the walls, splitting up of the elastica interna and fibrosis of the medium-sized arteries, sometimes also obstruction of the lumen and re-canalization

Autopsy 2 weeks later Similar changes were found also in the remaining kidney No s[illegible]s of vasculitis in other organs However, a muscle biopsy 8 months previously had [illegible] of the wall and abundant accumu-

[illegible]res



Fig 8 Case 5 Panarteritis nodosa class c form Multiple small arterial aneurysms of different sizes located predominantly at the bifurcations of the interlobular arteries

Comment The clinical picture and the microscopic appearances, particularly of the muscle specimen were compatible with panarteritis nodosa The intrarenal arterial aneurysms demonstrated at angiography are considered pathognomonic of this disease by many authors

Case 6 A 40-year old woman with transient arthritis and atrophic rhinitis In 1966 she had hypertonia eosinophilia haematuria and ESR of 110 mm and a serum creatinine level of 2 3 mg/100 ml serum Steroid treatment was started and the patient improved Two years later a new relapse with joint and muscle pain oedema and dyspnoea Serum creatinine was now 5 5 mg/100 ml serum In spite of treatment with prednisolone and azathioprine her uraemia progressed rapidly Dialysis was begun but was complicated by haemorrhages and shunt occlusions due to thrombophlebitis She died one year later

Nephroangiography The kidneys were of normal size In both kidneys several small aneurysms mainly located at arterial bifurcations The arteries were well outlined and without occlusions The cortex was of normal thickness but only faintly demarcated in the nephrographic phase

ap

th

in the kidneys nor in other organs On the other hand at muscle biopsies 3 years and 5 months respectively before death necrotizing vasculitis had been observed

Comment In spite of a slight involvement of the upper respiratory tract panarteritis nodosa without doubt is the correct diagnosis, symptoms and signs as well as microscopy and angiography were typical

Discussion

The first case of Wegener's granulomatosis was described already in 1931 by KLINGER who considered it as a variant of panarteritis nodosa The criteria for this type of granulomatosis were established after a detailed clinical and pathologic analysis of 7 patients as well as of 22 previously reported cases (GODMAN & CHURG 1954, FAHEY et coll 1954) Classical or generalized Wegener's granulomatosis is characterized by necrotizing granulomatous vasculitis of the upper and lower respiratory tracts together with glomerulonephritis and wide-spread disseminated vasculitis involving both small arteries and veins A localized form, limited primarily to the upper and lower respiratory tracts, has been described (CARRINGTON & LIEBOW 1966, DAVIS et coll 1972, GONZÁLEZ & ORDSTRAND 1973) A certain diagnosis is often difficult to establish in early or mild cases

The microscopic appearances are well-known and the kidney involvement has been described as a glomerulitis or a glomerulonephritis (GODMAN & CHURG, HORN et coll 1974) Since small arteries and veins are involved in the inflammatory process, it is to be expected that the angiographic abnormalities resemble those occurring in glomerulonephritis In the present 3 cases of granulomatosis angiography was performed at various stages of the disease Fig 3 a (Case 2) represents the acute stage with a large kidney, thick cortex, thin separated intrarenal arteries and poor peripheral circulation Fig 3 b (Case 2) and Fig 1 (Case 1) may be said to represent a subacute stage, the abnormalities mentioned being less evident Fig 4 (Case 3) resembles a subchronic form of glomerulonephritis with a kidney of normal size, thin cortex, tortuosity of the subcortical arteries and probably diminished cortical blood flow No occlusions or aneurysms were demonstrated

In panarteritis nodosa, on the other hand, larger vessels are involved, both in the classical type with intrarenal arterial aneurysms (Fig 7) as well as in the microscopic one (Fig 5) In the latter variant the intrarenal vascular outlines were blurred and several vascular occlusions were demonstrated in medium-sized arteries, i e interlobar and arcuate arteries, but no aneurysms In the nephrographic phase the kidneys had a mottled appearance most likely due to small multiple infarcts

The angiographic appearances may vary during different stages of panarteritis MCCLURE & WESTCOTT (1969) reported that intrarenal aneurysms could disappear, and they assumed that this could represent a regression of the disease Later, however, ROBINS & BOOKSTEIN (1972) found that the disappearance of aneurysms cannot be correlated with the clinical course When aneurysms had disappeared, segmental stenosis, occlusions of small arterial bifurcations and small infarcts remained Furthermore, they suggested that arterial aneurysms might occur in other types of necrotizing vasculitis However, this has not yet been demonstrated It seems as if

intrarenal arterial aneurysms occur in the classical type, while other vascular abnormalities consisting of lumen variations and occlusions occur in the microscopic form of the disease, as in Case 4 It is true that the differences in angiographic appearances between Wegener's granulomatosis, classical and microscopic panarteritis nodosa are based upon a small number of observations but they do indicate that nephroangiography might contribute to the differential diagnosis The microscopic appearances are not pathognomonic themselves, but together with symptoms and signs and angiography a diagnosis may be possible even in early cases This has become more important during recent years since modern treatment, particularly of early cases, has improved the prognosis

SUMMARY

Three cases of Wegener's granulomatosis with a classical course are described, 2 of which with fatal outcome in spite of immuno suppressive therapy Nephroangiography was performed during the oliguric or anuric phase The appearances were similar to those encountered in glomerulonephritis and were compared with those in three cases of pan arteritis nodosa Two of these represented the classical form with intrarenal arterial aneurysms, the third was a case of the microscopic type presenting blurred intrarenal arteries with lumen variations and occlusions These observations support the opinion that Wegener's granulomatosis and panarteritis nodosa are different diseases Nephroangiography seems to be of value in their differentiation

ZUSAMMENFASSUNG

Drei Falle von Wegener'scher Granulomatose mit einem klassischen Verlauf werden beschrieben zwei mit einem todlichen Ausgang trotz immunosuppressiver Therapie Nephroangiographie wurde während den oligurämischen und anuramischen Phasen vorgenommen Das Bild war ahnlich dem bei Glomerulonephritis und wurde mit dem bei drei Fallen mit Panarteritis nodosa verglichen Zwei von diesen reprasentierten die klassische Form mit intrarenalen arteriellen Aneurysmen, der dritte war ein Fall des mikroskopischen Typus mit unscharfen intrarenalen Arterien mit Variationen des Lumens und Okklusionen Diese Beobachtungen stutzen die Auffassung, dass die Wegener'sche Granulomatose und die Panarteritis nodosa verschiedene Erkrankungen sind Die Nephroangiographie scheint zu deren Differenzierung von Wert zu sein

RÉSUME

Présent [illegible]
2 o [illegible]
gra[illegible]
été [illegible]
ceu [illegible] ces cas présentaient la forme classique avec des anevrysmes arteriels intrarénaux, le troisième était un cas du type microscopique avec des artères intrarénales floues avec des variations de calibre de la lumière artérielle

Comment In spite of a slight involvement of the upper respiratory tract panarteritis nodosa without doubt is the correct diagnosis, symptoms and signs as well as microscopy and angiography were typical

Discussion

The first case of Wegener's granulomatosis was described already in 1931 by KLINGER who considered it as a variant of panarteritis nodosa The criteria for this type of granulomatosis were established after a detailed clinical and pathologic analysis of 7 patients as well as of 22 previously reported cases (GODMAN & CHURG 1954, FAHEY et coll 1954) Classical or generalized Wegener's granulomatosis is characterized by necrotizing granulomatous vasculitis of the upper and lower respiratory tracts together with glomerulonephritis and wide-spread disseminated vasculitis involving both small arteries and veins A localized form, limited primarily to the upper and lower respiratory tracts, has been described (CARRINGTON & LIEBOW 1966, DAVIS et coll 1972, GONZÁLEZ & ORDSTRAND 1973) A certain diagnosis is often difficult to establish in early or mild cases

The microscopic appearances are well-known and the kidney involvement has been described as a glomerulitis or a glomerulonephritis (GODMAN & CHURG, HORN et coll 1974) Since small arteries and veins are involved in the inflammatory process, it is to be expected that the angiographic abnormalities resemble those occurring in glomerulonephritis In the present 3 cases of granulomatosis angiography was performed at various stages of the disease Fig 3 a (Case 2) represents the acute stage with a large kidney, thick cortex, thin separated intrarenal arteries and poor peripheral circulation Fig 3 b (Case 2) and Fig 1 (Case 1) may be said to represent a subacute stage, the abnormalities mentioned being less evident Fig 4 (Case 3) resembles a subchronic form of glomerulonephritis with a kidney of normal size, thin cortex, tortuosity of the subcortical arteries and probably diminished cortical blood flow No occlusions or aneurysms were demonstrated

In panarteritis nodosa, on the other hand, larger vessels are involved, both in the classical type with intrarenal arterial aneurysms (Fig 7) as well as in the microscopic one (Fig 5) In the latter variant the intrarenal vascular outlines were blurred and several vascular occlusions were demonstrated in medium-sized arteries, i e interlobar and arcuate arteries, but no aneurysms In the nephrographic phase the kidneys had a mottled appearance most likely due to small multiple infarcts

The angiographic appearances may vary during different stages of panarteritis MCCLURE & WESTCOTT (1969) reported that intrarenal aneurysms could disappear, and they assumed that this could represent a regression of the disease Later, however, ROBINS & BOOKSTEIN (1972) found that the disappearance of aneurysms cannot be correlated with the clinical course When aneurysms had disappeared, segmental stenosis, occlusions of small arterial bifurcations and small infarcts remained Furthermore, they suggested that arterial aneurysms might occur in other types of necrotizing vasculitis However, this has not yet been demonstrated It seems as if

HORN R G, FAUCI A S ROSENTHAL A S and WOLFF S M Renal biopsy pathology in Wegener's granulomatosis Amer J Path 74 (1974) 423
KAPLAN S R HAYSLETT J P and CALABRESI P Treatment of advanced Wegener's granulomatosis with azathioprine and duazomycin A New Engl J Med 278 (1968) 239
KLINGER H Grenzformen der Periarteritis nodosa Frankfurt Z Path 42 (1931) 455
KUNTZ E BENEKE G and KNOTH W Die Wegenersche Granulomatose Med Welt 6 (1967) 295
LILIEQUIST B and LINK H Wegener's granulomatosis Report of a case Angiology 19 (1968) 215
MCCLURE P and WESTCOTT J L Periarteritis nodosa with perirenal hemorrhage a case report with angiographic findings J Urol 102 (1969) 126
MEADOWS R (Editor) Renal histopathology Oxford University Press, London 1973
PIRANI C L and MANALIGOD J R The kidney in collagen diseases *In* The Kidney, International Academy of Pathology monograph p 147 Edited by F K Mostofi and D E Smith Baltimore 1966
RAITT J W Wegener's granulomatosis Treatment with cytotoxic agents and adrenocorticoids Ann intern Med 74 (1971) 344
ROBINS J M and BOOKSTEIN J J Regressing aneurysms in periarteritis nodosa Radiology 104 (1972) 39
WEGENER F Über generalizierte septische Gefasserkrankungen Verh dtsch path Ges 29 (1936) 202
ZEEK P M Periarteritis nodosa A critical review Amer J clin Path 22 (1952) 777
— Periarteritis nodosa and other forms of necrotizing angiitis New Engl J Med 248 (1953) 764
— SMITH C C and WEETER J C Studies on periarteritis nodosa III The differentiation between the vascular lesions of periarteritis nodosa and of hypersensitivity Amer J Path 24 (1948) 889

et des occlusions Ces observations viennent à l'appui de l'opinion que la granulomatose de Wegener et la panartérite noueuse sont des affections différentes La néphroangiographie paraît avoir un intérêt pour leur differenciation

REFERENCES

BERGLUND G, HANSSON L, PERSSON B and VIKGREN P Combined chlorambucil and prednisolone treatment of five patients with Wegener's granulomatosis Acta med scand 191 (1972), 5

BOURONCLE B A, SMITH E J and CUPPAGE F. E Treatment of Wegener's granulomatosis with Imuran Amer J Med 42 (1967), 314

BRON K M, STROTT C A and SHAPIRO A P The diagnostic value of angiographic observations in polyarteritis nodosa Arch intern Med 116 (1965), 450

CARRINGTON C B and LIEBOW A A Limited forms of angiitis and granulomatosis of Wegener's type Amer J Med 41 (1966), 497

DAVIS R W, FETTER B F and YOUNG W G Wegener's granulomatosis Two patients presenting with solitary pulmonary lesions and review of eleven other cases Ann thoracic Surg 13 (1972), 427

DAWSON J, BALL J and PLATT R The kidney in periarteritis nodosa Quart J Med 17 (1948), 175

DORNFELD L, LECKY J W and PETER J B Polyarteritis and intrarenal artery aneurysms J Amer med Ass 215 (1971), 1950

EKELUND L, KAUDE J and LINDHOLM T Angiography in glomerular disease of the kidney A correlation with clinical findings and the stage of the disease Amer J Roentgenol 119 (1973), 739

EFSEN F and LORENZEN U Nephroangiography in periarteritis nodosa Report of a case Acta radiol Diagnosis 7 (1968), 225

ESSINGER A and BONARD M Panarteritis nodosa, an angiographic entity presentation of two cases Brit J Radiol 44 (1971), 184

FAHEY J, LEONARD E, CHURG J and GODMAN G Wegener's granulomatosis Amer J Med 17 (1954), 168

FAUCI A S and WOLFF S H Wegener's granulomatosis Studies in eighteen patients and a review of the literature Medicine 52 (1973), 535

FLEMING R J and STERN L Z Multiple intraparenchymal renal aneurysms in polyarteritis nodosa Radiology 84 (1965) 100

GODMAN G C and CHURG J Wegener's granulomatosis Pathology and review of the literature Arch Path 58 (1954), 533

GONZÁLEZ L and VAN ORDSTRAND H S Wegener's granulomatosis Review of eleven cases Radiology 107 (1973), 295

HALPERN M Angiography in chronic renal disease and renal failure Radiol Clin N Amer 10 (1972), 467

— and CITRON B P Necrotizing angiitis associated with drug abuse Amer J Roentgenol 111 (1971), 663

HOLLANDER D and MANNING R T The use of alkylating agents in the treatment of Wegener's granulomatosis Ann intern Med 67 (1967), 393

HOLLENBERG N K, EPSTEIN M, ROSEN S M, BASCH R I, OKEN D E and MERRILL J P Acute oliguric renal failure in man evidence for preferential renal cortical ischemia Medicine 47 (1968), 455



a



b

bule of the laby
tympanic part

Material and Methods

Isolated temporal bone specimens were macerated enzymatically and mounted in a plexiglass holder for tomography on the Polytome in routine projections (JENSEN & ROVSING 1971, MUNDNICH & FREY 1959) antero-posterior, half-axial, axial-pyramidal, Stenvers', true lateral and axial, exposure data 60 to 75 kV, 50 mA, 11 6 s (double hypocycloid movement), focal spot size 0 3 mm The radiographic system consisted of a cassette without intensifying screens and Structurix D 7 film (Figs 7–12)

Plastic moulds (Akemi) were prepared by filling the lumina of the inner ear and the facial canal of ... accoustic meatu ... were subsequer ... of the bone tissue with 5 M hydrochloric acid The moulds were smoked with ammonium chloride for photography

Roentgenographic remarks In conventional roentgenography the course of the facial canal is difficult to observe, owing to the complicated structure of the temporal

FROM THE DEPARTMENT OF DIAGNOSTIC RADIOLOGY, AKADEMISKA SJUKHUSET, UNIVERSITY OF UPPSALA, S-750 14 UPPSALA, SWEDEN

MULTIDIRECTIONAL TOMOGRAPHY OF THE FACIAL CANAL

H F WILBRAND

Advances in microsurgery of the ear necessitate increasingly accurate roentgenographic information preoperatively Modern tomographic equipment with hypocycloid or spiral movement (Polytome, Philips Massiot and Stratomatic, Koch & Sterzel) combined with tubes with small focal spots is able to meet this demand, and advances in the development of screen-film systems may be expected to increase the information further

The facial canal is of essential importance in otosurgery It is exposed in several operations (radical mastoidectomy, stapedectomy, reconstructive middle ear surgery and tumor surgery), in which injury to the facial nerve must be avoided High standard roentgen diagnosis therefore requires detailed knowledge of the anatomy of the facial canal and of the otosurgical problems involved in the individual case

A detailed technique for demonstrating the canal in conventional roentgenography has been presented by VAN DER BREKEL (1959) Tomography, however, has proved its superiority for demonstration of the facial canal, and techniques have been described by LUCARELLI & POMPILI (1961, 1966), BRÜNNER et coll (1963) BRÜNNER & PEDERSEN (1970), VIGNAUD et coll (1970), WILBRAND (1970), WRIGHT et coll (1967) and WRIGHT & TAYLOR (1968)

The present report, based on anatomic and radiographic investigations, is intended to complement previous descriptions of the appearances of the facial canal

Submitted for publication 19 February 1974

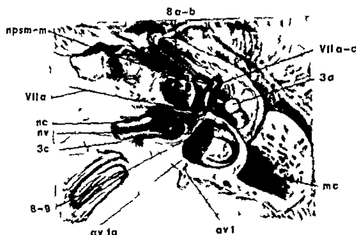


Fig. 3 R ght pyramid partly opened Axial view of the opened labyrinthine part of the facial cana w th the fac al nerve turned upwards and laterally Opened cochlea and vestibule with lateral semi circular canal and the opened epitympanum with the incus removed (Redrawn after Pernkopf)

av 1—vestibular aqueduct av 1 a—internal aperture of the vestibular aqueduct mc—mastoid cells nc—cochlear nerve npsm m—greater and minor superficial petrosal nerve nv—vestibular nerve, VII a—labyrinthine part of the facial canal VII a–c—labyrinthine and tympanic segment of the facial nerve 3 a—head of the malleus 3 c—stapedial footplate 8 a b—cochlear coils. 8 9—secon dary spiral lam na and vestibule

Anatomy The facial canal is divided into three parts corresponding to their directions It starts from the fundus of the internal acoustic meatus and ends with the stylomastoid foramen It is 24 to 30 mm long and conveys the facial and intermediate nerves together with blood vessels Each of the parts of the canal has an important topographic relationship to inner and middle ear structures (SENDULSKI 1928)

Labyrinthine part The labyrinthine, or first part (VII a b, Figs 1 a, 3, 6) is 2 5 to 6 mm long and about 1 mm in diameter It runs across the pyramid and starts at the lateral end of the internal acoustic meatus in the antero-superior division of the fundus above the transverse crest It then runs in a horizontal, antero-lateral course through the petrous bone above the cochlea and between the cochlear and vestibular parts of the labyrinth conveying the facial and intermediate nerves At the lateral end the lumen widens to form the 'upper knee' (Figs 1 a 2 a 6) which houses the geniculate ganglion (Figs 2 a 3) It has not a truly straight lateral course but forms an *obtuse angle with the long axis of the pyramid* (Figs 1 a, 2 a) From the 'upper knee' the tympanic part continues in an occipital direction In the knee (Figs 1, 3 4) sensory fibers form the ganglion (VII b), from which the great superficial petrosal nerve arises and continues in frontal direction through a channel of its own The labyrinthine part of the canal lies close to the cochlea

Anatomic variations Defects of the labyrinthine part are seldom encountered in cases where the pyramid is normal

a

b

Fig 2 a) Labyrinthine part of the left facial canal in the cranio caudal (axial) view in a temporal bone preparation (corresponding to Fig 1 a) the facial canal internal acoustic meatus basal turn of the cochlea and superior semicircular canal as well as mastoid air cells have been exposed by a dental drill b) Tympanic and mastoid parts of the left facial canal Temporal bone preparation View corresponding to Stenvers projection perpendicular to

c

'or the stape
post wall
s—foramen
nal acoustic
ᵔ of the
II a—
panic

bone, not even stereoscopy is of much help and essential details are still indiscernible Linear tomography improved the demonstration of the canal (AGAZZI et coll 1958, MUNTEAN 1941) but it cannot compete with multidirectional tomography (hypo cycloid or spiral) (JENSEN & ROVSING, KAUFMANN et coll 1973 MUNDNICH & FREY, VALVASSORI 1963)

Routine tomographic projections of the temporal bone give a complete survey of the facial canal, each of the three parts being most evident in a particular view (Figs 7–12)

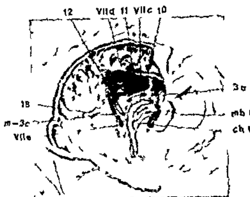


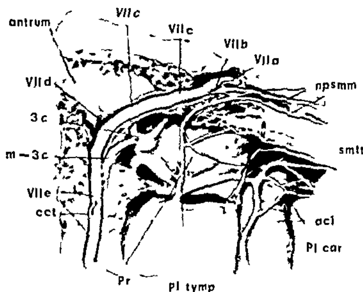
Fig 5 Right ear (lateral view) Opened tympanic cavity after almost complete resection of the mastoid cells and post parts of the external acoustic meatus Exposed tympanic part lateral wall and vertical part of the facial nerve canal with the chorda tympani and stapedius muscle in the post wall of the tympanic space (Redrawn after Pernkopf)

ch t—chorda tympani m—3 c—stapedius muscle and head of the stapes mb t—tympanic membrane VII c—tympanic segment of the facial nerve VII d—lateral knee VII e—mastoid segment of the *facial nerve* 3 a—head of the malleus 10—lateral semicircular canal 11—superior semicircular canal 12—post semicircular canal 18—sigmoid sinus

the long axis of the pyramid It continues the pathway for the nerve from the geniculate ganglion at the cochleariforme process in the direction towards the lateral (horizontal) semi circular canal It forms a part of the medial wall of the tympanum above the oval window and does not run quite horizontally (Figs 1 b, 2 b, 4) Its anterior part is *located* a little higher than the posterior part (DWORACEK 1960) and sometimes deviates peripherally laterally to the lateral semi circular canal (*Fig 1 a*) (*MIEHLKE 1972*, DE PONTVILLE et coll) In the medial wall of the tympanic cavity the canal protrudes over the oval window and usually forms a ledge projecting into the cavity (Figs 2 c *4 5*) *In* the middle ear the facial nerve is covered by an extremely thin bony layer (Fig 2 b) and may easily be injured by instruments or undue pressure during operation Posteriorly the wall bulges somewhat to form the prominence of the *facial canal* (Fig 2 c) Immediately above and posterior to this prominence lies the prominence of the lateral *semicircular canal* At the level of the pyramidal eminence in the posterior wall of the tympanic cavity, *the facial* canal forms a second bend the 'lateral knee' (VII d) beneath the lateral semicircular *canal* and proceeds in a vertical direction The bony lateral semicircular canal protrudes laterally over the facial canal (BOTMAN & JONGKEES 1955) (Figs 1 a, 2 b) The distance between the semicircular and the facial canals varies anteriorly *from 0 1 to 1* mm and posteriorly from 2 to 3 mm (Fig 1 b) The length of the lateral knee varies from 2 to 6 mm [illegible]

[illegible] lateral semicircular canal

Anatomic variations The tympanic part *sometimes* forms an overhanging ledge to such a degree that the oval window niche and the stapes are concealed from direct inspection in middle ear surgery Natural defects of the walls may also occur



aci—int carotid artery, cct—channel for the chorda tympani m 3 c—stapedius muscle npsmm— …—tympanic plexus Pr— …inthine part of the facial …al VII d—lateral knee VII e—mastoid part of the facial canal 3 c—stapes

Roentgenography In conventional roentgenography the labyrinthine part (VII a–b) is best demonstrated in the Chaussé IV projection (50° lateral inclination of the head) and appears above the cochlea and the lateral superior parts of the internal acoustic meatus (DE PONTVILLE et coll 1965) It may also be observed in Stenvers view at the lateral end of the meatus above the transverse crest

At tomography the labyrinthine part is best demonstrated in the axial pyramidal projection (Fig 9 a) Its longitudinal course and the orifice, and the more or less marked transverse crest, are well outlined due to the solid bony wall of the canal (in the otic capsule between the cochlear and vestibular parts of the labyrinth) In the a p and half axial views (Figs 7 a, 8 a) the labyrinthine part is sectioned obliquely but the wall of the canal is well demonstrated In the axial-pyramidal, half axial and a p views the wider lateral part at the 'upper knee must not be mistaken for the semi canal of the tensor tympani muscle (Fig 2 b, c), particularly as the latter may have the same dimension and appear as a closed canal The labyrinthine part is well demonstrated with the axial projection (Fig 12 a), but as this position is uncomfortable for the patient with the Polytome and Stratomatic, it ought to be used only on special indications

Tympanic part The tympanic, horizontal, or second part (VII c, Figs 1, 2, 4, 5, 6) is 8 to 11 mm long and 0 9 to 2 5 mm in diameter and runs approximately parallel to

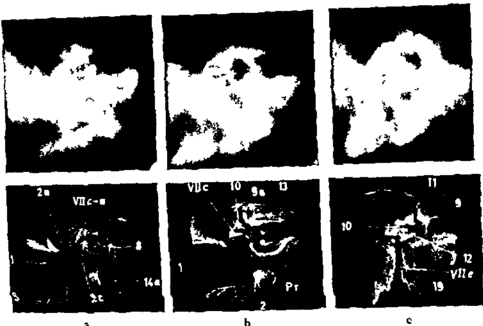


Fig 7 Tomography of the facial canal in the a p projection a) Section at the level of the chochlea b) Section at the level of the oval window Oblique section of the tympanic part of the facial canal beneath the lateral *semicircular canal* c) *Section immediately post to the post wall of the tympanic* cavity with the mastoid part of the facial canal in relation to post vestibular structures

cells and the wall between the canal and the cells may be only paper-thin or even defective in some places In such cases the lumen of the mastoid part is in direct connection with the mucoperiosteum of the cells, and thus indirectly with the middle ear

The mastoid part is connected to (1) the channel for the stapedius muscle, protruding into the tympanic cavity from its posterior wall as the pyramidal eminence (Figs 1 b, 2 b, c, 4, 5), and (2) a small channel for the chorda tympani (Figs 1 b, 2 c, 5)

The facial canal, besides carrying the facial nerve, also conveys blood vessels to the auditory ossicles In the labyrinthine and tympanic parts the nerve occupies more than 50 per cent of the lumen, but in the mastoid part only 25 to 50 per cent (SUNDERLAND & COSSAR 1953), the remainder being filled by connective tissue containing vessels The contents of the facial canal and its environment receive their blood supply from the stylomastoid, petrosal and labyrinthine arteries (BLUNT 1954, BOSATRA 1956, SUNDERLAND & COSSAR) The tympanum is situated in front of this part of the facial canal, as also is the posterior wall of the external meatus—at a distance of about 3 mm In its downward course towards the stylomastoid foramen, it is often

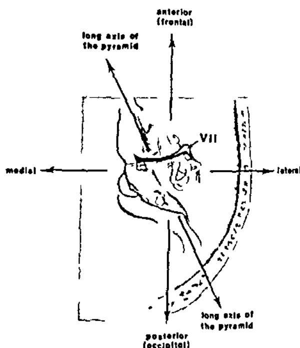


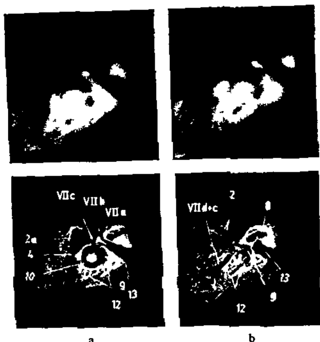
Fig 6 Schematic drawing of a right pyramid as seen in the cranio pcaudal (axial) view with the course of the facial nerve (VII)

and may be of importance if the nerve is surgically exposed to inadvertent instrumentation Their roentgenographic appearances have been discussed by WILBRAND & BERGSTRÖM (1975) and WRIGHT et coll

Roentgenographic positioning In conventional roentgenography the tympanic part (VII c) is best demonstrated in the Stenvers' and the transorbital projections

Tomographically the longitudinal course is best demonstrated in the Stenvers' projection (Fig 10), but because of the thin wall of the canal at the oval window niche, its finer details may be less well outlined Its transverse course is visible in the half-axial (Fig 8 b) or axial pyramidal (Fig 9 b) views, both permitting an assessment of its width In these views the thin tympanic portion of the wall is discernible in the healthy ear because of the favourable absorption difference (air/bone) The tympanic wall is not satisfactorily demonstrated with the a p projection (Fig 7 b) because of its oblique angle to the tomographic plane

Mastoid part The mastoid, vertical, or third part (VII e, Figs 1 b, 2 b, 4 5) has an average length of 12 2 mm (8 9 to 16) and a diameter of 4 mm It descends in a cranio caudal direction from the 'lateral knee' at the level of the pyramidal eminence to the stylomastoid foramen (Figs 1 b, 2 b, 4, 5) Its length is partly dependent on the shape of the temporal bone and partly on the extent of the pneumatization of the mastoid process The mastoid part has in its main extension a compact bony wall, it may, however, come into contact with mastoid cells at the level of the hypotympanum to a varying degree In some cases the canal may be completely surrounded by large



a b

a) Section at the level of the epi

cavity (the ossicles have been removed)

VII a—labyrinthine part of facial canal, VII b—upper knee, VII c—tympanic part of facial canal, VII d—lateral knee, 2—tympanic cavity, 2 a—epitympanic recess, 4—mastoid antrum, 8—cochlea, 9—vestibule, 10—lat semicircular canal, 12—post. semicircular canal, 13—int acoustic meatus

normal course, but just proximal to the chorda it forms a posteriorly convex curve before resuming its usual course forwards and medially The most prominent point of this posteriorly convex curve is located directly distally to the overhanging part of the lateral semicircular canal This explains why this portion of the nerve is especially exposed to injury during mastoidectomy (2) A dorsal displacement (2 to 4 mm along its vertical course), and (3) a combination of (1) and (2)

Besides these deviations in the course, splitting of the nerve into two vertical segments with a canal for each has been reported (BASEK 1962, FOWLER 1961, HAHLBROCK 1960, MIEHLKE 1960) and also of a tripartite course (BOTMAN & JONGKEES) Such splitting has been observed tomographically (TERRAHE 1972)

Marked anomalies of the course of the facial canal are generally associated with malformations

Substantial variations of the lumen of the mastoid part are normal and frequently [illegible] 1960) (Fig 1 b) They occur also, but to a lesser extent, in the







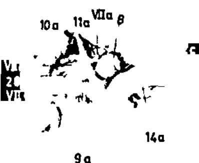


Fig 10

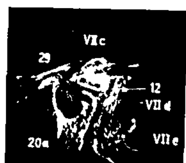


Fig 11 a



Fig 11 b

projection Section at the level of the oval win
icial canal and the lumen of the pyramidal emi

facial canal 2 c—hypotympanum 8—
—ant semicircular canal 14 a—carotid

Fig 11 Tomography of the facial canal in the lateral projection a) Section at the level of the lateral knee Mastoid part of the facial canal and part of the channel for the stapedius muscle in the post wall of the tympanum b) Section at the level of the oval window niche its relationship to the tympa nic and mastoid parts of the facial canal demonstrated

VII c—tympanic part of facial canal VII d—lateral knee VII e—mastoid part of facial canal 9 an—oval window niche 12—post semicircular canal 20 a—tympanic ring 29—channel for stapedius muscle

o the horizontal in the frontal plane and in 13 per cent this angle was 70 to 80° n 2 per cent it descended laterally at an angle of 60 to 70° In the sagittal plane it descended forwards at an angle of 100 to 110° in 9 per cent 80 to 100° in 80 per cent and 70° in 11 per cent Thus, three courses of the mastoid part have been distingu shed a flat, a steep and an oblique one (BOTMAN & JONGKEES) Under normal condi tions the mastoid part at the level of the posterior wall of the external meatus is located 10 to 15 mm medially to the suprameatal spine

The different courses may be explained by the development of the mastoid process They are not anomalies in the strict sense, but rather a result of unusual anatomic conditions in the immediate vicinity of the facial canal (POGANY 1922) An abnormal course may be manifested in three different ways (KETTEL 1946) (1) between the stylomastoid foramen and the origin of the chorda tympani the canal pursues its

Clinical aspects and pathology

Malformation In addition to anomalies in the course of the canal in the presence of otherwise normal bone anatomy, atypical courses occur, which are due to polymorphic bone malformations The course of the facial nerve and its length may be affected in cases with various grades of atresia of the external acoustic meatus A bevelled course and shortening of the canal are observed in severe dysplasia The part between the geniculate ganglion and the stylomastoid foramen is abnormal, the latter is wide (WRIGHT & TAYLOR), and the 'lateral knee' may be absent, the nerve maintaining a bevelled dorsal course If the mastoid process is hypoplastic, the canal is shorter, almost horizontal, and the facial nerve emerges laterally at the temporal bone In such cases the tympanic part cannot be outlined A steep facial canal indicates a sagittally short tympanum and stapedial dysplasia (TERRAHE)

Fractures Fractures of the skull base may continue into the labyrinthine segment of the facial canal with lesion of the nerve Very gracile fractures may remain undiagnosed in conventional roentgenography Usually, however, fractures can be revealed either by conventional roentgenography (LINDGREN 1943), or, with greater certainty, by tomography, where there is a high correlation between roentgen and clinical findings However, fractures of the canal do not necessarily lead to injury to the nerve, but only to vascular disturbances of the nerve Facial paralysis due to fractures of the skull may also occur, also without the fracture reaching the canal (JONGKEES 1965)

Temporal bone fractures are usually divided into three groups pyramido-transverse, pyramido-longitudinal and mastoid fractures The latter do not affect the inner ear, but may involve the mastoid part of the facial canal (RAMADIER & CAUSSÉ 1937, MIEHLKE 1960) Clinical methods for localization of the possible nerve lesion should always be supplemented by tomography

A *transverse fracture* of the pyramid is mostly a continuation of a posterior fossa fracture The position and direction vary considerably, they may be subdivided into two types (MCHUGH 1960), an internal and an *external* The internal one involves the internal acoustic meatus and the cochlea and in rare cases the labyrinthine part of the facial canal The external one mostly destroys the cochlea, vestibule and facial nerve When the facial canal is involved, immediate facial paralysis, loss of hearing and intense spontaneous nystagmus directed toward the opposite side occur

Longitudinal fractures involve the temporal squama or the mastoid process, often cross the external meatus and the roof of the tympanum and run forward along the pyramid The fracture often passes on either side of the otic capsule leaving [illegible]
Involvement [illegible]

[illegible] of impact indicates a direct facial nerve lesion,

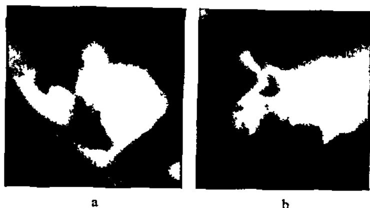


Fig 13 Tomography of the right ear of a 6-day-old girl a) Section in the semiaxial projection at the level of the oval windc
with a complete bony
the marrow cavity of t
from the labyrinthine to the mastoid part

tympanic part (Fig 1 b) The nerve occupies 10 to 45 per cent of the canal, in its narrower part 25 to 40 per cent (LINDEMAN) or 25 to 50 per cent (SULLIVAN) The variations of the lumen of the facial canal are a matter of discussion concerning their relationship to Bell's palsy At the junction of the tympanic to the mastoid part of the canal the lumen widens Considerable variations of the width are found at the point at which the chorda tympani joins the facial nerve It is usually stated that this point lies at a fixed distance above the stylomastoid foramen, but this has been con tradicted (LEGROS et coll 1972, ANSON et coll) Nowhere in its descent is the lumen of the canal circular, due to communication with the vascular channels in the bone (ANSON et coll) (Figs 1 b, 2 b, 7 c, 10, 11)

Defects of the walls occur and are of surgical importance like those of the tympanic part

Roentgenography With conventional roentgenography the mastoid part is best demonstrated in the lateral or modified lateral projection (VAN DER BREKEL) and may also be localized in the axial projection The 'lateral knee and the upper part may sometimes be seen in the transorbital and Chaussé III projection, but these give no detailed information

Tomographically the mastoid part may be demonstrated with all routine projections Stenvers' projection (Fig 10) gives the best survey of the whole course of the canal in a small series of sections In the true lateral view the channel of the chorda tympani may sometimes be observed In the axial view the mastoid part is best revealed in its relation to the mastoid cells, the tympanic ring and the posterior wall of the tympanic cavity The advantages of this view are not, however, sufficient to justify its routinely use as this position causes discomfort to the patient

Facial palsy can be caused by ultrasonic energy applied to the lateral semi circular canal in the treatment of Menière's disease (WALTNER 1965)

In reconstructive middle ear surgery much attention is paid to the tympanic part of the facial canal and accurate preoperative information about its course and appearance are required (WILBRAND & EKVALL 1975) In all cases where the canal appears normal (Figs 7 b, 8 b, 9 b, 10) its relation to the oval window must be revealed, since a narrow or deep oval window niche constitutes a surgical problem (Figs 2 b, c, 4, 5) Absence of a part of the wall may be regarded as an anomaly when the nerve has an aberrant course through the tympanic cavity, which pre operative tomograms may suggest (a free nerve traversing the tympanic cavity beneath the oval window, KAPLAN 1960, FOWLER, own case)

Surgical intervention in cases of fracture is intended either to restore the continuity of a torn nerve, relieve the nerve from compression or to remove bone fragments impinging upon it

Recommendation The three parts of the facial canal may be demonstrated in several of the routine tomographic projections For a complete examination of the canal a combination of two or three projections is recommended The labyrinthine part is best demonstrated with the axial pyramidal and the Stenvers' projections, the tympanic part with the Stenvers' and the half axial or axial pyramidal projections and the mastoid part with the true lateral and any other projection of choice The chorda tympani may be demonstrated with the true lateral projection In the author's opinion the facial canal as a whole is best evaluated with the half axial, Stenvers' and true lateral projections If detailed information is required a series of 0 5 mm sections apart is applied to the area of special interest The nature of the lesion must sometimes determine the choice of projection and distance between the sections

SUMMARY

The course of the facial canal in the complicated structure of the temporal bone is best demonstrated by multidirectional (hypocycloid or spiral) tomography A description of its normal anatomy is delivered, based on experiences from dissected temporal bone specimens, plastic moulds and tomograms Detailed knowledge of the anatomy is required for distinction of defects and anomalies, particularly pre-operatively (fractures reconstructive middle ear surgery) In malformation the pre-operative localization of the course of the facial canal is important since its relation to the oval window and the posterior wall of the tympanic cavity is decisive for surgical procedures

ZUSAMMENFASSUNG

Der Verlauf des Fazialiskanals im komplizierten, strukturreichen Felsenbein lässt sich am besten mit multidirektionaler (hypozykloider oder spiraliger) Tomographie abbilden Die normale Anatomie wird veranschaulicht mit Knochenpräparaten des Felsenbeins,

the nerve being either torn or compressed Late paralysis is caused by edema or hematoma of the nerve sheaths

In cases of deafness due to transverse or longitudinal fractures, hearing and the vestibular apparatus are completely destroyed once and for all If a facial nerve lesion is possible, an attitude of expectation is generally regarded as dangerous, and active intervention is recommended Bone spicules may impinge upon the nerve and may be demonstrated by tomography

Fractures through the mastoid process involve the mastoid cells and mastoid part of the facial canal without damaging the otic capsule structures

Inflammatory changes, including cholesteatoma Cholesteatoma, chronic granulation tissue and bony destructions due to infections are frequently found in the proximity of the upper mastoid part of the facial canal in the tympanic sinus, around the oval window or in the fossula of the round window Eradication of the growth without damage to the nerve requires close attention to anatomic details (KETTEL 1963, MIEHLKE 1960, SHAMBAUGH 1967) Defects of the tympanic and mastoid parts of the facial canal may be concealed by such tissue, which necessitates special care during operative instrumentation

In acute middle ear inflammation facial paralysis may arise either due to a direct effect on the tympanic part of the facial canal or as a result of involvement of cells in the direct vicinity of the posterior wall of the external meatus and cells beneath the lateral semicircular canal (Figs 2 b, c)

Tumors Destruction of the facial canal by tumor is rare Osteolysis due to tumor growth (eosinophilic granuloma, primary cholesteatoma, meningioma, neurinoma and chordoma) may be observed in conventional roentgenograms but are more evident in tomograms Besides carcinoma in the middle ear, neurinoma, rhabdomyosarcoma and glomus tumors occasionally may involve the facial canal

Surgical aspects The operation microscope has greatly diminished operation hazards When the course of the canal is atypical it is endangered when it forms a marked bulge beneath the lateral semicircular canal or when a long protracted dystopia of the mastoid part in the occipital direction is present

Many surgical procedures with the posterior approach to the middle ear imply risks to the facial canal removal of cells below and distal to the horizontal semicircular canal, removal of retrofacial cells in well pneumatized bone while operating close to the mastoid part of the canal (acute mastoiditis), and eradicating the surroundings of the cochleariform process

One indication for surgery on the mastoid part of the facial canal is long standing Bell's palsy Previously, nerve decompression within 5 to 6 weeks was recommended Nowadays the indications are more restrictive but preoperative tomography may be useful since such operations are still performed

JONGKEES L B W Facial paralysis complicating skull trauma Arch Otol 81 (1965), 518
KAPLAN J Congenital dehiscence of the Fallopian canal in middle ear surgery Arch Otolaryng 72 (1960), 197
KAUFMANN H, SCHMITT G und HACH G Schichtuntersuchungen mit spiralformiger und hypozykloidaler Systembewegung Radiologe 13 (1973), 82
KETTEL K Abnormal course of the facial nerve in the Fallopian canal Arch Otolaryng 44 (1946) 406
— Peripheral facial paralysis in fractures of the temporal bone Arch Otolaryngol 51 (1950), 25
— Surgery of the facial nerve Arch Otolaryng 77 (1963), 327
KODROS A and BUCKINGHAM R A The anatomy of the descending portion of the facial nerve Arch Otolaryng 66 (1957) 735
KULLMAN G L, DYCK P J and CODY D T Anatomy of the mastoid portion of the facial nerve Arch Otolaryng 93 (1973), 29
LEGROS M BEAUVILLAIN J and CHOUARD C Variations in the apparent origin of the chorda tympani Explanation of certain failures in chordial neurolysis Ann Oto-laryng Chir cerviofaciale 89 (1972), 349
LINDEMAN H The Fallopian canal, an anatomical study of its distal part Acta oto-laryng Suppl 158 (1960) 204
LINDGREN E Rontgenologische Gesichtspunkte zu Schädelfrakturen, die das Ohr betreffen Radiol clin 12 (1943), 1
LUCARELLI U e POMPILI G Indicazioni cliniche allo studio stratigrafico del canale del nervo facciale (In Italian) Arch ital Otol 72 (1961), 654
— — Anatomia e tecnica stratigraphice del canale del nervo faciale (In Italian) Radiol med 48 (1966), 729
MCHUGH H E The surgical treatment of facial paralysis and traumatic conductive deafness in fractures of the temporal bone Ann Otol 68 (1960), 855
MIEHLKE A Die Chirurgie des Nervus facialis Urban & Schwarzenberg, Munchen, Berlin 1960
— Probleme der Fazialisläsionen in der fachartzlichen Praxis Mschr Ohrenheilk (1972/3), 461
MUNTEAN E Der Wert der Tomographie fur die Erkennung pathologischer Veränderungen des Labyrinthes und des Fazialiskanals Fortschr Röntgenstr 64 (1941), 109
MUNDNICH K und FREY K-W Das Rontgenschichtbild des Ohres Georg Thieme, Stuttgart 1959
PLATZER W Zur Anatomie der Eminentia pyramidalis und des M stapedius Mschr Ohrenheilk 94–95 (1961) 553
POGANY E Einige anatomische Abnormitäten des Felsenbeines vom Gesichtspunkte der Otochirurgie Mschr Ohrenheilk 56 (1922), 35
DE PONTVILLE M PIGANIOL G et HOIROT J C l exploration radiologique du canal facial Techniques pratiques d examen Rev Laryng 86 (1965) 695
RAMADIER J A et CALSSÉ R Traumatismes de l oreille Masson & Cie, Paris 1937
SENDULSK J J Chirurgische Anatomie des Gesichtsnervenkanals Mschr Ohrenheilk 62 (1928) 175 280 426 512 704 1048 1268 1290 1490
SHAMBAUGH S E Surgery of the ear W B Saunders Comp, Philadelphia & London 1967
SULLIVAN J A Recent advances in the surgical treatment of facial paralysis and Bell's palsy Laryngoscope 62 (1952), 449
SUNDERLAND S and COSSAR D F The structure of the facial nerve Anat Rec 116 (1953), 147

plastischen Ausgussen und Tomogrammen Zur Darstellung und Erkennung von Dehiszenzen und Anomalien, insbesondere praoperativ (Frakturen und rekonstruktiver Mittelohrchirurgie), bedarf es einer Detailkenntnis der Anatomie in diesem Bereich Bei Missbildungen hat die tomographische Lokalisation und Darstellung des Verlaufes des Fazialiskanals ein besonderes Gewicht, zumal sein Verhaltnis zum ovalen Fenster und der hinteren Paukenhohlenwand für die Operation entscheidend ist

RÉSUMÉ

C'est la tomographie multidirectionnelle (hypocycloïde ou spirale) qui montre le mieux le trajet du canal facial dans la structure compliquée de l'os temporal L'auteur decrit son anatomie normale sur la base d'une experimentation faite sur des pièces d'os temporal dissequé, sur des moules plastiques et sur des tomographies Une connaissance détaillée de l'anatomie est nécessaire pour distinguer les pertes de substance osseuse et les anomalies, en particulier avant une opération (fracture, chirurgie reconstructive de l oreille moyenne) Dans les malformations il est important de localiser avant l'opération le trajet du canal facial car ses rapports avec la fenêtre ovale et la paroi postérieure de la cavité tympanique sont décisifs pour les traitements chirurgicaux

REFERENCES

AGAZZI C, COVA P L, e SENALDI M Semeiotica stratigrafica dell'osso temporale (In Italian) Relaz XVI Rad Gr Alta Italia O R L 1958

ANSON B J, DONALDSON J A and SCHILLING B B Surgical anatomy of the chorda tympani Ann Otol 81 (1972), 616

— — WARPEHA R L, RENSINK M J and SCHILLING B B Surgical anatomy of the facial nerve Arch Otolaryng 97 (1973), 201

BASEK M Anomalies of the facial nerve in normal temporal bones Ann Otol 71 (1962), 382

BLUNT M J The blood supply of the facial nerve J Anat 88 (1954), 520

BOSATRA A Some observations on the vascularization of the VII nerve J Laryng 70 (1956), 605

BOTMAN J W M and JONGKFES L B W Temporal branching of the facial nerve Acta oto laryng 45 (1955), 111

VAN DER BREKEL B A M Over de canalis facialis en zijn rontgenbeeld (In Dutch) Thesis, Amsterdam 1959

BRUNNER S and PEDERSEN C B Roentgen examination of the facial canal Acta radiol Diagnosis 10 (1970), 545

— PEDERSEN Ö and STOKSTED P Tomography of the facial canal in non rheumatic facial palsy Acta radiol Diagnosis 1 (1963), 90

...haltnisse des Mittelohres unter operationsmikrosko-
...ig 51 (1960), 15

...ral bone course of the facial nerve Laryngoscope 71 (1961), 937

HAHLBROCK K H Zweiteilung des N facialis im Warzenfortsatz Arch Ohr-Nas-, u Kehlk-Heilk 174 (1958-60), 465

... tomography Charles C Thomas, Spring-

FROM THE DEPARTMENTS OF DIAGNOSTIC RADIOLOGY (DIRECTOR PROF O OLSSON) AND THORACIC SURGERY (DIRECTOR O DAHLBÄCK), UNIVERSITY HOSPITAL, S 221 85 LUND, AND DEPARTMENT OF DIAGNOSTIC RADIOLOGY (DIRECTOR R SUNDGREN), CENTRAL-LASARETTET, S 291 85 KRISTIANSTAD, SWEDEN

INTRAPHRENIC ESOPHAGEAL LEIOMYOMA ASSOCIATED WITH DIVERTICULA PREOPERATIVELY DIAGNOSED BY ANGIOGRAPHY

J GÖTHLIN, R BLOCH and R SUNDGREN

The combination of benign esophageal tumor and diverticulum is uncommon, particularly in the lower esophageus Most reported cases have been found accidentally at autopsy while few have been diagnosed preoperatively Hiatal hernia has been the false diagnosis in some cases As the diagnosis benign tumor and diverticulum may be set accurately at angiography and barium meal, the present communication is forwarded, emphasizing the importance of selective angiography

Case reports

Case 1 Female age 26 Increasing difficulties in swollowing since 18 months Chest films revealed a mediastinal mass to the left just above the diaphragm Barium meal demonstrated a diverticulum at the same he gh r [illegible] ible,
a [illegible]
e [illegible]
d [illegible]

Submitted for publication 25 October 1974

TERRAHE K Diagnostik der Missbildungen des Ohres und des Ohrschädels Arch Ohr -Nas u Kehlk -Heilk 202 (1972) 85
VALVASSORI G E Laminagraphy of the ear Amer J Roentgenol 89 (1963) 1155
VIGNAUD J, BURLAMAQUE B J et AUBIN M L Étude tomographique de l aqueduc de Fallope J Radiol Electrol 51 (1970) 127
WALTNER J G Ultrasonic surgery in Meniere s disease Ann Otol 74 (1965) 174
WILBRAND H F Facialiskanalens rontgenanatomi (In Swedish) Nord Med 84 (1970) 1314
— and BERGSTROM B Multidirectional tomography of defects in the facial canal An experimental investigation Acta radiol Diagnosis 16 (1975) 223
— and EKVALL L Multidirectional tomography in reconstructive middle ear surgery Acta radiol Diagnosis 16 (1975) 436
WRIGHT J W and TAYLOR C E *Tomography and the facial nerve Trans Amer Acad* Ophtol Otolaryng 72 (1968) 103
— — and McKAY D C Variations in the course of the facial nerve as illustrated by tomography Laryngoscope 77 (1967) 717



Fig 2 Case 1 The gas filled diverticulum (↔) and the mass (→) 1 = left inferior phrenic artery anterior branch 2 left inferior phrenic artery posterior branch 3 = anterior esophageal branch 4 posterior esophageal branch 5 esophageal branch 6 = ascending branch of the left gastric artery

it was subphrenically located but more cranially than the one in case 1 No abnormal vessels were demonstrated

Thoracotomy revealed immediately above the main part of the diaphragm a tumor covered by the top layer of the diaphragm Associated with the tumor was a diverticulum

Discussion

Epiphrenal diverticula are rare (JULIAN 1953 GALVAO & GALVAO 1960) GOODMAN & PARNESS (1952) reviewed the literature finding 126 cases and adding three of their own A recent analysis of 80 cases was made by BRUGGEMAN & SEAMAN (1973) stating epiphrenic diverticula to be pulsion diverticula except the rare congenital cases They also found an unexplained association of diverticula and hiatal hernias



Fig 1 a) Case 1 b) Case 2 Divert culum in the lower part of the esophagus with a mass lateral to it

artery has an anterior and a posterior branch The latter followed the cranial surface of the diverticulum indicating its at least partly subphrenical localization No abnormal vessles were demonstrated

aphragm was situated over the upper
own into the abdominal cavity The
m the widened hiatus repaired Micro
mass
scopy revealed a leiomyoma and a diverticulum with unspecific inflammation The post

Esophagoscopy demonstrated narrow
walled diverticulum resembling a hiatal hernia Selective angiography the left lobe of the liver was vascularized by the left gastric artery (Fig 3 b) Only the posterior branch of the left inferior phrenic artery came from the left gastric artery while the origin of the anterior branch was not demonstrated The anterior and posterior esophageal branches passed into the anterior portion of the mass which was vascularized mainly by the posterior branch from the inferior phrenic artery It passed into the caudal part of the mass indicating that

diaphragm covering the proximal portion of the tumor and the term intraphrenic leiomyoma is suggested The two tumors had probably their origin between the two layers of the diaphragm pushing the parietal layer upwards In the first case the tumor extended through the hiatus into the abdominal cavity presumably by secondary growth Some of the previously reported leiomyomas may have grown in the same fashion but there is no such information in the reports This may be due to difficulties in observing intraphrenic growth when the anatomy has not been clarified preoperatively by angiography. This is easily performed with the technique described by SUNDGREN (1970), who also gives a detailed report of the vascular anatomy

Why esophageal diverticula develop in connection with tumors is not known Most authors believe that there is a congenital defect or mechanical traction by the tumor or a combination of these factors

As the tumors associated with diverticula reported in the literature have been fairly large, the mechanical factor may be important By heaviness, but mainly by rotation and pulsion at swollowing, a traction by the tumor on the esophageal wall seems to be quite possible

The angiographic appearance differs in malignant and benign lesion If a mass in the vicinity of the lower esophagus is detected on chest films and barium meal reveals connection with the esophagus, selective angiography of the left gastric artery should be performed GRIFF & COOPER found masses in the mediastinum of five patients all being leiomyomas, but GREEN et coll (1959), on the other hand, state that it is unusual for leiomyomas to present as masses on chest films

Conclusion Leiomyomas may grow intraphrenically Selective angiography of the left gastric artery may give the differential diagnosis between diverticula and hiatal hernia and disclose a benign tumor

SUMMARY

Two cases of esophageal leiomyoma associated with diverticulum are described Angiography demonstrated an intraphrenic location

ZUSAMMENFASSUNG

Zwei Fälle eines Leiomyoms verbunden mit Divertikeln werden beschrieben Die Angiographie zeigte eine intrahepatische Lokalisation

RÉSUMÉ

Description de deux cas de leiomyome associé à des diverticules L'angiographie a mis en évidence une localisation intraphrénique

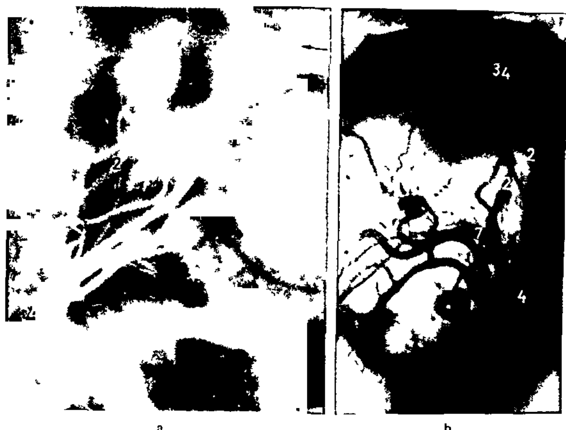


Fig 3 Case 2 The gas filled diverticulum (↔) and the mass (→) (The same abbreviations and symbols as in Fig 2) 7 = left hepatic artery

Leiomyoma is the most common solid benign tumor of the esophagus (KIRILUK 1967), despite the fact that less than 10 per cent of the leiomyomas of the alimentary tract are located in the esophagus (GRAY et coll 1961) The leiomyomas are rare in the upper esophagus, presumably due to less amount of smooth musculature (BOGEDAIN et coll 1963) Seven per cent of the leiomyomas occur in the upper third of the esophagus, 35 per cent in the middle and 55 per cent in the lower third (GRIFF & COOPER 1967) Nearly 10 per cent of the latter tumors involved the stomach

Benign tumors associated with diverticula in the lower esophagus have been found at autopsy by MILOVANIC (1914) and STEWART (1931) and at operation by among others HARRINGTON & MOERSCH (1955), PECHATNIKOVA (1950), NESE (1957), GALVAO & GALVAO, KÖHLE & SUCHANEK (1964), GAETINI et coll (1968) and BOTTGER (1970) Few of the leiomyomas were diagnosed preoperatively

In the material of DILLOW et coll (1970), two leiomyomas were masked by the epiphrenic diverticula and one by diverticulum and hiatal hernia HODGE (1970) reported one case with leiomyoma, diverticulum and hiatal hernia and MARTINS & ARDUINO (1959) one case with leiomyoma and diverticulum simulating hiatal hernia

All these diverticula were located 1 to 5 cm above the cardia and were thus classified as either epiphrenic or subphrenic The two present cases had a thin layer of the

diaphragm covering the proximal portion of the tumor and the term intraphrenic leiomyoma is suggested The two tumors had probably their origin between the two layers of the diaphragm pushing the parietal layer upwards In the first case the tumor extended through the hiatus into the abdominal cavity presumably by secondary growth Some of the previously reported leiomyomas may have grown in the same fashion but there is no such information in the reports This may be due to difficulties in observing intraphrenic growth when the anatomy has not been clarified preoperatively by angiography This is easily performed with the technique described by SUNDGREN (1970), who also gives a detailed report of the vascular anatomy

Why esophageal diverticula develop in connection with tumors is not known Most authors believe that there is a congenital defect or mechanical traction by the tumor or a combination of these factors

As the tumors associated with diverticula reported in the literature have been fairly large, the mechanical factor may be important By heaviness, but mainly by rotation and pulsion at swollowing, a traction by the tumor on the esophageal wall seems to be quite possible

The angiographic appearance differs in malignant and benign lesion If a mass in the vicinity of the lower esophagus is detected on chest films and barium meal reveals connection with the esophagus, selective angiography of the left gastric artery should be performed GRIFF & COOPER found masses in the mediastinum of five patients all being leiomyomas, but GREEN et coll (1959), on the other hand, state that it is unusual for leiomyomas to present as masses on chest films

Conclusion Leiomyomas may grow intraphrenically Selective angiography of the left gastric artery may give the differential diagnosis between diverticula and hiatal hernia and disclose a benign tumor

SUMMARY

Two cases of esophageal leiomyoma associated with diverticulum are described Angiography demonstrated an intraphrenic location

ZUSAMMENFASSUNG

Zwei Falle eines Leiomyoms verbunden mit Divertikeln werden beschrieben Die Angiographie zeigte eine intrahepatische Lokalisation

RÉSUMÉ

Description de deux cas de léiomyome associé à des diverticules L'angiographie a mis en évidence une localisation intraphrénique

REFERENCES

BOGEDAIN W, CARPATHIOS I and NOJIB A Leiomyoma of the esophagus Dis Chest 44 (1963), 391
BRUGGEMAN L L and SEAMAN W B Epiphrenic diverticula An analysis of 80 cases Amer J Roentgenol 119 (1973), 266
BOTTGER G Ringformig wachsendes Leiomyom des abdominalen Oesophagus Chirurg 41 (1970), 284
DILLOW B M, NEIS D D and SELLERS R D Leiomyoma of the esophagus Amer J Surg 120 (1970) 615
GAETINI A, DEI POLI M e PIAZZA L Due casi di leiomioma dell esofago (In Italian) Minerva chir 23 (1968), 753
GALVAO L e GALVAO I Diverticulo epifrenico do esofago (In Portuguese) Rev bras Cirurg 40 (1960) 103
GOODMAN H I and PARNESS I H Epiphrenic diverticula of the oesophagus J thorac Surg 23 (1952) 145
GRAY S W, SKANDALAKIS J E and SHEPARD D Smooth muscle tumors of the oesophagus Int Abstr Surg 113 (1961), 205
GREEN A E JR, BROGDON B G, CROW N E and SWEARINGEN A G Leiomyoma of esophagus Amer J Roentgenol 82 (1959), 1058
GRIFF L C and COOPER J Leiomyoma of the esophagus presenting as a mediastinal mass Amer J Roentgenol 101 (1967) 472
HARRINGTON S W and MOERSCH H J Surgical treatment and clinical manifestation of benign tumors of the esophagus with a report of 7 cases J thorac Surg 19 (1955) 800
HODGE G B Esophageal leiomyoma associated with an epiphrenic diverticulum and hiatus hernia Amer Surg 36 (1970), 538
JULIAN D G Epiphrenic oesophageal diverticulum with cardiac pain Lancet II (1953), 915
KIRILUK L B Leiomyoma of the esophagus North Med 66 (1967) 551
KÖHLE W und SUCHANEK E Leiomyom und Divertikel der Speiserohre Wien med Wschr 114 (1964) 312
MARTINS J D and ARDUINO E Leiomioma do esofago Rev bras Med (In Portuguese) 16 (1959), 30
MILOVANOVIC M Über Leiomyome des Oesophagus und der Kardia Wien klin Wschr 26 (1914), 753
NESE G Benign tumours and cysts of the oesophagus Acta chir scand 114 (1957), 165
PECHATNIKOVA E A A case of benign tumour of the esophagus complicated by diverticulum (In Russian with summary in English) Khirurgiya (Mosk) 5 (1950), 61
STEWART J B Myoma of the esophagus with associated diverticula Arch Path 12 (1931), 77
SUNDGREN R Selective angiography of the left gastric artery Acta radiol (1970) Suppl No 299

FROM THE DEPARTMENTS OF SURGERY I (DIRECTOR PROF L-E GELIN) AND II (DIRECTOR PROF R ROMANUS) AND THE DEPARTMENTS OF DIAGNOSTIC RADIOLOGY I (DIRECTOR PROF O BARTLEY) AND III (DIRECTOR PROF C-G HELANDER), SAHLGRENSKA SJUKHUSET, UNIVERSITY OF GOTHENBURG, S 413 45 GOTHENBURG, SWEDEN

ANGIOGRAPHY OF THE DILATOR RESPONSE IN EXTREMITY TRAUMA

D H LEWIS J SANDEGÅRD, T SEEMAN and B E ZACHRISSON

Injury to the soft tissue of the dog hind leg has been reported to be followed by a marked increase of blood flow to the injured extremity (LIU 1968, LEWIS & LIM 1970, SANDEGARD et coll 1974 a) In addition a marked dilatation of the vascular bed occurred in the traumatized leg extending proximally into the non traumatized areas Major arteries were dilated up to the bifurcation of the aorta The immediate increase of the blood flow was followed by gradual decrease of flow reaching pre-trauma levels approximately 60 to 90 min after the trauma Despite the decrea[illegible]

[illegible]

The increased blood flow was followed by a significant decrease of peripheral vascular resistance in the traumatized region, which cannot be explained as being solely of neurogenic origin, since a further increase of blood flow occurred following trauma to a limb after denervation (LIU) or post ganglionic sympathectomy (LEWIS & LIM) Moreover, the precapillary vessels displaying the vascular regions responsible for the decreasing flow resistance are strongly influenced by local stimuli as for

Submitted for publication 27 May 1974

example vasodilating substances A dilatation of larger arteries up to 30 per cent has been demonstrated angiographically during the hyperemia following muscular exercise (D'SILVA & FOUCHÉ 1960) This dilatation was even apparent when the flow increase was produced by an arterio-venous fistula from the contra-lateral leg It was concluded that changes in the caliber of these arteries were related to the flow However, the proximal spread of the dilatation of the femoral artery in response to contraction of muscles of the lower limb was abolished by division of the artery or by direct application of cocaine (HILTON 1959) It was therefore concluded that the response is mediated by a conducting system in the wall of the artery This system is activated by a variety of stimuli and ensures a reasonably widespread vascular response to local stimuli This mechanism seems to be related to the flow, whereas the dilatation following soft tissue trauma remained, despite return of flow to pre-trauma levels Several agents with vasodilating property have been demonstrated in the venous blood, draining the traumatized region (SANDEGÅRD et coll 1974 a, b) The occurrence of such factors may possibly explain the dilatation in the traumatized region but can hardly cause its proximal spread Therefore, the nature of the dilatation of the larger arteries after extensive trauma to the soft tissue of the hind leg was investigated and the possible role of the arterial conducting mechanism evaluated

Material and Methods

The experiments were carried out in twelve mongrel dogs (14 to 20 kg) of both sexes anesthetized intravenously with repeated small doses of sodium Pentobarbital, breathing spontaneously through a tracheal tube The operative preparation included small catheters for the recording of arterial blood pressure (mercury manometer) and for sampling and injections were introduced into one carotid artery and one jugular vein, respectively Following laparotomy through a lower midline incision, the internal iliac artery of one side and the medium sacral artery were ligated A catheter (Bardic adult feeding tube, length 107 cm, size 2 7 mm CR Bard International Ltd, England) for the injection of contrast medium was introduced through the contra-lateral internal iliac artery The tip of the catheter was placed just above the aortic bifurcation All branches of the external iliac and femoral artery including the deep and the cranial femoral arteries were ligated thus leaving the main artery to the traumatized region without major branches from the region to be traumatized up to the aortic bifurcation To exclude the circulation of the foot, with its rich net of arterio-venous anastomoses, a tourniquet was placed around the ankle

The trauma consisted of either (1) 200 blows with a padded hammer to one thigh, causing contusion of the soft tissues distal to the inguinal ligament and down to the knee or (2) gentle dissection of the soft tissues ventral to the junction of the lower thirds of the femur, thereby exposing the diaphysis of the femur Thirty minutes later a comminuted fracture was made by manipulating of a pair of bone tongs, or by an oscillating saw Two of the fractured dogs received an additional trauma of 100 blows to the fractured thigh



[illegible] moral arteries on the traumatized side proximal and distal to the suture line

For angiography the dogs were held in the supine position Serial angiography was performed with the same apparatus and technique described previously (SANDEGÅRD & ZACHRISSON) Fifteen ml Isopaque Cerebral (Nyegaard & Co, Oslo) was injected manually during 1 5 to 3 s Each series consisted of 30 films exposed at 2 films/s for 10 seconds, followed by 1 film/s for 10 seconds The angiography was performed before trauma, 1, 10, 30 and 60 min after the trauma

The flow increase and the dilatation of the major arteries were evaluated from the films by measuring the contrast medium transit time and the internal diameters of the external iliac and femoral arteries at corresponding levels (SANDEGÅRD & ZACHRISSON 1975 a) A measuring loupe with a built-in scale permitting readings within 0 1 mm was used The magnifying factor was × 7 The error of a single measurement at the iliac level was ±0 07 mm and at the different levels of the femoral artery ±0 05 mm

In seven animals the external iliac or the proximal part of the femoral artery was divided before the trauma and proximal to the region to be traumatized In four of these dogs resuture of the vessel was performed with single sutures In two of the animals 3 cm of the artery on the side to be traumatized was resected and thereafter the continuity of the vessel was reestablished by cannulating the vessel with a 4 cm siliconized plastic tube of slightly larger diameter than the vessel In one dog this grafting procedure was performed on both sides The anstomoses were secured by tight ligatures at each end

In three of the dogs with transection of the artery 0 5 ml nor-epinephrine (1m g/ml)



Fig 2 Angiography 30 min after trauma to the left thigh Division and reanastomosing the *femoral artery was made by a graft* (⇄) *before* trauma The spread of the dilatation was not abolished by the graft

was applied immediately after the trauma topically to the external iliac artery of both the traumatized and non-traumatized sides or injected into the vascular bed of the hind legs via the distal aortic catheter (1 mg/10 ml NaCl) In two animals repeated clamping with a pair of forceps was performed on the external iliac and femoral arteries of both the traumatized and non traumatized sides In two dogs following fracture and trauma to the soft tissue displacement of the fracture was produced

Results

Following soft tissue contusion trauma the systemic arterial pressure decreased moderately during the first 15 min and thereafter stabilized at a level slightly less than before trauma It was not affected by the preparation of the operative procedure to the arteries The fracture was followed by a less marked decrease of arterial pressure during the first 15 min and remained slightly lower than before fracture The addition of soft tissue contusion trauma did not further change the arterial pressure in comparison to that following trauma performed in non-fractured dogs

Angiography before trauma demonstrated equal filling and diameters of the larger arteries in both hind legs except in those subjected to division and reanastomosis of the iliac or femoral artery In these dogs slight narrowing of the vessel corresponding to the suture line and for about one cm proximal to the anastomoses occurred In the dogs with resected and grafted femoral artery the vessel proximal to the graft was slightly widened

In seven dogs, the vascular bed was markedly dilated one minute after the contusion trauma to the thigh distal to the suture line of the artery This dilatation involved the vessels both in the region traumatized and proximal to it The widening of the femoral artery extended proximally across the suture line and included the



Fig 3 Angiography 10 min after fracture of the right femur made with an oscillating saw (a) and 10 minutes after an additional contusion trauma to the thigh (b) which produced a widespread dilatation of the vessels in the traumatized region Segmental narrowing of the arteries overriding the fracture

iliac artery up to the aorta (Fig 1) It was not abolished by the resection and grafting of the vessel In comparison to the condition before trauma, a further widening even of the segment proximal to the graft had occurred (Fig 2)

In the five dogs with fracture neither the preparative procedure of the soft tissues nor the fracturing of the bone caused any widening of the diameters of the external iliac or the femoral arteries However, the addition of a contusion trauma consisting of 100 blows with the padded hammer distal to the suture level, was followed by a marked dilatation of the vessels within and proximal to the traumatized region (Fig. 3) Displacement of the fracture subsequent to the contusion trauma which caused an encroachment upon the vessel wall by sharp fragments could not abolish the dilatation provoked by the soft tissue trauma

Repeated clamping with a pair of forceps to the iliac or the femoral artery was followed by a marked segmental narrowing of the artery on the non traumatized side but did not affect the dilatation on the traumatized side (Fig 4 a) The topical administration of 0 5 mg nor-epinephrine to the iliac or femoral arteries caused a marked segmental contraction of the vessels Following contusion trauma this re

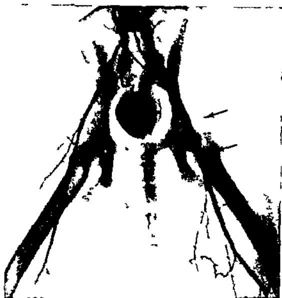


Fig 2 Angiography 30 min after trauma to the left thigh Division and reanastomosing the femoral artery was made by a graft (=) before trauma The spread of the dilatation was not abolished by the graft

was applied immediately after the trauma topically to the external iliac artery of both the traumatized and non-traumatized sides or injected into the vascular bed of the hind legs via the distal aortic catheter (1 mg/10 ml NaCl) In two animals repeated clamping with a pair of forceps was performed on the external iliac and femoral arteries of both the traumatized and non-traumatized sides In two dogs following fracture and trauma to the soft tissue displacement of the fracture was produced

Results

Following soft tissue contusion trauma the systemic arterial pressure decreased moderately during the first 15 min and thereafter stabilized at a level slightly less than before trauma It was not affected by the preparation of the operative procedure to the arteries The fracture was followed by a less marked decrease of arterial pressure during the first 15 min and remained slightly lower than before fracture The addition of soft tissue contusion trauma did not further change the arterial pressure in comparison to that following trauma performed in non-fractured dogs

Angiography before trauma demonstrated equal filling and diameters of the larger arteries in both hind legs except in those subjected to division and reanastomosis of the iliac or femoral artery In these dogs slight narrowing of the vessel corresponding to the suture line and for about one cm proximal to the anastomoses occurred In the dogs with resected and grafted femoral artery the vessel proximal to the graft was slightly widened

In seven dogs, the vascular bed was markedly dilated one minute after the contusion trauma to the thigh distal to the suture line of the artery This dilatation involved the vessels both in the region traumatized and proximal to it The widening of the femoral artery extended proximally across the suture line and included the



Fig 5 Angiography 30 min after trauma to the right thigh Immediately before angiography 1 mg nor-epinephrine was injected into the distal aorta Impaired passage of contrast medium on the non traumatized side

experimental set-up implies a comparison of the traumatized and non traumatized limbs in each animal

The dilator response following extended soft tissue contusion trauma to the dog hind leg was not affected by either mechanical or pharmacologic stimuli In an experimental set-up in which the flow in the femoral artery could be intermittently changed by the regulation of a distal arterio venous fistula to the contra lateral leg, D SILVA & FOUCHÉ could demonstrate angiographically the relation of the arterial diameter to the flow Increased flow widened the artery This mechanism might well agree with the condition early after the trauma when the blood flow to the traumatized region was markedly increased (SANDEGÅRD et coll a) However, it does not explain the persistent dilatation when the blood flow has returned to pre trauma value or even lower, as was demonstrated previously (SANDEGÅRD & ZACHRISSON b) A decreased sensitivity to pressor stimuli is in agreement with the results of LEWIS & KERSTEIN (1970), who in hemodynamic measurements demonstrated the inability of sympathetic nerve stimulation or close intra arterial injection of nor-epinephrine to increase the peripheral vascular resistance in the traumatized extremity following contusion trauma This inability of the major arteries to respond to contractile stimuli, could also be demonstrated in the present angiographies to involve the femoral and iliac arteries proximal to the traumatized area LEWIS & KERSTEIN suggested the release of some vasoactive substance from the muscle which overcame the sympathetic contracting stimuli However, the occurrence of the proximal dilatation cannot reasonably be explained by the activity of vasodilatory substances released in the injured tissues

The release of a vasodilator property from the traumatized region into the venous outflow (SANDEGÅRD et coll b), can hardly cause the dilatation seen on the arterial side Recirculation of the vasodilatory property cannot be a factor either, since the



Fig 4 Angiography 20 min after trauma to the right thigh of two dogs In (a) the external iliac arteries on both sides were repeatedly clamped 10 times with a pair of forceps at the arrows In (b) nor epinephrine was administered topically at the arrows immediately before the angiography Narrowing on the non traumatized side in both dogs

sponse could not be obtained on the traumatized side for up to 60 min after the trauma (Fig 4 b)

Intra-arterial injection of nor-epinephrine via the catheter in the distal aorta, mainly impaired the passage of contrast medium to the non-traumatized side, on the traumatized side a retarded passage was observed in the femoral artery, which was not markedly narrowed following the injection of nor-epinephrine (Fig 5)

Discussion

Vascular spasms in an injured extremity has been much debated in the absence of a true lesion to a major vessel Clinical reports of this phenomenon exist (Leriche 1928, Foisie 1947, Lumpkin et coll 1958, Smith et coll 1963), but many authors claim the cause of distal ischemia to be invariably due to an injury to the main vessel (Kirkup 1963, Brøyn & Bie 1966, Makin et coll 1966, MacGowan 1968, McQuillan & Nolan 1968, Shuck et coll 1972) The discrepancy may be related to the varying time intervals from trauma to the time of examination

Only the immediate reactions of the major vessels were analysed in the present experiments, corresponding to the previously reported increase of blood flow following soft tissue trauma (Lewis & Lim, Sandegård et coll a) The transient dilator response to the intra-arterial injection of contrast medium (Lindgren & Törnell 1958, Boijsen et coll 1971, Lewis et coll 1974) may be disregarded, as the present



Fig 5 Angiography 30 min after trauma to the right thigh Immediately before angiography 1 mg nor-epinephrine was injected into the distal aorta Impaired passage of contrast medium on the non traumatized side

experimental set up implies a comparison of the traumatized and non-traumatized limbs in each animal

The dilator response following extended soft tissue contusion trauma to the dog hind leg was not affected by either mechanical or pharmacologic stimuli In an experimental set up in which the flow in the femoral artery could be intermittently changed by the regulation of a distal arterio-venous fistula to the contra-lateral leg, D SILVA & FOUCHÉ could demonstrate angiographically the relation of the arterial diameter to the flow Increased flow widened the artery This mechanism might well agree with the condition early after the trauma when the blood flow to the traumatized region was markedly increased (SANDEGÅRD et coll a) However, it does not explain the persistent dilatation when the blood flow has returned to pre-trauma value or even lower, as was demonstrated previously (SANDEGÅRD & ZACHRISSON b) A decreased sensitivity to pressor stimuli is in agreement with the results of LEWIS & KERSTEIN (1970), who in hemodynamic measurements demonstrated the inability of sympathetic nerve stimulation or close intra arterial injection of nor-epinephrine to increase the peripheral vascular resistance in the traumatized extremity following contusion trauma This inability of the major arteries to respond to contractile stimuli could also be demonstrated in the present angiographies to involve the femoral and iliac arteries proximal to the traumatized area LEWIS & KERSTEIN suggested the release of some vasoactive substance from the muscle which overcame the sympathetic contracting stimuli However, the occurrence of the proximal dilatation cannot reasonably be explained by the activity of vasodilatory substances released in the injured tissues

The release of a vasodilator property from the traumatized region into the venous outflow (SANDEGÅRD et coll b), can hardly cause the dilatation seen on the arterial side Recirculation of the vasodilatory property cannot be a factor either, since the

arteries on the non-traumatized side were unaffected The transport of vasodilatory substances in lymph has been demonstrated following scalding (ARTURSSON 1969, EDERY & LEWIS 1963) The present trauma dose not necessarily impair the flow of lymph from the traumatized region (unpublished own data) However, it is not likely that lymph with its possible content of vasodilatory substances would account for the marked dilatation proximally, not even considering the known capability of kinins, histamine or serotonin to increase the permeability of the vascular walls (SPECTOR 1958)

The fact that the dilatation could not be abolished by division and reanastomosis of the vessel suggests that the dilator response in trauma involves another mechanism or mechanisms than conduction in the vascular smooth muscles of the vessel wall, as described in hyperemia following muscular contraction or excercise (HILTON) LIE et coll have reported that transection of the femoral artery in the dog did not abolish dilatation of the artery associated with increased flow, which was obtained by peripheral injection of acetylcholine or histamine, opening up of an arterio-venous shunt or tetanic stimulation of the sciatic nerve

In addition to the influence of local vasodilatory substances, the impaired contractility of the vascular smooth muscles may be caused by a disturbance of the cellular function called forth by the trauma The present experimental set-up was, however, not designed for information of this question, but such an investigation has been performed and the results are reported elsewhere (SANDEGÅRD et coll 1974 c)

The presents results have further supported the thesis that the dilator response following extensive soft tissue trauma is strong in nature and that the wall of the vessel may not be affected by pressor stimuli The occurrence of distal ischemia in extensive injury to the soft tissues of the extremities suggests other reasons than spasm of the involved major arteries as the cause The presence of distal ischemia clinically, should therefore, initiate further investigations

SUMMARY

The dilatation of major arteries following early after extensive soft tissue trauma was demonstrated angiographically not to be affected by pharmacologic or mechanical contractile stimuli The proximal spread of the dilatation was not abolished by the division and a reanastomosis of the vessel before the trauma These results suggest loss or impairment of the contractile ability of the major arteries following early after the trauma

ZUSAMMENFASSUNG

Die Dilatation der grosseren Arterien nach einer ausgedehnten Weichtteilverletzung die angiographisch nachgewiesen wurden, konnen nicht durch pharmakologische oder mechanische kontraktile Stimuli beeinflusst werden Das proximale Fortschreiten der Dilatation

war nicht durch eine Abtrennung und eine Reanastomose der Gefasse vor dem Trauma zu verhindern Diese Ergebnisse lassen auf einen Verlust oder eine Schadigung des kontraktilen Vermogens der grosseren Arterien fruhzeitig nach einem Trauma schliessen

RESUMÉ

Ce travail a montre angiographiquement que la dilatation des grosses artères apparaissant precocement après un traumatisme étendu des parties molles n est pas modifiée par des stimuli vaso-constricteurs pharmacologiques ou mecaniques L'extension proximale de la dilatation n a pas ete empêchee par la section et la reanastomose de ce vaisseau avant le traumatisme Ces resultats font penser que la contractilité des grosses artères est abolie ou diminuee dans la periode qui suit de pres le traumatisme

REFERENCES

ARTURSSON G The plasma kinins in thermal injury Scand J Clin Lab Invest (1969) Suppl No 107 p 153

BOIJSEN E DAHN I and HALLBOOK T Hemodynamic effect of contrast medium in arteriography of legs Acta radiol Diagnosis 11 (1971), 295

BROYN T and BIE K Peripheral arterial occlusion following traumatic intimal rupture Acta chir scand 131 (1966) 167

D SILVA J L and FOUCHE R F The effect of changes in blood flow on the calibre of large arteries J Physiol 150 (1960) 23 P

EDERY H and LEWIS G P Kinin forming activity and histamine in lymph after tissue injury J Physiol 169 (1963) 568

FOISIE P S Traumatic arterial vasospasm New Engl J Med 237 (1947), 295

HILTON S M A peripheral arterial conducting mechanism underlying dilatation of the femoral artery and concerned in functional vasodilatation in skeletal muscle J Physiol 149 (1959) 93

KIRKUP J R Major arterial injury complicating fracture of the femoral shaft J Bone Jt Surg 45 B (1963) 337

LERICHE R The problem of osteo-articular diseases of vasomotor origin J Bone Jt Surg 10-B (1928) 492

LEWIS D H and KERSTEIN M D Trauma and sympathetic nerve stimulation in the dog Europ Surg Res 2 (1970) 12

— and LIM JR R C (a) Studies on the circulatory pathophysiology of trauma I Effect of acute soft tissue injury on nutritional and non nutritional [illegible]

— [illegible]

— SANDEGÅRD J SEEMAN T and ZACHRISSON B E Effects of intraarterial injection of contrast medium on regional circulation in soft tissue trauma Acta radiol Diagnosis 16 (1975) 373

LIE M SEJERSTED O M and KIIL F Local regulation of vascular cross section during changes in femoral arterial blood flow in dogs Circulat Res 27 (1970), 727

LINDGREN P and TÖRNELL G Blood circulation during and after peripheral arteriography Acta radiol 49 (1958), 425
LIU C T Circulatory response to muscle trauma following denervation and hemorrhage in dogs J Trauma 8 (1968), 75
LUMPKIN M B, LOGAN W D, COUVES C M and HOWARD J M Arteriography as an aid in the diagnosis and localization of acute arterial injuries Ann Surg 147 (1958), 353
MACGOWAN W Acute ischemia complicating limb trauma J Bone Jt Surg 50-B (1968), 472
MAKIN G S, HOWARD J M and GREEN R L Arterial injuries complicating fractures and dislocations The necessity for a more aggressive approach Surgery 59 (1966), 203
MCQUILLAN W M and NOLAN B Ischemia complicating injury J Bone Jt Surg 50-B (1968), 482
SANDEGÅRD J and ZACHRISSON B E (a) Circulatory disturbances after experimental fracture Acta radiol Diagnosis 16 (1975) 181
— — (b) Angiography and hemodynamic measurements in extensive soft tissue trauma to the extremity Acta radiol Diagnosis 16 (1975), 279
— NOLTE J, LEWIS D H and SEEMAN T (a) Early hemodynamic and biochemical changes following soft tissue trauma Europ Surg Res 6 (1974), 233
— LEWIS D H and SEEMAN T (b) Vasodilator property of venous blood from trauma region Europ Surg Res 6 (1974), 265
— JONSSON O and ZACHRISSON B E (c) The ionic distribution in arterial smooth muscle and the persistent vasodilation after soft tissue trauma Europ Surg Res 6 (1974) 321
SHUCK J M, OMER G E and LEWIS C E Arterial obstruction due to intimal disruption in extremity fractures J Trauma 12 (1972), 481
SMITH R F, SZILAGY D E and PFEIFER J R Arterial trauma Arch Surg 86 (1963), 825
SPECTOR W G Substances which affect capillary permeability Pharmacol Rev 10 (1958), 475